NUREG/CR-1882
PNL-3681

Prototypic Thermal-Hydraulic Experiment in NRU to Simulate Loss-of-Coolant Accidents

Prepared by C. L. Mohr, G. M. Hesson, G. E. Russcher, R. K. Marshall
L. L. King, N. J. Wildung, W. N. Rausch, W. D. Bennett

Pacific Northwest Laboratory
Operated by
Battelle Memorial Institute

Prepared for
U.S. Nuclear Regulatory
Commission

NOTICE

This report was prepared as an account of work sponsored by an agency of the United States Government. Neither the United States Government nor any agency thereof, or any of their employees, makes any warranty, expressed or implied, or assumes any legal liability or responsibility for any third party's use, or the results of such use, of any information, apparatus product or process disclosed in this report, or represents that its use by such third party would not infringe privately owned rights.

Available from

GPO Sales Program
Division of Technical Information and Document Control
U. S. Nuclear Regulatory Commission
Washington, D. C. 20555

Printed copy price: $8.00

and

National Technical Information Service
Springfield, Virginia 22161

NUREG/CR-1882
PNL-3681
R3

Prototypic Thermal-Hydraulic Experiment in NRU to Simulate Loss-of-Coolant Accidents

Manuscript Completed: December 1980
Date Published: April 1981

Prepared by
C. L. Mohr, G. M. Hesson, G. E. Russcher, R. K. Marshall,
L. L. King, N. J. Wildung, W. N. Rausch, W. D. Bennett

Pacific Northwest Laboratory
Richland, WA 99352

Prepared for
Division of Reactor Safety Research
Office of Nuclear Regulatory Research
U.S. Nuclear Regulatory Commission
Washington, D.C. 20555
NRC FIN B2277

ACKNOWLEDGMENTS

The authors would like to thank the Chalk River, Nuclear Laboratories (CRNL) for their assistance in performing this test series. A special acknowledgment is due to CRNL staff members S. Z. Hart, D. T. Nishimura, P. E. Kelly, S. H. Kendrick, J. W. Logie, C. A. Herriot, and B. Debrau, who made a major contribution in keeping this work on schedule.

The assistance of R. Van Houten, NRC/RSR/FBR, Project Manager is also acknowledged for providing helpful directives to the program.

The authors would also like to thank S. L. Lilly for preparation of this manuscript.

SUMMARY

Quick-look test results are reported for the initial test series of the Loss-of-Coolant Accident (LOCA) Simulation in the National Research Universal (NRU) test program, conducted by Pacific Northwest Laboratory (PNL) for the U.S. Nuclear Regulatory Commission (NRC). This test was devoted to evaluating the thermal-hydraulic characteristics of a full-length light water reactor (LWR) fuel bundle during the heatup, reflood, and quench phases of a LOCA. Experimental results from 28 tests cover reflood rates of 0.74 in./sec to 11 in./sec and delay times to initiate reflood of 3 sec to 66 sec. The results indicate that current analysis methods can predict peak temperatures within 10% and measured quench times for the bundle were significantly less than predicted. For reflood rates of 1 in./sec where long quench times were predicted (>2000 sec), measured quench times of 200 sec were found.

CONTENTS

	ACKNOWLEDGMENTS	iii
	SUMMARY	v
1.0	INTRODUCTION	1
	1.1 PROGRAM SCOPE AND OBJECTIVES	1
	1.2 APPLICATION OF RESULTS	2
2.0	TEST SERIES DESCRIPTION AND ORGANIZATION	4
	2.1 TEST TRAIN AND INSTRUMENTATION DESCRIPTION	4
	2.2 TEST SERIES ORGANIZATION	9
3.0	REPORT SCOPE AND ORGANIZATION	11
4.0	SUMMARY OF TEST CONDITIONS AND MAJOR RESULTS	12
	4.1 TEST ASSEMBLY TEMPERATURES	12
	4.2 TEST OUTLET TEMPERATURES	17
	4.3 NEUTRON FLUX	17
	4.4 COOLANT DENSITY VARIATIONS	19
	4.5 POWER COUPLING	20
	4.6 INSTRUMENTATION FAILURE	22
	4.7 SHROUD LEAK RATE CHARACTERISTICS	22
	4.8 REFLOOD CHARACTERISTICS FOR FLECHT COMPARISON TESTS	26
5.0	REFERENCES	28
	APPENDIX - QUICK-LOOK REPORT DATA	
	PART 1 - TEMPERATURE PROBES	A.1
	PART 2 - NEUTRON FLUX DISTRIBUTIONS	A.121
	PART 3 - STEAM TEMPERATURE PROBE DISTRIBUTIONS	A.175
	PART 4 - SHROUD LEAK RATE CHARACTERISTICS	A.235
	PART 5 - FLOWMETER RATES FOR THE FLECHT COMPARISON TEST SERIES	A.263

1.0 INTRODUCTION

The Loss-of-Coolant Accident (LOCA) Simulation in NRU test program is being conducted in the National Research Universal (NRU) reactor at Chalk River Nuclear Laboratories (CRNL)[a] by Pacific Northwest Laboratory (PNL).[b] The project is sponsored by the Fuel Behavior Research Branch of the U.S. Nuclear Regulatory Commission (NRC) to evaluate the thermal-hydraulic and mechanical deformation behavior of a full-length fuel rod bundle during heatup, reflood, and quench phases of a LOCA. The tests are driven by low-level fission heat and simulate the temperature gradients in the fuel and cladding typical of a LOCA.

1.1 PROGRAM SCOPE AND OBJECTIVES

The program's current scope calls for the irradiation of six full-length test assemblies. The geometric configuration of each assembly represents a 6x6 segment of a 17x17 pressurized water reactor (PWR) fuel bundle. The tests, which are being performed in the U-2 loop of the NRU reactor, provide the following data:

- temperature distributions in a full-length bundle as a function of time
- interaction between thermal-hydraulics and cladding deformation
- quench front propagation
- quenching characteristics of nuclear-heated Zircaloy-clad rods for comparison with electrically heated Inconel or stainless-clad rods
- temperature-stress-time of cladding deformation
- distribution of cladding strain within bundle and information on failure propagation
- axial distribution of diametral strain in test fuel rods
- flow area reduction from cladding expansion.

(a) Operated by Atomic Energy of Canada, Limited (AECL).
(b) Operated for the U.S. Department of Energy (DOE) by Battelle Memorial Institute.

The test matrix for the program is broken into a thermal-hydraulic test series (using a single test assembly) and five materials deformation tests (using a separate assembly for each test). The thermal-hydraulic test series results[a] are reported and consist of 28 tests using unpressurized fuel rods that did not deform or rupture during the test series. The results of this experiment provide a reference for evaluating the quenching characteristics of Zircaloy nuclear fuel rods (Hann 1979).

The subsequent five materials deformation tests will concentrate on evaluating not only ballooning and rupture but also the added effects on the thermal-hydraulic behavior of flow blockage.

1.2 APPLICATION OF RESULTS

The data will be used to assess various calculational models for reactor safety analyses and conclusions derived from the large series of electrically heated tests and smaller scale in-pile tests being conducted elsewhere. The test data provide information for evaluating cooling-degraded cores as a result of either an accident or an off-normal operating transient. The experimental results of the program address 17 specific items outlined in the Code of Federal Regulations 10 CFR 50.46 and 10 CFR 50, Appendix K. These 17 areas are generally characterized by the following seven more general groups:

- Peak Cladding Temperature — 50.46 (b)(1)
- Evaluation Model Assessment — 50.46 (b)(5)(2)
- Swelling and Rupture — Appendix (K)(I)(B)
- Flow Blockage — Appendix (K)(I)(C)(2)
- Droplet Entrainment — Appendix (K)(I)(C)(1)(C)(2)
- Reflood Rate — Appendix (K)(I)(D)(3)
- Refill and Reflood Heat Transfer — Appendix (K)(I)(D)(5)

(a) Designated prototypic thermal-hydraulic (PTH).

The results of the program will be used to provide data for model calibration or to help define the primary heat transfer mechanisms for new analytical models. The geometry, mass flux, heat capacity, and materials are all prototypic, which eliminates much of the uncertainty of prior test results from other programs. Major concerns of other programs, such as length of fuel bundle or type of heating (nuclear versus electrical), should be answered by these test results.

2.0 TEST SERIES DESCRIPTION AND ORGANIZATION

2.1 TEST TRAIN AND INSTRUMENTATION DESCRIPTION

A schematic of the overall test train is depicted in Figure 1. The total length of the test train, including both the closure head and the test region, is 9.18 m (30 ft, 1-1/2 in.). The closure region provides the primary pressure boundary and includes penetrations for 183 instrumentation leads. The hanger tube is used to suspend the test bundle and shroud from the closure plug, and instrument leads are attached to the hanger to protect them during testing and transport. The shroud supports the fuel bundle; it serves as a protective liner during the experiment and transfer operations and provides proper flow distribution during various stages of the experiment. The stainless steel (SS) shroud consists of two halves clamped together at 17.78-cm (7-in.) intervals and attached at the end fittings. The split shroud design will make it possible to disassemble, reassemble, and examine the test train underwater. The shroud assembly is approximately 4.27 m (14 ft) long and is instrumented with 22 self-powered neutron detectors (SPNDs) and 38 thermocouples (TCs).

The fuel bundle consists of a 6x6 segment of a 17x17 PWR design with the four corner rods removed for easier insertion in the shroud. This provides a basic test array of 6x6-4 or 32 rods. The outer row of rods, including the corner rods of the next inner ring, will not be pressurized and will serve as guard rod heaters during the test. The test section consists of 11 fuel rods and 1 instrument thimble tube arranged in a cruciform pattern. The test rods in the test section were unpressurized for the thermal-hydraulic test series; subsequent tests will use pressurized rods. The fuel rod design variables are:

Cladding Material Specification	=	Zircaloy-4		
Cladding Outside Diameter (OD)	=	0.963	cm	(0.379 in.)
Cladding Inside Diameter (ID)	=	0.841	cm	(0.331 in.)
Pitch	=	1.275	cm	(0.502 in.)
Fuel Pellet Diameter	=	0.826	cm	(0.325 in.)
Fuel Pellet Length	=	0.953	cm	(0.375 in.)
Active Fueled Length	=	365.76	cm	(144 in.)
Total Shroud Length	=	423.1	cm	(170.125 in.).

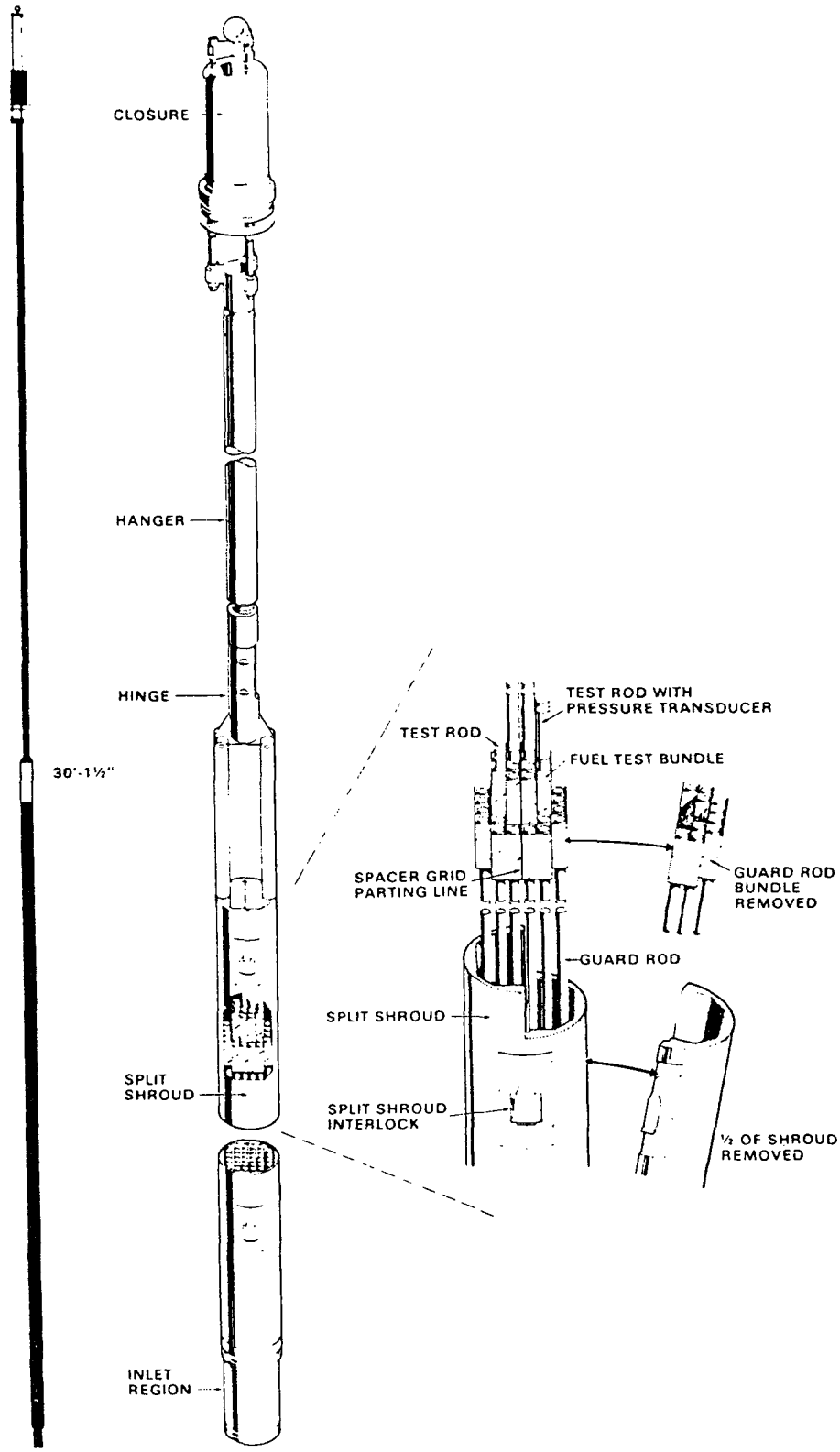

FIGURE 1. Schematic of the NRU LOCA Test Train

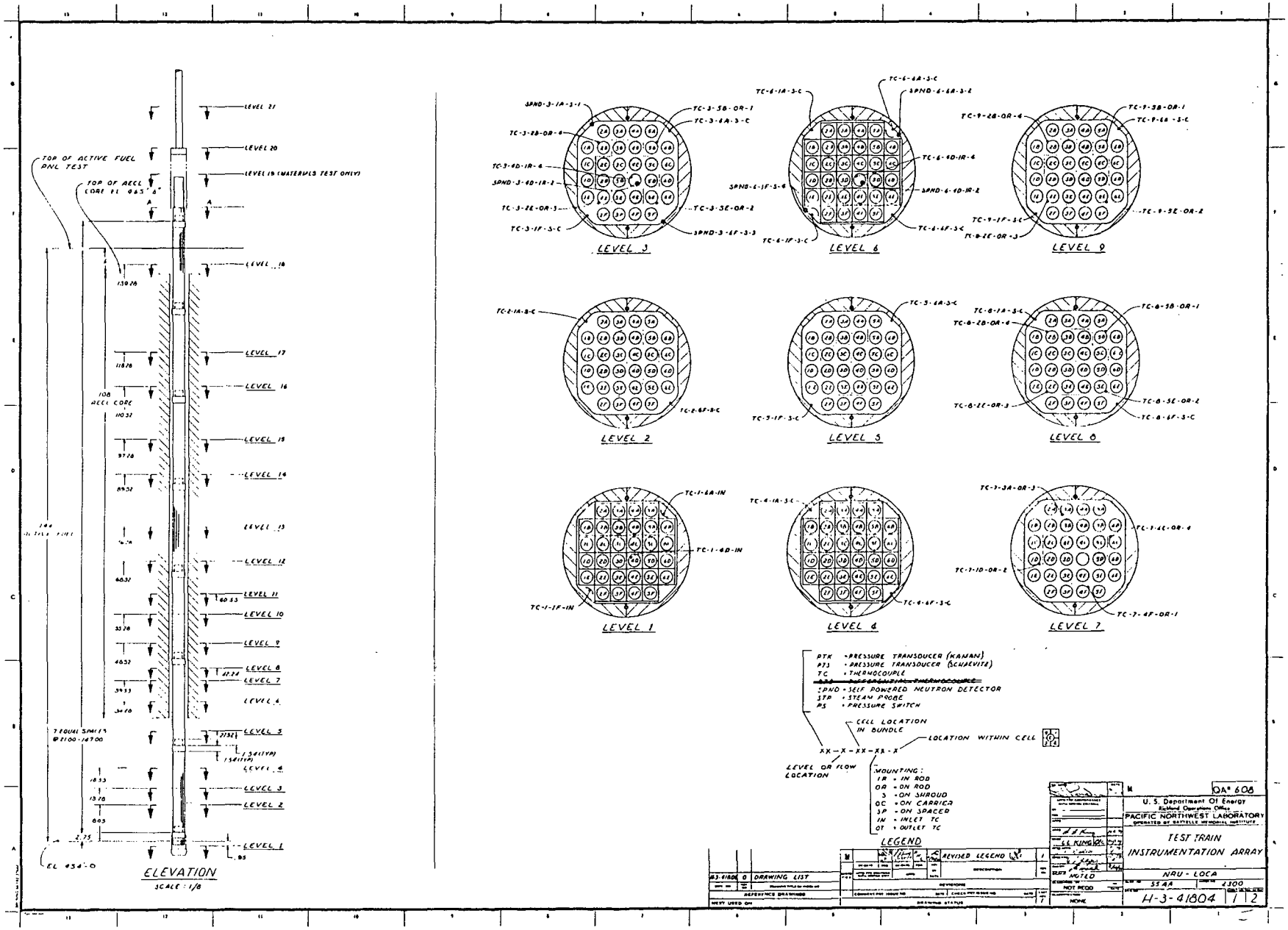

FIGURE 2. Axial Instrumentation Elevations and Instrumentation Cross Sections for Levels 1 through 9

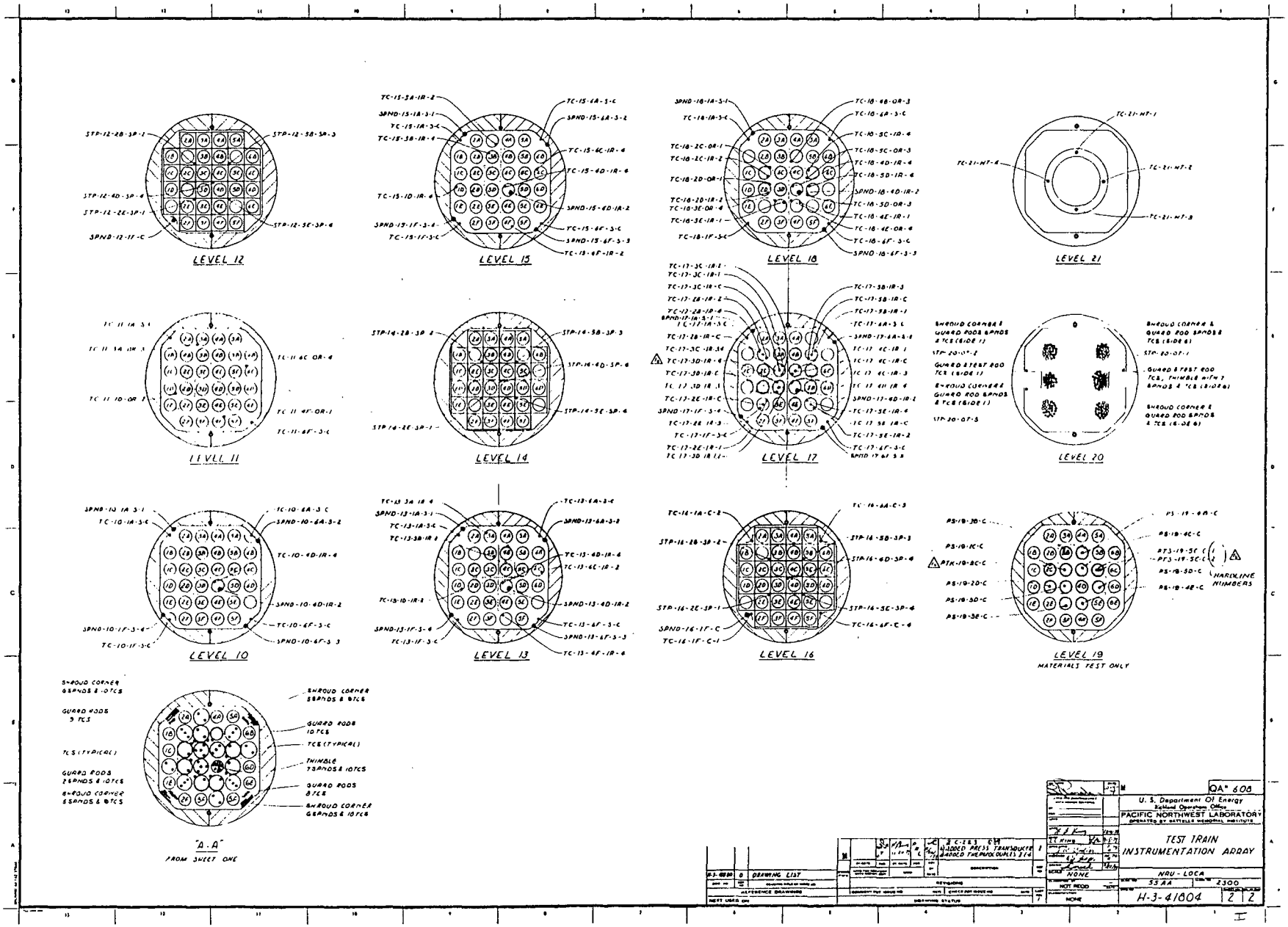

FIGURE 3. Instrumentation Cross Sections for Levels 10 through 21

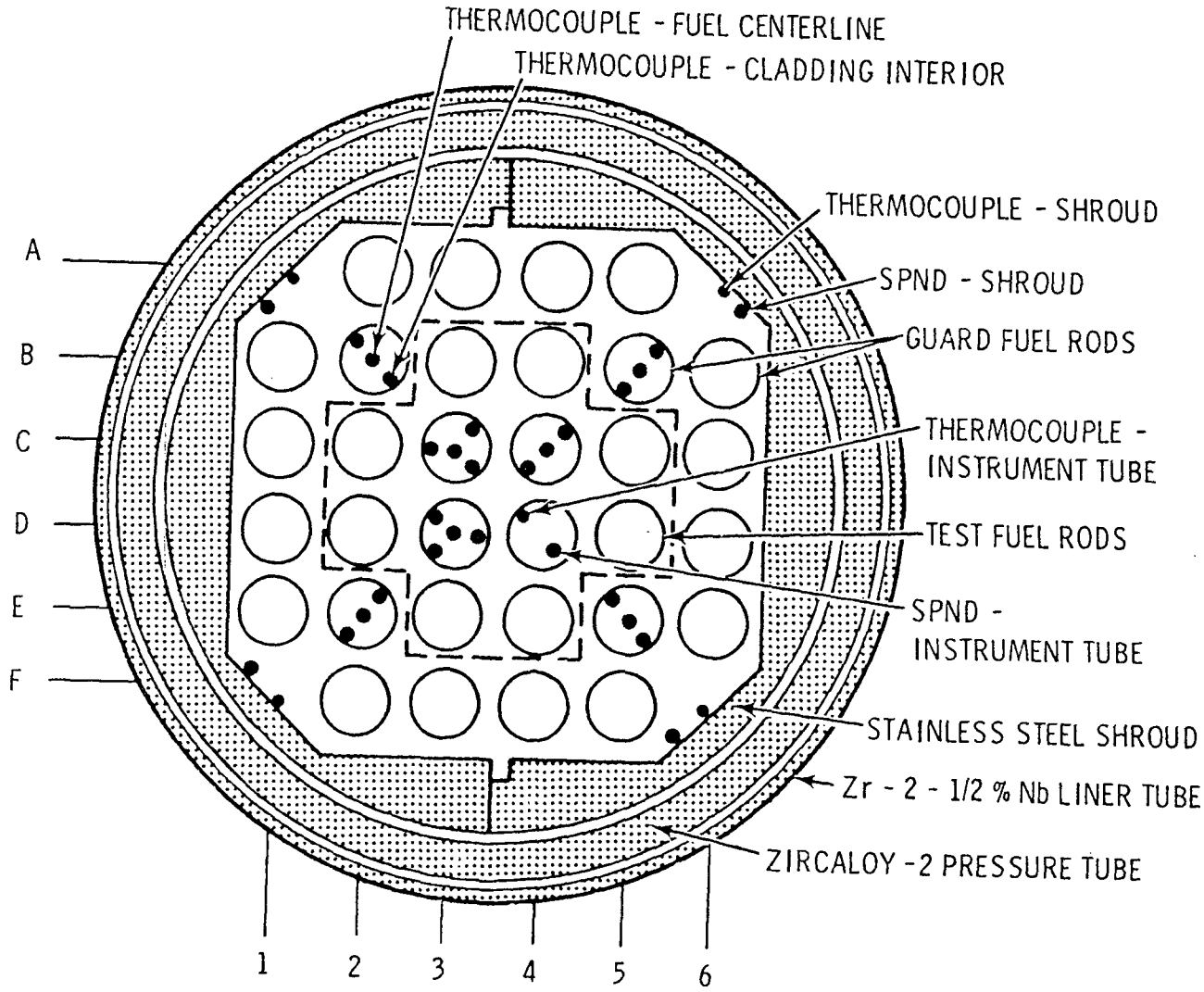

FIGURE 4. Cross Section of Test Assembly, Pressure Tube, Linear Tube, and Instrumentation Channel Identification

The test train instrumentation includes SPNDs (31), thermocouples (120), steam temperature probes (STPs) (18), and pressure transducers (11)[a] and/or pressure switches. These instruments were monitored on a real-time basis by the Data Acquisition and Control System (DACS). The data received allowed the temperature, power, and time history of the test train to be determined and provided an indication of when cladding rupture occurs.

TC measurements provide the main source of the thermal-hydraulic information. Measurement of quench front velocities and indications of water entrainment are determined from the steam probe (TC) instruments. TCs are also placed inside the cladding surface to measure azimuthal temperature variations.

The SPNDS provide relative power measurements within the fuel bundle during steady-state operation. These cobalt detectors are also able to detect density variations associated with the froth front that is present during the reflood phase of the transient.

A total of 21 levels along the axial length of the assembly have been defined where instrumentation is located. Figures 2 and 3 define the axial elevation of each of these levels and the associated instruments at each level. The nomenclature used to identify the instrumentation channels is keyed to a set of coordinate indicators defined in Figure 4.

2.2 TEST SERIES ORGANIZATION

The PTH test series was composed of three phases: preconditioning, pretransient, and transient operations (Mohr 1980; Russcher 1980). The preconditioning phase was conducted with the U-2 loop operating with water cooling and at an average fuel rod power of 187 W/cm (5.7 kW/ft). Two rises to full power were made in an attempt to allow the fuel to crack and relocate within the fuel cladding in a prototypic manner.

(a) Pressure transducers and/or pressure switches were not used on the PTH test but will be used on all deformation and rupture tests.

The pretransient phase was conducted with steam cooling at a flow rate of about 0.378 kg/s (3000 lb_m/hr) and an average rod power of 12.2 W/cm (0.37 kW/ft). This phase was used to initiate each of the specific 28 transient test runs in this test series. The operation consisted of bringing the assembly to power with a maximum measured cladding temperature of 700K (800°F) in preparation for the transient phase.

Both the pretransient and transient phases of operation were repeated for each test in the thermal-hydraulic test series. In the transient phase, the cladding was allowed to heat up in stagnant steam. At a preselected delay time, reflood water was introduced at a specified rate. At the point where either the loop was reflooded or all of the TCs were quenched, the test was terminated and the reactor power was tripped.

3.0 REPORT SCOPE AND ORGANIZATION

This report presents the most significant experimental results of the thermal-hydraulic test series in a timely manner without the benefit of supporting analysis or evaluation. Subsequent reports will provide more in-depth analysis of the neutronic and thermal-hydraulic behavior represented by the data presented in this report.

The remainder of the text portion of this report discusses the test conditions and major results from the following general areas:

- test assembly temperatures
- test outlet temperatures
- neutron flux
- coolant density variations
- power coupling
- instrumentation failure
- shroud leak rate characteristics
- reflood characteristics for FLECHT comparison tests.

The extensive Appendix of this report contains computer-generated plots of the data from the thermal-hydraulic test series. The data have been divided into five general parts: temperature profiles, neutron flux distributions, steam probe temperature distributions, shroud leak rate characteristics, and flowmeter rates for the FLECHT comparison test series.

No explanation is offered for apparent anomalies or differences between subsequent test data of the series. The data test series number for each test is clearly identified on each figure (e.g., PTH-101) along with the real time when the first data of the set were recorded.

4.0 SUMMARY OF TEST CONDITIONS AND MAJOR RESULTS

A summary of the test conditions used in each of the 28 PTH experiments is detailed in Tables 1 and 2.

Table 1 describes the test conditions, including reflood rate, reflood delay time, and peak cladding temperatures measured during the test. The peak cladding temperatures reported are those at the start of the transient (at the start of the adiabatic heatup), at the start of reflood, and at turnaround. The peak cladding temperatures were measured by TCs on the inside surface of the fuel rods. Calculations have shown that the measured temperatures of these TCs are probably 11-22K (2040°F) higher than the clad temperatures. The peak clad temperatures predicted by the Combustion Engineering proprietary THERM code and by use of the Westinghouse FLECHT correlation in the TRUMP heat transfer code are also shown in Table 1; predicted and experimental results show reasonable agreement.

Table 2 gives the quench times for both the peak temperature rod and the bundle as well as the quench times predicted by the THERM code. The measured values are significantly shorter than the predicted values.

The remainder of this section consists of summaries of the data results from the thermal-hydraulic test series. Computergenerated data plots for each general section can be found in the Appendix.

4.1 TEST ASSEMBLY TEMPERATURES

Test assembly temperatures were measured in four major components: test assembly shroud, instrument tube, guard fuel rods, and test fuel rods. Data for each of these components can be found in Part 1 of the Appendix where the preconditioning, pretransient, and transient test operations are summarized.

TABLE 1. Experimental Heat Cladding Temperatures

TEST NO.	REFLOOD RATE IN/SEC	DELAY TIME SEC	PEAK CLAD TEMP AT START OF TRANSIENT DEG F	PEAK CLAD TEMP AT START OF REFLOOD DEG F	PEAK CLAD TEMP AT TURNAROUND MEASURED DEG F	PEAK CLAD TEMP AT TURNAROUND PREDICTED FLECHT-TRUMP DEG F	PEAK CLAD TEMP AT TURNAROUND PREDICTED THERM DEG F
101	3.8	28 (1)	871	881	1403	1350	1365
104	3.8	37	853	1336	1487	1400	1445
105	1.9	7	858	907	1364	1400	1370
106	10.5 (2)	19	873	1101	1223	1100	1150
107	1.9	19	891	1154	1578	1500	1420
108	1.4	11	891	1010	1676	1700	1500
109	1.3	22	865	1158	1881	1800	1580
110	1.9	30	895	1314	1665	1600	1525
111	1.4 (3)	11	817	962	1696	1700	1500
112	3.8	37	843	1330	1589	1400	1425
113	7.6	37	845	1408	1526	1400	1395
114	7.6	32	858	1368	1477	1300	1300
115	9.5	66	795	1666	1758	1800	1720
116	3.8	51	836	1500	1707	1600	1605
117	3.8	66	817	1599	1788	1800	1800
118	2.9	52	844	1480	1756	1700	1675
119	2.9	46	862	1451	1673	1600	1620
120	5.9	51	847	1460	1611	1600	1580
121	3.8	36	833	1304	1579	1400	1425
122	7.6	52	866	1486	1611	1600	1575
123	2.9	51	848	1532	1788	1700	1675
124	5.9	52	861	1556	1688	1600	1580
125	1.4	20	872	1138	1802	1800	1565
126	1.2	3	797	800	1644	1700	1530
127	1.0	3	943	966	1991	1900	1650
128	2.0	50	911	1604	1991	1800	1735
129	1.4	32	940	1371	1898	1900	1670
130	0.7 (4)	5	929	998	2040		

(1) Unplanned delay caused by problems in prefill
(2) Malfunctioning equipment caused greater reflood rate than planned
(3) 1st two seconds of data missing
(4) Reactor tripped at ~1850 ^{o}F

TABLE 2. Comparisons of Predicted and Measured Quench Times

TEST NO.	REFLOOD RATE IN/SEC	DELAY TIME SEC	QUENCH OF PEAK POINT MEASURED TIME, s	QUENCH OF PEAK POINT PREDICTED TIME, s	QUENCH OF BUNDLE MEASURED TIME, s	QUENCH OF BUNDLE PREDICTED TIME, s
101	3.8	28 (1)	85		120	180
104	3.8	37	101	150	138	200
105	1.9	7	125	255	155	780
106	10.5 (2)	19	42	50		
107	1.9	19	154	290	173	800
108	1.4	11	189	410	276	1800
109	1.3	22	268	440	292	1700
110	1.9	30	173	315	193	810
111	1.4 (3)	11	205	410	235	1800
112	3.8	37	109	150	138	200
113	7.6	37	82	115	93	120
114	7.6	32	73	185	83	280
115	9.5	66	107	140	107	160
116	3.8	51	148	180	159	240
117	3.8	66	150	210	163	270
118	2.9	52	170	230	172	320
119	2.9	46	141	220	165	310
120	5.9	51	113	150	120	170
121	3.8	36	122	150	126	200
122	7.6	52	100	135	108	140
123	2.9	51	157	230	165	320
124	5.9	52	113	150	122	170
125	1.4	20	219	440	269	1700
126	1.2	3	207	450	257	>2000
127	1.0	3	344	625	344	>2000
128	2.0	50	162	355	220	830
129	1.4	32	216	470	287	1700
130	0.7 (4)	5				

(1) Unplanned delay caused by problems in prefill
(2) Malfunctioning equipment caused greater reflood rate than planned
(3) 1st two seconds of data missing
(4) Reactor tripped at ~1850 ^{o}F

4.1.1 Preconditioning Test Assembly Temperatures

Data were recorded as test PRECTH during the full-power steady-state Preconditioning Phase of NRU reactor operation. The average axial temperature profile for the shroud is shown (see Part 1.1 of the Appendix) as are the individual corner channel axial temperature profiles. Inlet piping 27.4 m (1080 in.) upstream from the test assembly, the outlet region (Level 20), the hanger tube (Level 21), and the outlet piping 8.2 m (324 in.) downstream from the test assembly are also provided in the profile. Coolant temperature gradients across the test assembly are also shown.

The instrument tube (see location 4D of Figure 4) has two types of temperature sensors. TCs are located on the inside radius (IR) of the tube, and steam probes with protective hoods removed are mounted on the outer radius (OR) of the tube. These sensors supplied the data (see Appendix, Part 1.1.2) for axial temperature profiles during the water-cooled preconditioning phases for comparison with grid-mounted STP data.

Guard fuel rod temperatures during preconditioning are summarized in Part 1.1 of the Appendix. TC sensors were located on both the interior and exterior of the guard fuel rods, and axial temperature distributions are provided by both types of sensor. Data for the same type and instrument level are either averaged or plotted independently to show power stress. Temperature gradients across the test assembly are also shown at several levels.

Test fuel rod temperatures during preconditioning are also provided by several IR, three center Level 17, and one Level 18 exterior TCs. The average IR axial temperature profiles are also shown in the Appendix for comparison with average fuel center and exterior cladding temperatures; individual test fuel rod temperatures are also compared with their center temperature. A diagonal temperature profile across the test assembly at Level 17 clearly shows the temperature gradient. The instrument tube (location shown in Figure 4) is adjacent to the test fuel rod locations plotted (3D and 4C); the effect of the tube is evident.

4.1.2 Pretransient and Transient Test Assembly Temperatures

Temperature data summaries are presented in the Appendix, Part 1.2, for four major test assembly components: shroud, instrument tube, guard fuel rods, and test fuel rods. Pretransient (steady-state) operation in the NRU uses steam cooling at higher temperatures than preconditioning. During transient operation, several additional sensors failed, and when erratic behavior was obvious, they were deleted from the data graphs. Some suspicious data remain, however. The test assembly coolant temperature profile across the diagonal at Level 16 is shown for the pretransient operation, which is typical of the many transient tests; it is a combination of STP and lead carrier TC data. An axial temperature profile of the shroud during pretransient operation is also provided, showing typical channel wall temperatures for each corner of the shroud. A set of elapsed time temperature profiles is also provided that shows the (measured) axial temperature gradients and peak temperatures of the shroud at 10 time intervals between the time when reflooding was started and when the shroud was quenched. TC data at the TA inlet (Level 1), the TA outlet (Level 20), and the hanger tube (Level 21) provide temperature data continuity over the entire test train, although none of these are contained in the instrument tube.

Guard fuel rod temperatures recorded during each transient test are presented in the Appendix, Part 1.2.3, as time histories averaged at each of the sensor levels (13, 15, and 17). These data are from interior TCs located between the fuel pellets and cladding. Typical temperature differences between these guard fuel rods can be seen in the preconditioning data summary (Appendix, Part 1.1.3).

Appendix, Part 1.2.4, contains time histories of the test fuel rod temperatures at the same sensor levels (13, 15, and 17) used for guard fuel rods. These data are from interior TCs with the addition of a central TC from instrumentation Level 17 for comparison. It is noted that the last Level 13 TC failed during test PTH-117 when the temperature exceeded 1255K (1800°F). Level 15 TCs remained operational even though the temperature reached 1350K (1970°F) in test PTH-130.

4.2 TEST OUTLET TEMPERATURES

A special section of outlet temperature data is not provided in the Appendix. Rather, this information is included in sections that present data summaries for the test assembly shroud, instrument tube, and test train.

4.2.1 Preconditioning Outlet Temperatures

During water-cooled preconditioning operation, the test assembly outlet region, hanger tube, and outlet piping operate at about 544K (520°F) as shown in Figures 1.1.1.3, 1.1.2.1, and 1.1.2.2 in the Appendix.

4.2.2 Pretransient and Transient Outlet Temperatures

The axial temperature profile of the test assembly during pretransient operation is shown in Appendix Figure 1.2.1.2; the outlet region temperatures do not exceed 589K (600°F). During the transients, the test train axial temperature profiles (see Figures 1.2.1.3.01 through 1.2.2.30) show that the maximum temperatures of the test assembly outlet region (Level 20) and hanger tube (Level 21) were about 716k (830°F) and 658K (725°F), respectively.

4.3 NEUTRON FLUX

The neutron flux is measured by SPNDs mounted in the instrument tube and on the test assembly shroud at several locations. Typical locations are shown in Figure 4. Similar data are provided for preconditioning (water-cooled), pretransient, and transient (steam-cooled) operations for comparison.

4.3.1 Preconditioning Neutron Flux

Full-powered NRU reactor operation provided the steady-state environment that is summarized on neutron flux distributions in the Appendix, Part 2.0. Neutron flux axial profiles are provided for the instrument tube and each corner channel of the shroud. The areas under

each curve of Appendix Figures 2.1.1 and 2.1.2 were integrated to provide an average neutron flux for each location. They are:

Test Assembly Location	Neutron Flux
IT 4D	2.71
Corner 1A	4.97
Corner 1F	5.28
Corner 6A	4.50
Corner 6F	4.97

When normalized to these averages, the five flux distributions collapse into one curve, which conforms to the neutronic design distribution (Heaberlin et al. 1979). That neutron flux axial profile has a peak-to-average ratio of 1.53 with the peak at an elevation of 2.13 m (84 in.). The ratio of the average flux at the shroud corners to the neutron flux at the instrument tube is a measure of flux depression and is measured to be 1.82; the ratio of maximum to minimum flux is 1.68 for the design neutron distribution extrapolated to the radius of the shroud SPNDs. The ratio of the shroud corner flux provides a measure of the flux tilt across the test assembly. It is 1.17 from corner 1F to corner 6A with a tilt axis along the 1A to 6F diagonal.

4.3.2 Pretransient and Transient Neutron Flux

Reactor operation at nominally 6% of full power provides the steady-state heat source for pretransient operation and the transient LOCA test series. These data are summarized in the Appendix, Part 2.2. For a comparison between water- and steam-cooled neutron flux distributions, the diagonal neutron flux profile across the test assembly is shown in Appendix Figure 2.2.1.1 for pretransient operation.

The axial neutron flux profile is provided in Figure 2.2.1.2 for each corner of the shroud for comparison with preconditioning data. The average pretransient neutron flux for each location is:

Test Assembly Location	Neutron Flux
IT 40	0.213
Corner 1A	0.300
Corner 1F	0.311
Corner 6A	0.271
Corner 65	0.304

The normalized axial flux distribution for each channel collapses to the same curve that conforms to the neutronic design distribution. The maximum to minimum flux depression ratio is 1.4, which is somewhat less than in the preconditioning operation; however, it is only 11% less than predicted in the neutronic design distribution. The flux tilt is 1.15 or 2% less than in the preconditioning operation, and the flux tilt orientation is the same.

Subtle changes in the neutron flux are caused by the neutron absorption effects of the reflood water. To evaluate the changing density of the coolant, the changing neutron flux is presented for various instrument tube levels during each transient test. The plotted delta flux is the difference between the current flux and the average flux calculated for at least 10 sec before the reflood began. In addition to the problem of SPND failures, the data presented may include the effects of the NRU reactor control system response to the reflood water neutronic absorption. For comparison with real-time histories of changing neutron flux, instrument tube axial flux profiles are also provided at several intervals after the time reflooding begins. Because some shroud SPNDs survived longer than instrument tube SPNDs, a comparable set of real-time histories of changing neutron flux at the shroud corner 6F are also provided in the Appendix, Part 2.2.

4.4 COOLANT DENSITY VARIATIONS

The evaluation of coolant density variations as a function of time during the transient operation is based on TC and SPND data (see Appendix, Part 2.2). The test assembly coolant changes from superheated steam during the pretransient operation to stagnant steam at the start of the transient. This condition changes to stagnant steam with entrained

water droplets, water froth, and saturated steam during the reflooding and quench periods. The results obtained from these instruments have been given a preliminary review; however, no conclusions have been drawn as to how much density information can be developed from these readings.

The evaluation of the coolant density throughout the test assembly as a function of time has an axial dependence based on reflood the test assembly from the lower end and upper dependence in the upper hanger bar region due to potential fall-back and condensation. TCs on the hanger rod as well as high-pressure instrument connectors located in the same region provide some time/temperature information that can be used to help evaluate density variations.

4.4.1 Preconditioning Coolant Density Variations

The STP response to steady-state (full-power) operation is shown in the Appendix, Part 3.1. Data from each instrument level are averaged to provide the axial temperature profile in water. Thermocouple data for the high-pressure connectors located on the upper region of the hanger bar are also included. Air TCs monitor the environment inside the connector and wall TCs are mounted on the connector walls. These data are included to indicate the bulk outlet temperature.

4.4.2 Pretransient and Transient Coolant Density Variations

Average STP data are shown for instrument levels 12, 14, 16, and 20 in the Appendix, Part 3.2. These, together with high-pressure connector TC data, are comparable with the preconditioning data summary. A temperature history of STP data is provided for each transient as is a temperature history of the high-pressure connectors.

4.5 POWER COUPLING

4.5.1 NRU Power

The NRU reactor power indication is provided by the normal reactor instrumentation and is given both as percentage of full reactor power

and as MW. The calculations presented here are based on percentage values.

4.5.2 Test Assembly Preconditioning Power

The test assembly power during preconditioning was determined by calorimetric methods at several power levels during the two rises to power. The data used were the flow rate provided by the loop instrumentation and an inlet temperature obtained by averaging the three test assembly TCs below the fueled region and the three test assembly TCs above the fueled region. Using TCs rather than loop instrumentation eliminated concern over heat losses in the loop piping. The powers calculated in this manner are:

Reactor Power, %	Test Assembly Power, kW	Coupling[a]
20	425	21.3
40	898	22.4
50	936	18.7
98	2058	21.5
97	2113	21.8
	Average	21.1

(a) Coupling is defined as Test Assembly Power/% Reactor Power

4.5.3 Test Assembly Pretransient Power

The test assembly powers were determined in the same manner as the caluclations for preconditioning power for runs PTH-COM and PTH-106. The powers were 138 and 135 kW, respectively. The nominal reactor power was 6%, which gives coupling values (test assembly power/% reactor power) of 23.0 and 22.5, which may be compared to the average coupling value of 21.1 determined for the preconditioning operation. This implies a 9% decrease in assembly power upon going from steam-filled to water-filled operation.

Some uncertainty exists concerning the accuracy of the nominal reactor power percentages used in the foregoing calculations, and the problem is being investigated and will be resolved.

4.6 INSTRUMENTATION FAILURE

During the course of the testing, many of the sensors including TCs, STPs, and neutron detectors behaved in odd ways. In many cases, a sensor appeared to have failed but later in the same test or in a later test it was once again performing as expected. This behavior was especially prevalent among the SPNDs.

More analysis will be required to determine the difference between actual instrument failure and instrument behavior that is real but not currently understood. Table 3 presents a preliminary list of the sensors whose output showed inexplicable response patterns when plotted versus time. Although Table 3 is listed in chronological order of failure, the tests were not always performed in the direct numerical sequence of the test identification number.

4.7 SHROUD LEAK RATE CHARACTERISTICS

The shroud leak rate tests were designed to test both the shroud integrity and to verify the reflood rate calibration. Each test consisted of one reflood cycle with the reactor at essentially zero power. The data consist of STP measurements plotted versus time. Identical leak rate tests were performed at different times during the thermal-hydraulic test series. Optimally, each of these tests would result in identical instrument responses. The data from STPs at different elevations are presented for tests at 2 in./sec and 3 in./sec nominal reflood rates in Appendix Figures 5.1.1 through 5.7.4. Table 4 contains the elevations of these instruments to be used in evaluating the actual reflood rates.

4.7.1 Low Reflood Rate (2 in./sec)

The first shroud leak tests were performed early in the test series to set a base response curve. The reflood rate as measured by

TABLE 3. Failed Sensors

Test Number	Sensor Designation
101	TC-13-6C-IR-2
	TC-13-1F-S-C
	TC-15-6F-S-C
	TC-17-4C-IR-C
	TC-17-3C-IR-7
	TC-17-5B-IR-C
	TC-18-1A-S-C
	SPND-15-1F-S-4
	SPND-3-6F-S-3
	SPND-15-1A-S-1
114	SPND-13-1F-S-4
107	TC-17-6F-S-C
110	SPND-17-4D-1R-2
	SPND-17-1A-S-1
108	TC-3-6A-S-C
	STP-14-5E-SP-4
109	SPND-15-4D-IR-2
	SPND-15-6F-S-3
	SPND-15-6A-S-2
	SPND-18-4D-1R-2
	TC-11-1D-OR-2
	SPND-17-6A-S-C
	STP-12-2B-SP-2
	SPND-17-6F-S-C
	STP-14-58-SP-3
	SPND-13-6F-S-3
	SPND-13-6A-S-2
	SPND-13-4D-IR-2
	SPND-16-IF-S-C
112	TC-11-4F-OR-1

TABLE 3. Failed Sensors (continued)

Test Number	Sensor Designation
116	TC-7-3A-OR-3 TC-20-OT-3
117	STP-14-2E-SP-1 TC-11-3A-OR-3 TC-13-3B-1R-2
118	TC-7-6C-OR-4
119	STP-16-5E-SP-4
122	STP-14-2B-SP-2
124	STP-16-2E-SP-1
125	STP-12-5B-SP-3 TC-11-6C-OR-4
127	TC-6-1A-S-C STP-12-5E-SP-4 STP-12-2E-SP-1 SPND-18-6F-S-3
128	SPND-13-1A-S-1
130	SPND-10-6F-S-3

TABLE 4. Steam Probe Identification and Axial Locations

	Elevation	
	in.	(m)
STP-12-4D-SP-4	68.8	(1.748)
STP-12-5E-SP-4	68.8	(1.746)
STP-12-5B-SP-3	68.8	(1.746)
STP-12-2B-SP-2	68.8	(1.746)
STP-12-2E-SP-1	68.8	(1.746)
STP-14-4D-SP-4	89.8	(2.282)
STP-14-5E-SP-4	89.8	(2.281)
STP-14-5B-SP-3	89.8	(2.281)
STP-14-2B-SP-2	89.8	(2.281)
STP-14-2E-SP-1	89.8	(2.281)
STP-16-4D-SP-4	110.8	(2.815)
STP-16-5E-SP-4	110.8	(2.814)
STP-16-5B-SP-3	110.8	(2.814)
STP-15-2B-SP-2	110.8	(2.814)
STP-16-2E-SP-1	110.8	(2.814)
STP-20-OT-2	160	(4.06)

the turbine flowmeter is shown in Appendix Figure 5.1.1. The temperature responses for the three STPs mounted on the instrument tube are shown in Appendix Figure 5.1.2. Appendix Figures 5.1.3 and 5.1.4 show the temperatures measured by the STPs mounted on the grid spacers in the bundle. Two figures were used to show the large number of instruments.

It can be seen that as the coolant reached the level of each instrument, the temperature dropped suddenly. By using the times at which different elevations were reached, it is possible to determine the actual rate at which the shroud filled with water. Appendix Figures 5.2.1 to 5.3.3 show information from the second and third shroud leak tests at 2 in./sec. Changing flow conditions may be determined by comparing these measurements with the first test.

4.7.2 Nominal Reflood Rate (3 in./sec)

Shroud leak test data from tests at 3 in./sec are presented in the same manner as those for the low reflood rate data. Results from the first test at 3 in./sec are shown in Appendix Figures 5.4.1 through 5.4.4; and tests 2, 3, and 4 are presented in Appendix Figures 5.5.1 through 5.7.4. These plots indicate that very little, if any, shroud leakage was experienced during these tests. Further evaluations are being performed to better define the leakage.

4.8 REFLOOD CHARACTERISTICS FOR FLECHT COMPARISON TESTS

Three pairs of tests were designed to provide data for comparison with FLECHT data: PTH-108, PTH-111, PTH-118, PTH-123; and PTH-120, PTH-124. Tests PTH-108, PTH-118, and PTH-120 used a normal prefill that introduced reflood water up to the bottom of the fuel rod at a fast rate of 0.229-0.254 m/sec (9-10 in./sec) followed by the preselected reflood rate for the duration of the test. The companion tests used a fast-filled sequence to insert reflood water at the fast rate up to the 0.305-m (1-ft) level on the fuel column, followed by the preselected reflood rate for the duration of the test. A reflooding rate history is provided in Part 5 of the Appendix for each of these FLECHT comparison tests.

In addition, the reflood rate history is provided for three replicable tests that were conducted between the FLECHT comparison test pairs. Those tests (PTH-104, PTH-112, and PTH-121) all used normal prefill reflooding sequences and compared very well. Because the remaining tests of the series used this normal prefill sequence, additional reflood rate history graphs are not provided.

5.0 REFERENCES

1. Hann, C. R. 1979. Program Plan LOCA Simulation in the National Research Universal (NRU) Reactor. PNL-3056, Pacific Northwest Laboratory, Richland, Washington.

2. Mohr, C. L., et al. 1981. Safety Analysis Report: Loss-of-Coolant Accident Simulations in the National Research Universal Reactor. PNL-3093, NUREG/CR-1208, Pacific Northwest Laboratory, Richland, Washington.*

3. Heaberlin, S. W., et al. 1979. Design Basis Neutronics Calculations for NRU-LOCA Experiments. PNL-3113, NUREG/CR-1025, Pacific Northwest Laboratory, Richland, Washington.*

*Available for purchase from the NRC/GPO Sales Program, U.S. Nuclear Regulatory Commission, Washington, DC 20555, and/or the National Technical Information Service, Springfield, VA 22161.

APPENDIX

QUICK-LOOK REPORT DATA

PART 1

TEMPERATURE PROFILES

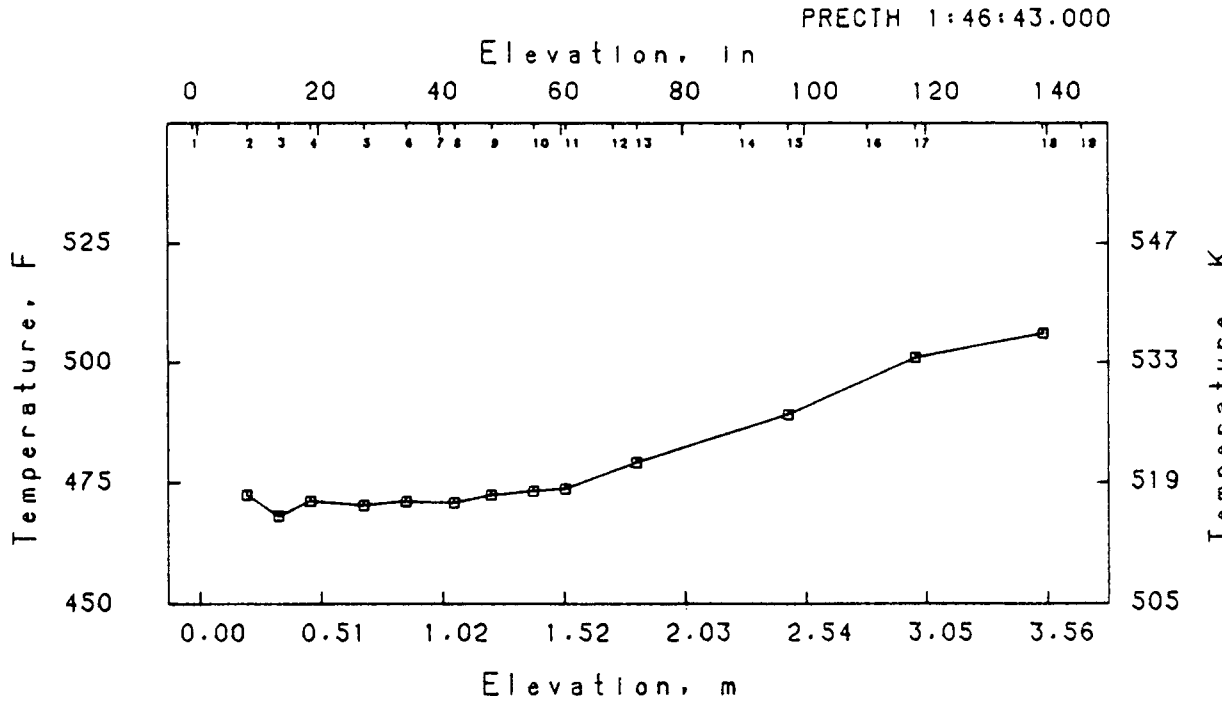

FIGURE 1.1.1.1 AVERAGE SHROUD AXIAL TEMPERATURE PROFILE

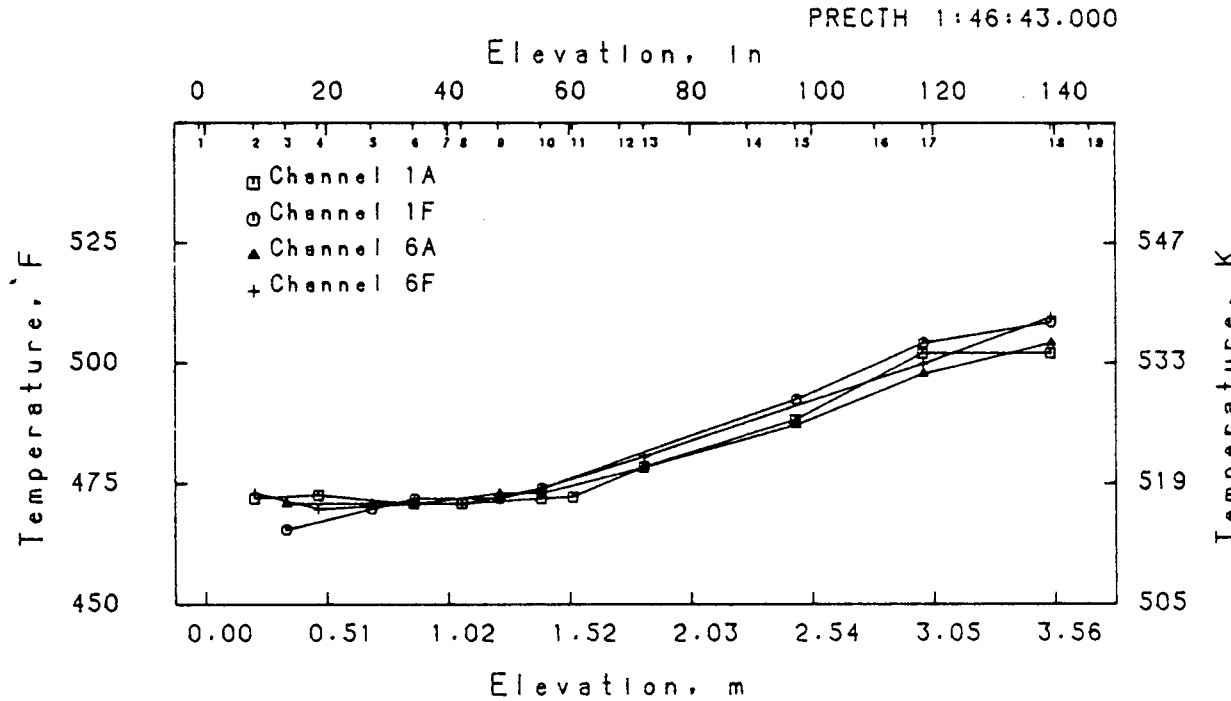

FIGURE 1.1.1.2 SHROUD AXIAL TEMPERATURE PROFILE

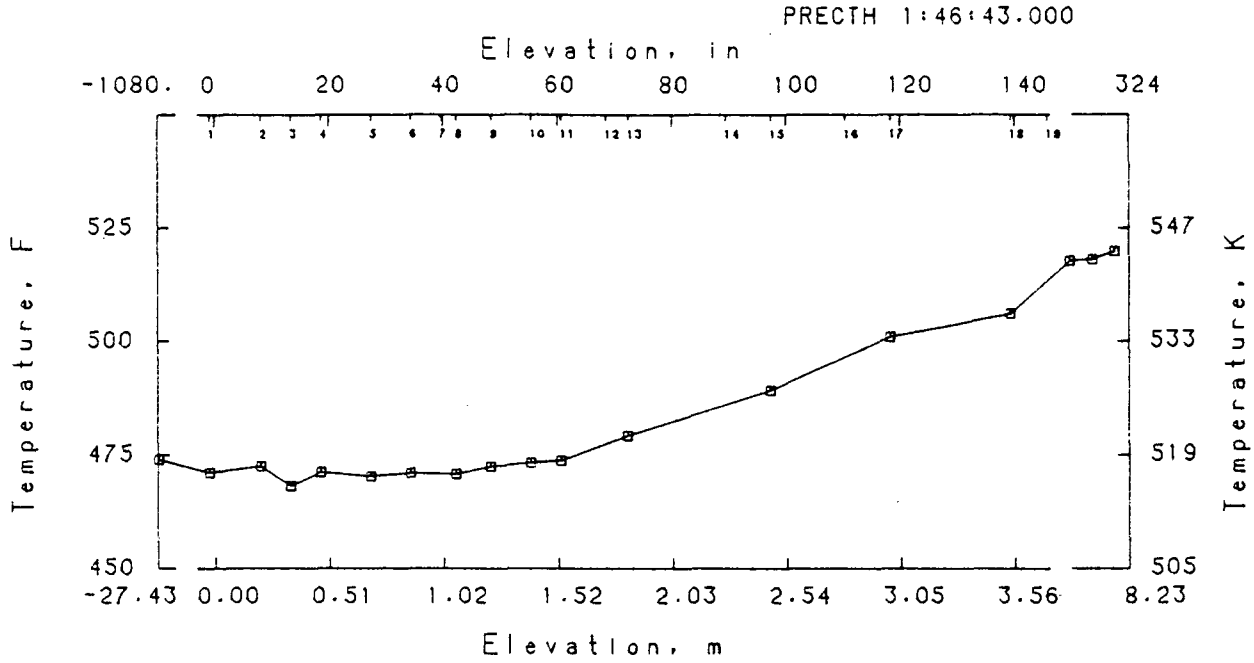

FIGURE 1.1.1.3 SHROUD AND TEST TRAIN COOLANT TEMPERATURES

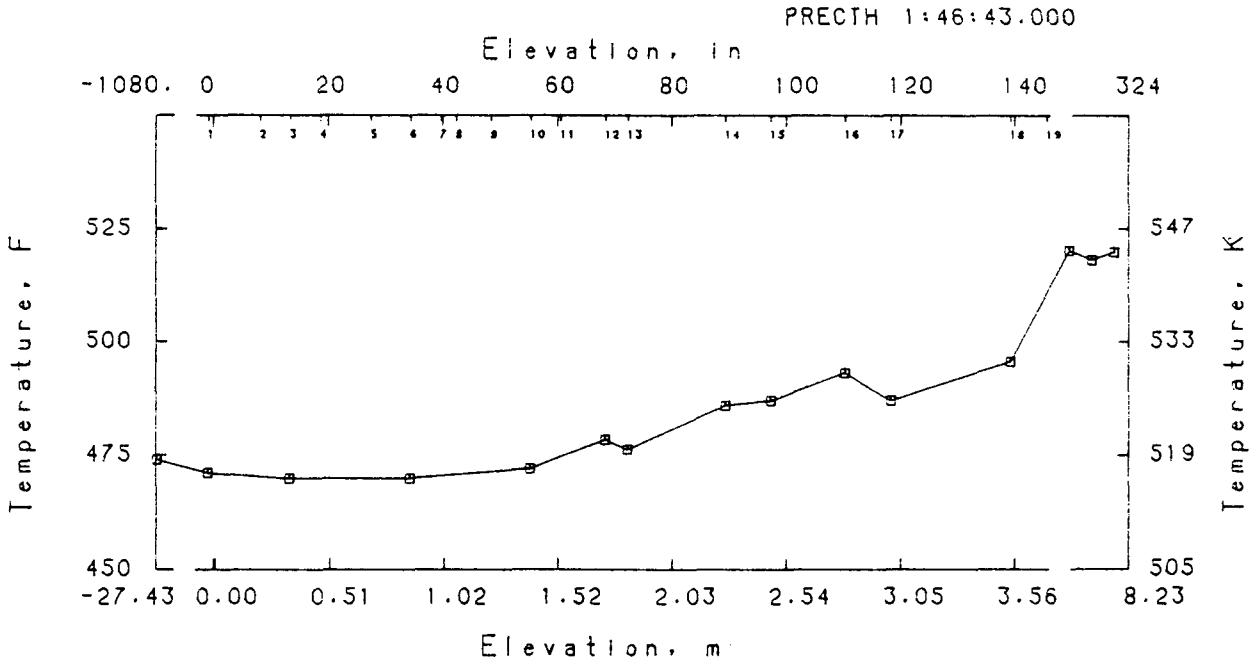

FIGURE 1.1.2.1 INSTRUMENT TUBE AND TEST TRAIN COOLANT TEMPERATURE PROFILE

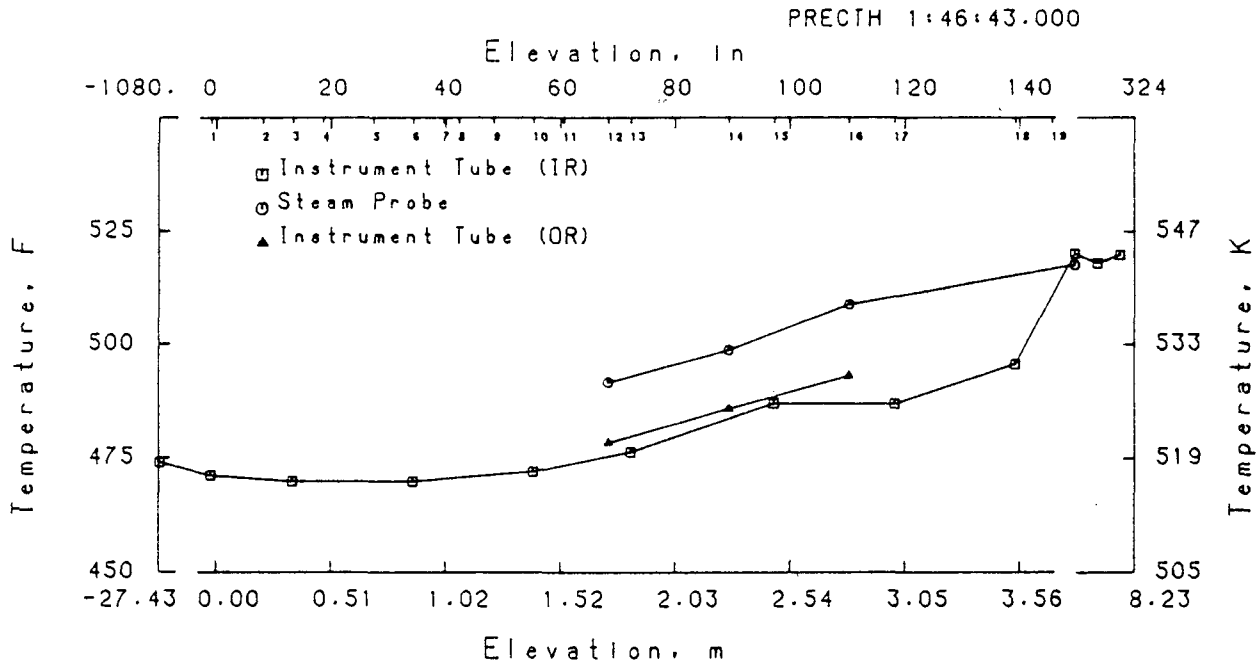

FIGURE 1.1.2.2 COMPARISON OF STEAM PROBE WITH INSTRUMENT TUBE AND TEST TRAIN TEMPERATURE PROFILES

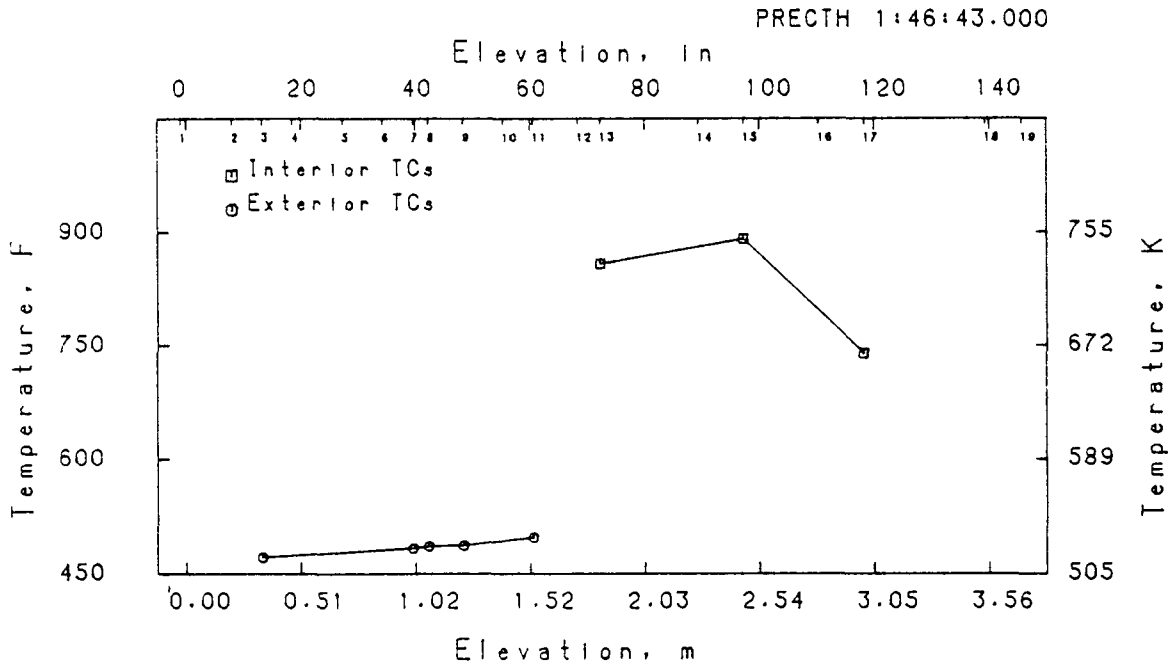

FIGURE 1.1.3.1 AVERAGE GUARD FUEL ROD CLADDING TEMPERATURE PROFILES - INTERIOR AND EXTERIOR TC'S

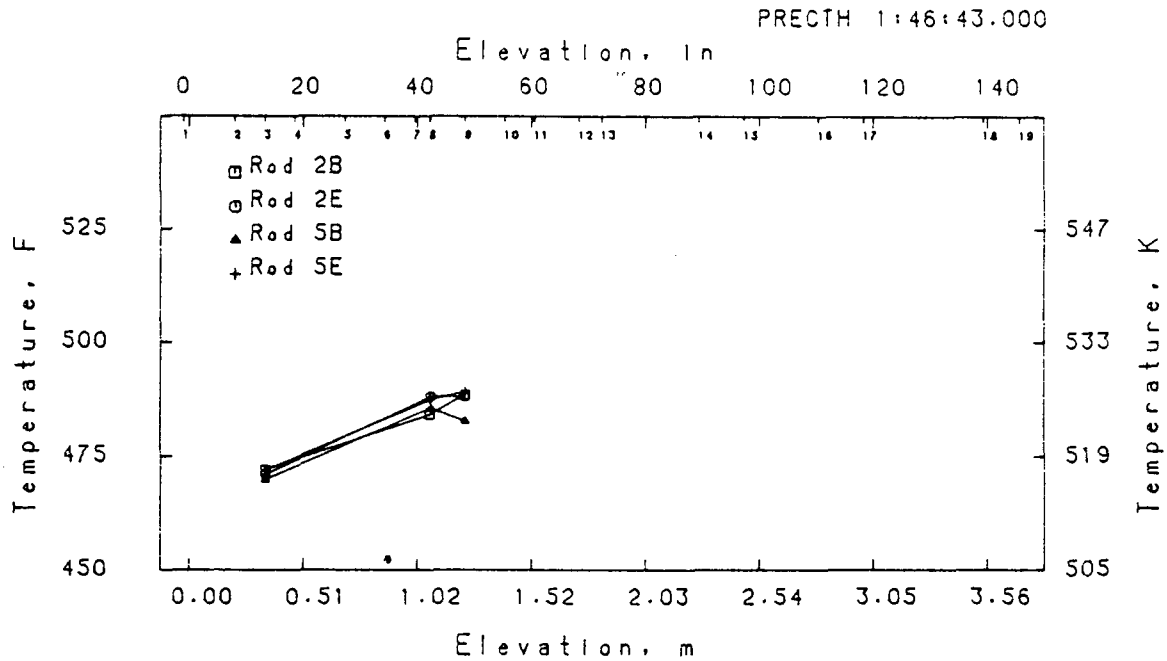

FIGURE 1.1.3.2 INDIVIDUAL GUARD FUEL ROD CLADDING EXTERIOR TEMPERATURE PROFILES

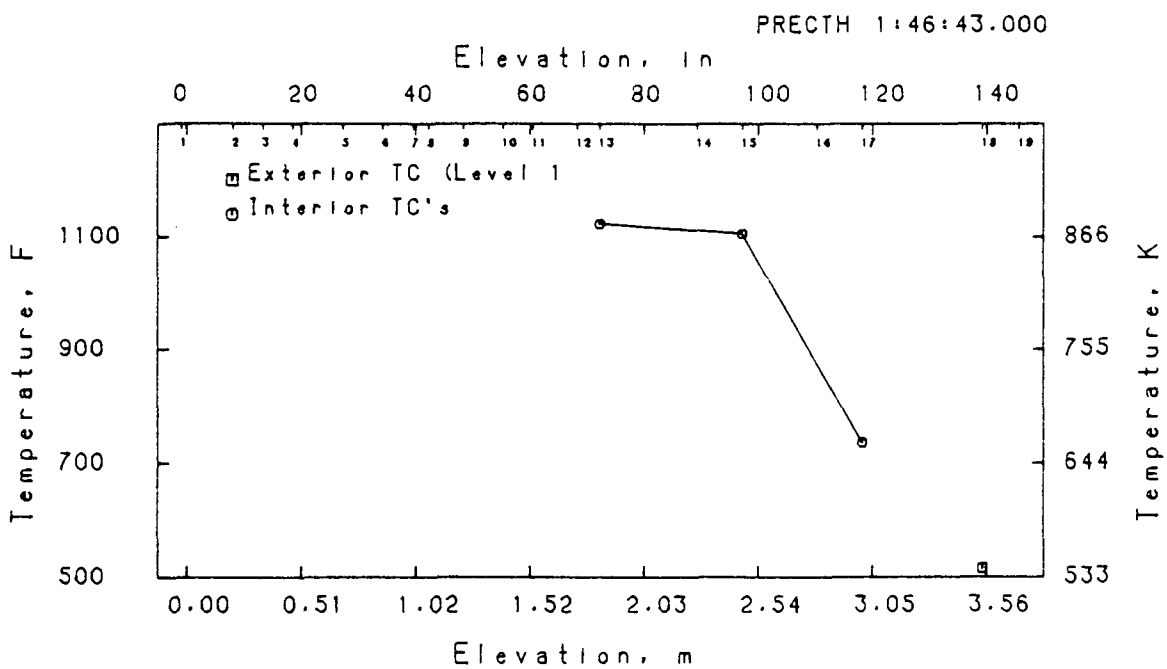

FIGURE 1.1.4.1 AVERAGE TEST FUEL ROD CLADDING TEMPERATURE PROFILE - EXTERIOR AND INTERIOR TC'S

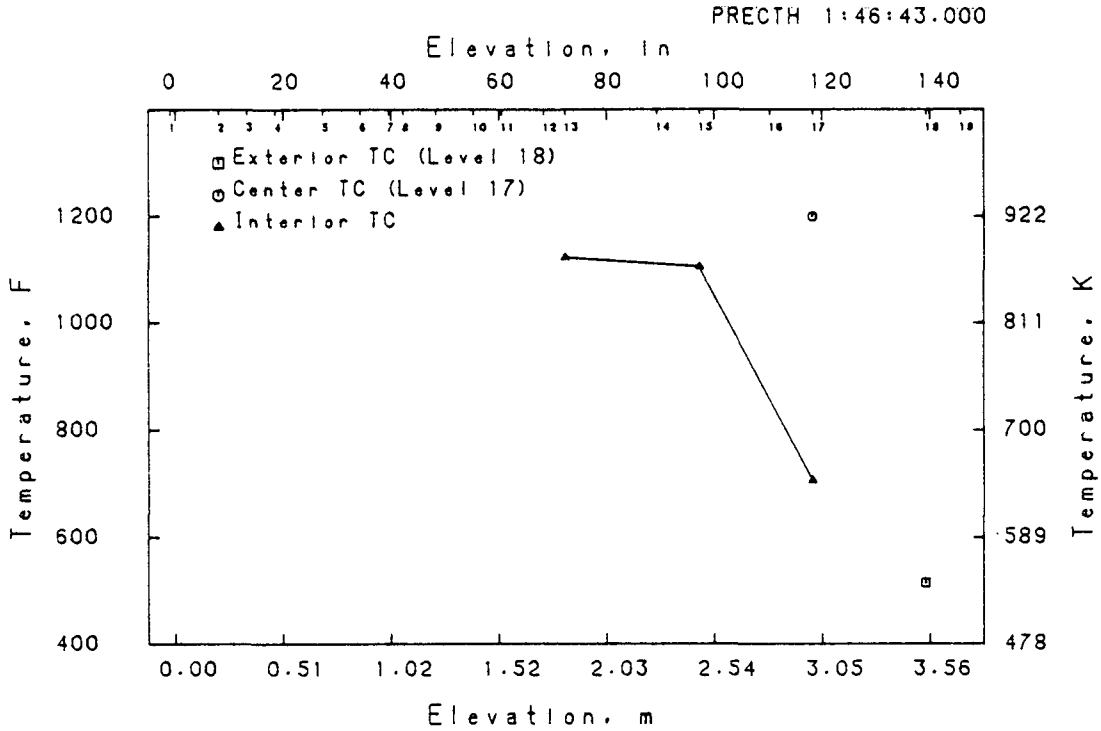

FIGURE 1.1.4.2 AVERAGE TEST FUEL ROD TEMPERATURE PROFILES - EXTERIOR, INTERIOR, AND CENTER TC

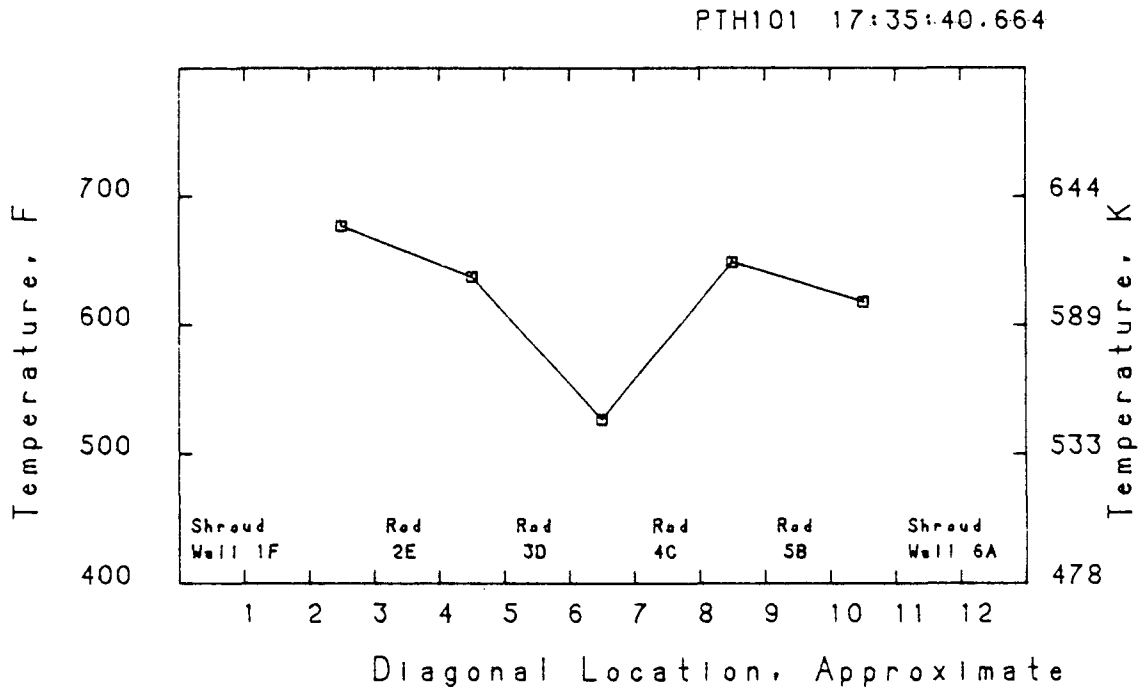

FIGURE 1.2.1.1 DIAGONAL TEMPERATURE PROFILE ACROSS TEST ASSEMBLY COOLANT DURING PRETRANSIENT - LEVEL 16

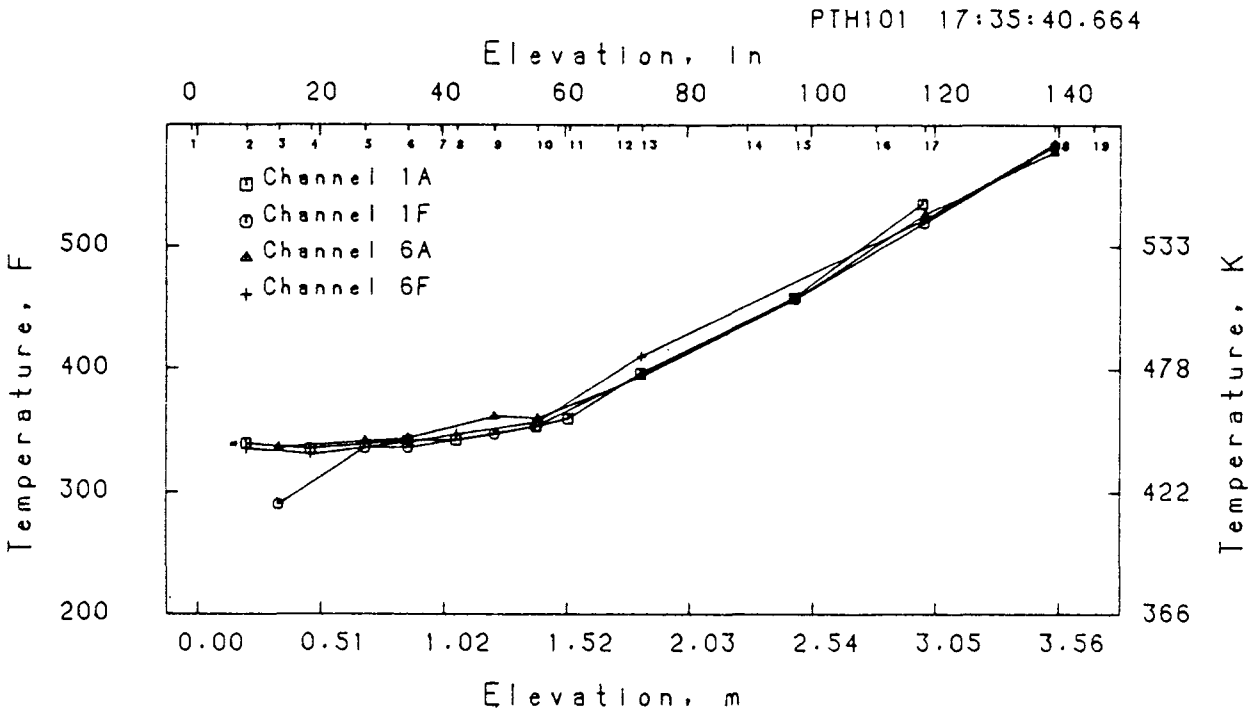

FIGURE 1.2.1.2 SHROUD AXIAL TEMPERATURE PROFILE - PRETRANSIENT PTH101

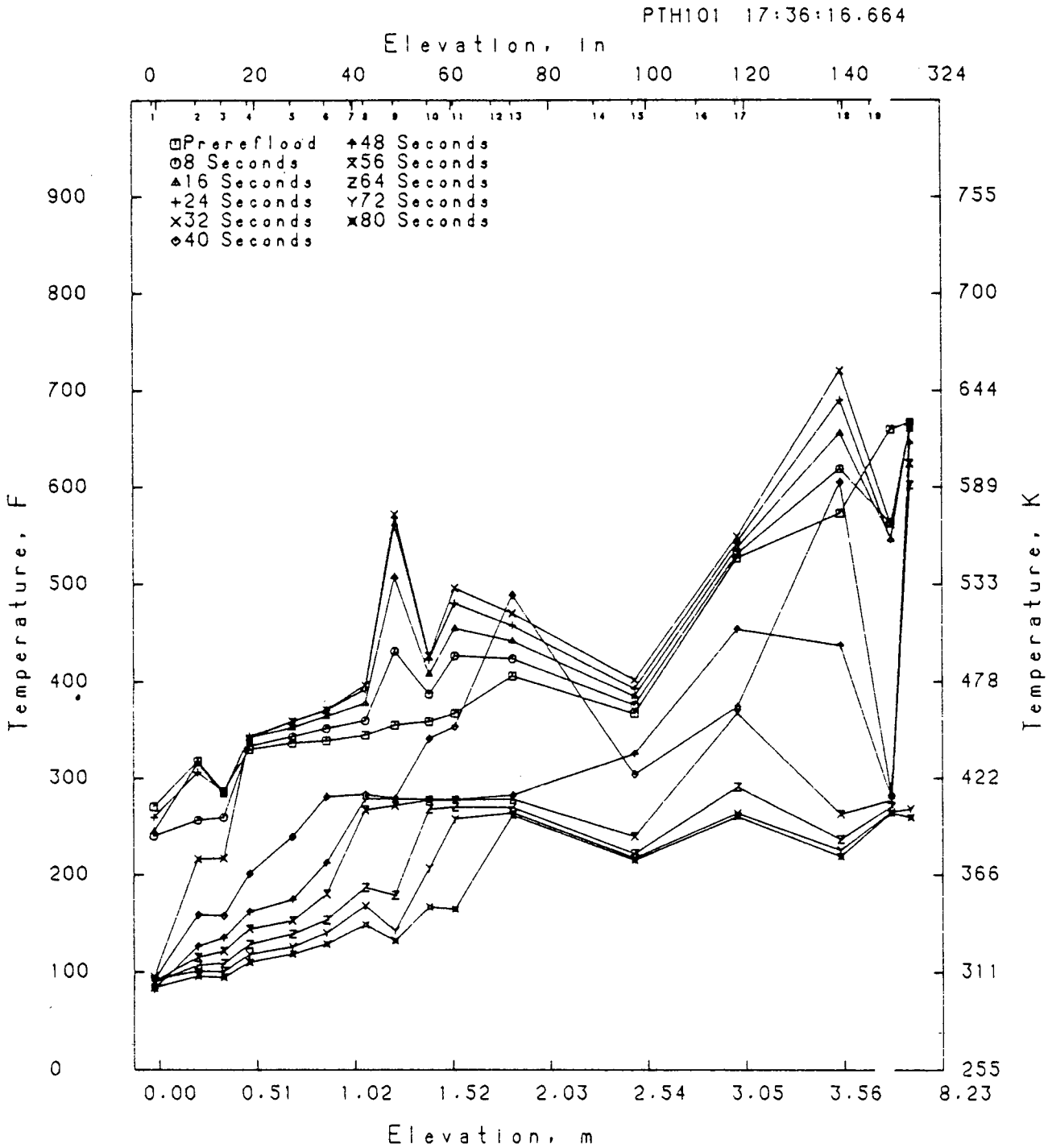

FIGURE 1.2.1.3.01 SHROUD AND TEST TRAIN TEMPERATURE PROFILES DURING REFLOODING AT 8 S INTERVALS - PTH101

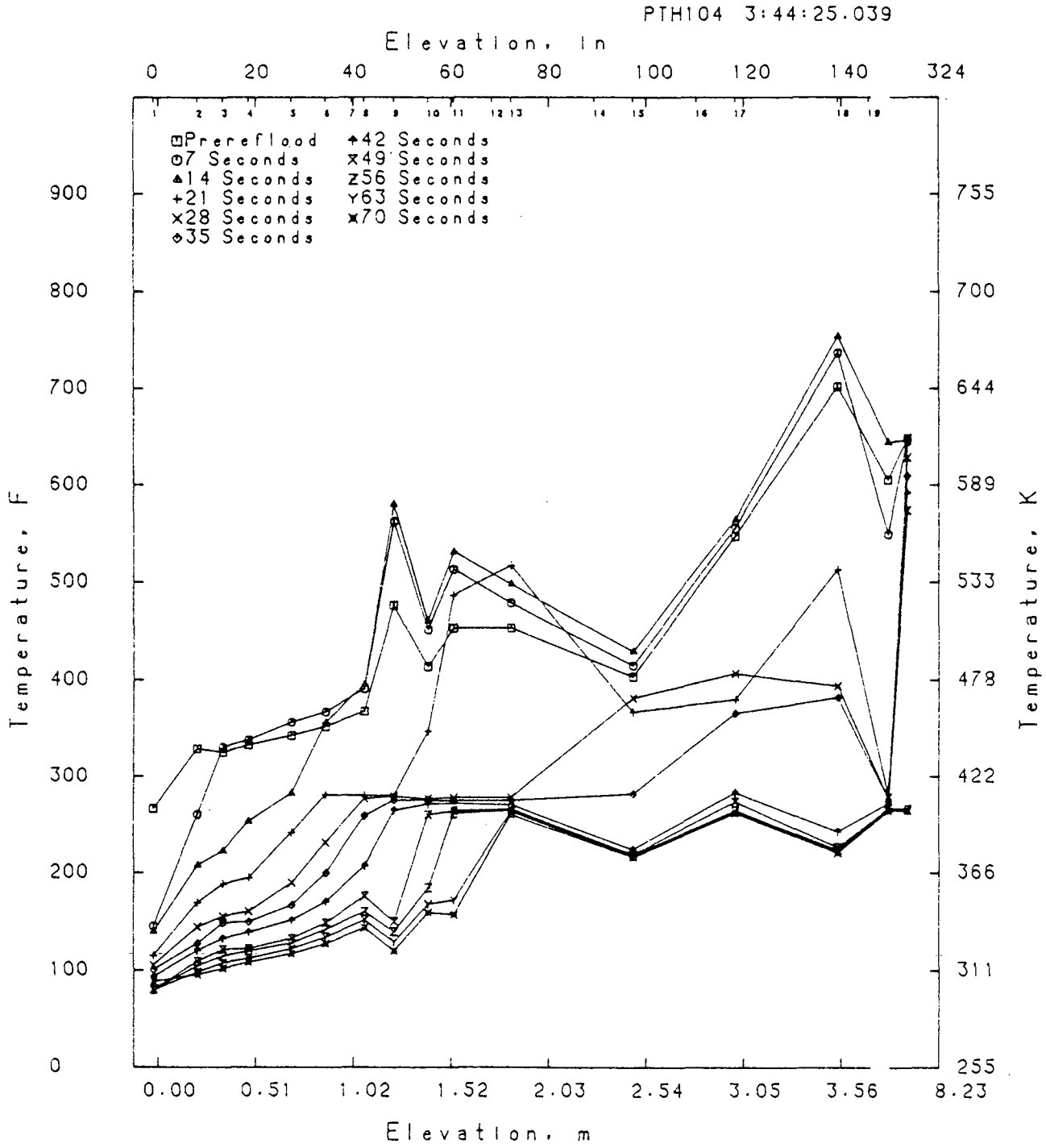

FIGURE 1.2.1.3.04 SHROUD AND TEST TRAIN TEMPERATURE PROFILES DURING REFLOODING AT 7S INTERVALS - PTH104

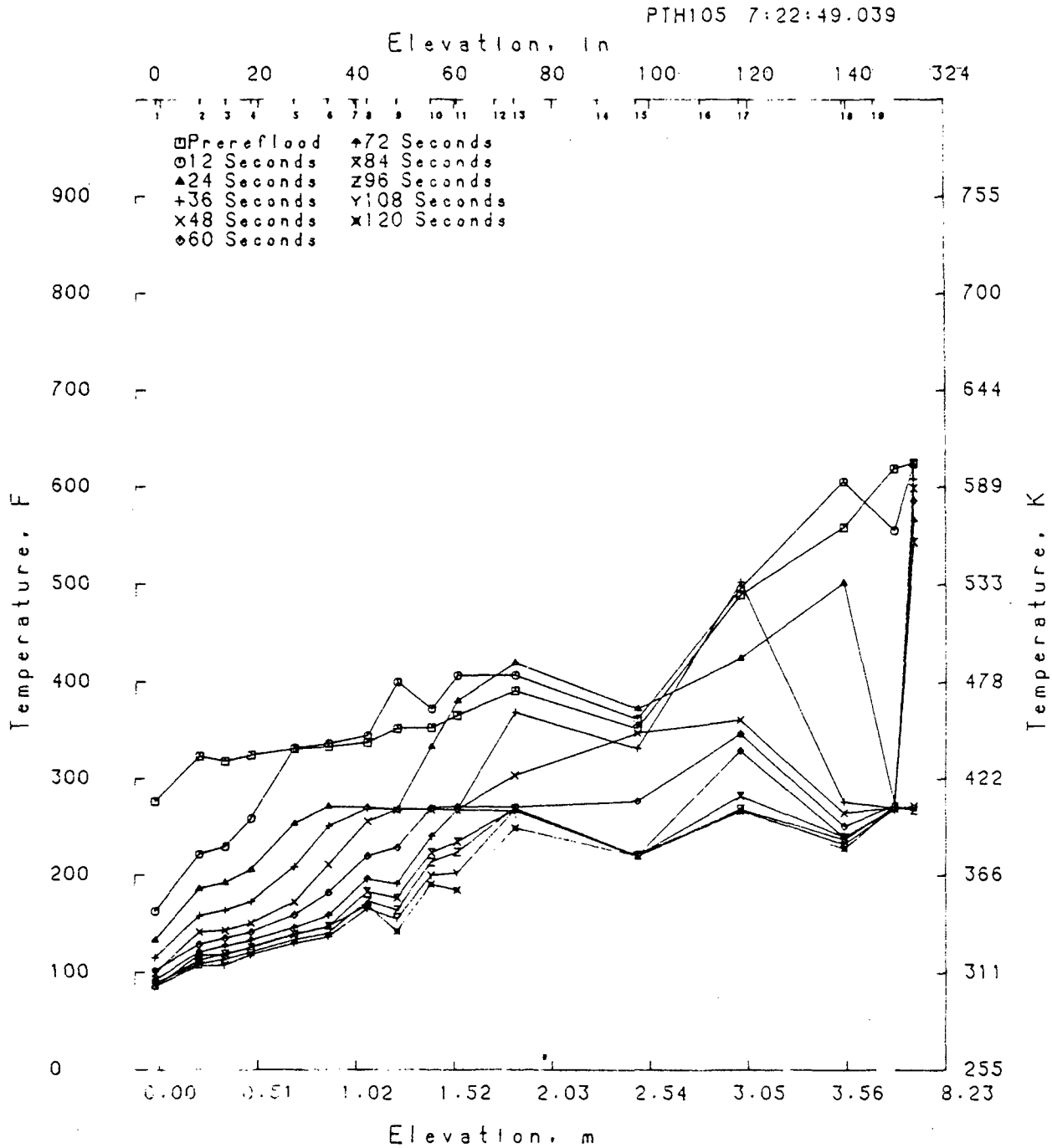

FIGURE 1.2.1.3.05 SHROUD AND TEST TRAIN TEMPERATURE PROFILES DURING REFLOODING AT 12S INTERVALS - PTH105

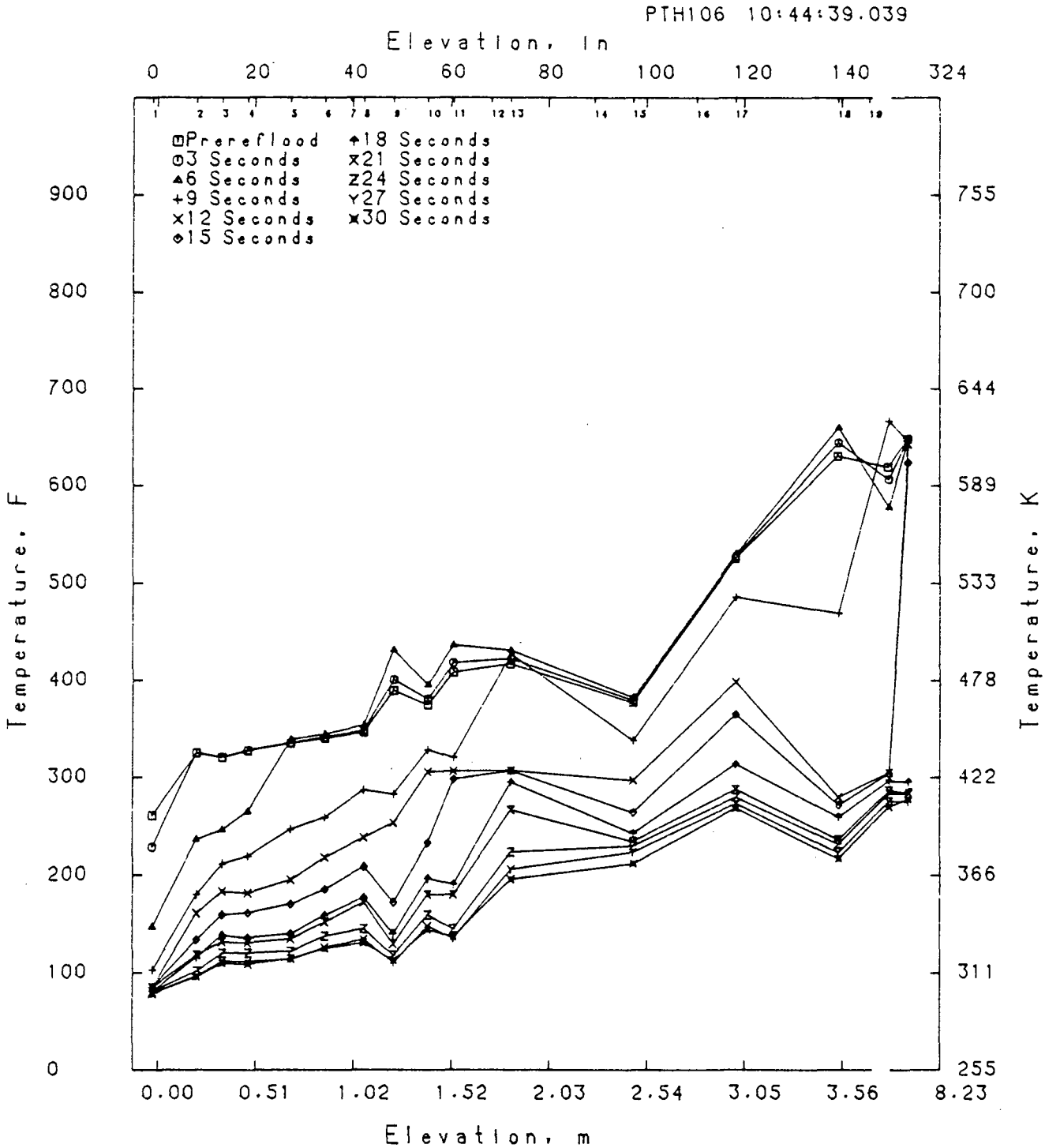

FIGURE 1.2.1.3.06 SHROUD AND TEST TRAIN TEMPERATURE PROFILES DURING REFLOODING AT 3S INTERVALS - PTH106

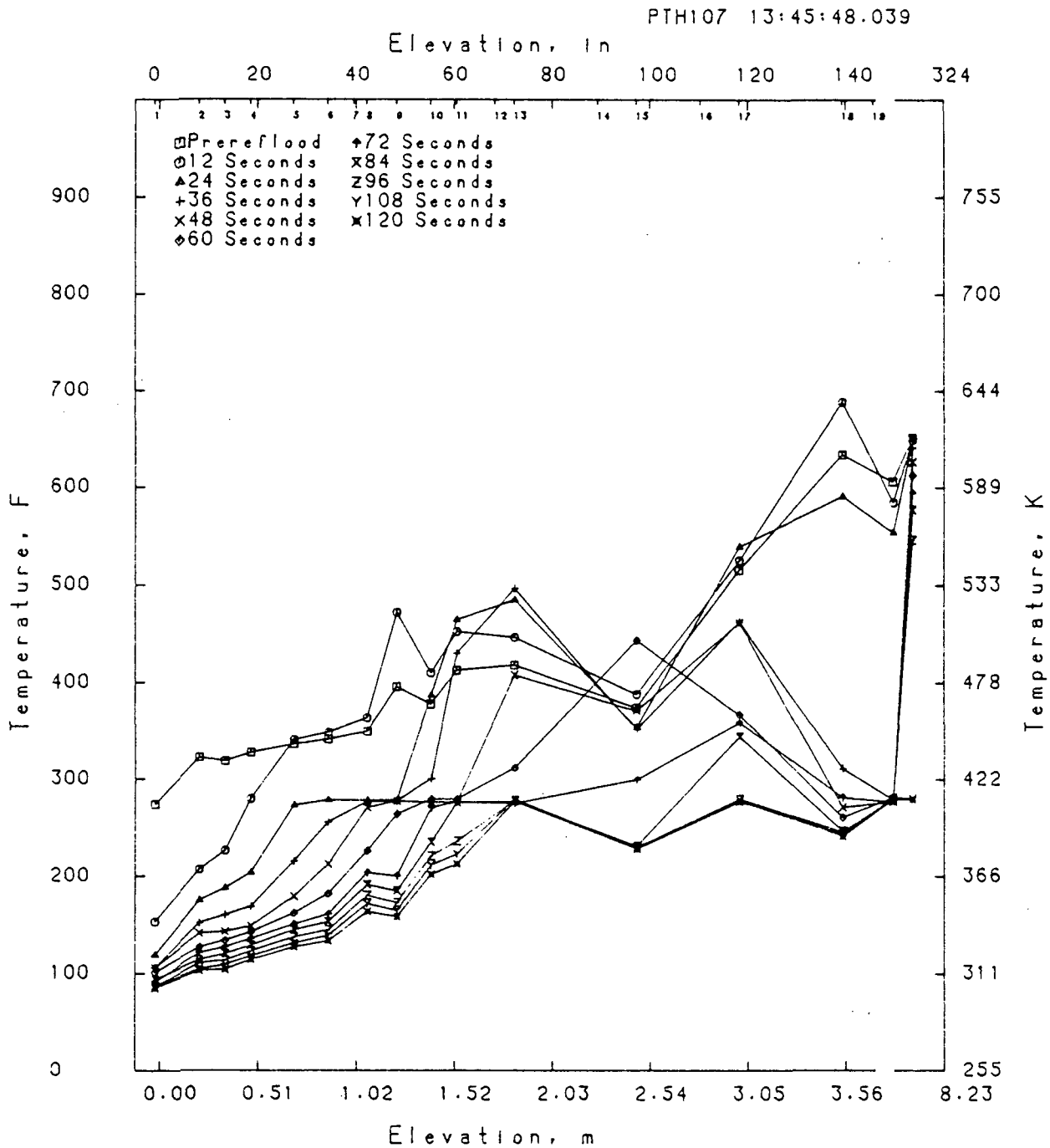

FIGURE 1.2.1.3.07 SHROUD AND TEST TRAIN TEMPERATURE PROFILES DURING REFLOODING AT 12S INTERVALS

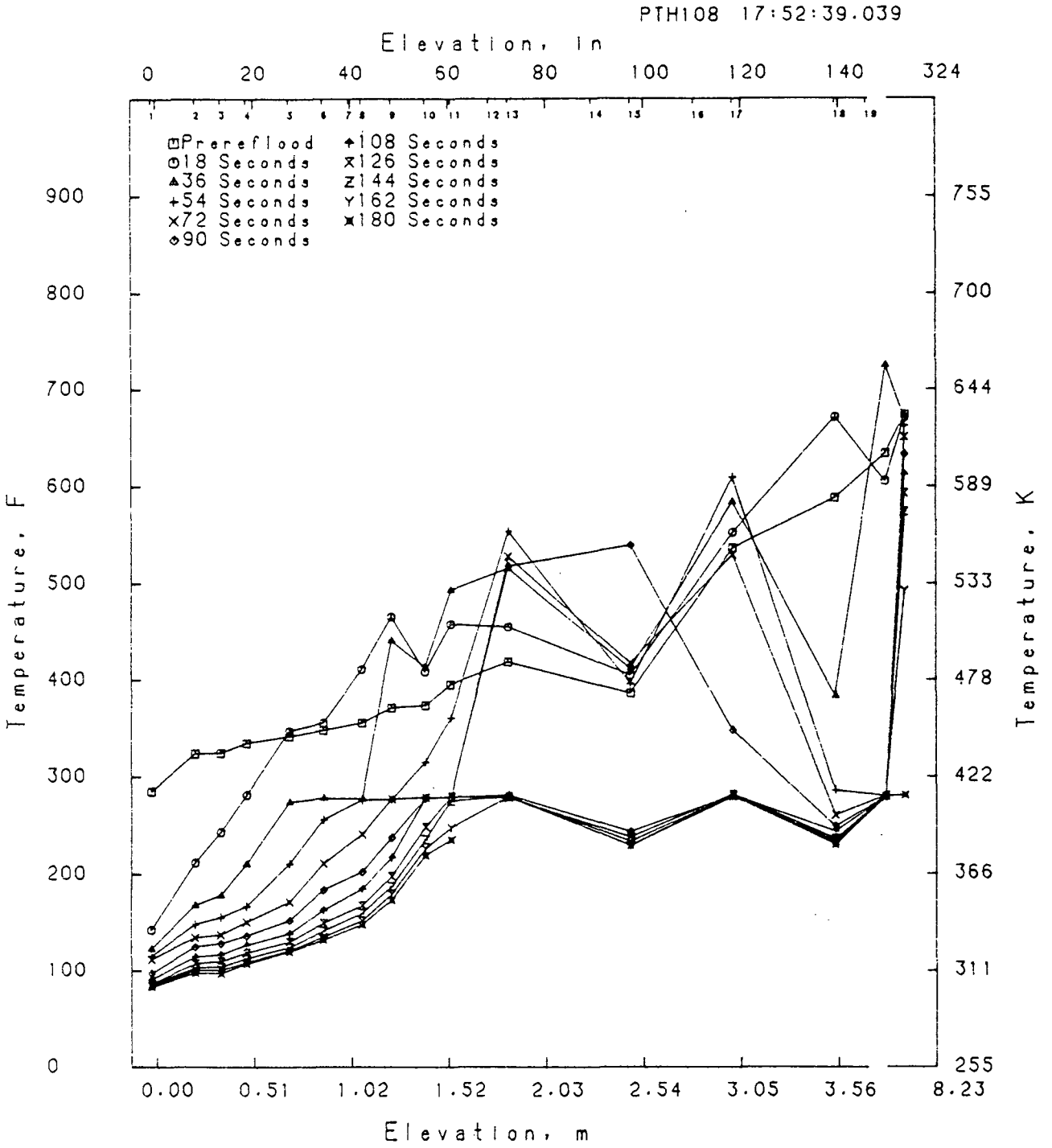

FIGURE 1.2.1.3.08 SHROUD AND TEST TRAIN TEMPERATURE PROFILES DURING REFLOODING AT 18S INTERVALS - PTH108

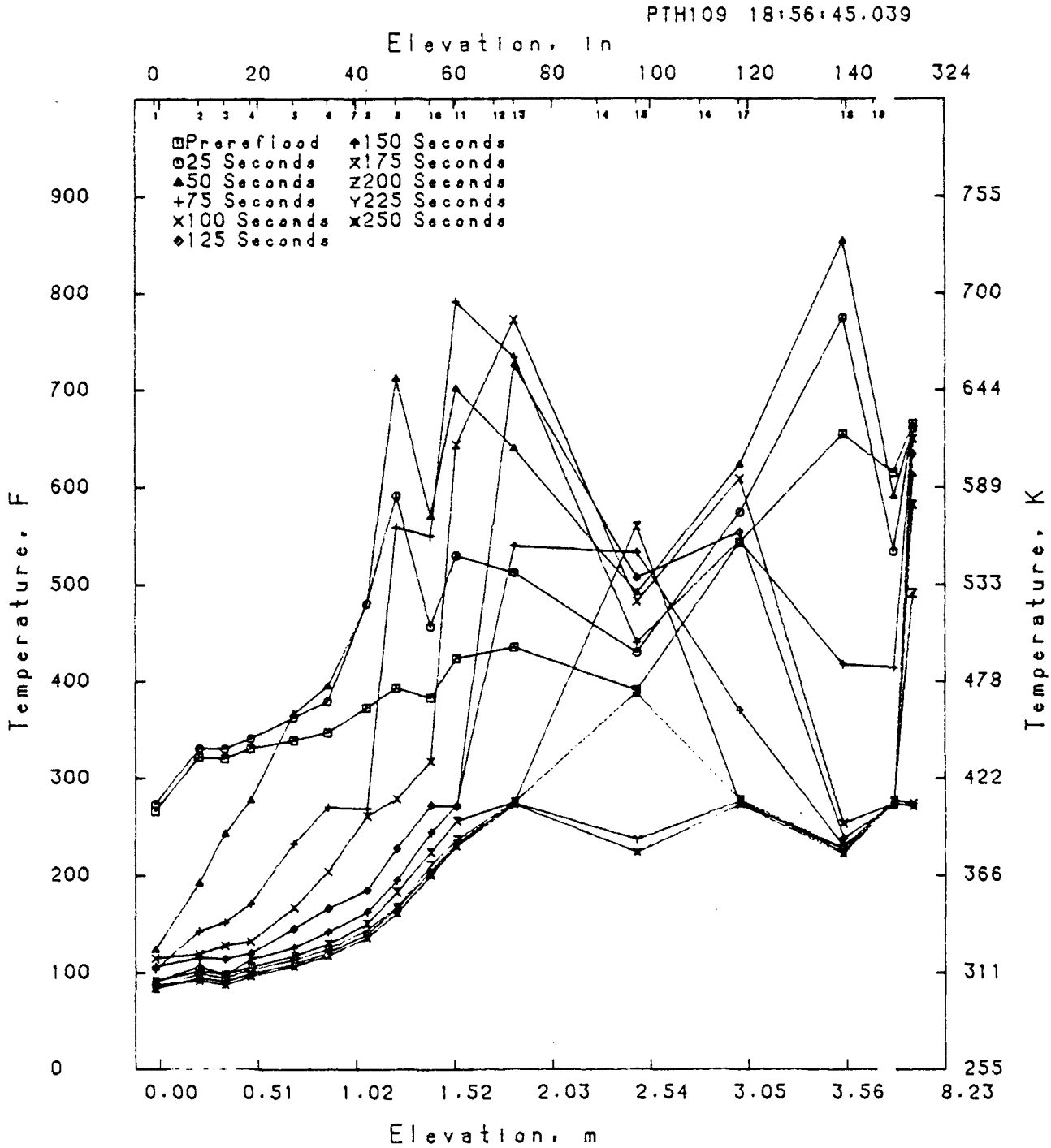

FIGURE 1.2.1.3.09 SHROUD AND TEST TRAIN TEMPERATURE PROFILES DURING REFLOODNG AT 25 S INTERVALS

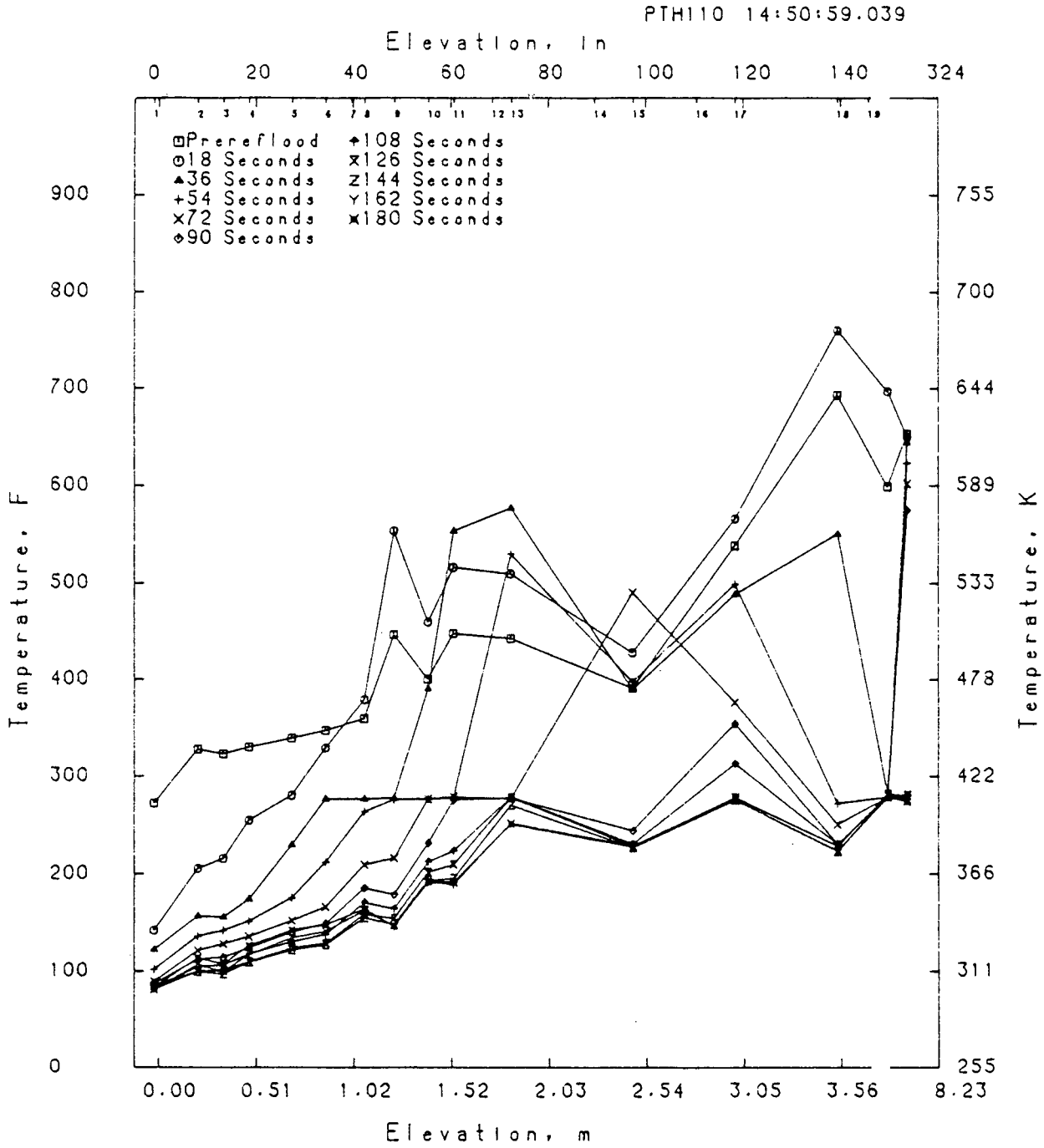

FIGURE 1.2.1.3.10 SHROUD AND TEST TRAIN TEMPERATURE PROFILES DURING REFLOODING AT 18S INTERVALS - PTH110

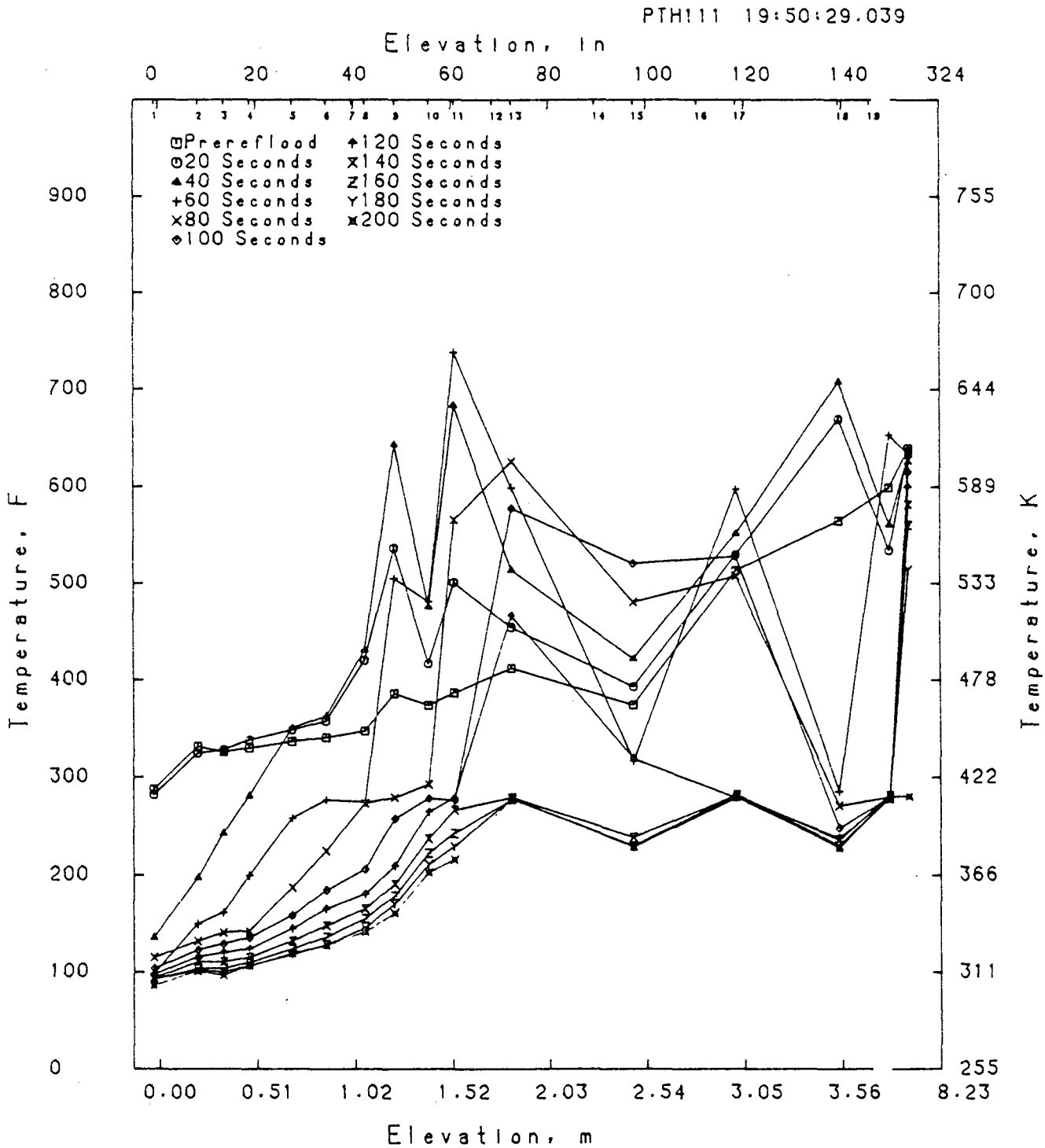

FIGURE 1.2.1.3.11 SHROUD AND TEST TRAIN TEMPERATURE PROFILES DURING REFLOODNG AT 20S INTERVALS - PTH111

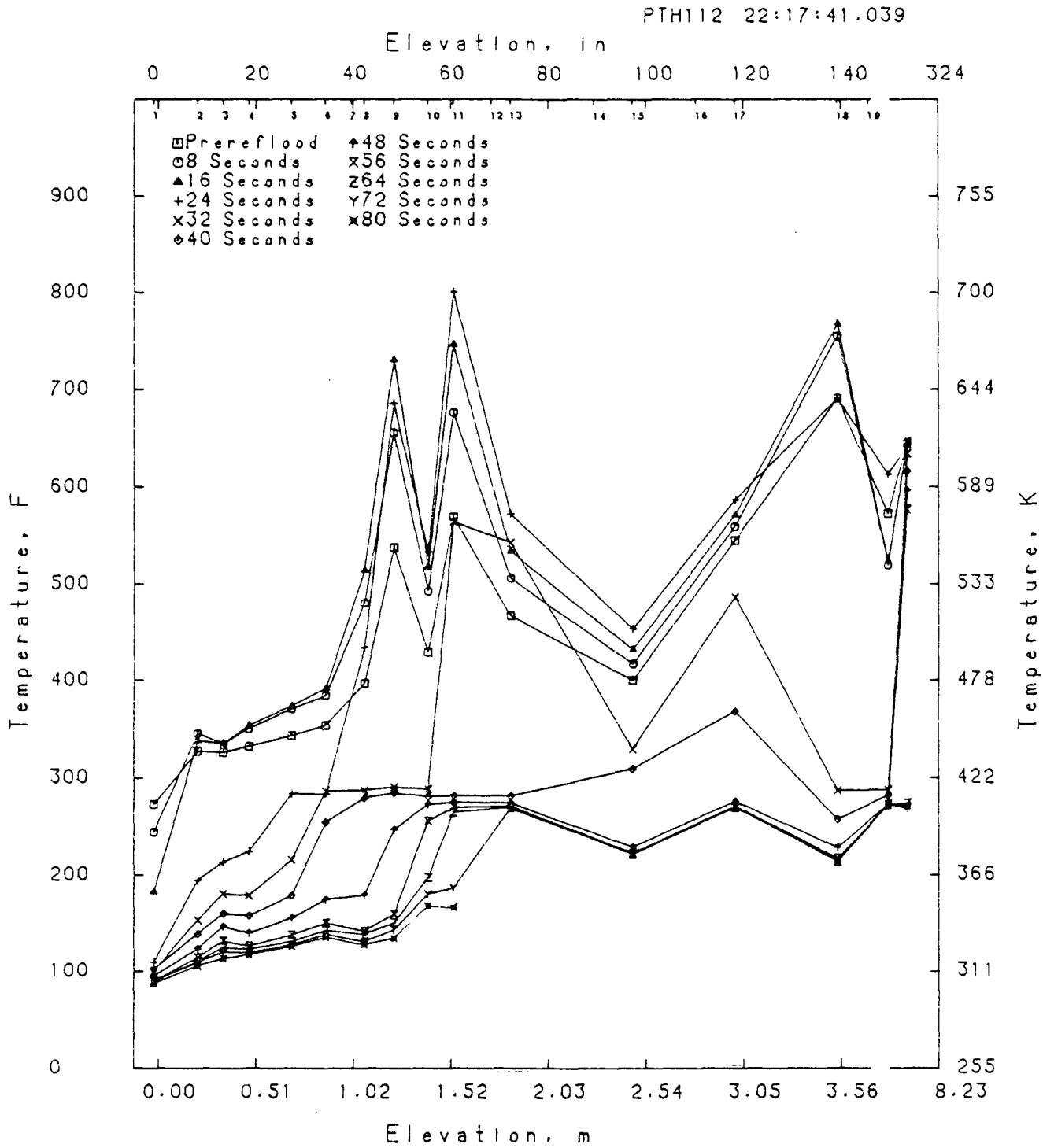

FIGURE 1.2.1.3.12 SHROUD AND TEST TRAIN TEMPERATURE PROFILES DURING REFLOODING AT 8S INTERVALS - PTH112

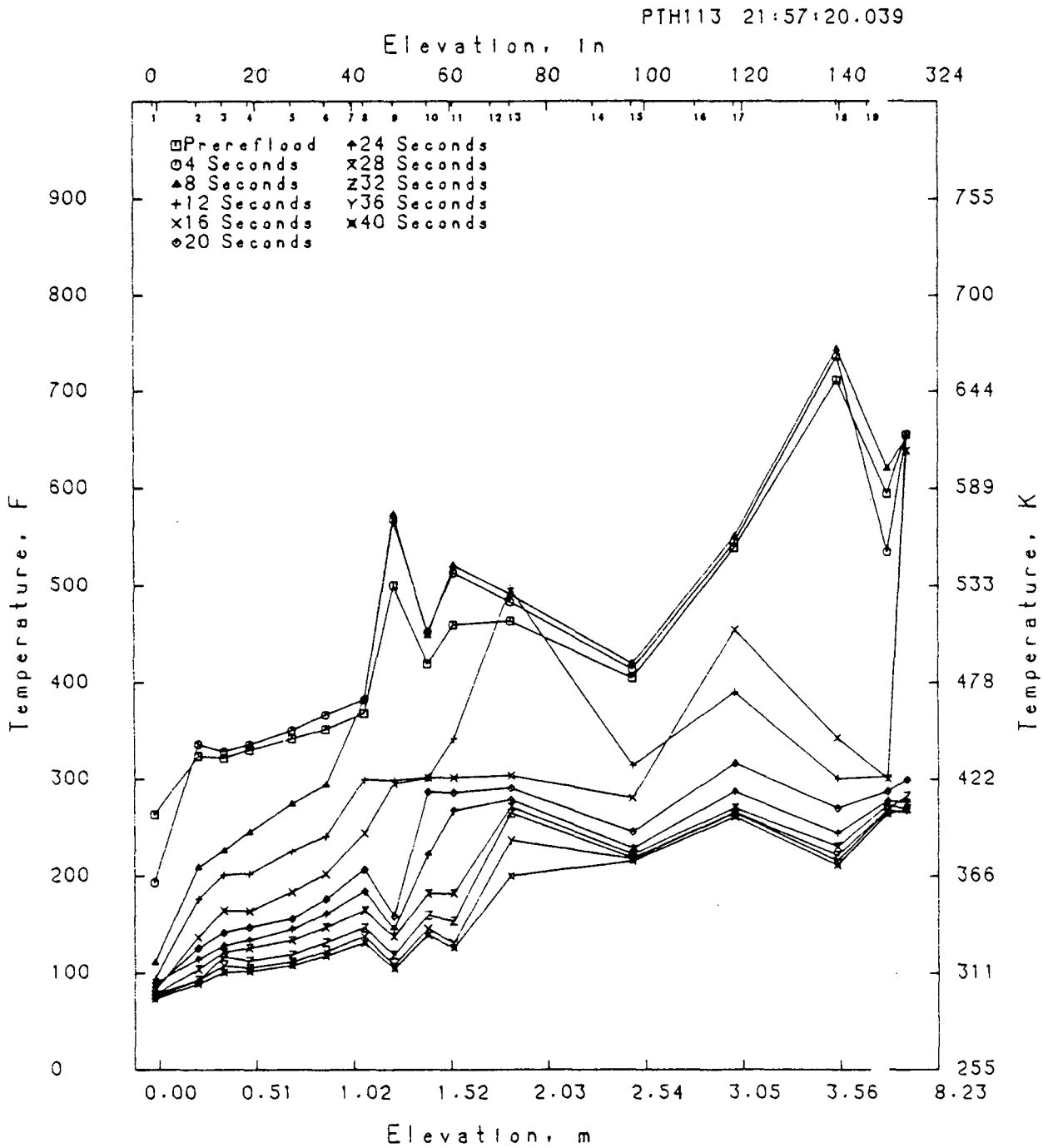

FIGURE 1.2.1.3.13 SHROUD AND TEST TRAIN TEMPERATURE PROFILES DURING REFLOODING AT 4S INTERVALS - PTH113

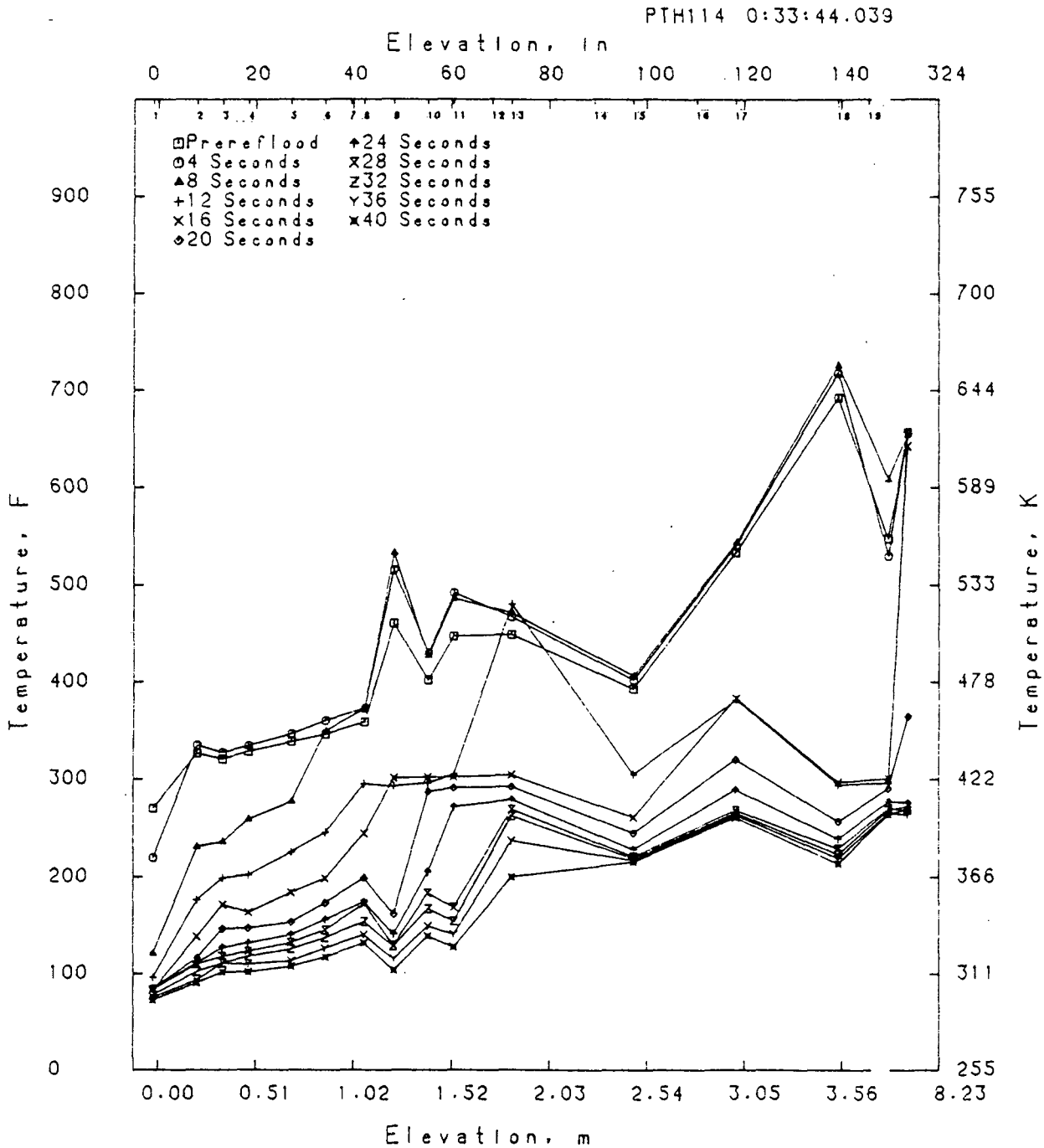

FIGURE 1.2.1.3.14 SHROUD AND TEST TRAIN TEMPERATURE PROFILES DURING REFLOODING AT 4S INTERVALS

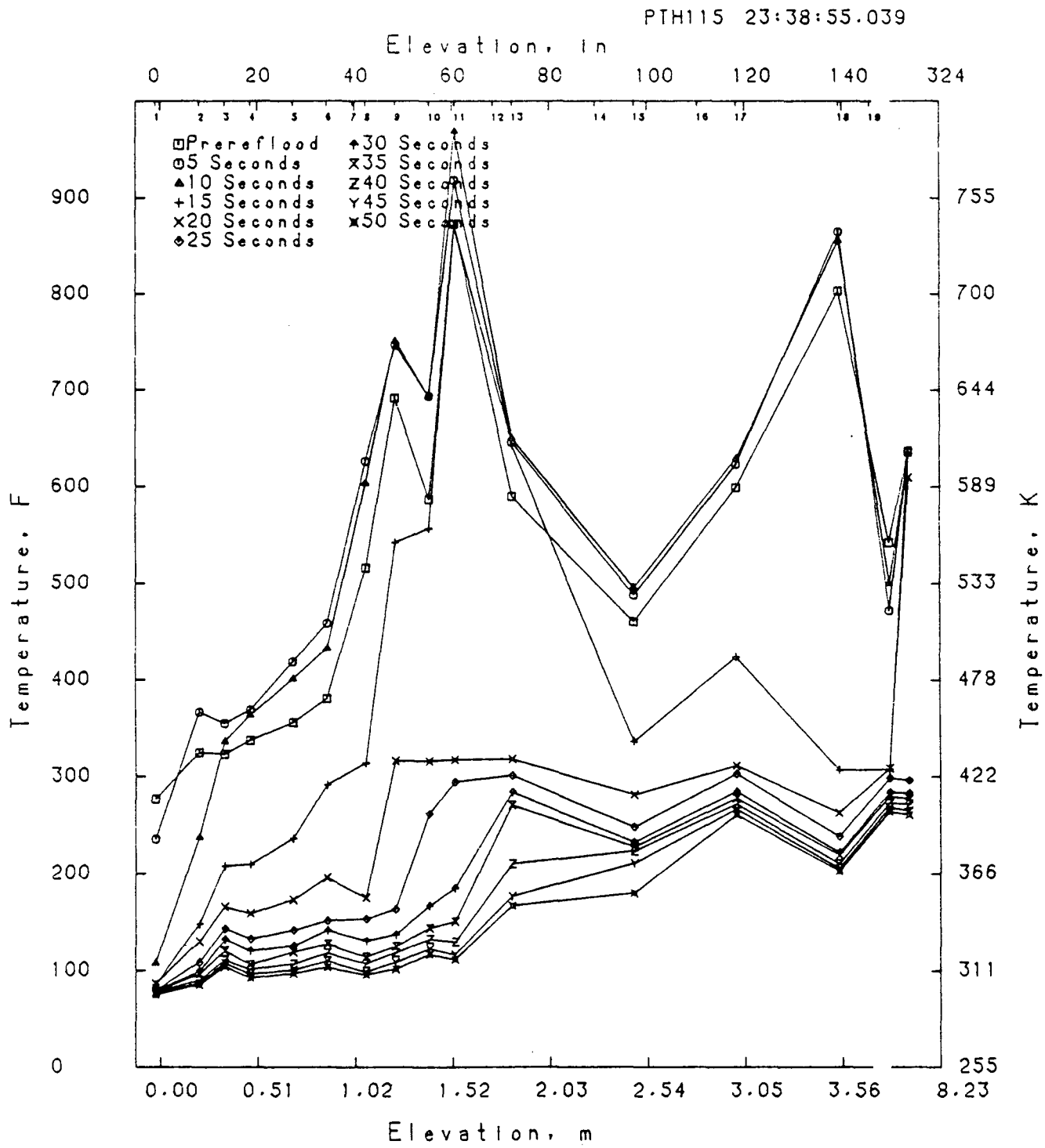

FIGURE 1.2.1.3.15 SHROUD AND TEST TRAIN TEMPERATURE PROFILES DURING REFLOODING AT 5S INTERVALS - PTH115

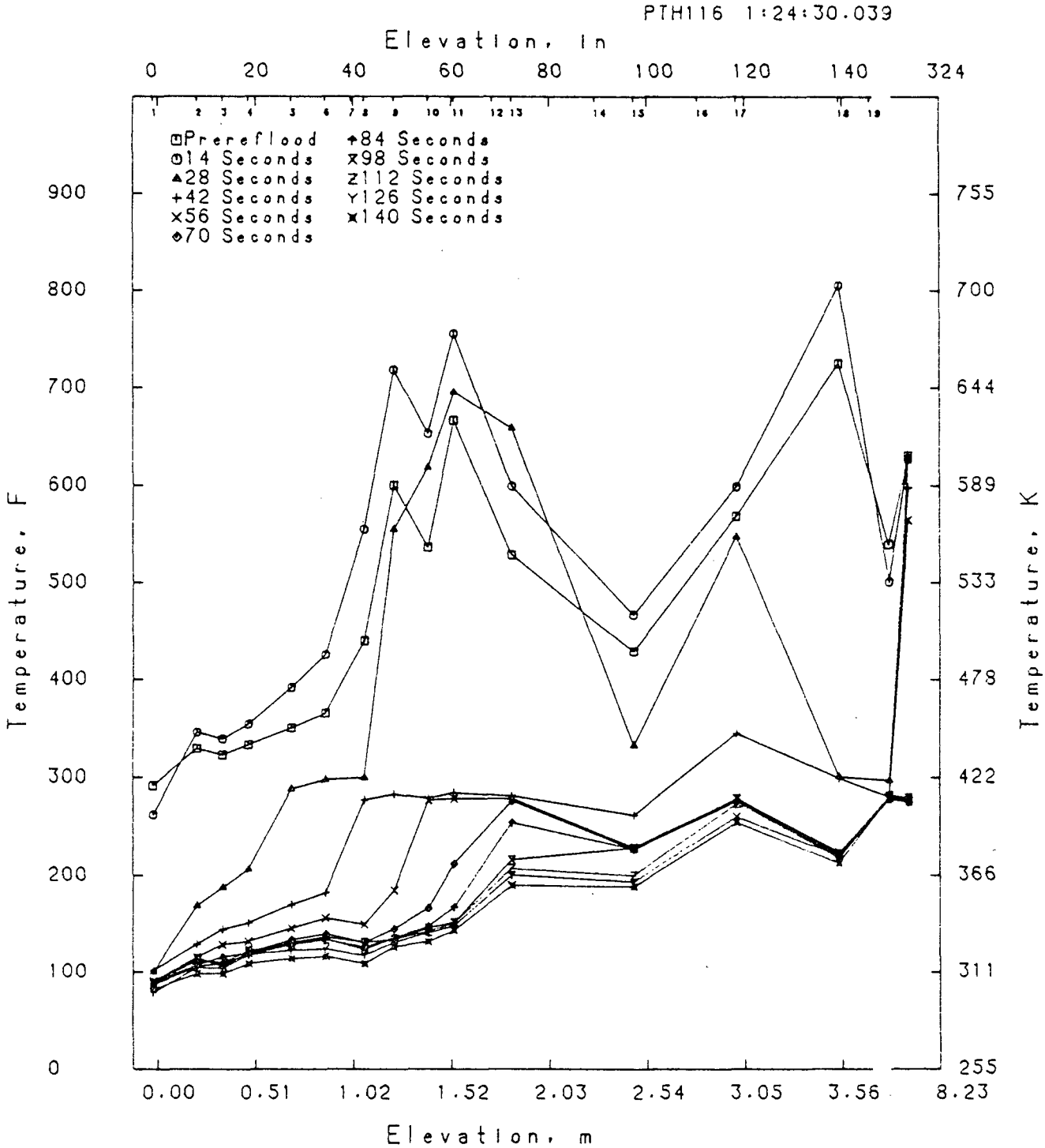

FIGURE 1.2.1.3.16 SHROUD AND TEST TRAIN TEMPERATURE PROFILES DURING REFLOODING AT 14S INTERVALS - PTH116

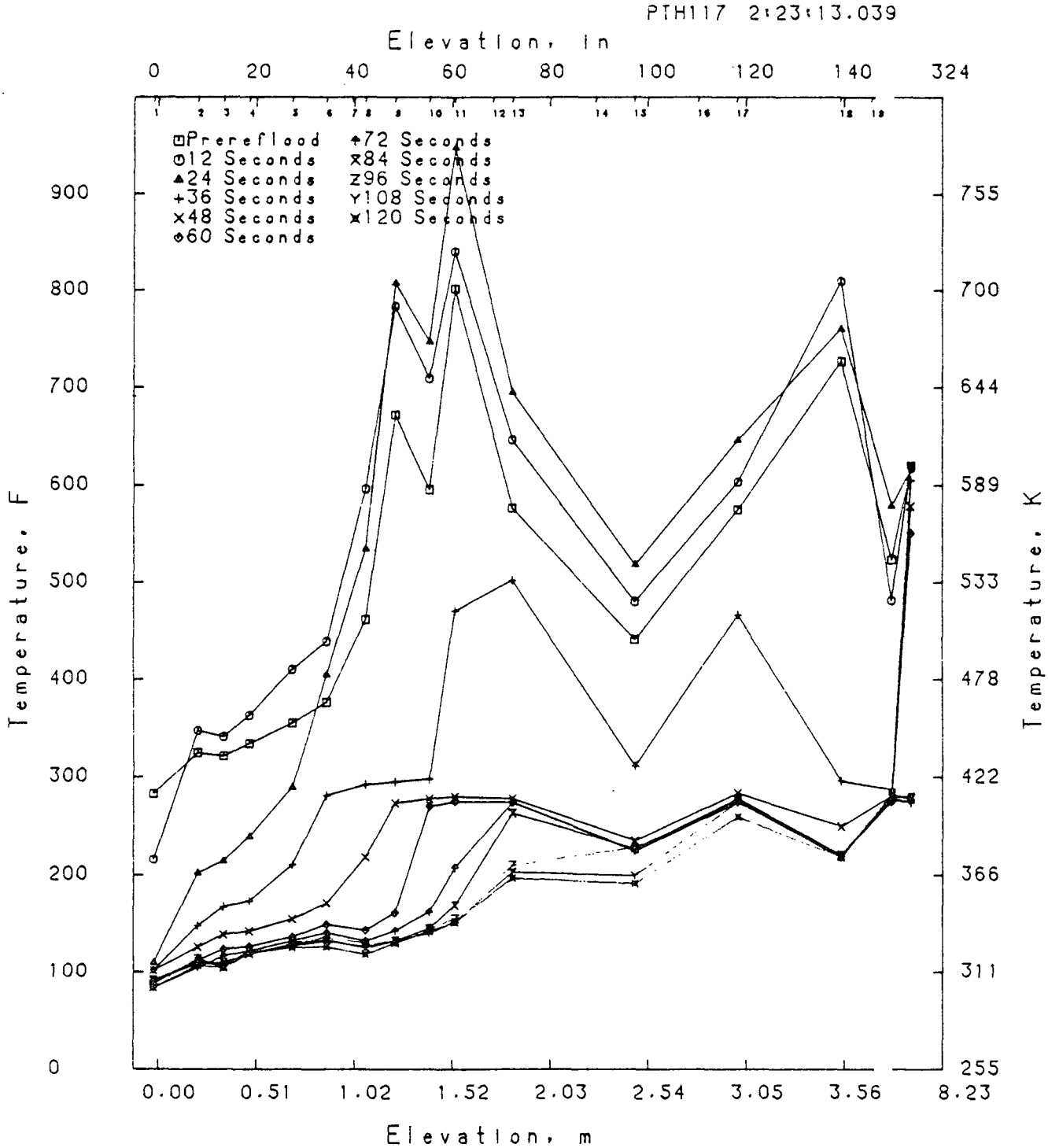

FIGURE 1.2.1.3.17 SHROUD AND TEST TRAIN TEMPERATURE PROFILES DURING REFLOODING AT 12S INTERVALS - PTH117

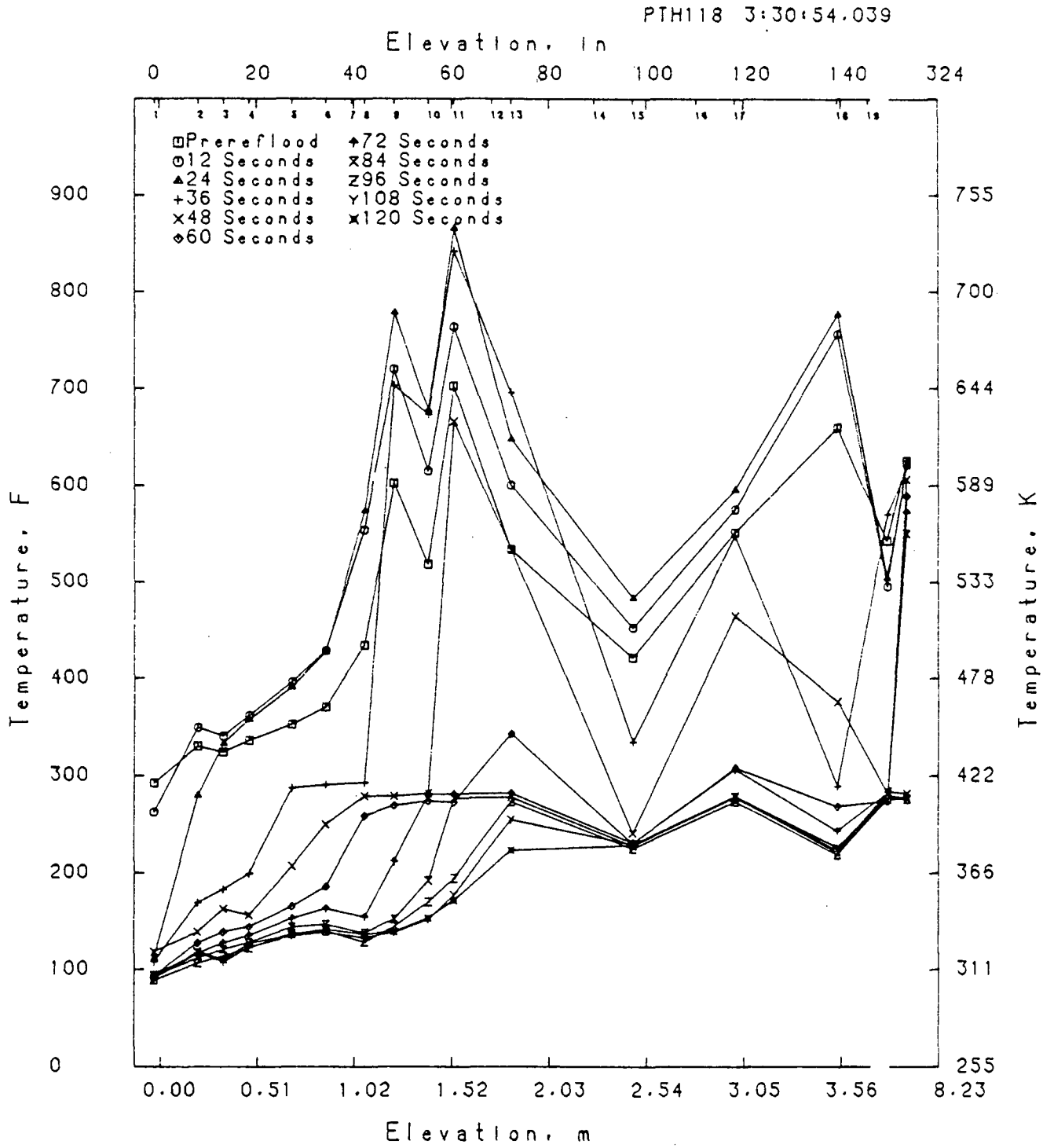

FIGURE 1.2.1.3.18 SHROUD AND TEST TRAIN TEMPERATURE PROFILES DURING REFLOODING AT 12S INTERVALS

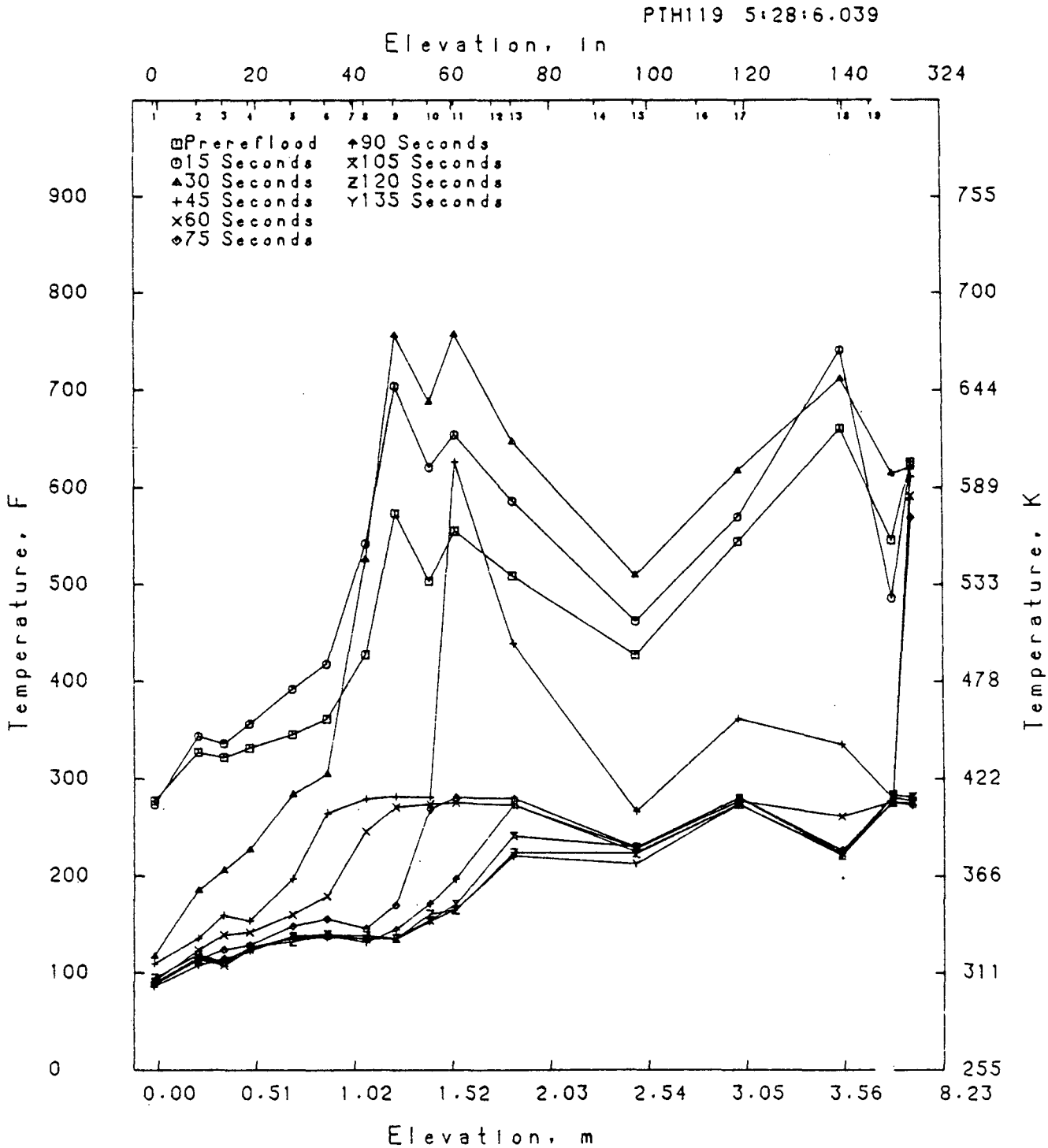

FIGURE 1.2.1.3.19 SHROUD AND TEST TRAIN TEMPERATURE PROFILES DURING REFLOODING AT 15S INTERVALS - PTH119

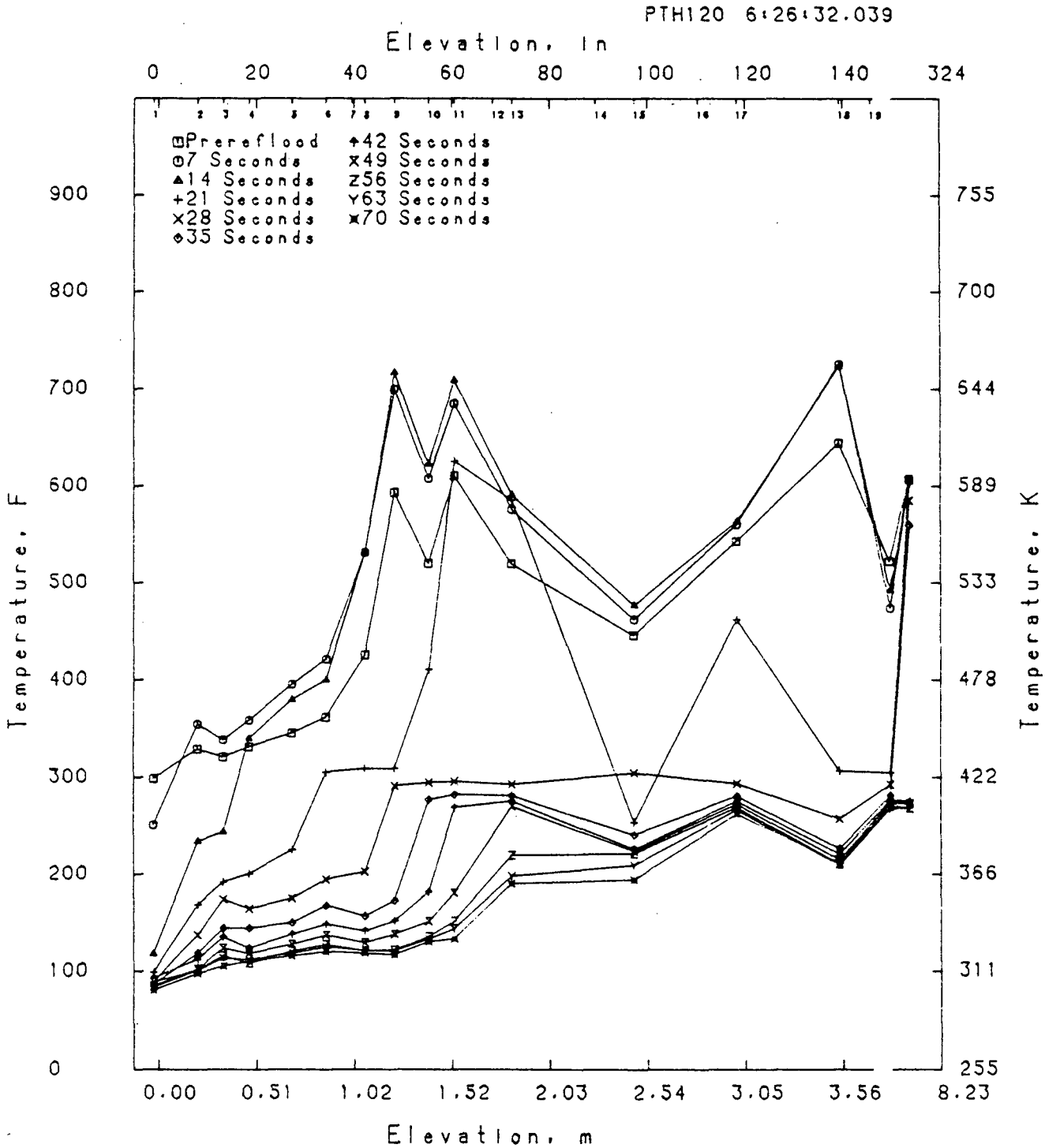

FIGURE 1.2.1.3.20 SHROUD AND TEST TRAIN TEMPERATURE PROFILES DURING REFLOODING AT 7S INTERVALS

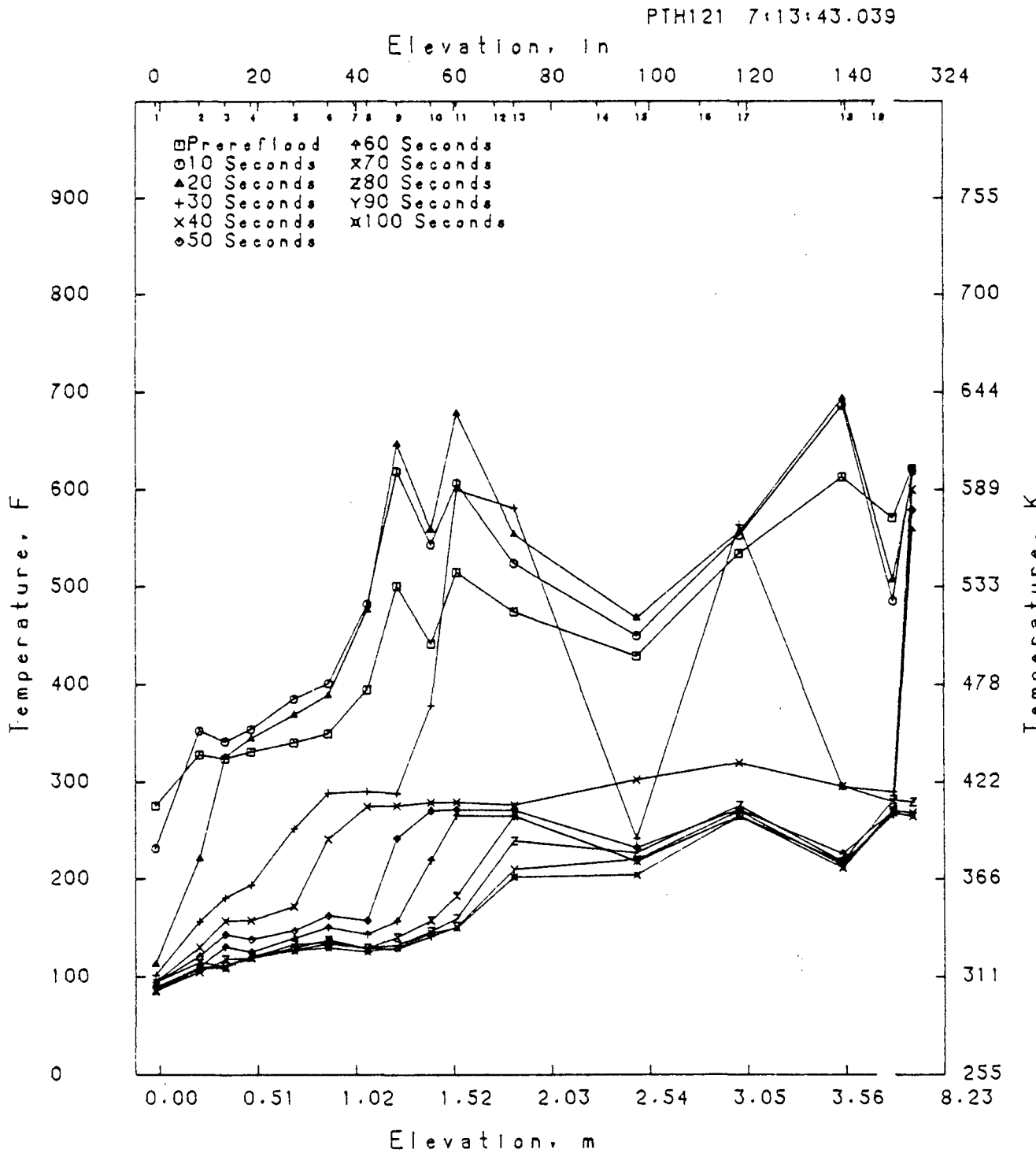

FIGURE 1.2.1.3.21 SHROUD AND TEST TRAIN TEMPERATURE PROFILES DURING REFLOODING AT 10S INTERVALS - PTH121

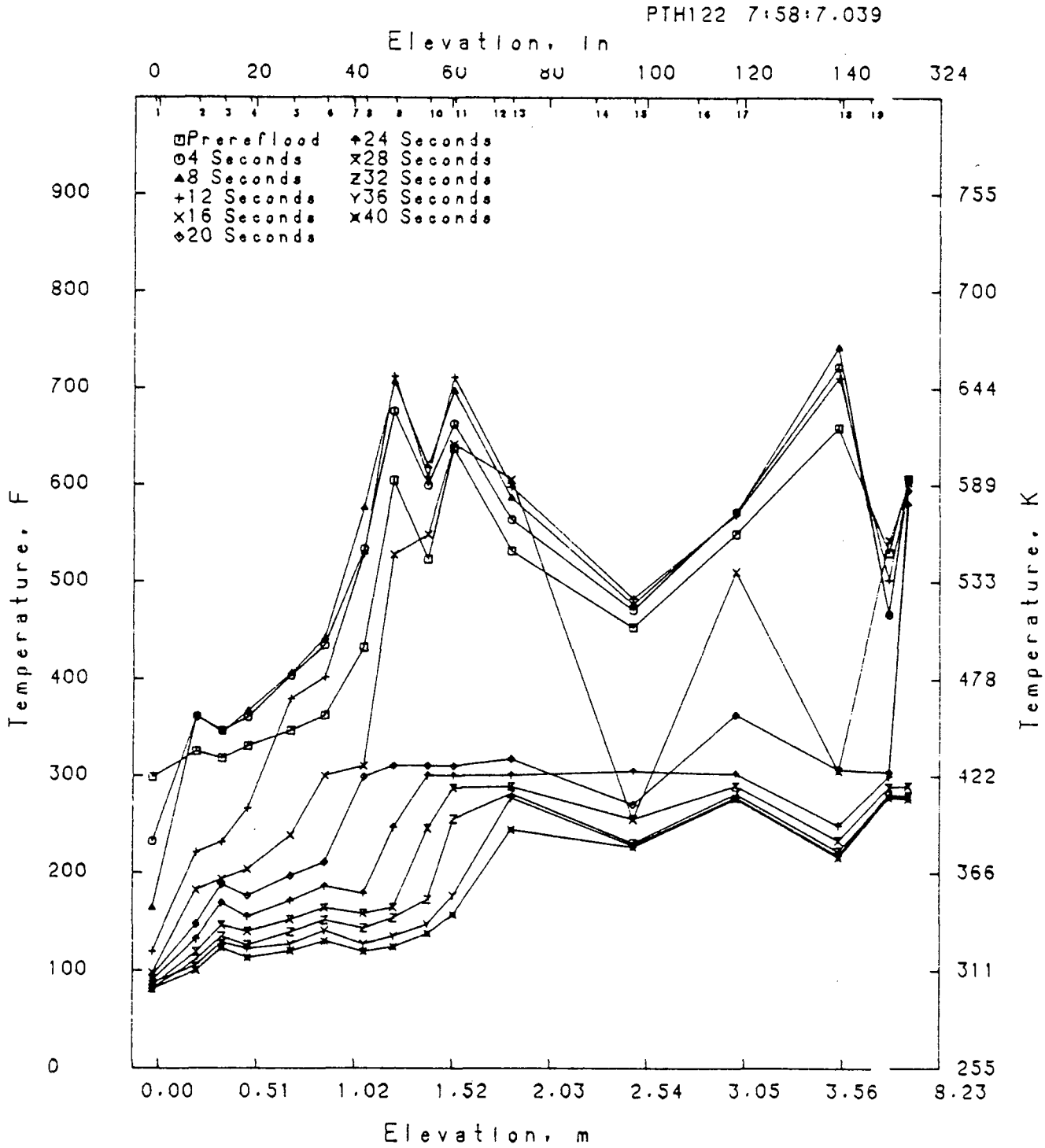

FIGURE 1.2.1.3.22 SHROUD AND TEST TRAIN TEMPERATURE PROFILES DURING REFLOODING AT 4S INTERVALS - PTH122

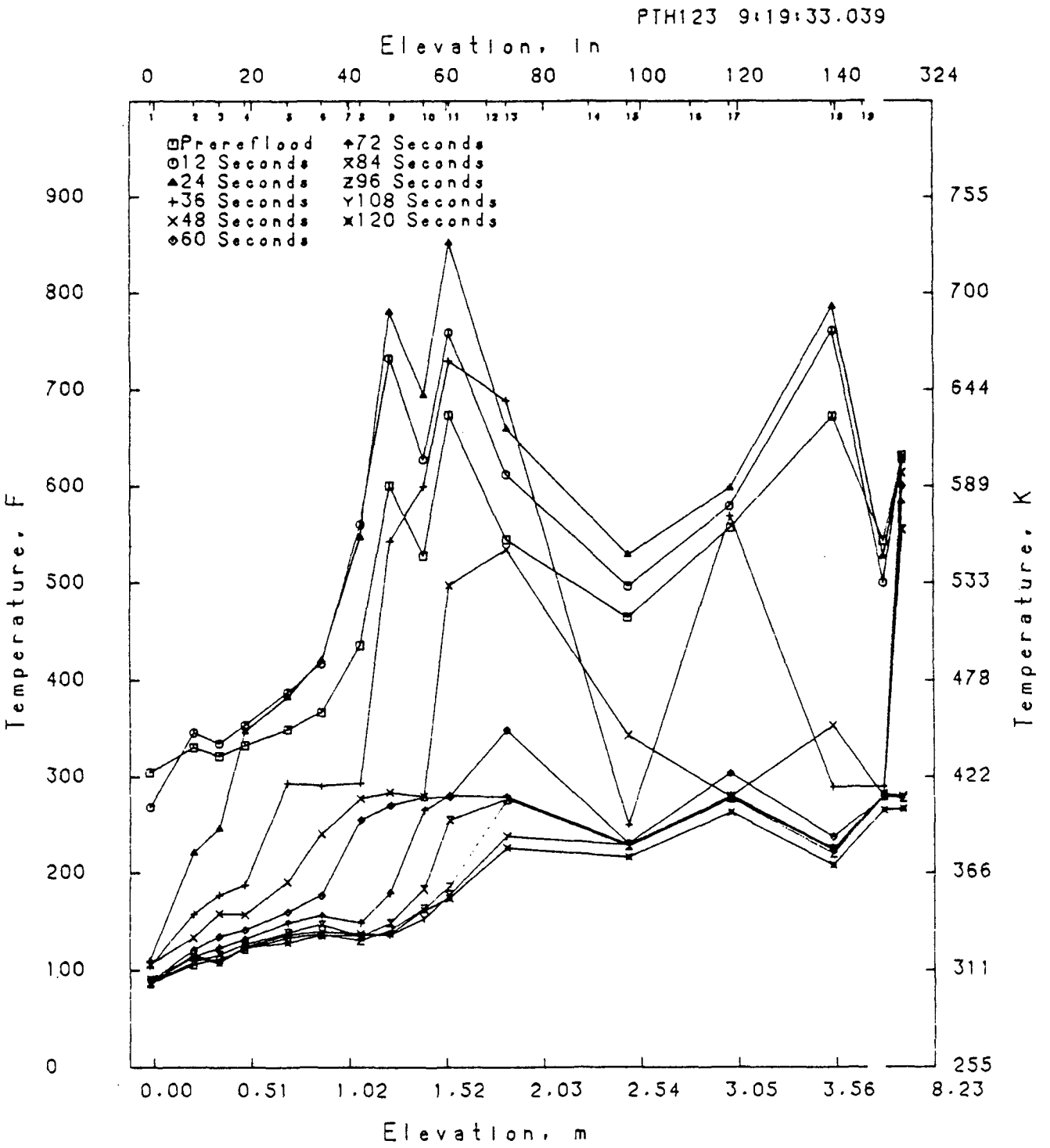

FIGURE 1.2.1.3.23 SHROUD AND TEST TRAIN TEMPERATURE PROFILES DURING REFLOODING AT 12S INTERVALS - PTH123

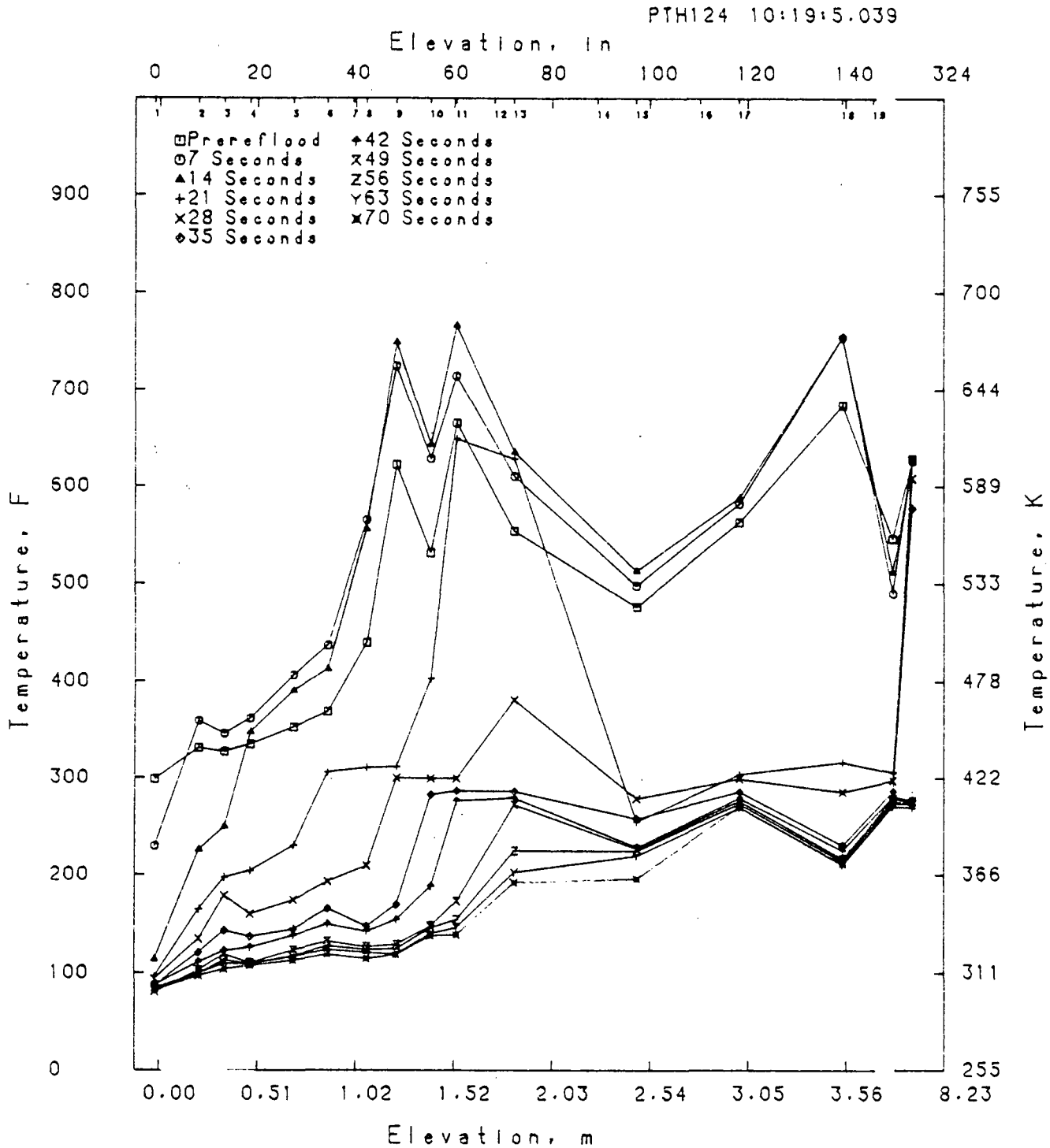

FIGURE 1.2.1.3.24 SHROUD AND TEST TRAIN TEMPERATURE PROFILES DURING REFLOODING AT 7S INTERVALS - PTH124

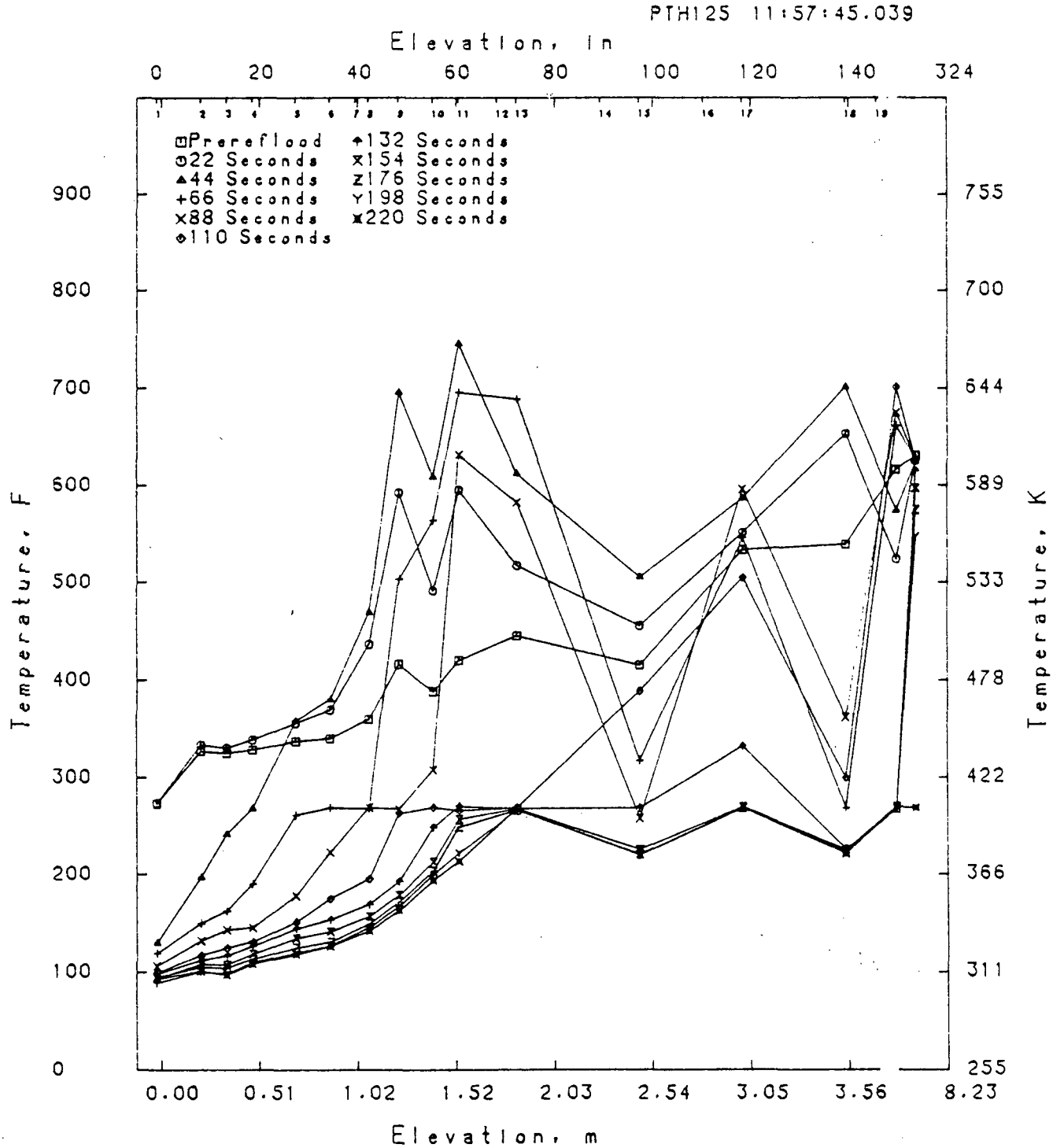

FIGURE 1.2.1.3.25 SHROUD AND TEST TRAIN TEMPERATURE PROFILES DURING REFLOODING AT 22S INTERVALS

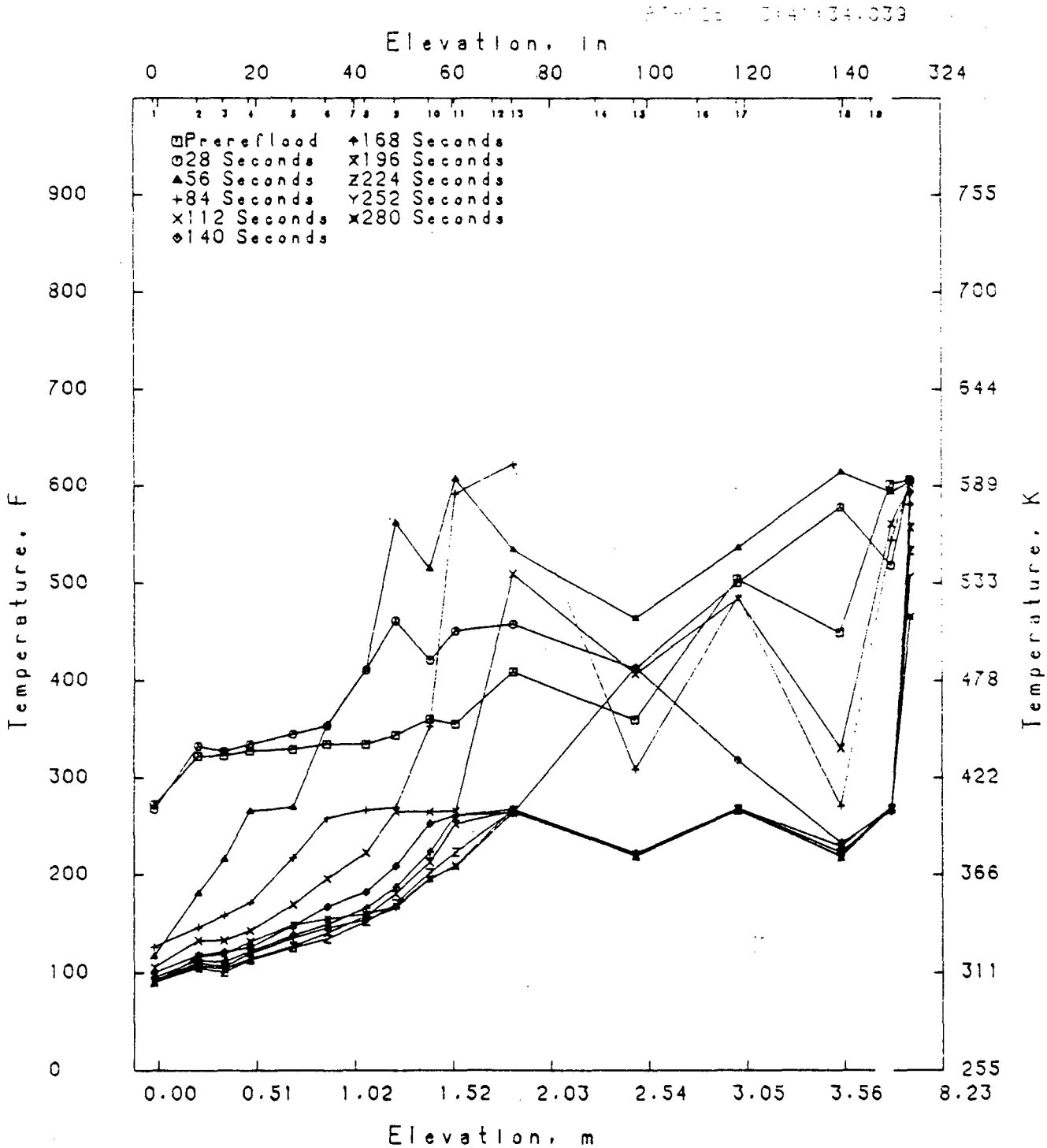

FIGURE 1.2.1.3.26 SHROUD AND TEST TRAIN TEMPERATURE PROFILES DURING REFLOODING AT 28S INTERVALS - PTH128

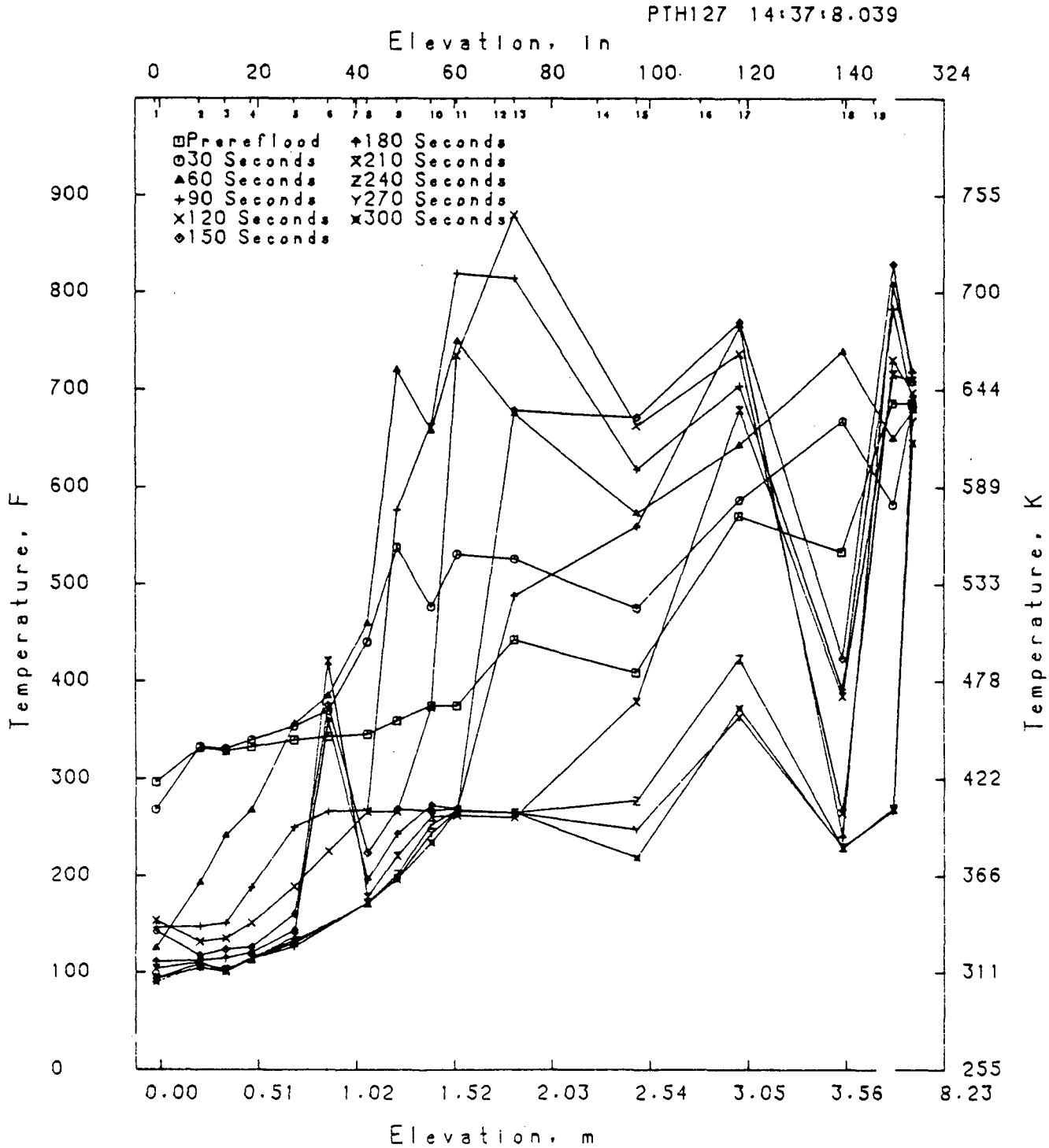

FIGURE 1.2.1.3.27 SHROUD AND TEST TRAIN TEMPERATURE PROFILES DURING REFLOODING AT 30 S INTERVALS

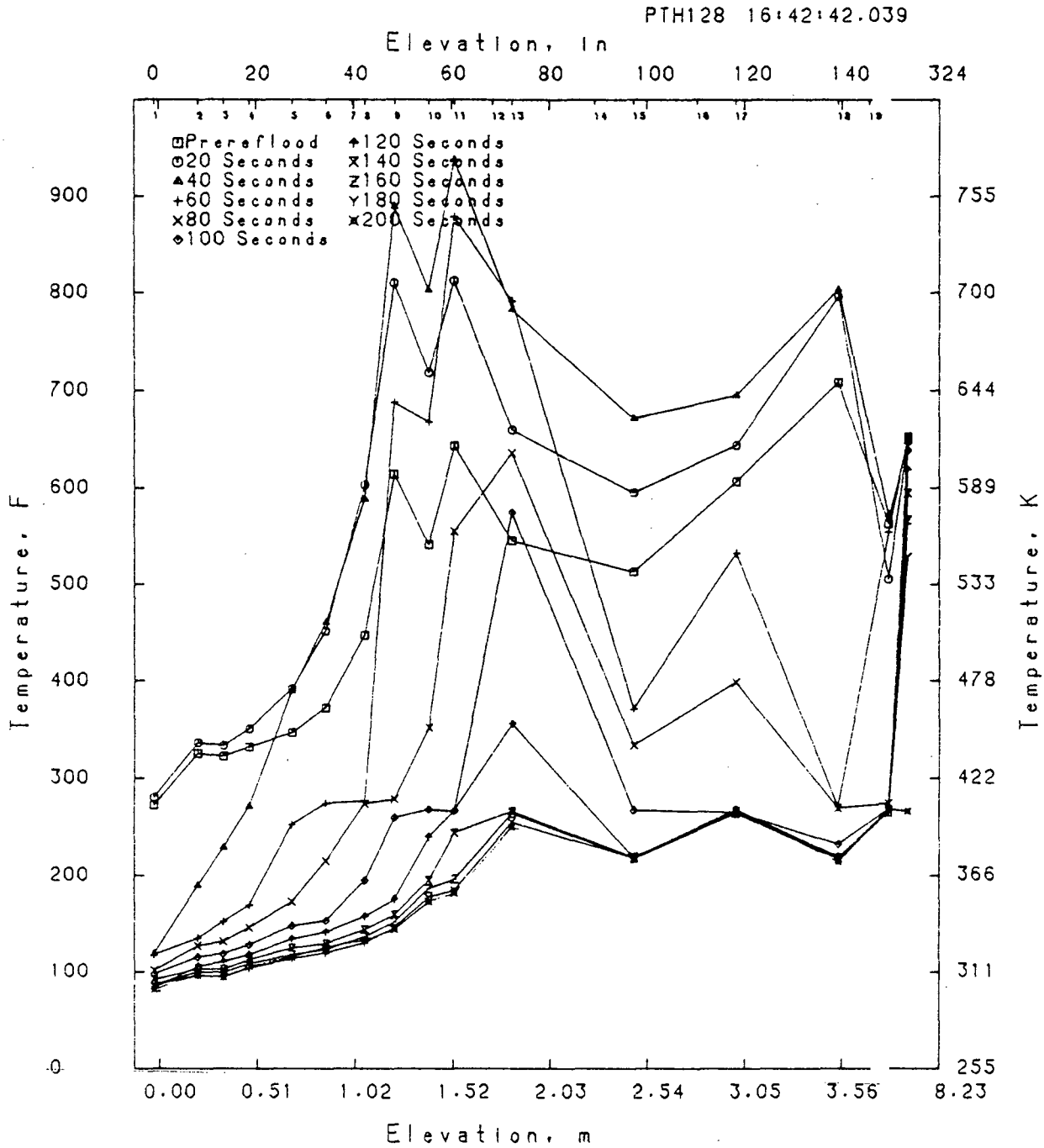

FIGURE 1.2.1.3.28 SHROUD AND TEST TRAIN TEMPERATURE PROFILES DURING REFLOODING AT 20S INTERVALS - PTH128

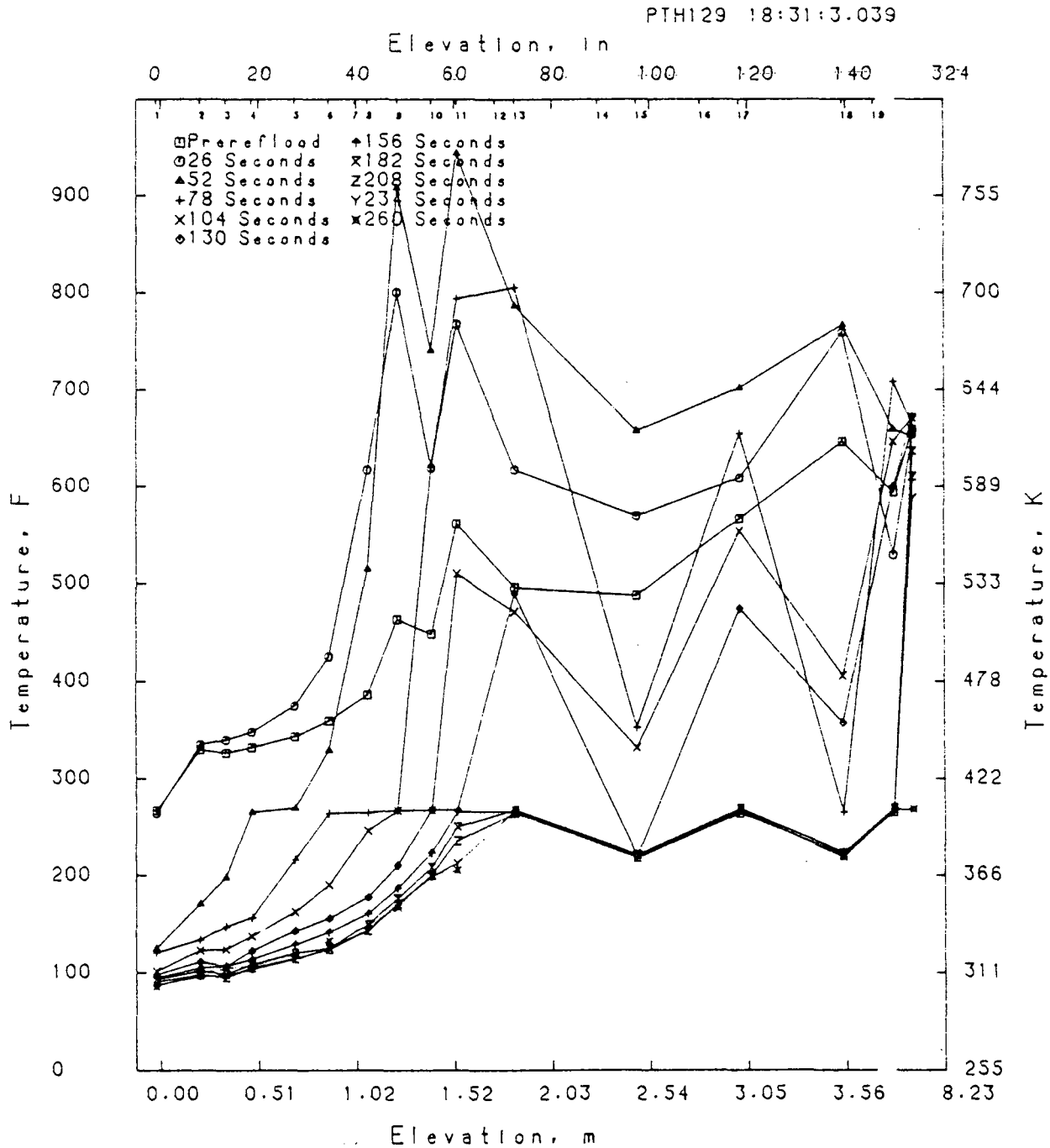

FIGURE 1.2.1.3.29 SHROUD AND TEST TRAIN TEMPERATURE PROFILES DURING REFLOODING AT 26S INTERVALS - PTH129

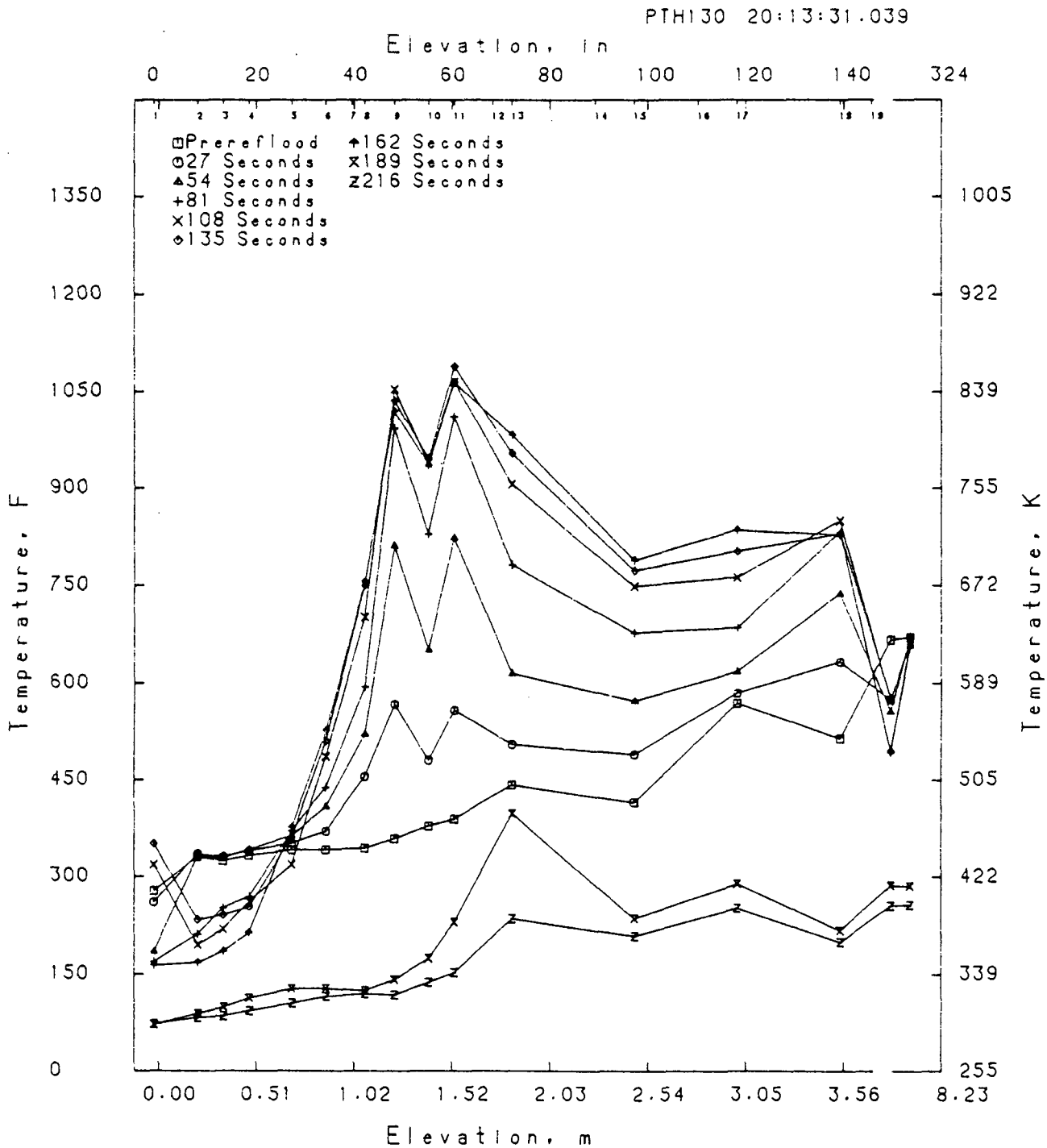

FIGURE 1.2.1.3.30 SHROUD AND TEST TRAIN TEMPERATURE PROFILES DURING REFLOODING AT 27S INTERVALS - PTH130

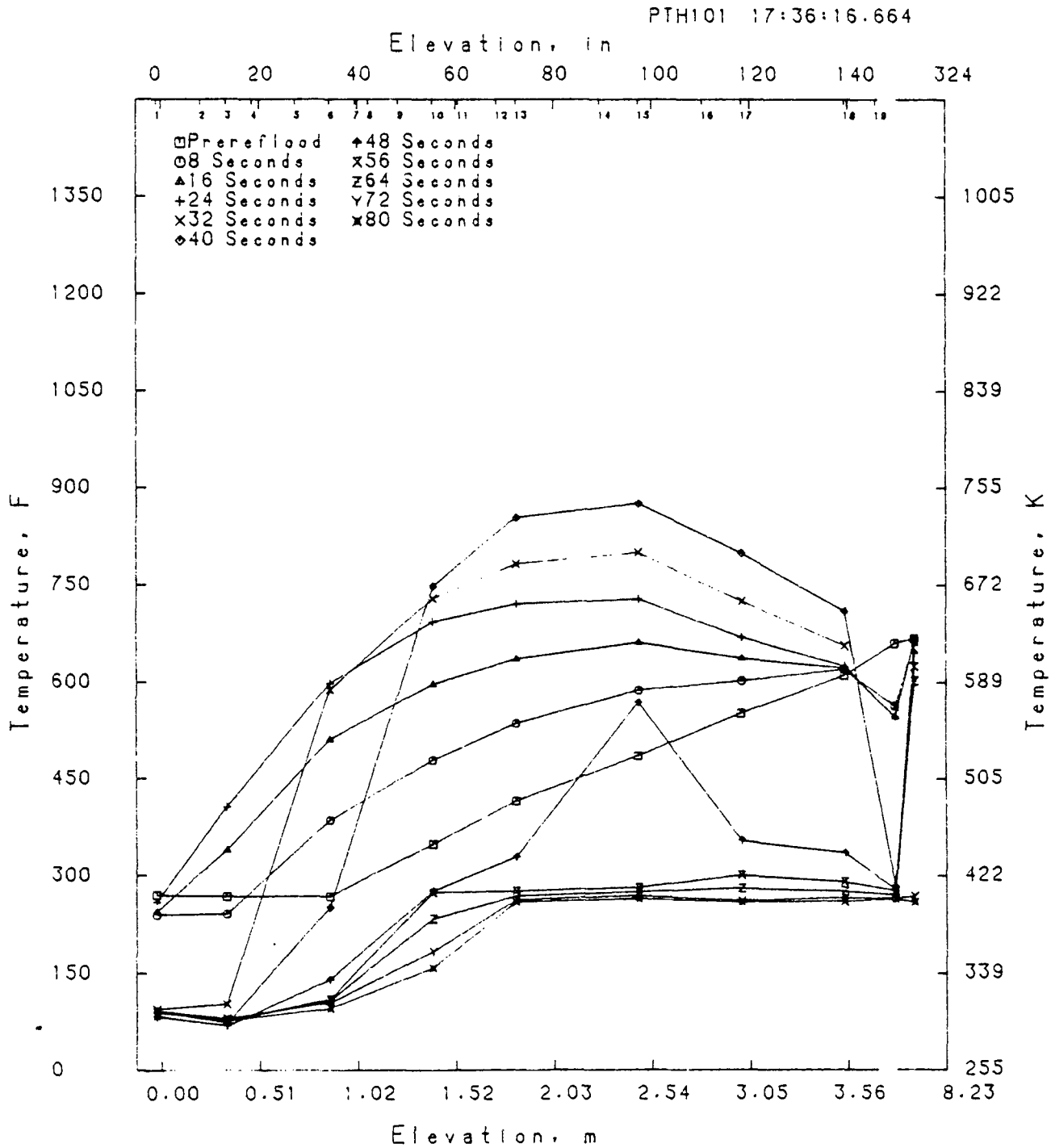

FIGURE 1.2.2.01 INSTRUMENT TUBE AND TEST TRAIN TEMPERATURE PROFILES DURING REFLOODING AT 8S INTERVALS - PTH101

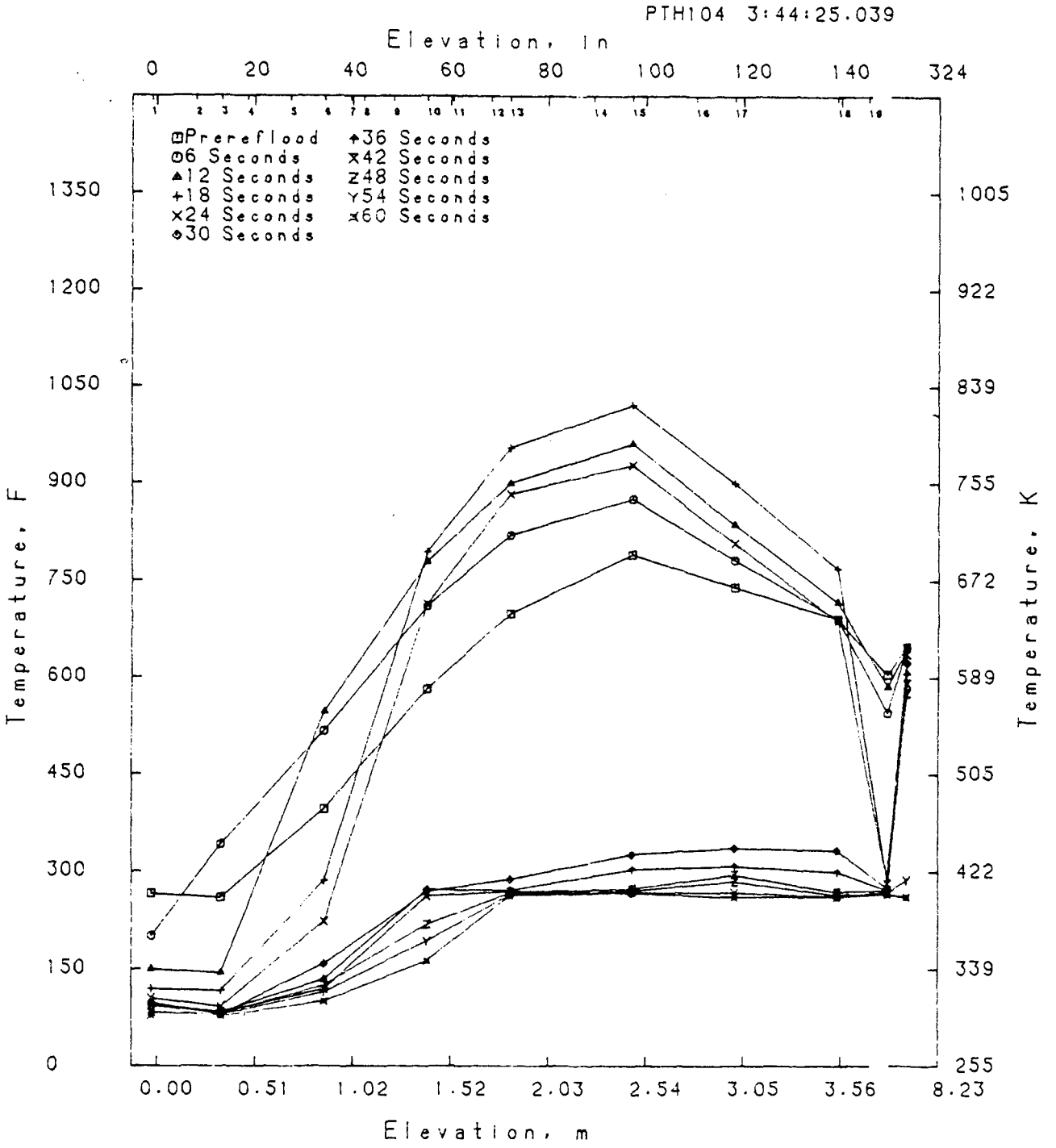

FIGURE 1.2.2.04 INSTRUMENT TUBE AND TEST TRAIN TEMPERATURE PROFILES DURING REFLOODING AT 6S INTERVALS - PTH104

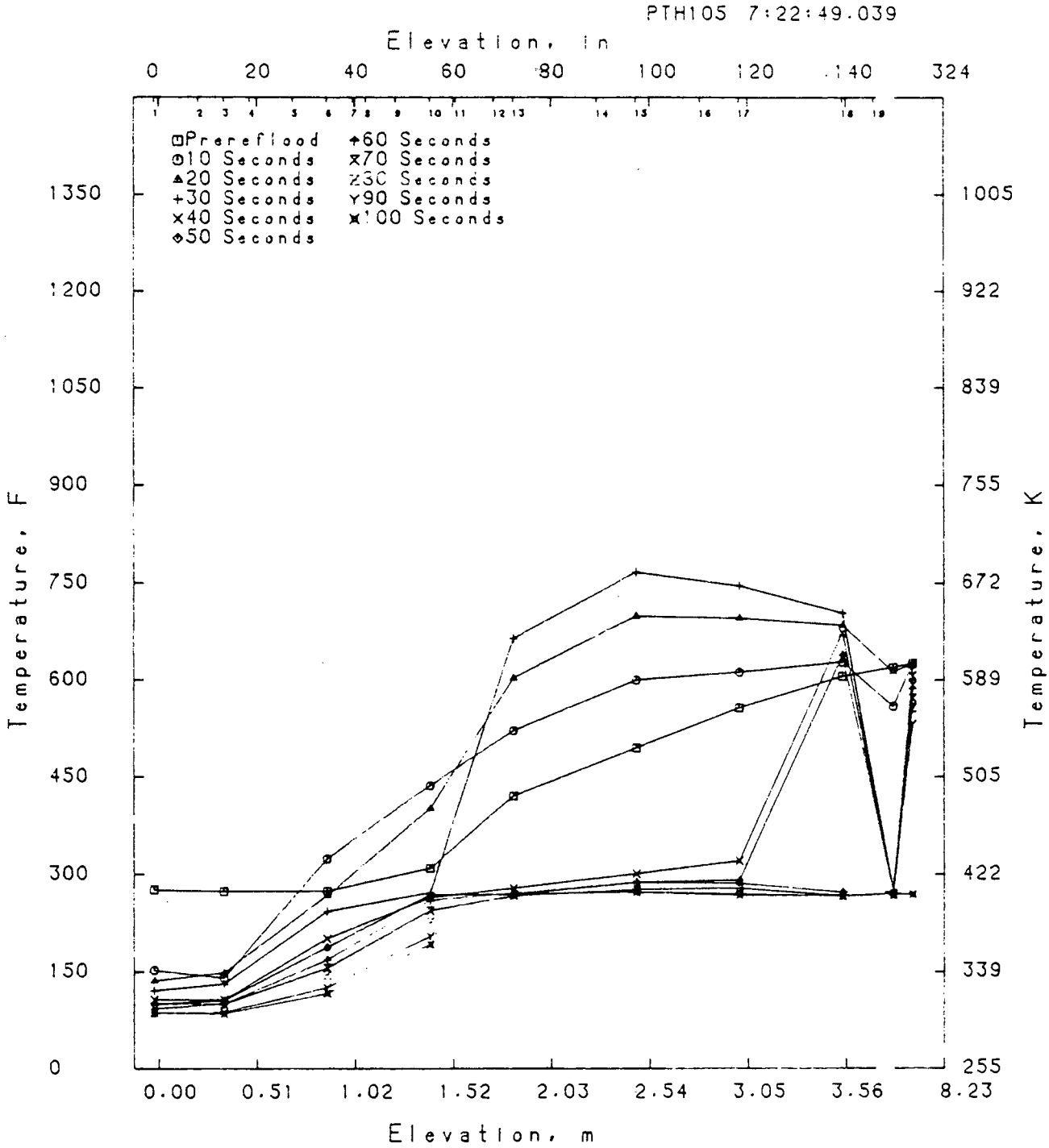

FIGURE 1.2.2.05 INSTRUMENT TUBE AND TEST TRAIN TEMPERATURE PROFILES DURING REFLOODING AT 10S INTERVALS - PTH105

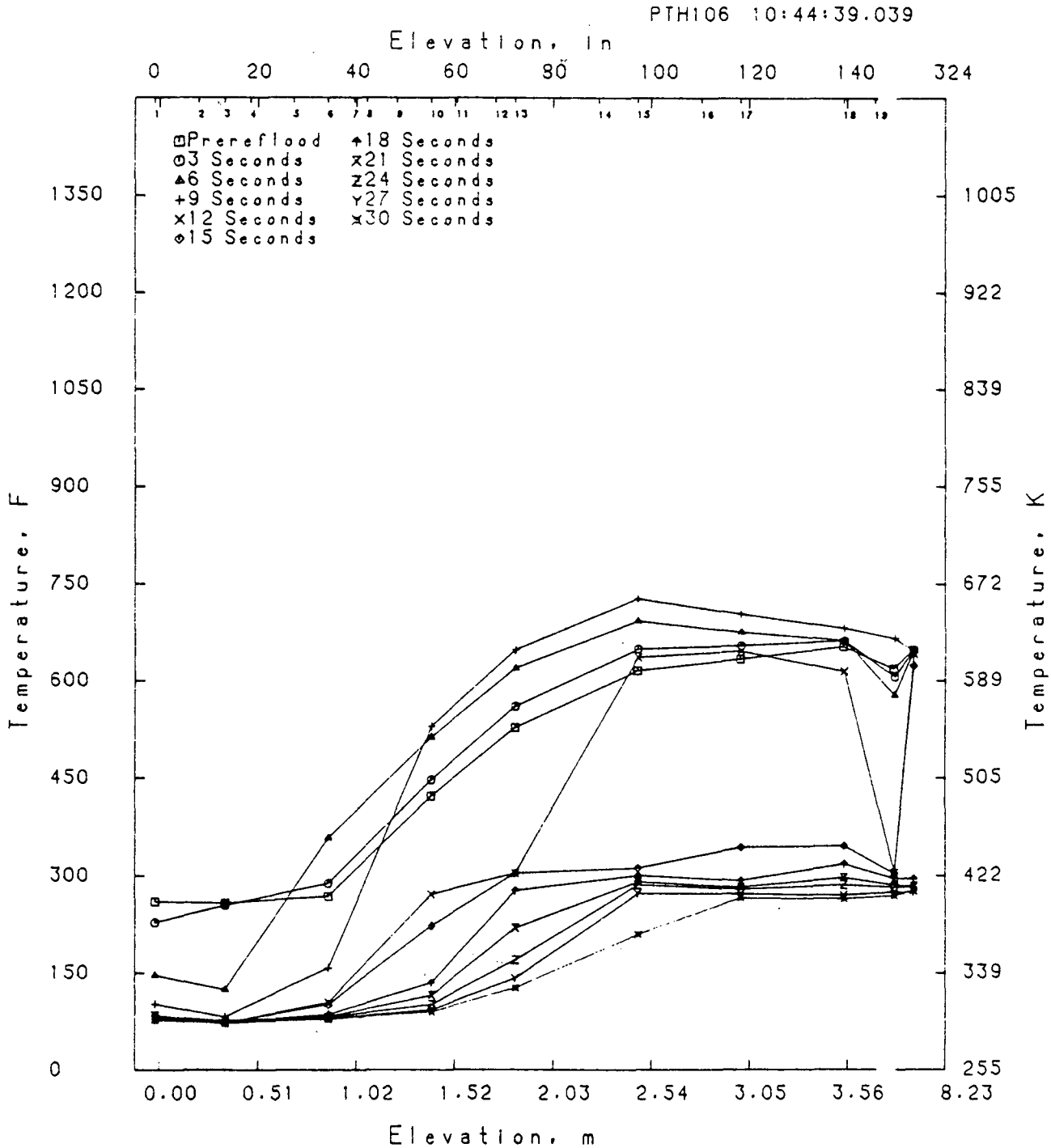

FIGURE 1.2.2.06 INSTRUMENT TUBE AND TEST TRAIN TEMPERATURE PROFILES DURING REFLOODING AT 3S INTERVALS - PTH106

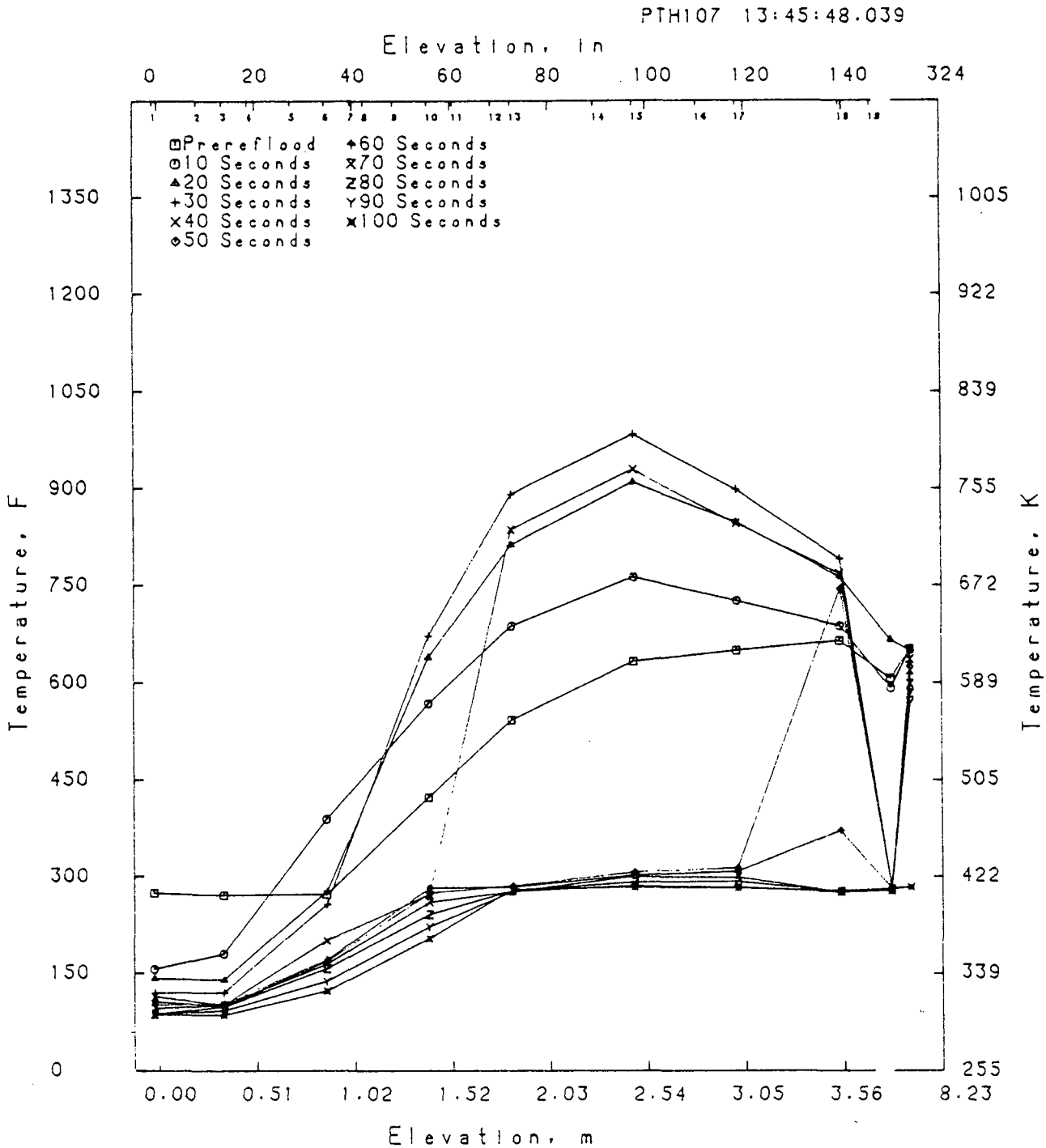

FIGURE 1.2.2.07 INSTRUMENT TUBE AND TEST TRAIN TEMPERATURE PROFILES DURING REFLOODING AT 10S INTERVALS - PTH107

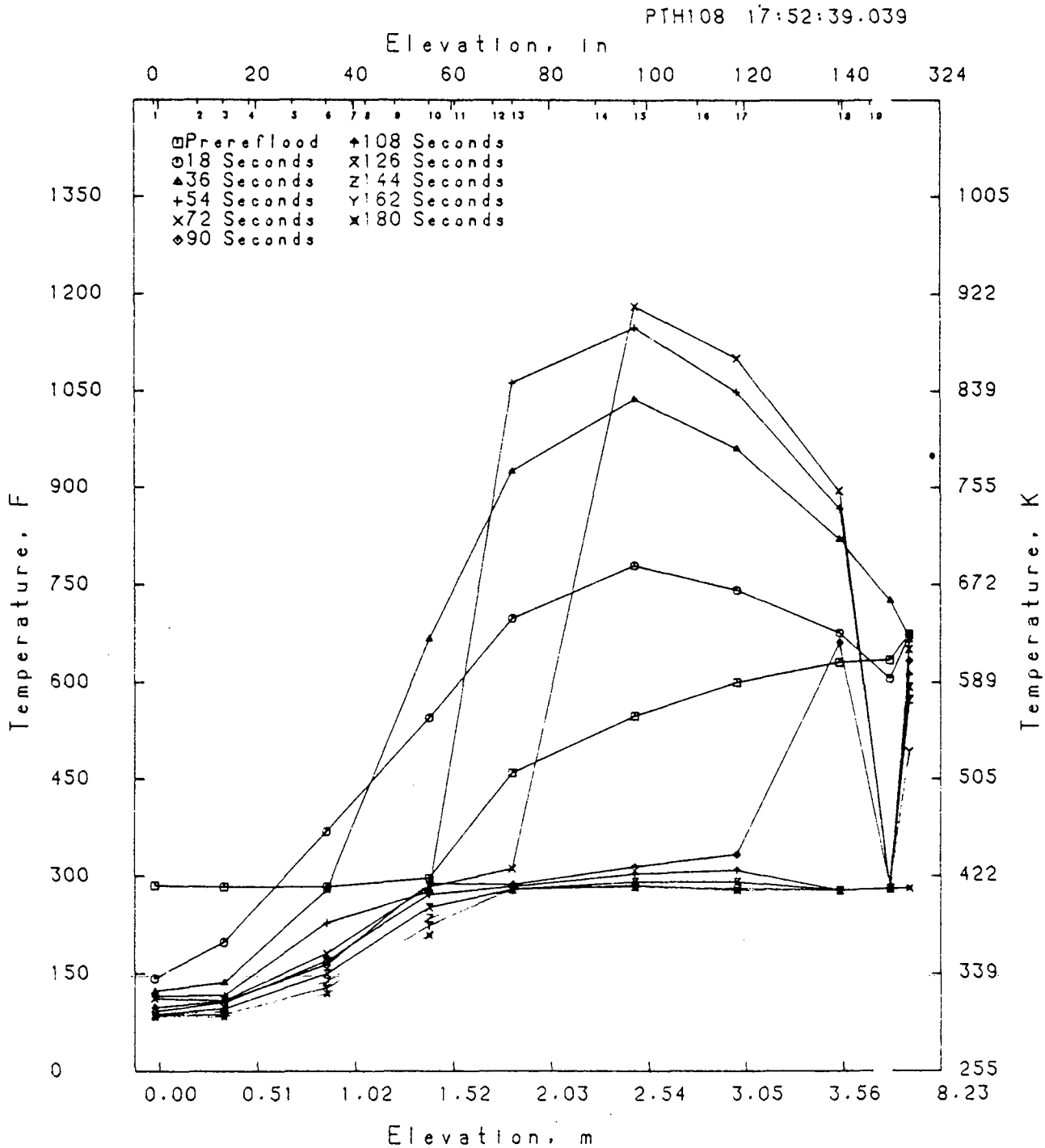

FIGURE 1.2.2.08 INSTRUMENT TUBE AND TEST TRAIN TEMPERATURE PROFILES DURING REFLOODING AT 18S INTERVALS - PTH108

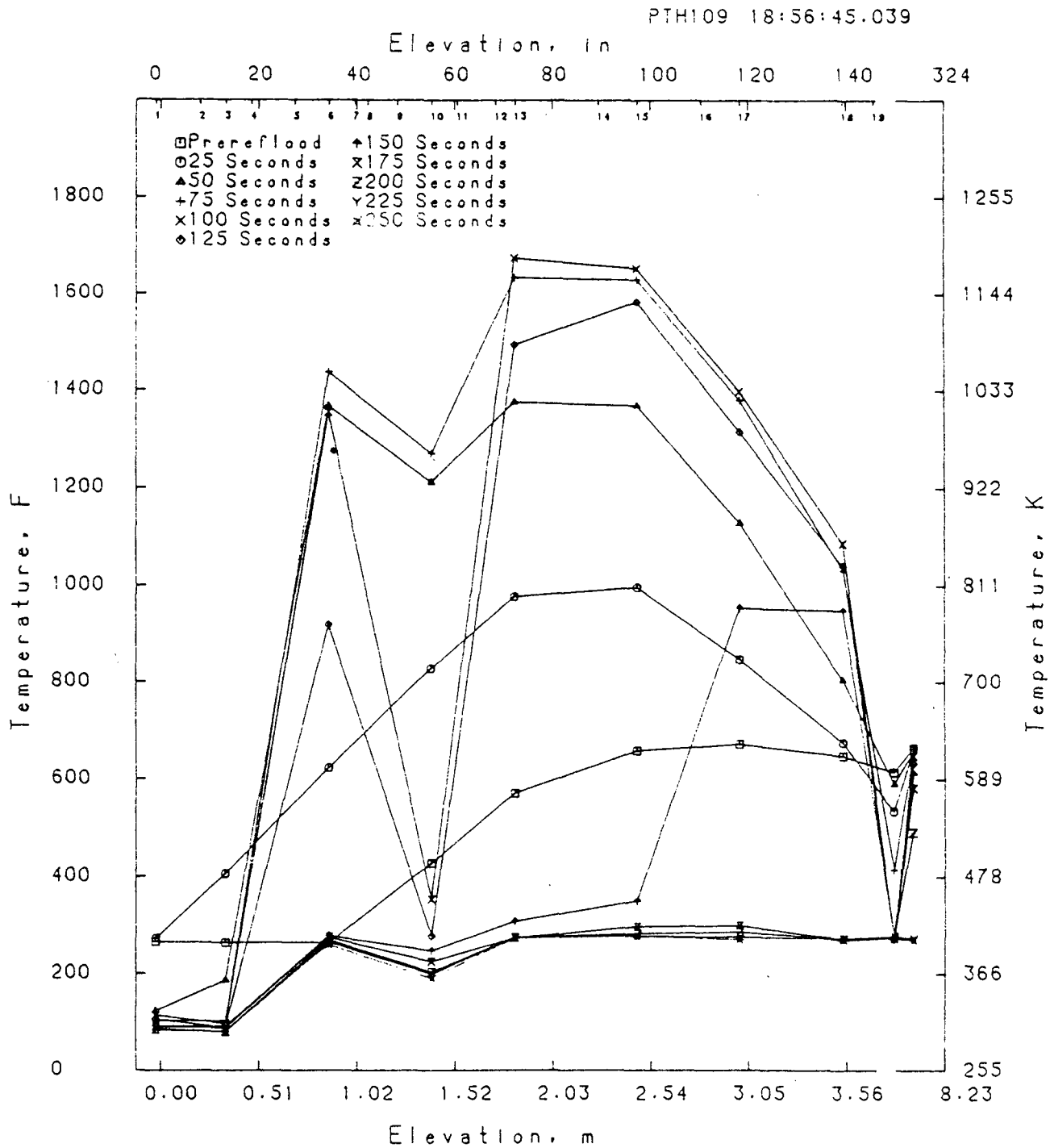

FIGURE 1.2.2.09 INSTRUMENT TUBE AND TEST TRAIN TEMPERATURE PROFILES DURING REFLOODING AT 25S INTERVALS - PTH109

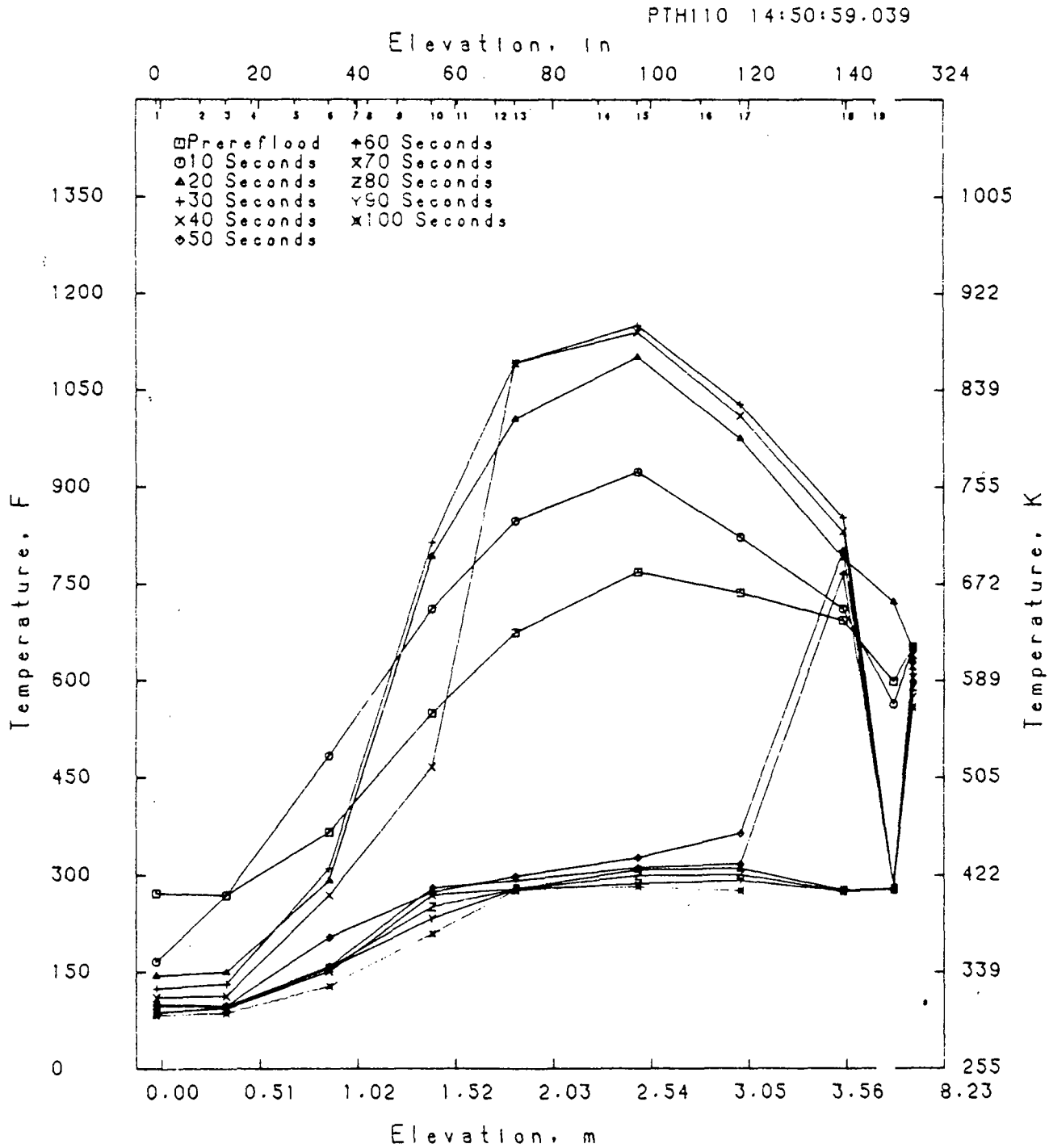

FIGURE 1.2.2.10 INSTRUMENT TUBE AND TEST TRAIN TEMPERATURE PROFILES DURING REFLOODING AT 10S INTERVALS - PTH110

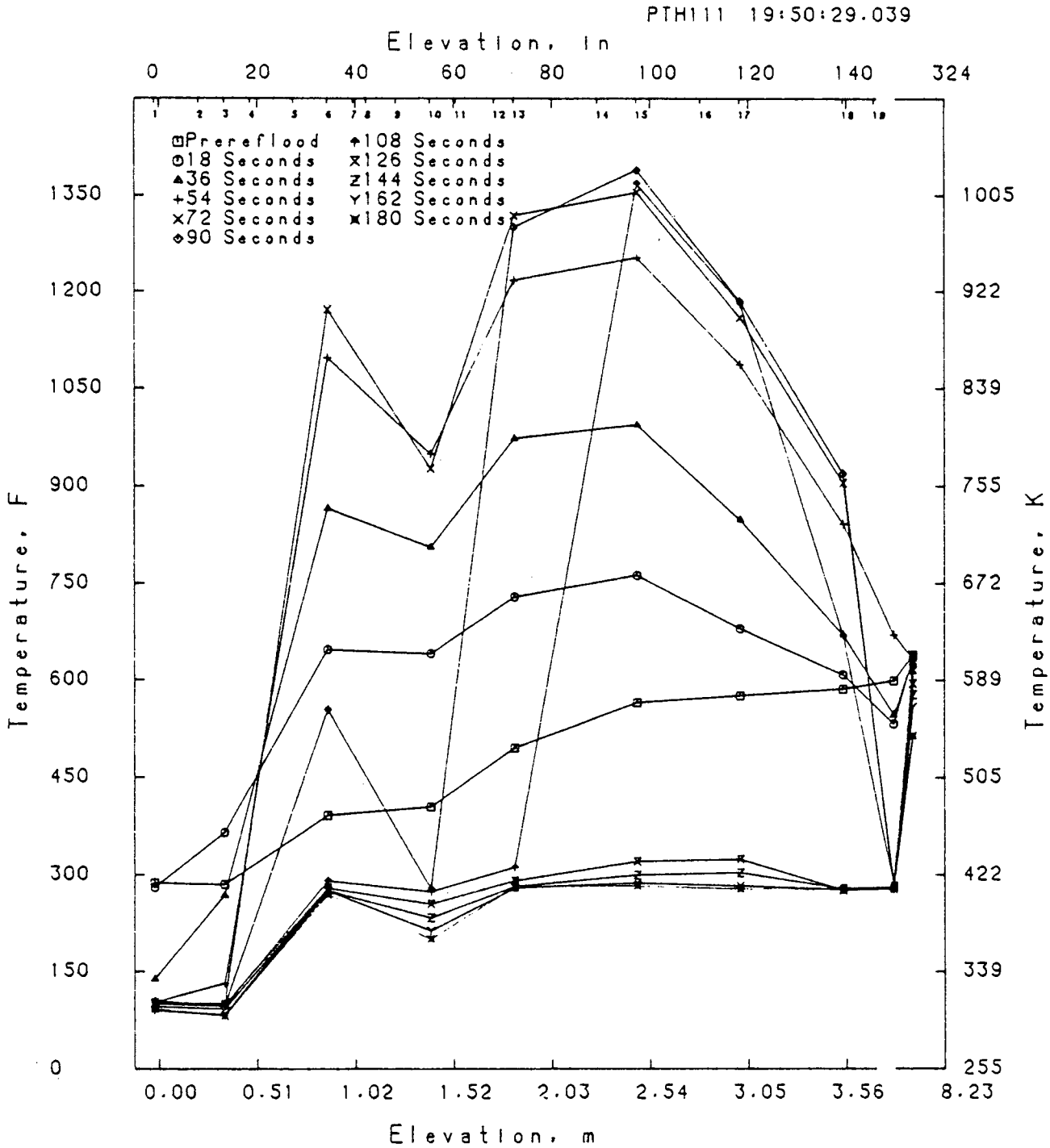

FIGURE 1.2.2.11 INSTRUMENT TUBE AND TEST TRAIN TEMPERATURE PROFILES DURING REFLOODING AT 18S INTERVALS - PTH111

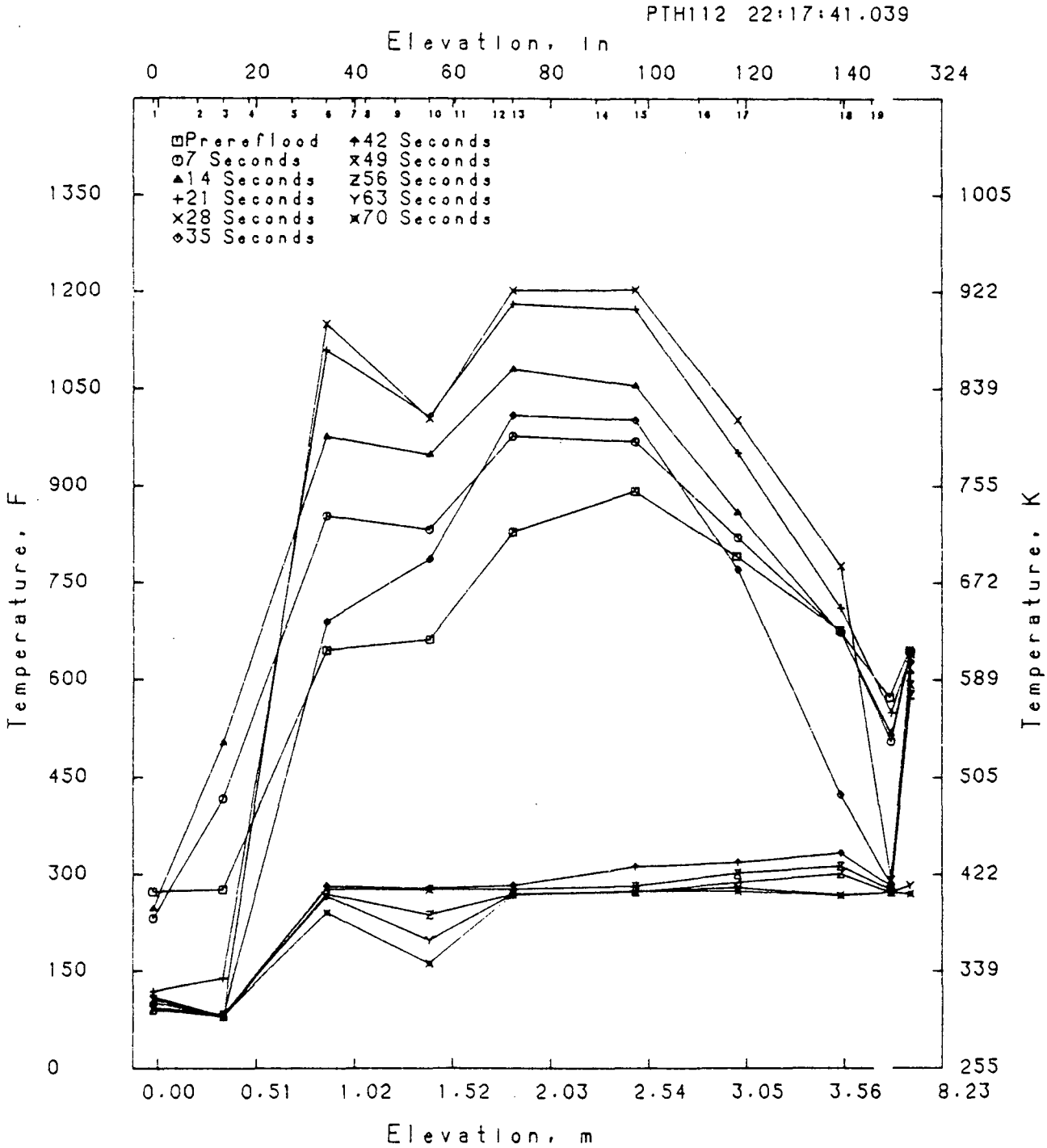

FIGURE 1.2.2.12 INSTRUMENT TUBE AND TEST TRAIN TEMPERATURE PROFILES DURING REFLOODING AT 7S INTERVALS - PTH112

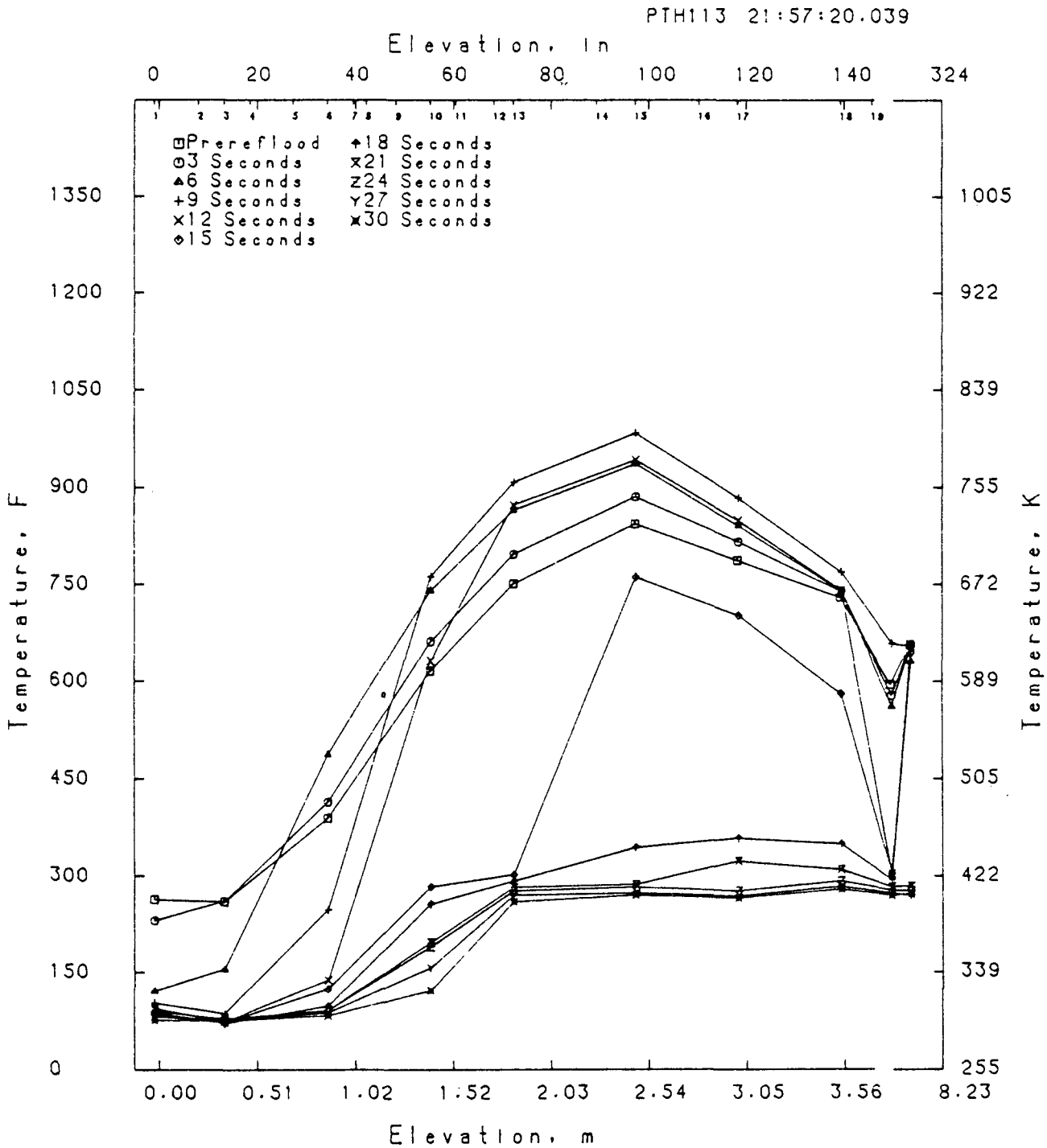

FIGURE 1.2.2.13 INSTRUMENT TUBE AND TEST TRAIN TEMPERATURE PROFILES DURING REFLOODING AT 3S INTERVALS - PTH113

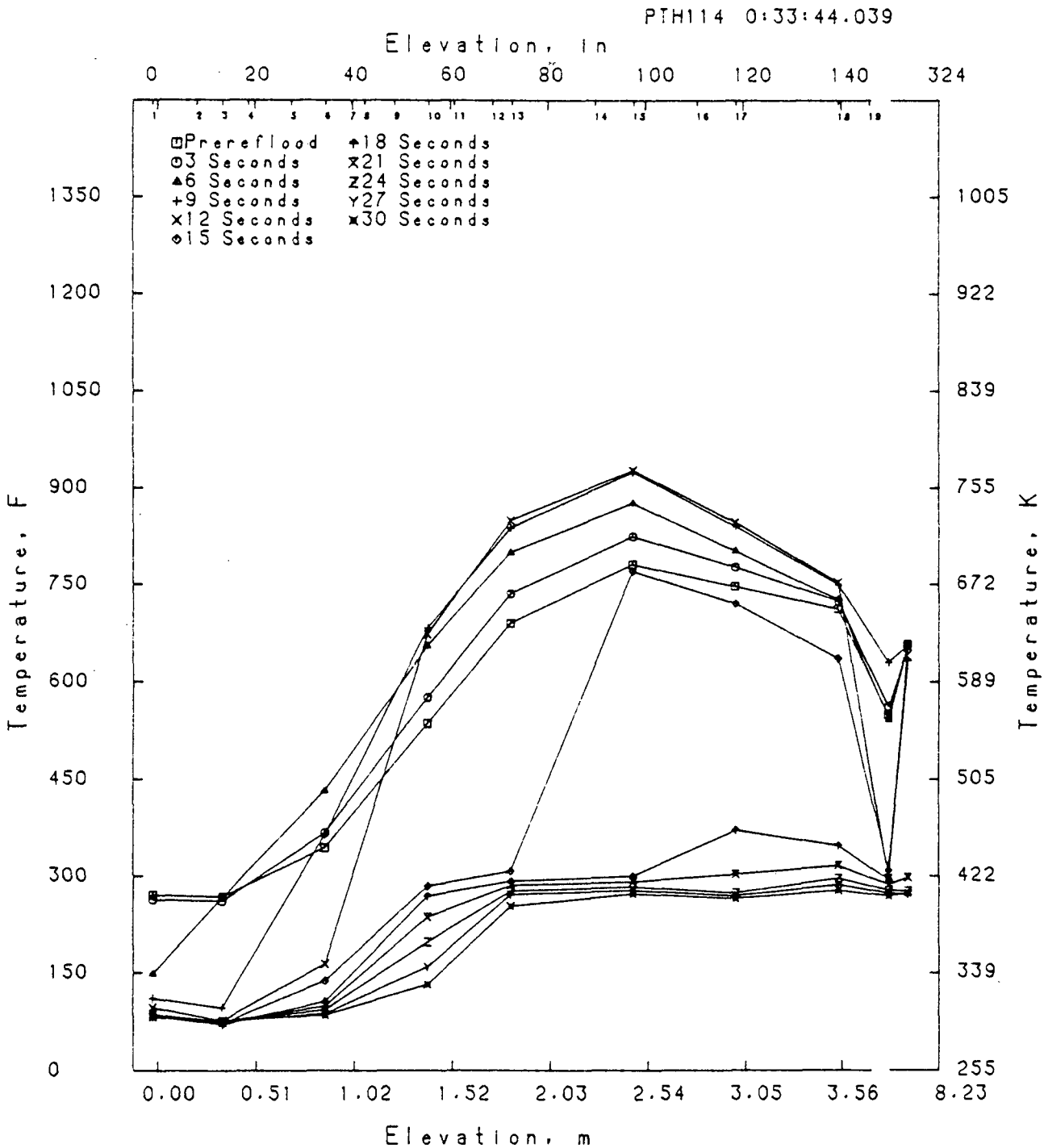

FIGURE 1.2.2.14 INSTRUMENT TUBE AND TEST TRAIN TEMPERATURE PROFILES DURING REFLOODING AT 3S INTERVALS - PTH114

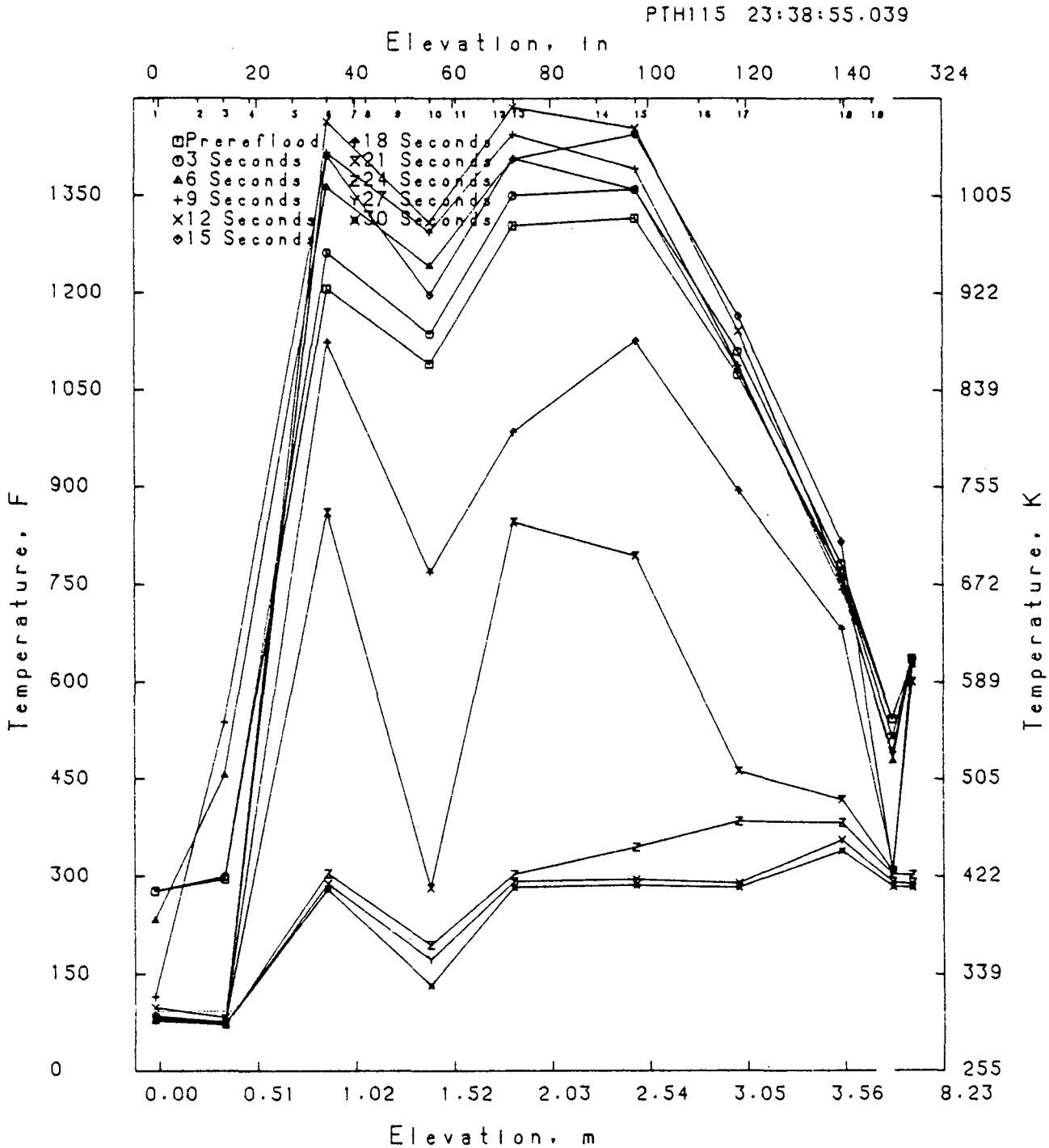

FIGURE 1.2.2.15 INSTRUMENT TUBE AND TEST TRAIN TEMPERATURE PROFILES DURING REFLOODING AT 3S INTERVALS - PTH115

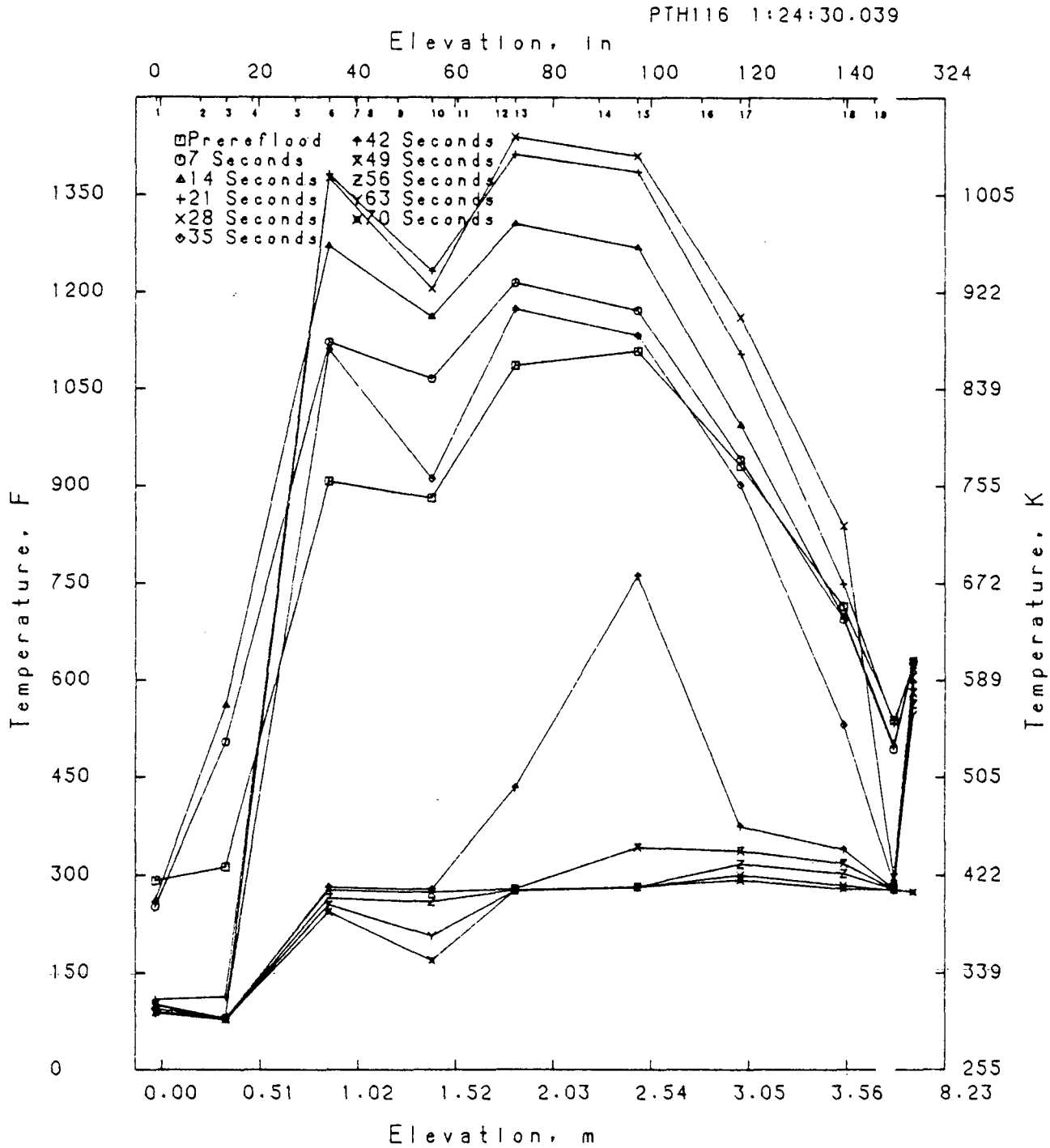

FIGURE 1.2.2.16 INSTRUMENT TUBE AND TEST TRAIN TEMPERATURE PROFILES DURING REFLOODING AT 7S INTERVALS - PTH116

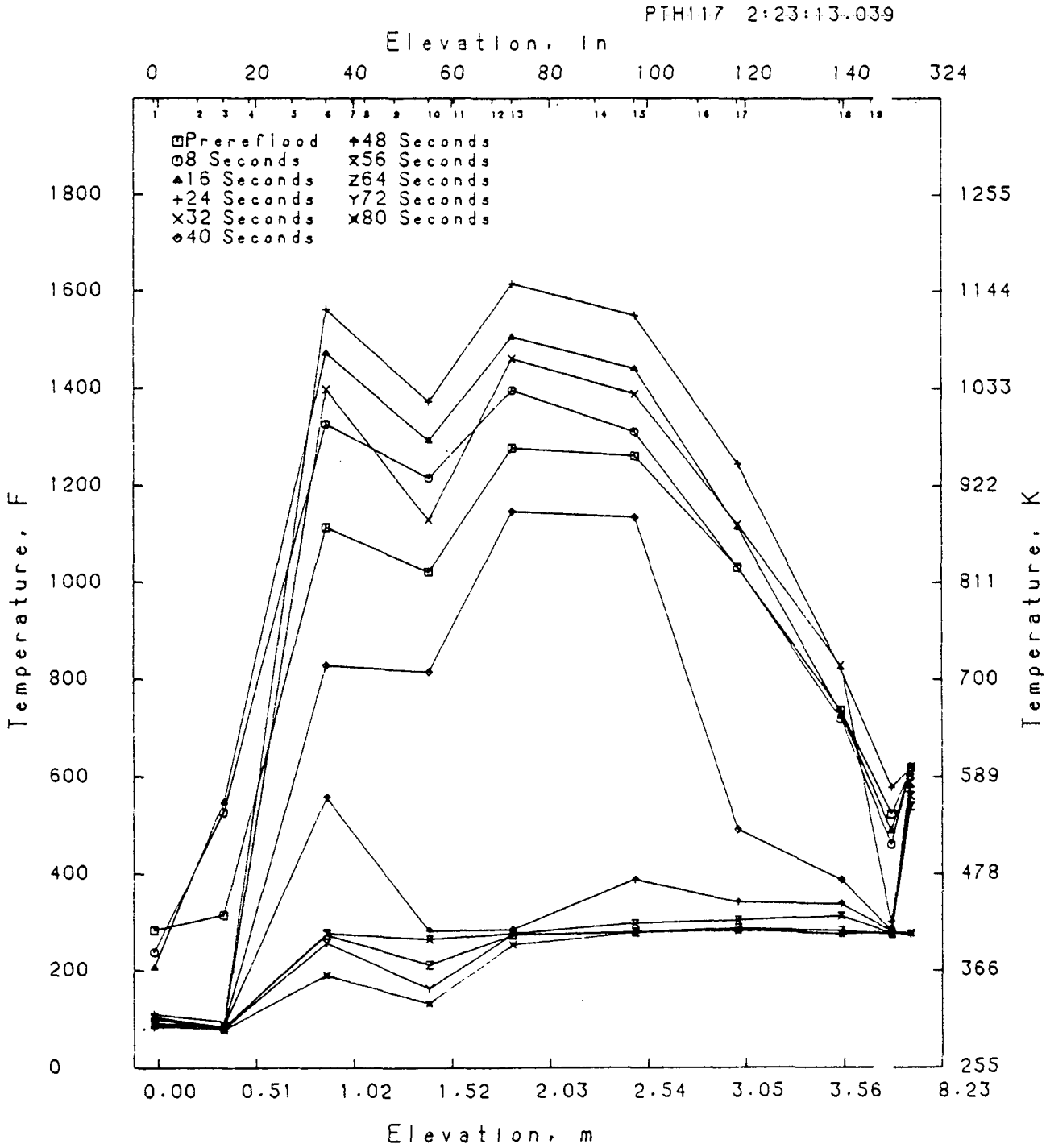

FIGURE 1.2.2.17 INSTRUMENT TUBE AND TEST TRAIN TEMPERATURE PROFILES DURING REFLOODING AT 8S INTERVALS - PTH117

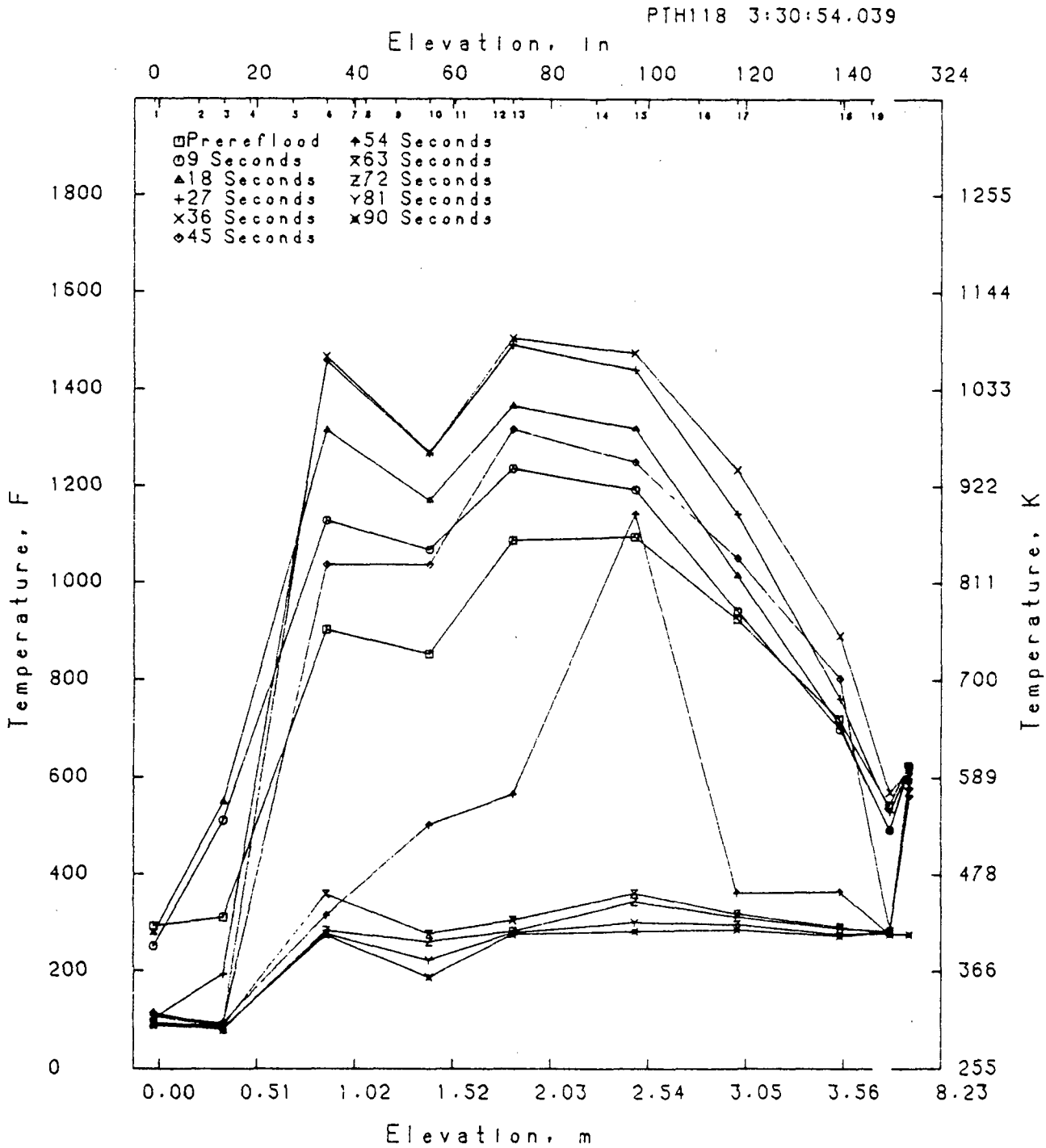

FIGURE 1.2.2.18 INSTRUMENT TUBE AND TEST TRAIN TEMPERATURE PROFILES DURING REFLOODING AT 9S INTERVALS - PTH118

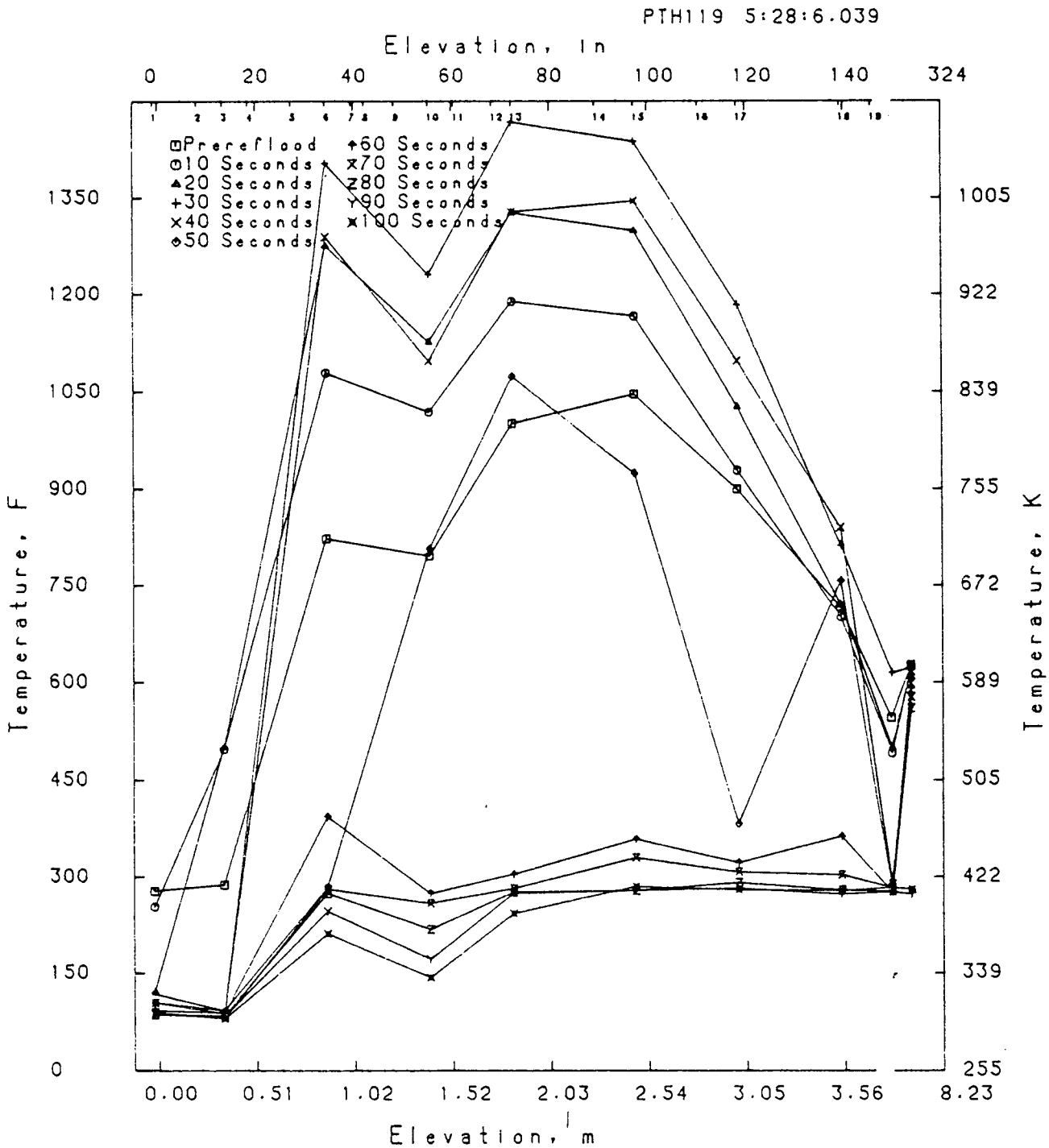

FIGURE 1.2.2.19 INSTRUMENT TUBE AND TEST TRAIN TEMPERATURE PROFILES DURING REFLOODING AT 10S INTERVALS - PTH119

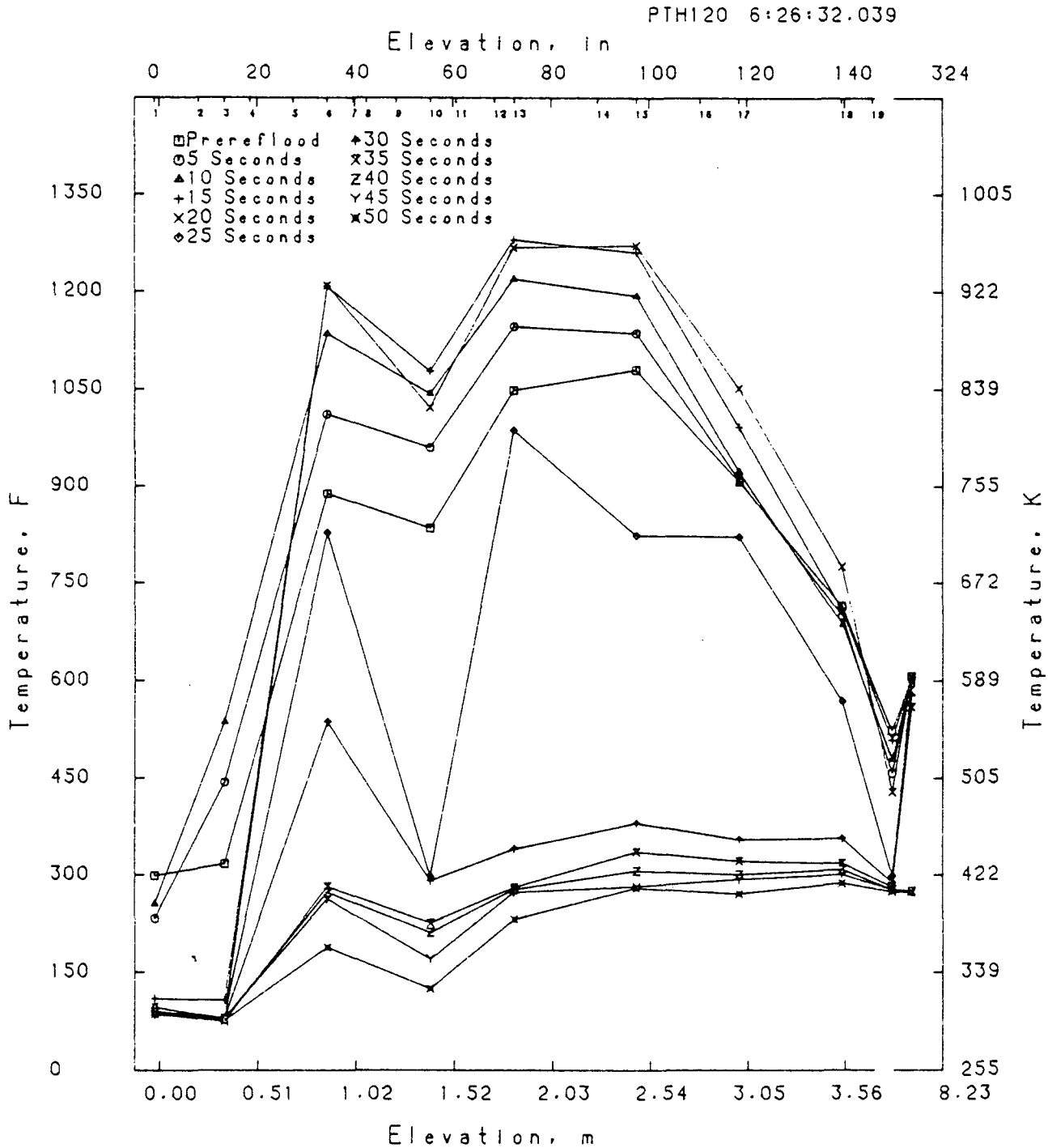

FIGURE 1.2.2.20 INSTRUMENT TUBE AND TEST TRAIN TEMPERATURE PROFILES DURING REFLOODING AT 5S INTERVALS - PTH120

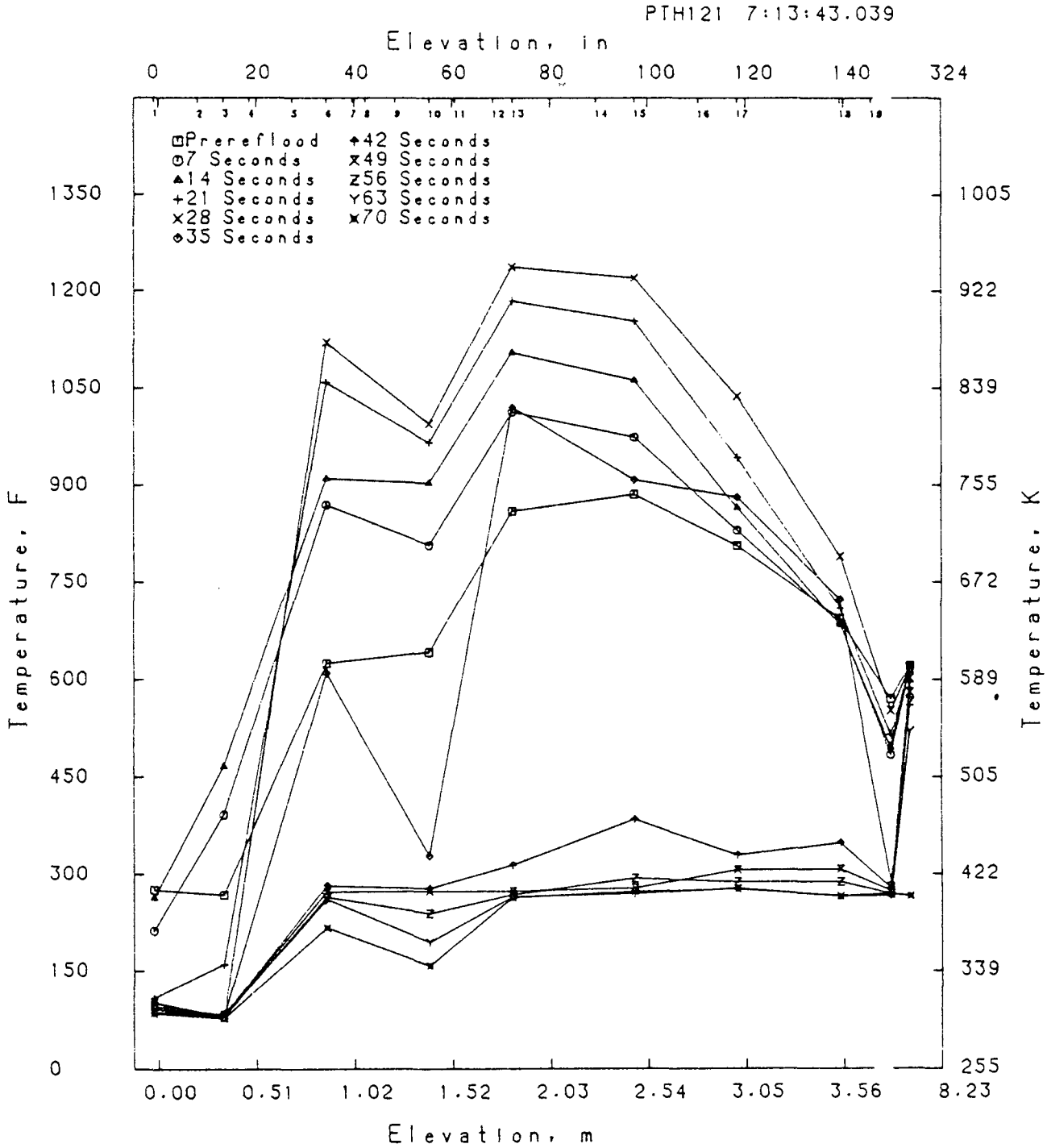

FIGURE 1.2.2.21 INSTRUMENT TUBE AND TEST TRAIN TEMPERATURE PROFILES DURING REFLOODING AT 7S INTERVALS - PTH121

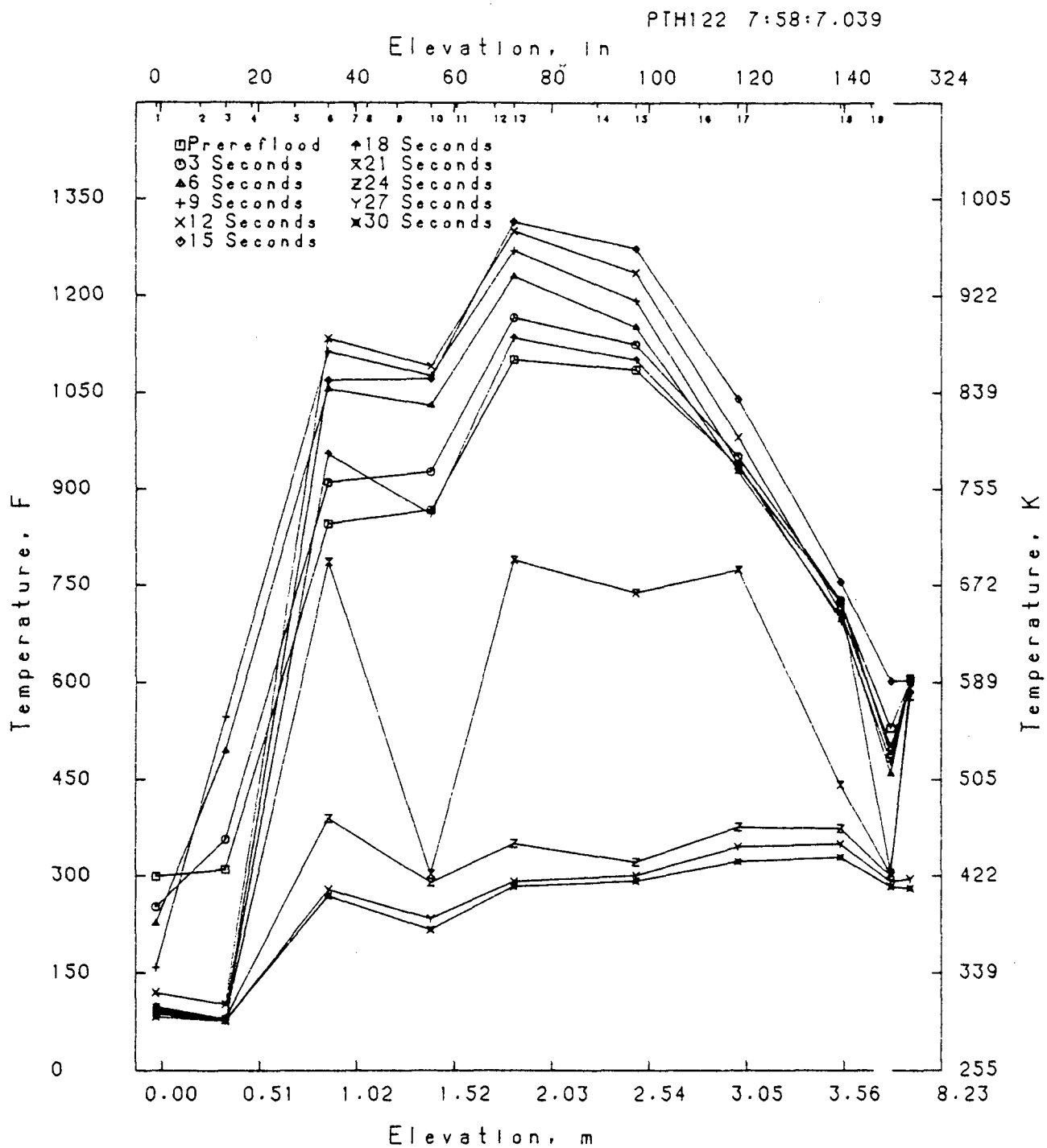

FIGURE 1.2.2.22 INSTRUMENT TUBE AND TEST TRAIN TEMPERATURE PROFILES DURING REFLOODING AT 3S INTERVALS - PTH122

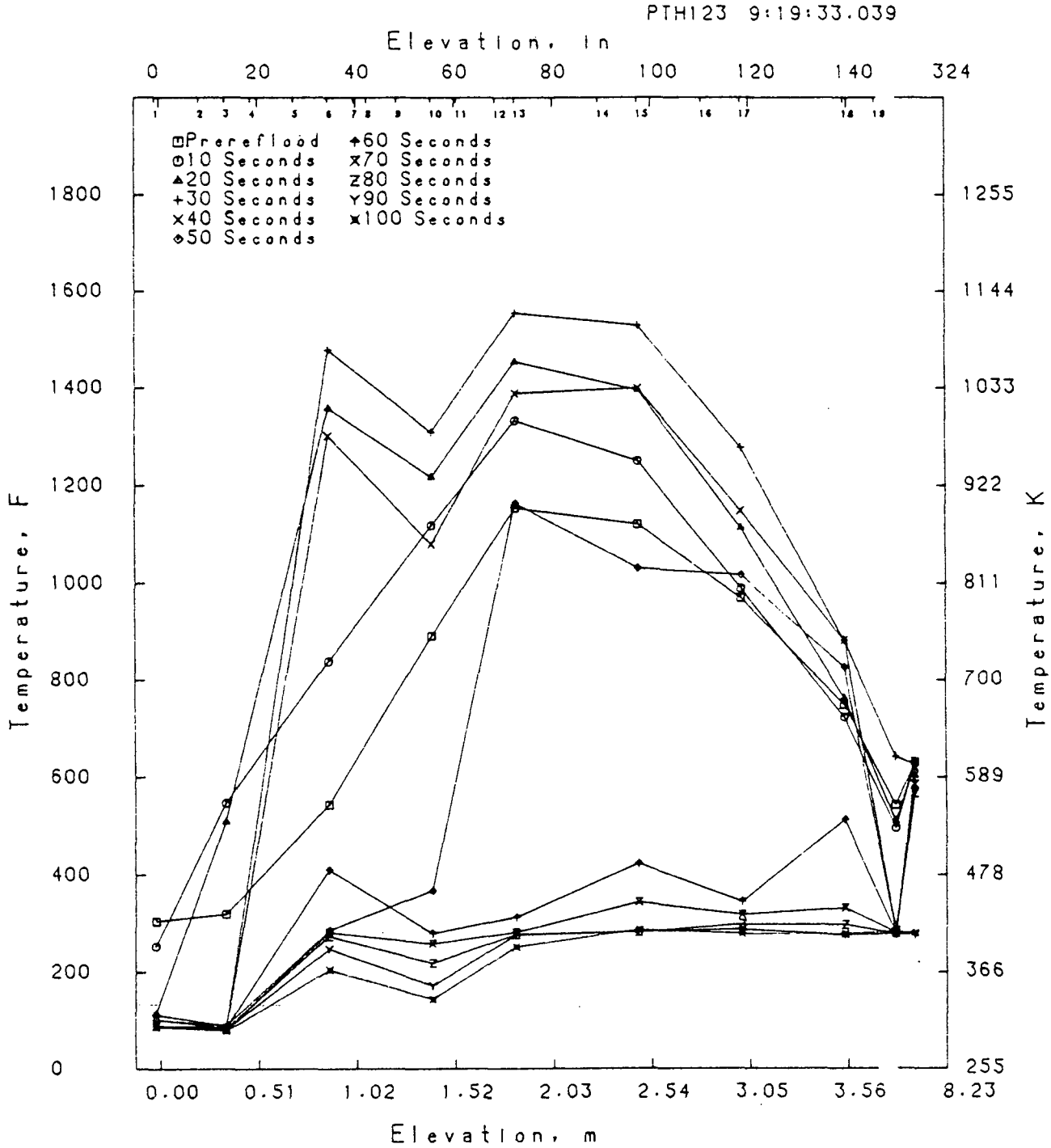

FIGURE 1.2.2.23 INSTRUMENT TUBE AND TEST TRAIN TEMPERATURE PROFILES DURING REFLOODING AT 10S INTERVALS - PTH123

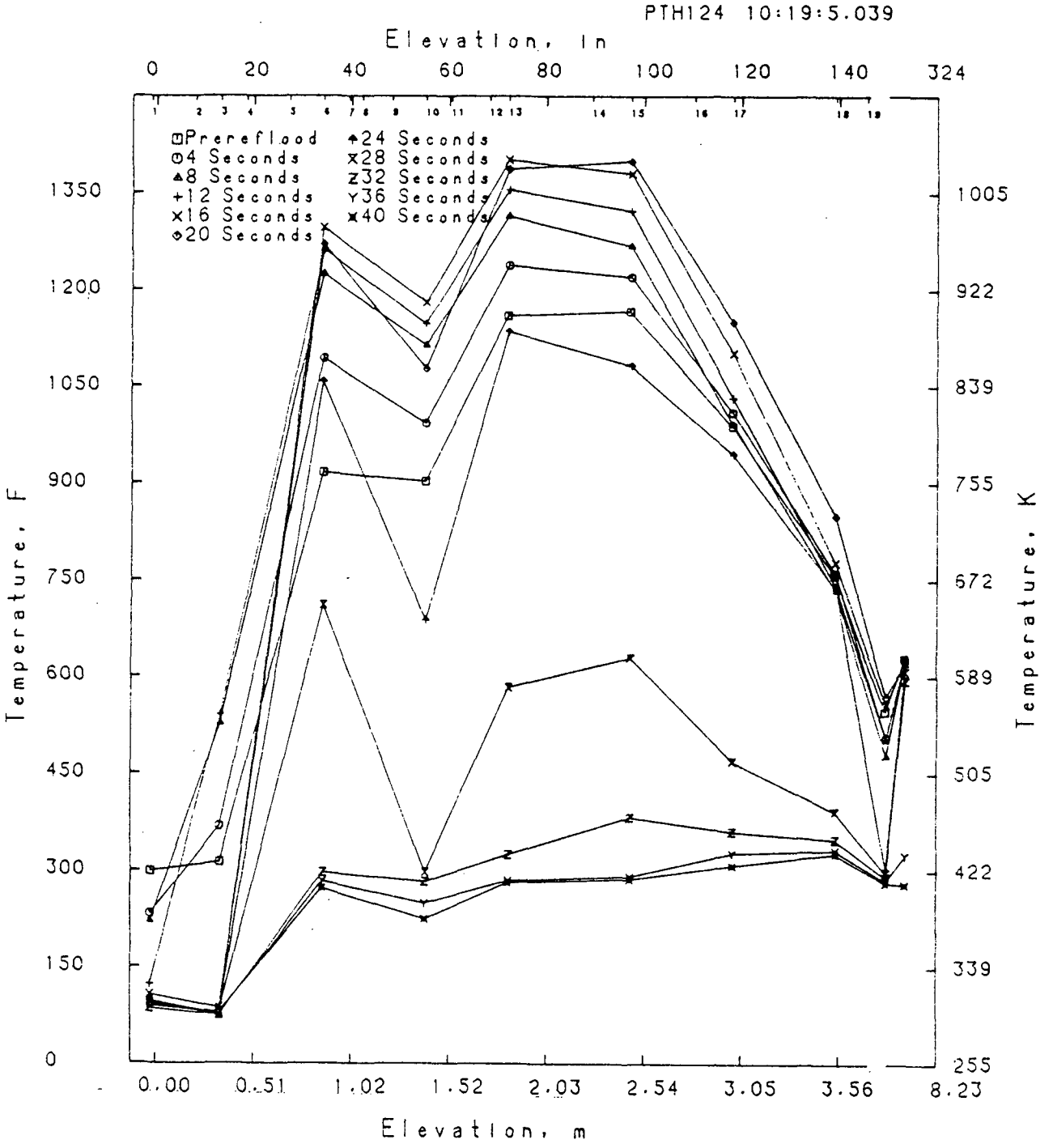

FIGURE 1.2.2.24 INSTRUMENT TUBE AND TEST TRAIN TEMPERATURE PROFILES DURING REFLOODING AT 4S INTERVALS - PTH124

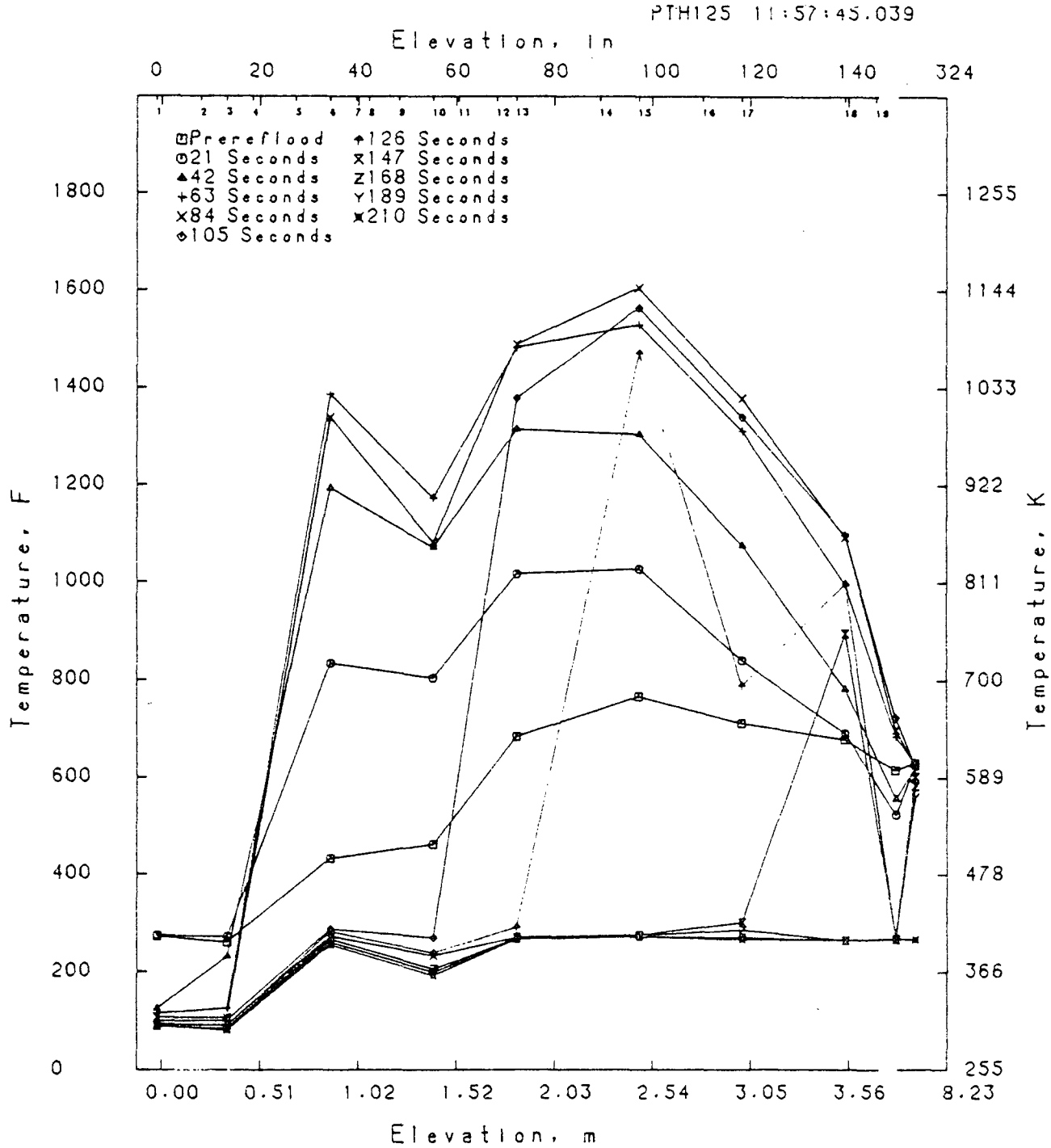

FIGURE 1.2.2.25 INSTRUMENT TUBE AND TEST TRAIN TEMPERATURE PROFILES DURING REFLOODING AT 21S INTERVALS - PTH125

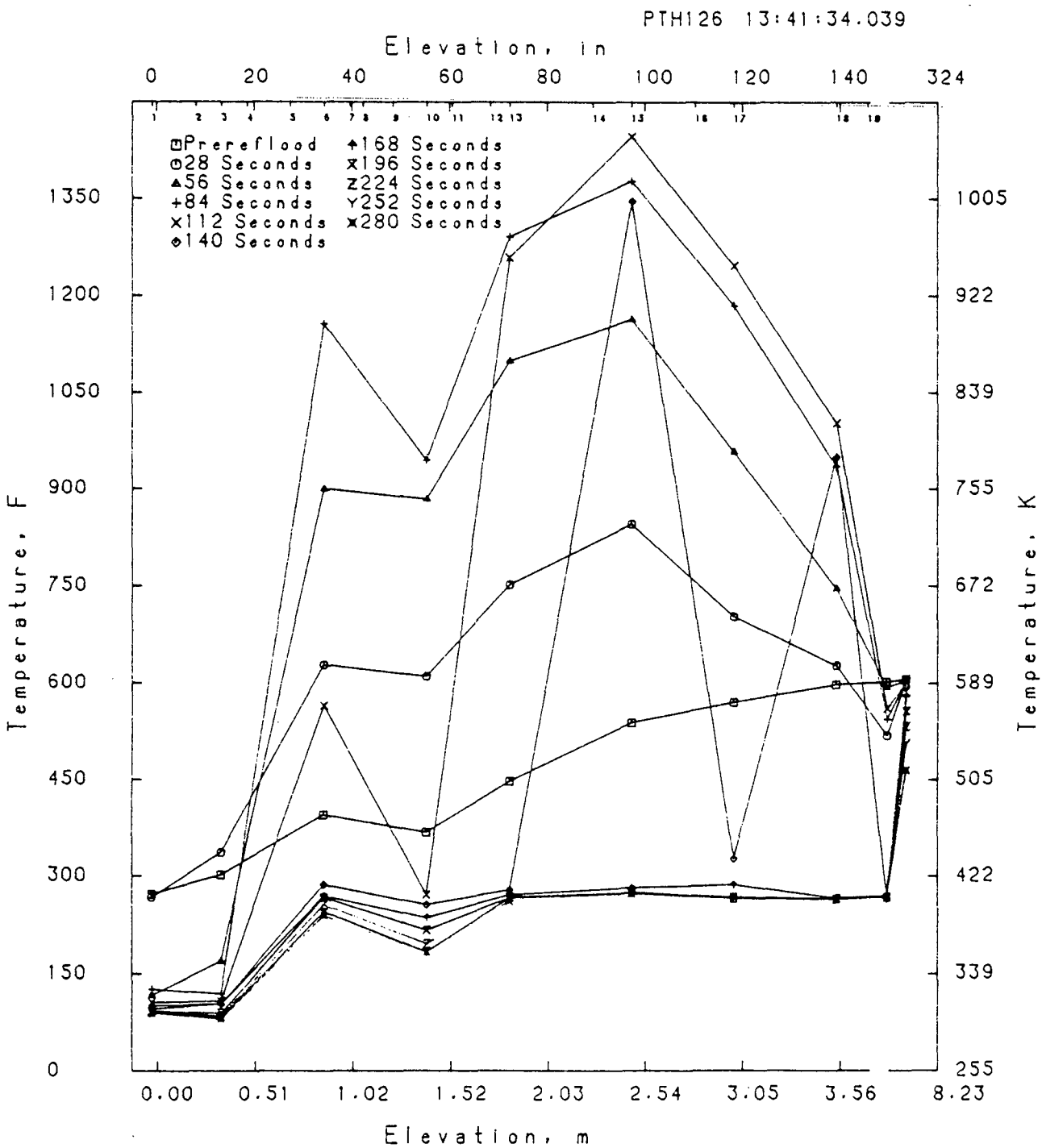

FIGURE 1.2.2.26 INSTRUMENT TUBE AND TEST TRAIN TEMPERATURE PROFILES DURING REFLOODING AT 28S INTERVALS - PTH126

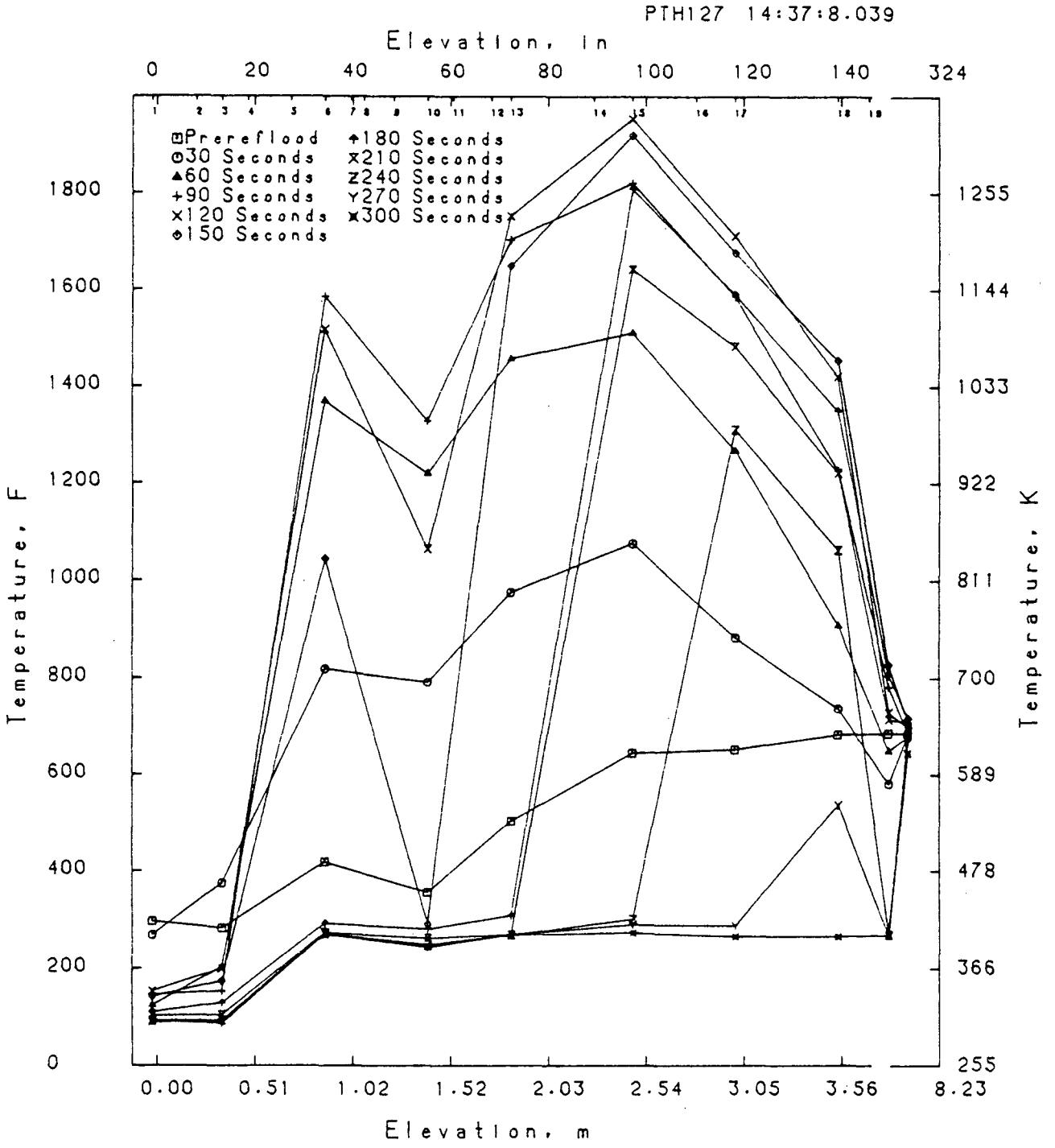

FIGURE 1.2.2.27 INSTRUMENT TUBE AND TEST TRAIN TEMPERATURE PROFILES DURING REFLOODING AT 30S INTERVALS - PTH127

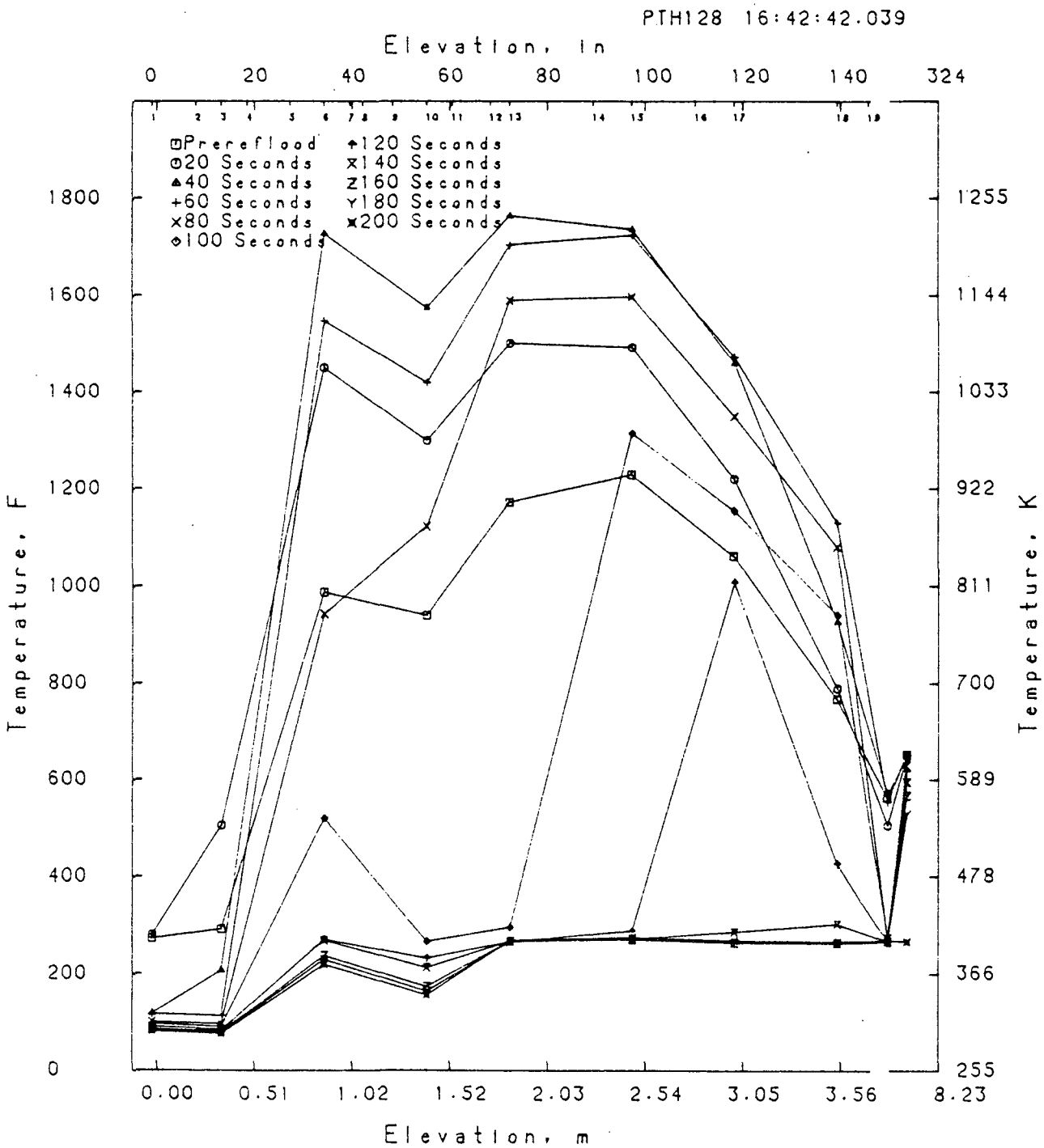

FIGURE 1.2.2.28 INSTRUMENT TUBE AND TEST TRAIN TEMPERATURE PROFILES DURING REFLOODING AT 20S INTERVALS - PTH128

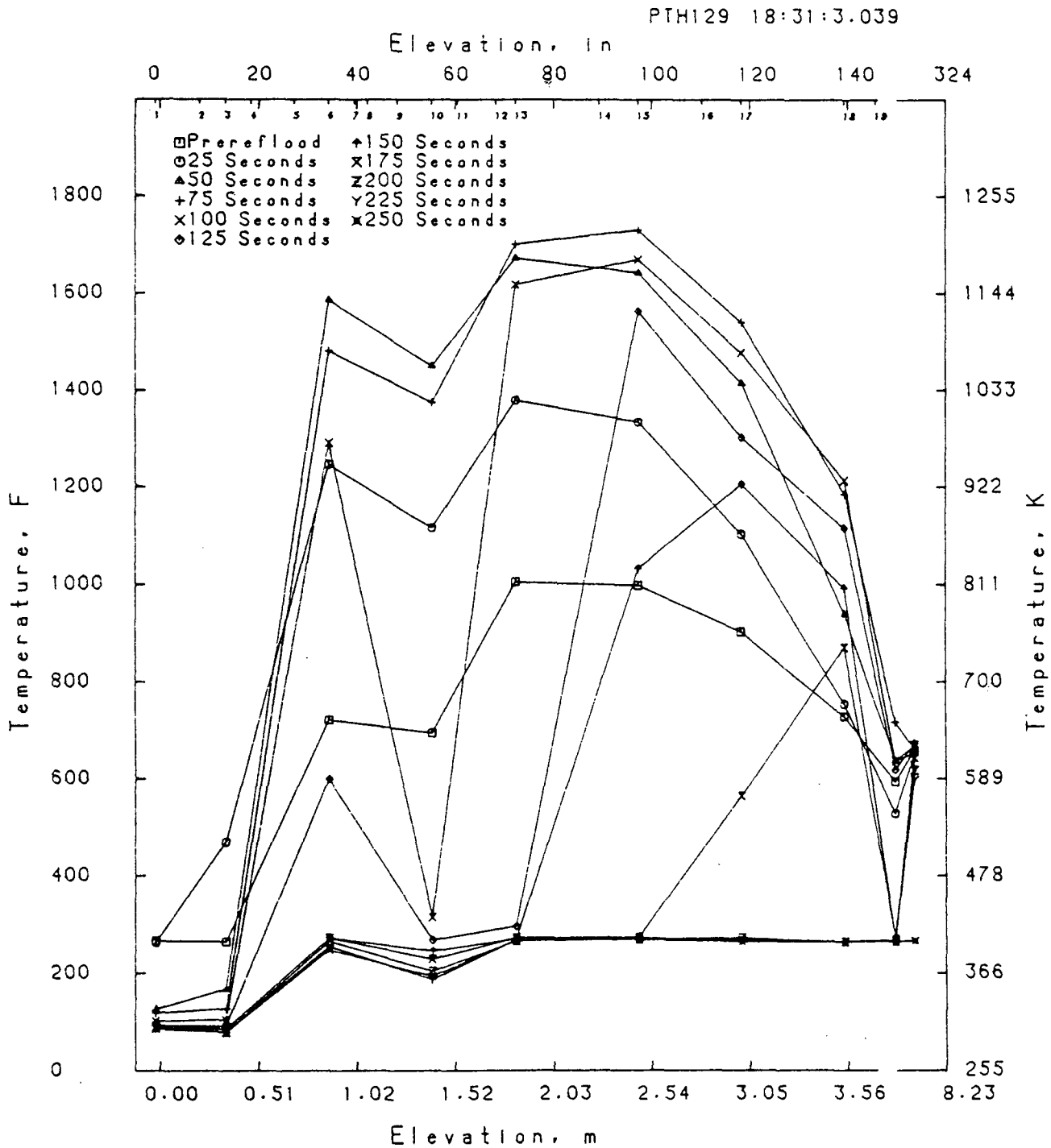

FIGURE 1.2.2.29 INSTRUMENT TUBE AND TEST TRAIN TEMPERATURE PROFILES DURING REFLOODING AT 25S INTERVALS - PTH129

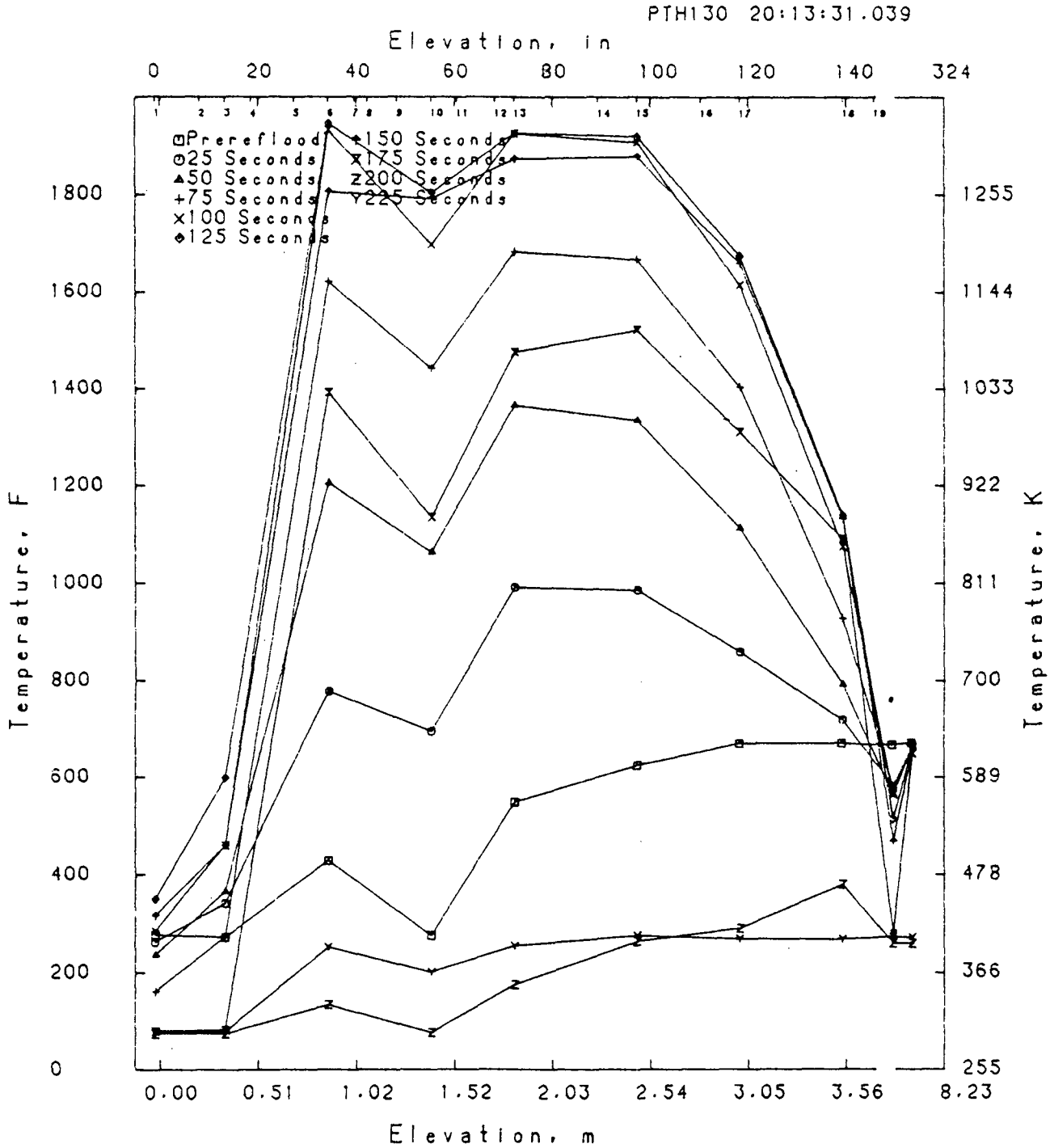

FIGURE 1.2.2.30 INSTRUMENT TUBE AND TEST TRAIN TEMPERATURE PROFILES DURING REFLOODING AT 25S INTERVALS - PTH130

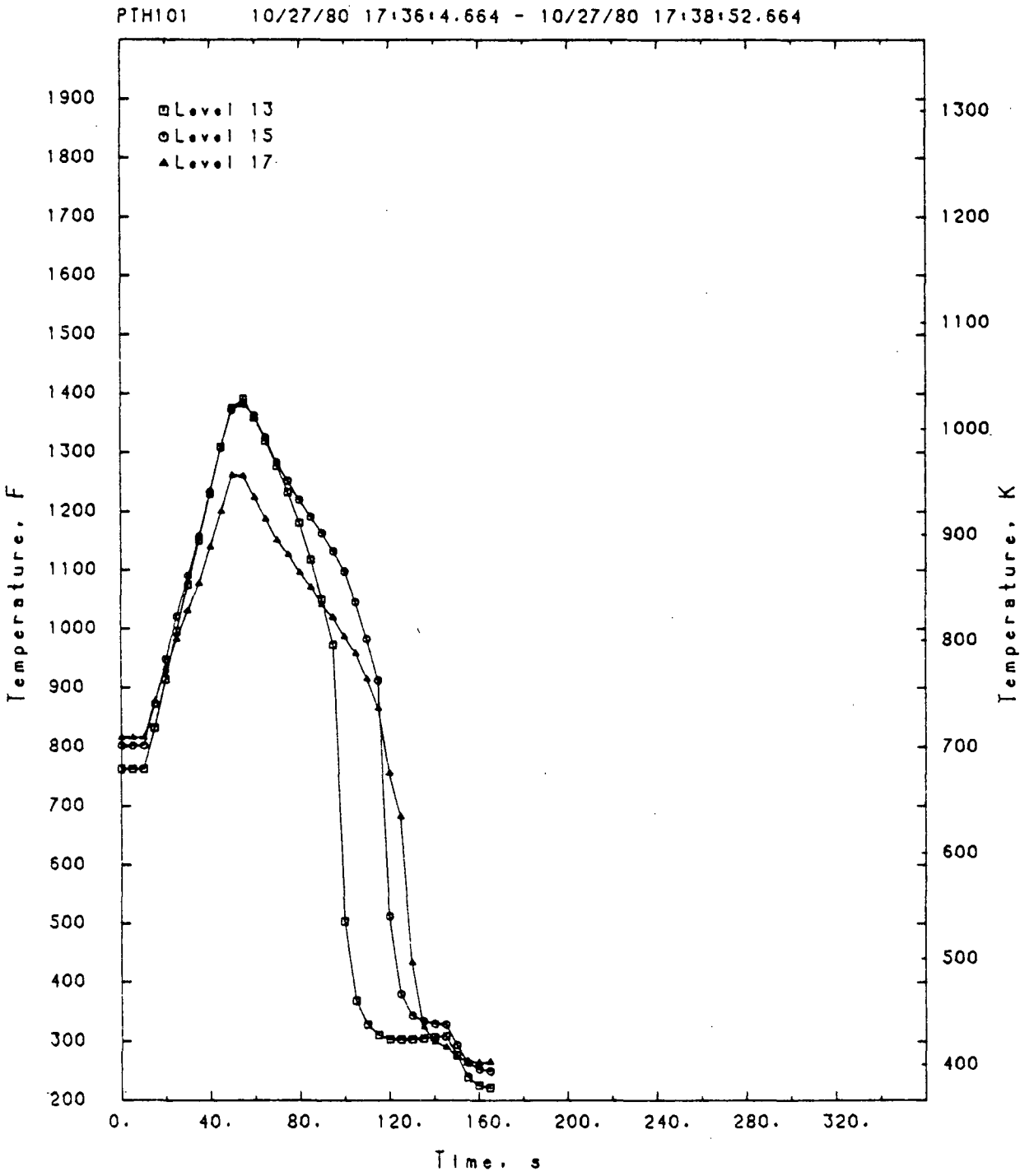

FIGURE 1.2.3.01 AVERAGE GUARD FUEL ROD CLADDING TEMPERATURE HISTORIES (INTERIOR TC'S) DURING TRANSIENT PTH101

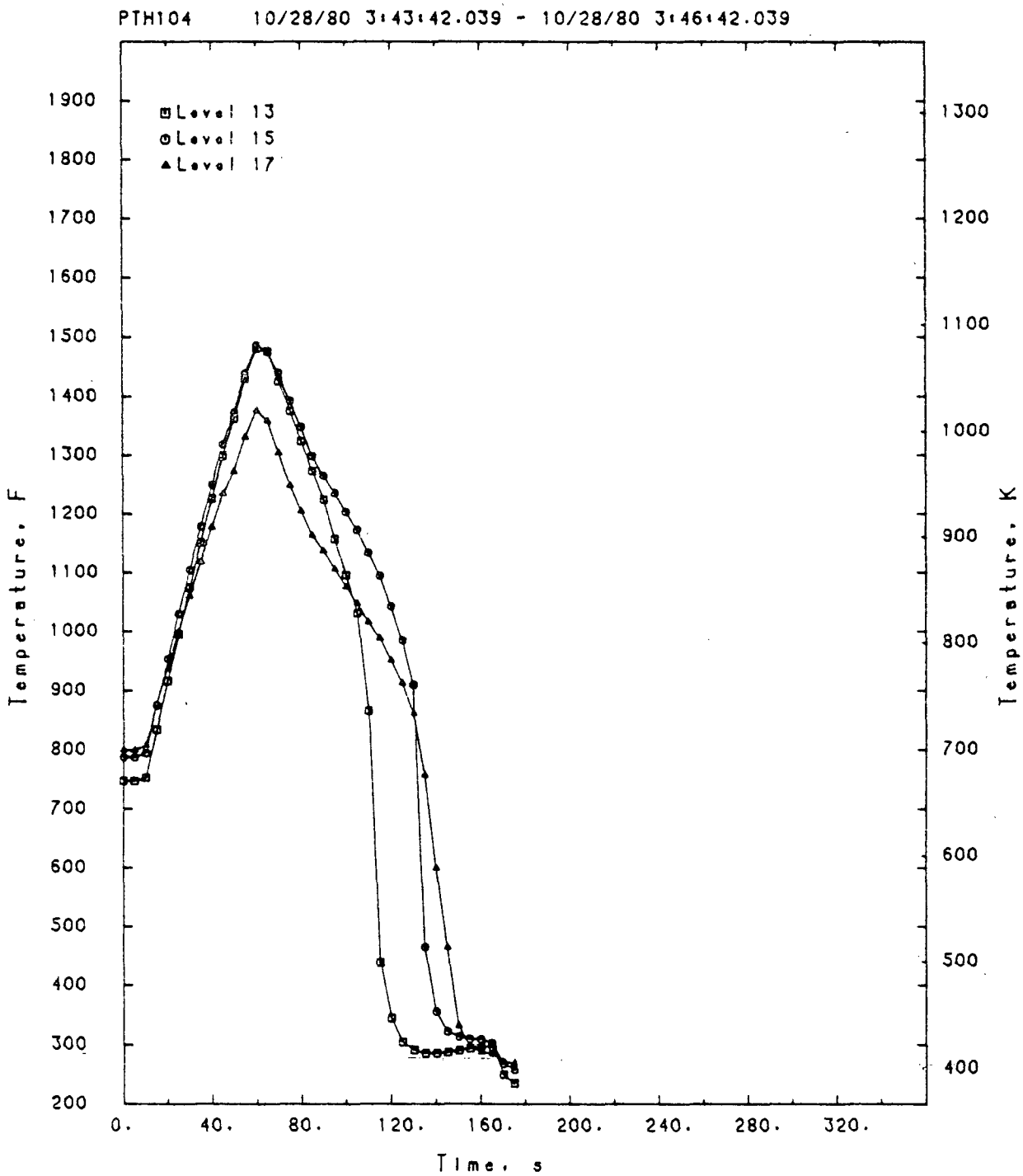

FIGURE 1.2.3.04 AVERAGE GUARD FUEL ROD CLADDING TEMPERATURE HISTORIES (INTERIOR TC'S) DURING TRANSIENT PTH104

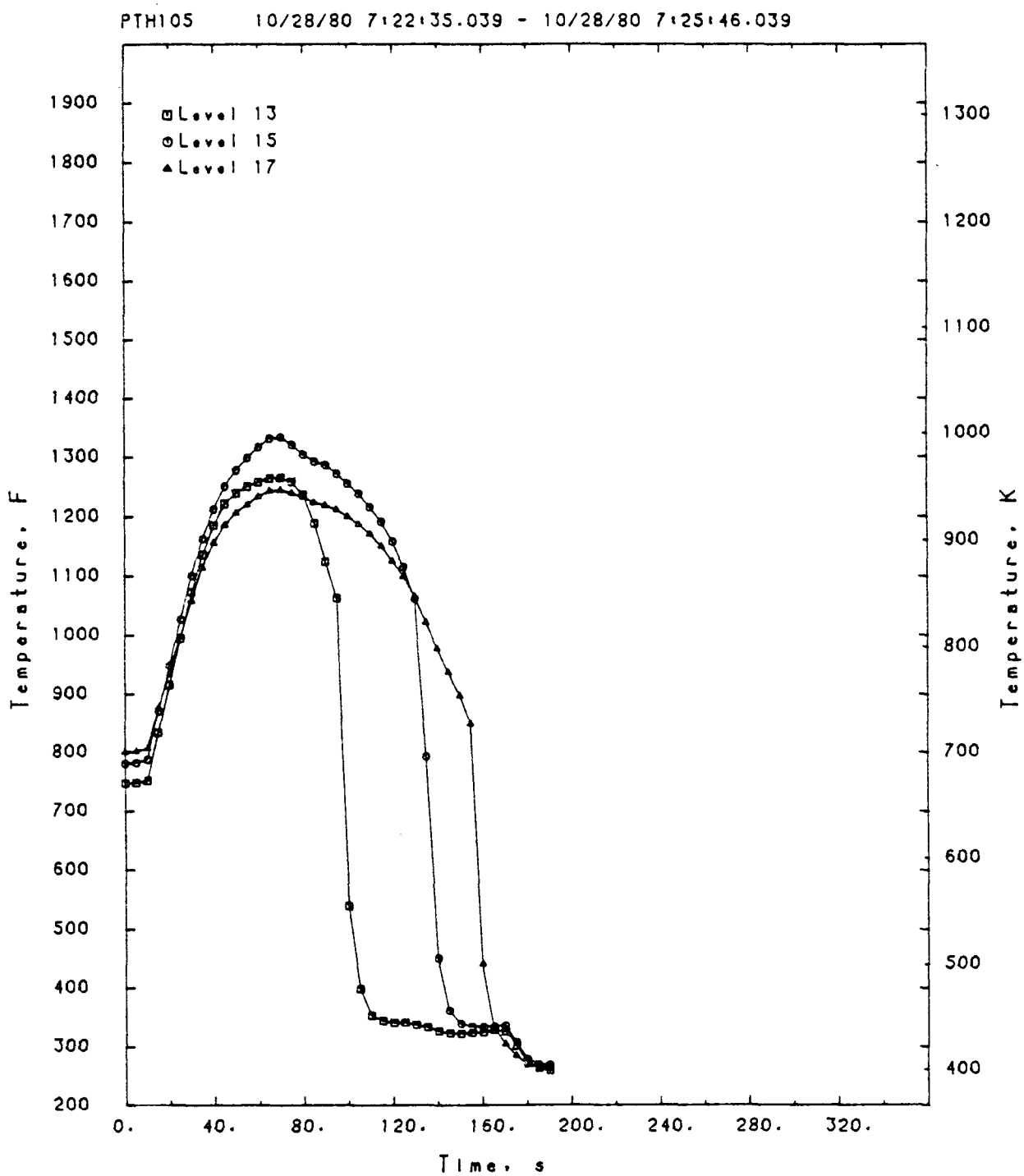

FIGURE 1.2.3.05 AVERAGE GUARD FUEL ROD CLADDING TEMPERATURE HISTORIES (INTERIOR TC'S) DURING TRANSIENT PTH105

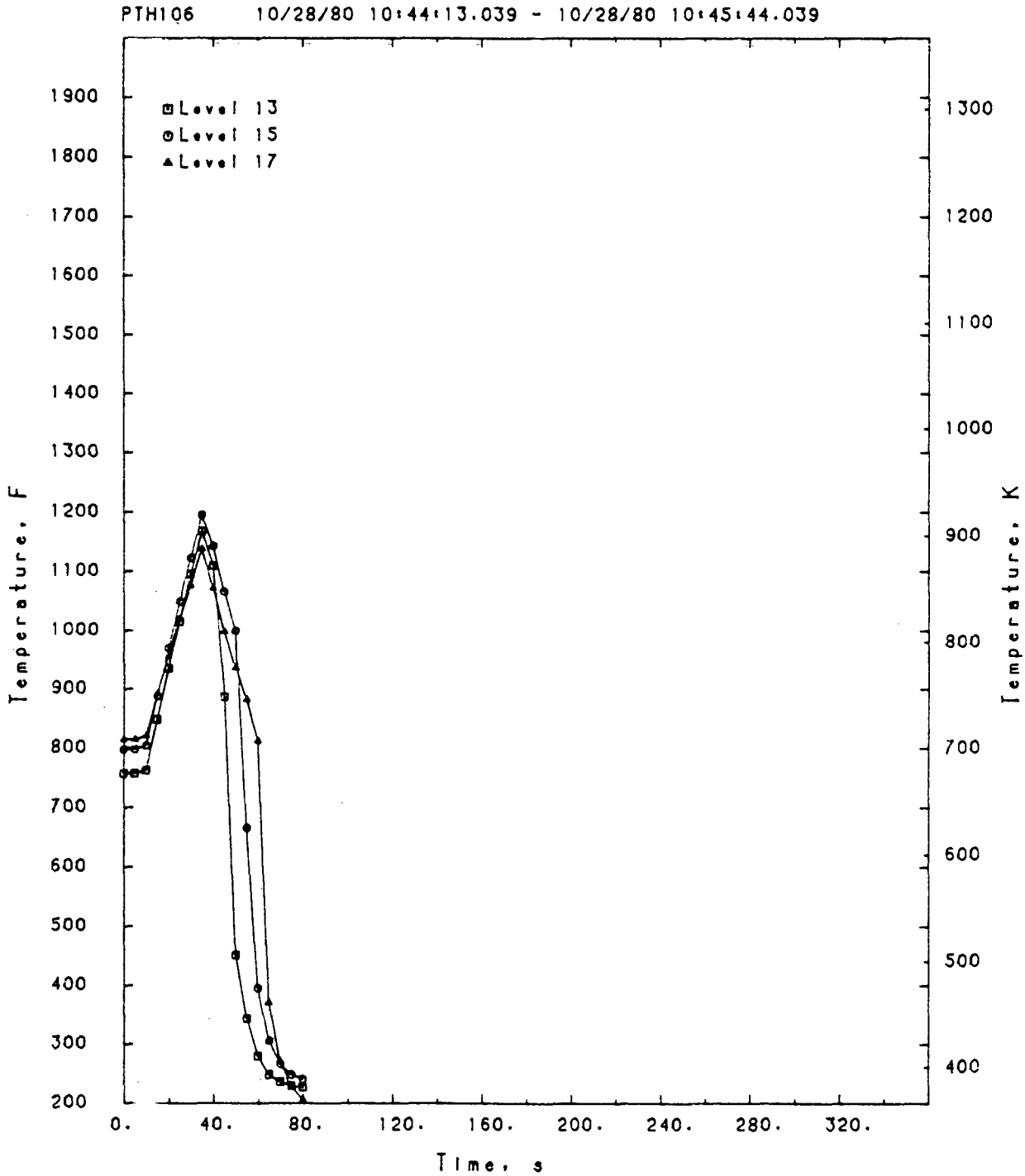

FIGURE 1.2.3.06 AVERAGE GUARD FUEL ROD CLADDING TEMPERATURE HISTORIES (INTERIOR TC'S) DURING TRANSIENT PTH106

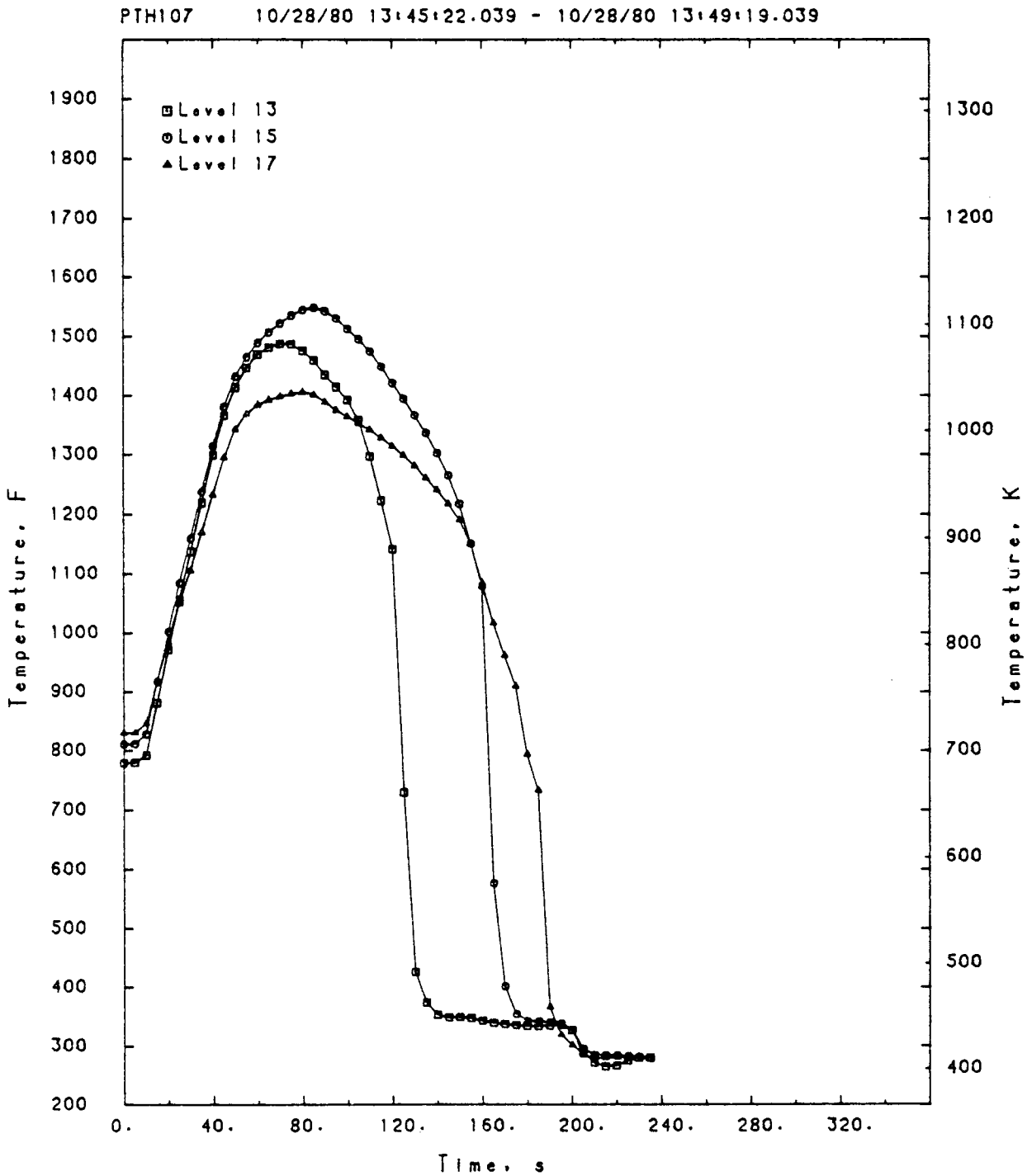

FIGURE 1.2.3.07 AVERAGE GUARD FUEL ROD CLADDING TEMPERATURE HISTORIES (INTERIOR TC'S) DURING TRANSIENT PTH107

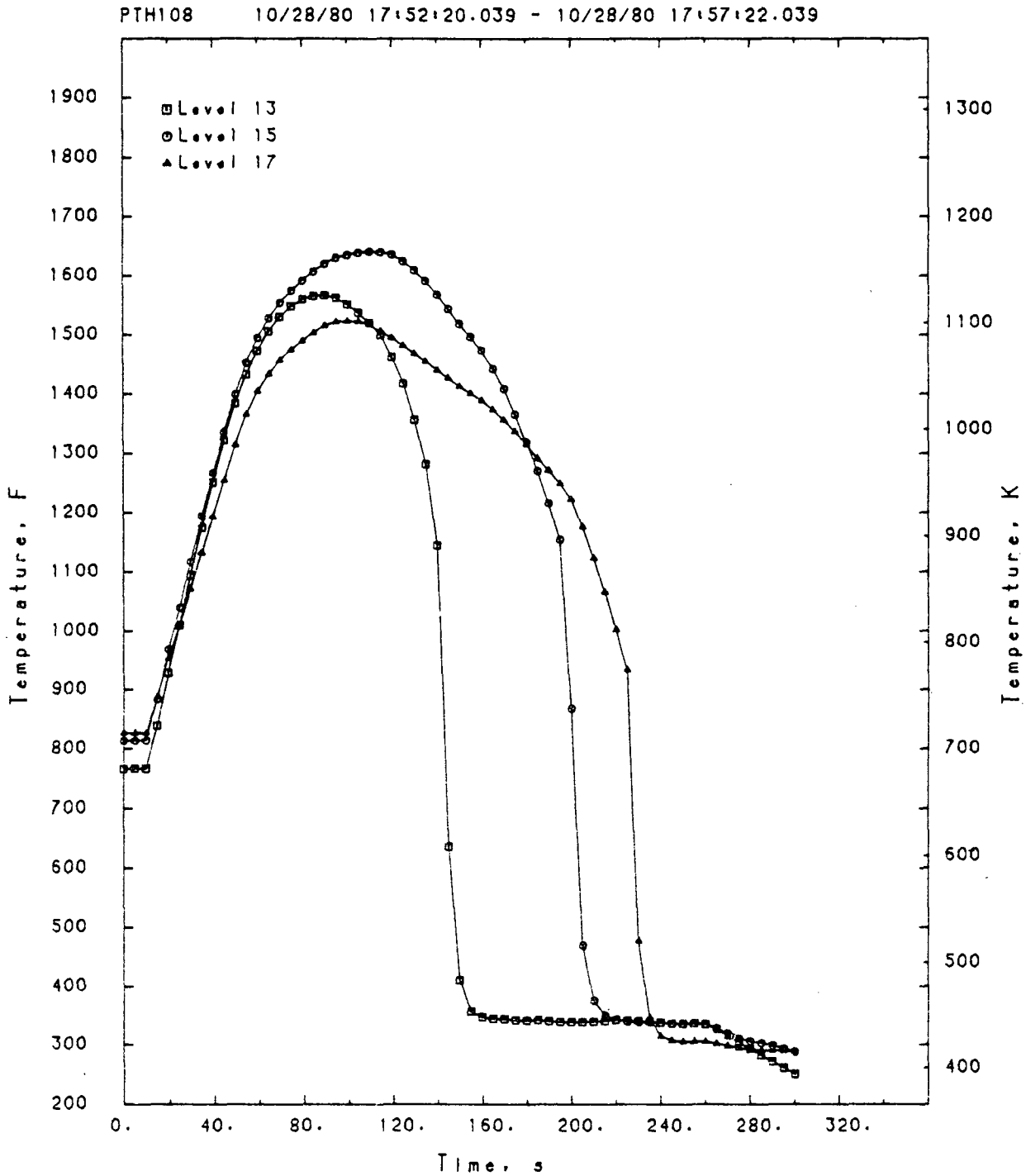

FIGURE 1.2.3.08 AVERAGE GUARD FUEL ROD CLADDING TEMPERATURE HISTORIES (INTERIOR TC'S) DURING TRANSIENT PTH108

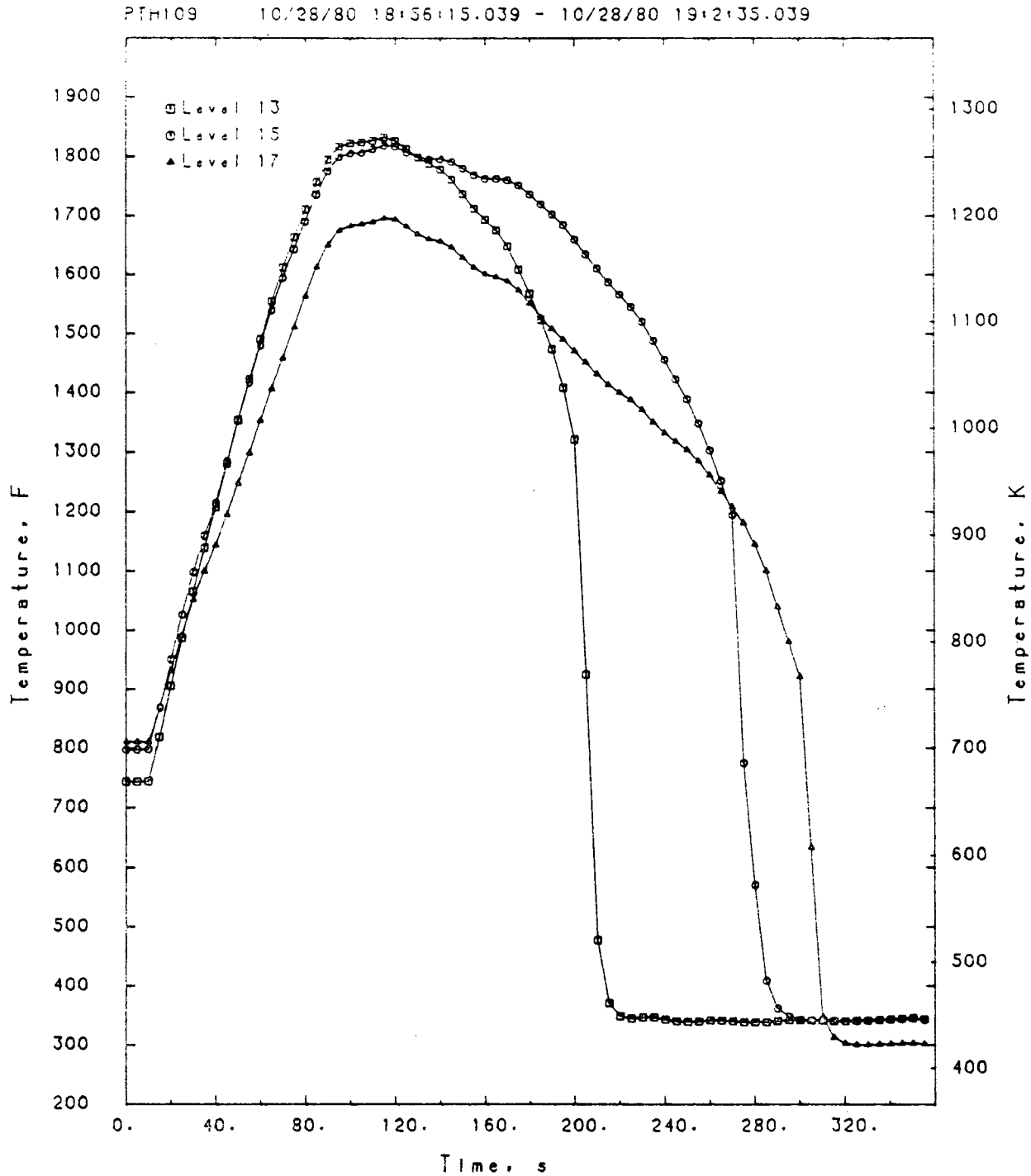

FIGURE 1.2.3.09 AVERAGE GUARD FUEL ROD CLADDING TEMPERATURE HISTORIES (INTERIOR TC'S) DURING TRANSIENT PTH109

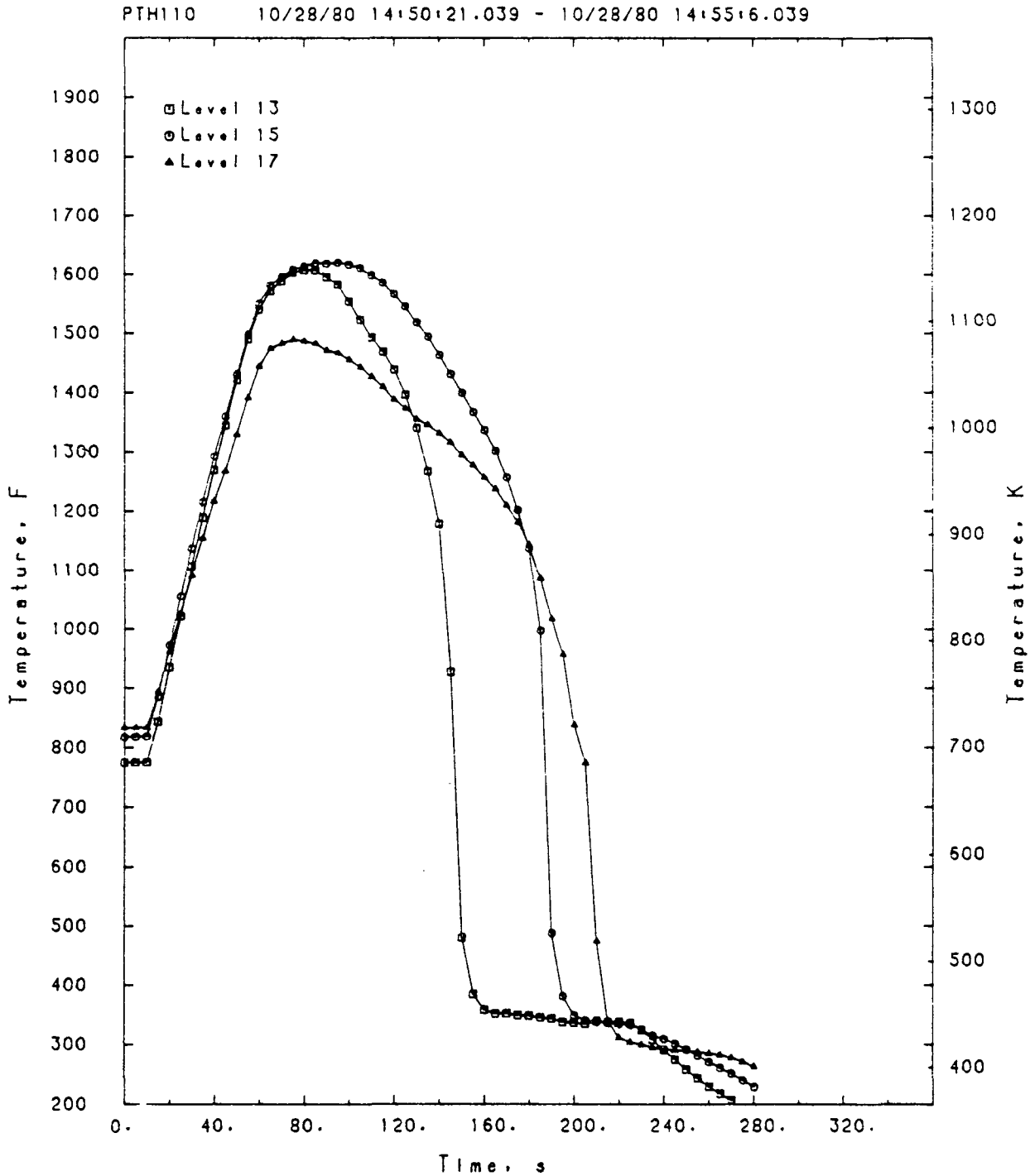

FIGURE 1.2.3.10 AVERAGE GUARD FUEL ROD CLADDING TEMPERATURE HISTORIES (INTERIOR TC'S) DURING TRANSIENT PTH110

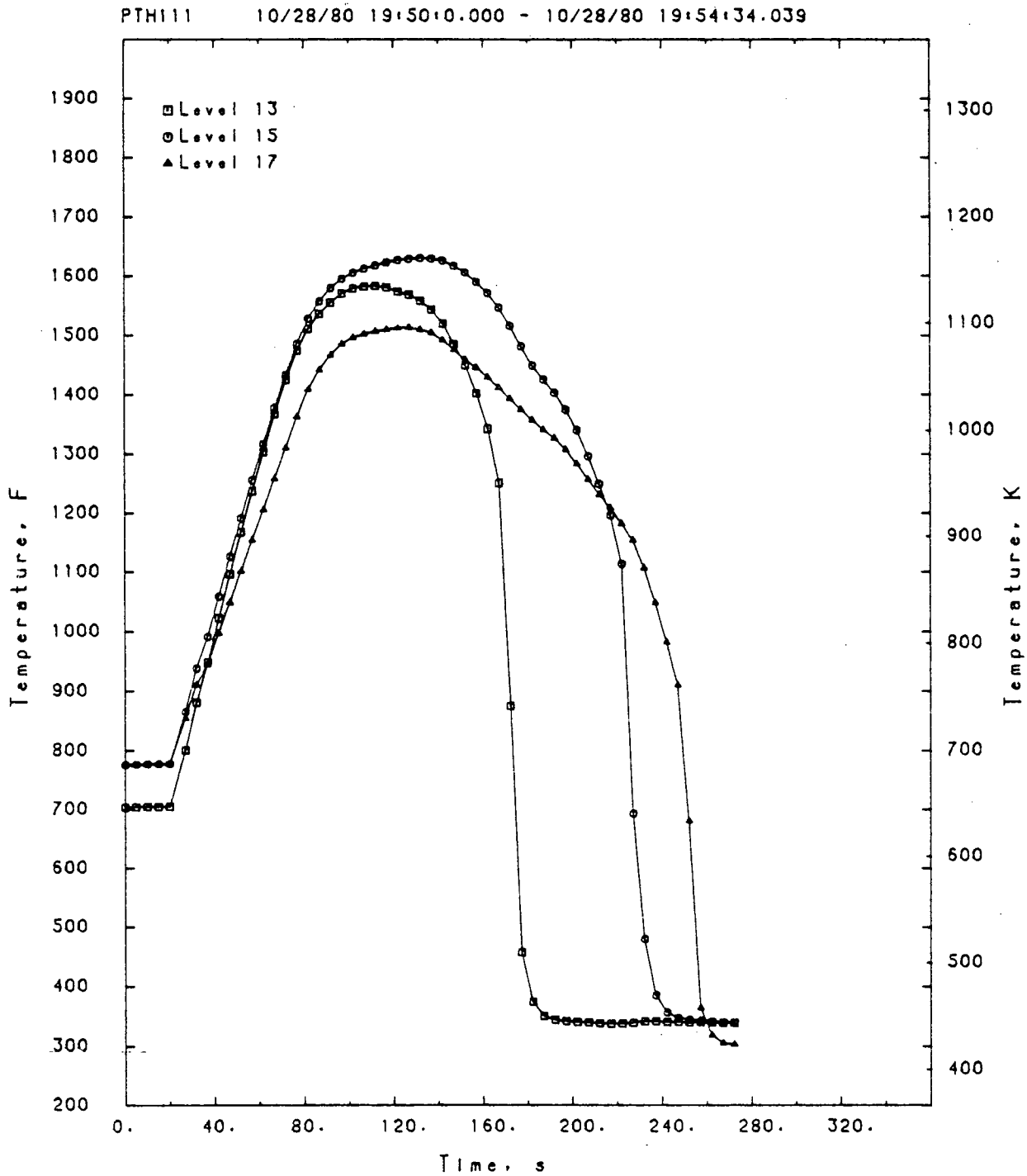

FIGURE 1.2.3.11 AVERAGE GUARD FUEL ROD CLADDING TEMPERATURE HISTORIES (INTERIOR TC'S) DURING TRANSIENT PTH111

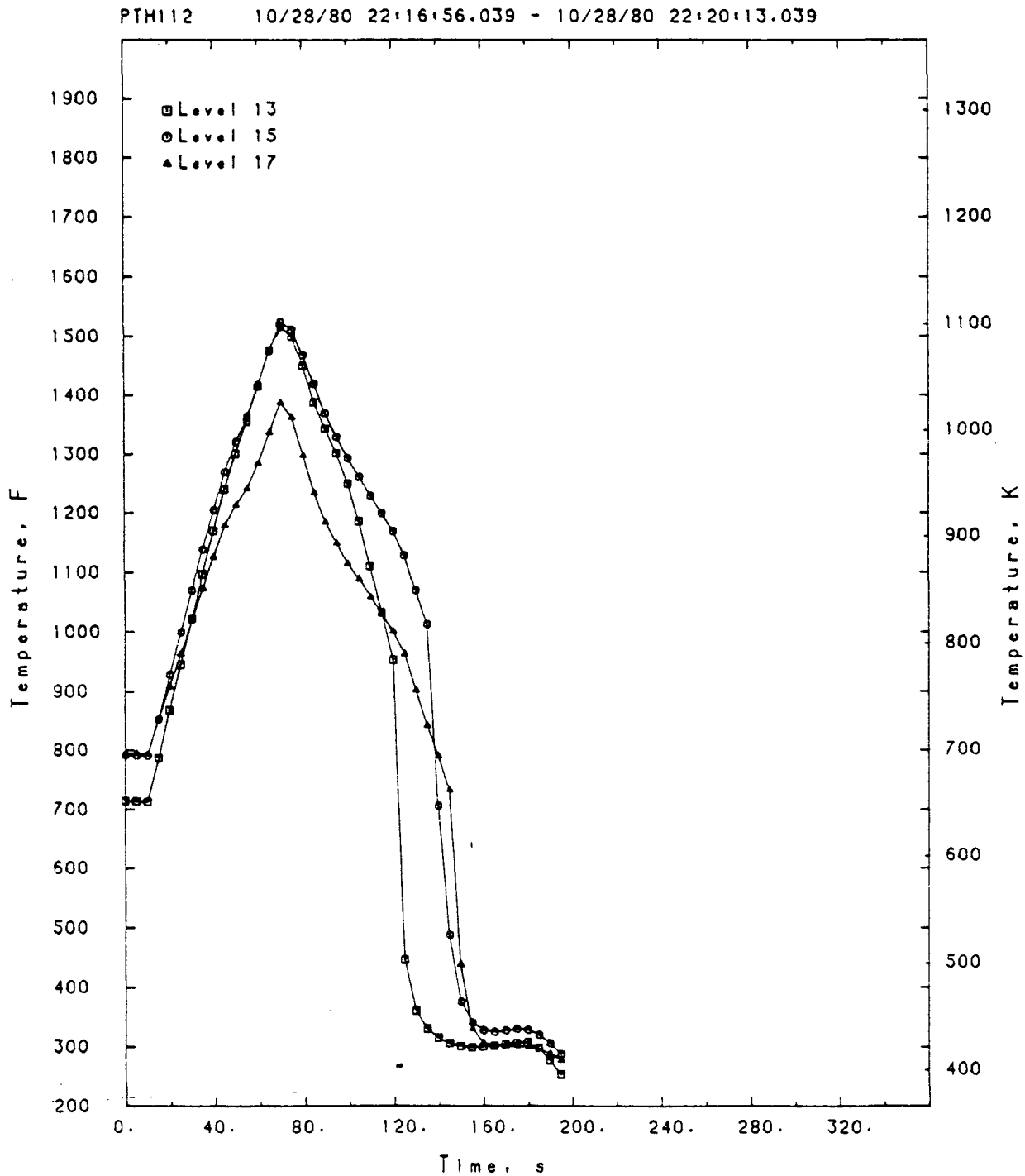

FIGURE 1.2.3.12 AVERAGE GUARD FUEL ROD CLADDING TEMPERATURE HISTORIES (INTERIOR TC'S) DURING TRANSIENT PTH112

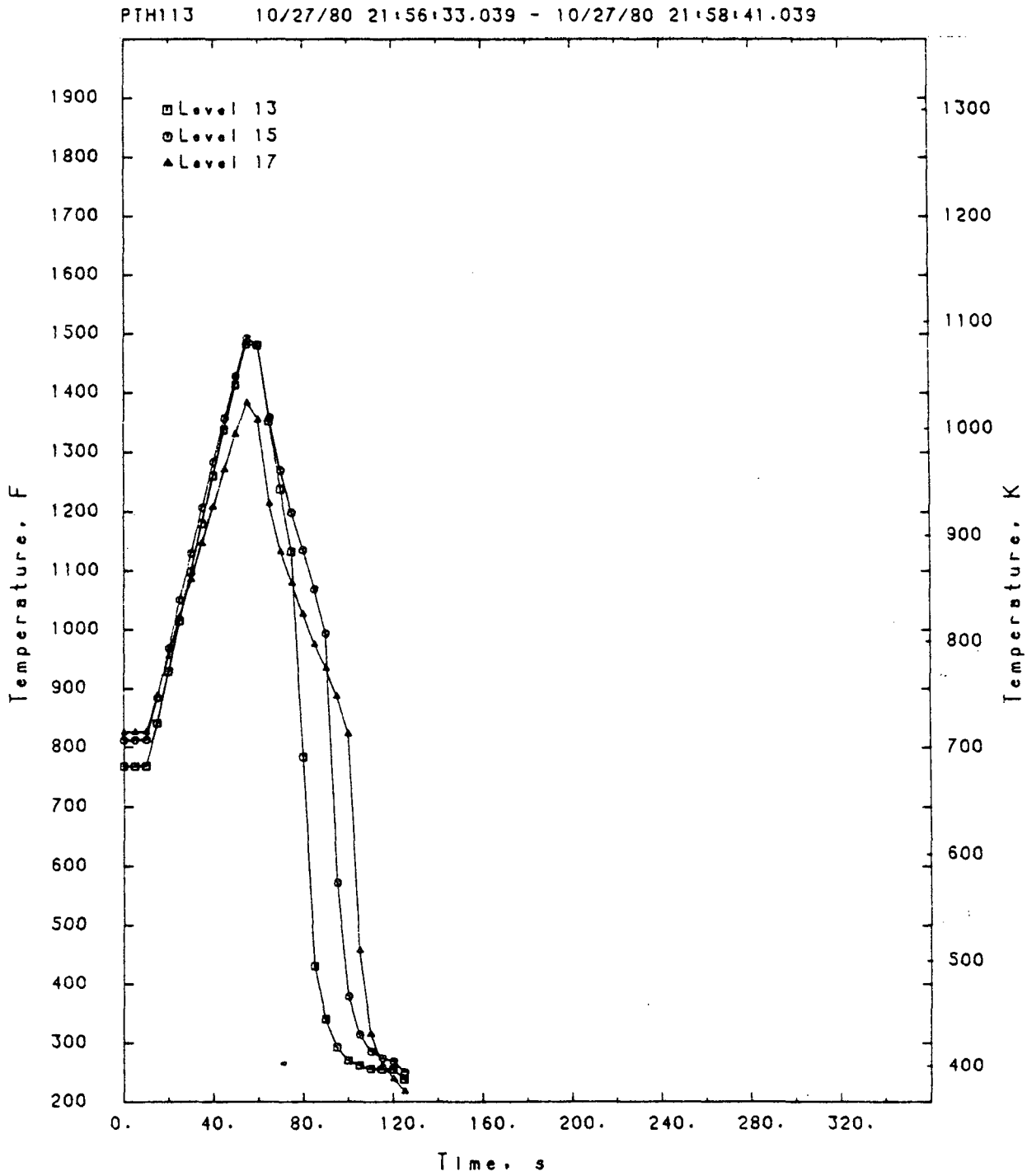

FIGURE 1.2.3.13 AVERAGE GUARD FUEL ROD CLADDING TEMPERATURE HISTORIES (INTERIOR TC'S) DURING TRANSIENT PTH113

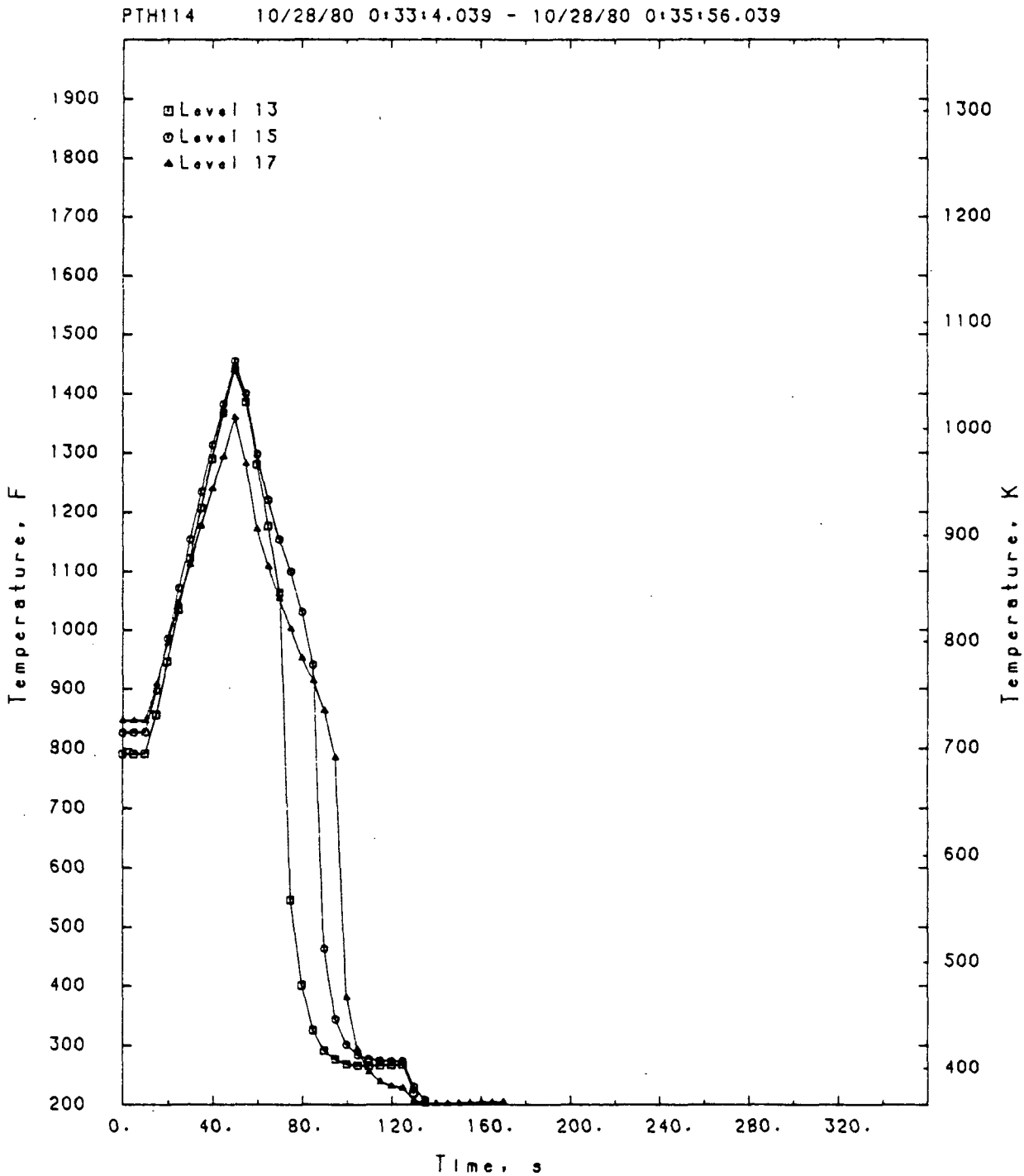

FIGURE 1.2.3.14 AVERAGE GUARD FUEL ROD CLADDING TEMPERATURE HISTORIES (INTERIOR TC'S) DURING TRANSIENT PTH114

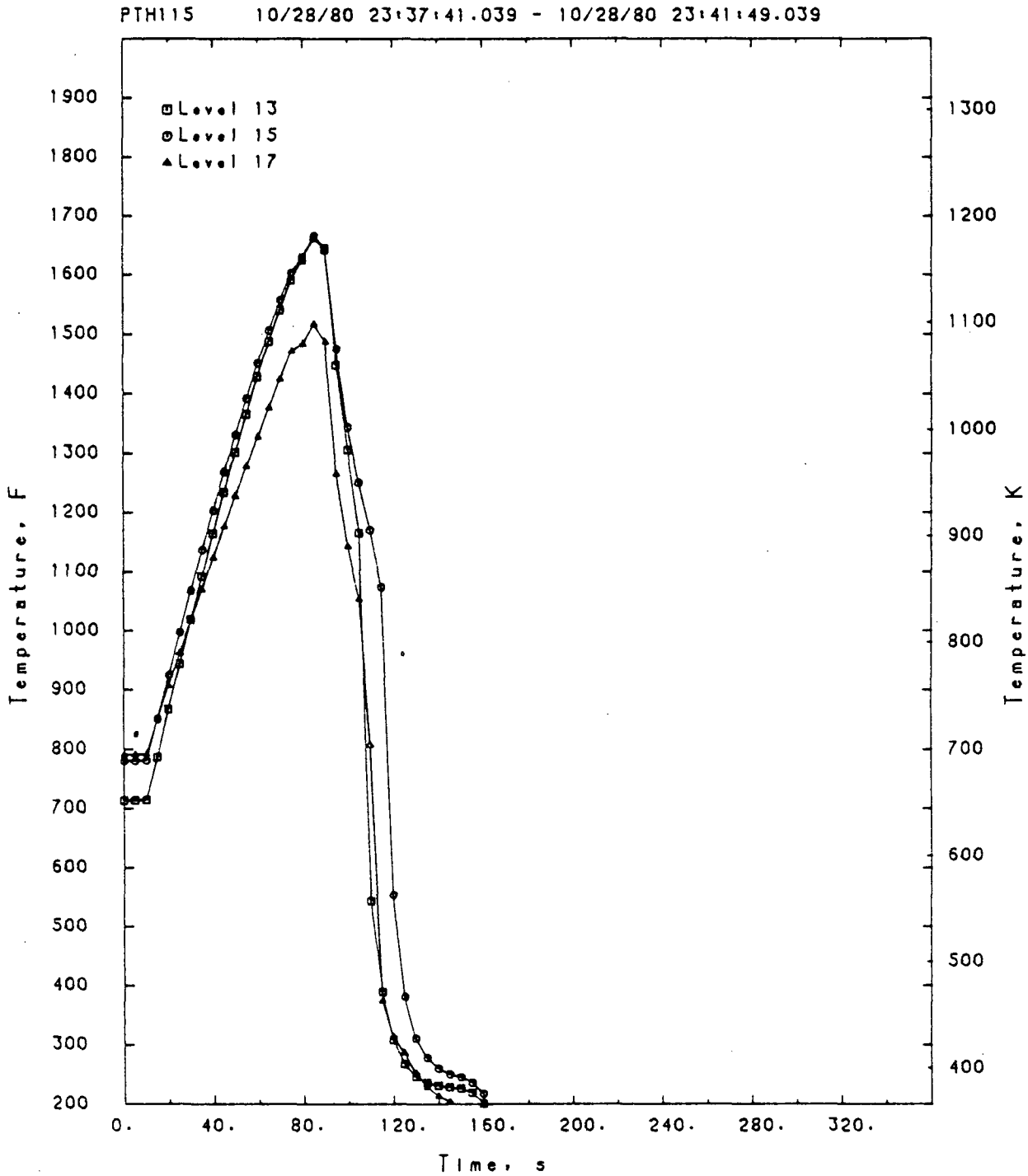

FIGURE 1.2.3.15 AVERAGE GUARD FUEL ROD CLADDING TEMPERATURE HISTORIES (INTERIOR TC'S) DURING TRANSIENT PTH115

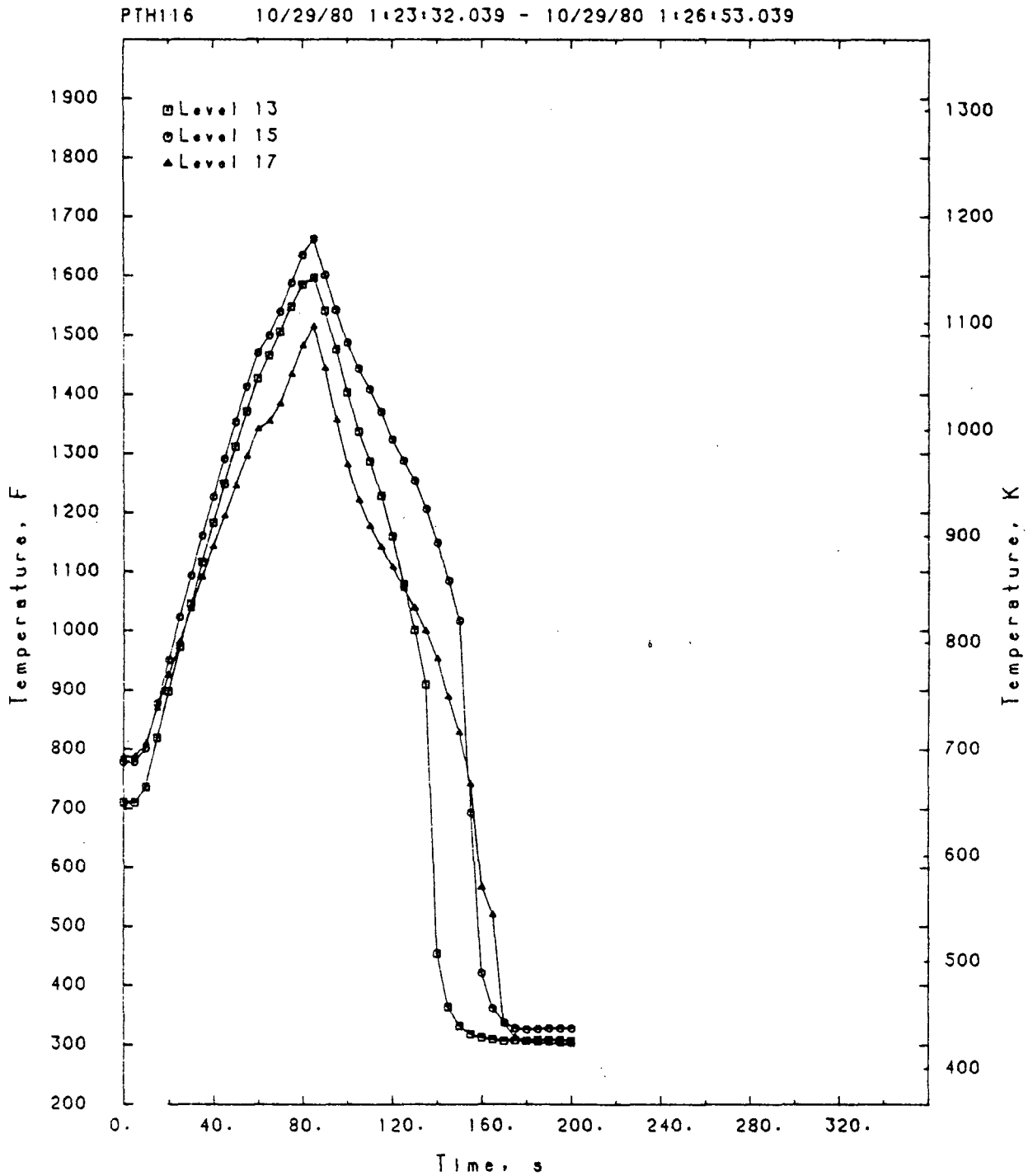

FIGURE 1.2.3.16 AVERAGE GUARD FUEL ROD CLADDING TEMPERATURE HISTORIES (INTERIOR TC'S) DURING TRANSIENT PTH116

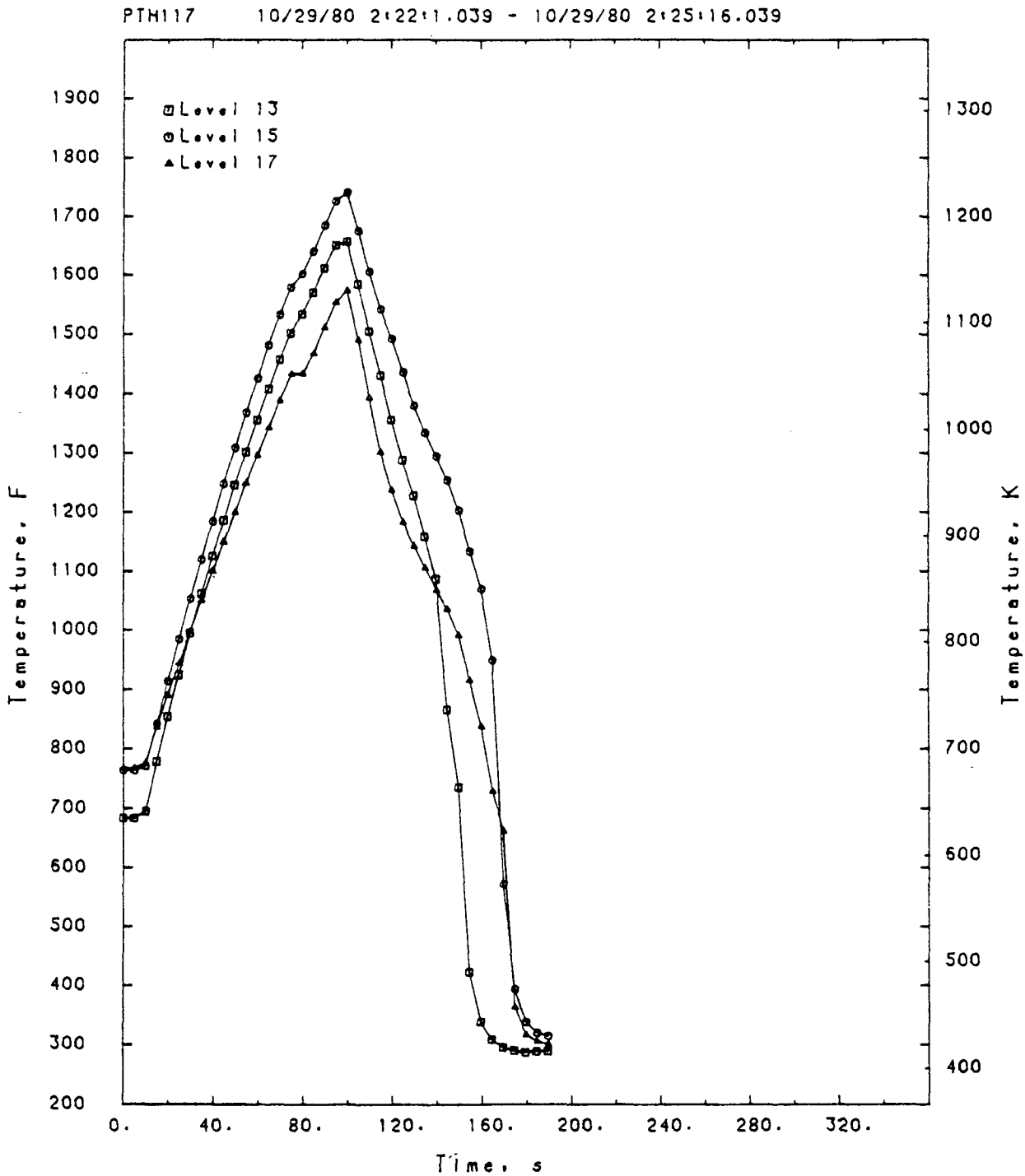

FIGURE 1.2.3.17 AVERAGE GUARD FUEL ROD CLADDING TEMPERATURE HISTORIES (INTERIOR TC'S) DURING TRANSIENT PTH117

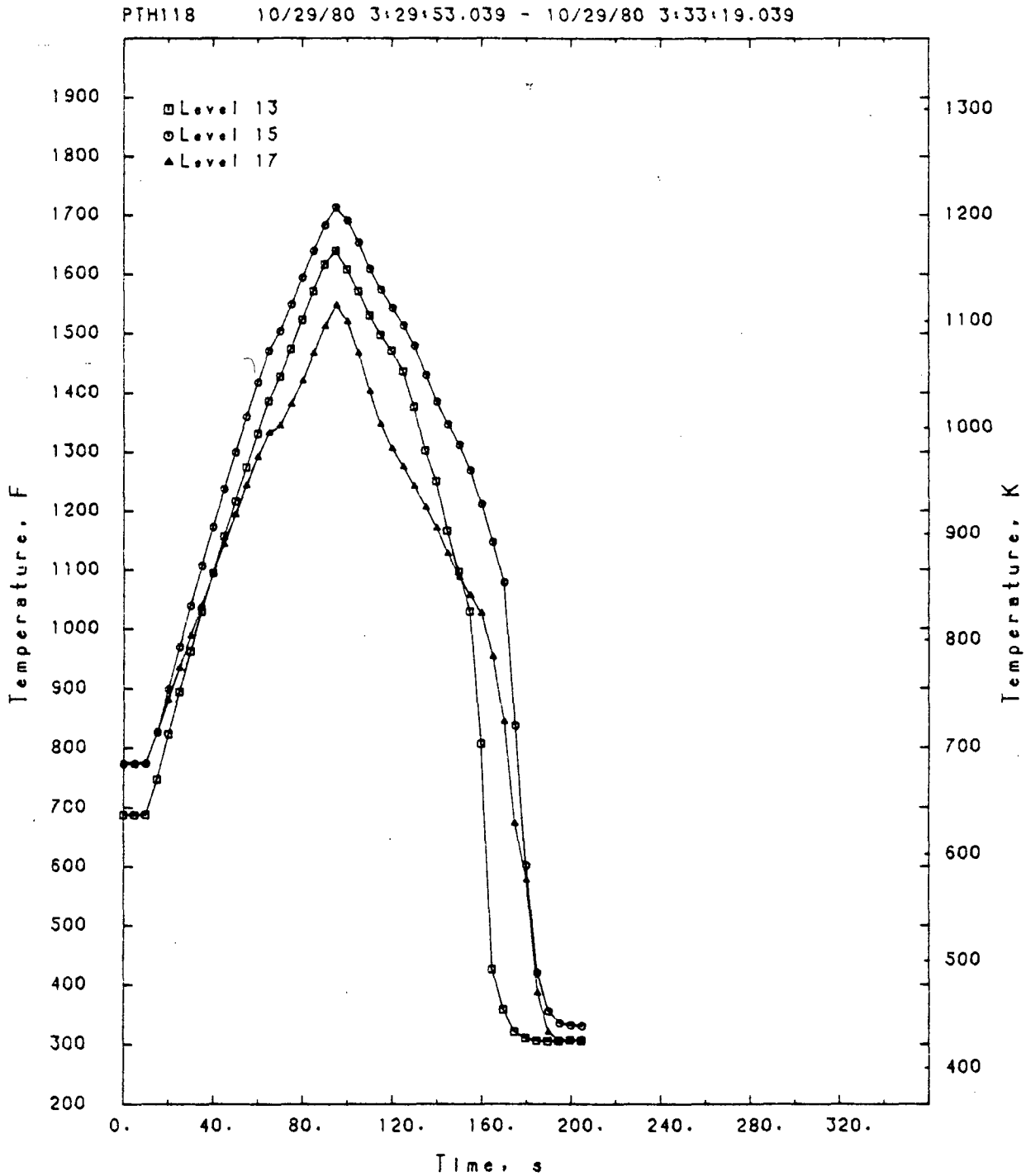

FIGURE 1.2.3.18 AVERAGE GUARD FUEL ROD CLADDING TEMPERATURE HISTORIES (INTERIOR TC'S) DURING TRANSIENT PTH118

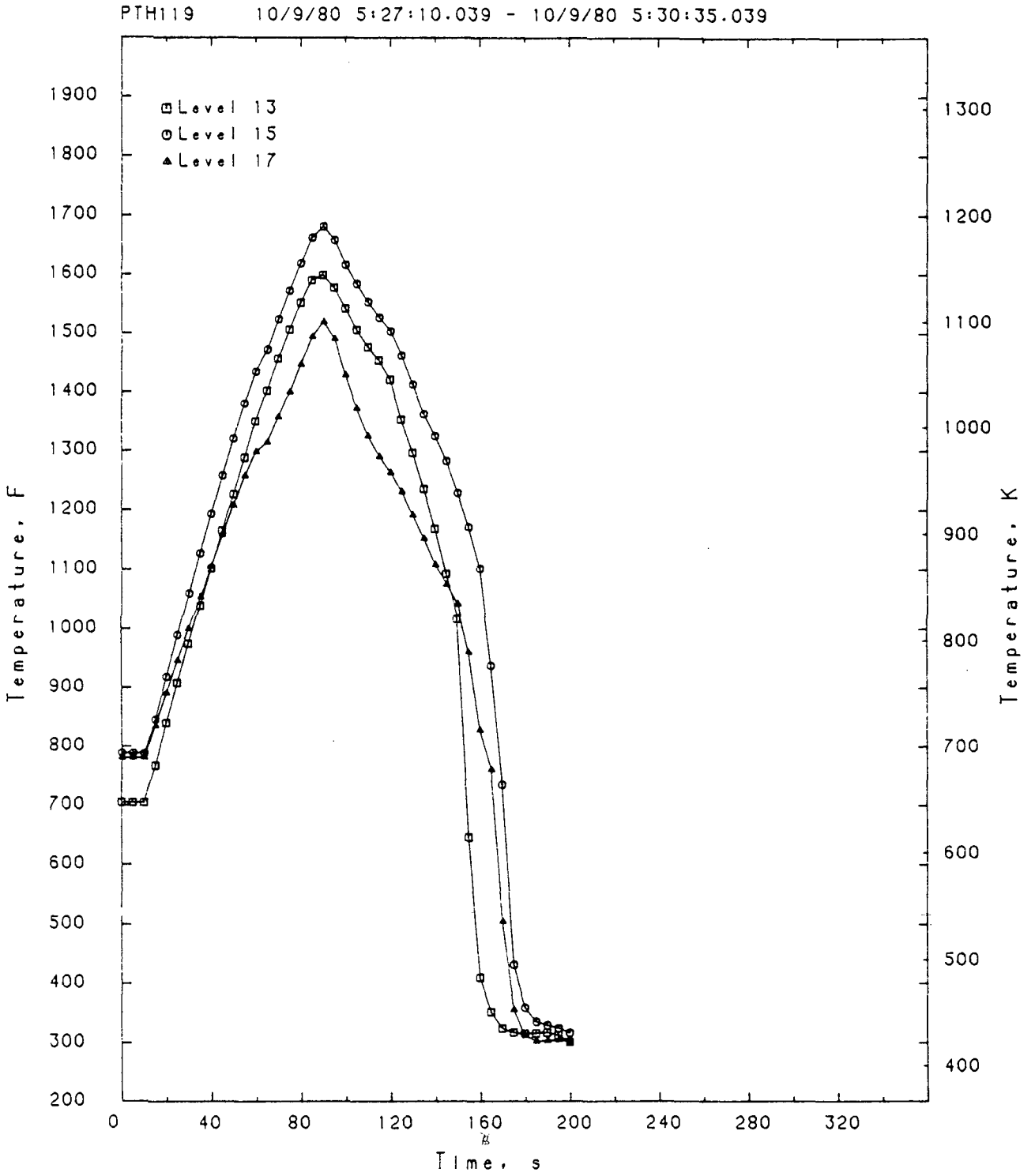

FIGURE 1.2.3.19 AVERAGE GUARD FUEL ROD CLADDING TEMPERATURE HISTORIES (INTERIOR TC'S) DURING TRANSIENT PTH119

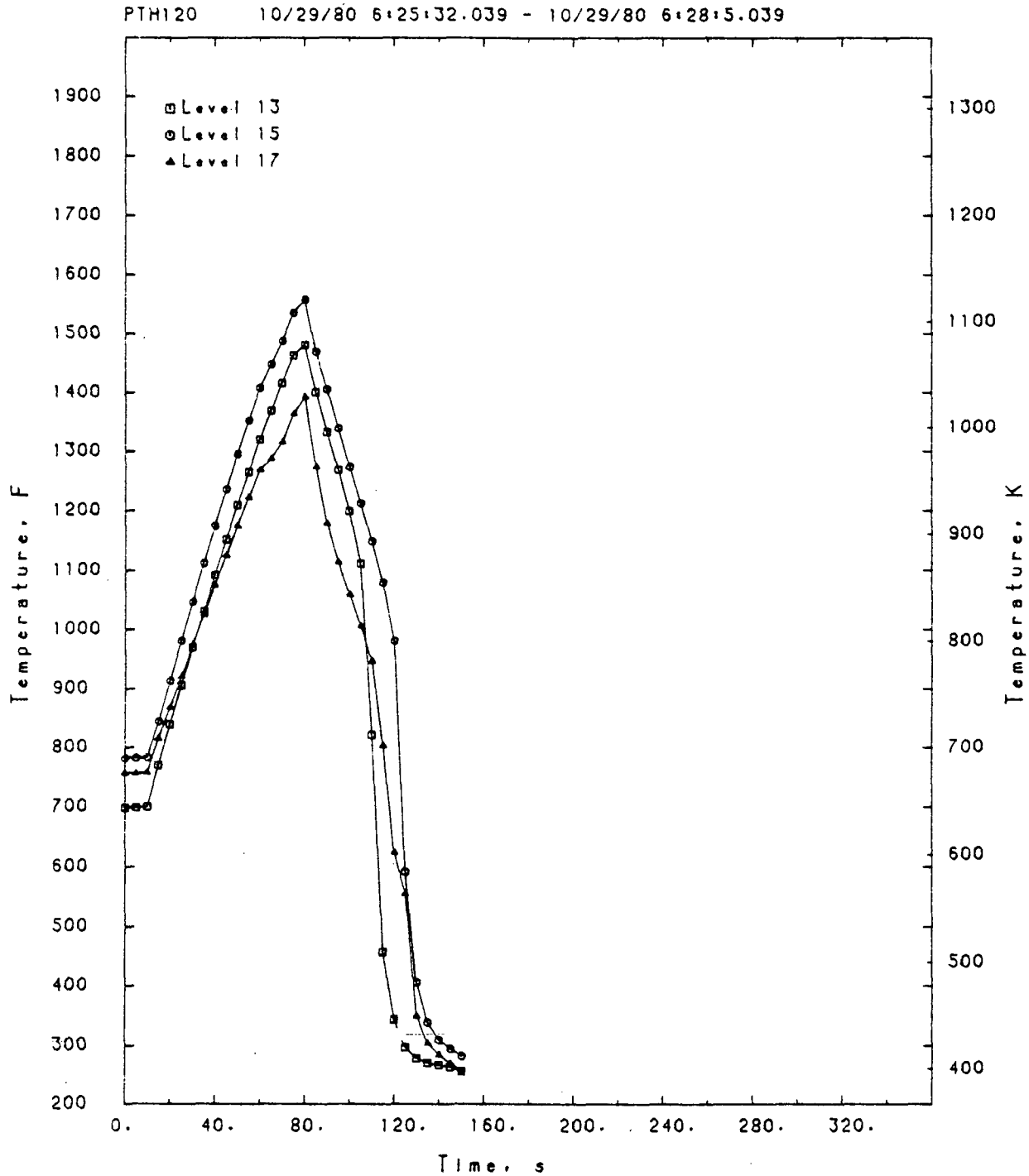

FIGURE 1.2.3.20 AVERAGE GUARD FUEL ROD CLADDING TEMPERATURE HISTORIES (INTERIOR TC'S) DURING TRANSIENT PTH120

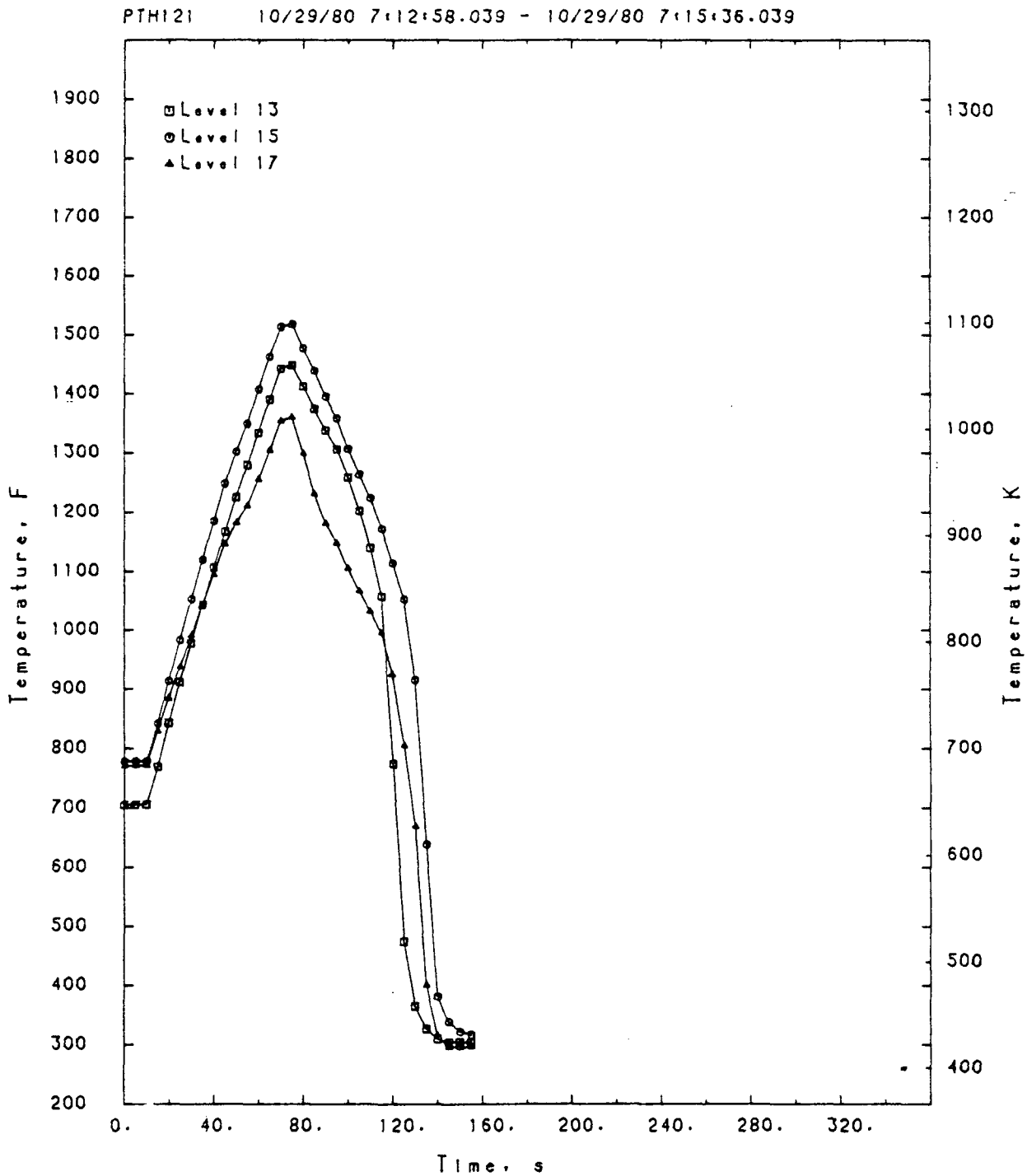

FIGURE 1.2.3.21 AVERAGE GUARD FUEL ROD CLADDING TEMPERATURE HISTORIES (INTERIOR TC'S) DURING TRANSIENT PTH121

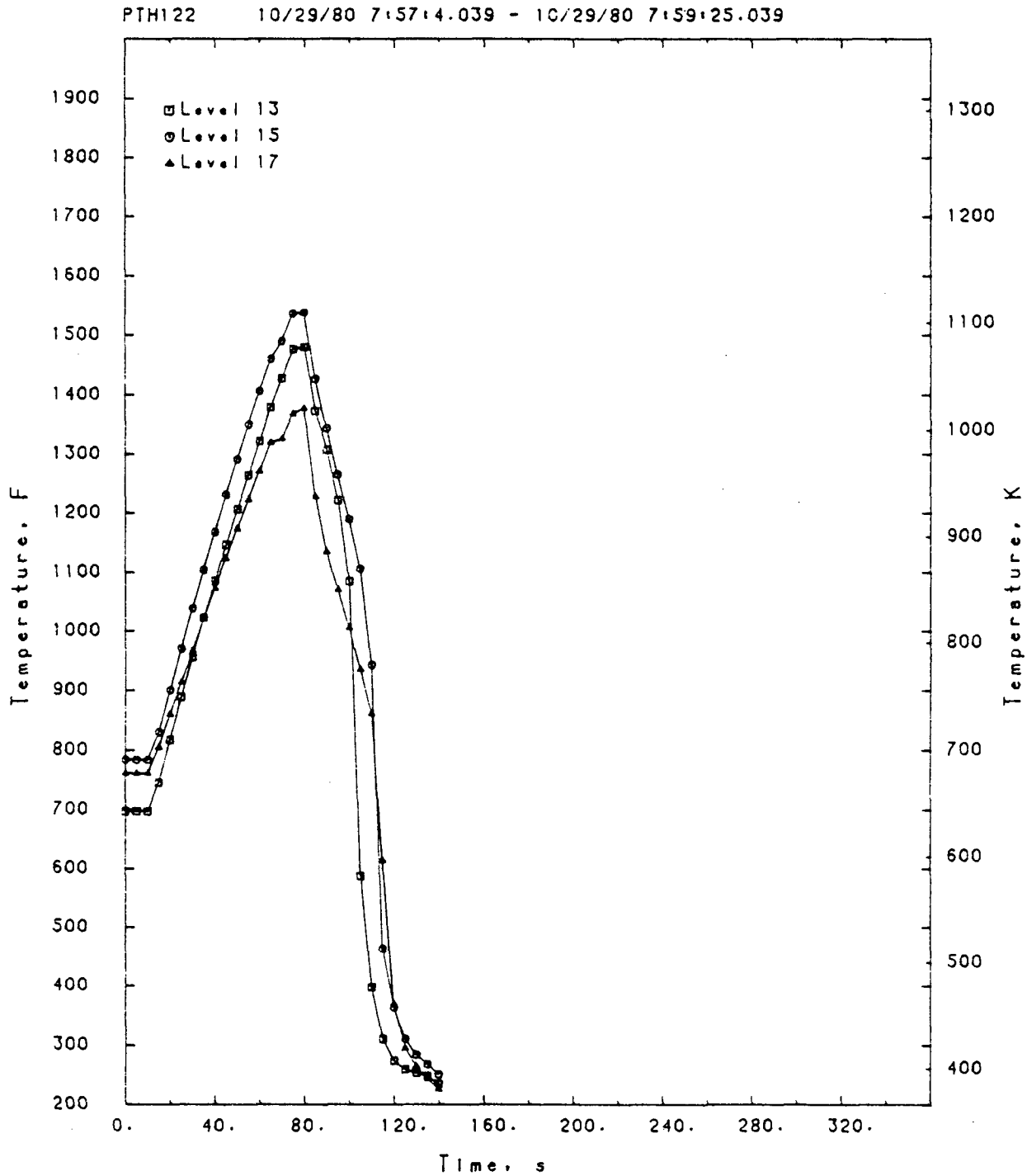

FIGURE 1.2.3.22 AVERAGE GUARD FUEL ROD CLADDING TEMPERATURE HISTORIES (INTERIOR TC'S) DURING TRANSIENT PTH122

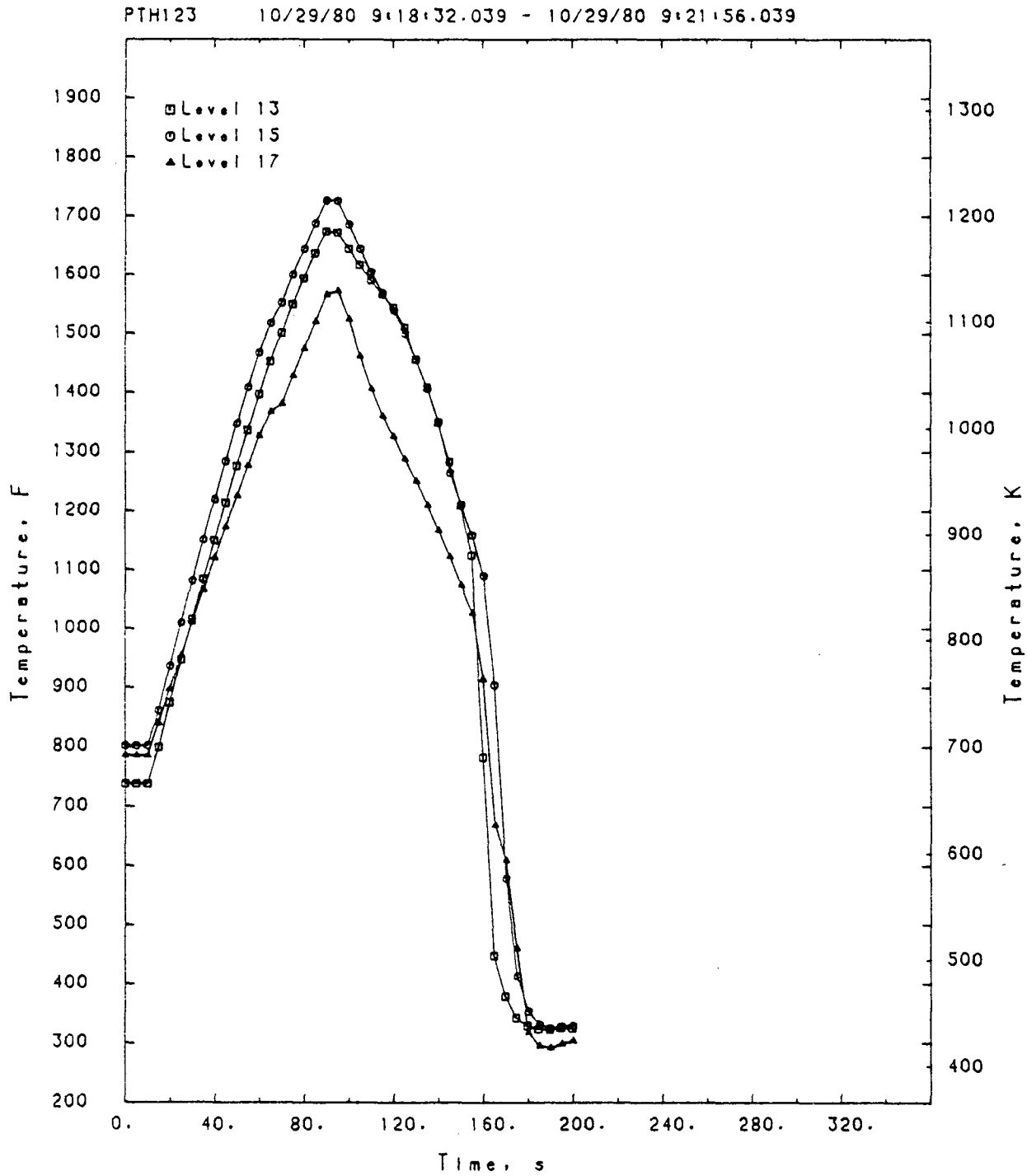

FIGURE 1.2.3.23 AVERAGE GUARD FUEL ROD CLADDING TEMPERATURE HISTORIES (INTERIOR TC'S) DURING TRANSIENT PTH123

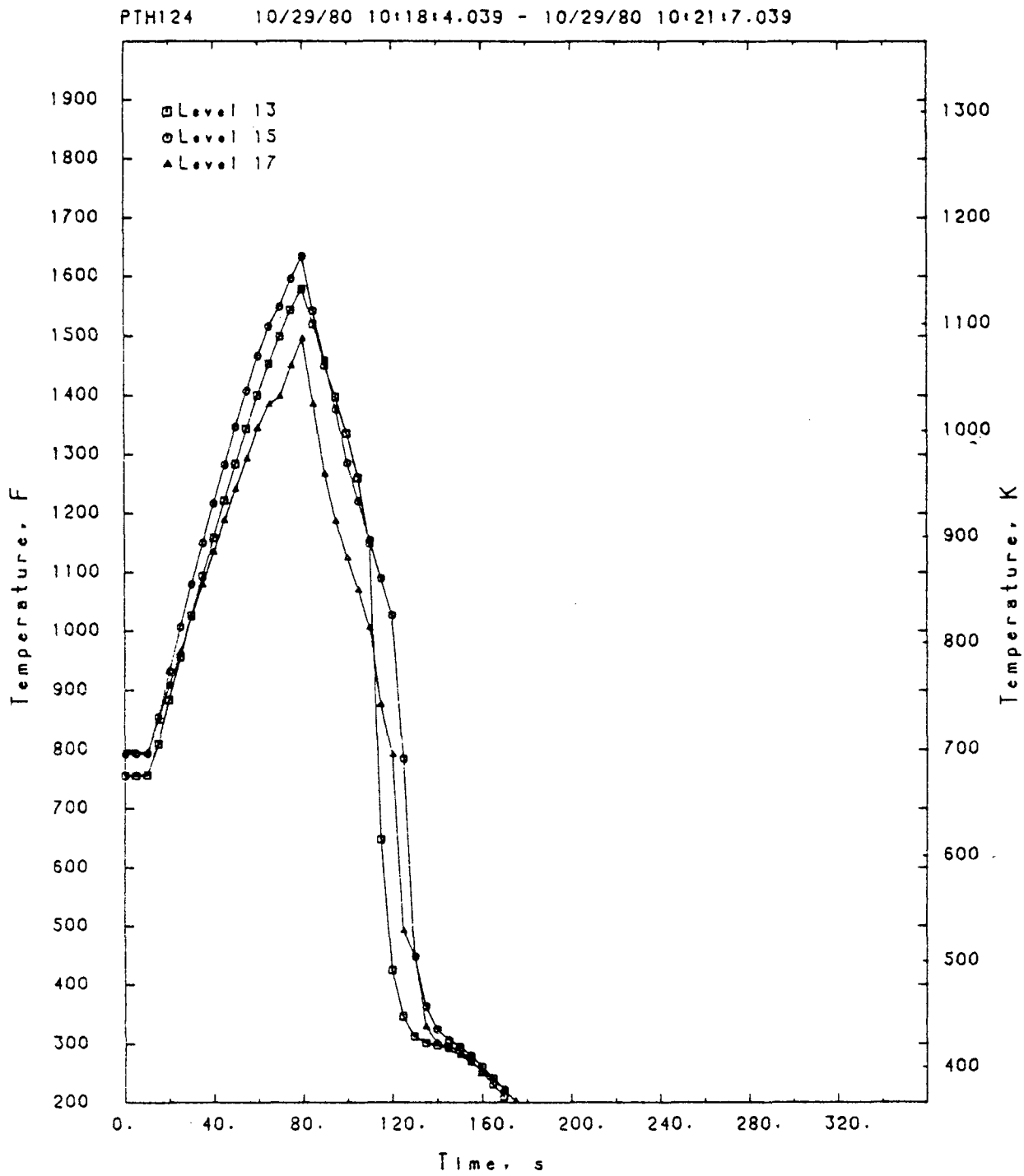

FIGURE 1.2.3.24 AVERAGE GUARD FUEL ROD CLADDING TEMPERATURE HISTORIES (INTERIOR TC'S) DURING TRANSIENT PTH124

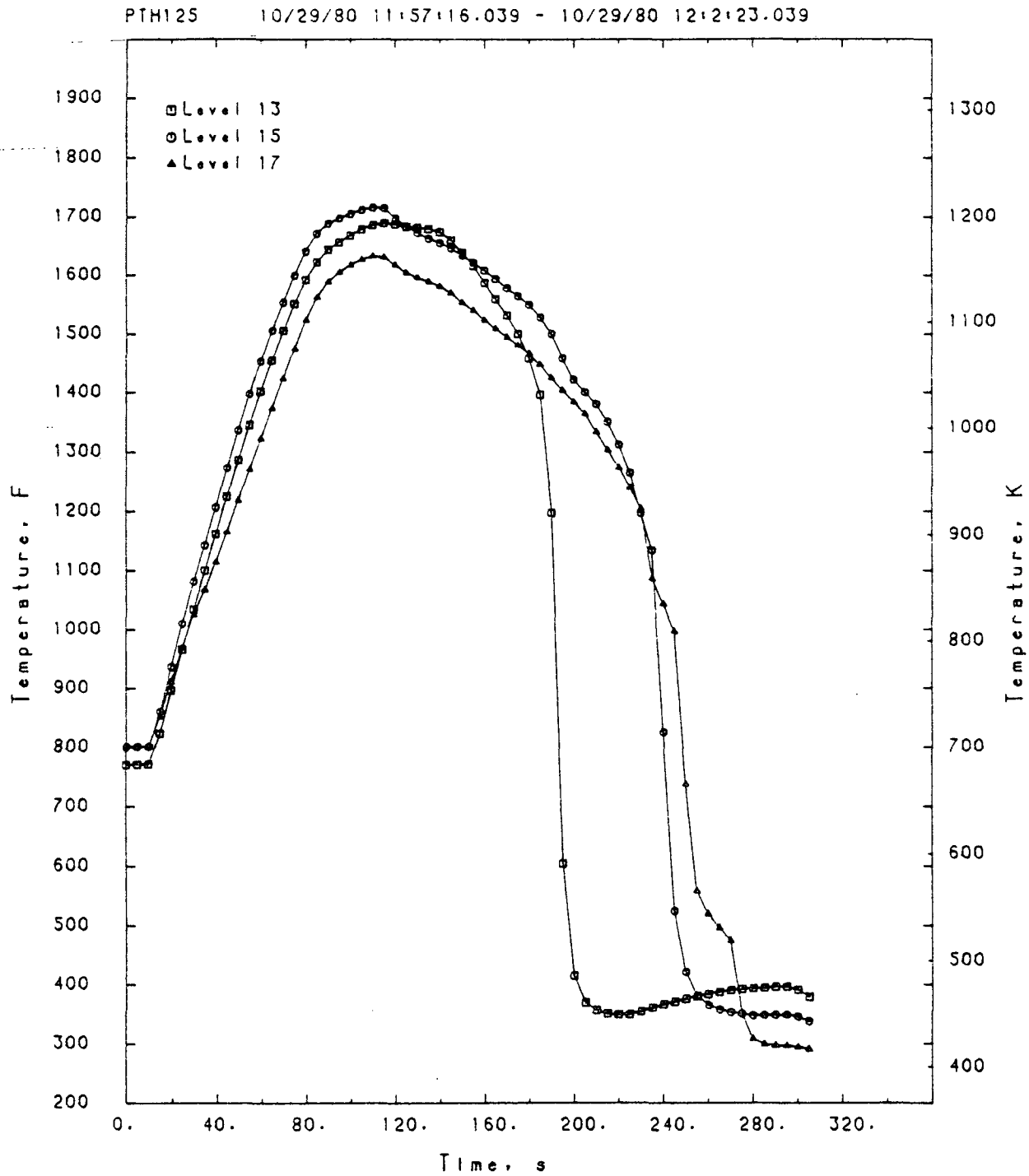

FIGURE 1.2.3.25 AVERAGE GUARD FUEL ROD CLADDING TEMPERATURE HISTORIES (INTERIOR TC'S) DURING TRANSIENT PTH125

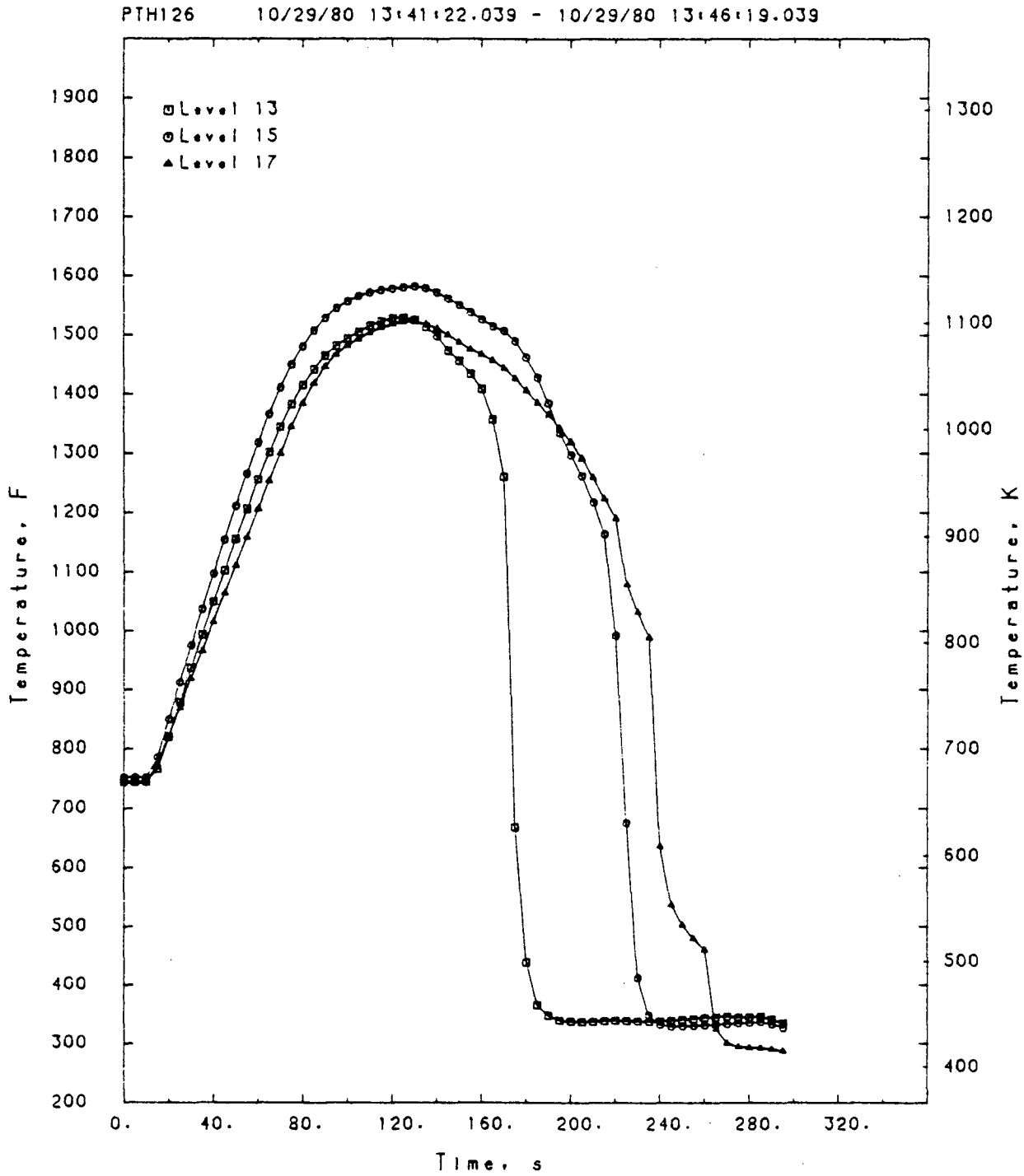

FIGURE 1.2.3.26 AVERAGE GUARD FUEL ROD CLADDING TEMPERATURE HISTORIES (INTERIOR TC'S) DURING TRANSIENT PTH126

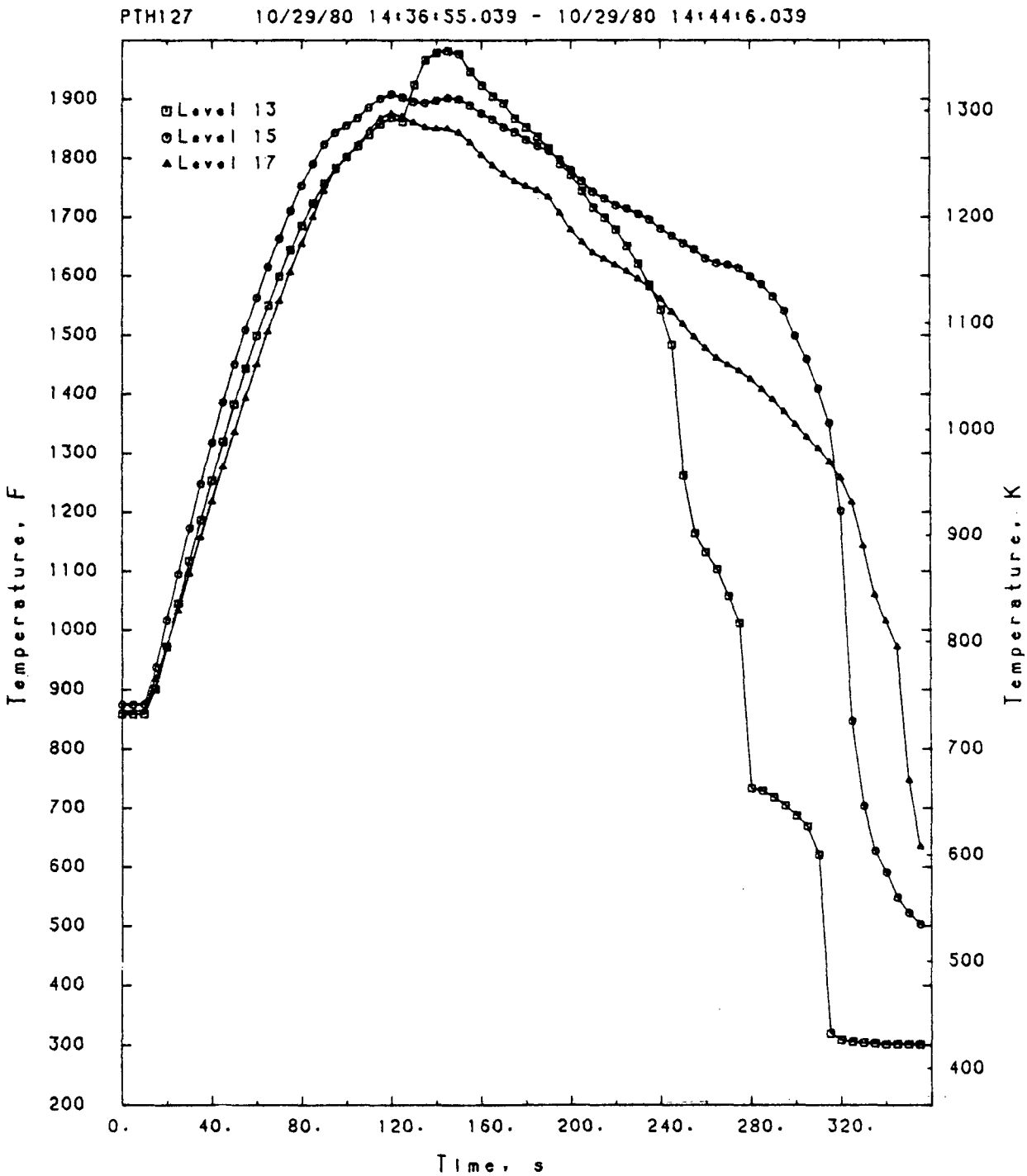

FIGURE 1.2.3.27 AGERAGE GUARD FUEL ROD CLADDING TEMPERATURE HISTORIES (INTERIOR TC'S) DURING TRANSIENT PTH127

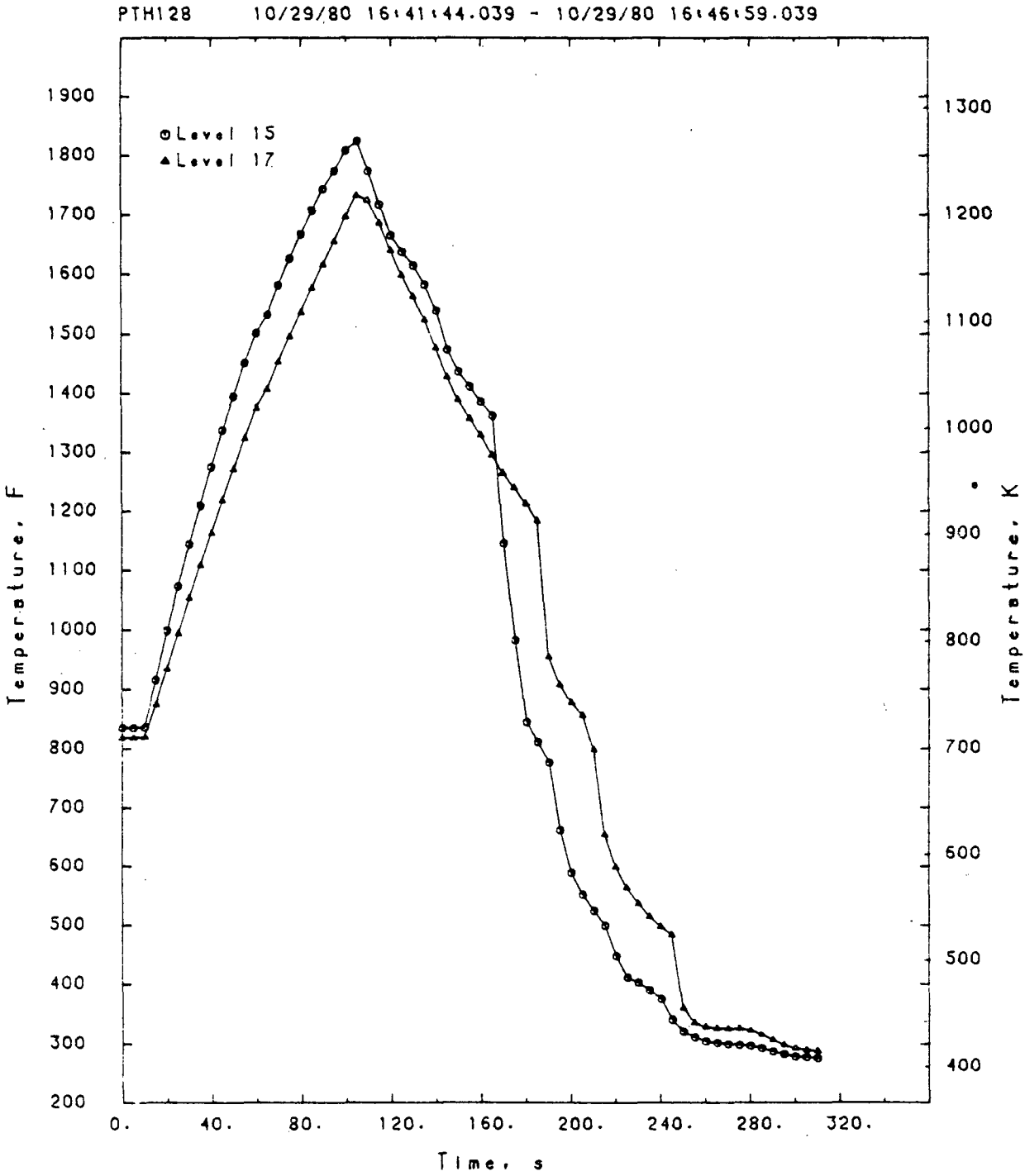

FIGURE 1.2.3.28 AVERAGE GUARD FUEL ROD CLADDING TEMPERATURE HISTORIES (INTERIOR TC'S) DURING TRANSIENT PTH128

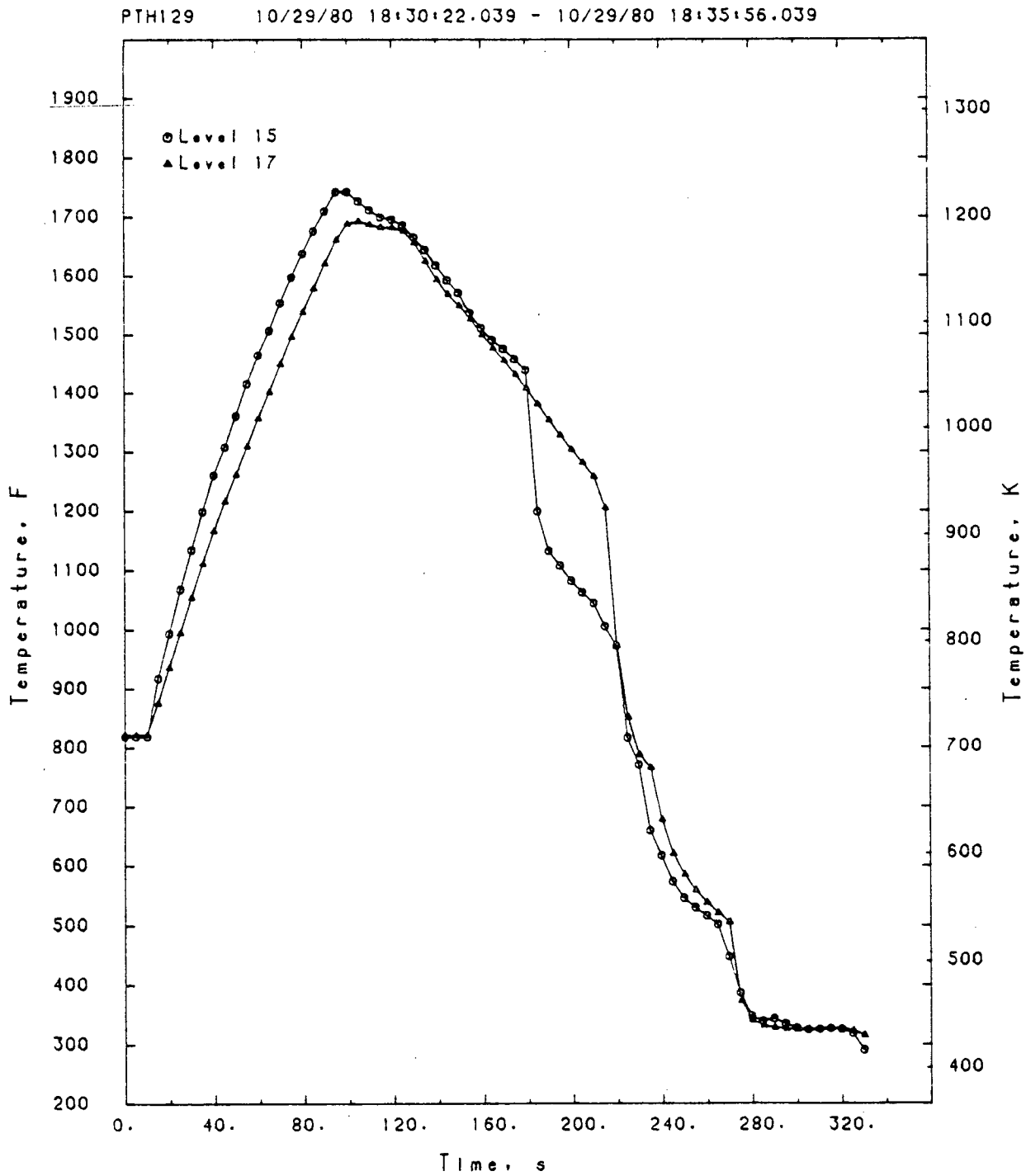

FIGURE 1.2.3.29 AVERAGE GUARD FUEL ROD CLADDING TEMPERATURE HISTORIES (INTERIOR TC'S) DURING TRANSIENT PTH129

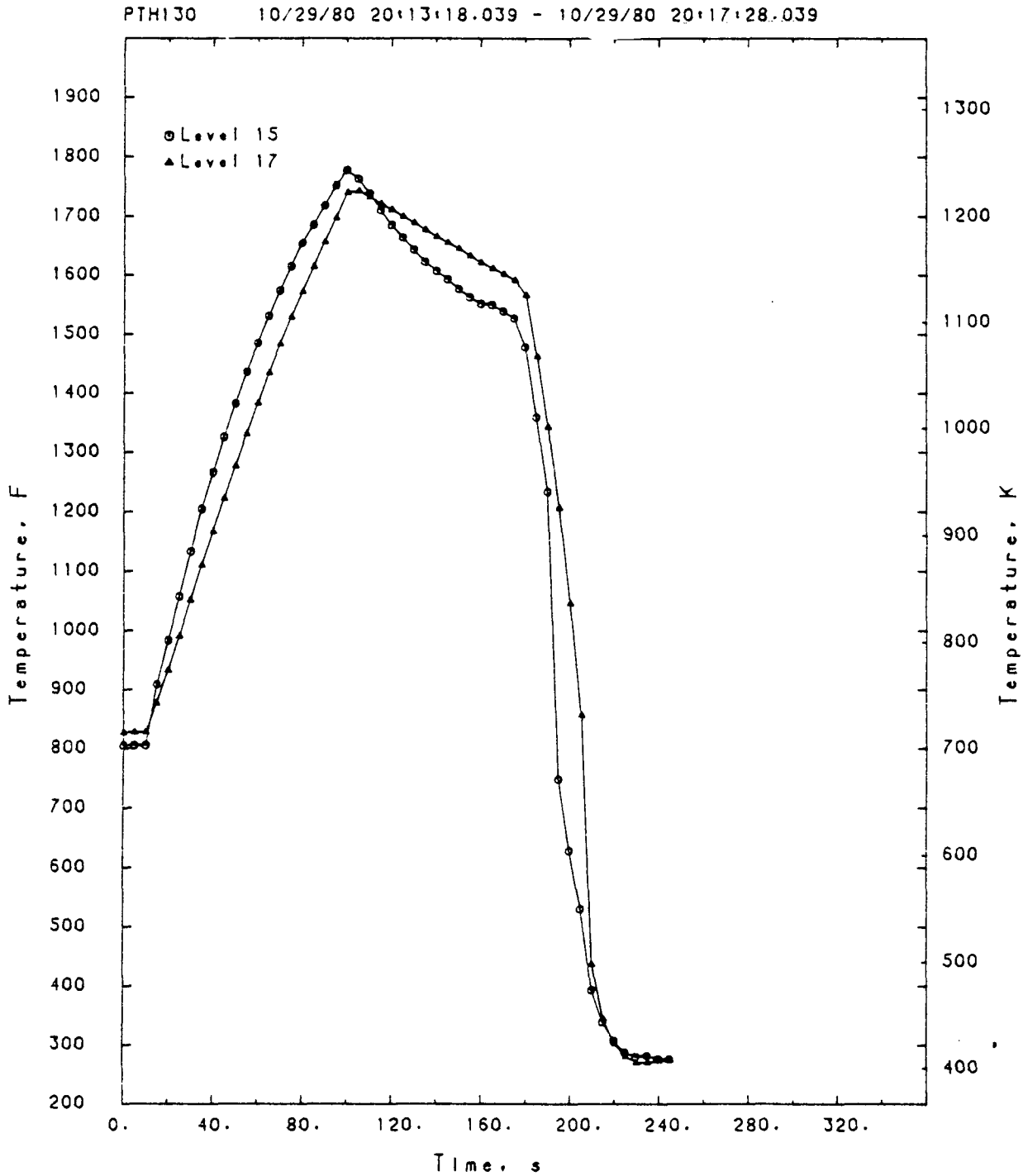

FIGURE 1.2.3.30 AVERAGE GUARD FUEL ROD CLADDING TEMPERATURE HISTORIES (INTERIOR TC'S) DURING TRANSIENT PTH130

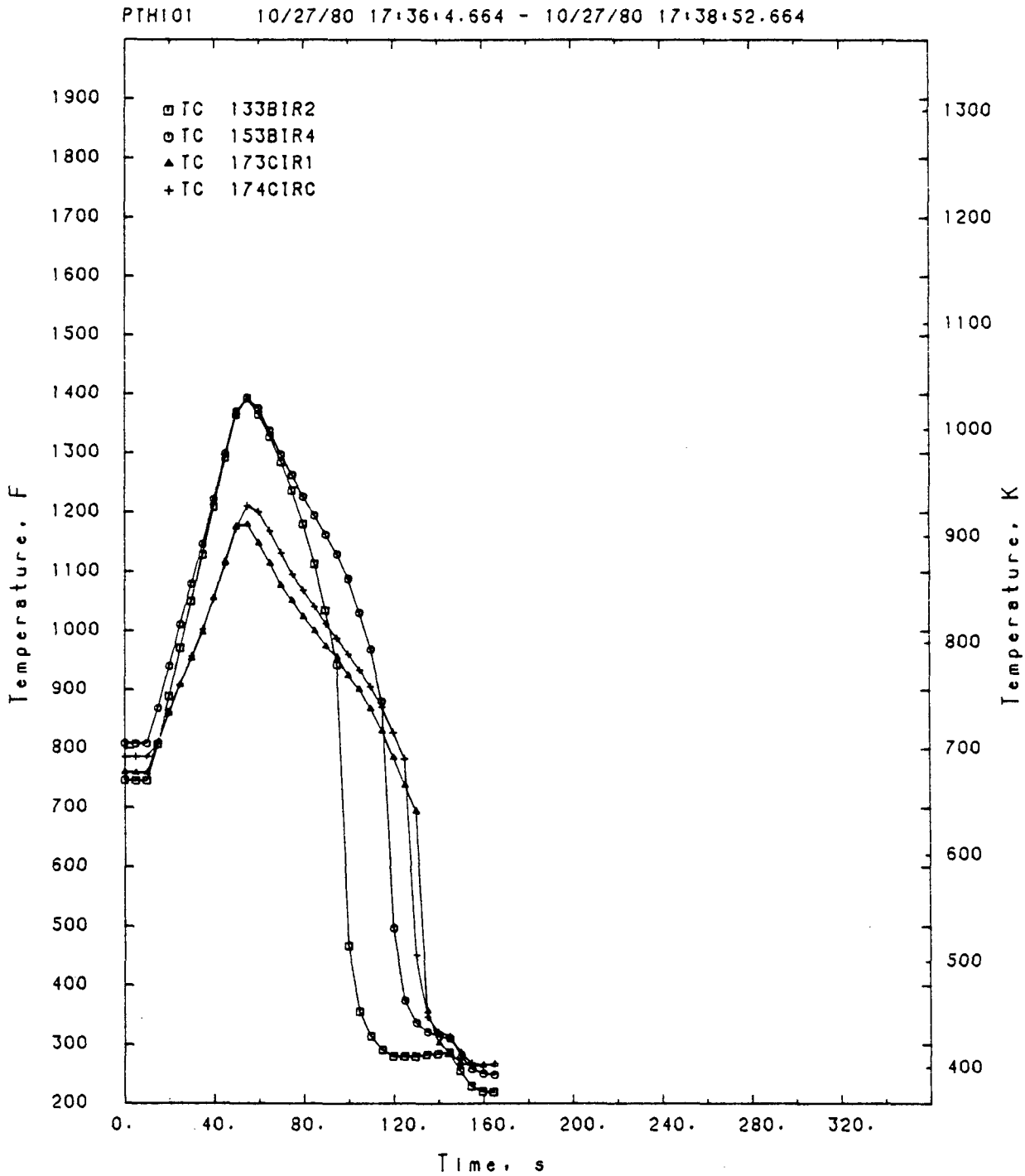

FIGURE 1.2.4.01 TEST FUEL ROD CENTER AND INTERIOR CLADDING TEMPERATURE HISTORIES DURING TRANSIENT PTH101

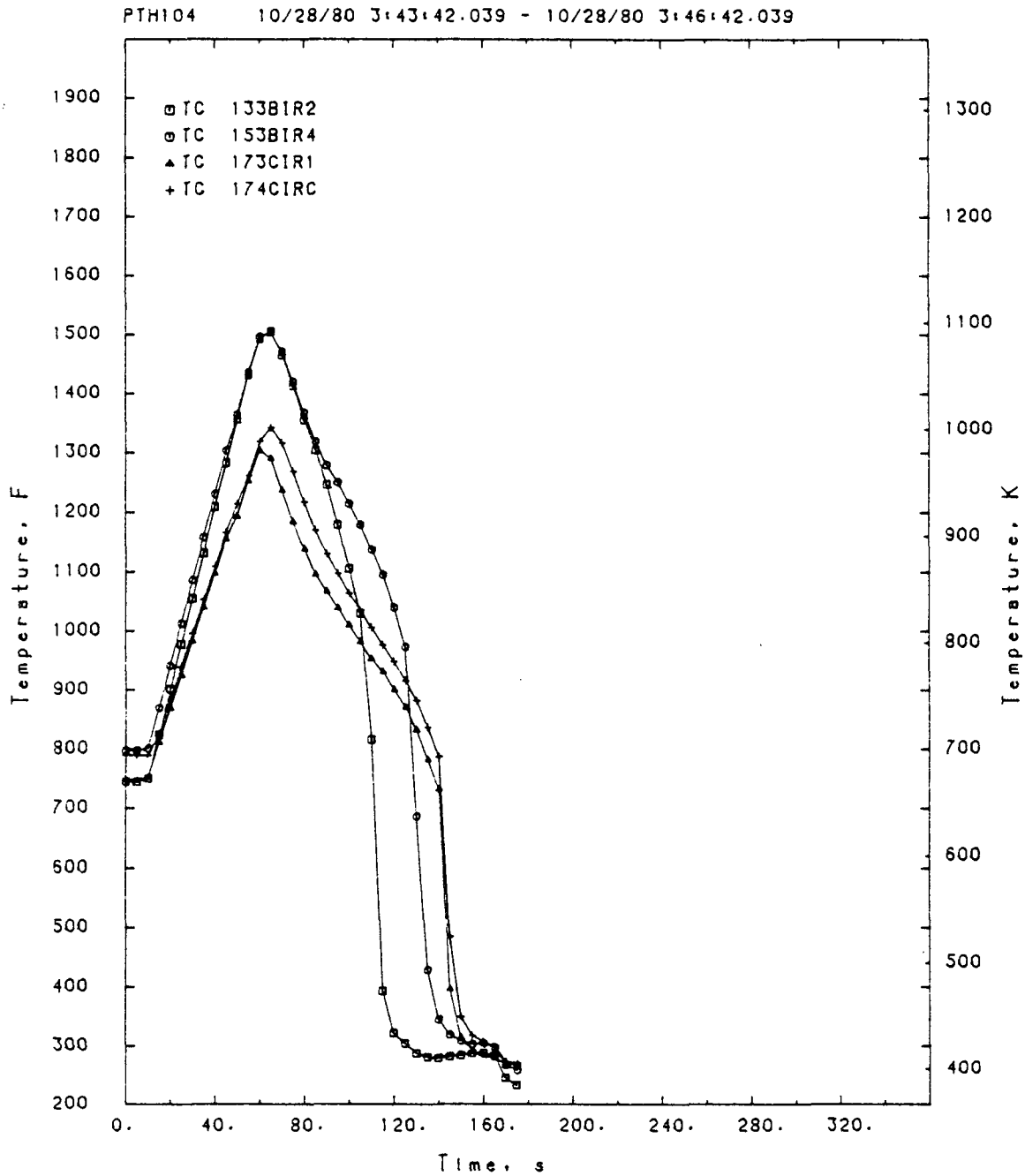

FIGURE 1.2.4.04 TEST FUEL ROD CENTER AND INTERIOR CLADDING TEMPERATURE HISTORIES DURING TRANSIENT PTH104

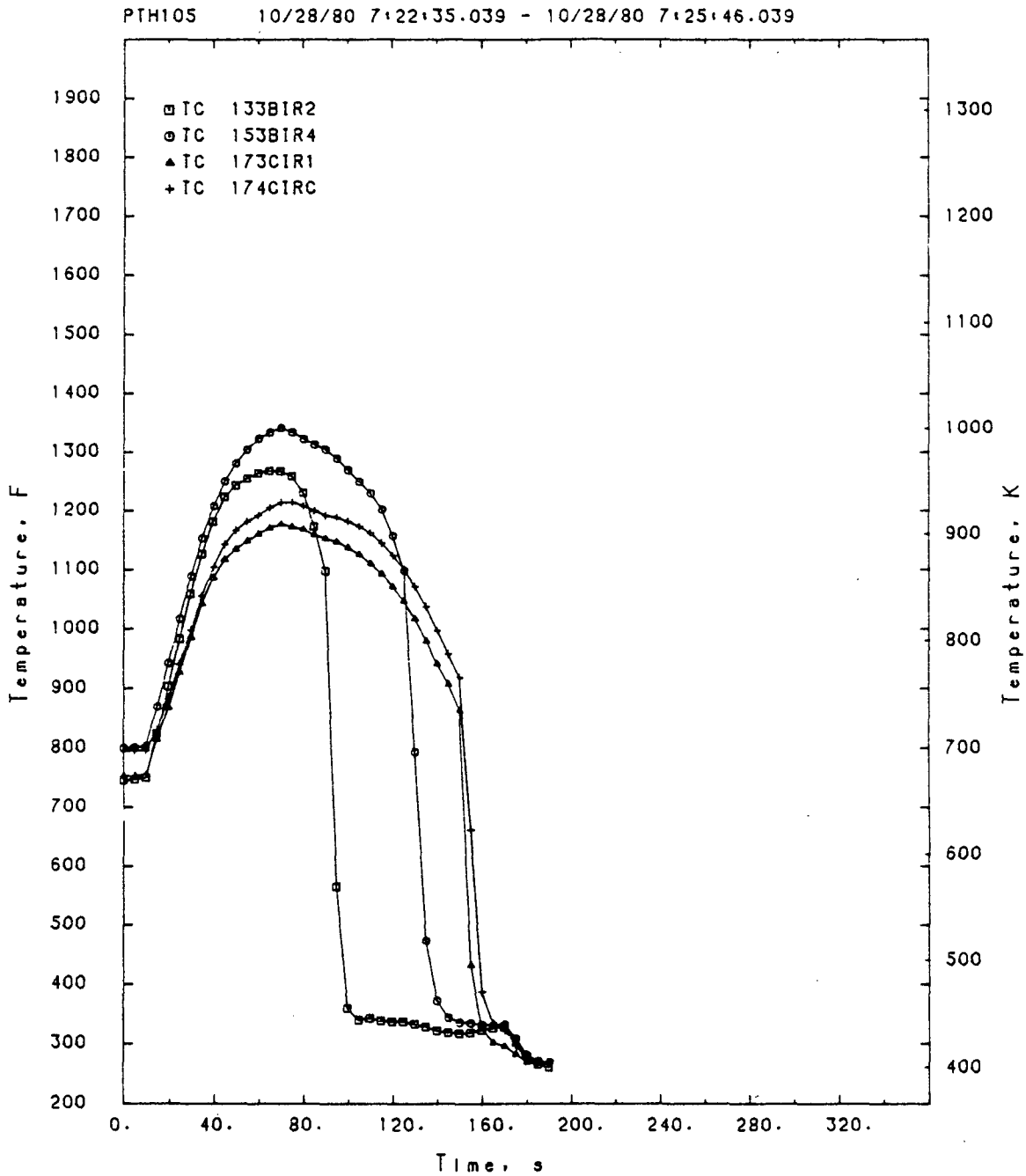

FIGURE 1.2.4.05 TEST FUEL ROD CENTER AND INTERIOR CLADDING TEMPERATURE HISTORIES DURING TRANSIENT PTH105

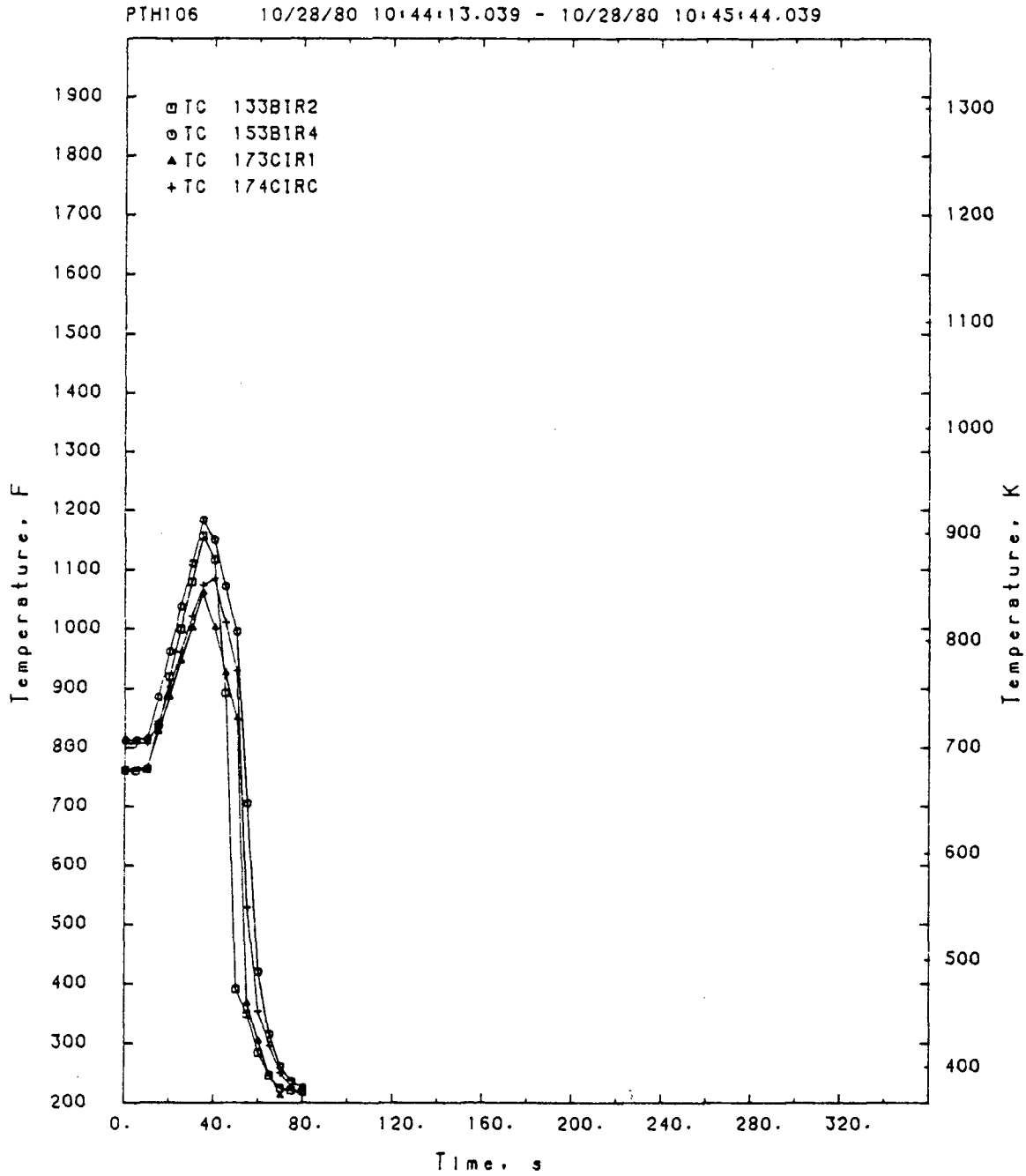

FIGURE 1.2.4.06 TEST FUEL ROD CENTER AND INTERIOR CLADDING TEMPERATURE HISTORIES DURING TRANSIENT PTH106

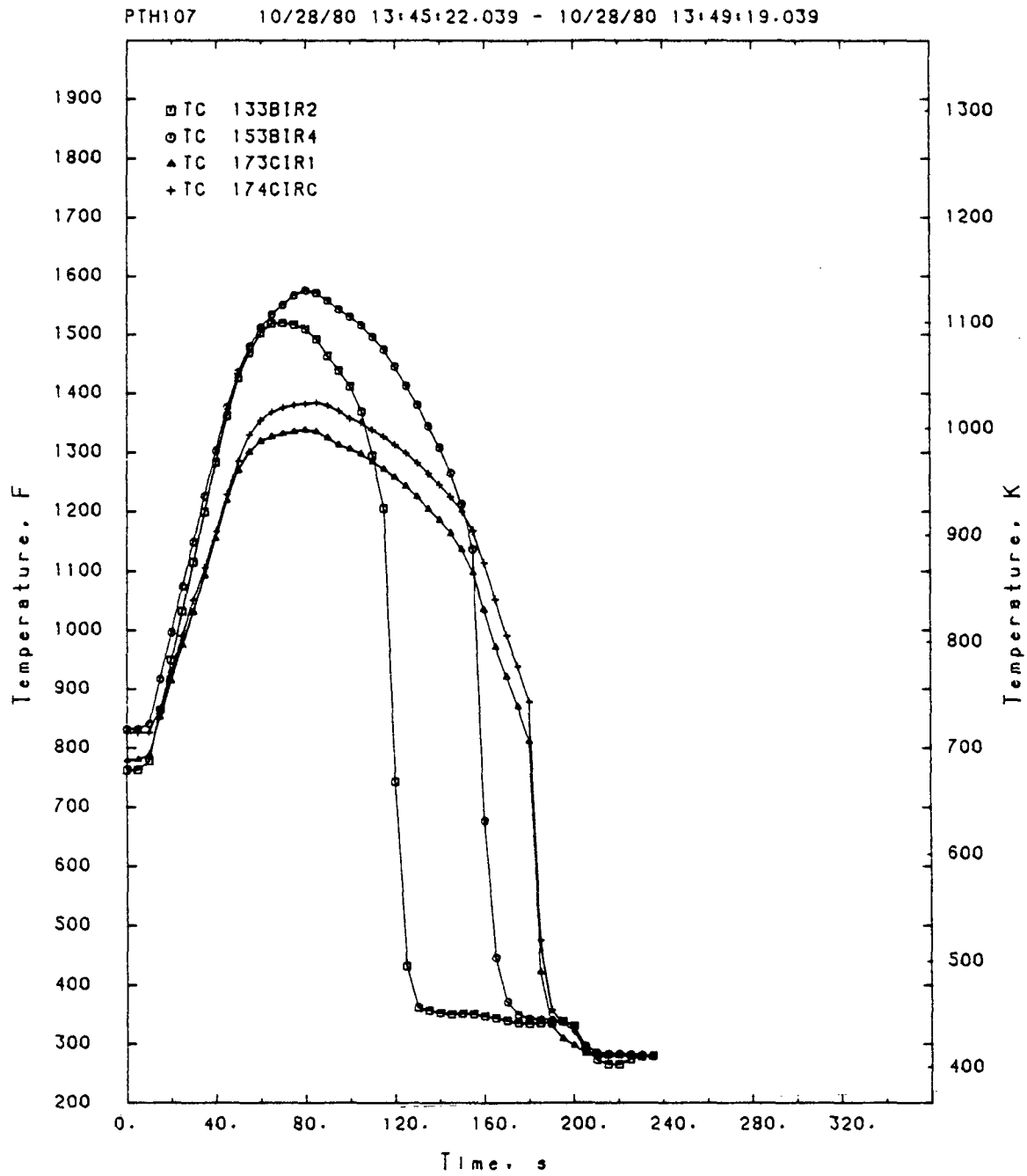

FIGURE 1.2.4.07 TEST FUEL ROD CENTER AND INTERIOR CLADDING TEMPERATURE HISTORIES DURING TRANSIENT PTH107

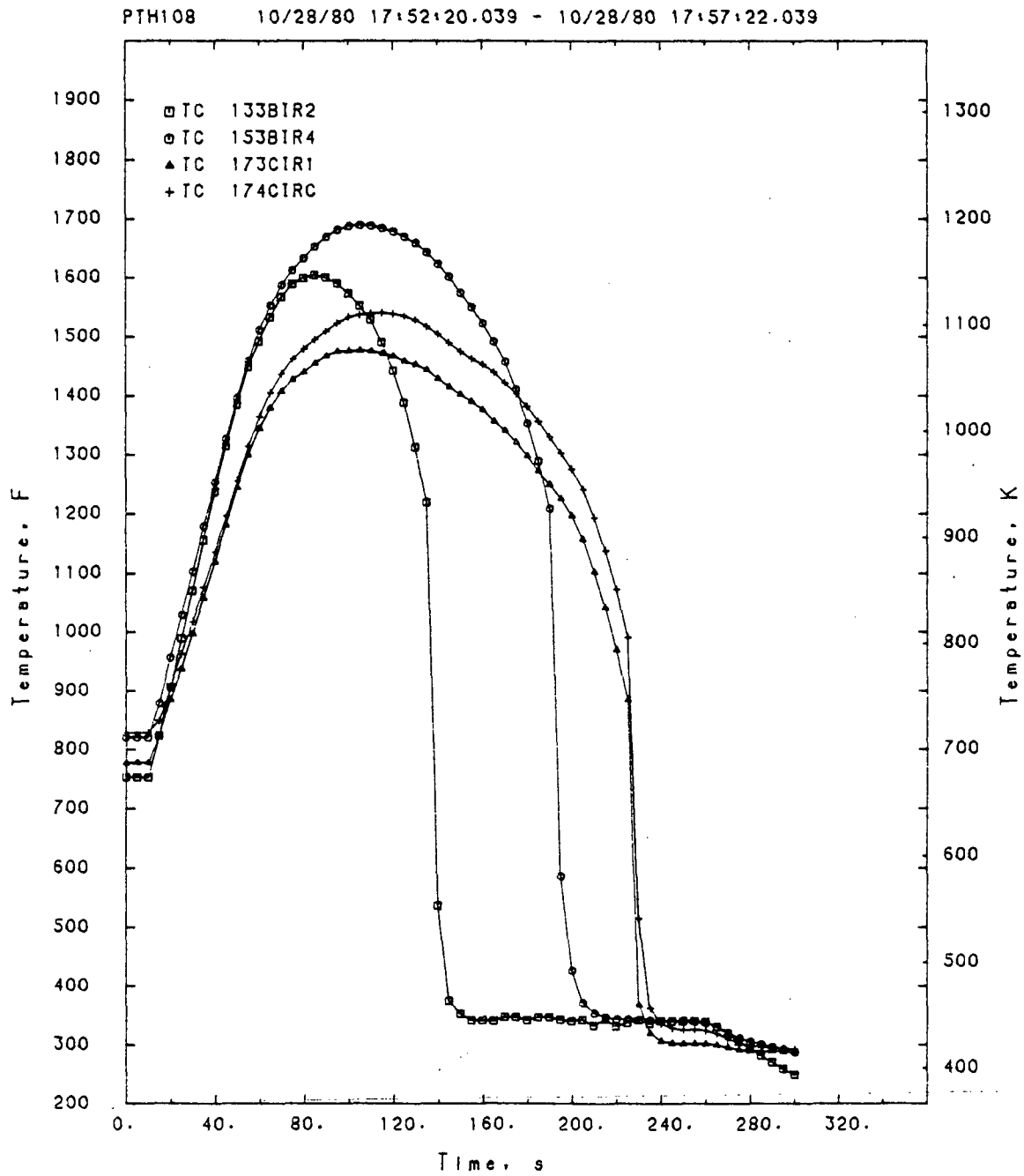

FIGURE 1.2.4.08 TEST FUEL ROD CENTER AND INTERIOR CLADDING TEMPERATURE HISTORIES DURING TRANSIENT PTH108

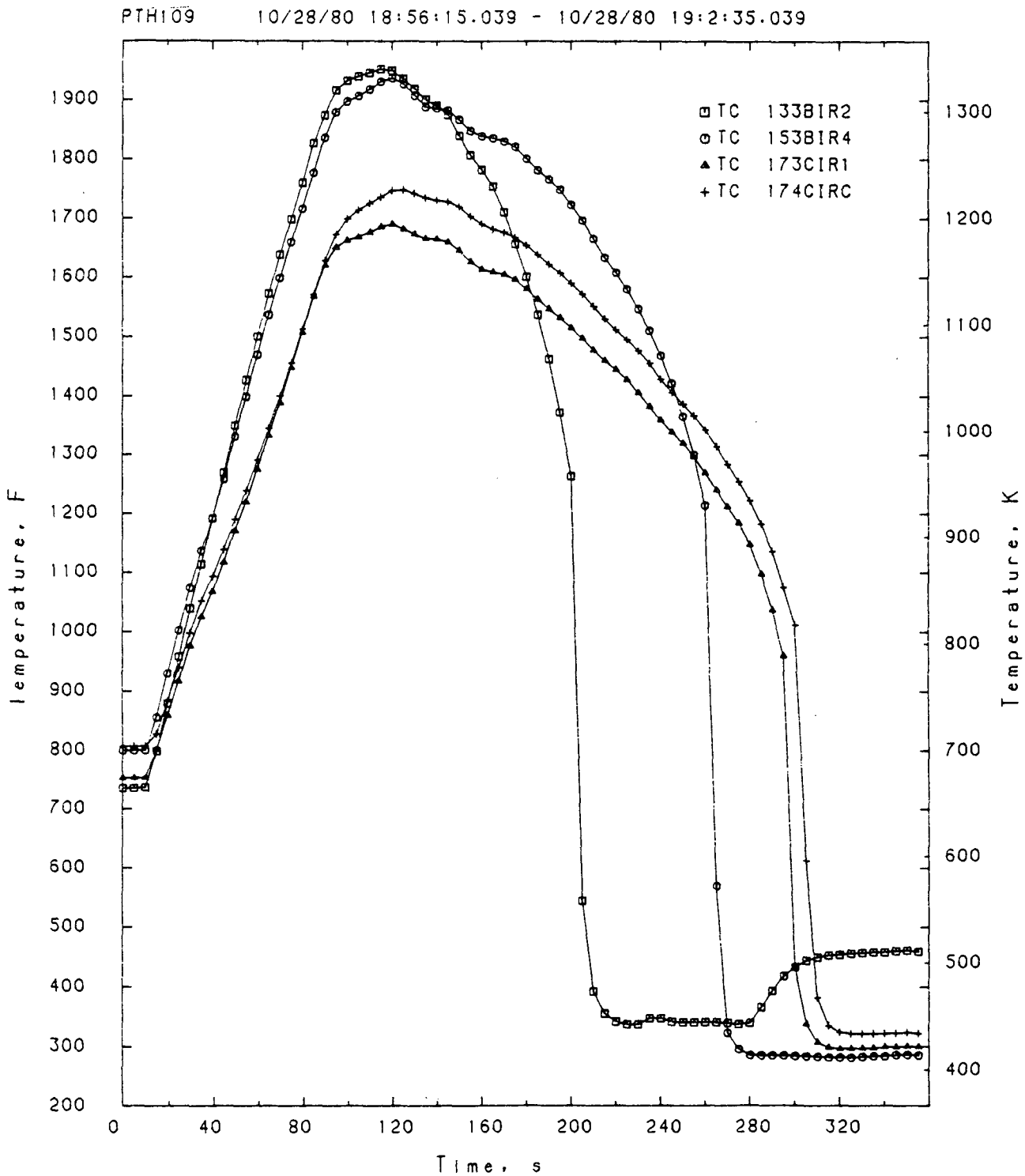

FIGURE 1.2.4.09 TEST FUEL ROD CENTER AND INTERIOR CLADDING TEMPERATURE HISTORIES DURING TRANSIENT PTH109

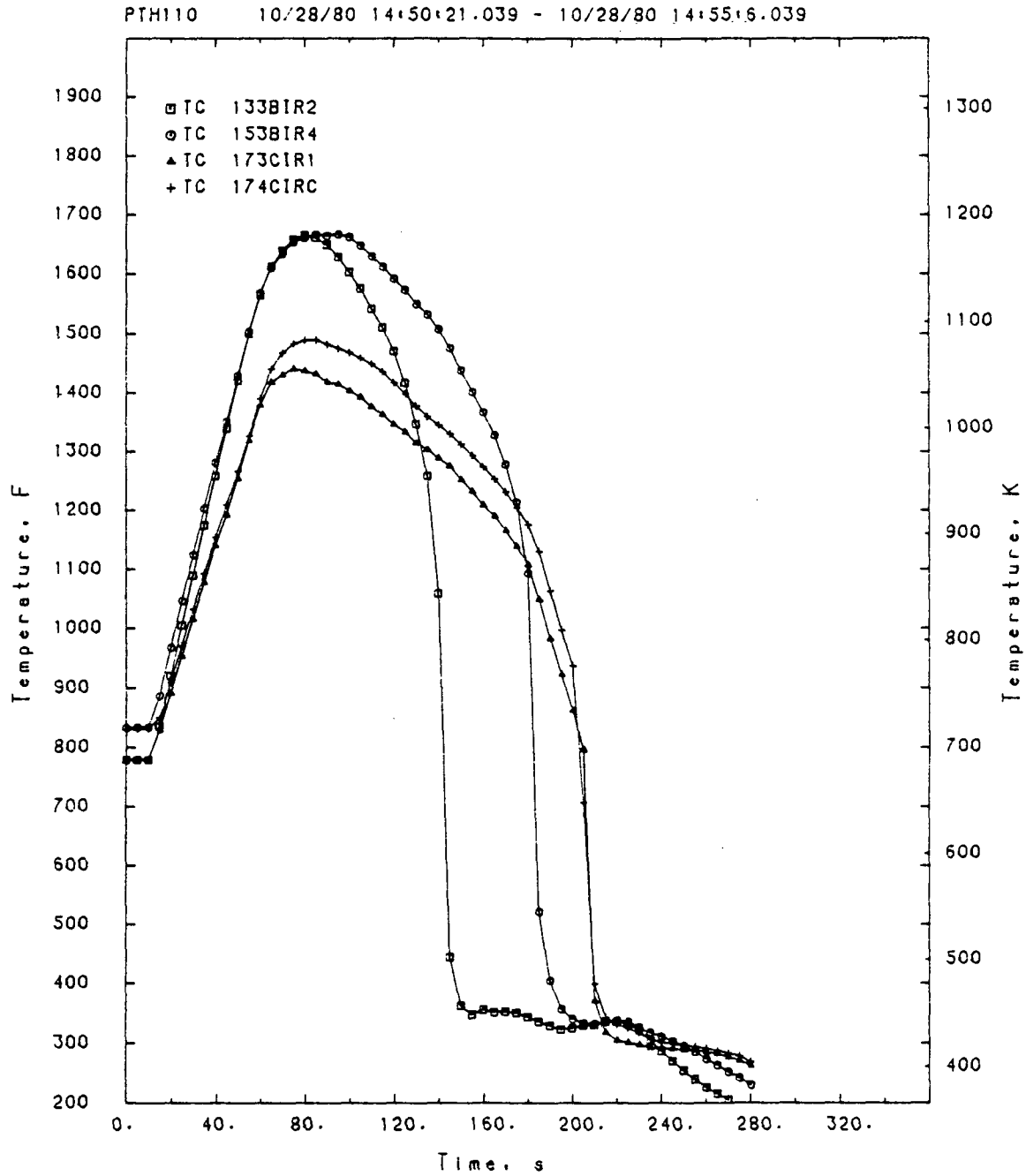

FIGURE 1.2.4.10 TEST FUEL ROD CENTER AND INTERIOR CLADDING TEMPERATURE HISTORIES DURING TRANSIENT PTH110

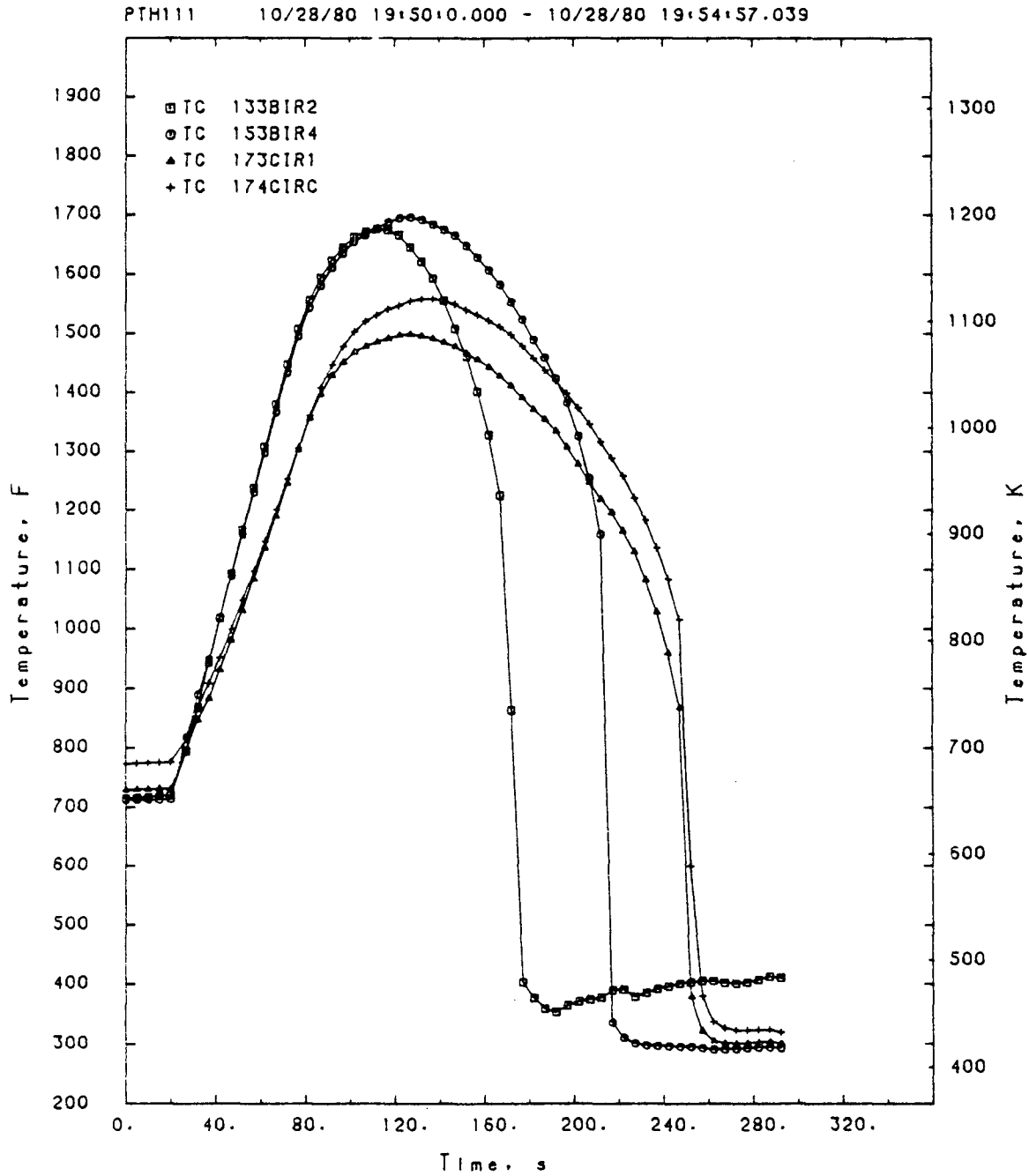

FIGURE 1.2.4.11 TEST FUEL ROD CENTER AND INTERIOR CLADDING TEMPERATURE HISTORIES DURING TRANSIENT PTH111

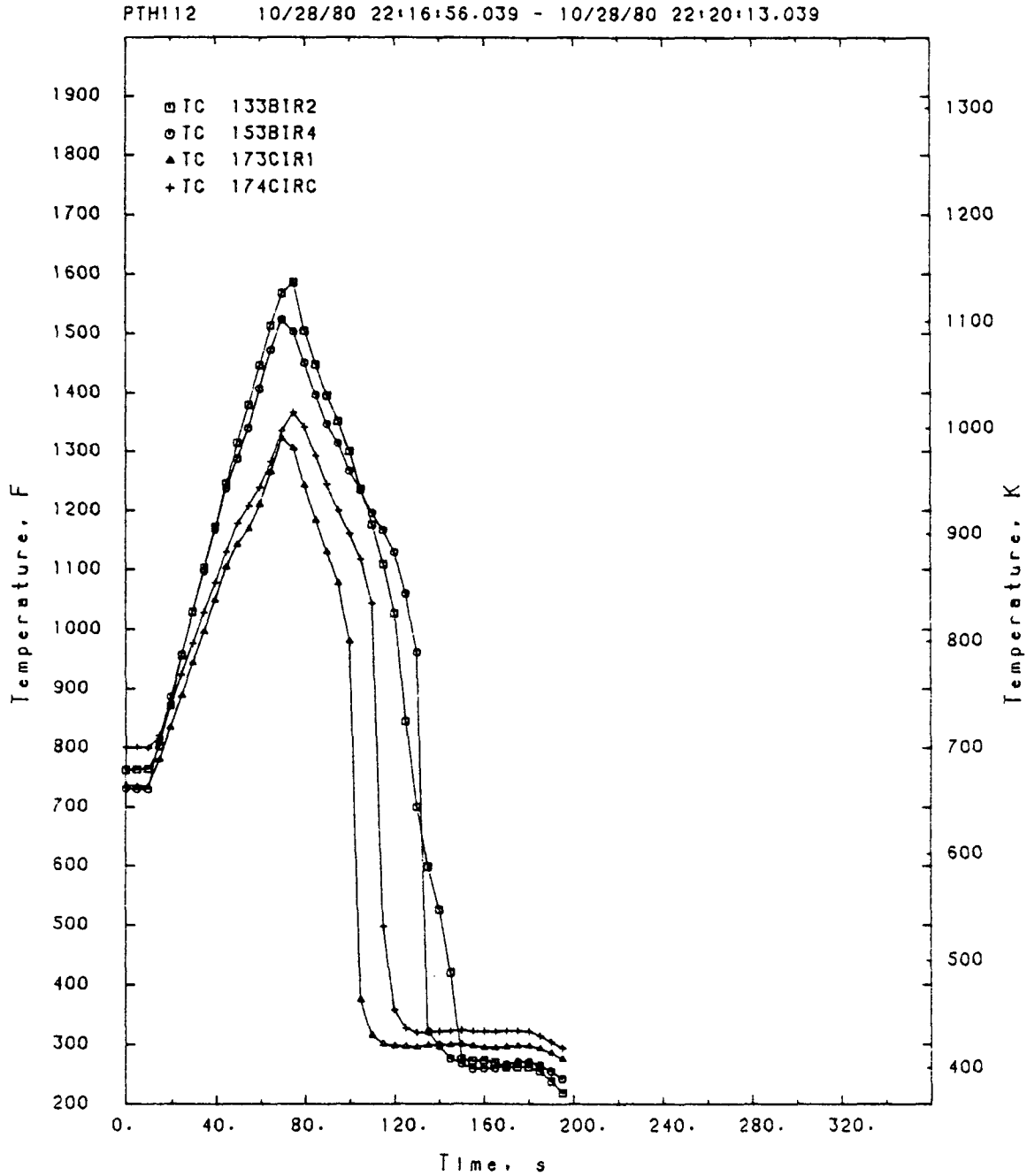

FIGURE 1.2.4.12 TEST FUEL ROD CENTER AND INTERIOR CLADDING TEMPERATURE HISTORIES DURING TRANSIENT PTH112

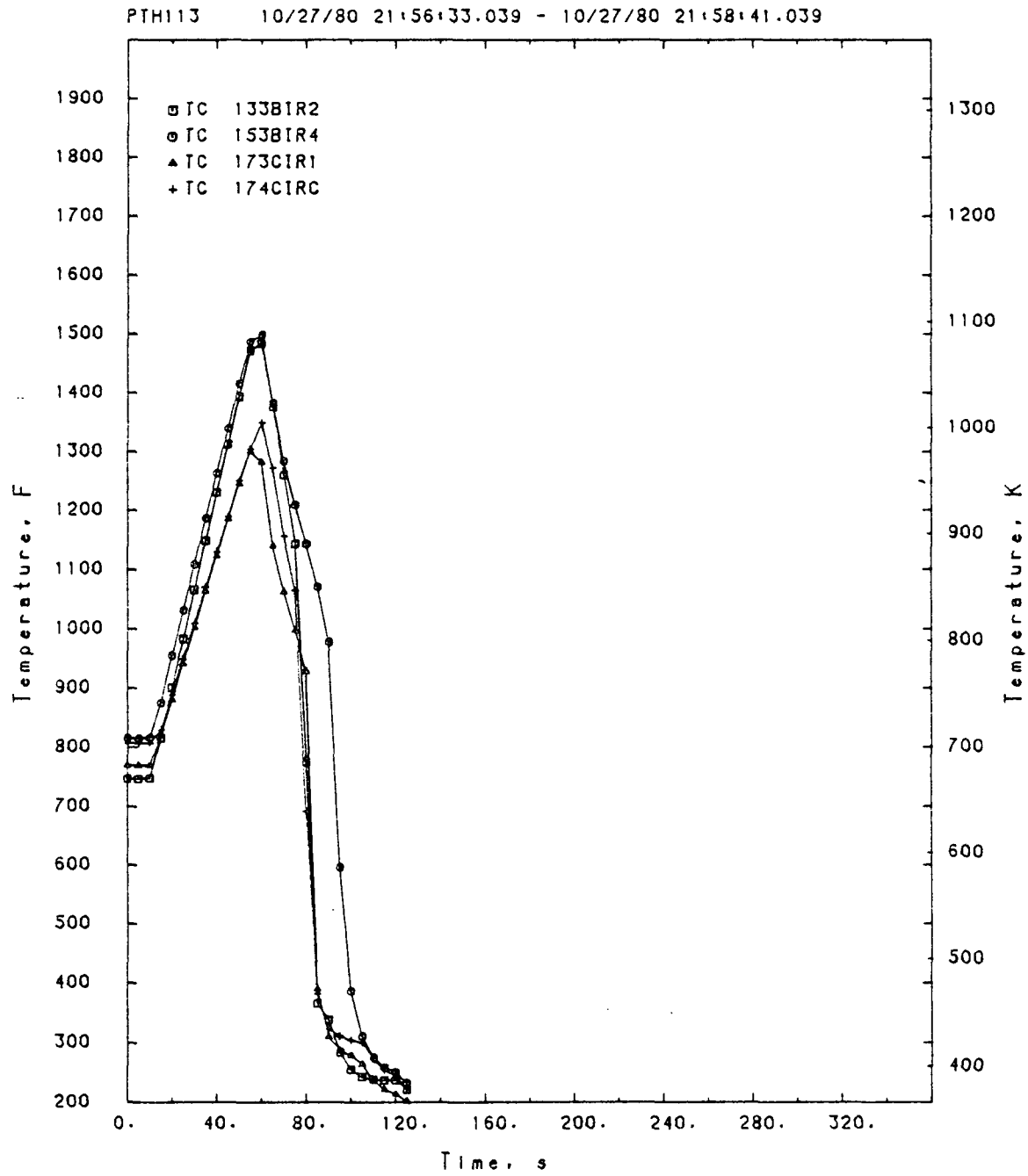

FIGURE 1.2.4.13 TEST FUEL ROD CENTER AND INTERIOR CLADDING TEMPERATURE HISTORIES DURING TRANSIENT PTH113

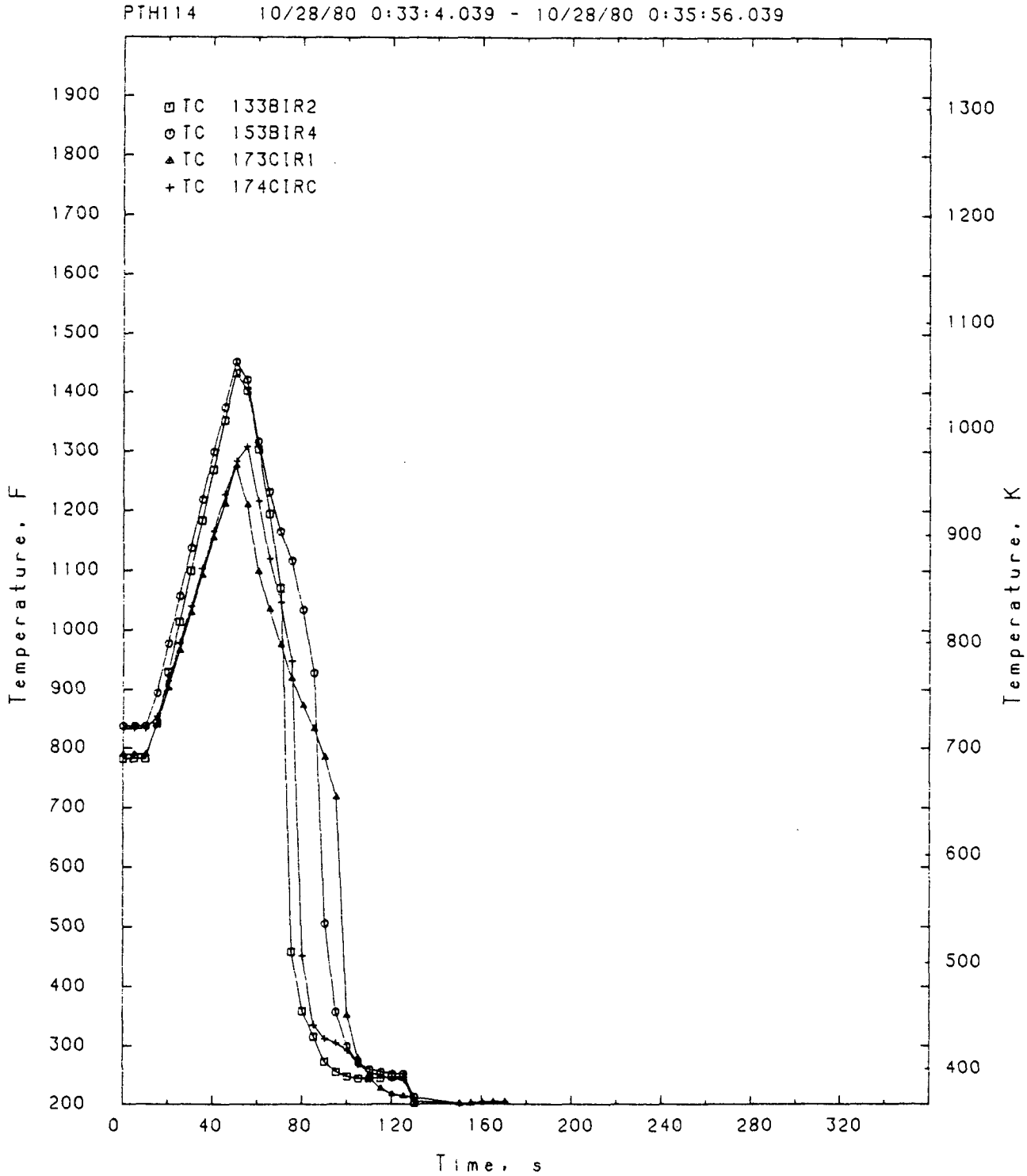

FIGURE 1.2.4.14 TEST FUEL ROD CENTER AND INTERIOR CLADDING TEMPERATURE HISTORIES DURING TRANSIENT PTH114

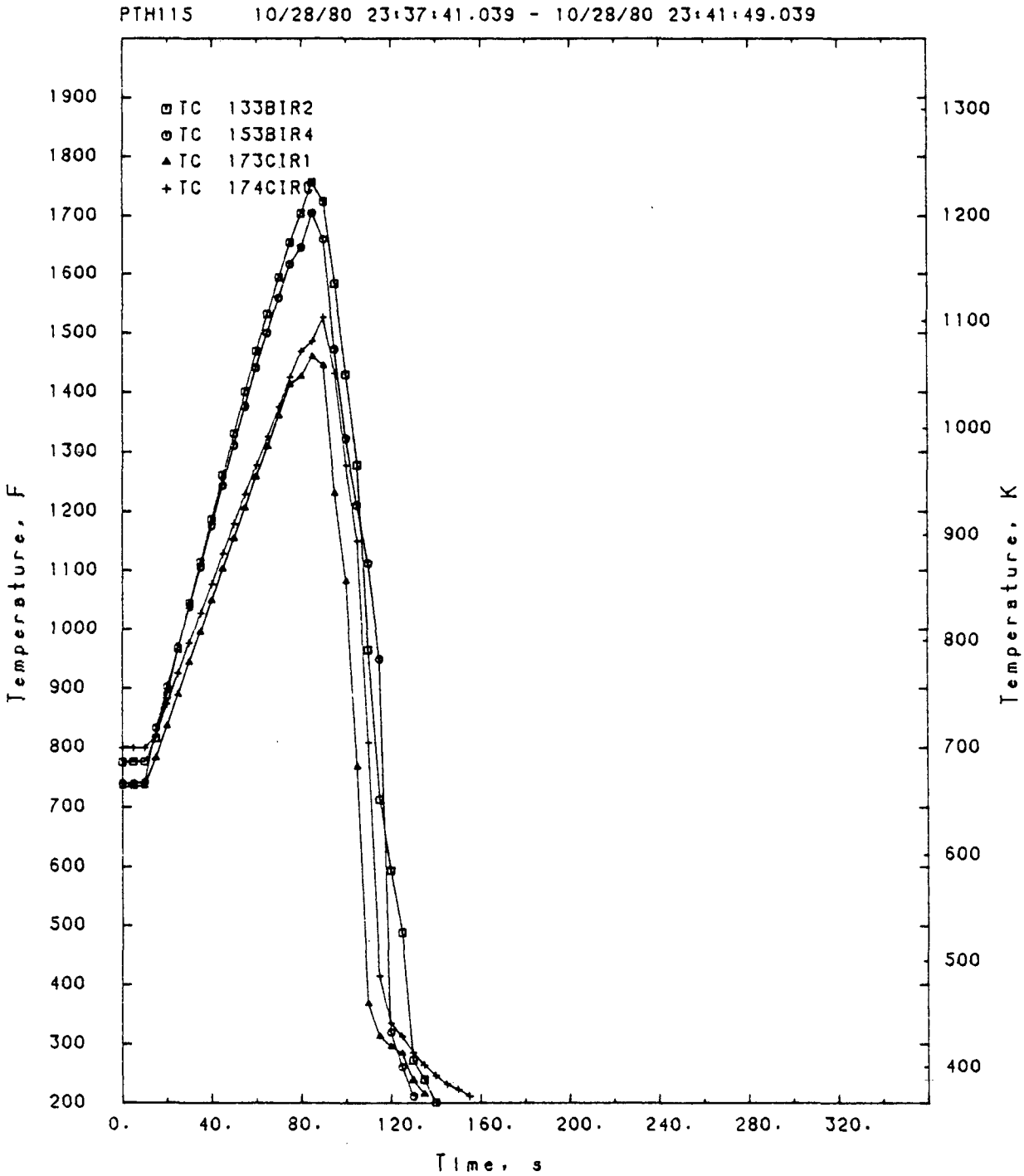

FIGURE 1.2.4.15 TEST FUEL ROD CENTER AND INTERIOR CLADDING TEMPERATURE HISTORIES DURING TRANSIENT PTH115

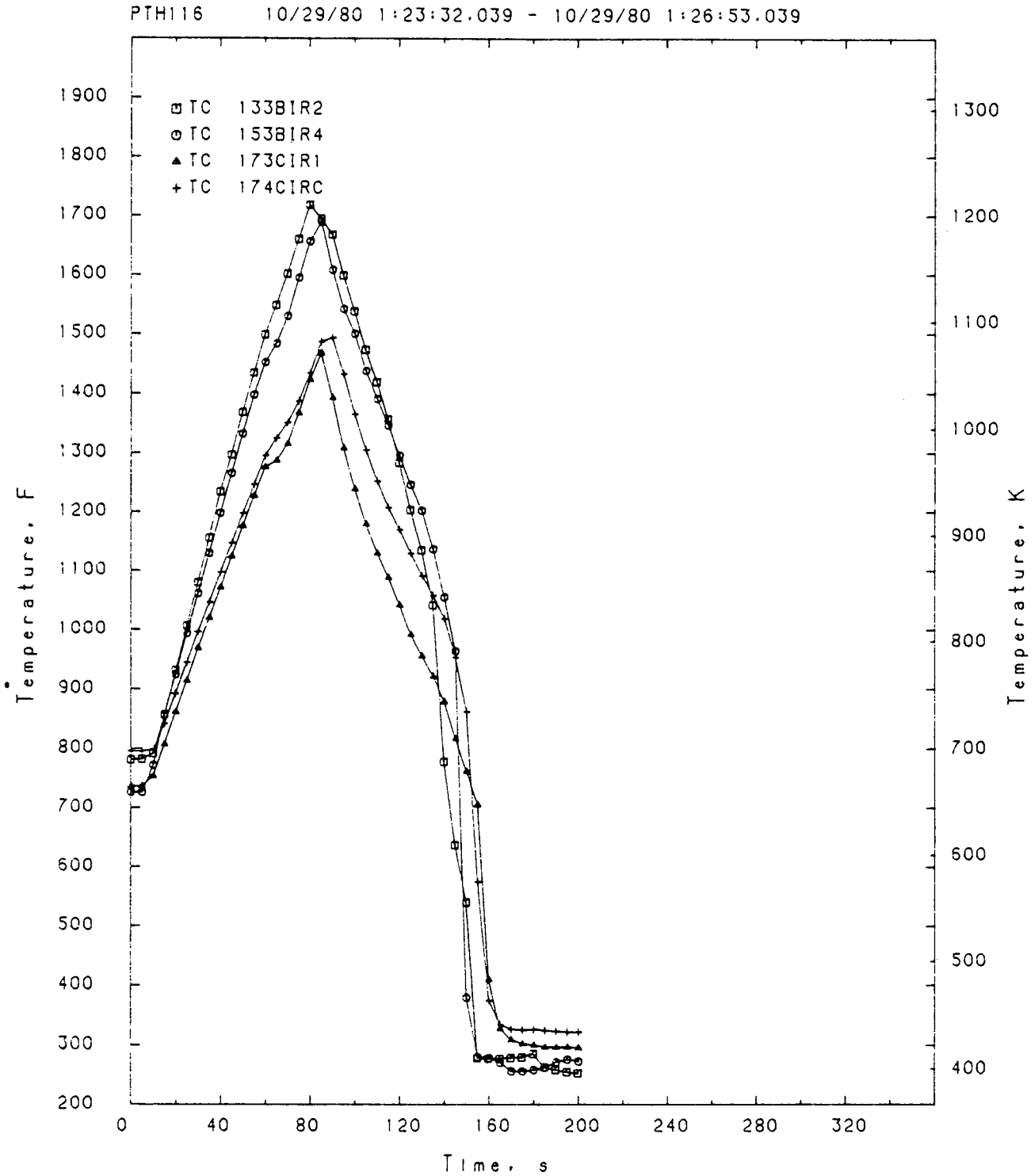

FIGURE 1.2.4.16 TEST FUEL ROD CENTER AND INTERIOR CLADDING TEMPERATURE HISTORIES DURING TRANSIENT PTH116

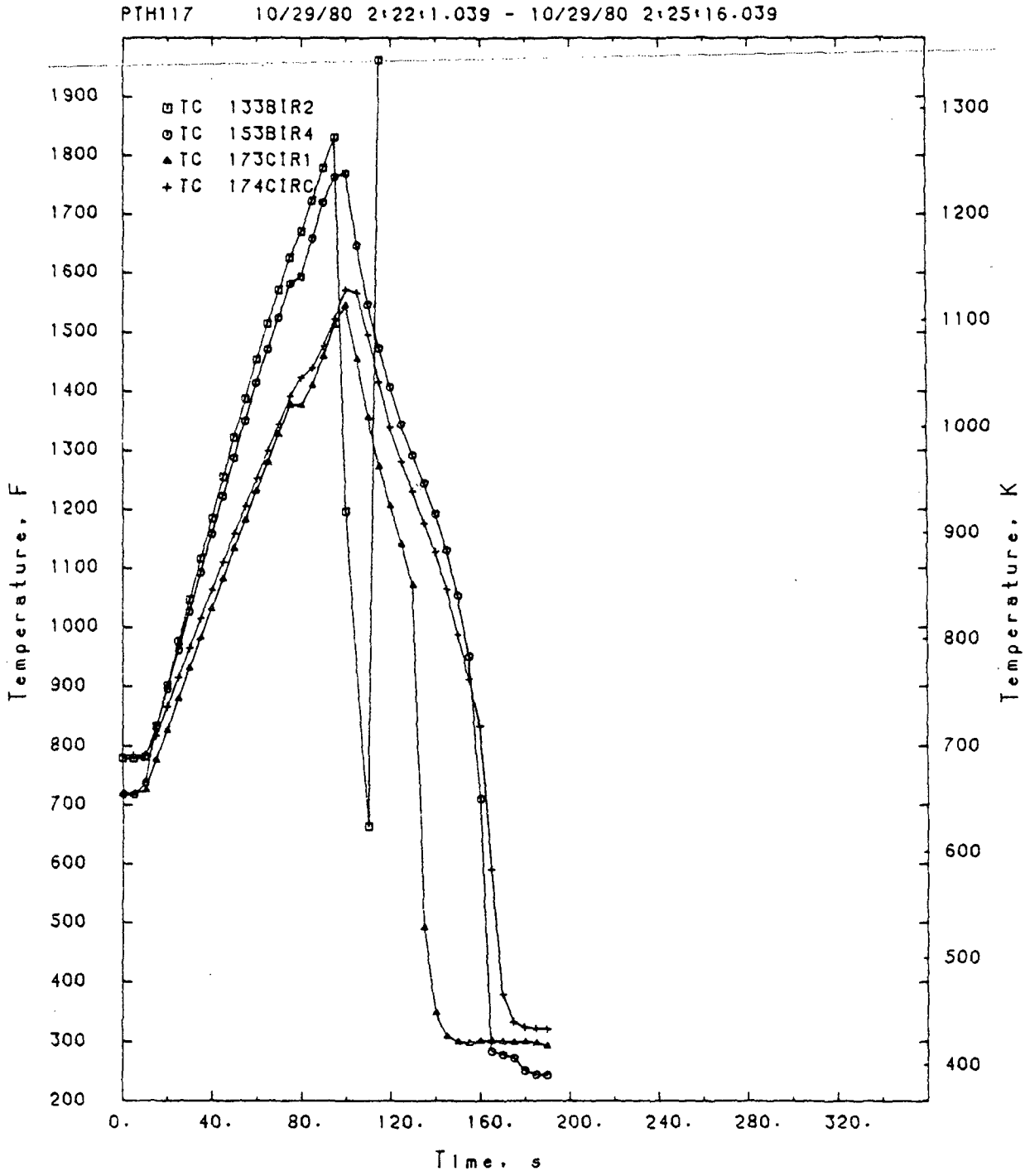

FIGURE 1.2.4.17 TEST FUEL ROD CENTER AND INTERIOR CLADDING TEMPERATURE HISTORIES DURING TRANSIENT PTH117

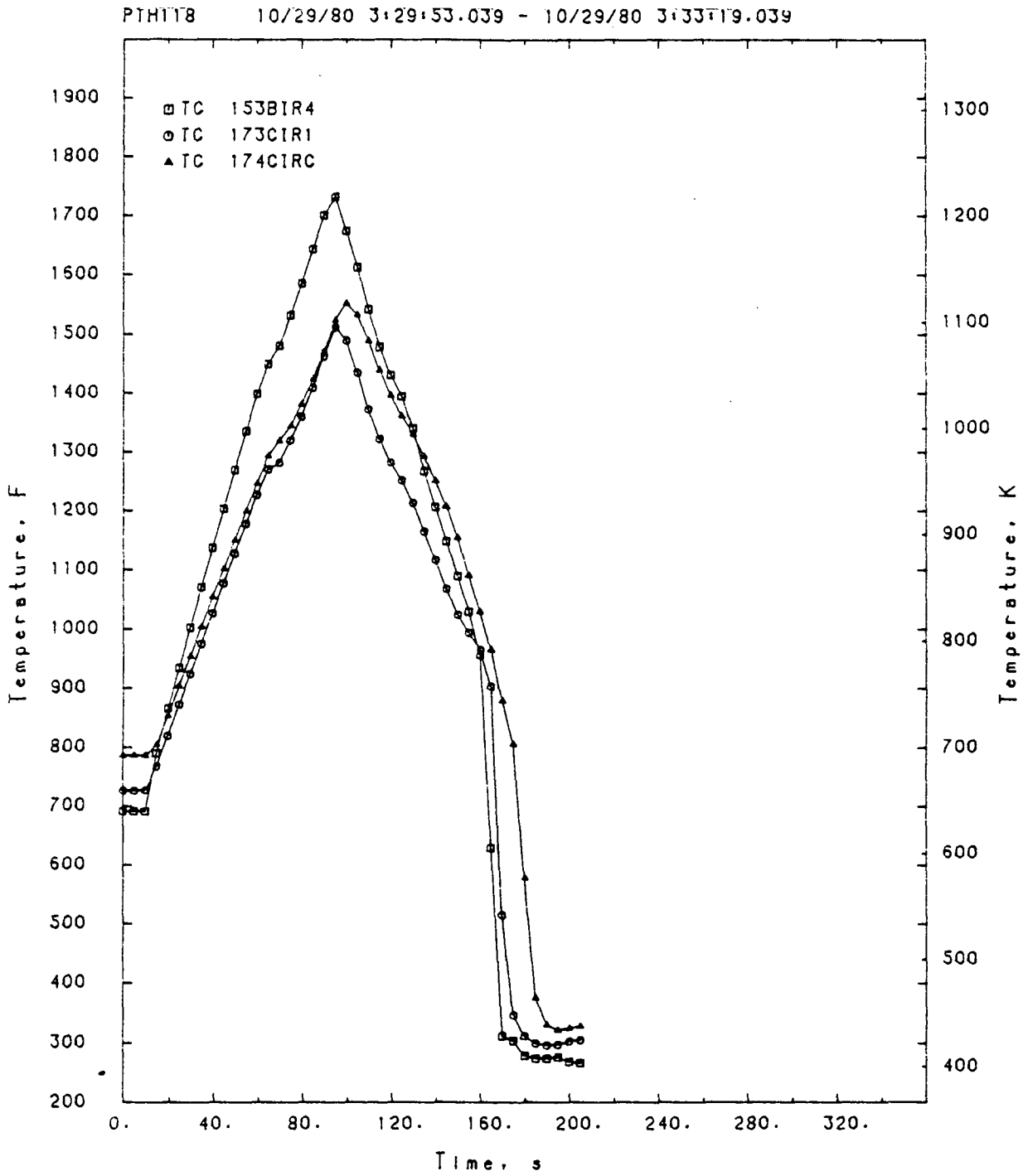

FIGURE 1.2.4.18 TEST FUEL ROD CENTER AND INTERIOR CLADDING TEMPERATURE HISTORIES DURING TRANSIENT PTH118

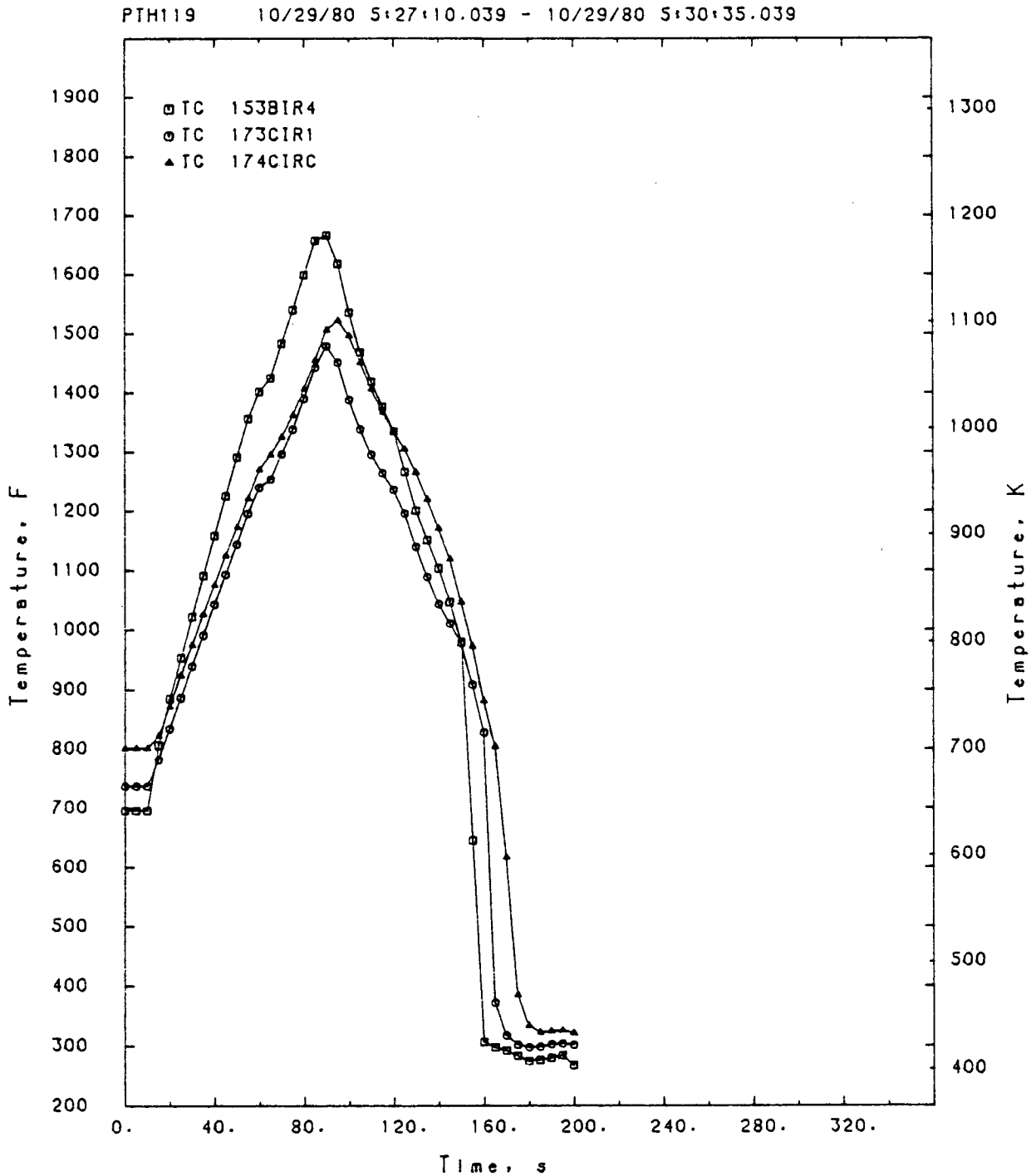

FIGURE 1.2.4.19 TEST FUEL ROD CENTER AND INTERIOR CLADDING TEMPERATURE HISTORIES DURING TRANSIENT PTH119

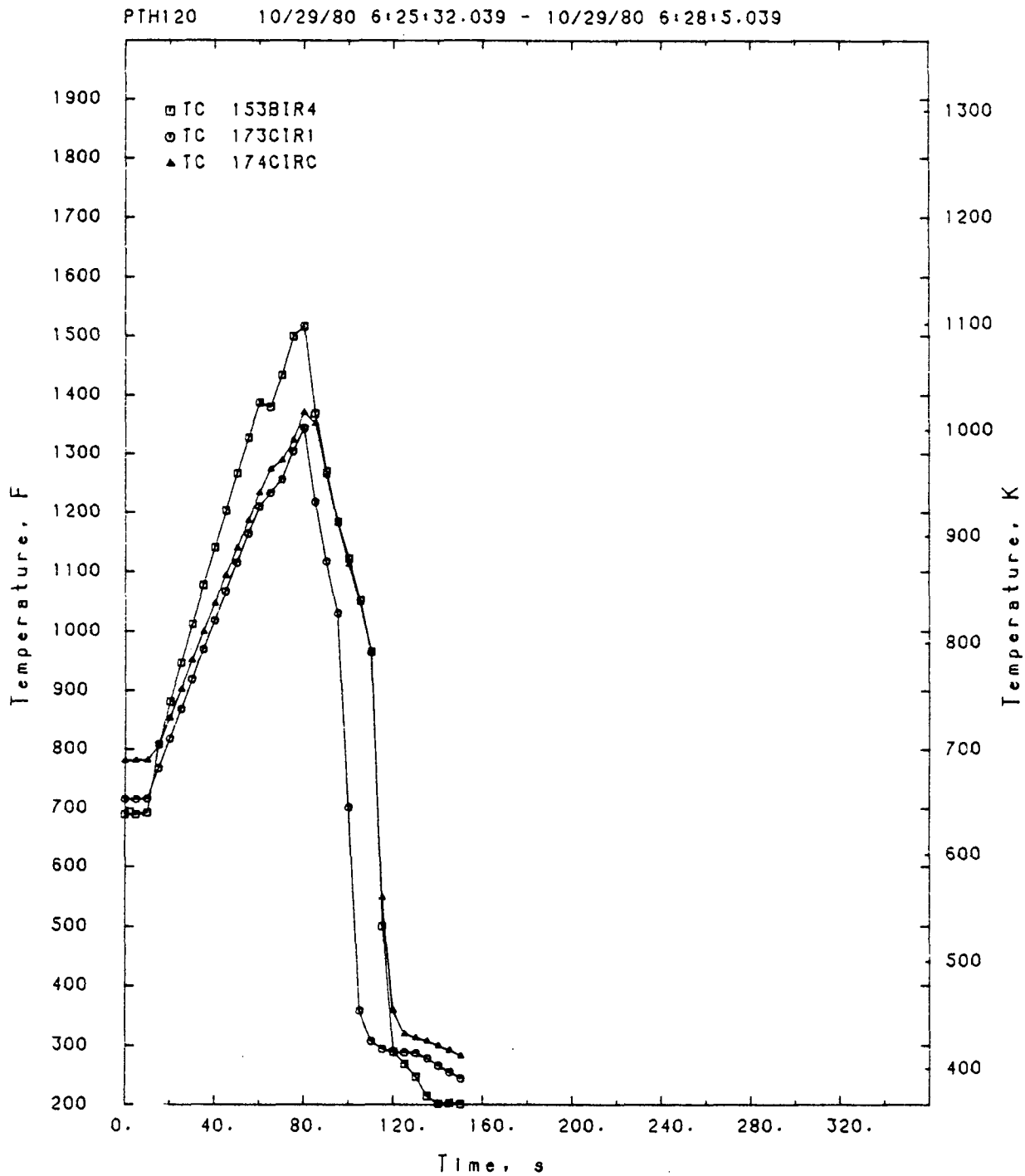

FIGURE 1.2.4.20 TEST FUEL ROD CENTER AND INTERIOR CLADDING TEMPERATURE HISTORIES DURING TRANSIENT PTH120

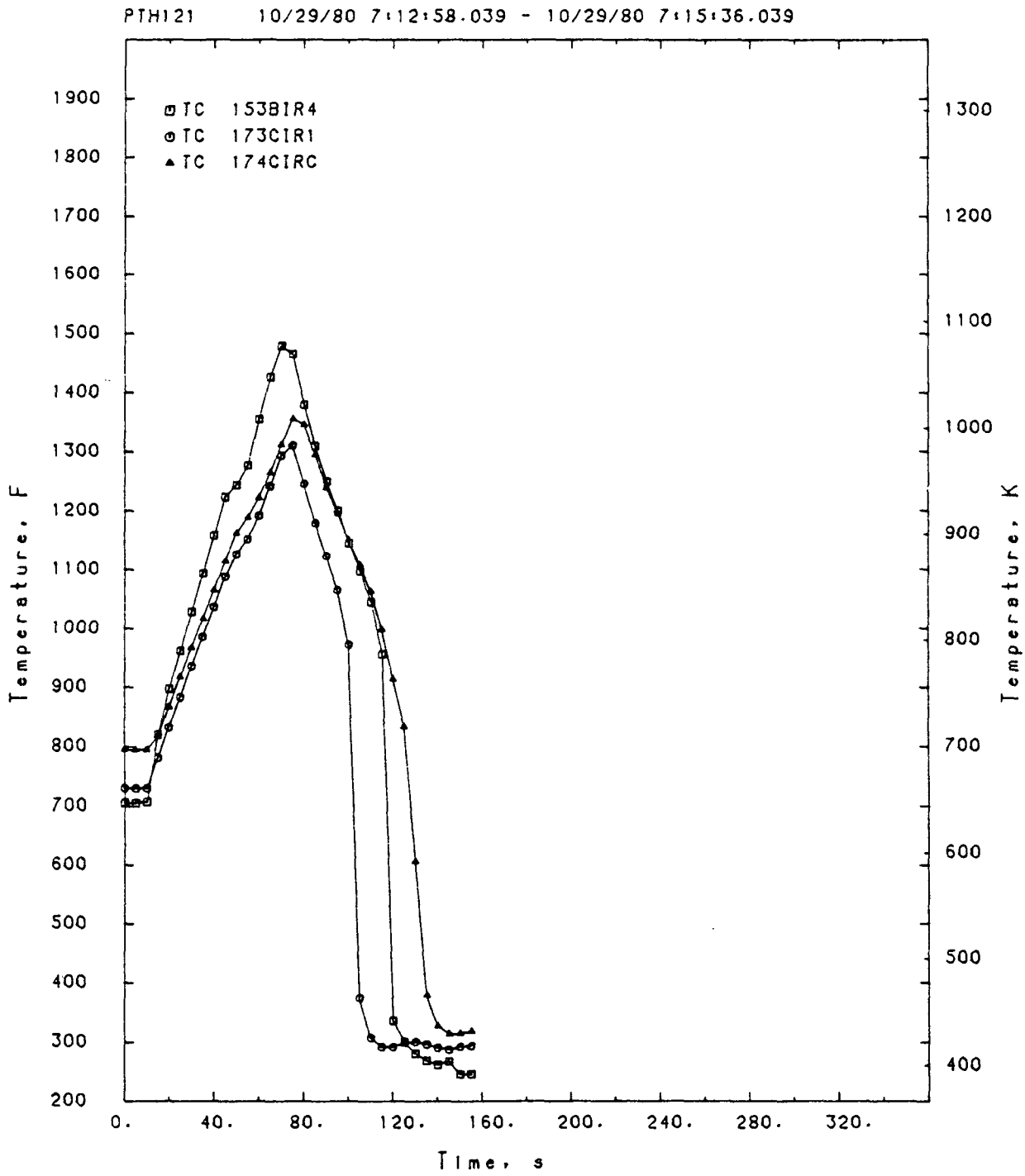

FIGURE 1.2.4.21 TEST FUEL ROD CENTER AND INTERIOR CLADDING TEMPERATURE HISTORIES DURING TRANSIENT PTH121

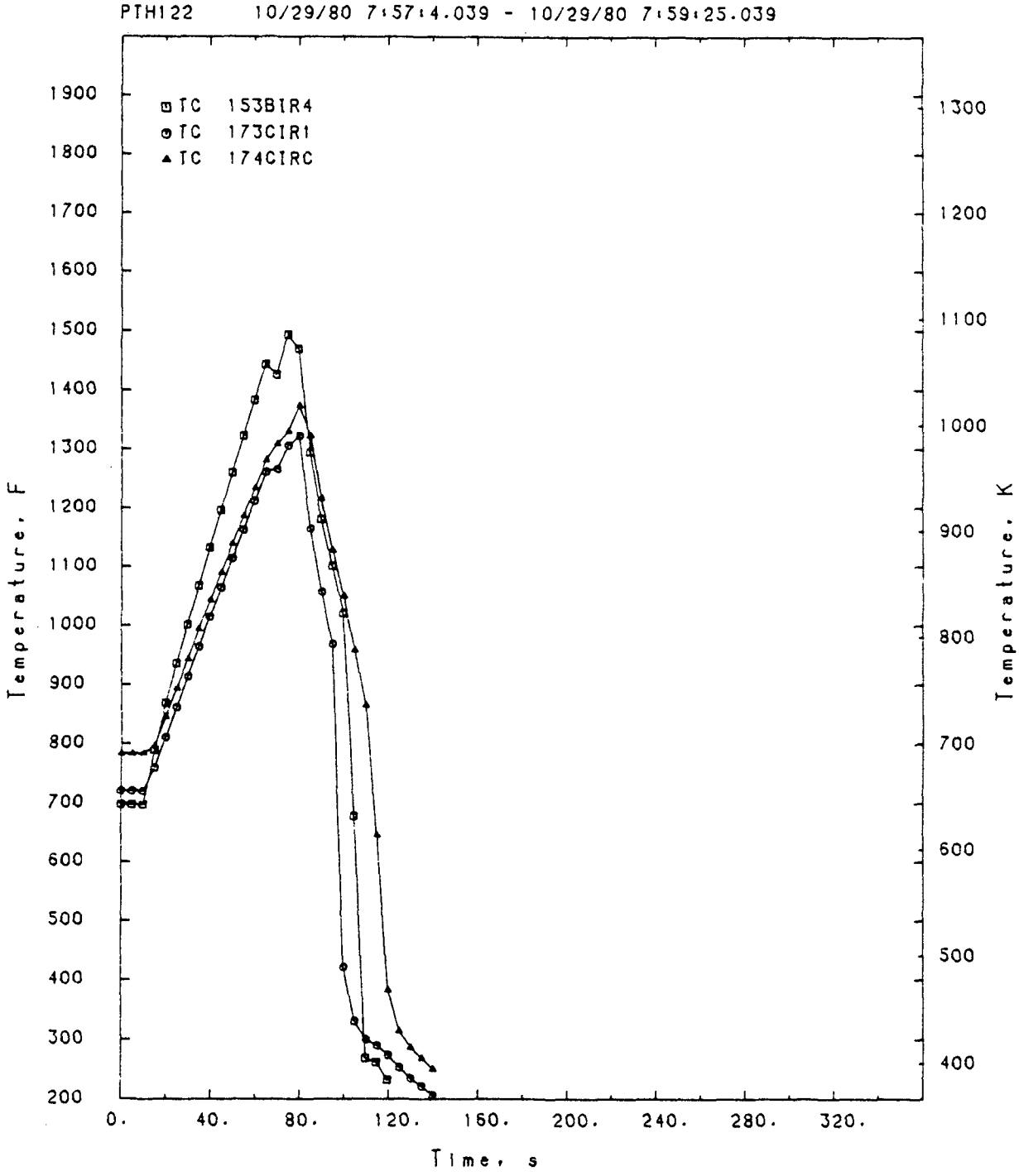

FIGURE 1.2.4.22 TEST FUEL ROD CENTER AND INTERIOR CLADDING TEMPERATURE HISTORIES DURING TRANSIENT PTH122

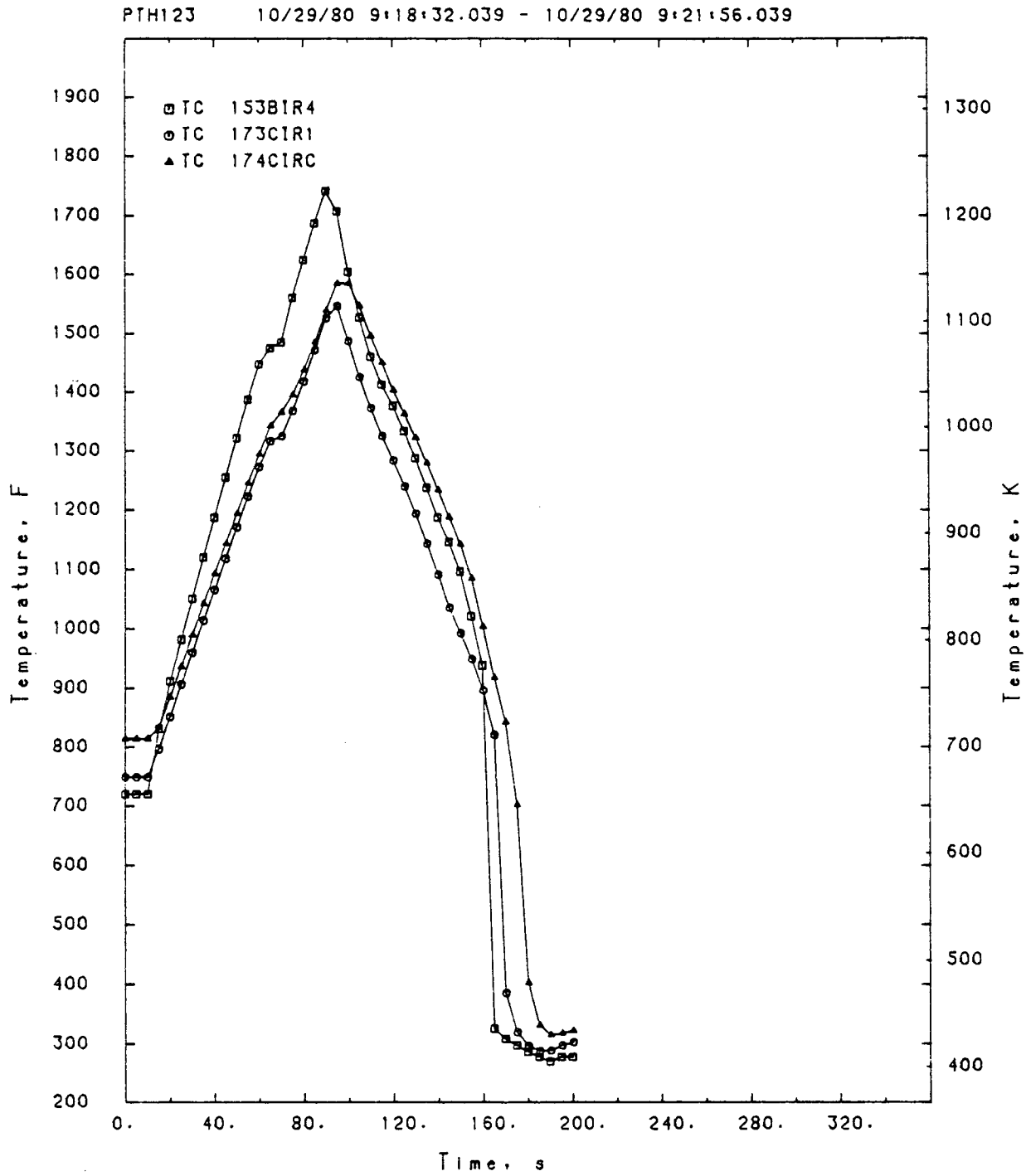

FIGURE 1.2.4.23 TEST FUEL ROD CENTER AND INTERIOR CLADDING TEMPERATURE HISTORIES DURING TRANSIENT PTH123

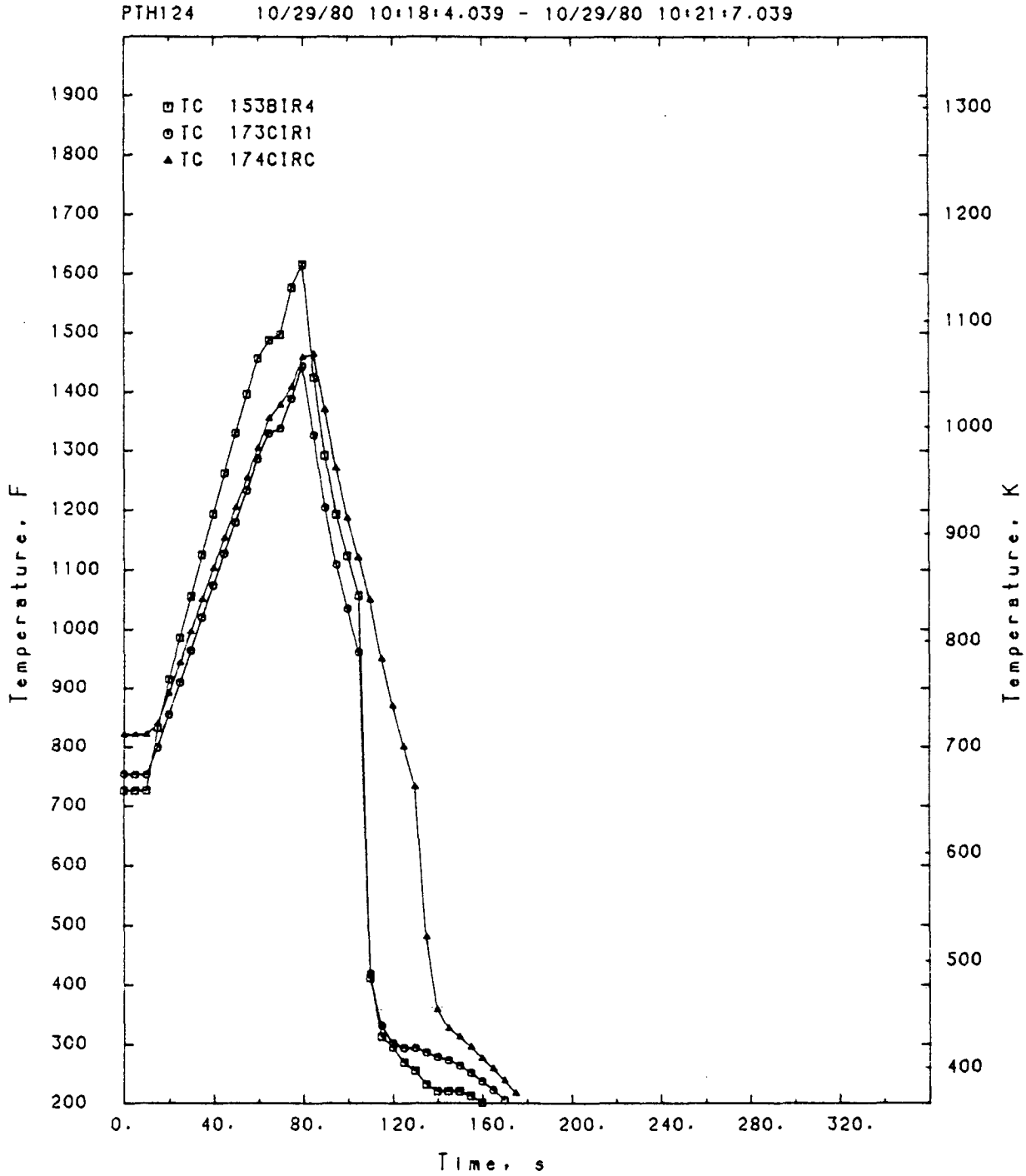

FIGURE 1.2.4.24 TEST FUEL ROD CENTER AND INTERIOR CLADDING TEMPERATURE HISTORIES DURING TRANSIENT PTH124

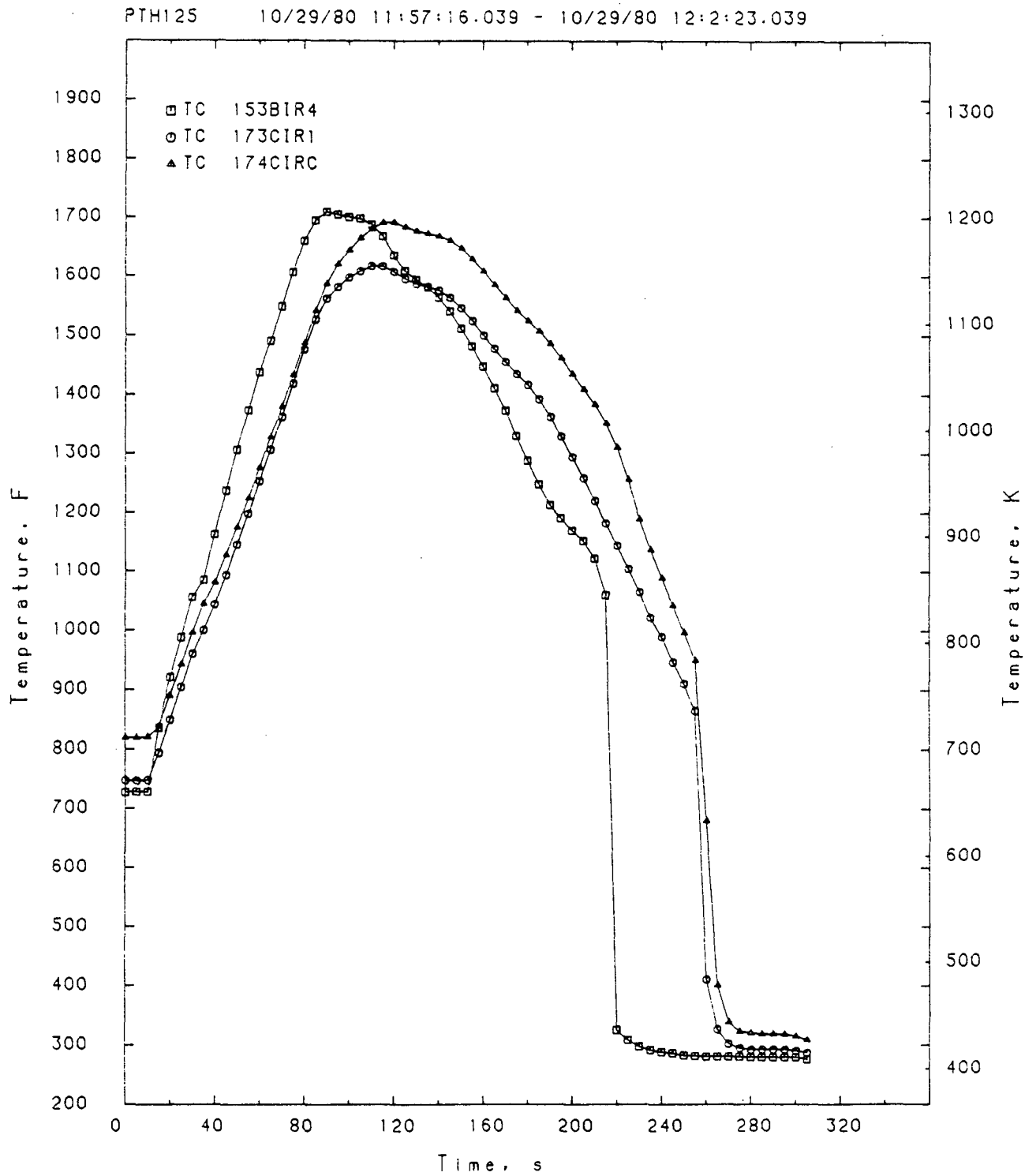

FIGURE 1.2.4.25 TEST FUEL ROD CENTER AND INTERIOR CLADDING TEMPERATURE HISTORIES DURING TRANSIENT PTH125

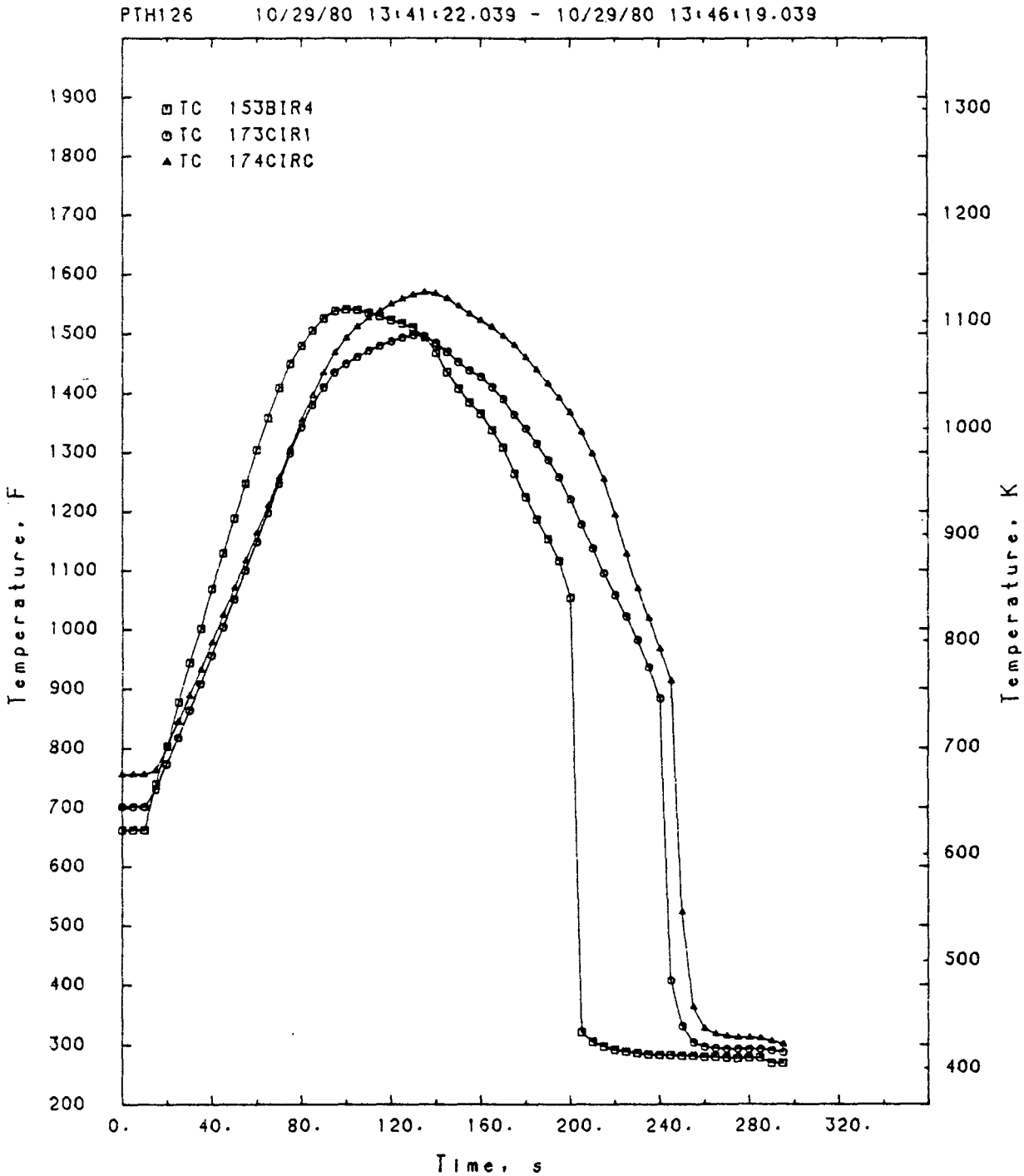

FIGURE 1.2.4.26 TEST FUEL ROD CENTER AND INTERIOR CLADDING TEMPERATURE HISTORIES DURING TRANSIENT PTH126

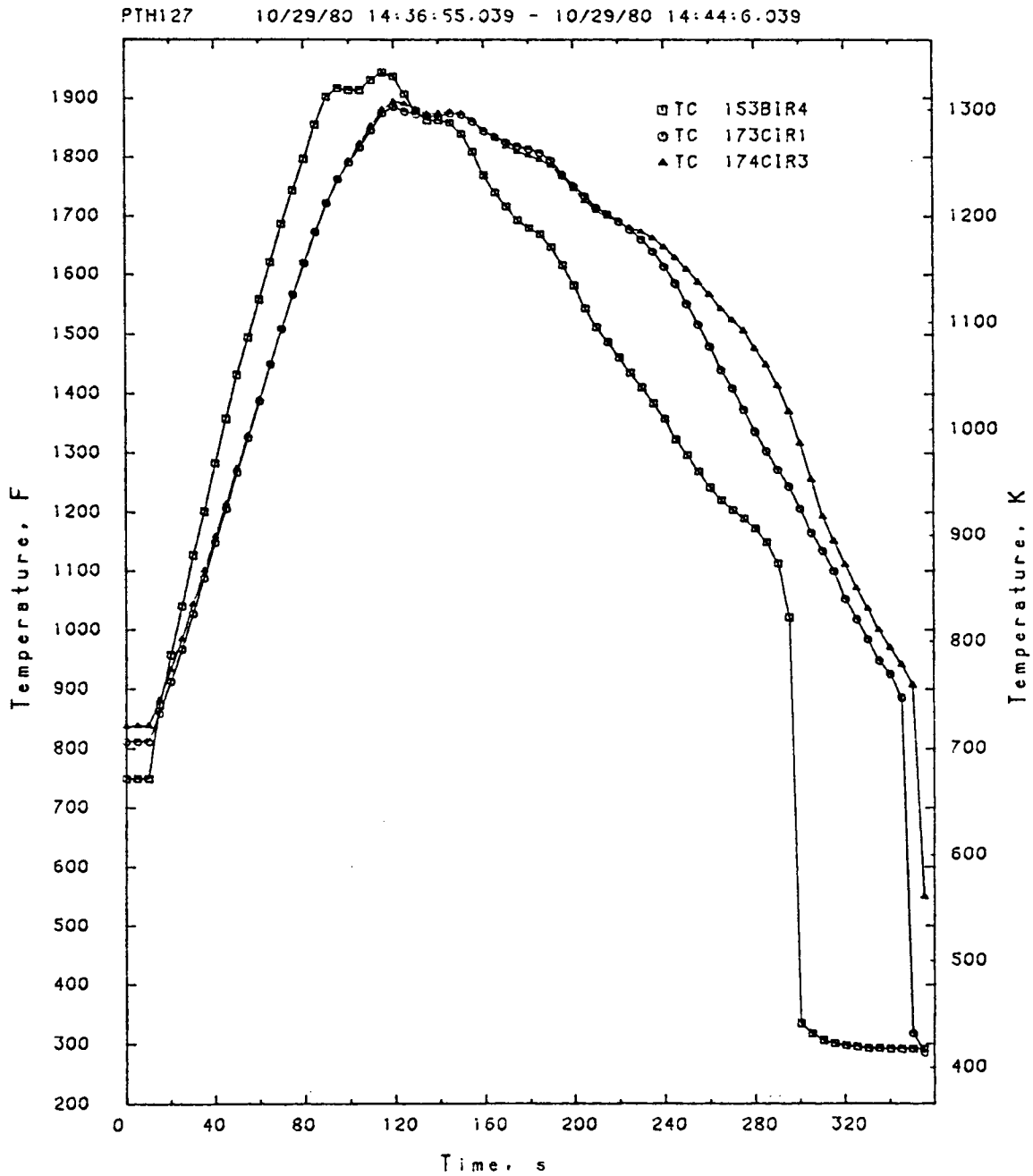

FIGURE 1.2.4.27 TEST FUEL ROD CENTER AND INTERIOR CLADDING TEMPERATURE HISTORIES DURING TRANSIENT PTH127

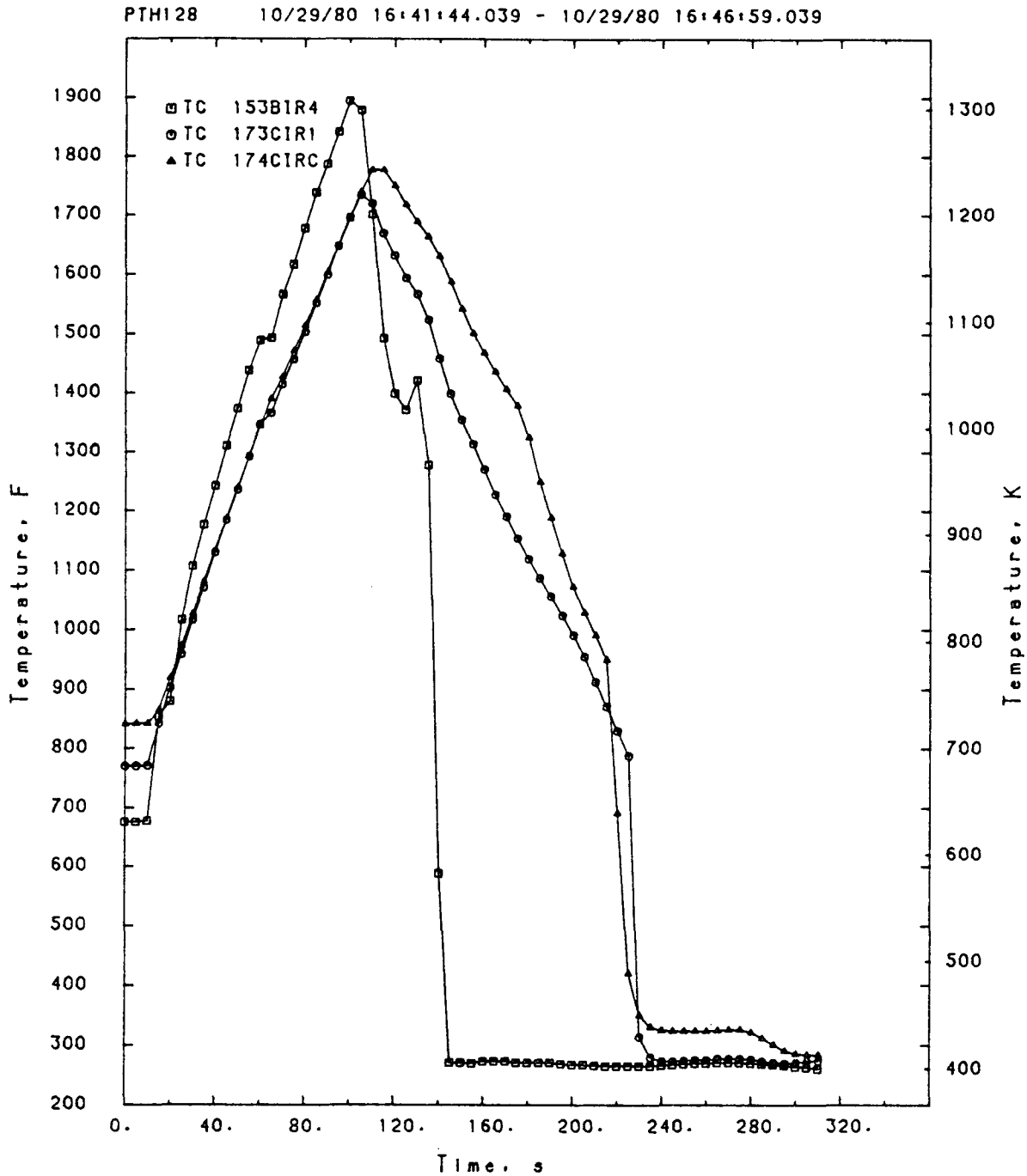

FIGURE 1.2.4.28 TEST FUEL ROD CENTER AND INTERIOR CLADDING TEMPERATURE HISTORIES DURING TRANSIENT PTH128

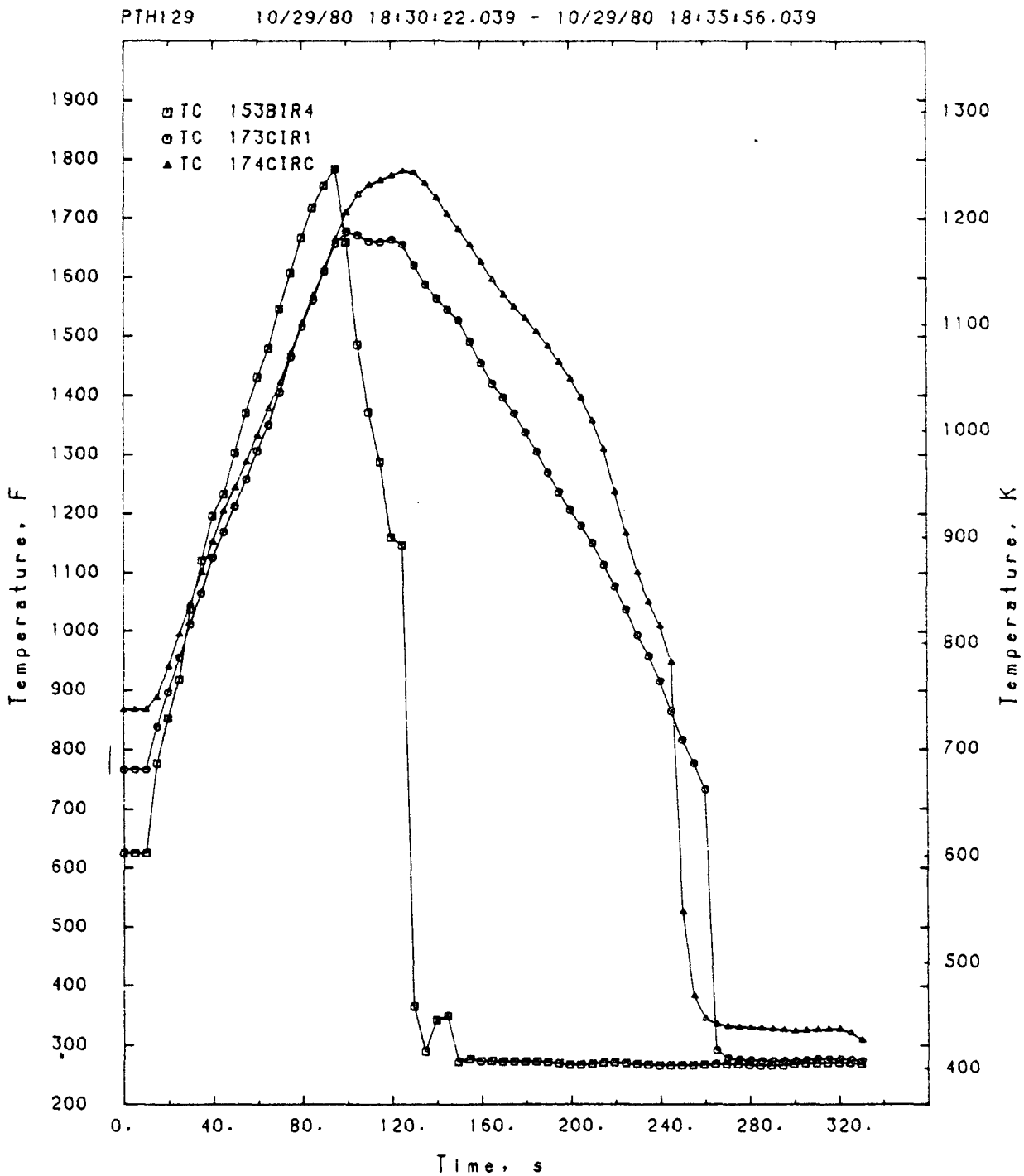

FIGURE 1.2.4.29 TEST FUEL ROD CENTER AND INTERIOR CLADDING TEMPERATURE HISTORIES DURING TRANSIENT PTH129

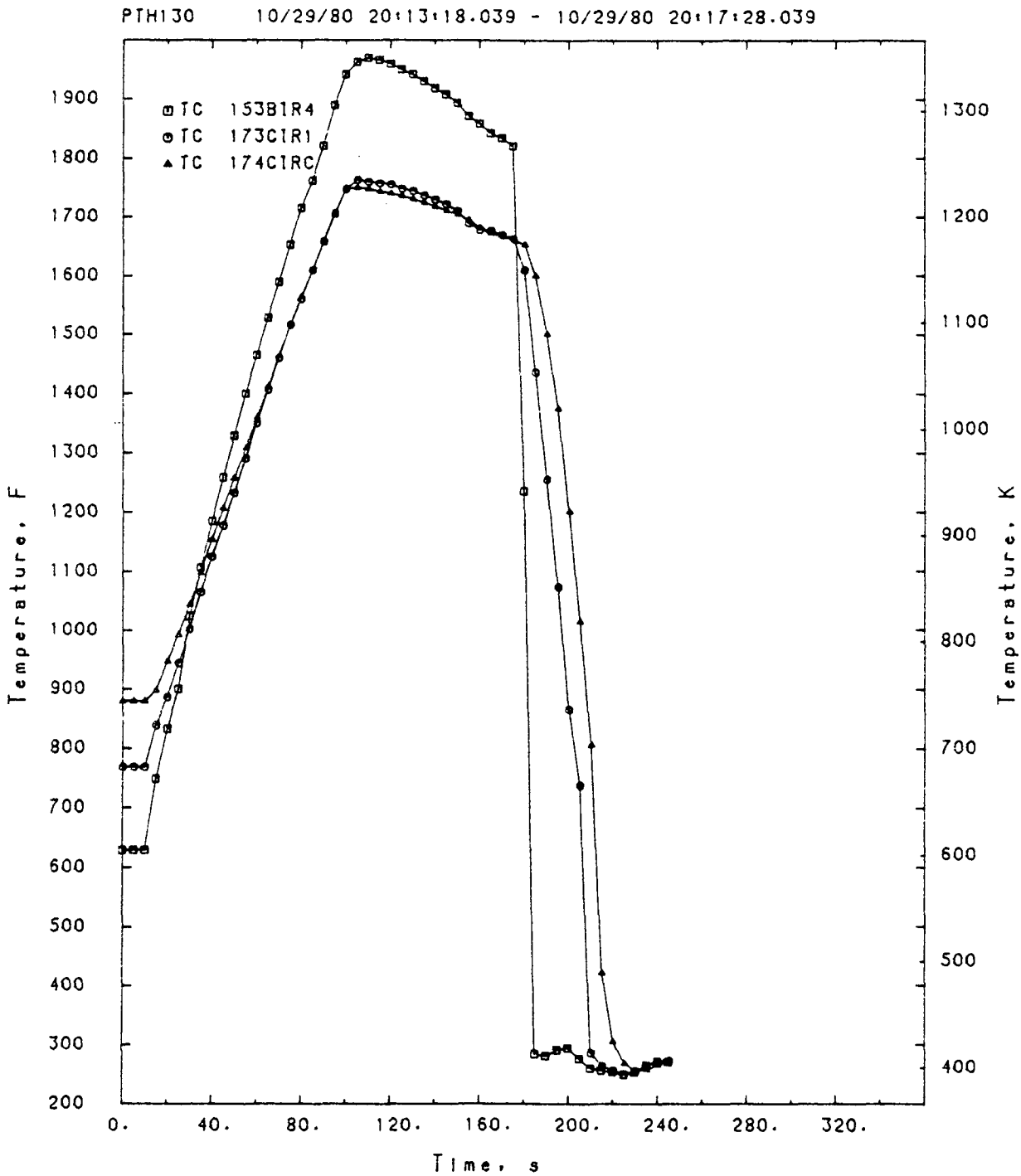

FIGURE 1.2.4.30 TEST FUEL ROD CENTER AND INTERIOR CLADDING TEMPERATURE HISTORIES DURING TRANSIENT PTH130

PART 2

NEUTRON FLUX DISTRIBUTIONS

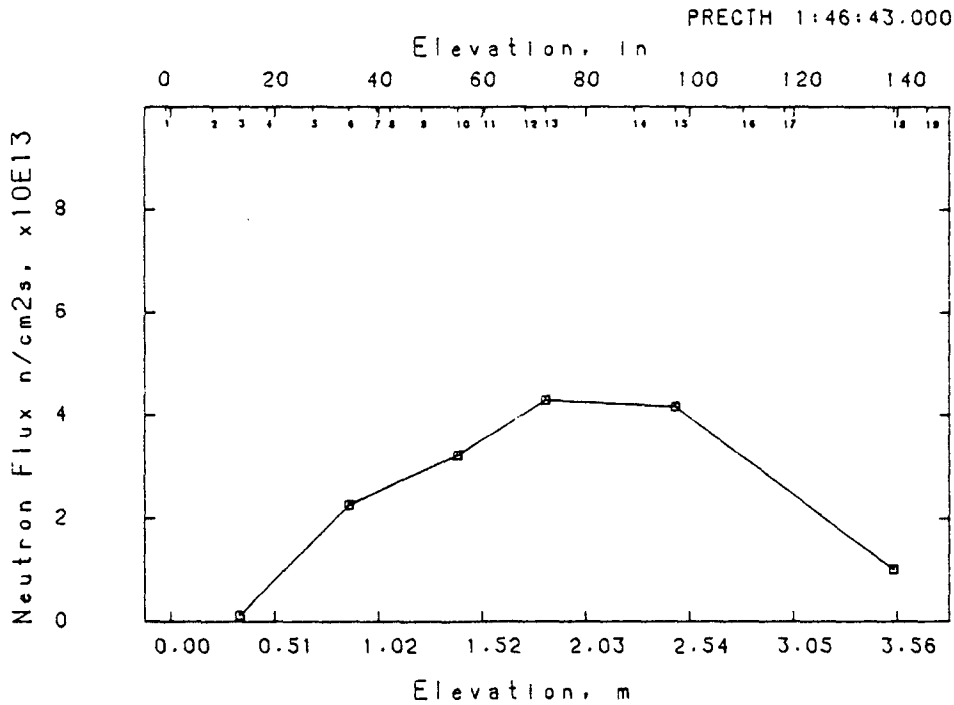

FIGURE 2.1.1 PRECONDITIONING (INSTRUMENT TUBE) NEUTRON FLUX AXIAL PROFILE

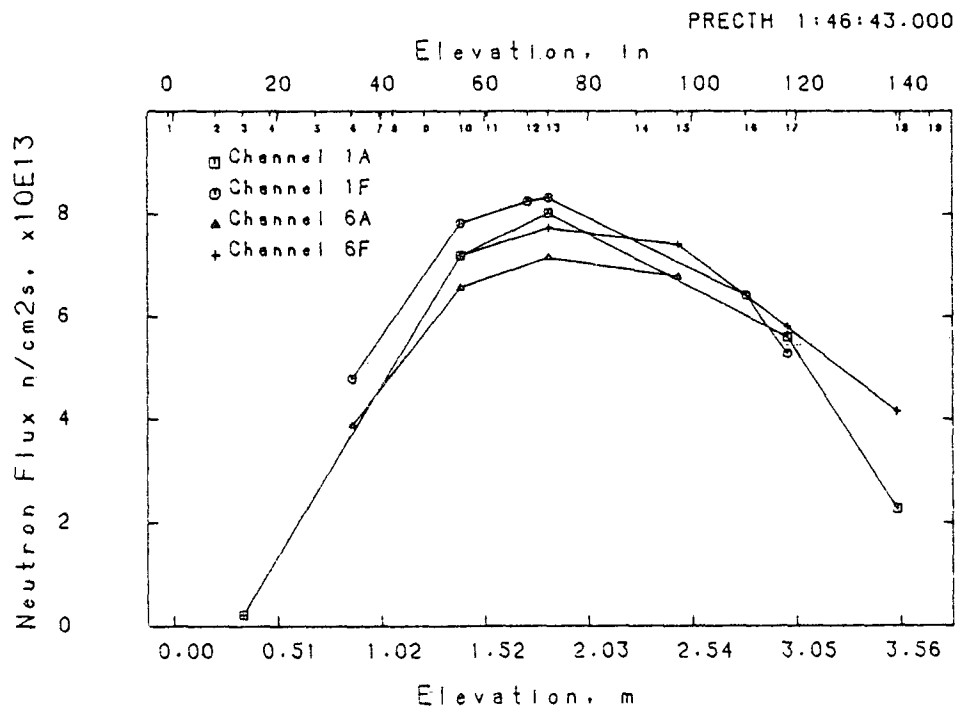

FIGURE 2.1.2 PRECONDITIONING (SHROUD) NEUTRON FLUX AXIAL PROFILES

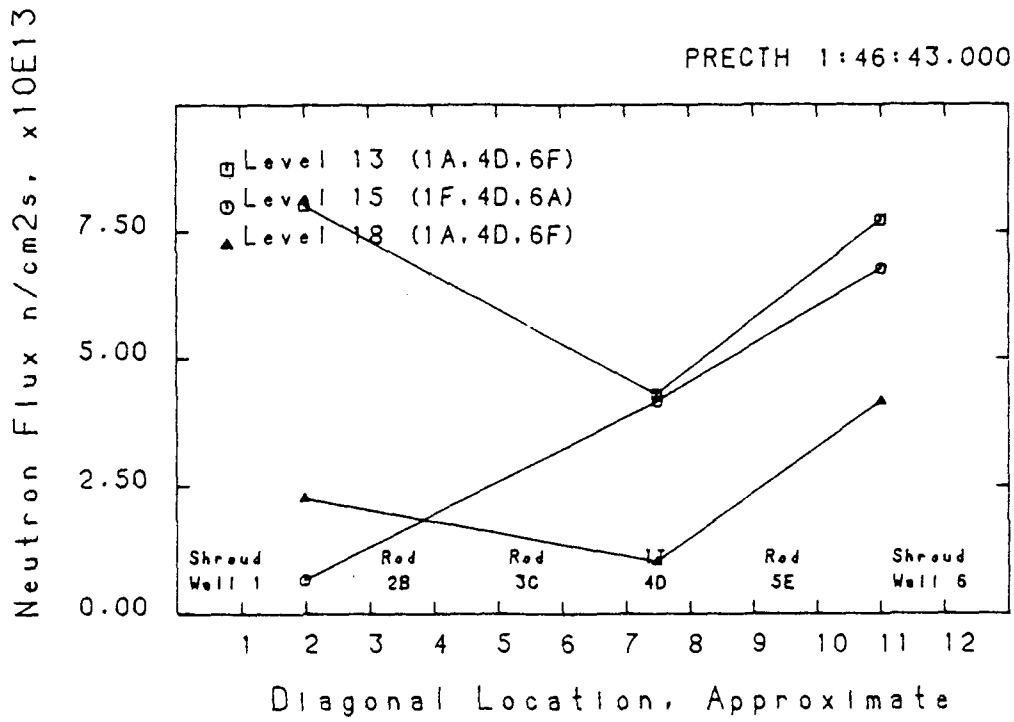

FIGURE 2.1.3 DIAGONAL NEUTRON FLUX PROFILE ACROSS TEST ASSEMBLY - PRECONDITIONING

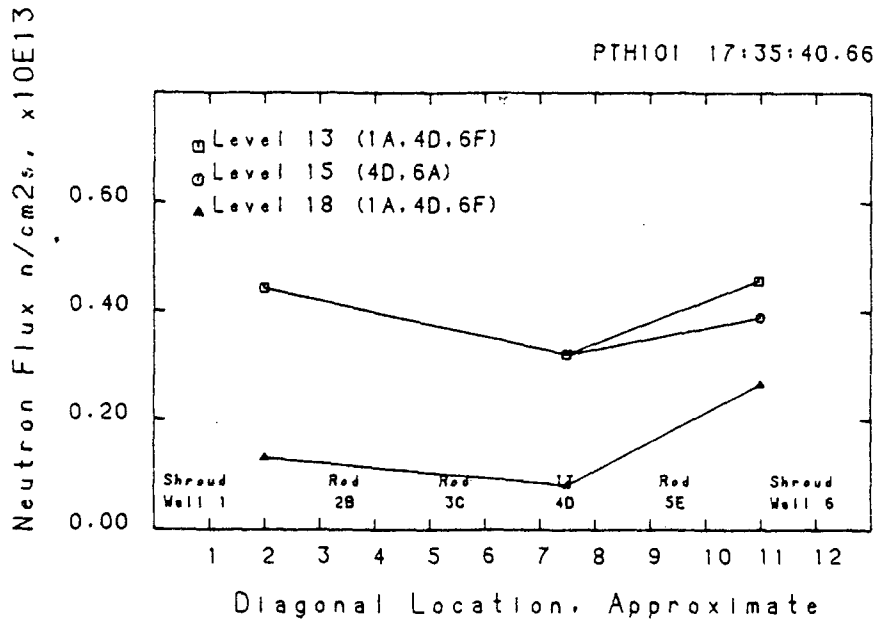

FIGURE 2.2.1.1 DIAGONAL NEUTRON FLUX PROFILE ACROSS THE TEST ASSEMBLY - PRETRANSIENT - PTH101

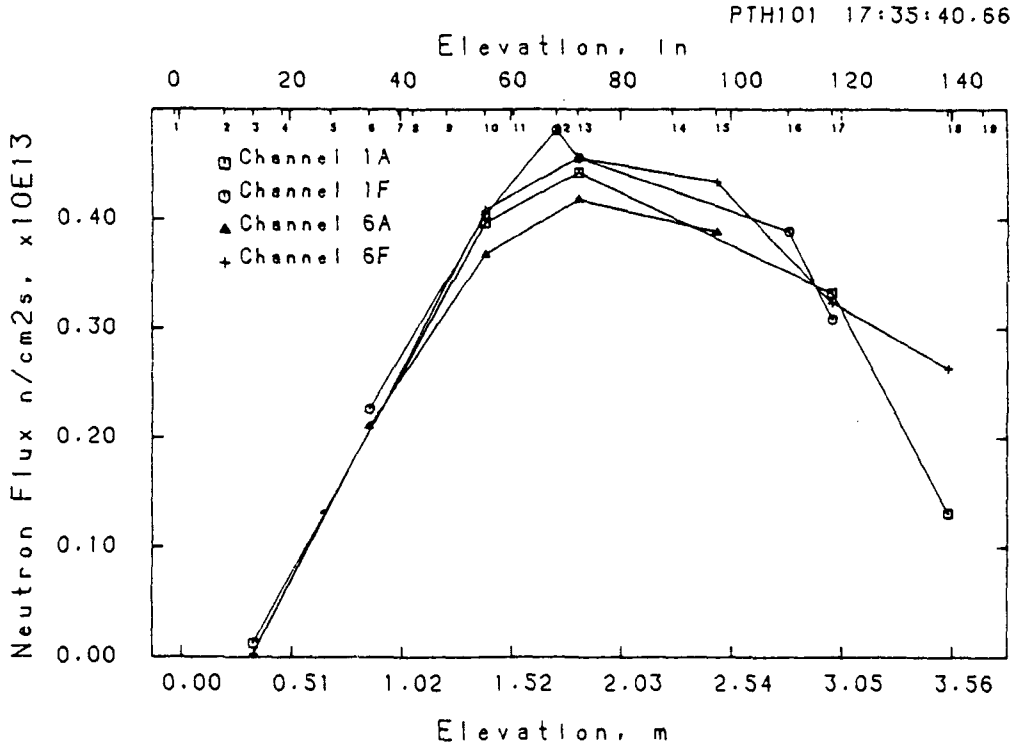

FIGURE 2.2.1.2 PRETRANSIENT SHROUD NEUTRON FLUX AXIAL PROFILE

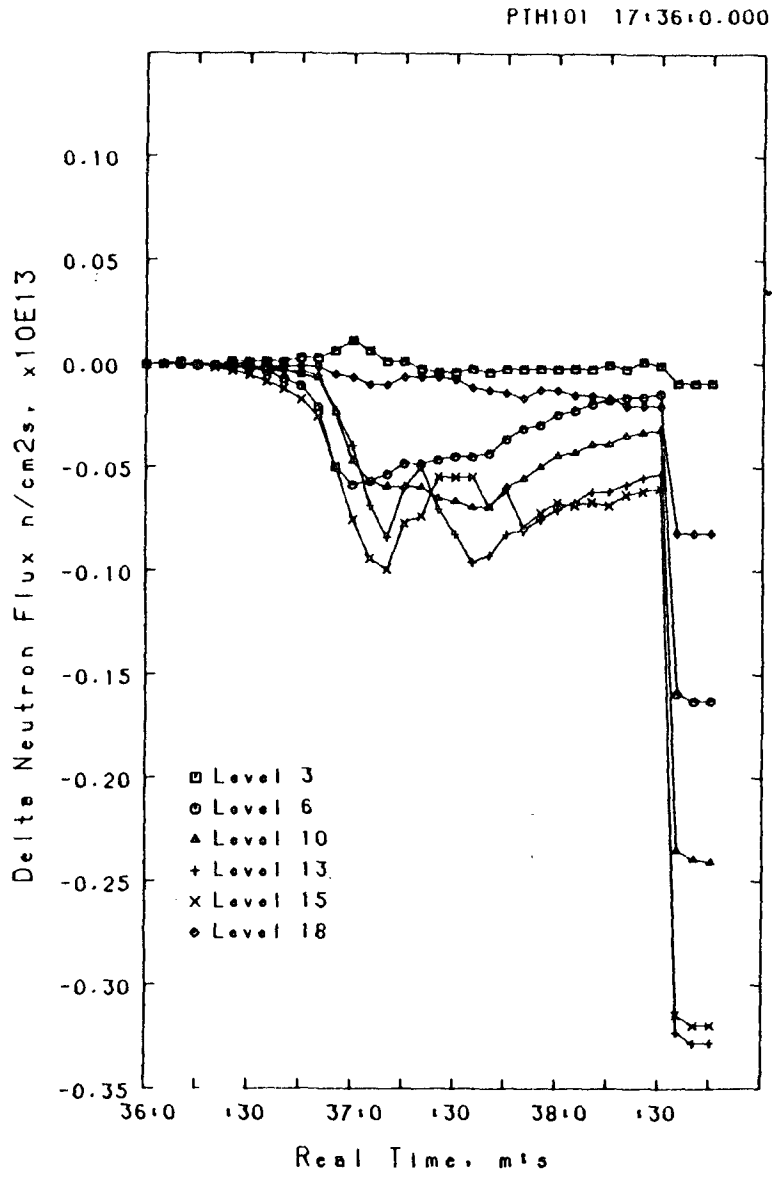

FIGURE 2.2.2.01 CHANGING IT NEUTRON FLUX AFTER PTH101 REFLOODING BEGINS. T=36:18S

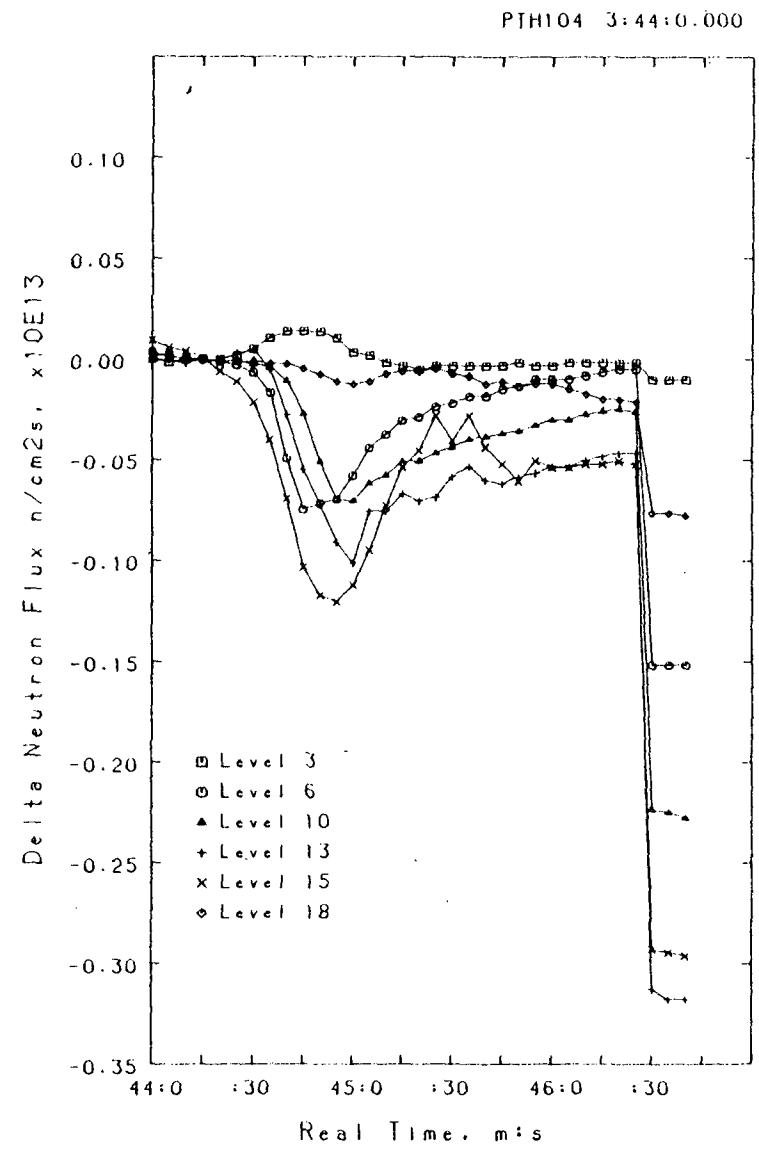

FIGURE 2.2.2.04 CHANGING IT NEUTRON FLUX AFTER PTH104 REFLOODING BEGINS. T=44M:27S

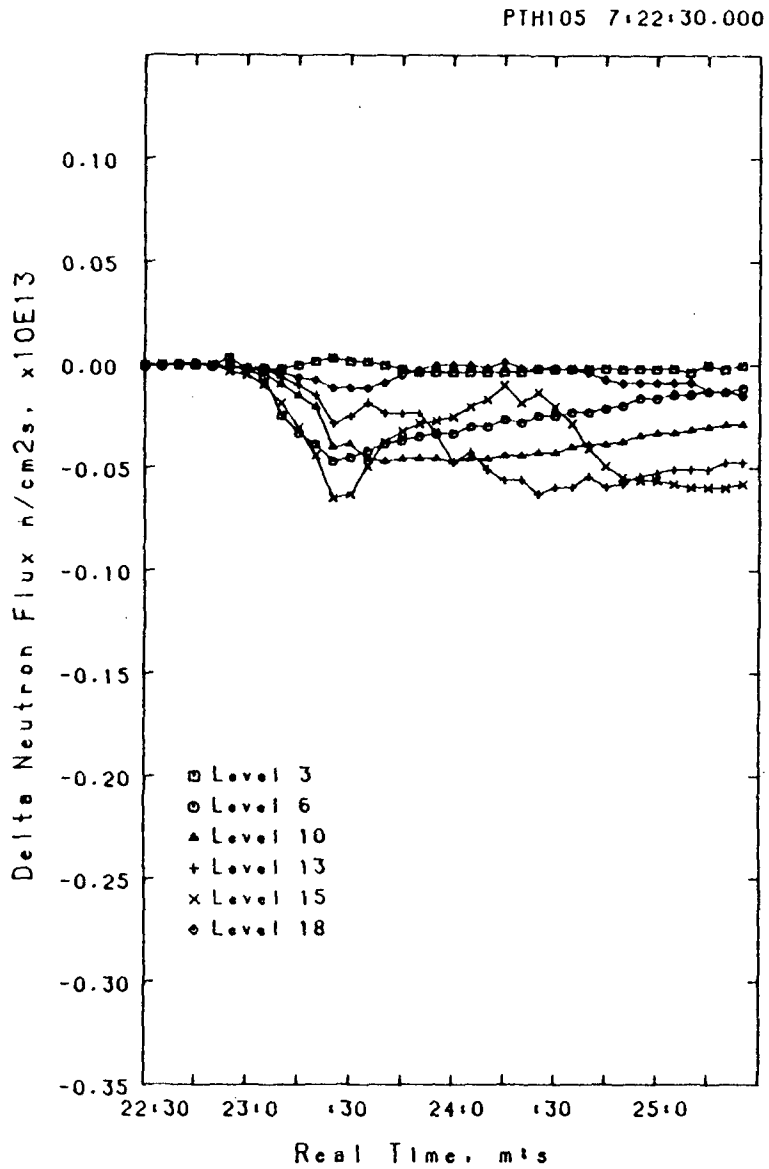

FIGURE 2.2.2.05 CHANGING IT NEUTRON FLUX AFTER PTH105 REFLOODING BEGINS. T=22:51S

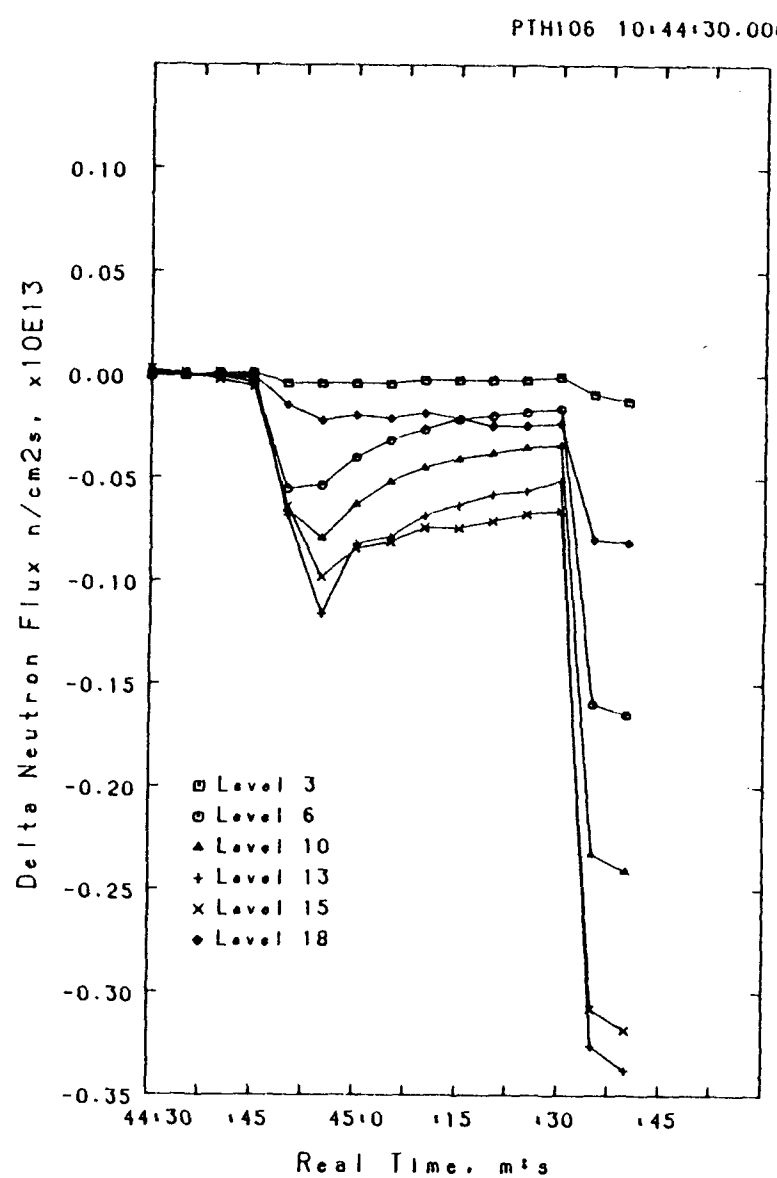

FIGURE 2.2.2.06 CHANGING IT NEUTRON FLUX AFTER PTH106 REFLOODING BEGINS. T=44:41S

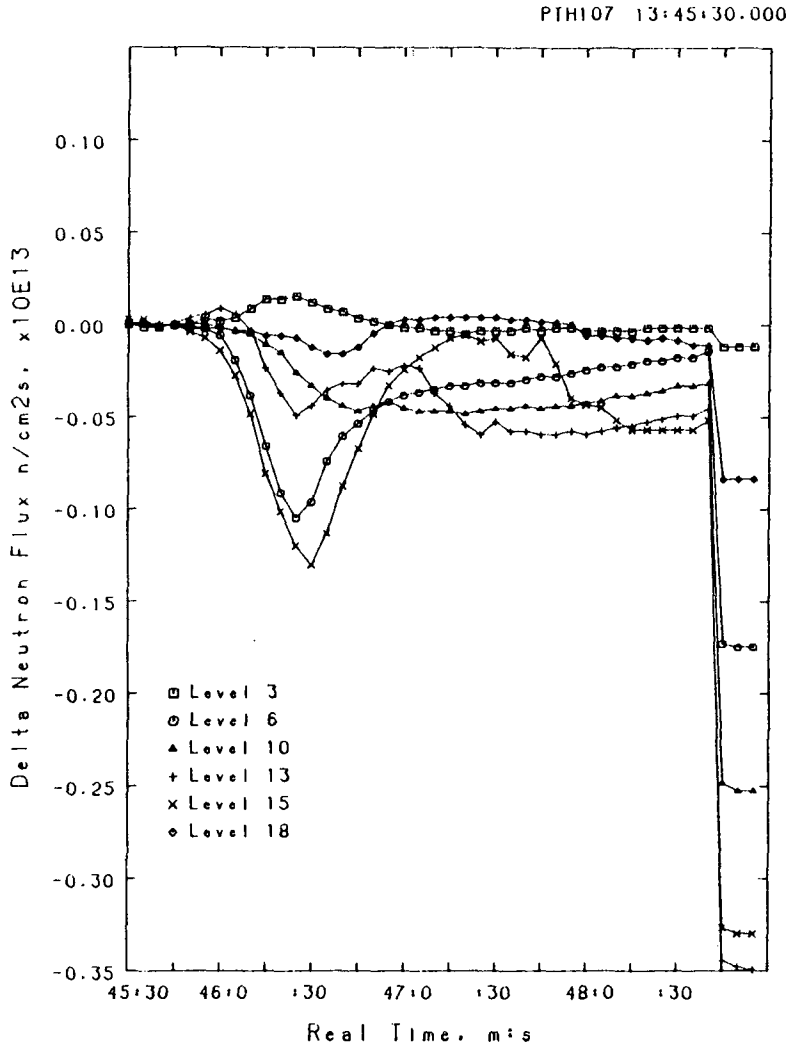

FIGURE 2.2.2.07 CHANGING IT NEUTRON FLUX AFTER PTH107 REFLOODING BEGINS, T=45M:50S

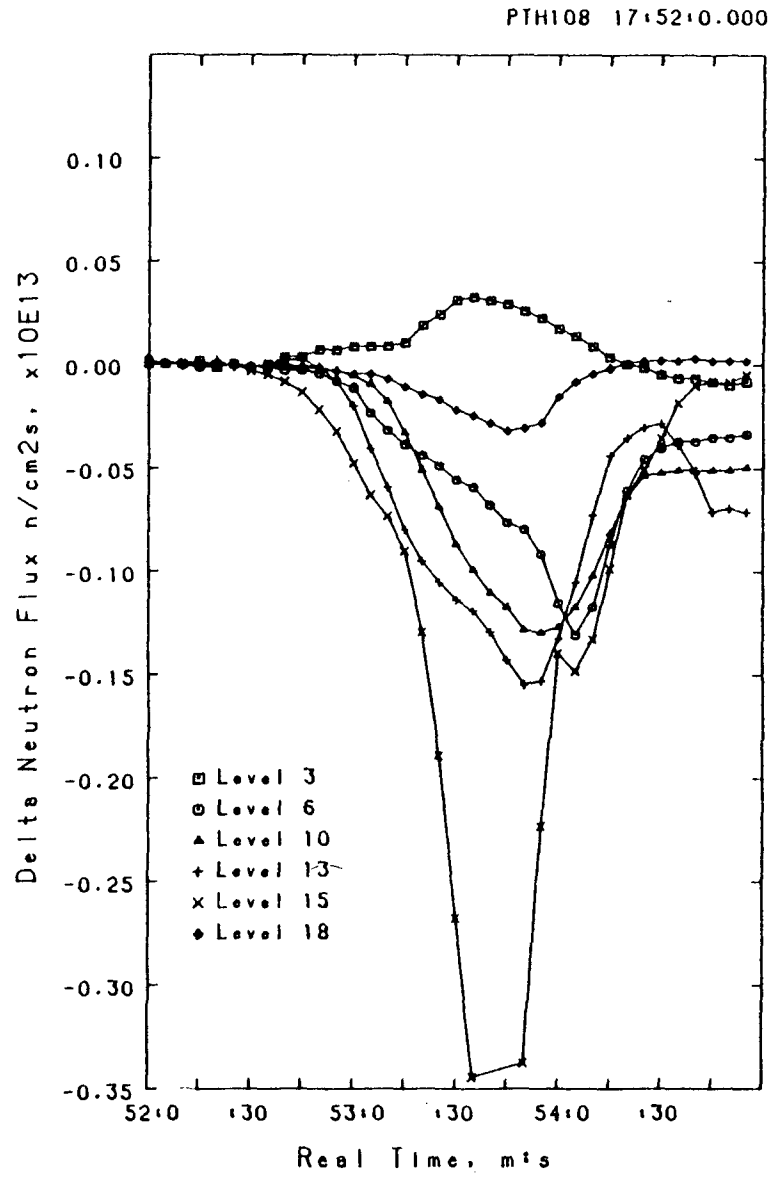

FIGURE 2.2.2.08 CHANGING IT NEUTRON FLUX AFTER PTH108 REFLOODING BEGINS, T=52:41S

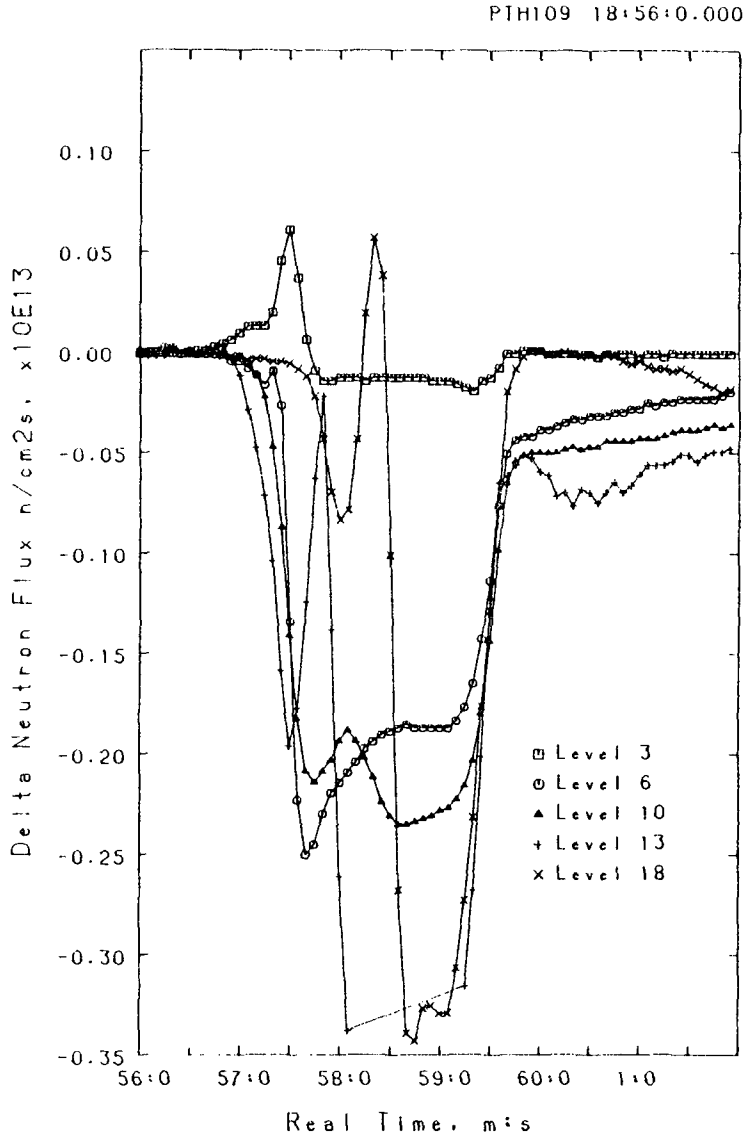

FIGURE 2.2.2.09 CHANGING IT NEUTRON FLUX AFTER PTH109 REFLOODING BEGINS. T=56M:47S

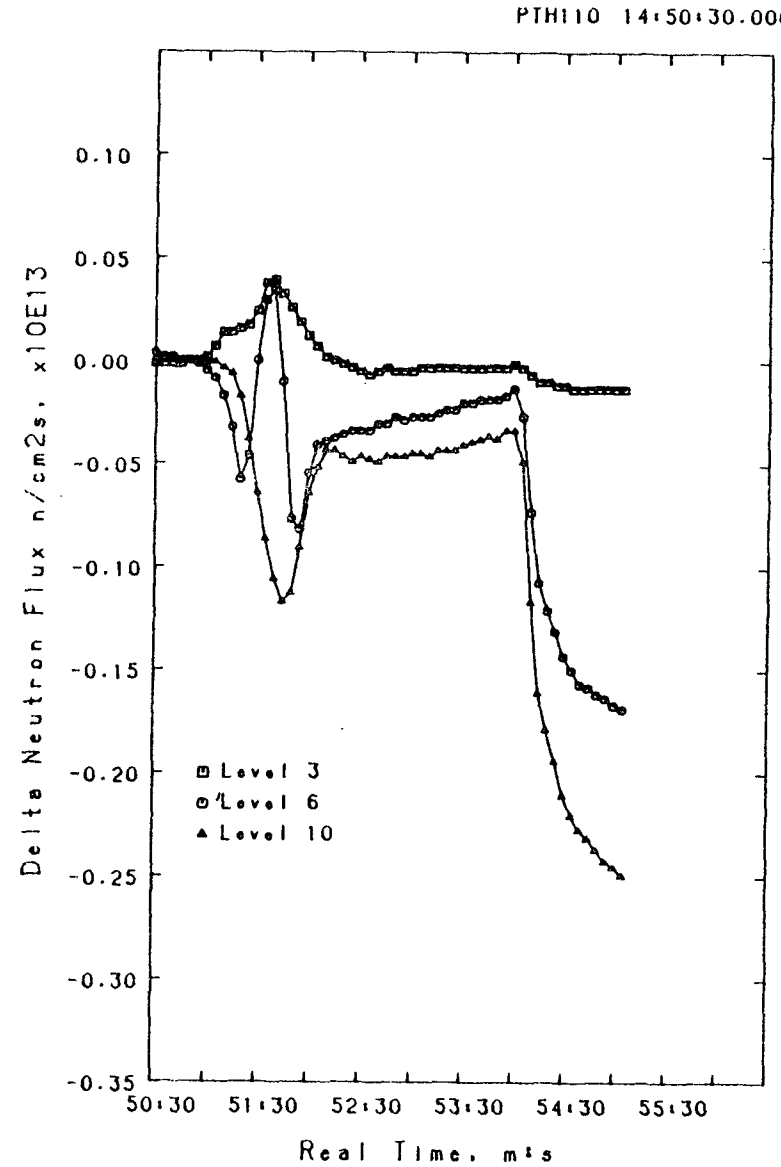

FIGURE 2.2.2.10 CHANGING IT NEUTRON FLUX AFTER PTH110 REFLOODING BEGINS. T=51:02S

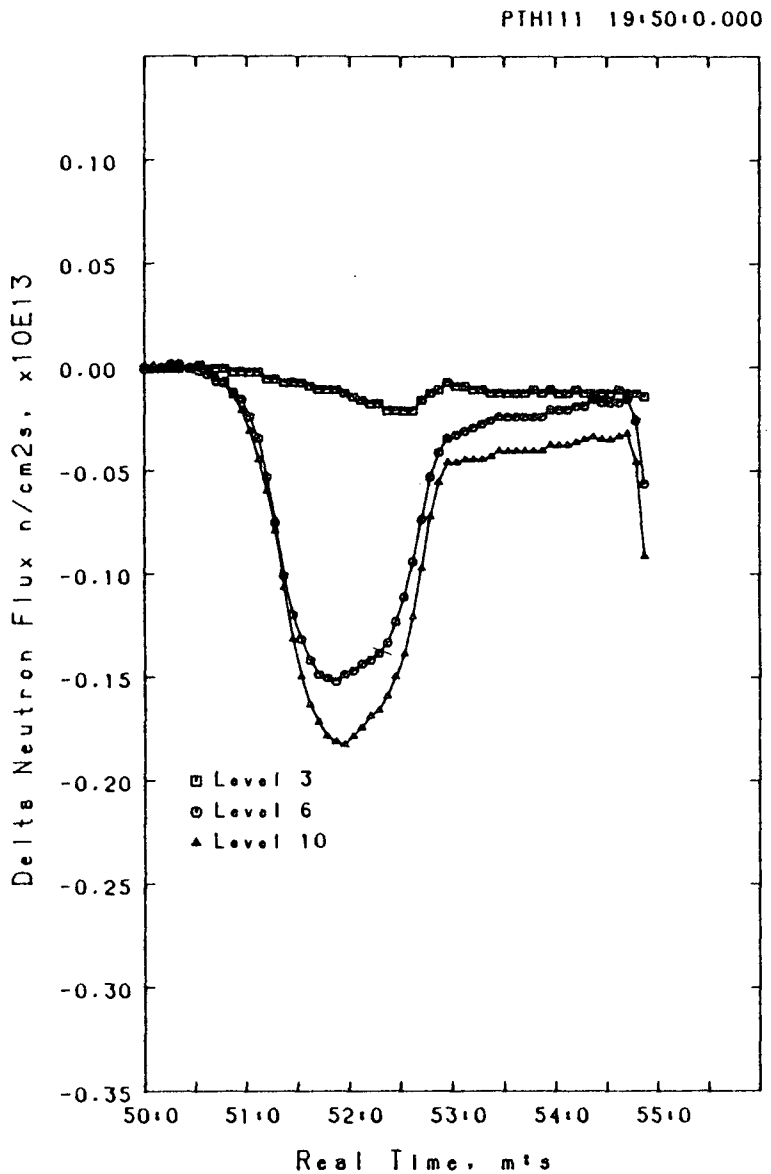

FIGURE 2.2.2.11 CHANGING IT NEUTRON FLUX AFTER PTH111 REFLOODING BEGINS, T=50:31S

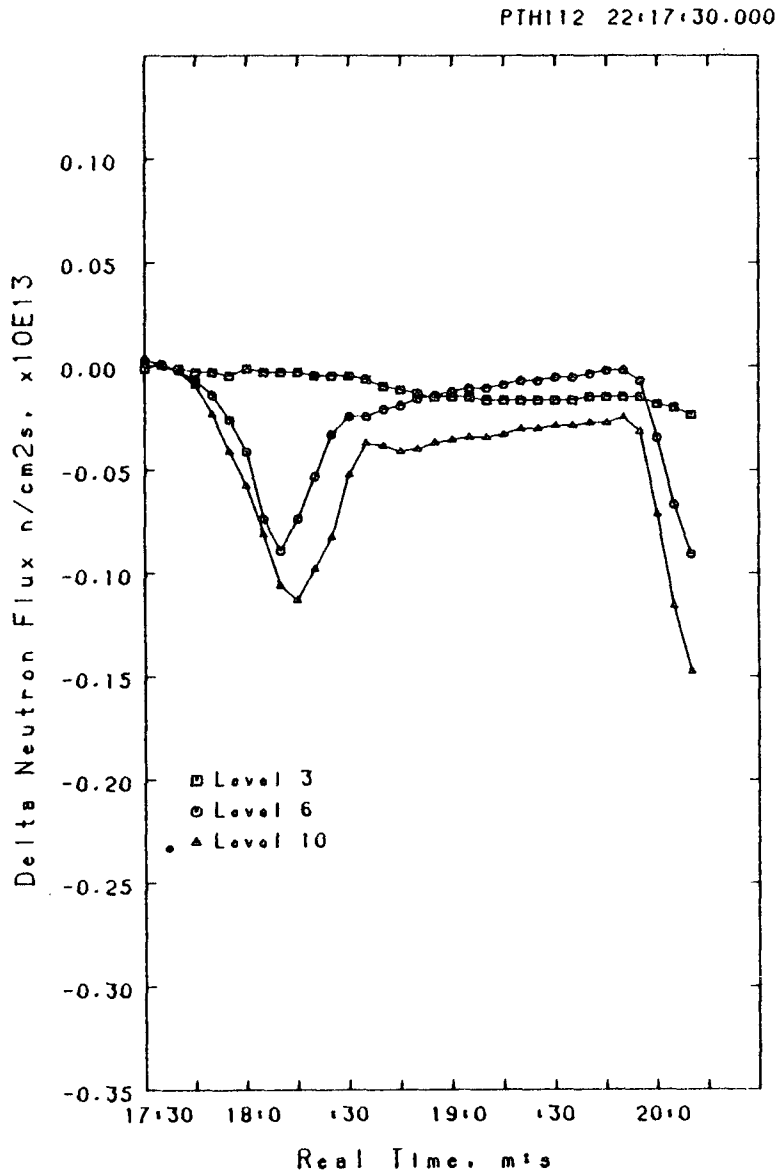

FIGURE 2.2.2.12 CHANGING IT NEUTRON FLUX AFTER PTH112 REFLOODING BEGINS, T=17:43S

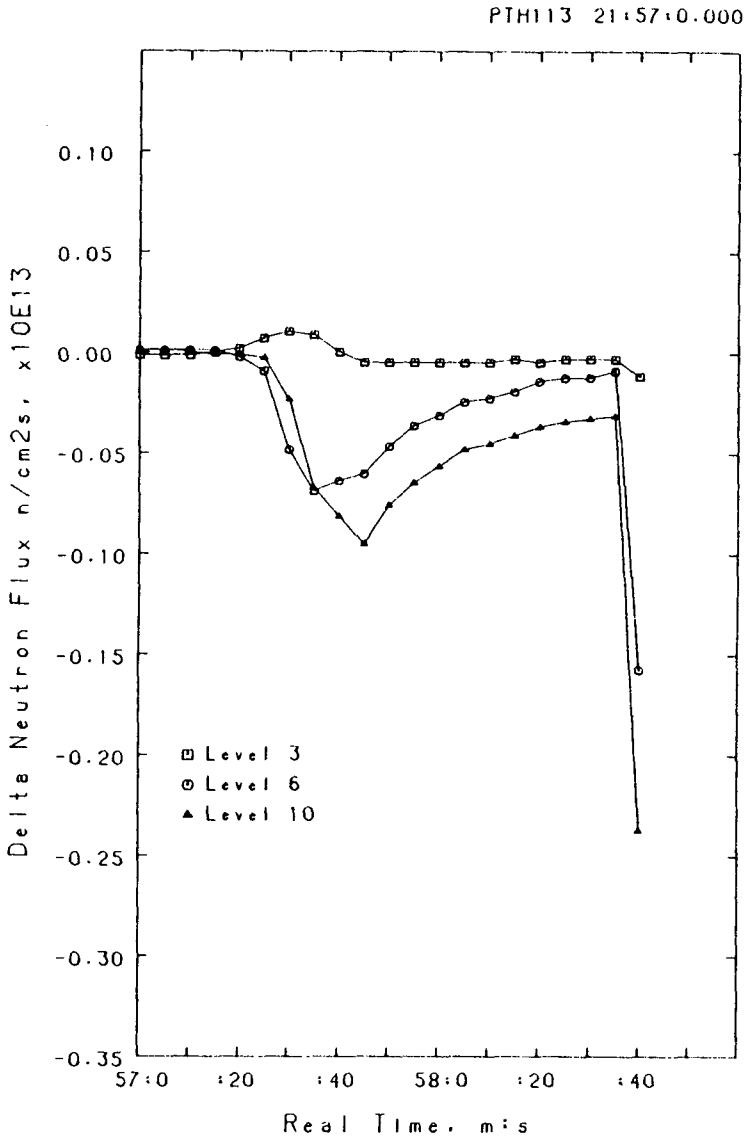

FIGURE 2.2.2.13 CHANGING IT NEUTRON FLUX AFTER PTH113 REFLOODING BEGINS. T=57M:22S

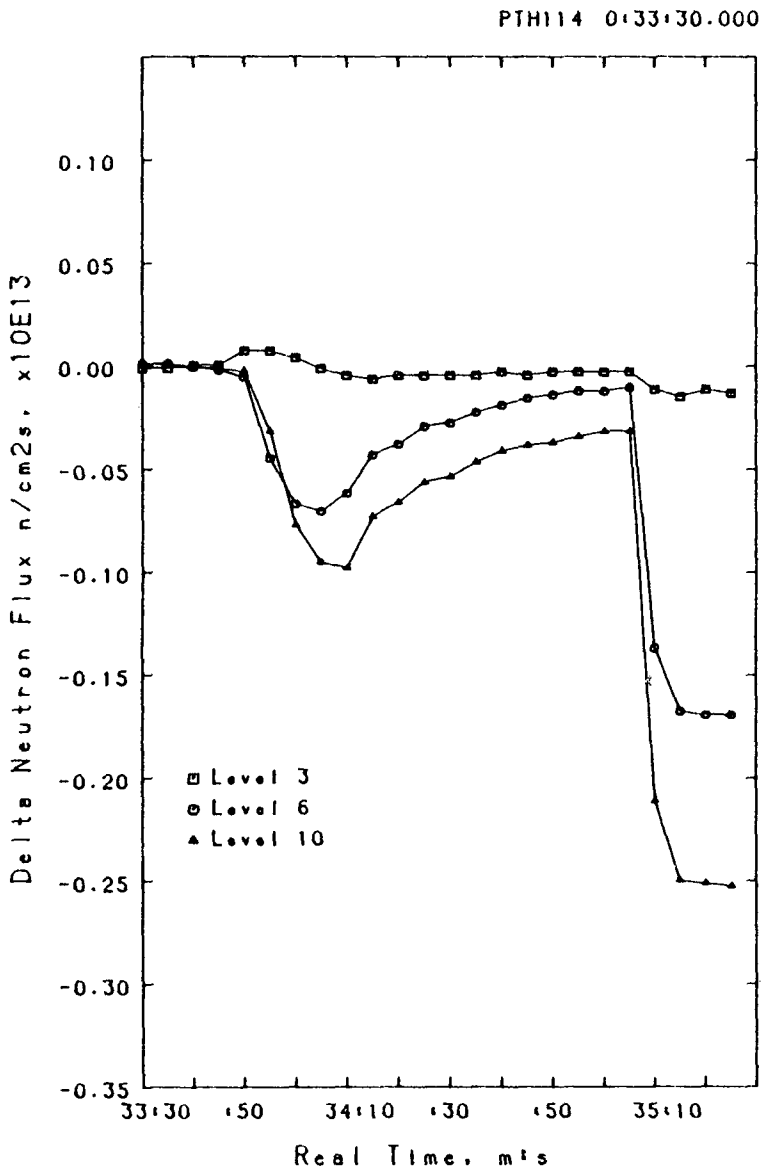

FIGURE 2.2.2.14 CHANGING IT NEUTRON FLUX AFTER PTH114 REFLOODING BEGINS. T=33:46S

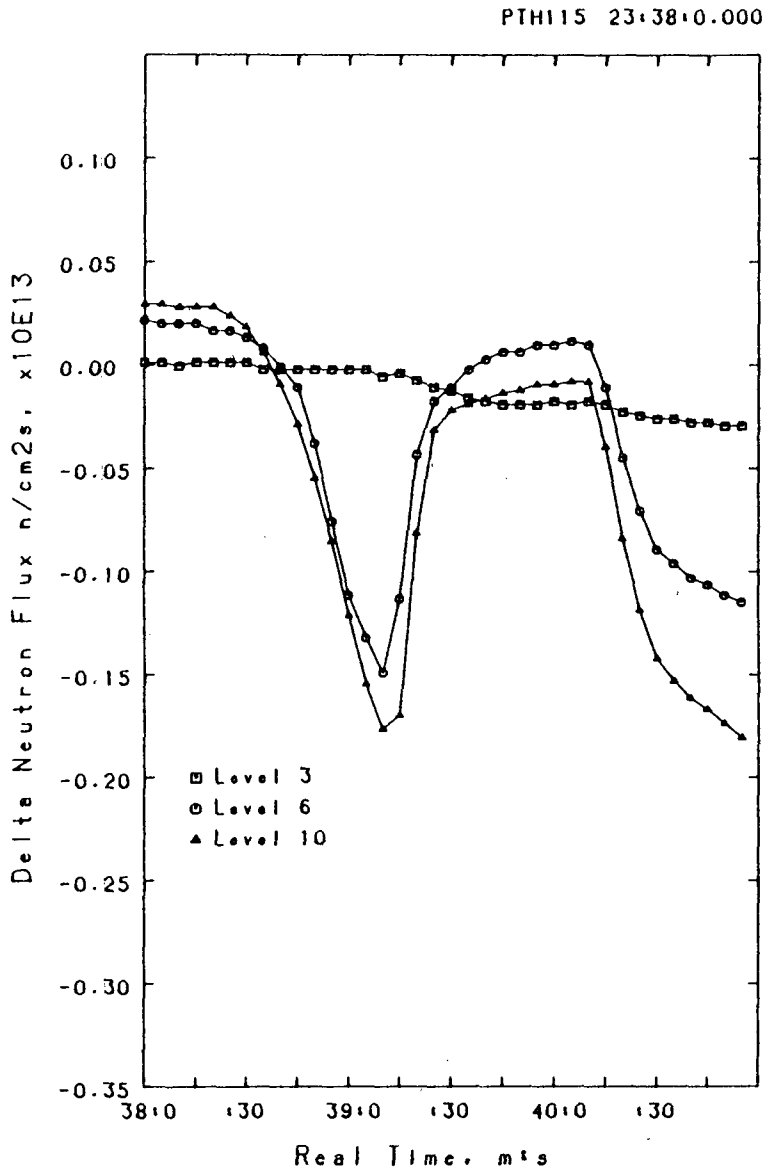

FIGURE 2.2.2.15 CHANGING IT NEUTRON FLUX AFTER PTH115 REFLOODING BEGINS. T:38:57S

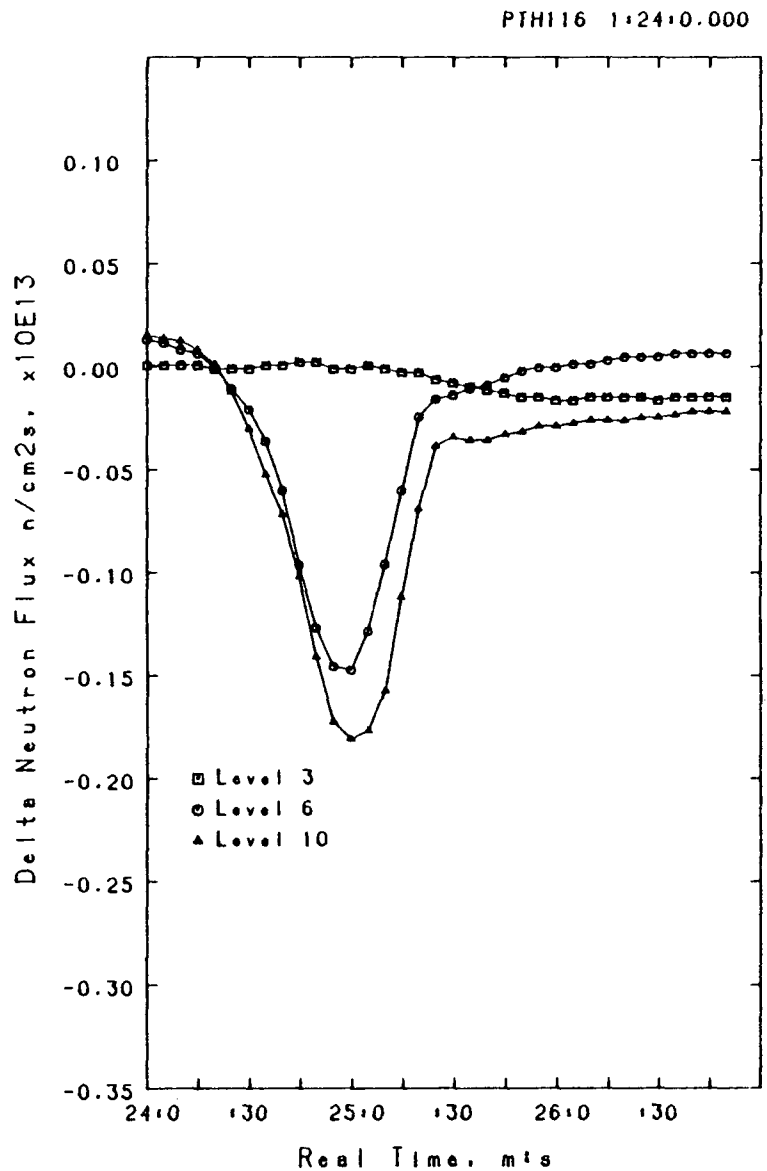

FIGURE 2.2.2.16 CHANGING IT NEUTRON FLUX AFTER PTH116 REFLOODING BEGINS. T=24:32S

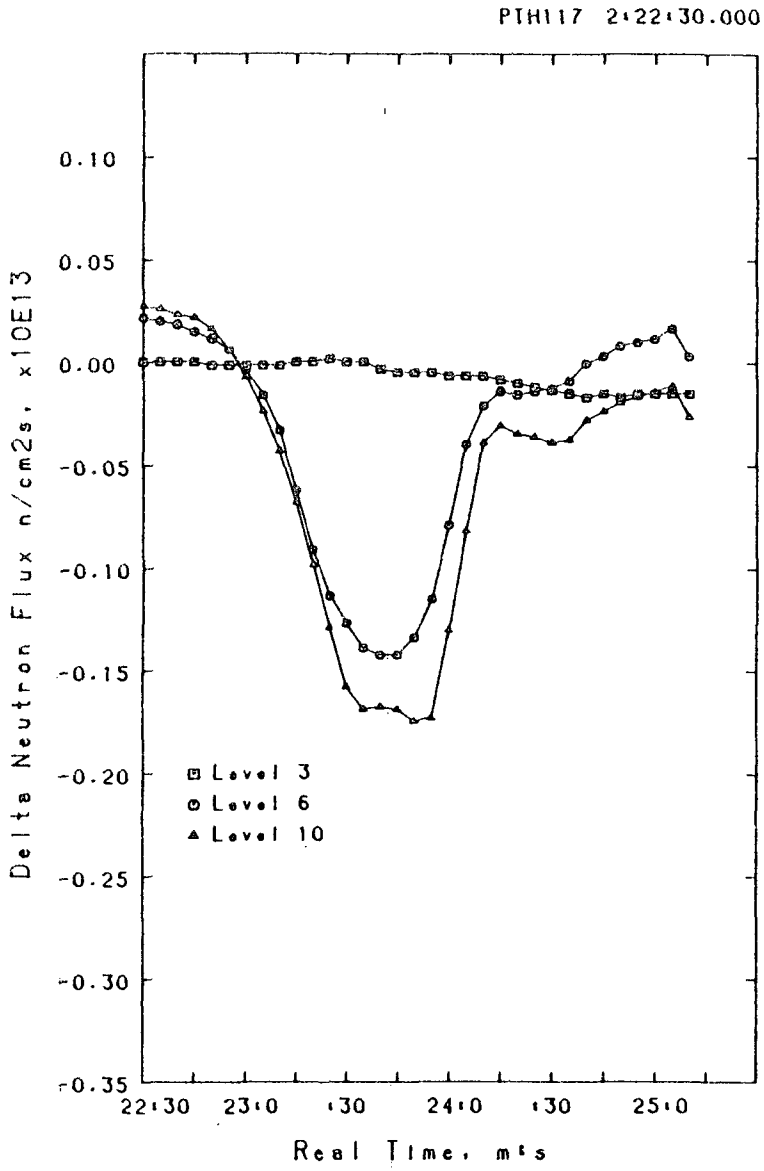

FIGURE 2.2.2.17 CHANGING IT NEUTRON FLUX AFTER PTH117 REFLOODING BEGINS. T=23:15S

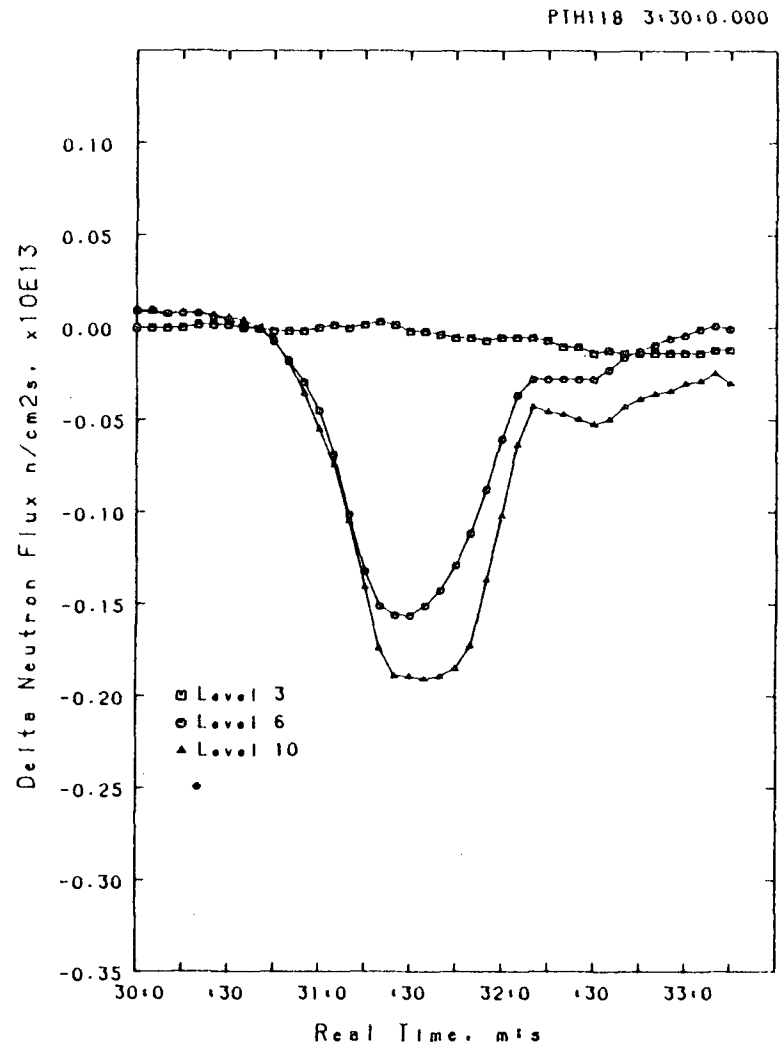

FIGURE 2.2.2.18 CHANGING IT NEUTRON FLUX AFTER PTH118 REFLOODING BEGINS. T=30:56S

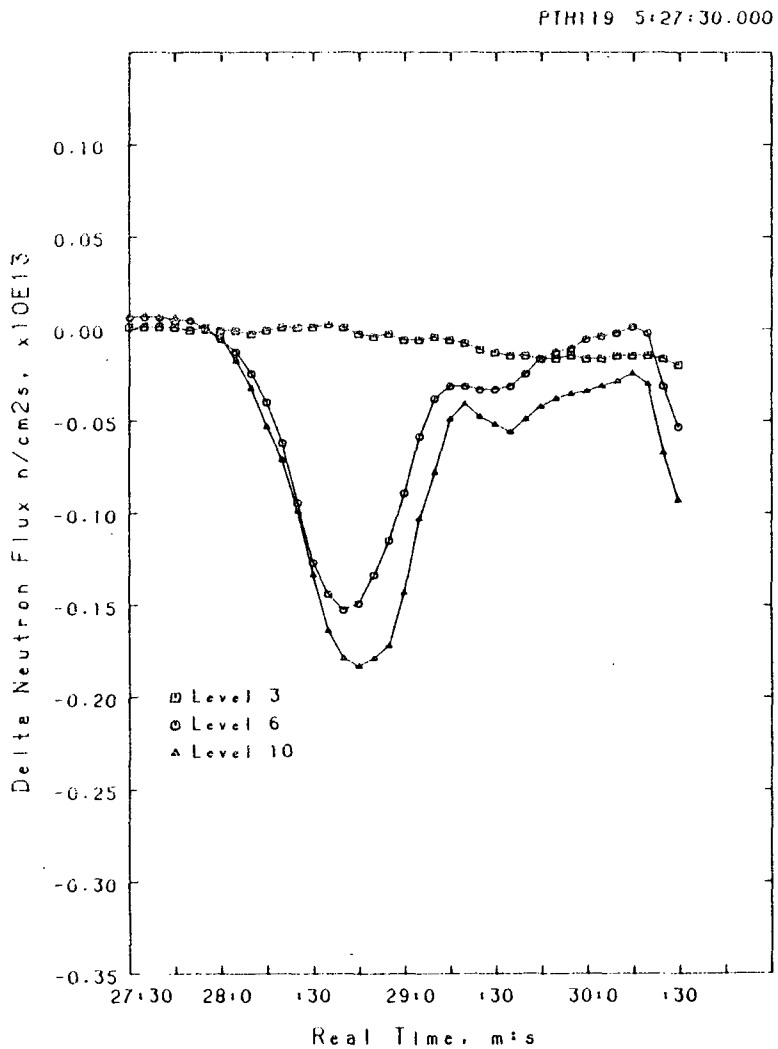

FIGURE 2.2.2.19 CHANGING II NEUTRON FLUX AFTER PTH119 REFLOODING BEGINS. T=28M:8S

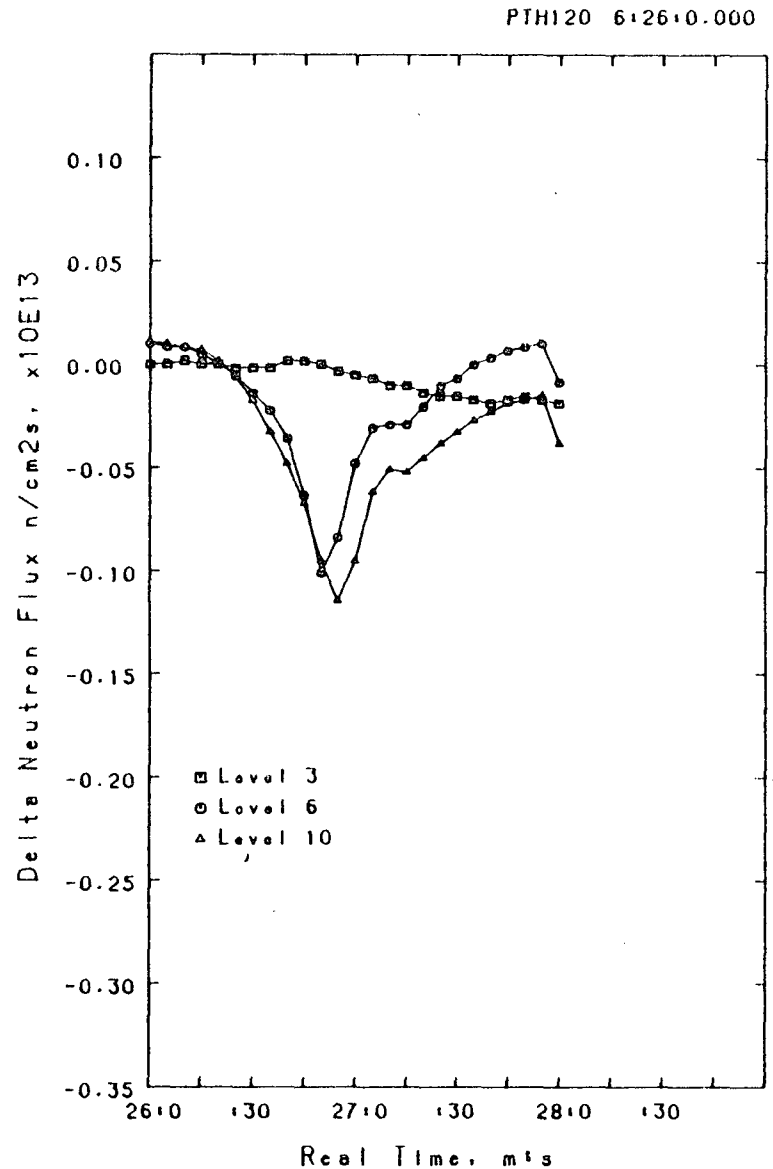

FIGURE 2.2.2.20 CHANGING II NEUTRON FLUX AFTER PTH120 REFLOODING BEGINS. T=26:34S

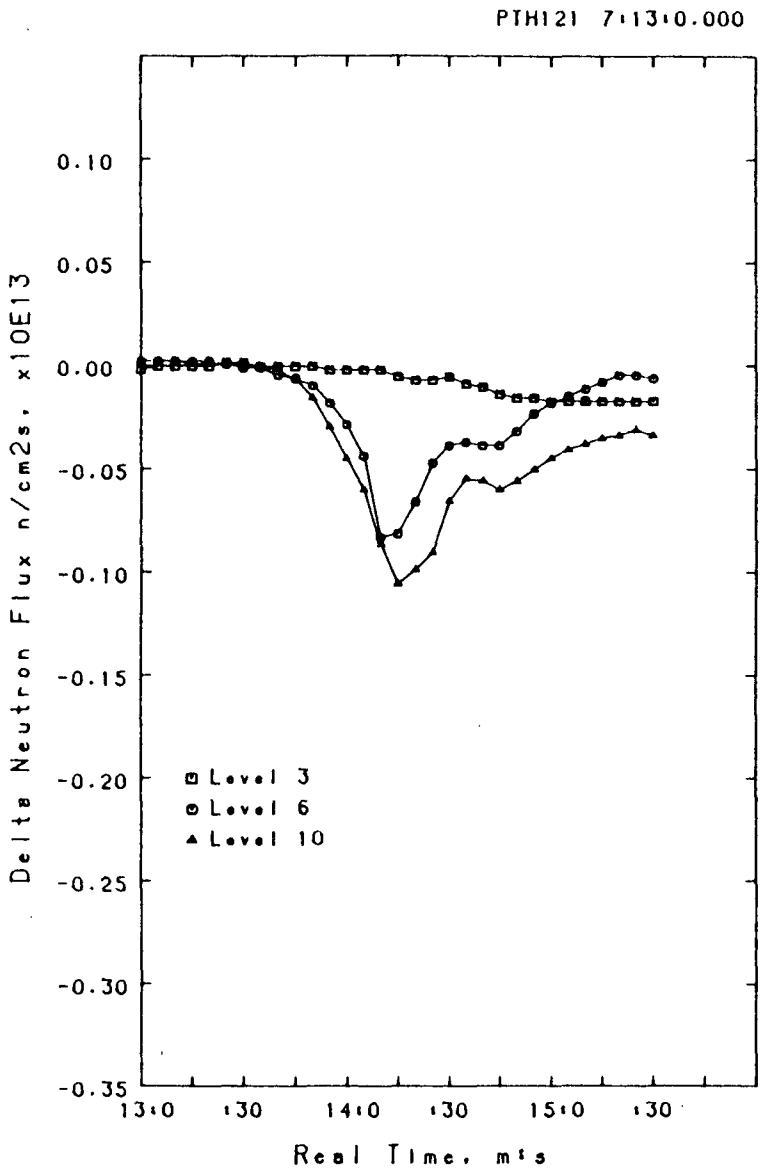

FIGURE 2.2.2.21 CHANGING IT NEUTRON FLUX AFTER PTH121 REFLOODING BEGINS, T=13:45S

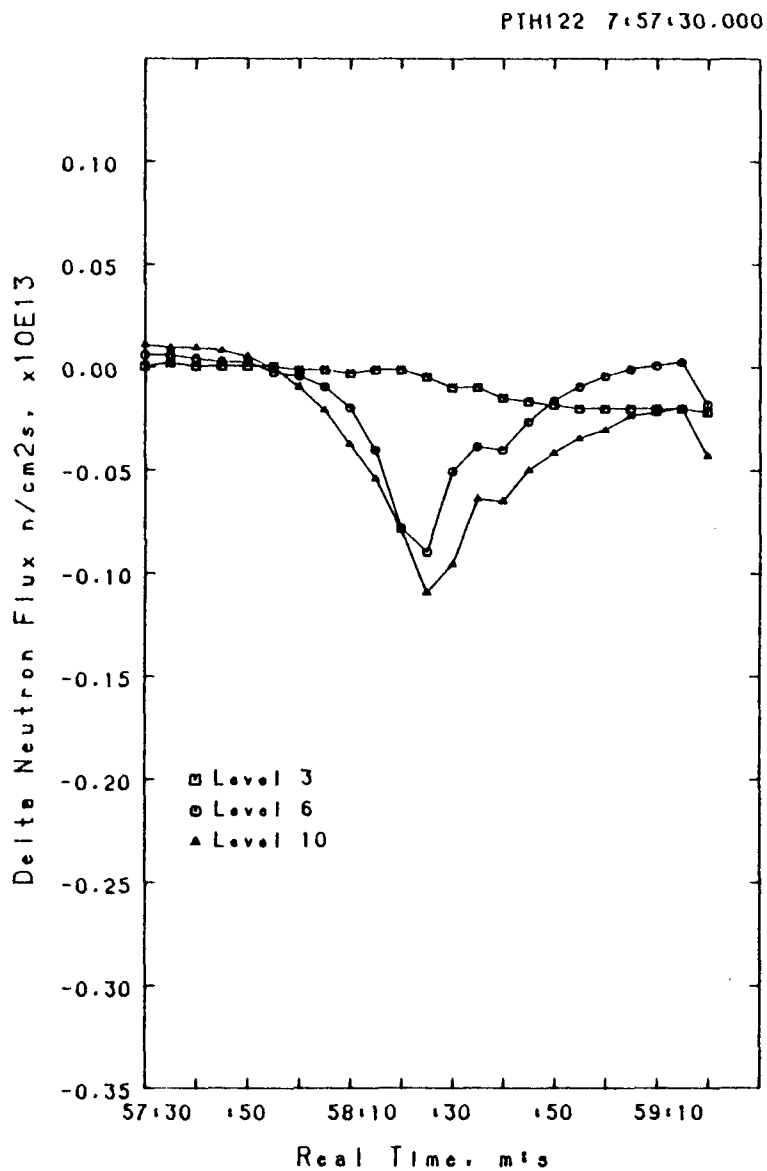

FIGURE 2.2.2.22 CHANGING IT NEUTRON FLUX AFTER PTH122 REFLOODING BEGINS, T=58:8S

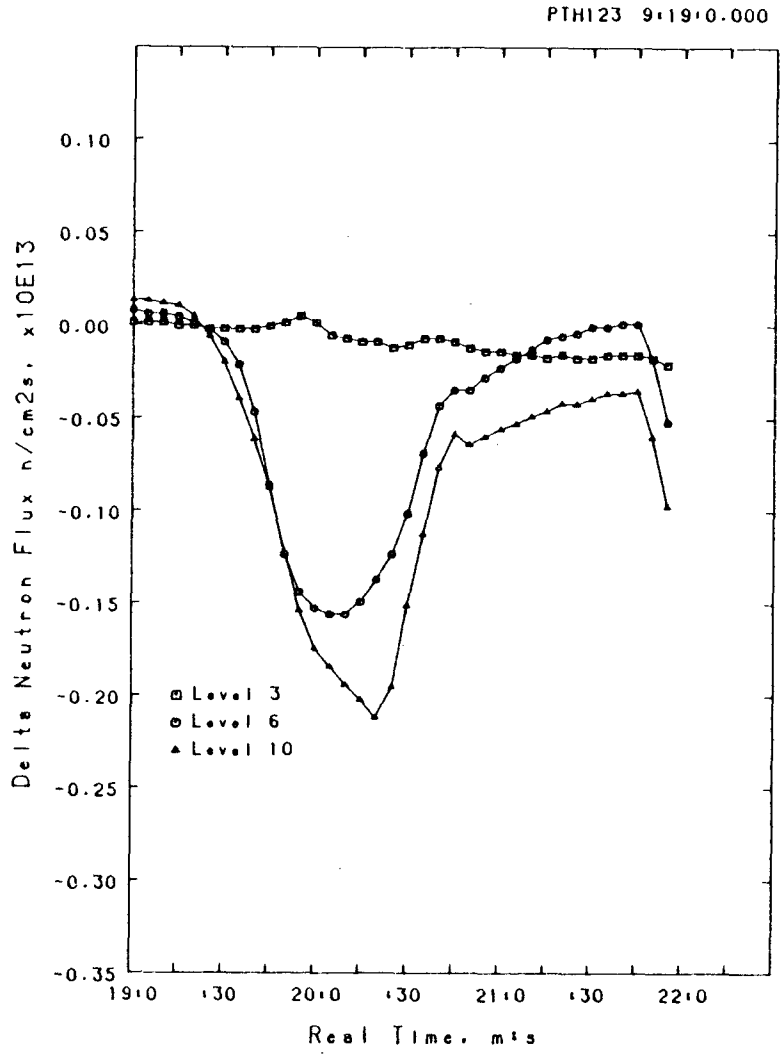

FIGURE 2.2.2.23 CHANGING IT NEUTRON FLUX AFTER PTH123 REFLOODING BEGINS, T=19:35S

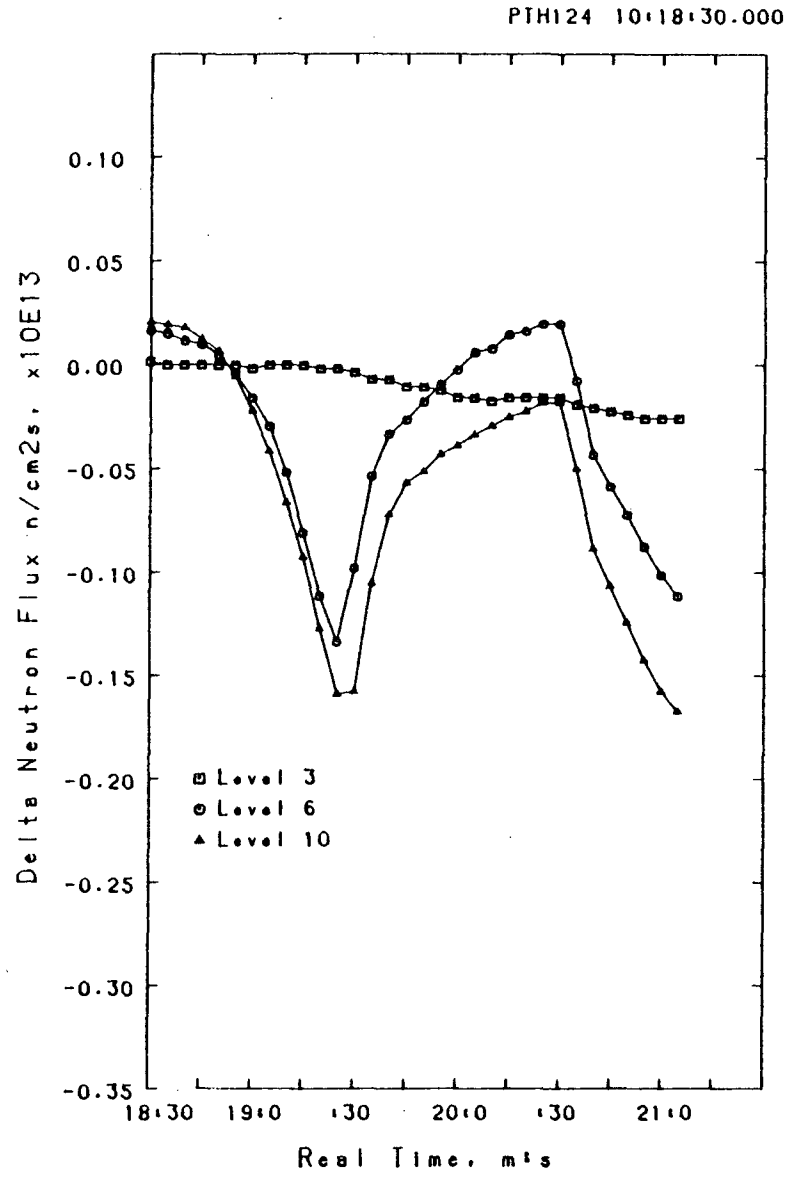

FIGURE 2.2.2.24 CHANGING IT NEUTRON FLUX AFTER PTH124 REFLOODING BEGINS, T=19:07S

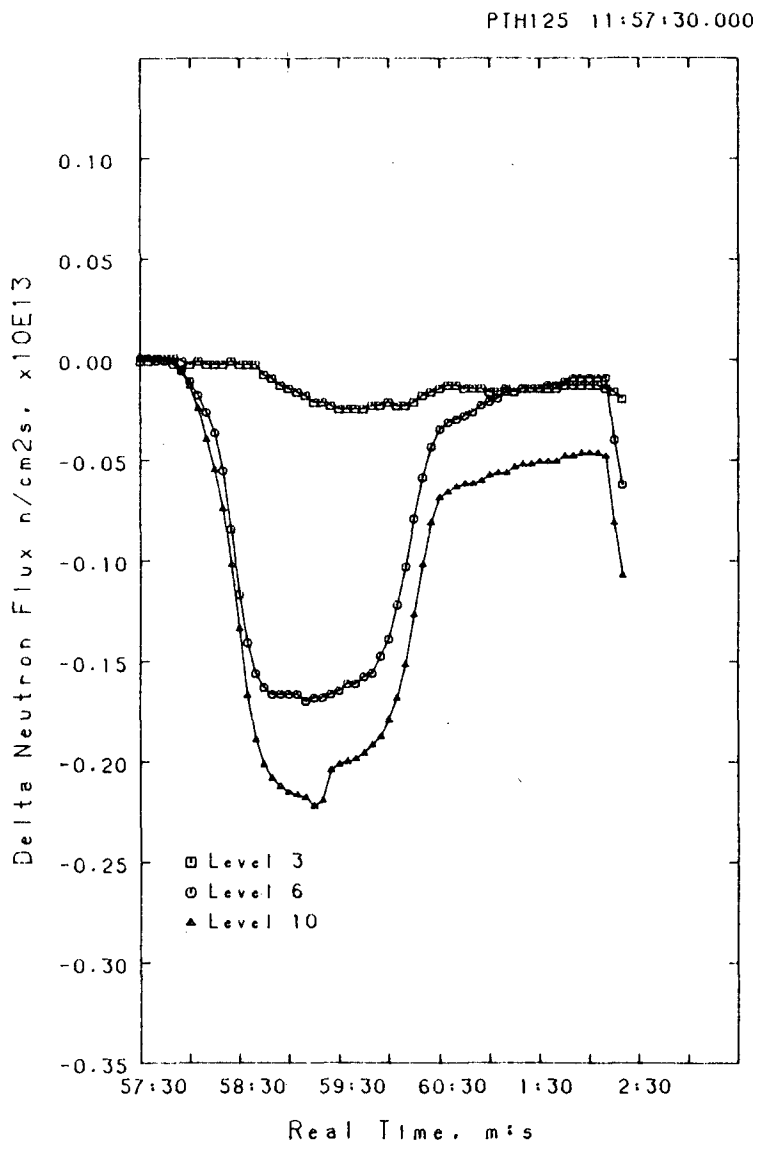

FIGURE 2.2.2.25 CHANGING IT NEUTRON FLUX AFTER PTH125 REFLOODING BEGINS. T=57M:46S

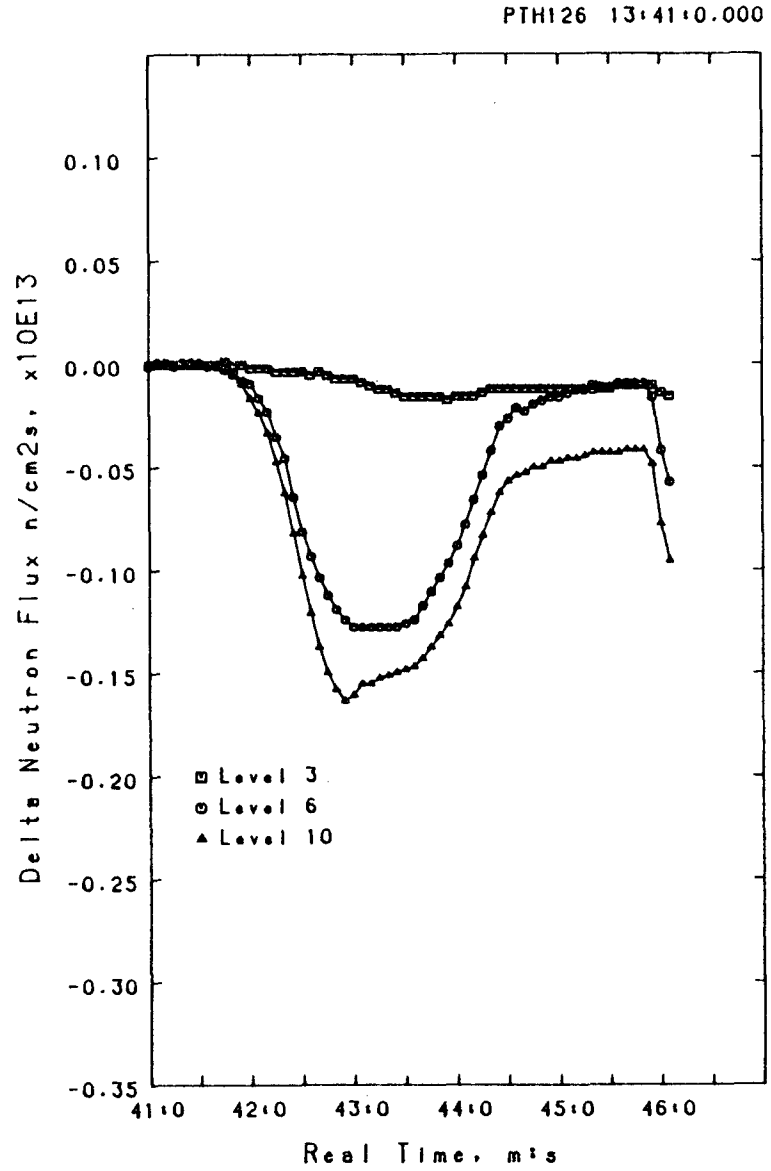

FIGURE 2.2.2.26 CHANGING IT NEUTRON FLUX AFTER PTH126 REFLOODING BEGINS. T=41.36S

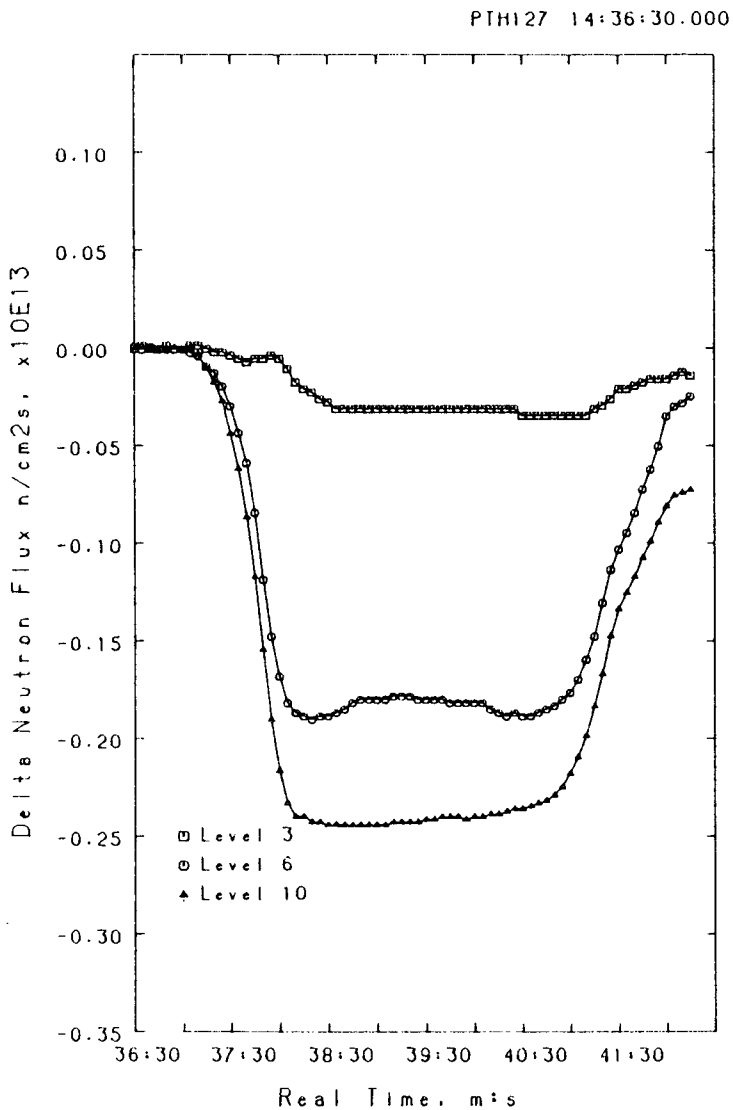

FIGURE 2.2.2.27 CHANGING IT NEUTRON FLUX AFTER PTH127 REFLOODING BEGINS, T=37:09S

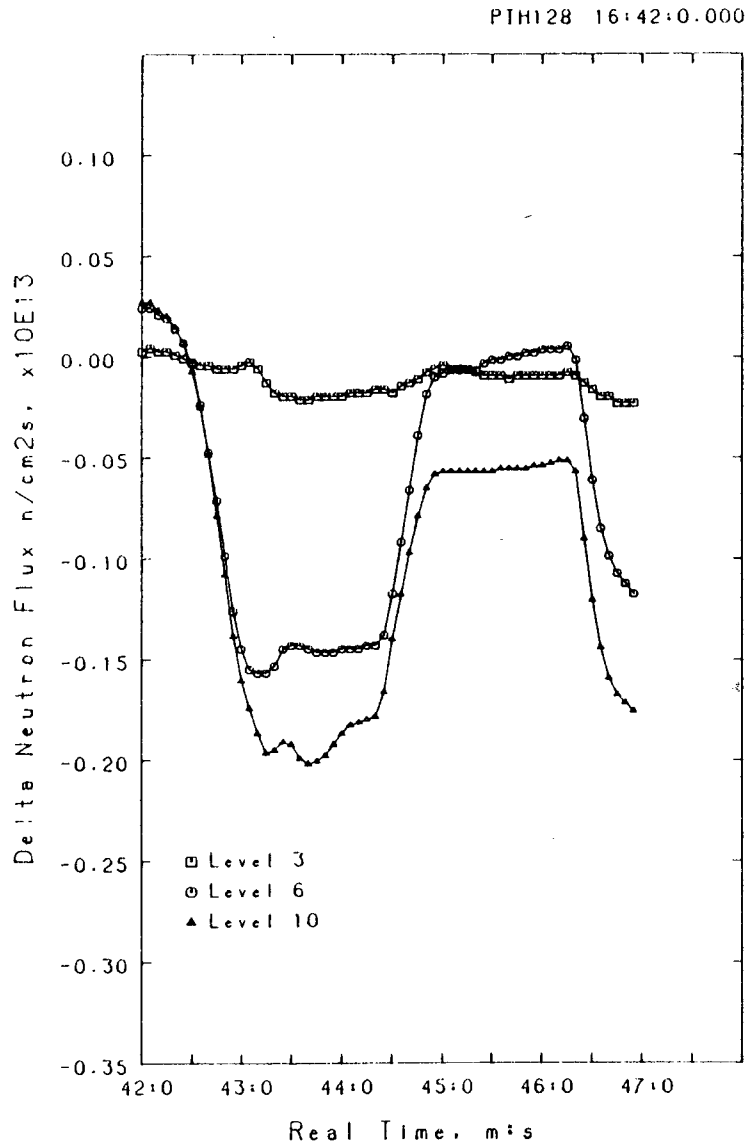

FIGURE 2.2.2.28 CHANGING IT NEUTRON FLUX AFTER PTH128 REFLOODING BEGINS, T=42M:44S

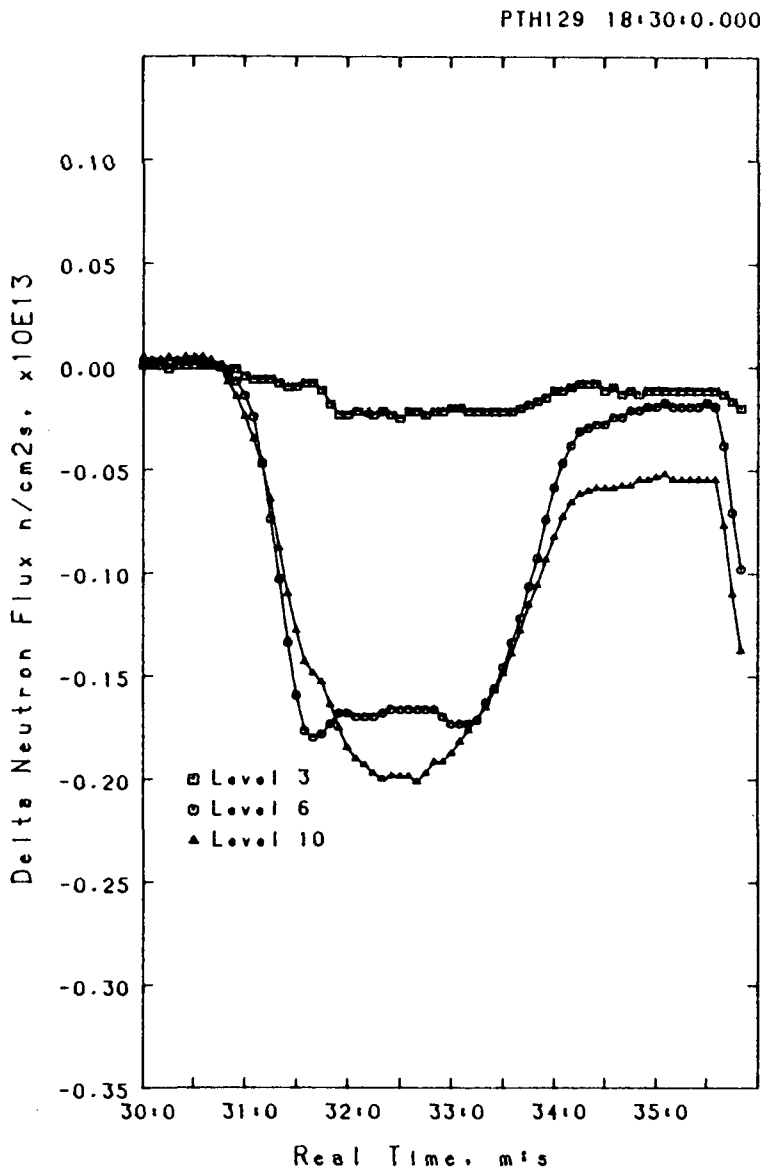

FIGURE 2.2.2.29 CHANGING IT NEUTRON FLUX AFTER PTH129 REFLOODING BEGINS, T=31.05S

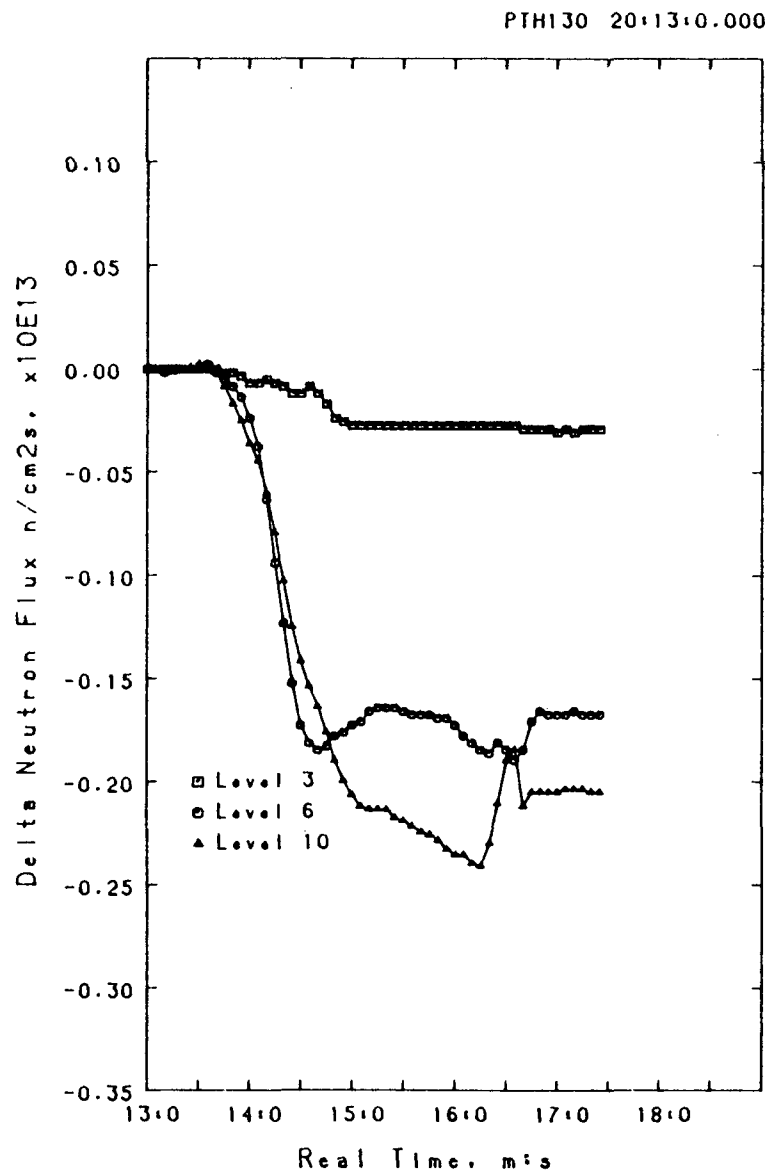

FIGURE 2.2.2.30 CHANGING IT NEUTRON FLUX AFTER PTH130 REFLOODING BEGINS, T=13:33S

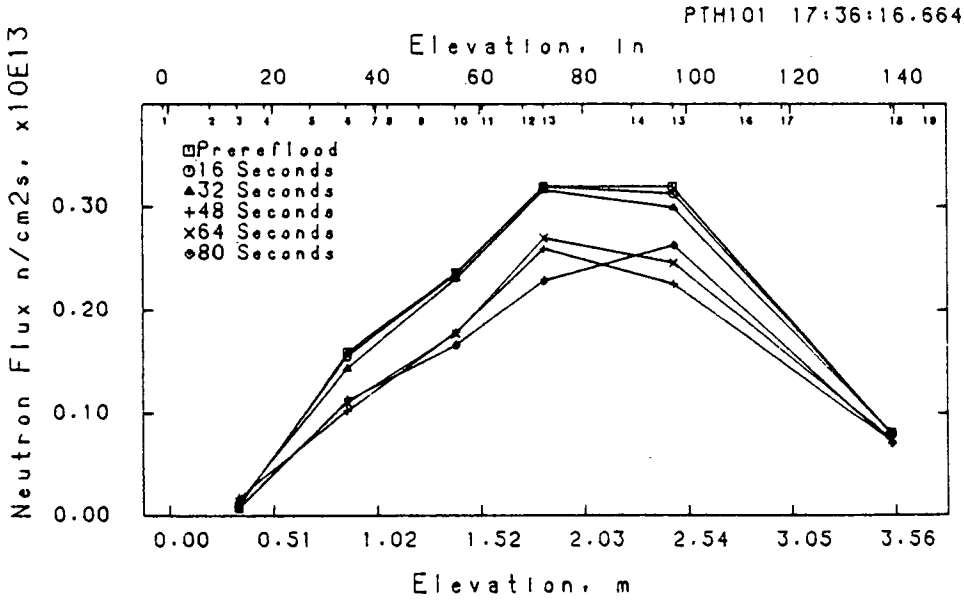

FIGURE 2.2.3.01 IT NEUTRON FLUX AXIAL PROFILES AFTER REFLOODING, AT 16S INTERVALS - PTH101

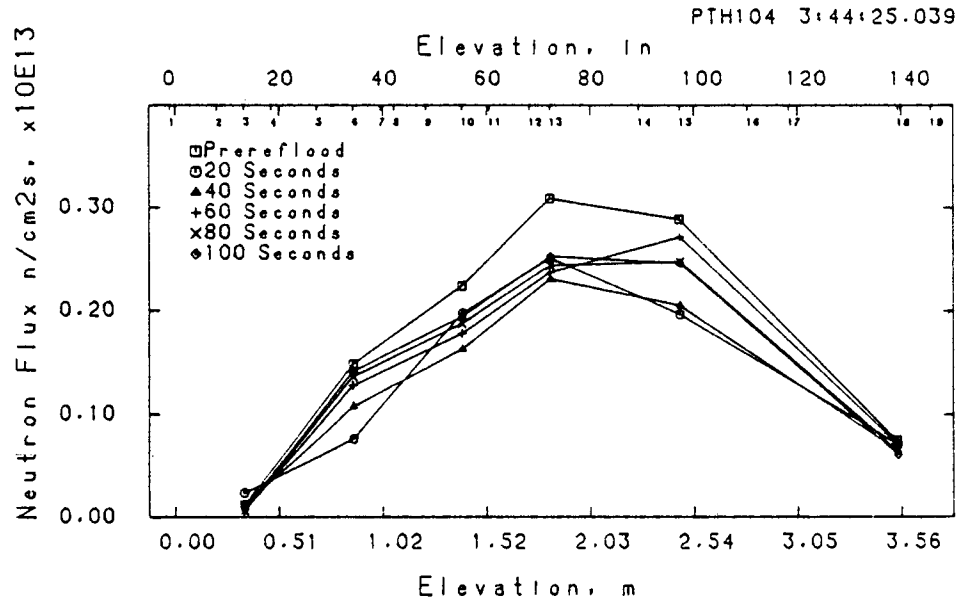

FIGURE 2.2.3.04 IT NEUTRON FLUX AXIAL PROFILES AFTER REFLOODING, AT 20S INTERVALS - PTH104

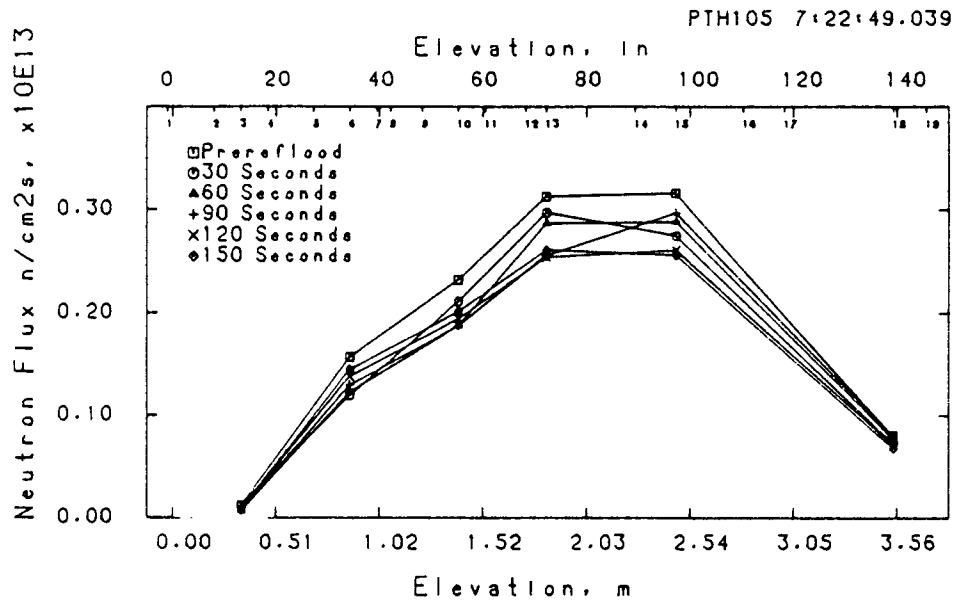

FIGURE 2.2.3.05 IT NEUTRON FLUX AXIAL PROFILES AFTER REFLOODING, AT 30S INTERVALS - PTH105

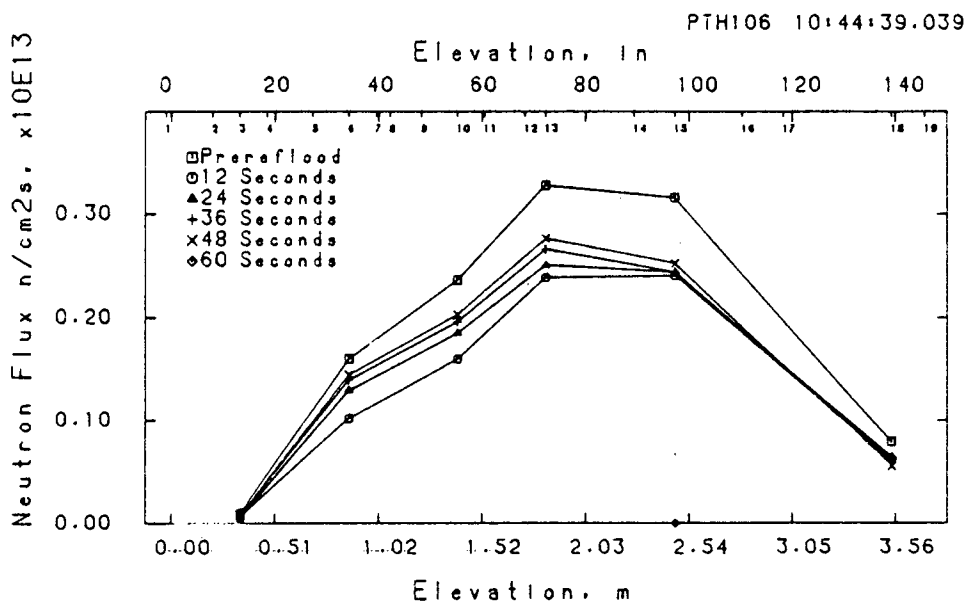

FIGURE 2.2.3.06 IT NEUTRON FLUX AXIAL PROFILES AFTER REFLOODING, AT 12S INTERVALS - PTH106

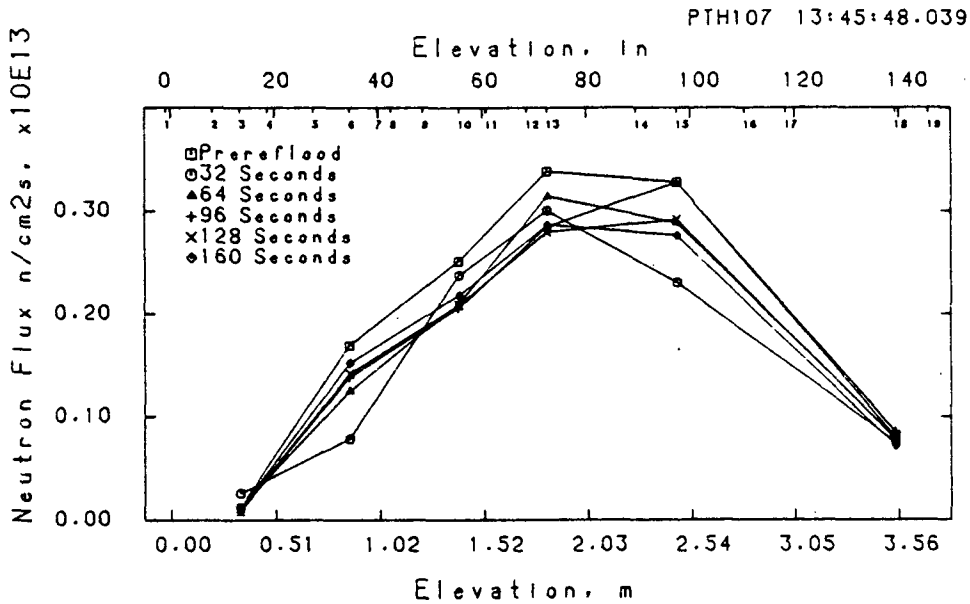

FIGURE 2.2.3.07 IT NEUTRON FLUX AXIAL PROFILES AFTER REFLOODING, AT 32S INTERVALS - PTH107

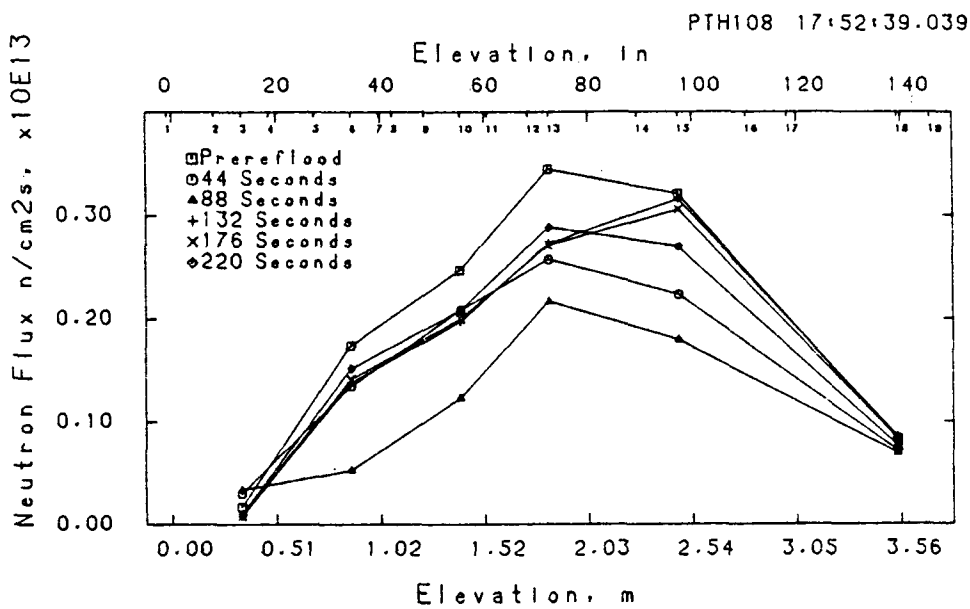

FIGURE 2.2.3.08 IT NEUTRON FLUX AXIAL PROFILES AFTER REFLOODING, AT 44S INTERVALS - PTH108

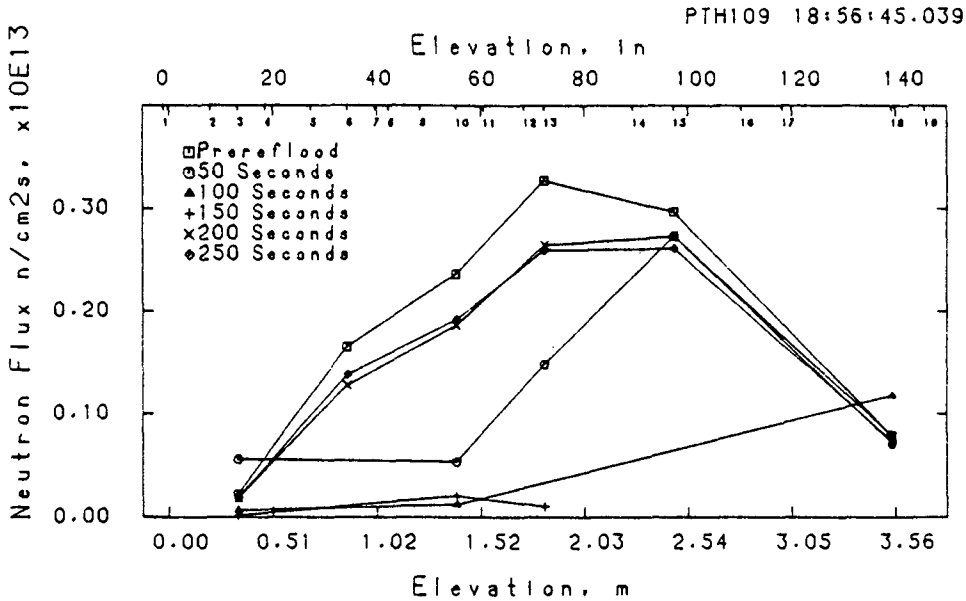

FIGURE 2.2.3.09 IT NEUTRON FLUX AXIAL PROFILES AFTER REFLOODING AT 50S INTERVALS - PTH109

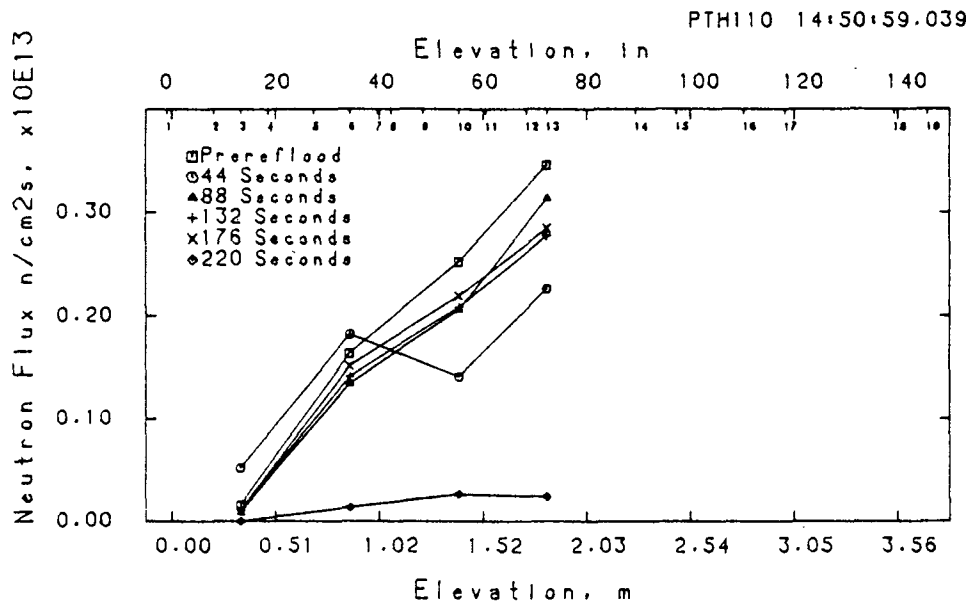

FIGURE 2.2.3.10 IT NEUTRON FLUX AXIAL PROFILES AFTER REFLOODING AT 44S INTERVALS - PTH110

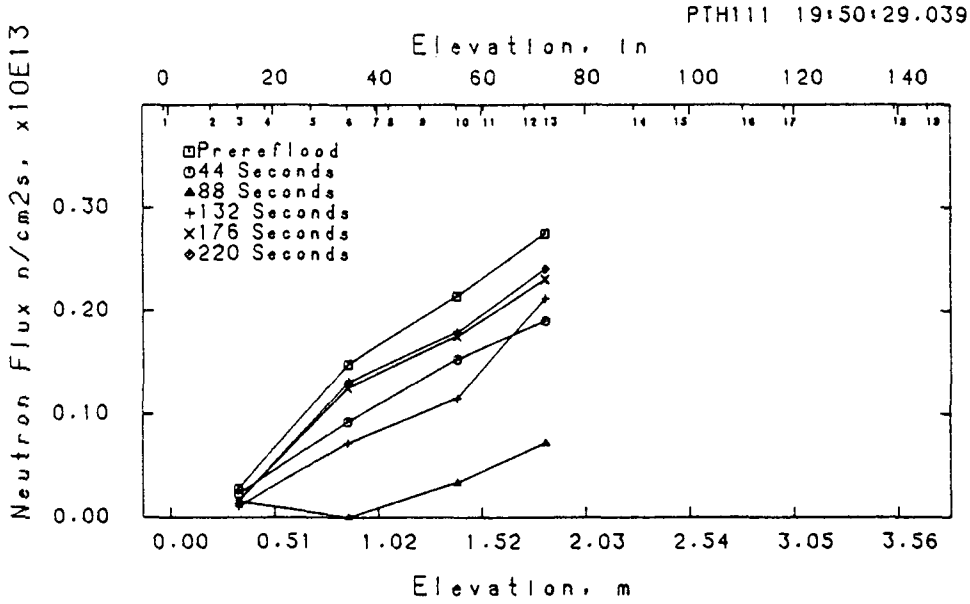

FIGURE 2.2.3.11 IT NEUTRON FLUX AXIAL PROFILES AFTER REFLOODING AT 44S INTERVALS - PTH111

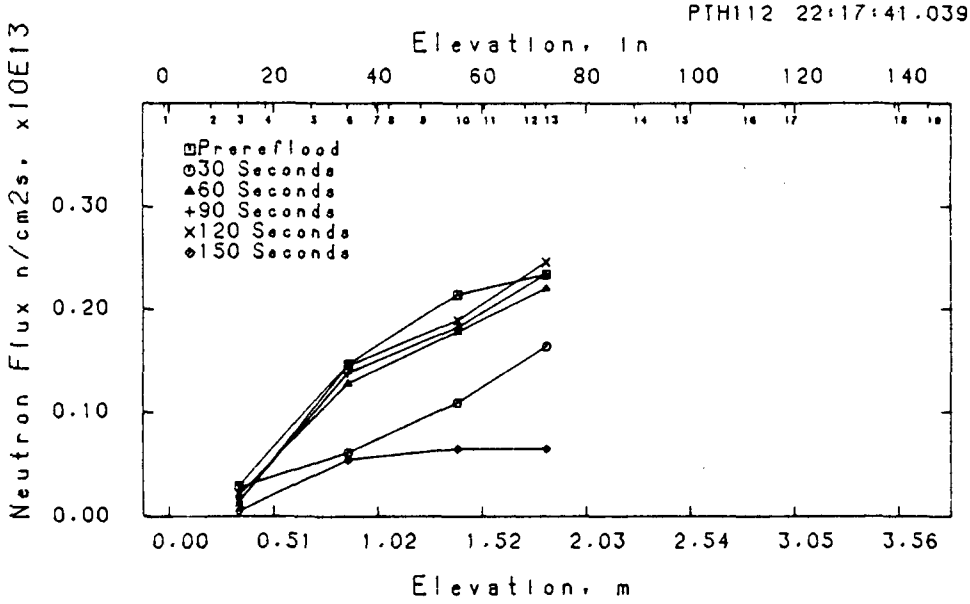

FIGURE 2.2.3.12 IT NEUTRON FLUX AXIAL PROFILES AFTER REFLOODING AT 30S INTERVALS - PTH112

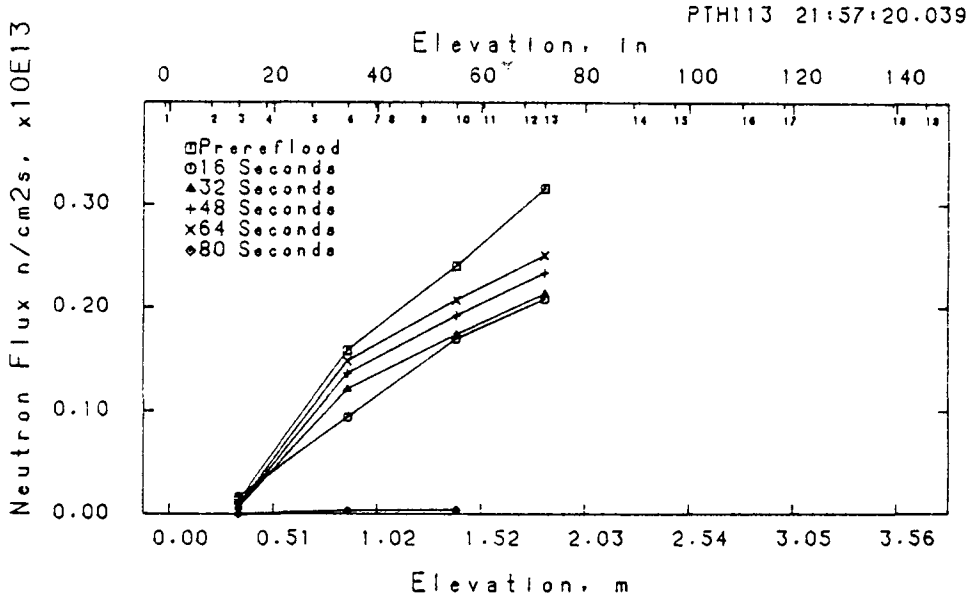

FIGURE 2.2.3.13 IT NEUTRON FLUX AXIAL PROFILES AFTER REFLOODING AT 16S INTERVALS - PTH113

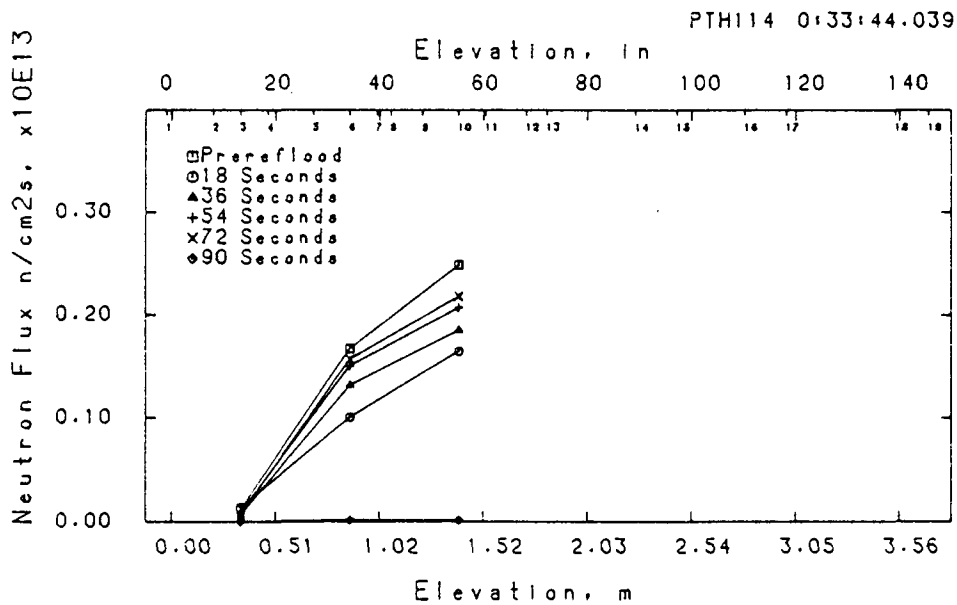

FIGURE 2.2.3.14 IT NEUTRON FLUX AXIAL PROFILES AFTER REFLOODING AT 18S INTEVALS - PTH114

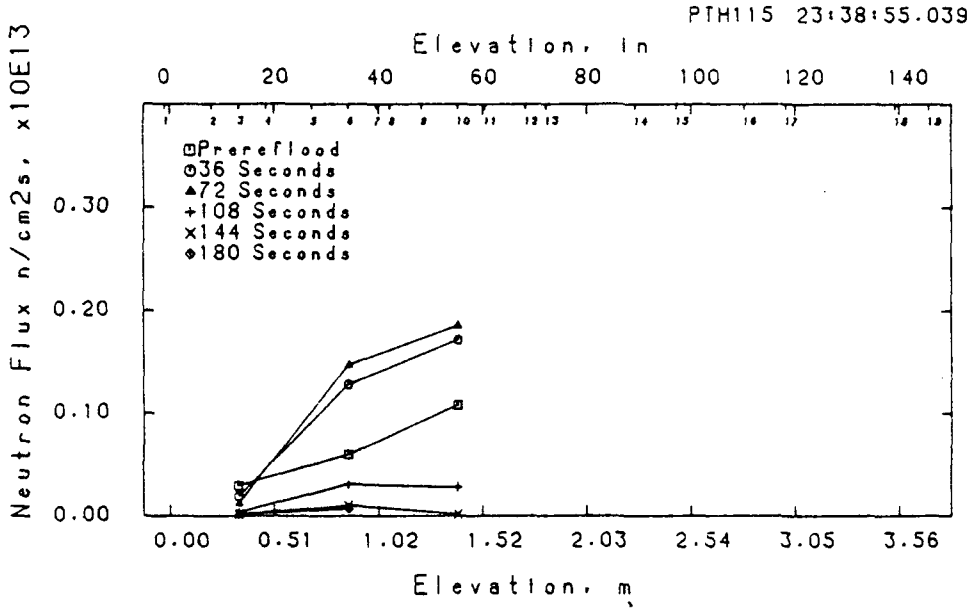

FIGURE 2.2.3.15 IT NEUTRON FLUX AXIAL PROFILES AFTER REFLOODING AT 36S INTERVALS - PTH115

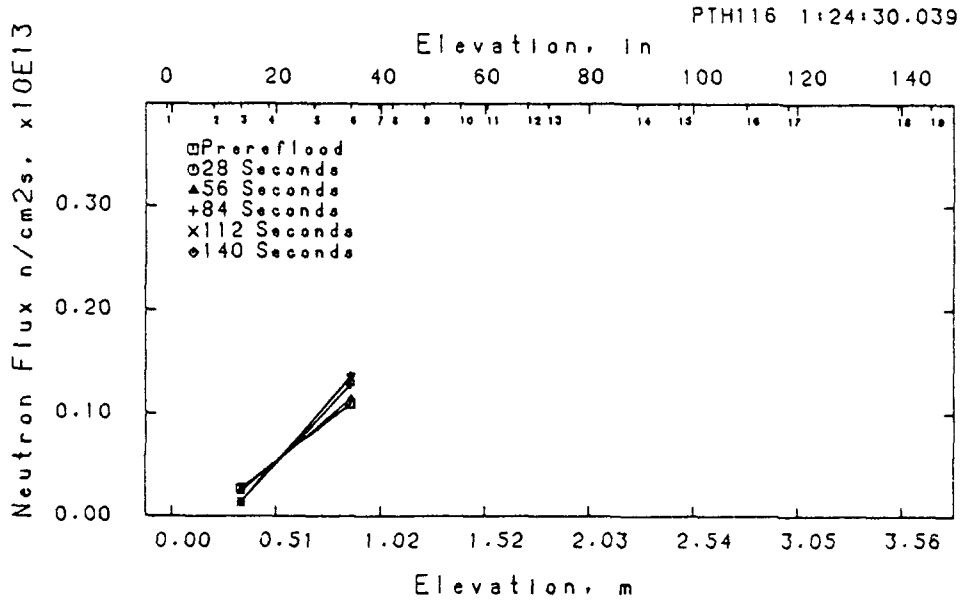

FIGURE 2.2.3.16 IT NEUTRON FLUX AXIAL PROFILES AFTER REFLOODING AT 28S INTERVALS - PTH116

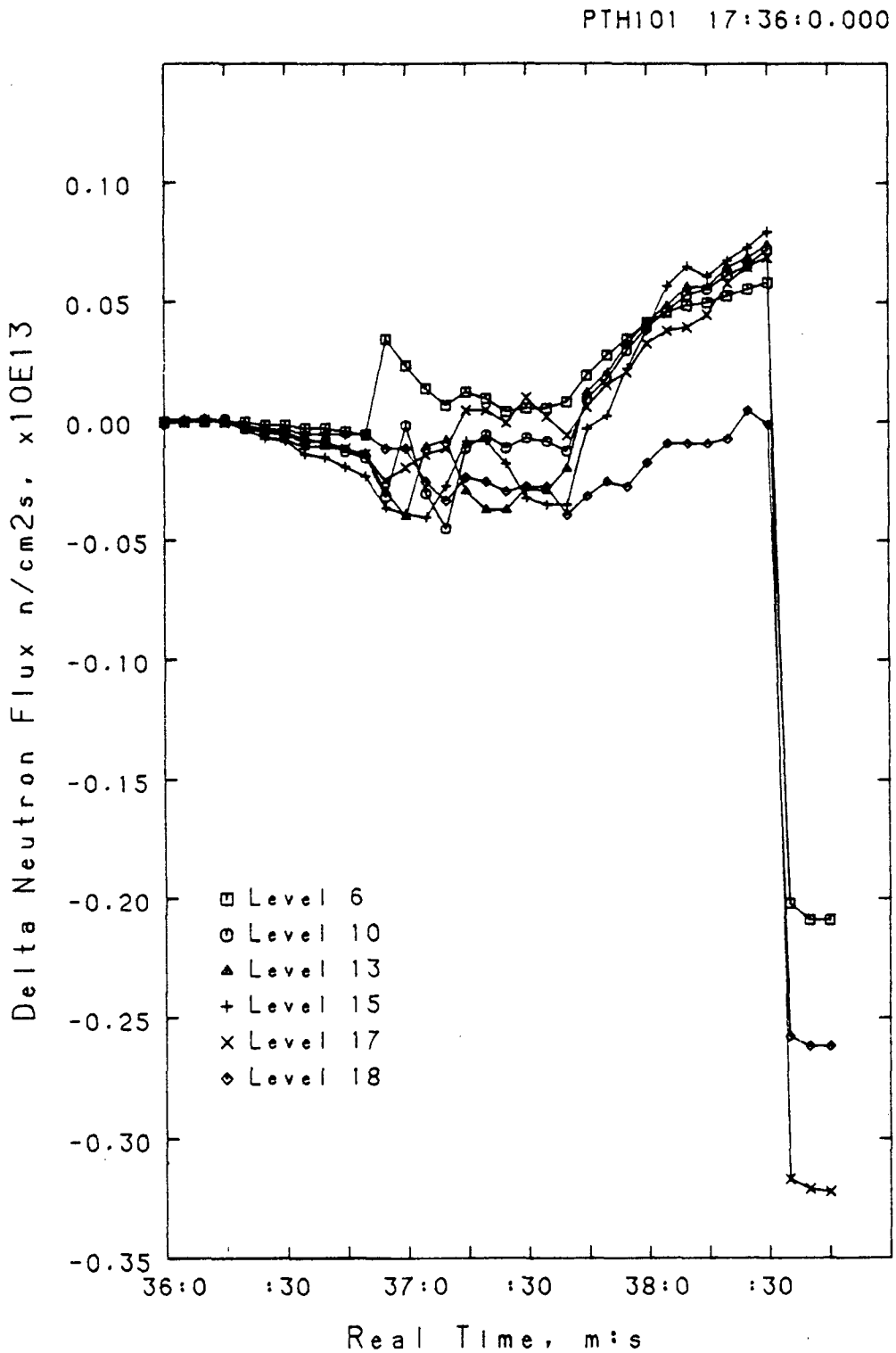

FIGURE 2.2.4.01 CHANGING NEUTRON FLUX (SHROUD) AFTER REFLOODING BEGINS, T=36:18S

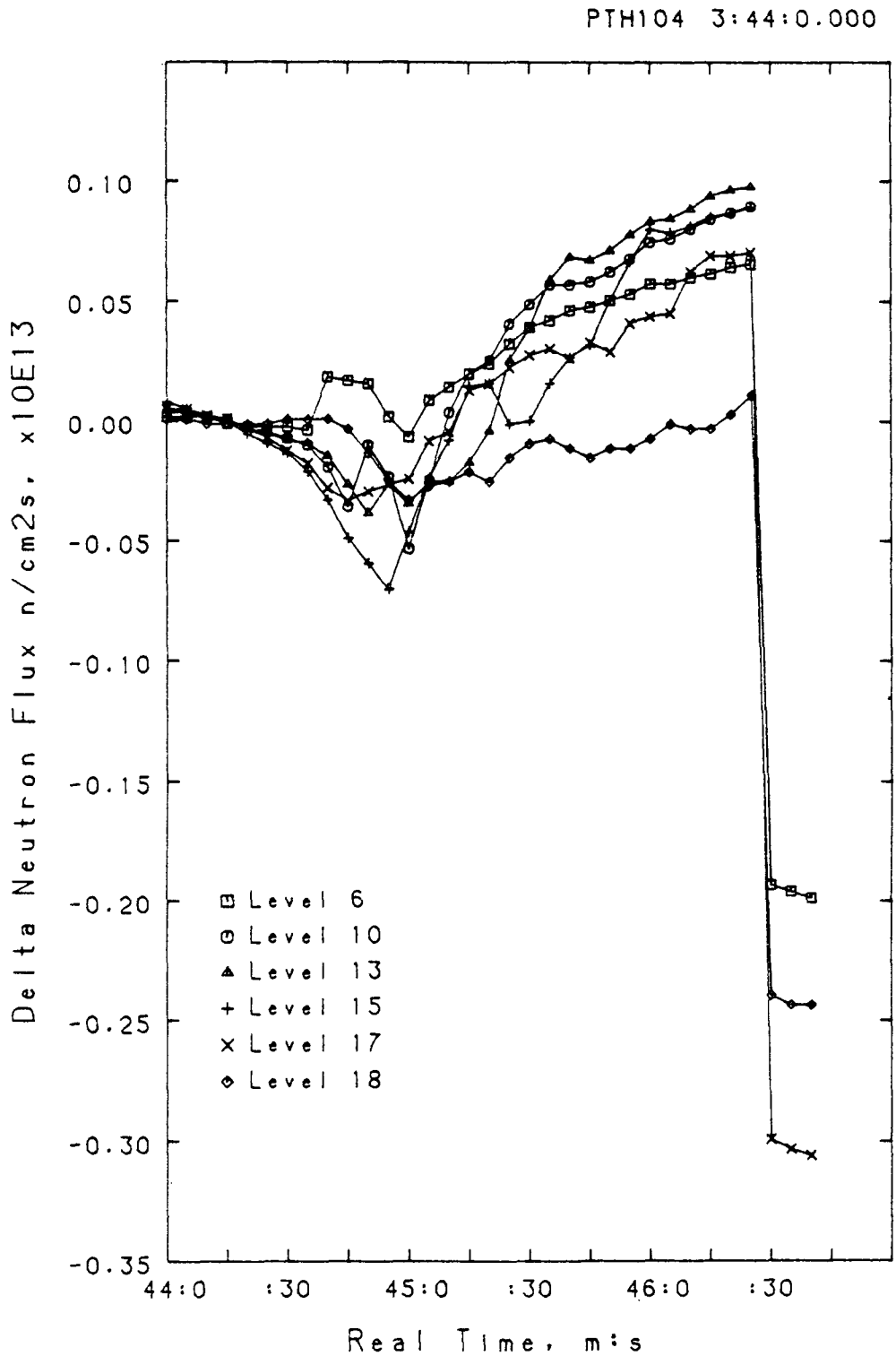

FIGURE 2.2.4.04 CHANGING NEUTRON FLUX (SHROUD) AFTER REFLOODING BEGINS, T=44:27S

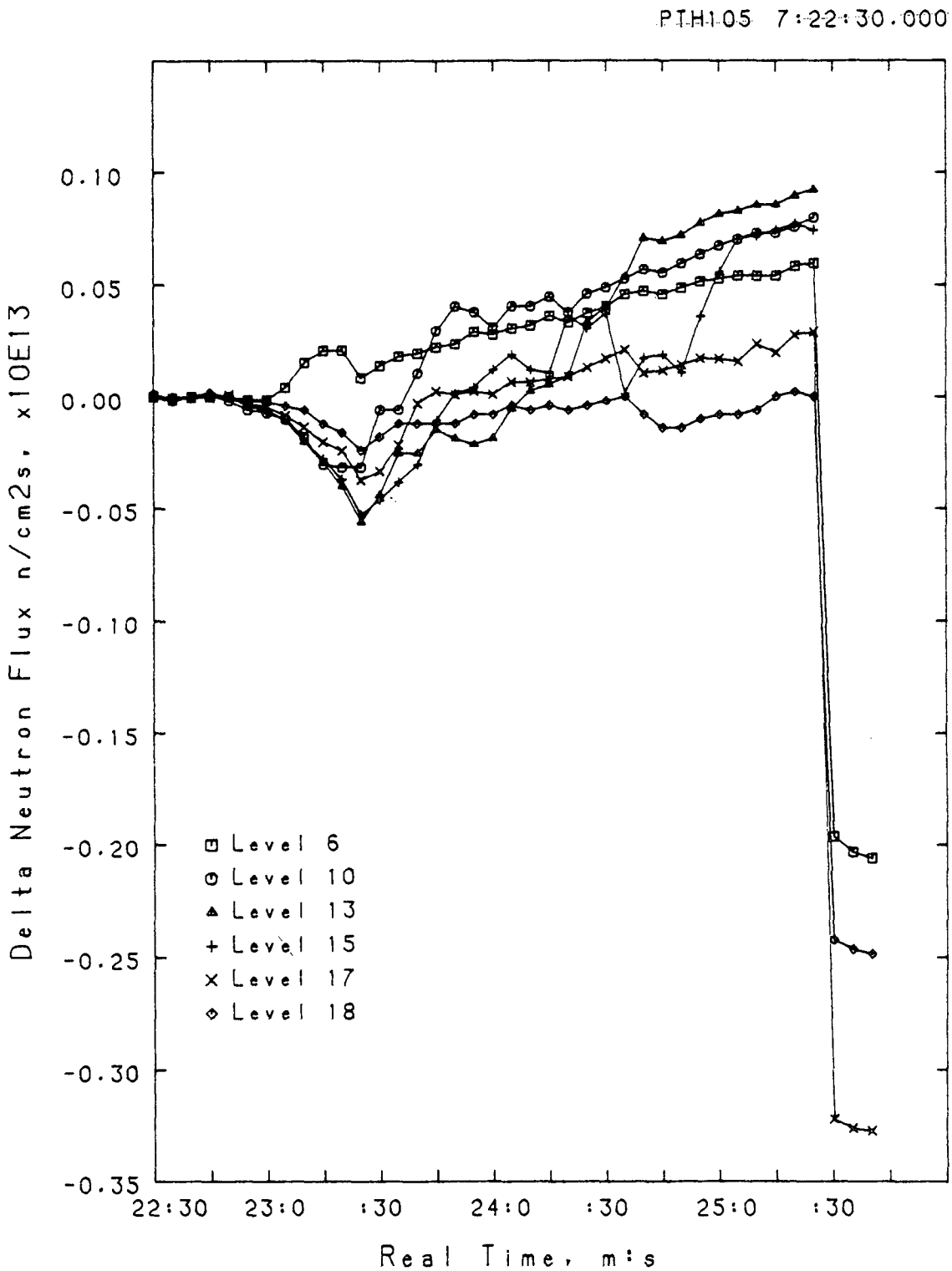

FIGURE 2.2.4.05 CHANGING NEUTRON FLUX (SHROUD) AFTER REFLOODING BEGINS, T=22:51S

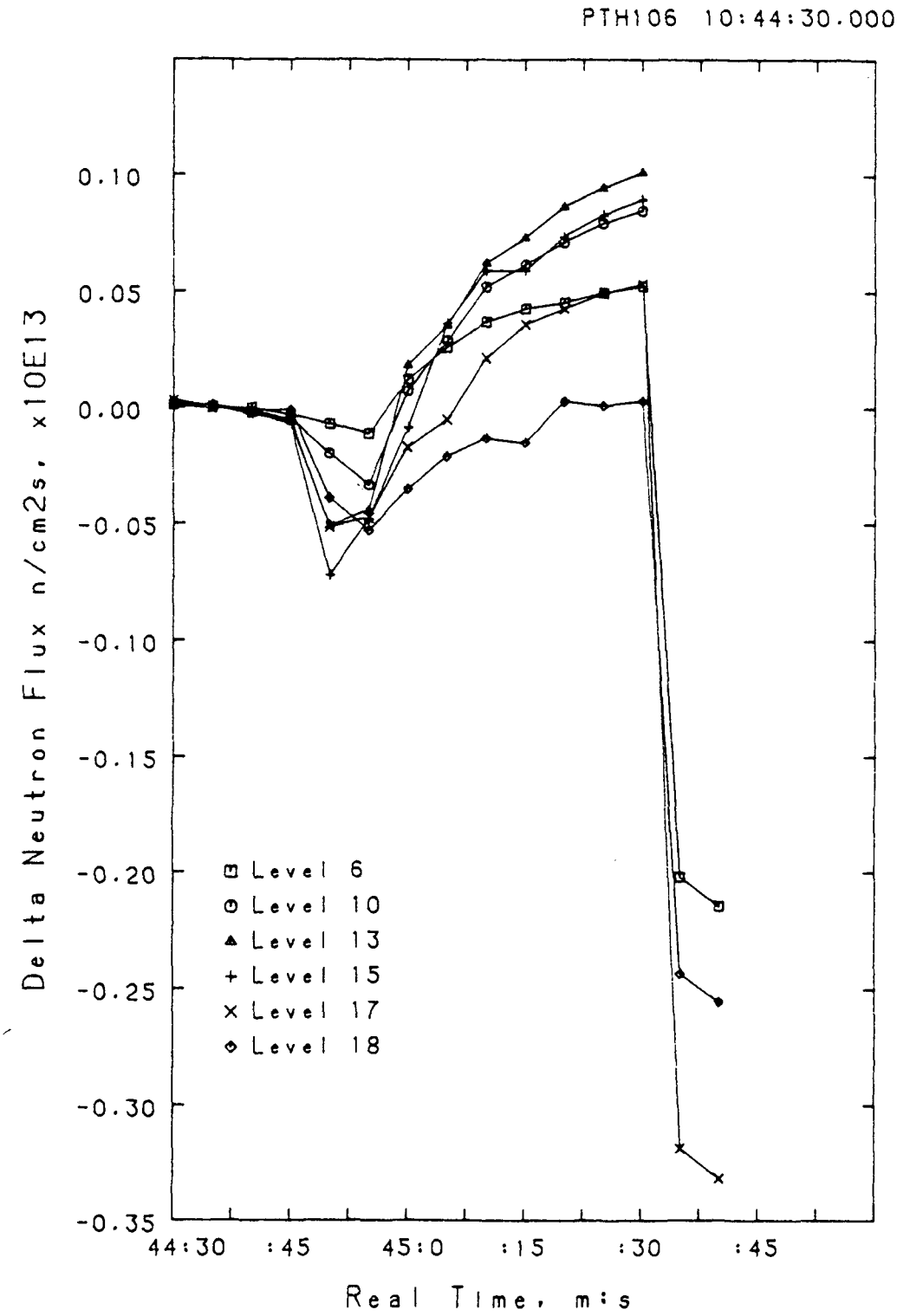

FIGURE 2.2.4.06 CHANGING NEUTRON FLUX (SHROUD) AFTER REFLOODING BEGINS. T=44:41S

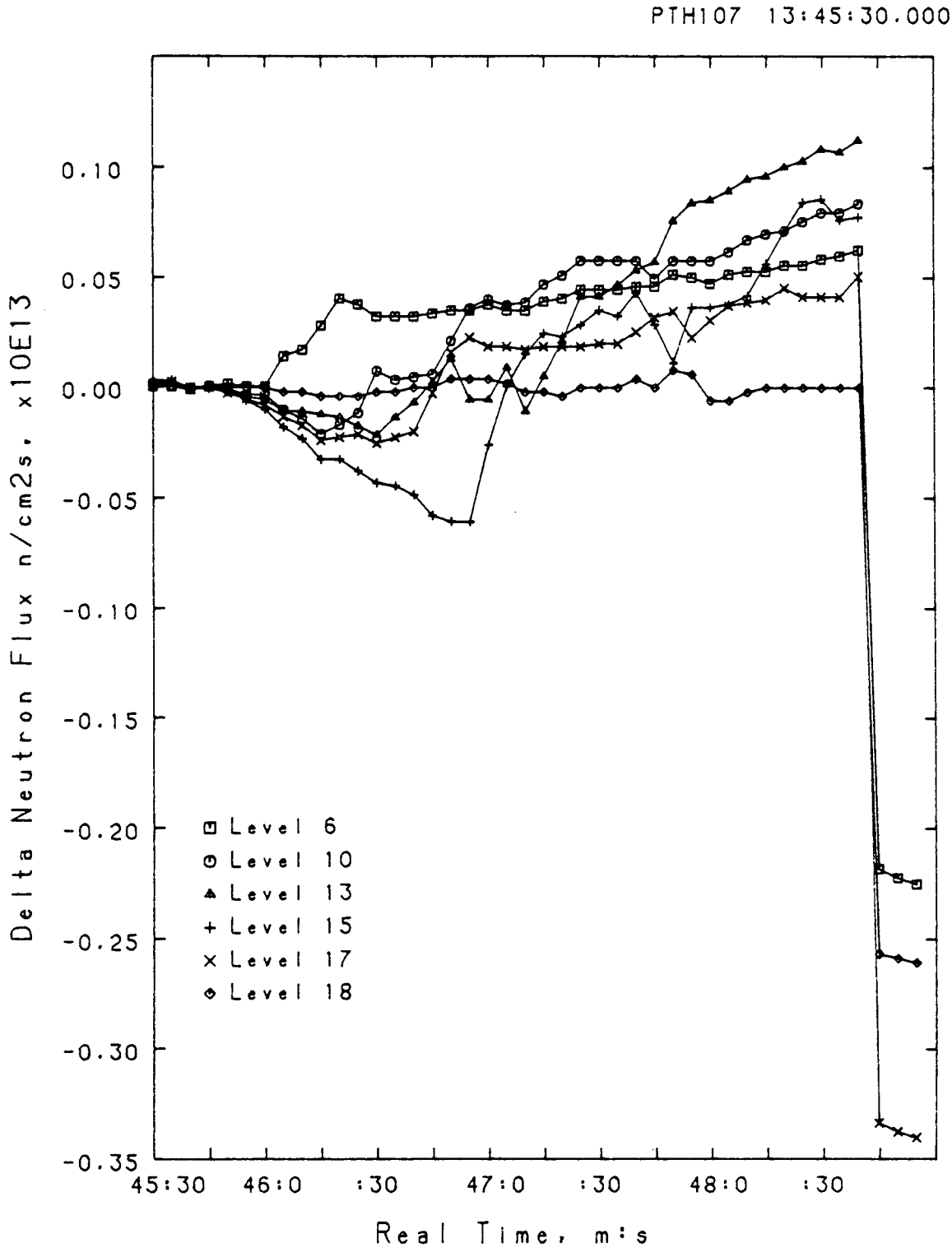

FIGURE 2.2.4.07 CHANGING NEUTRON FLUX (SHROUD) AFTER REFLOODING BEGINS, T=45:50S

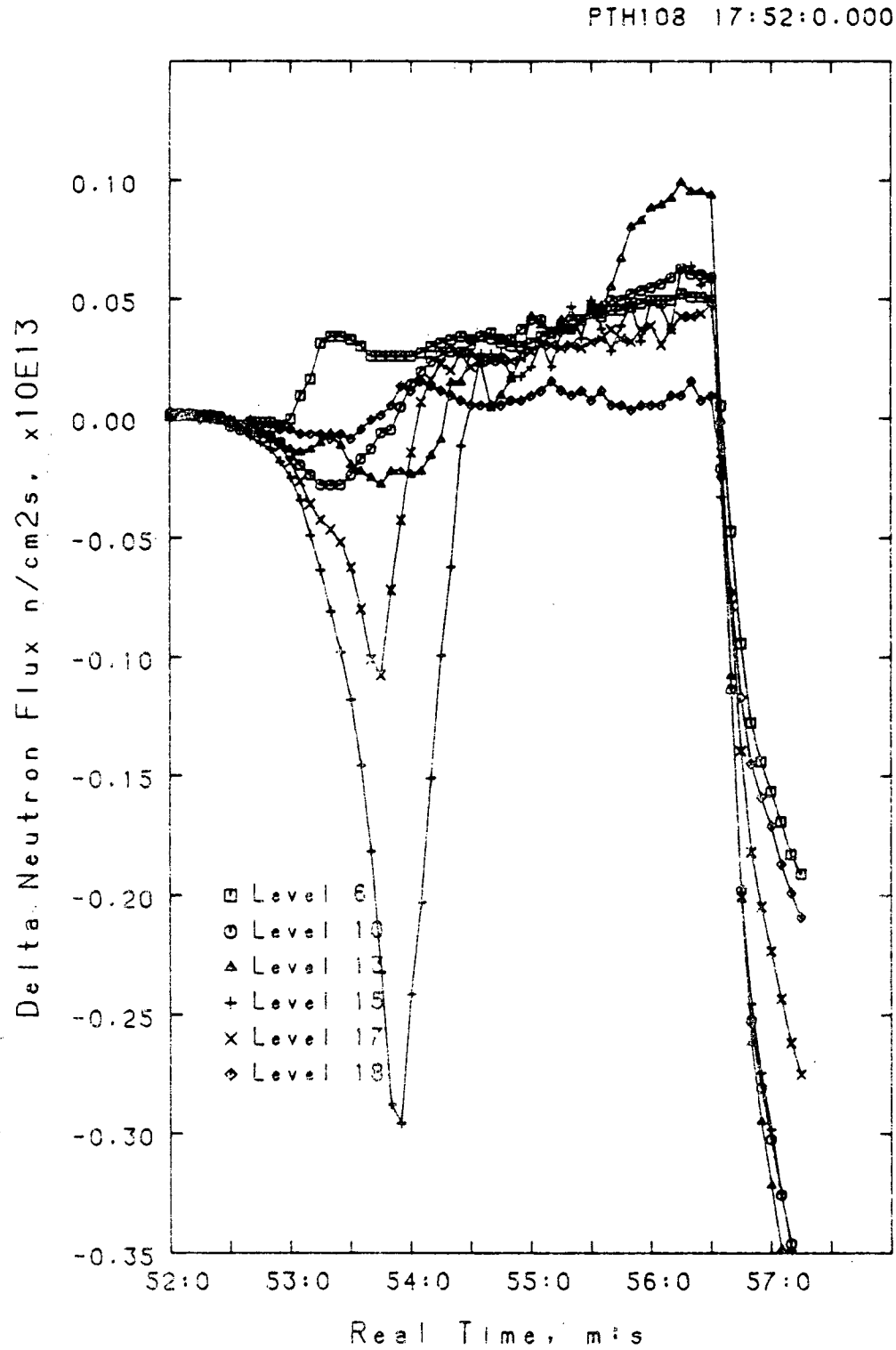

FIGURE 2.2.4.08 CHANGING NEUTRON FLUX (SHROUD) AFTER REFLOODING BEGINS. T=52:41S

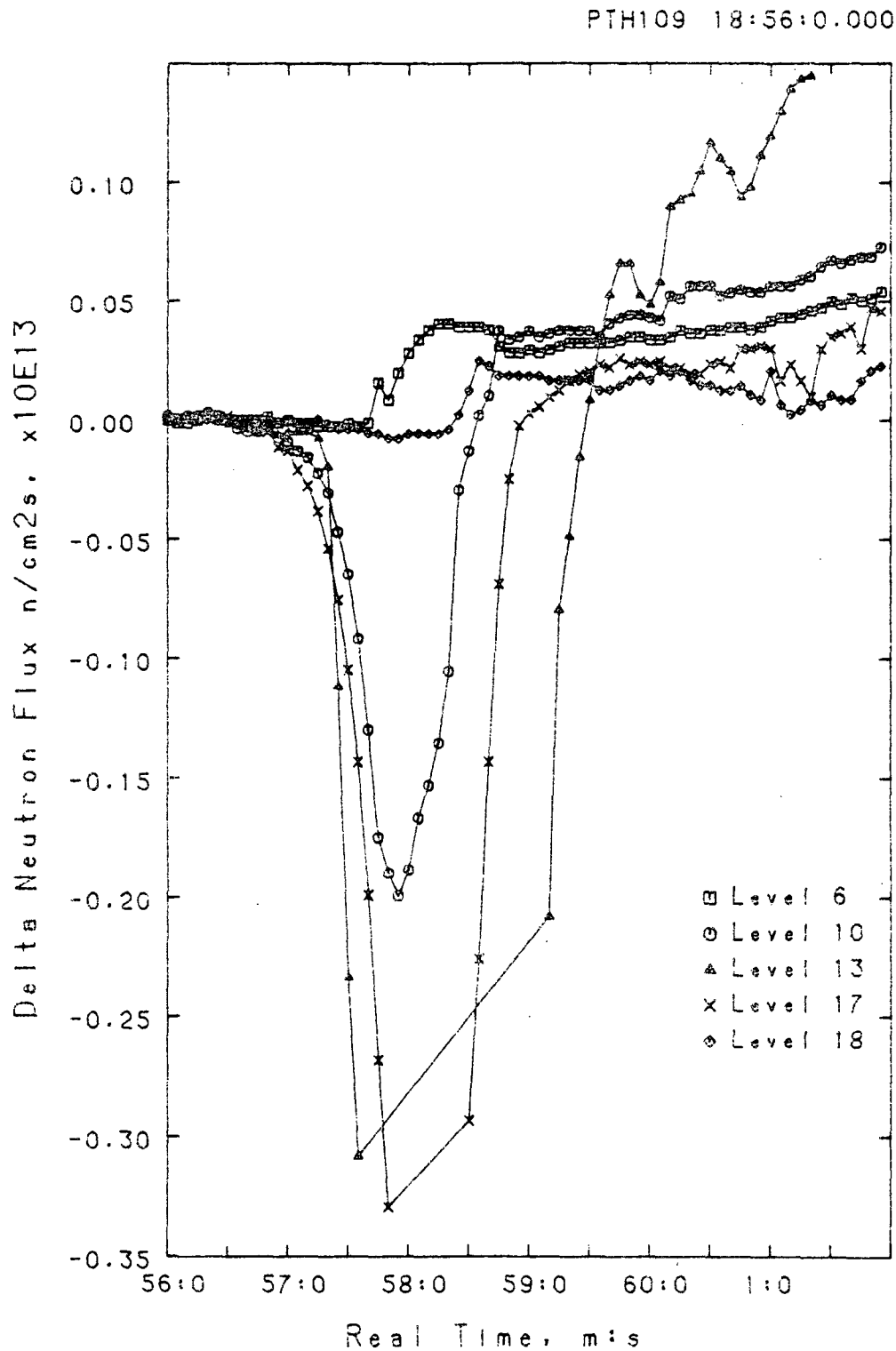

FIGURE 2.2.4.09 CHANGING NEUTRON FLUX (SHROUD) AFTER REFLOODING BEGINS, T=56M:47S

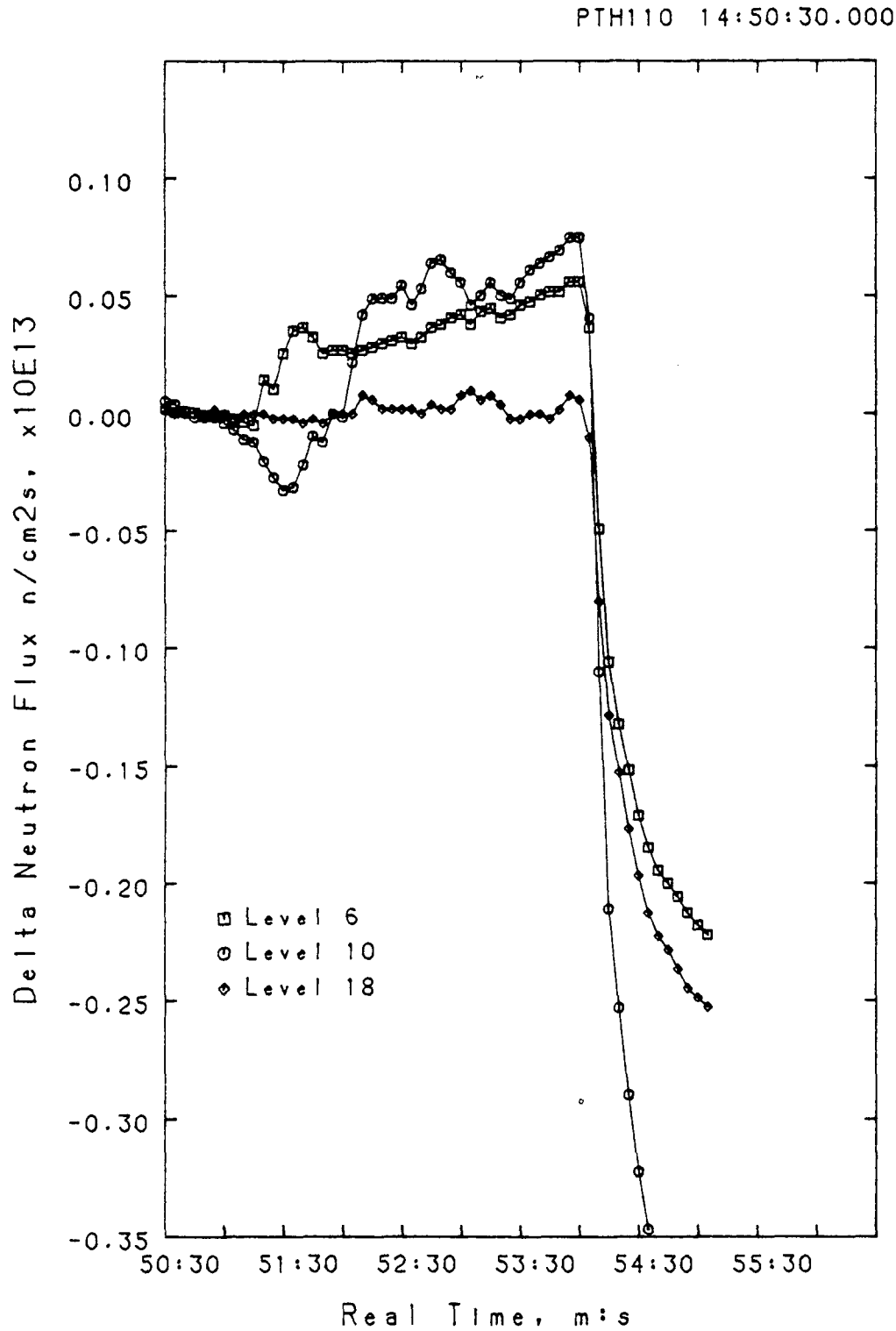

FIGURE 2.2.4.10 CHANGING NEUTRON FLUX (SHROUD) AFTER REFLOODING BEGINS, T=51M:02S

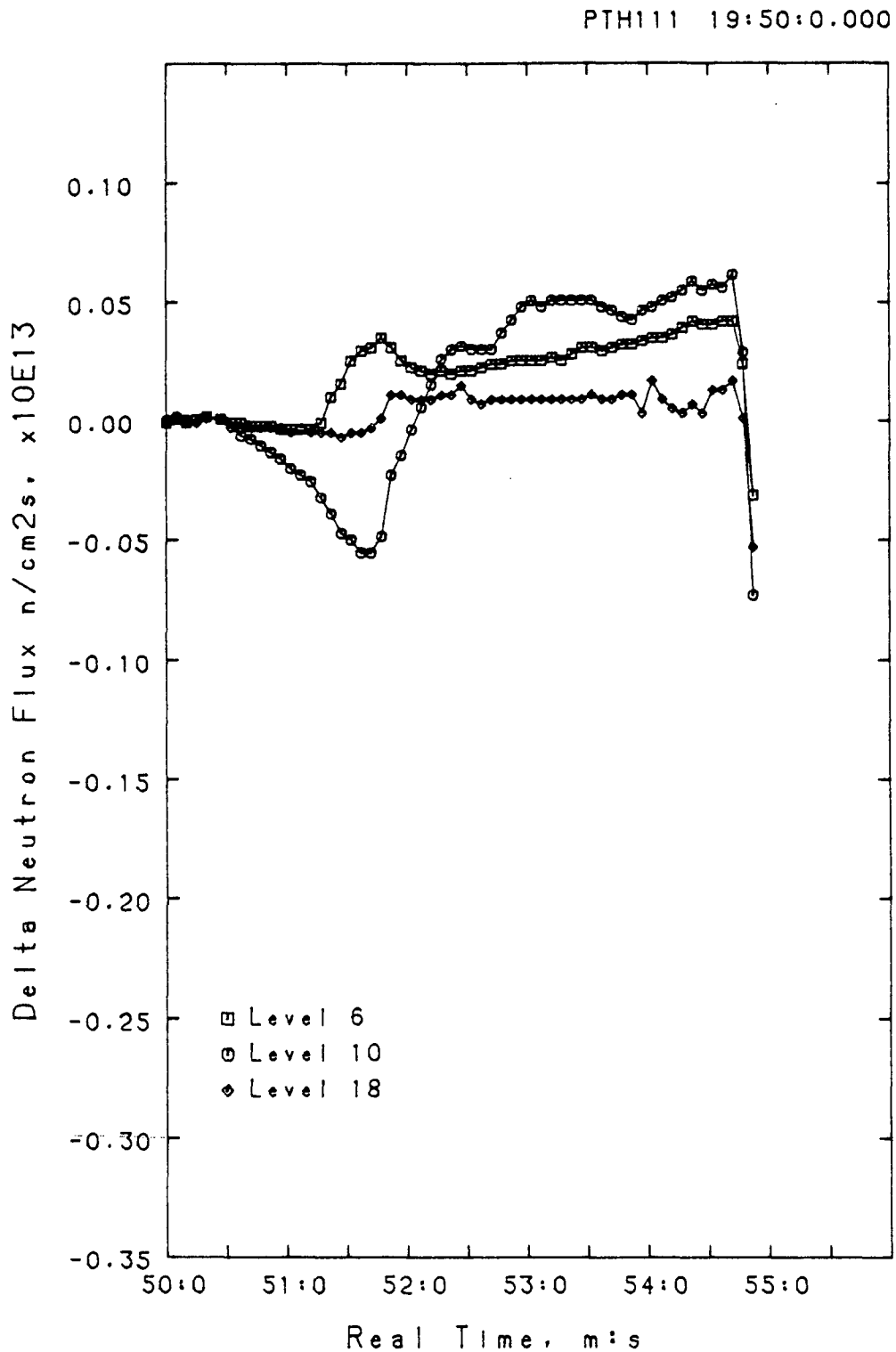

FIGURE 2.2.4.11 CHANGING NEUTRON FLUX (SHROUD) AFTER REFLOODING BEGINS, T=50m:31S

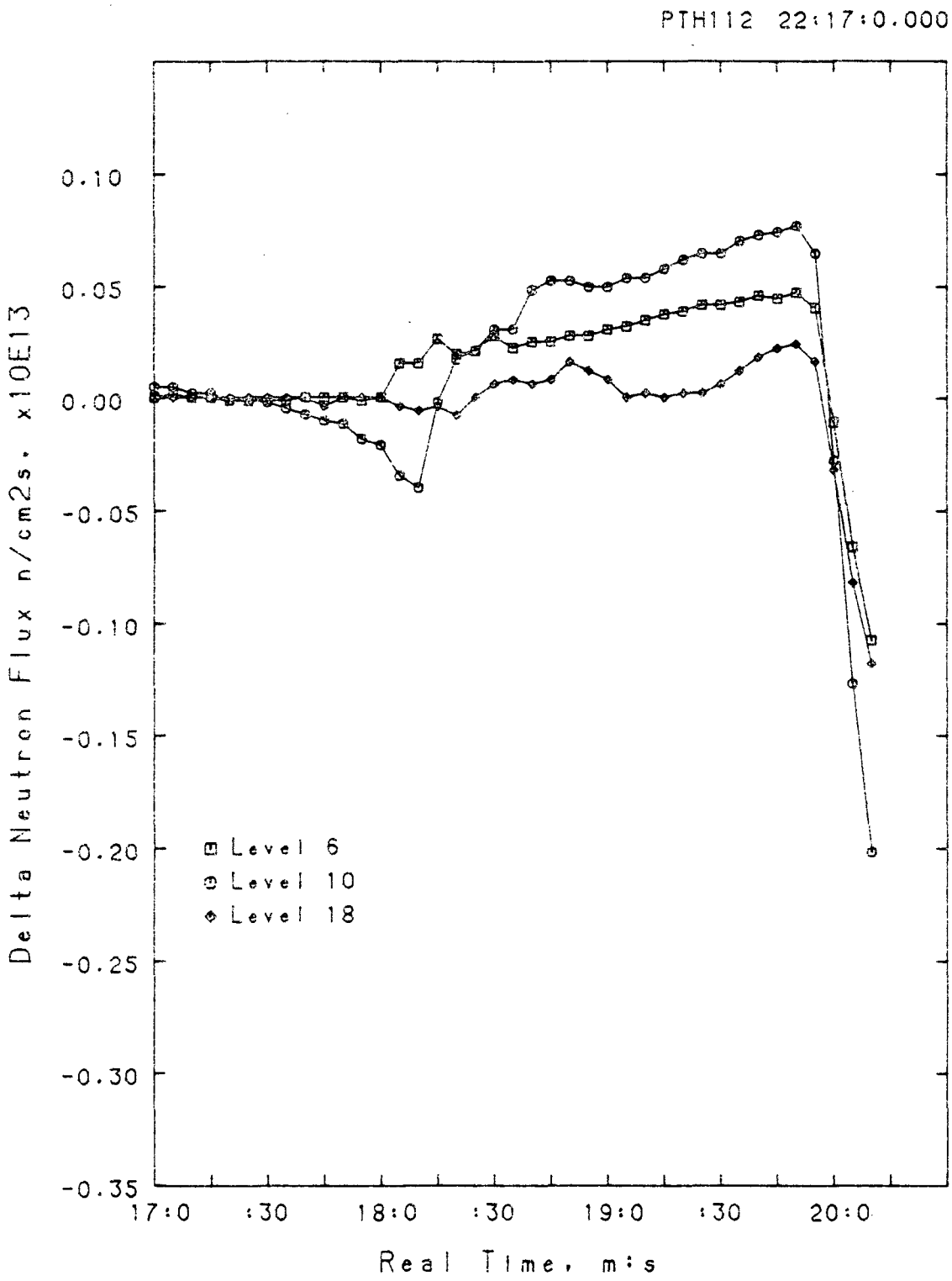

FIGURE 2.2.4.12 CHANGING NEUTRON FLUX (SHROUD) AFTER REFLOODING BEGINS, T=17M:43S

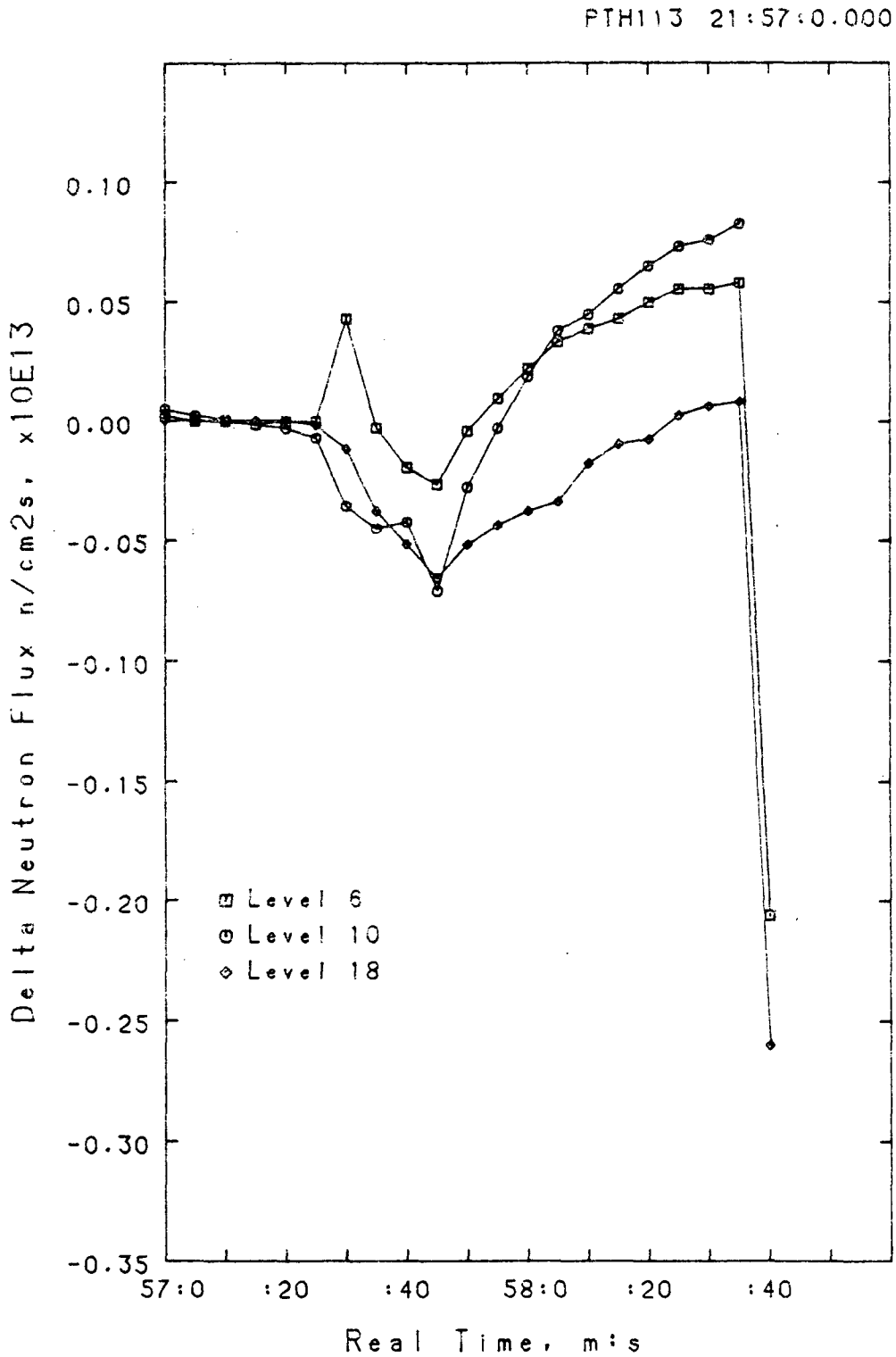

FIGURE 2.2.4.13 CHANGING NEUTRON FLUX (SHROUD) AFTER REFLOODING BEGINS, T=57M:22S

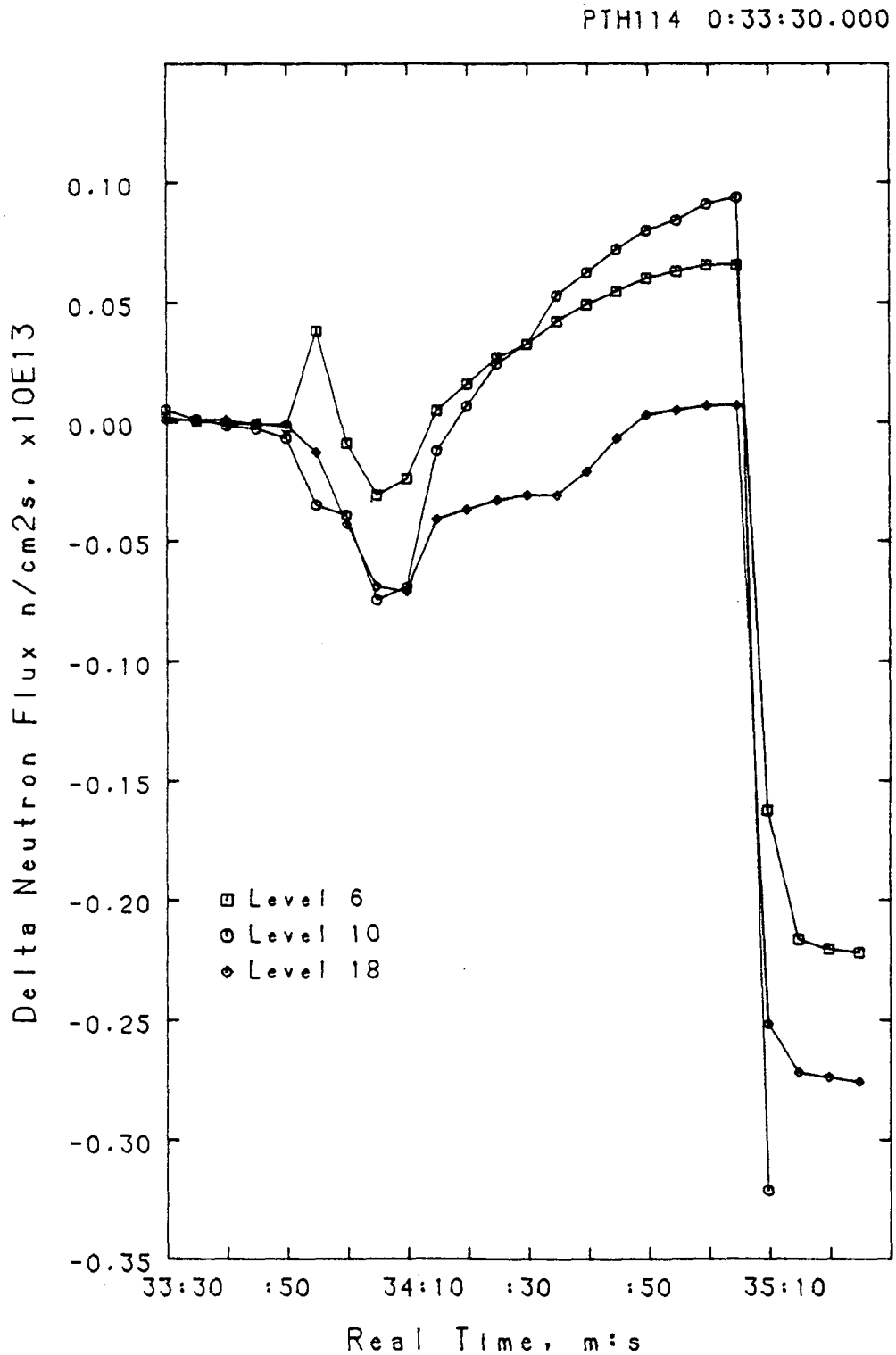

FIGURE 2.2.4.14 CHANGING NEUTRON FLUX (SHROUD) AFTER REFLOODING BEGINS, T=33M:46S

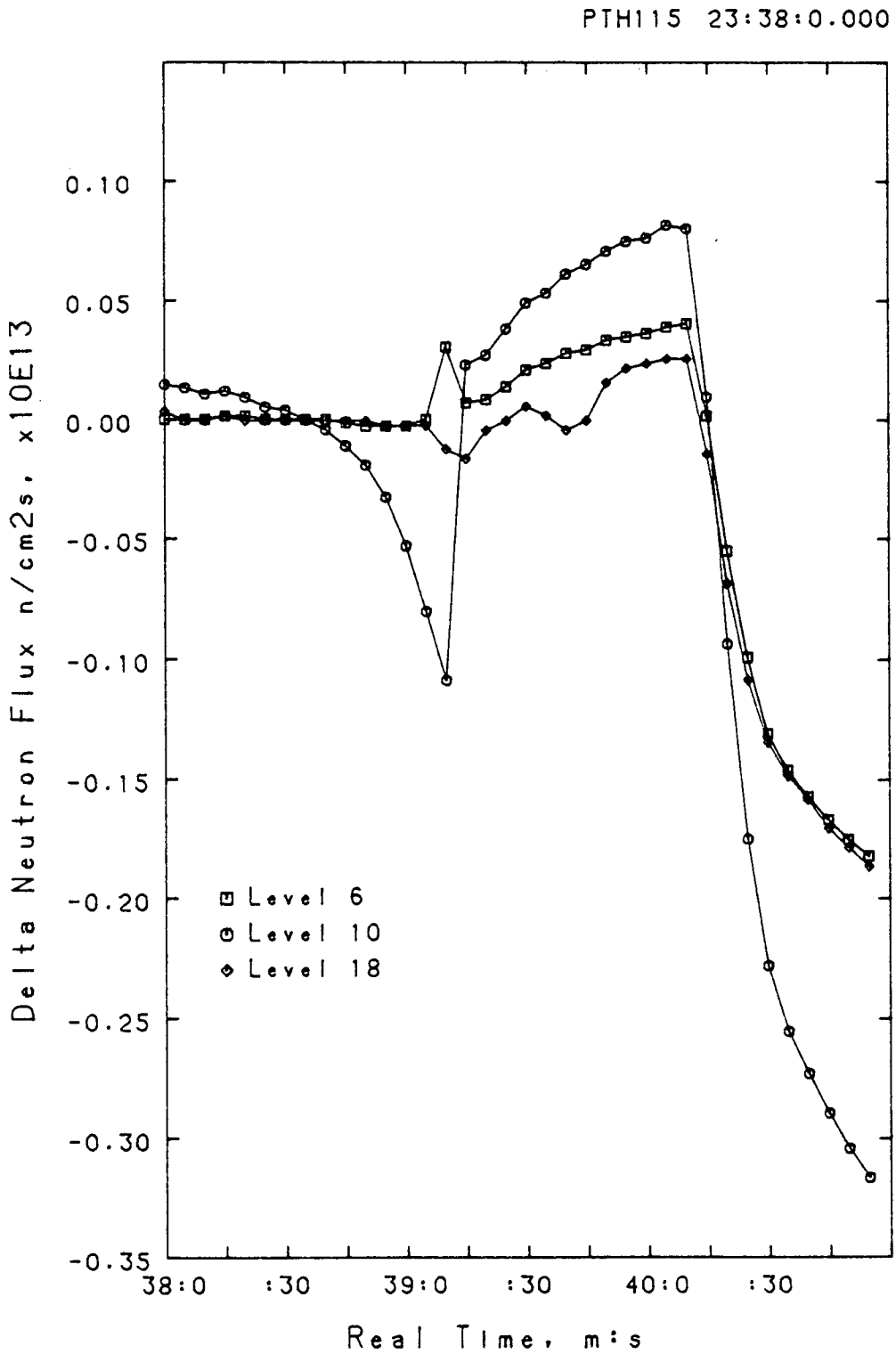

FIGURE 2.2.4.15 CHANGING NEUTRON FLUX (SHROUD) AFTER REFLOODING BEGINS, T=38M:57S

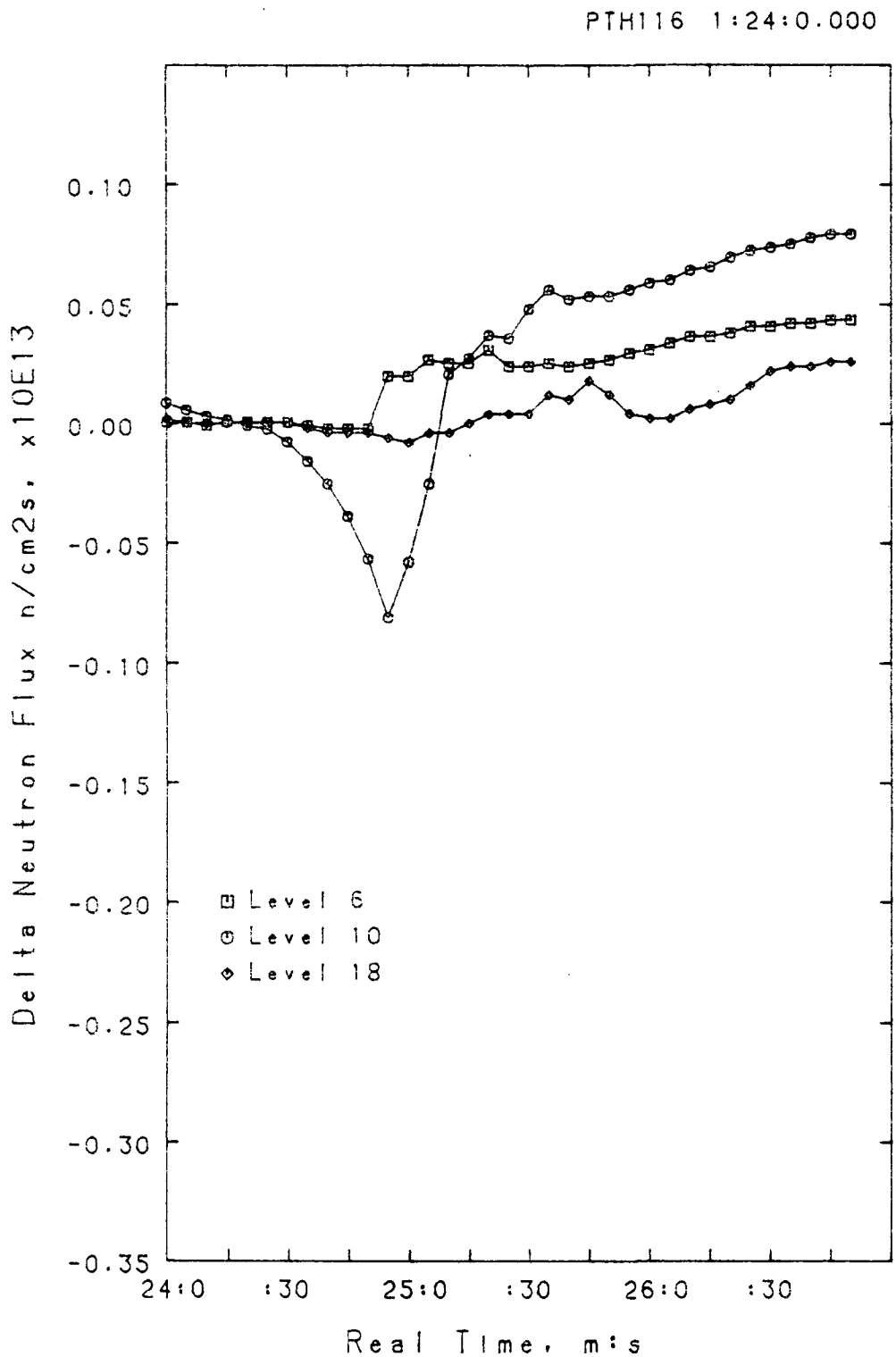

FIGURE 2.2.4.16 CHANGING NEUTRON FLUX (SHROUD) AFTER REFLOODING BEGINS, T=24M:32S

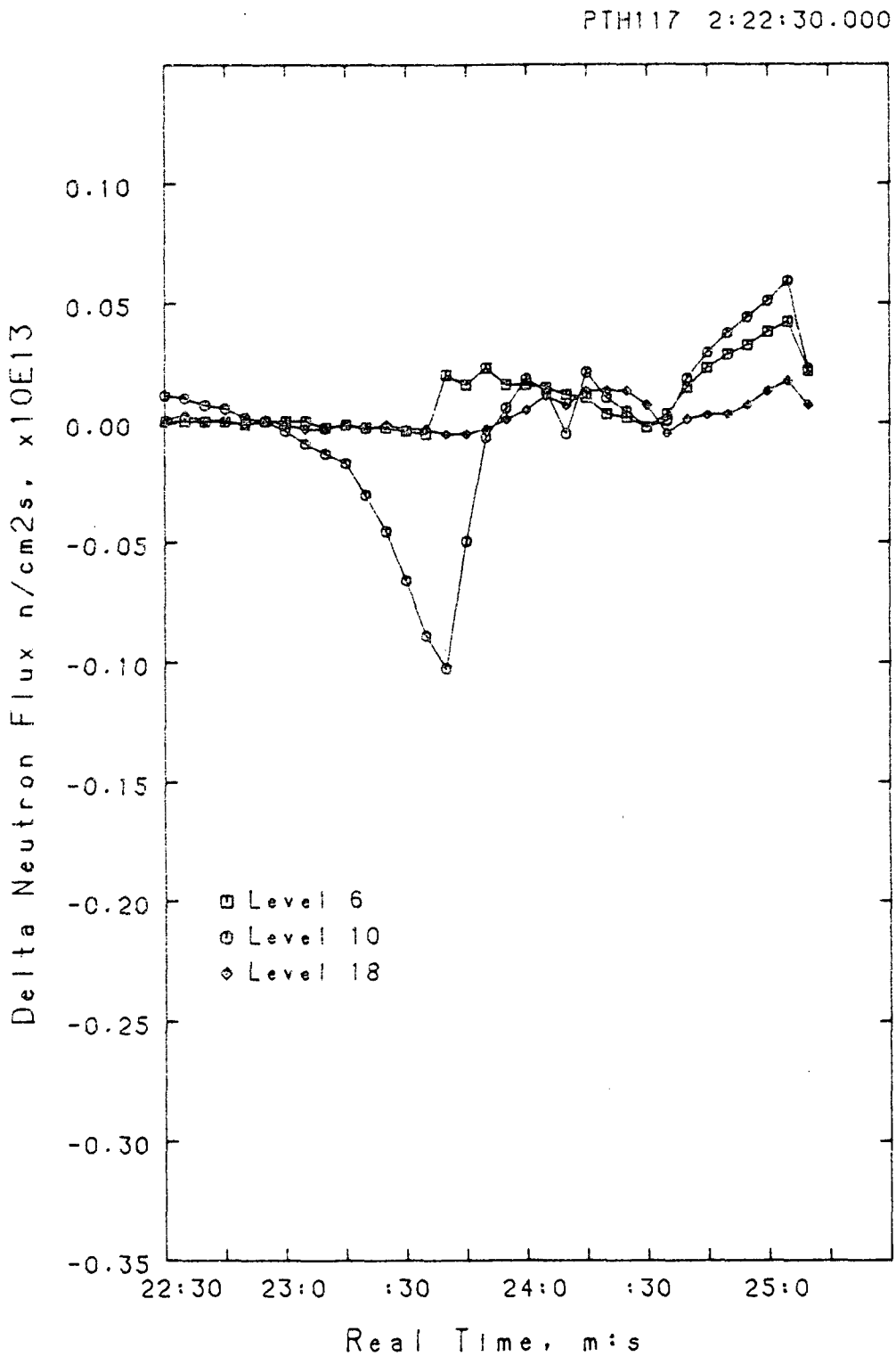

FIGURE 2.2.4.17 CHANGING NEUTRON FLUX (SHROUD) AFTER REFLOODING BEGINS, T=23M:15S

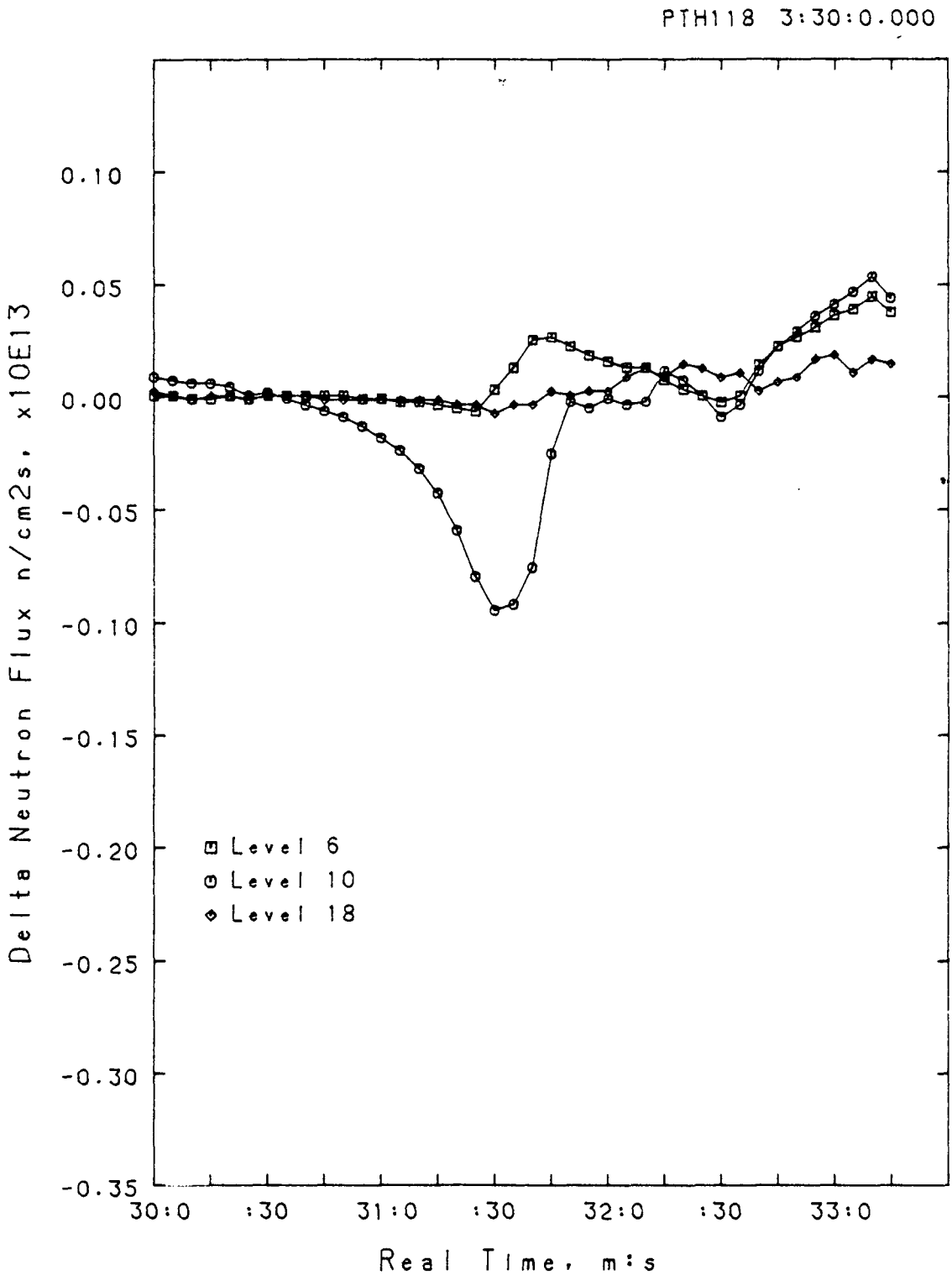

FIGURE 2.2.4.18 CHANGING NEUTRON FLUX (SHROUD) AFTER REFLOODING BEGINS, T=30M:56S

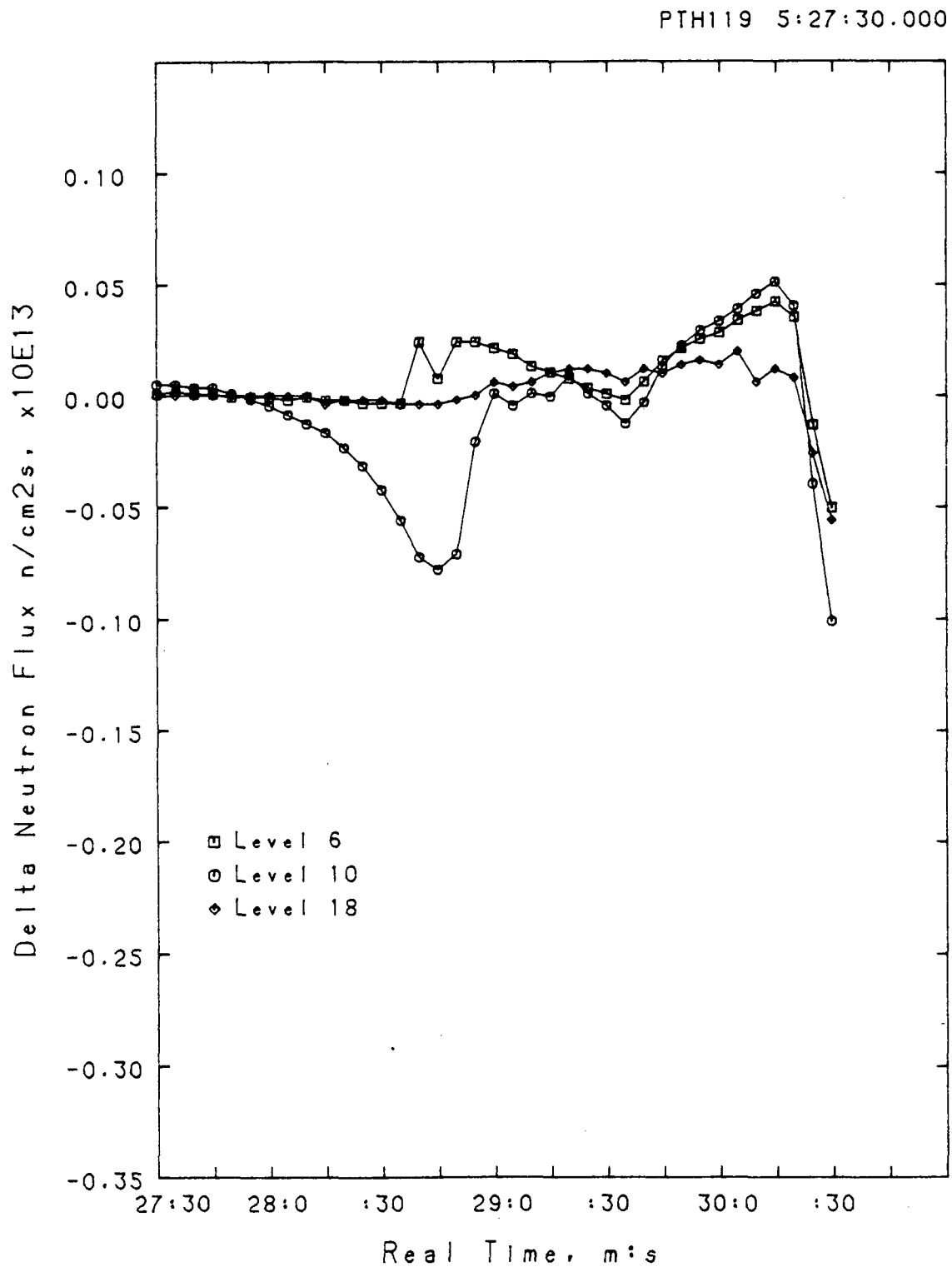

FIGURE 2.2.4.19 CHANGING NEUTRON FLUX (SHROUD) AFTER REFLOODING BEGINS, T=28M:8S

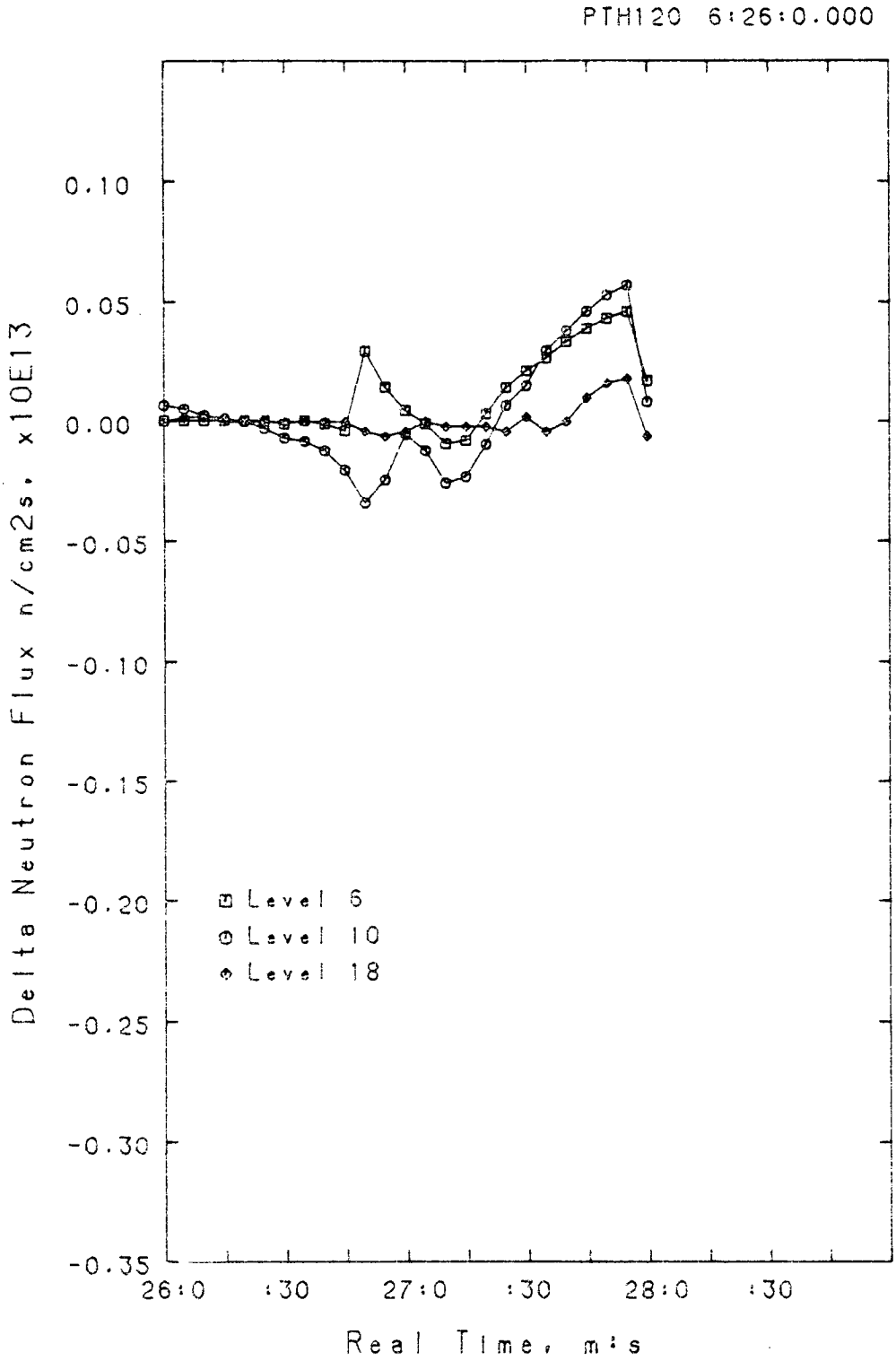

FIGURE 2.2.4.20 CHANGING NEUTRON FLUX (SHROUD) AFTER REFLOODING BEGINS, T=26M:34S

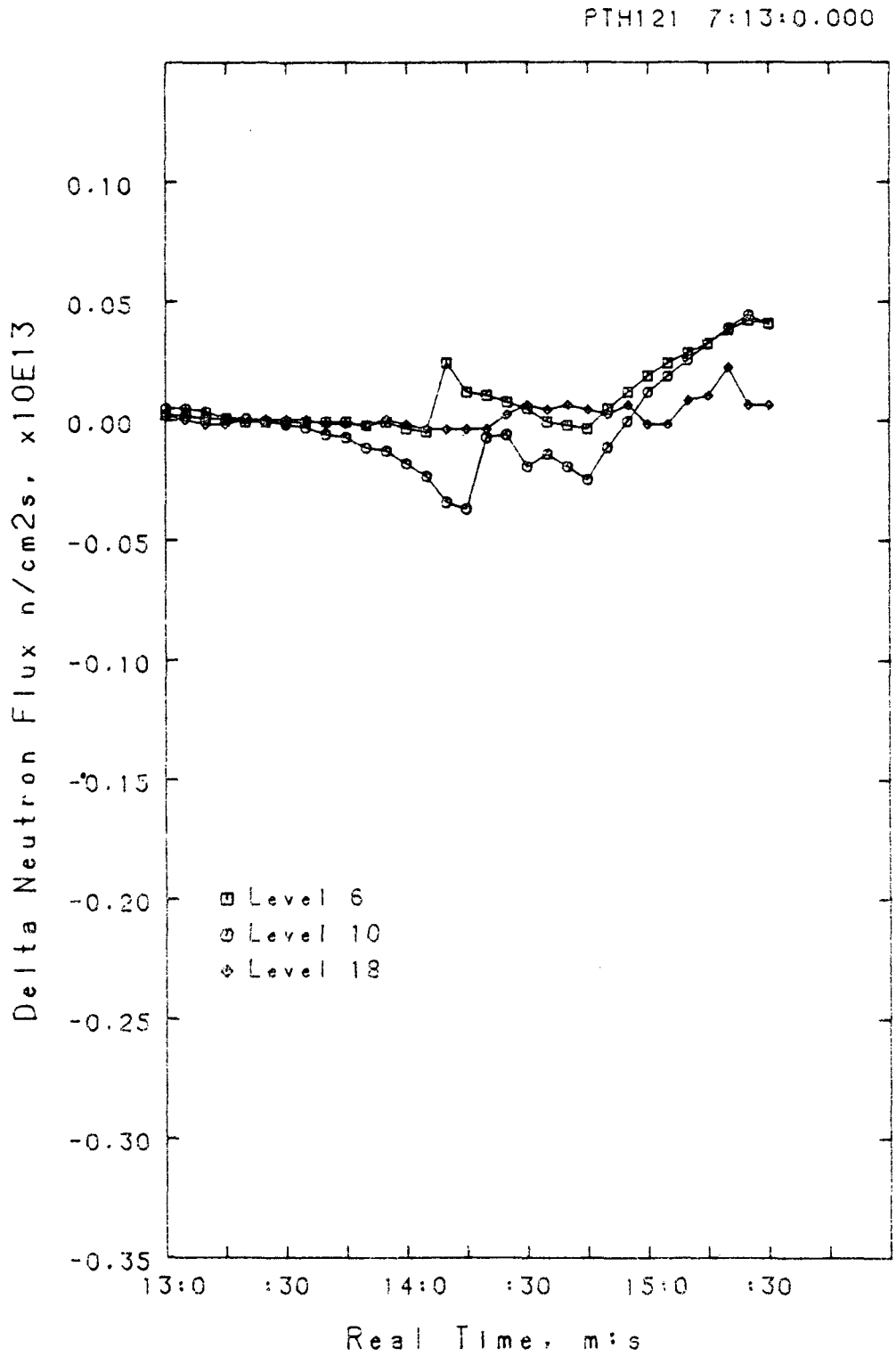

FIGURE 2.2.4.21 CHANGING NEUTRON FLUX (SHROUD) AFTER REFLOODING BEGINS, T=13M:45S

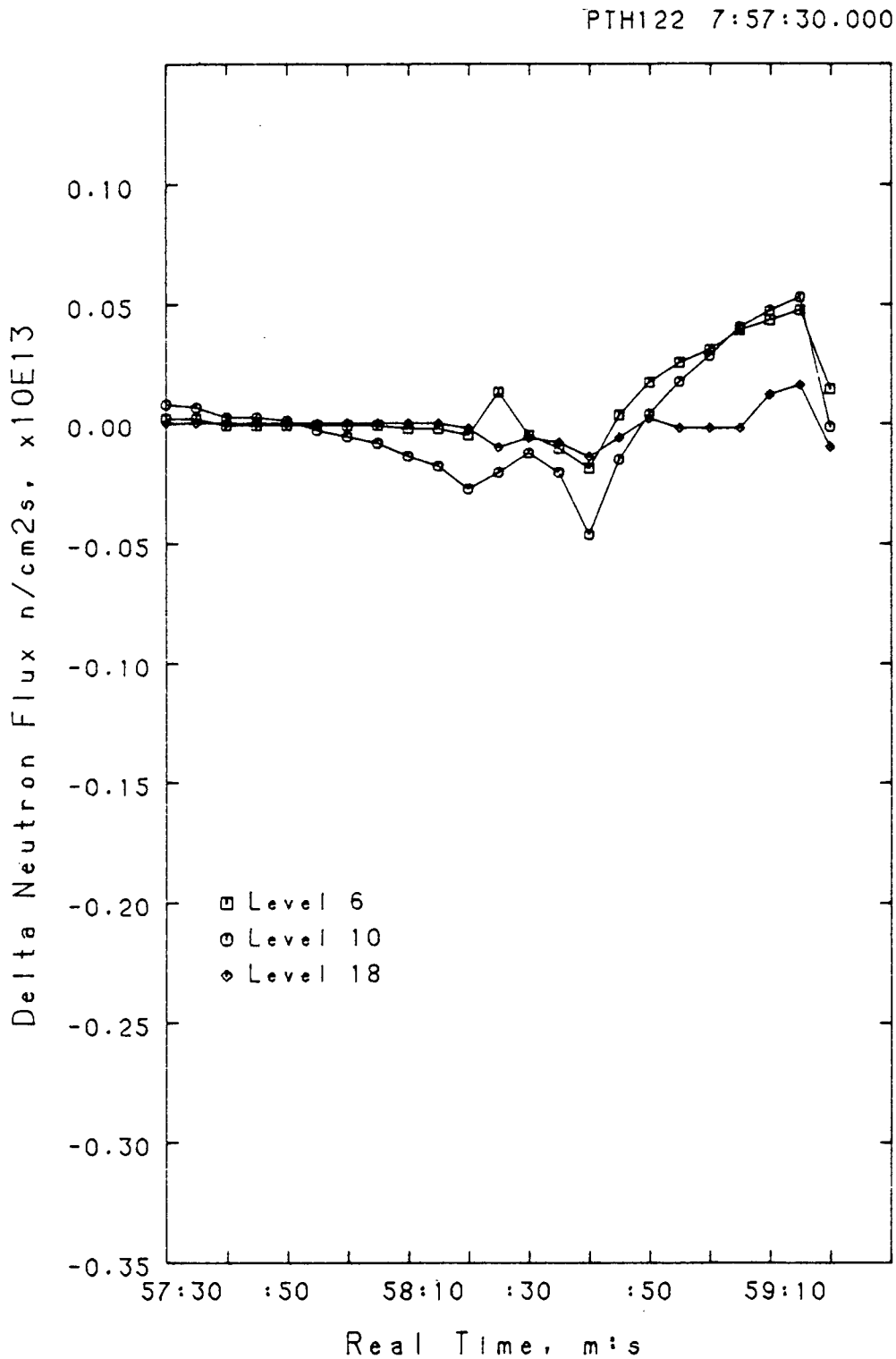

FIGURE 2.2.4.22 CHANGING NEUTRON FLUX (SHROUD) AFTER REFLOODING BEGINS, T=58M:5S

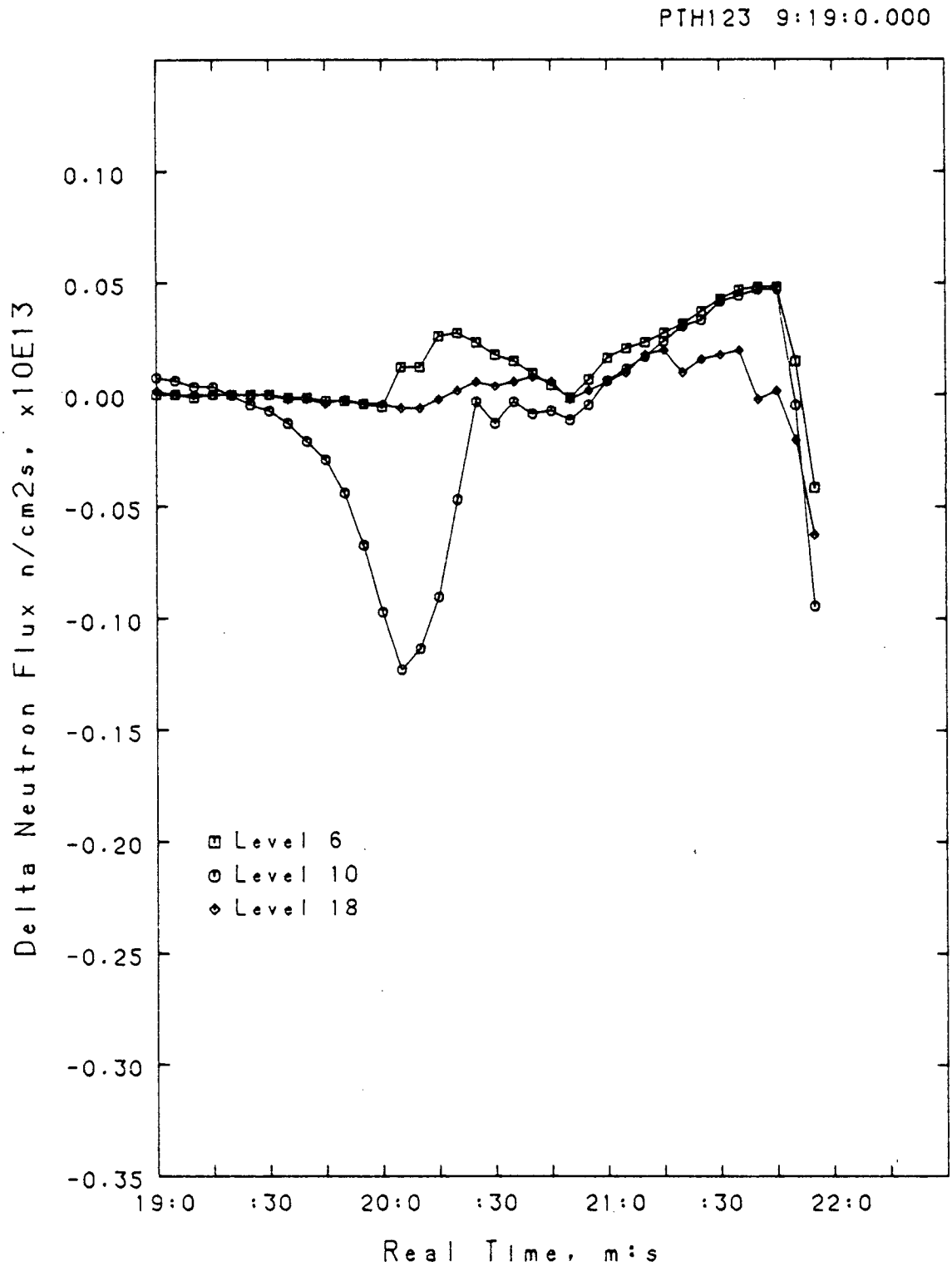

FIGURE 2.2.4.23 CHANGING NEUTRON FLUX (SHROUD) AFTER REFLOODING BEGINS. T=19M:35S

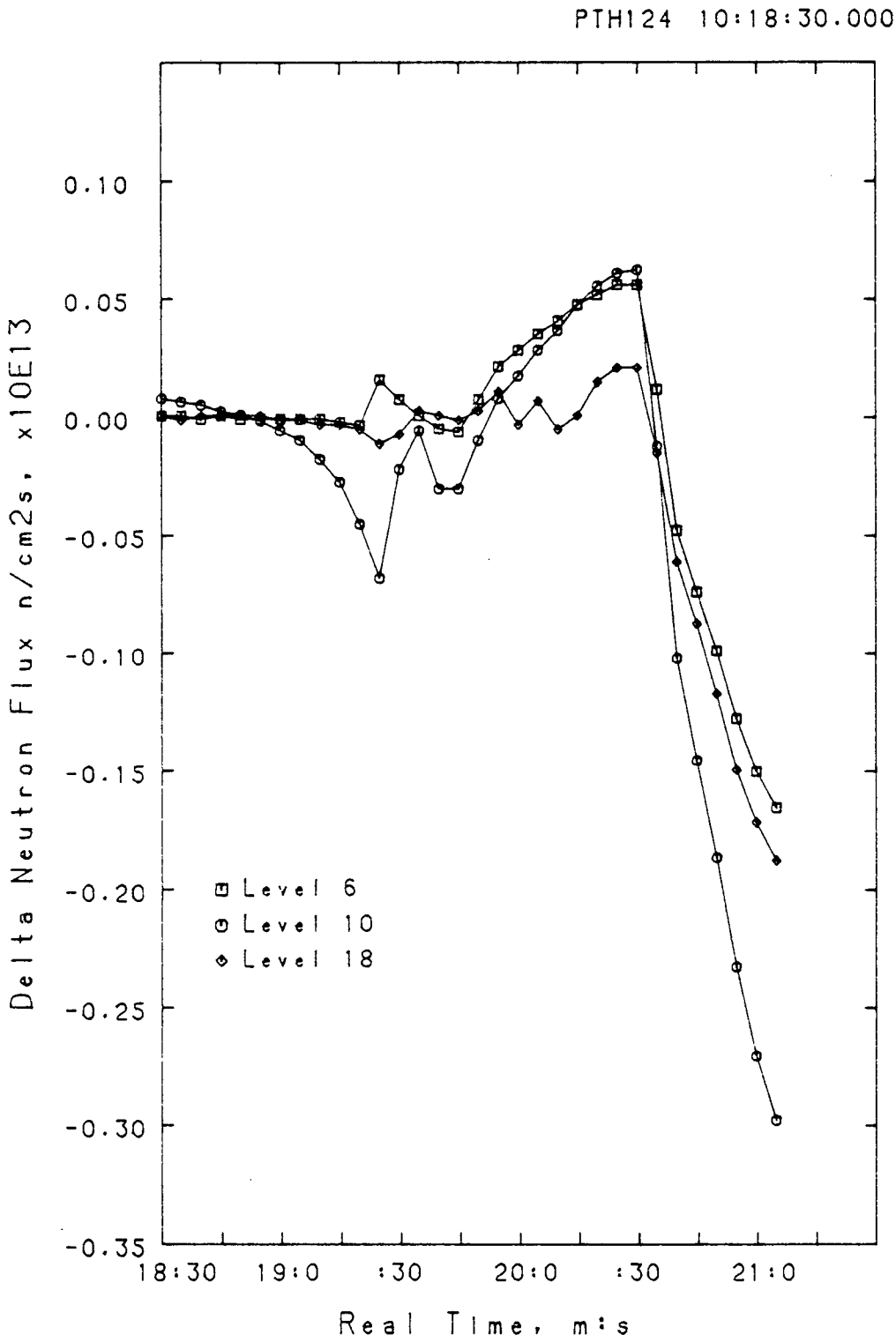

FIGURE 2.2.4.24 CHANGING NEUTRON FLUX (SHROUD) AFTER REFLOODING BEGINS, T=19M:07S

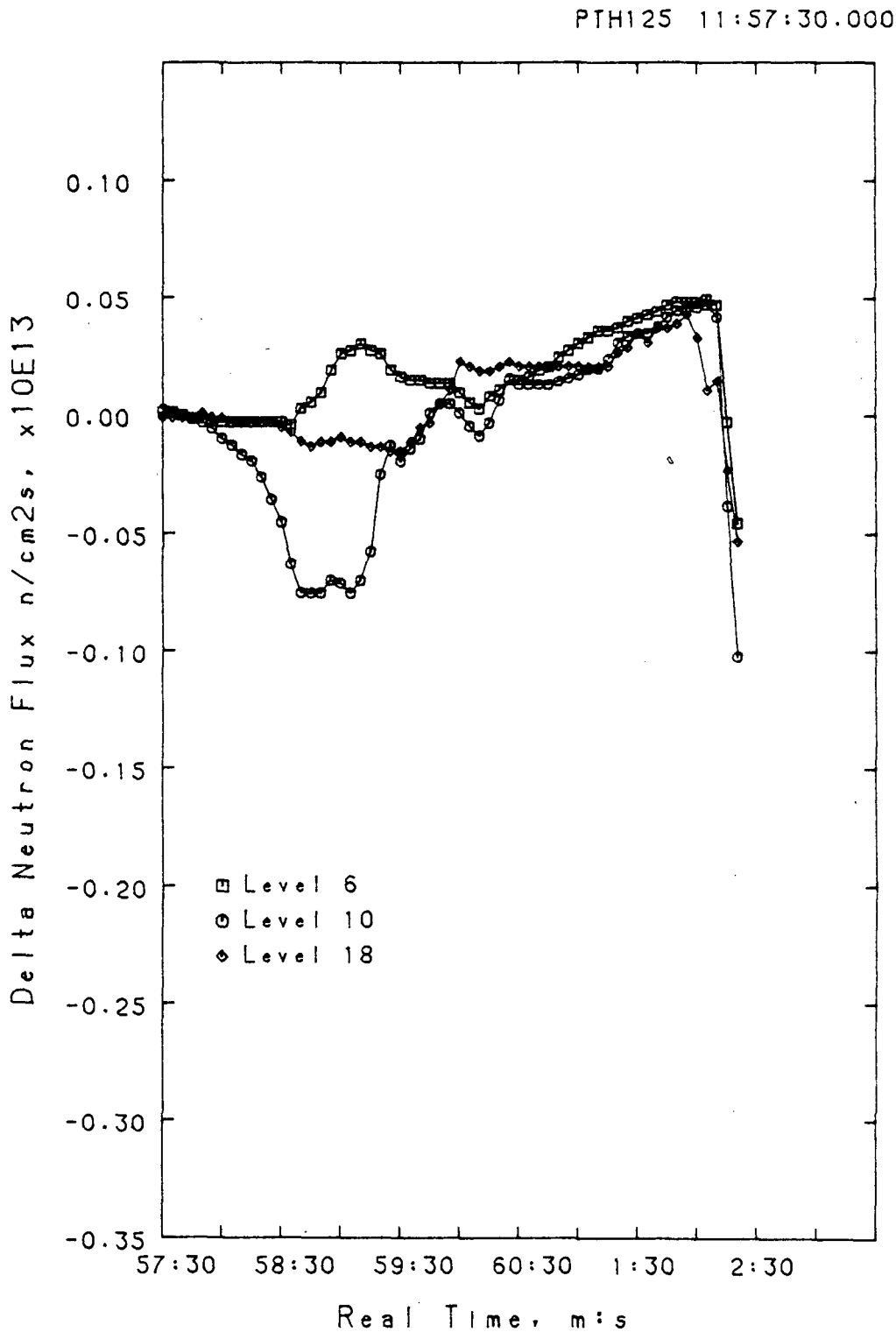

FIGURE 2.2.4.25 CHANGING NEUTRON FLUX (SHROUD) AFTER REFLOODING BEGINS, T=57M:46S

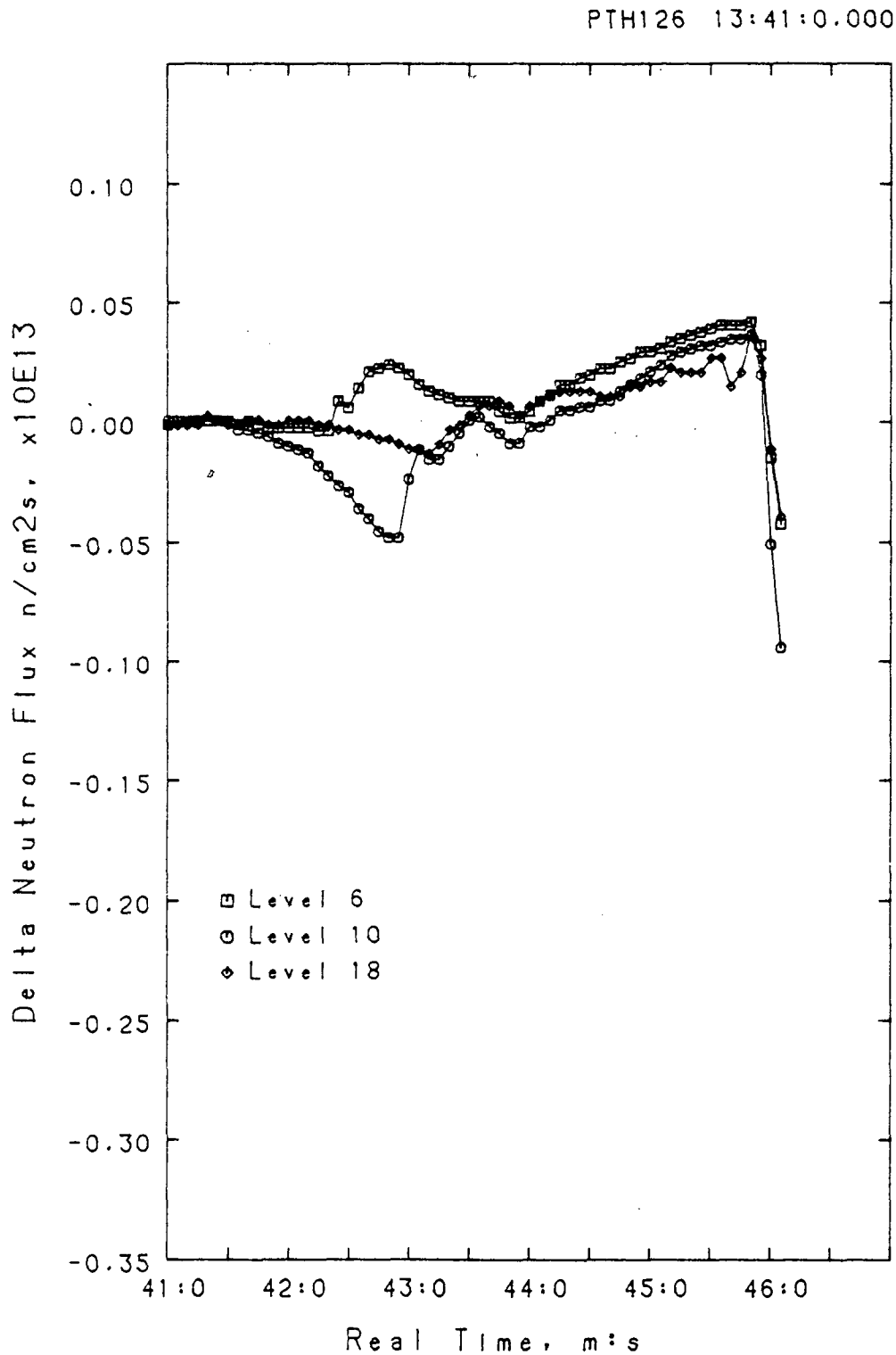

FIGURE 2.2.4.26 CHANING NEUTRON FLUX (SHROUD) AFTER REFLOODING BEGINS, T=41M:36S

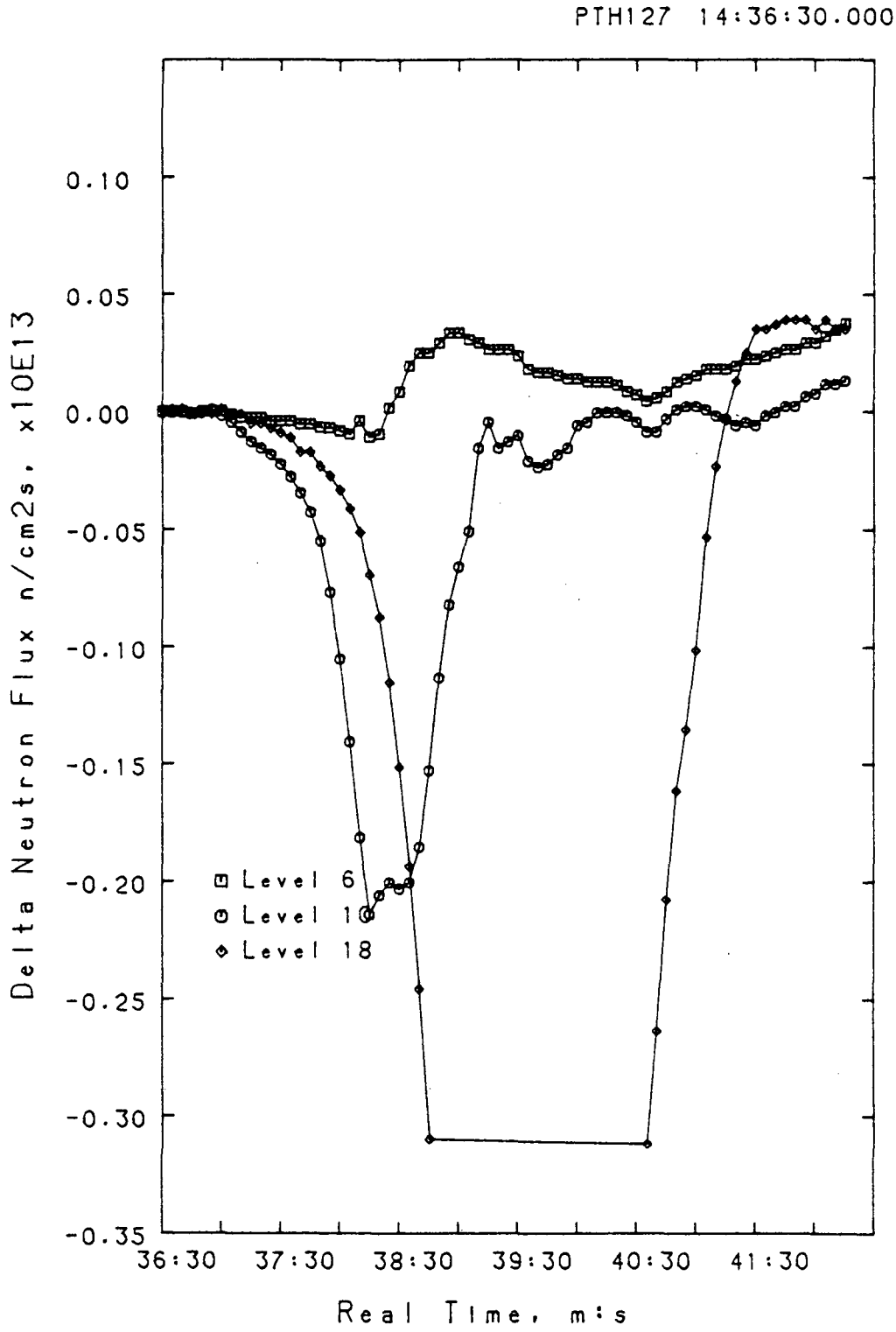

FIGURE 2.2.4.27 CHANGING NEUTRON FLUX (SHROUD) AFTER REFLOODING BEGINS, T=37M:09S

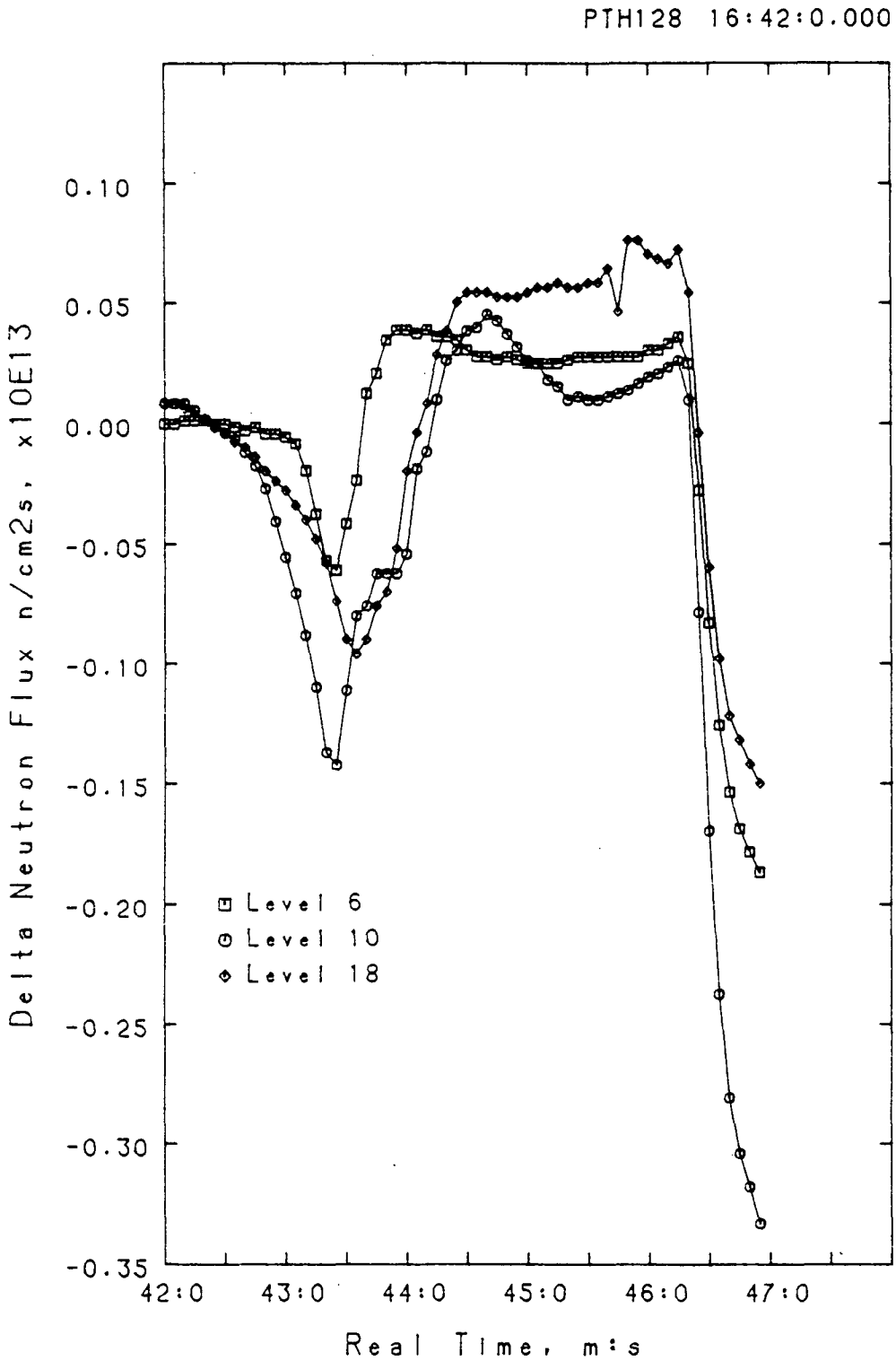

FIGURE 2.2.4.28 CHANGING NEUTRON FLUX (SHROUD) AFTER REFLOODING BEGINS, T=42M:44S

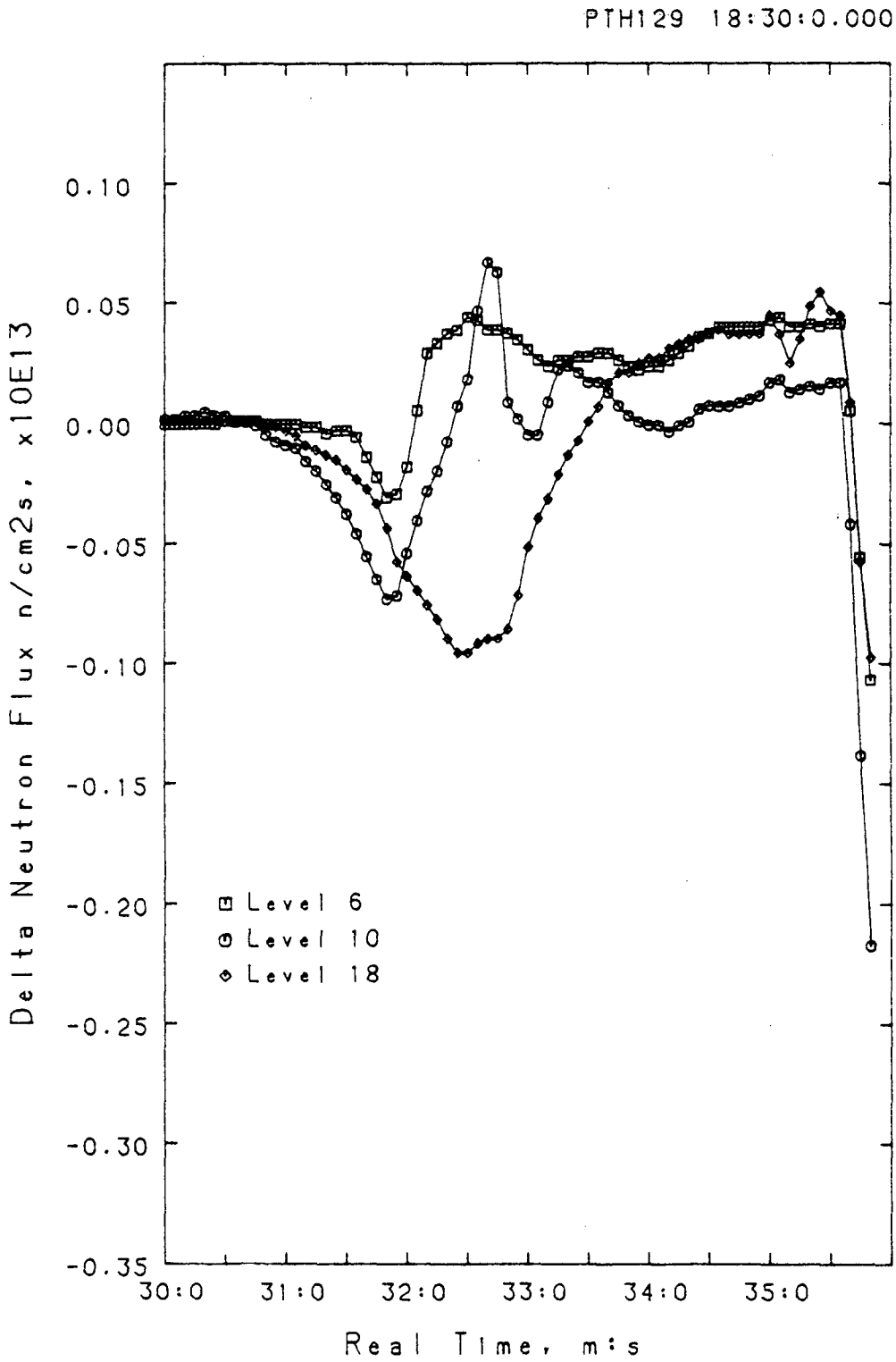

FIGURE 2.2.4.29 CHANGING NEUTRON FLUX (SHROUD) AFTER REFLOODING BEGINS, T=31M:05S

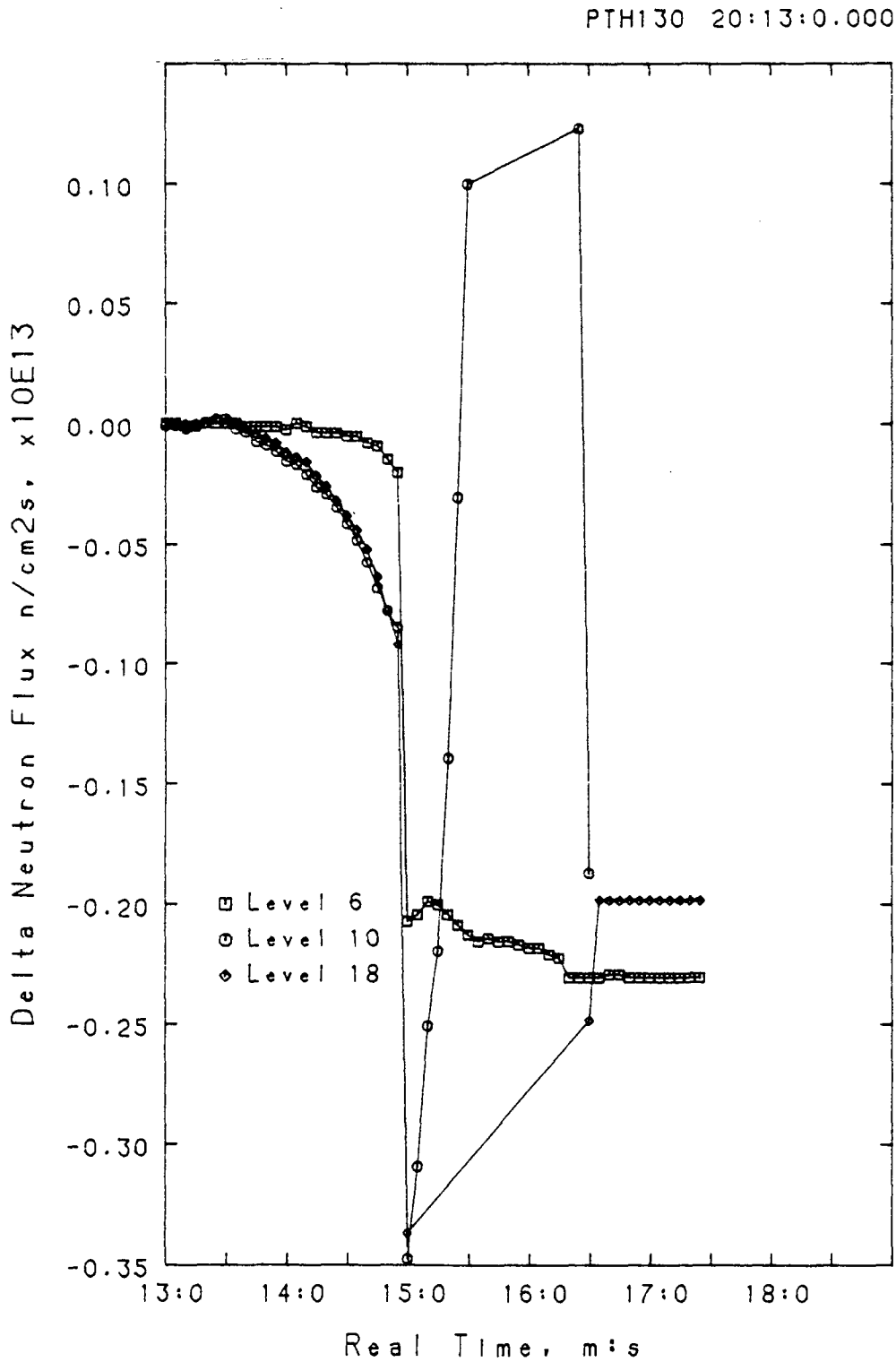

FIGURE 2.2.4.30 CHANGING NEUTRON FLUX (SHROUD) AFTER REFLOODING BEGINS, T=13M:33S

PART 3

STEAM TEMPERATURE PROBE DISTRIBUTIONS

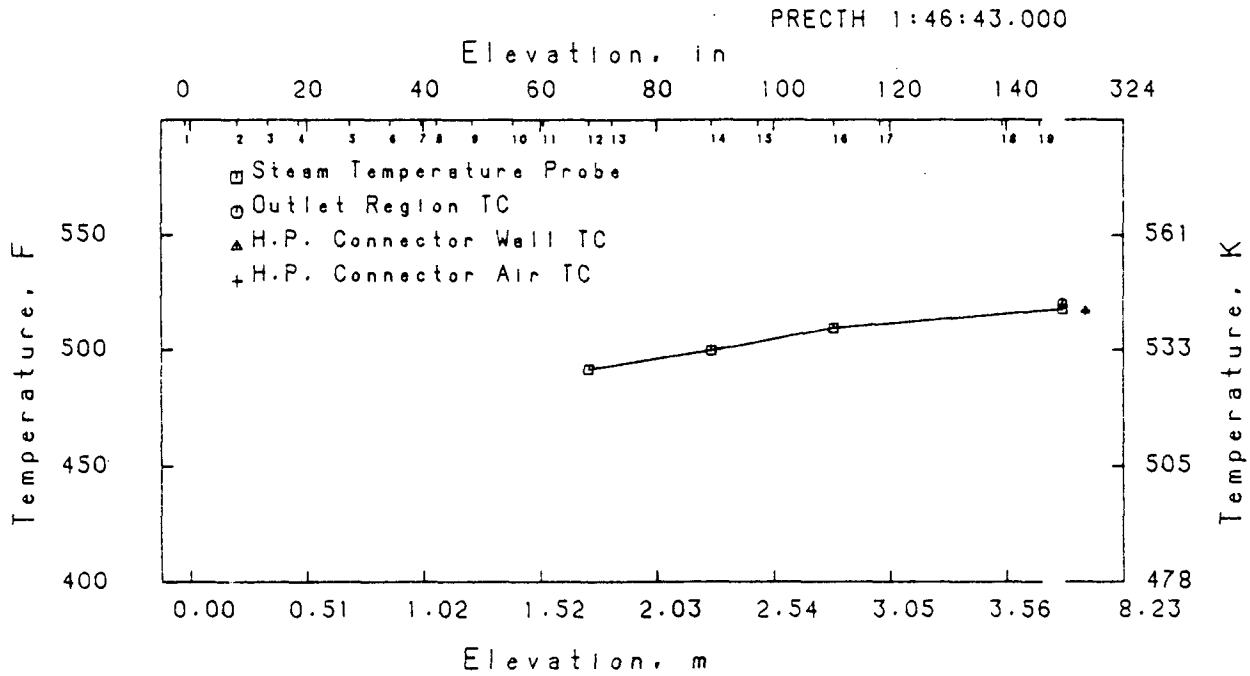

FIGURE 3.1.1 AVERAGE STEAM PROBE AND HP CONNECTOR TEMPERATURE PROFILE (IN WATER-PRECONDITIONING)

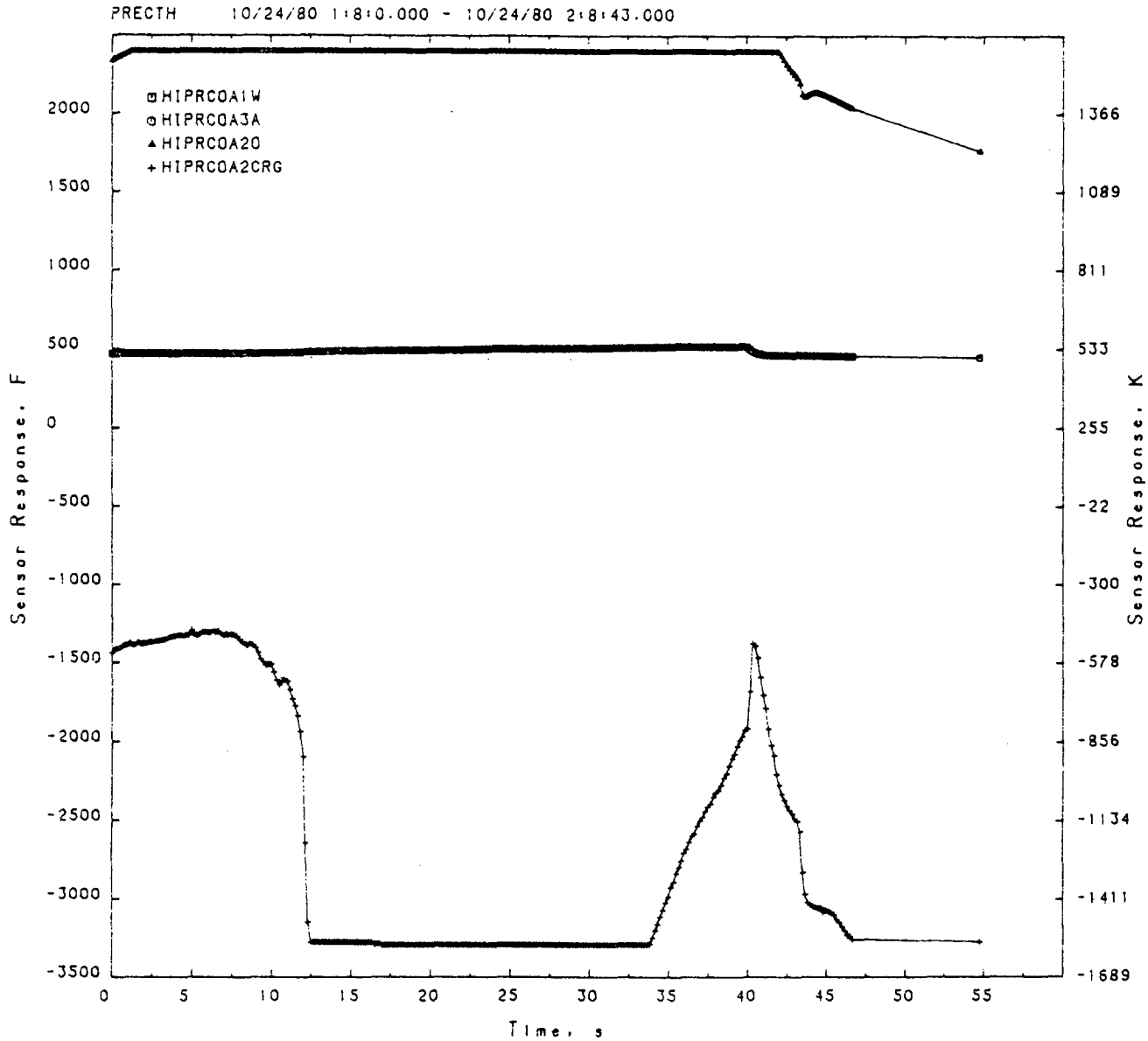

FIGURE 3.1.2 HIGH PRESSURE CONNECTOR TC RESPONSE HISTORY DURING PRECONDITIONING OPERATION

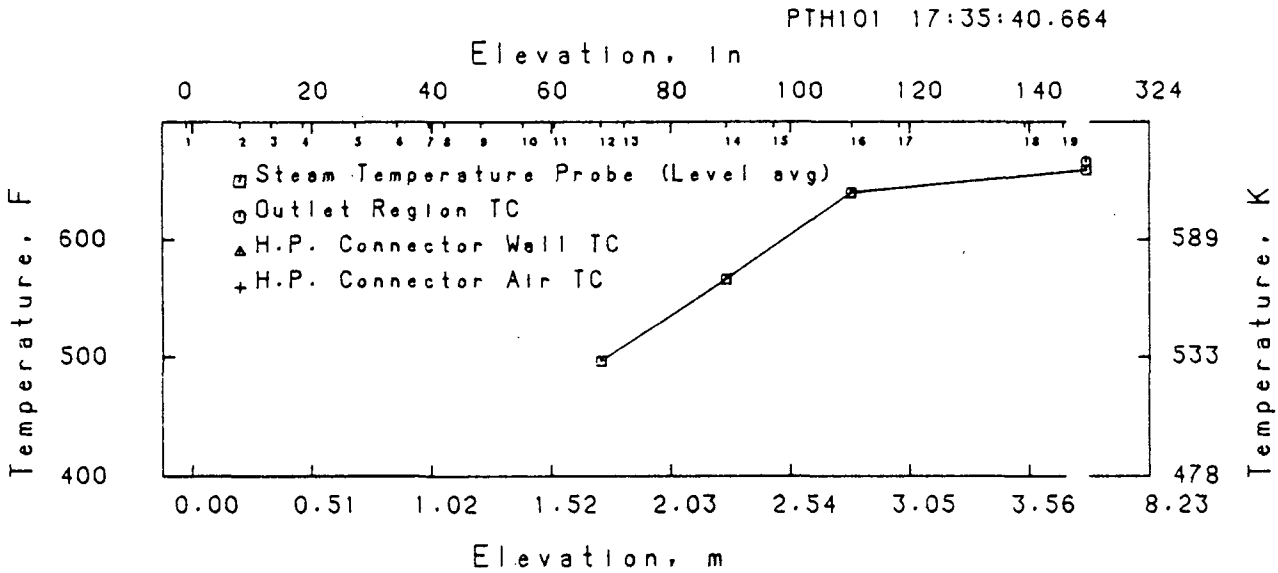

FIGURE 3.2.1 STEAM PROBE AND CONNECTOR TEMPERATURE PROFILE (IN STEAM-PRETRANSIENT)

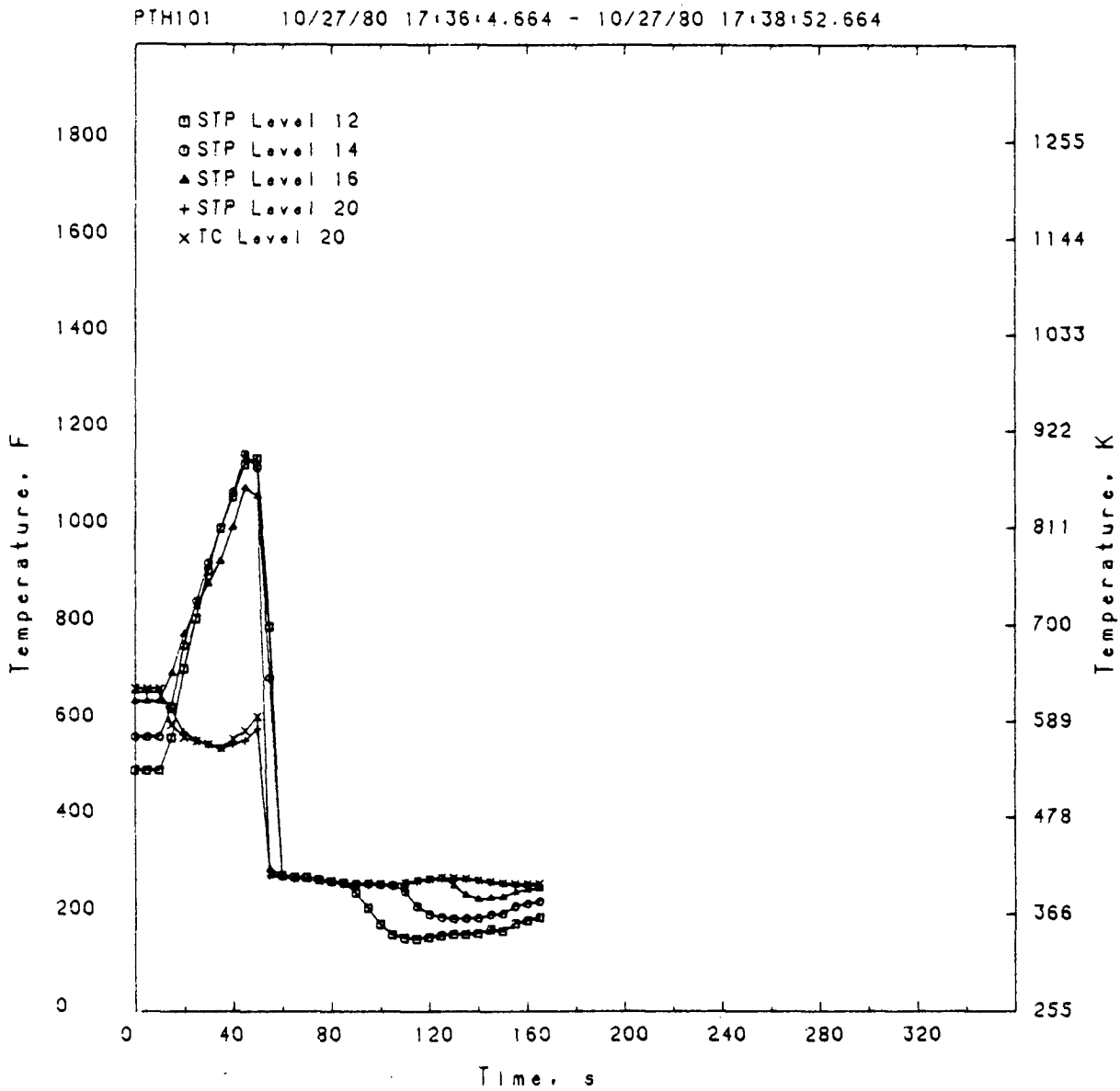

FIGURE 3.2.2.01 STEAM TEMPERATURE PROBE HISTORY DURING TRANSIENT PTH101

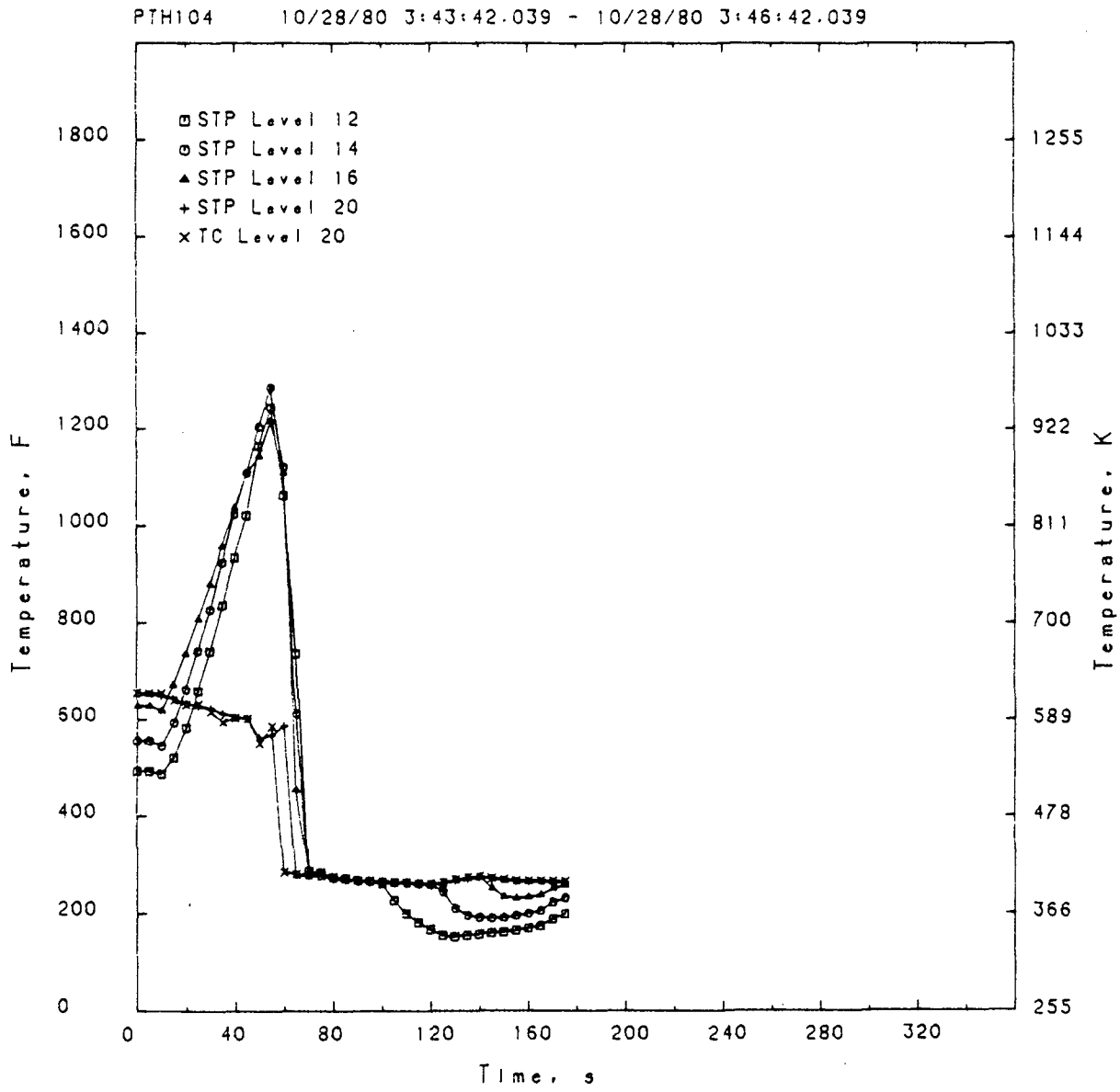

FIGURE 3.2.2.04 STEAM TEMPERATURE PROBE HISTORY DURING TRANSIENT PTH104

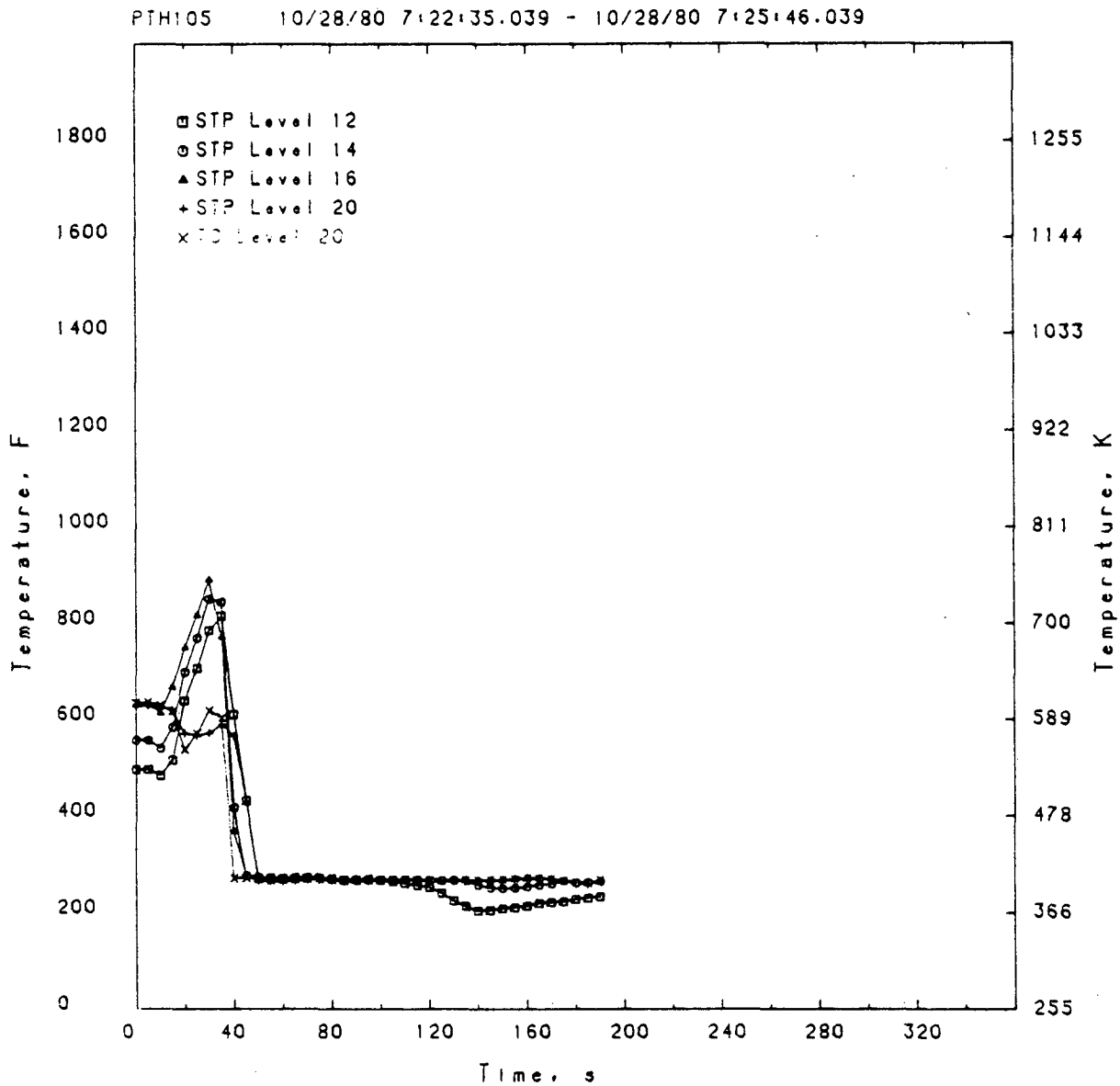

FIGURE 3.2.2.05 STEAM TEMPERATURE PROBE HISTORY DURING TRANSIENT PTH105

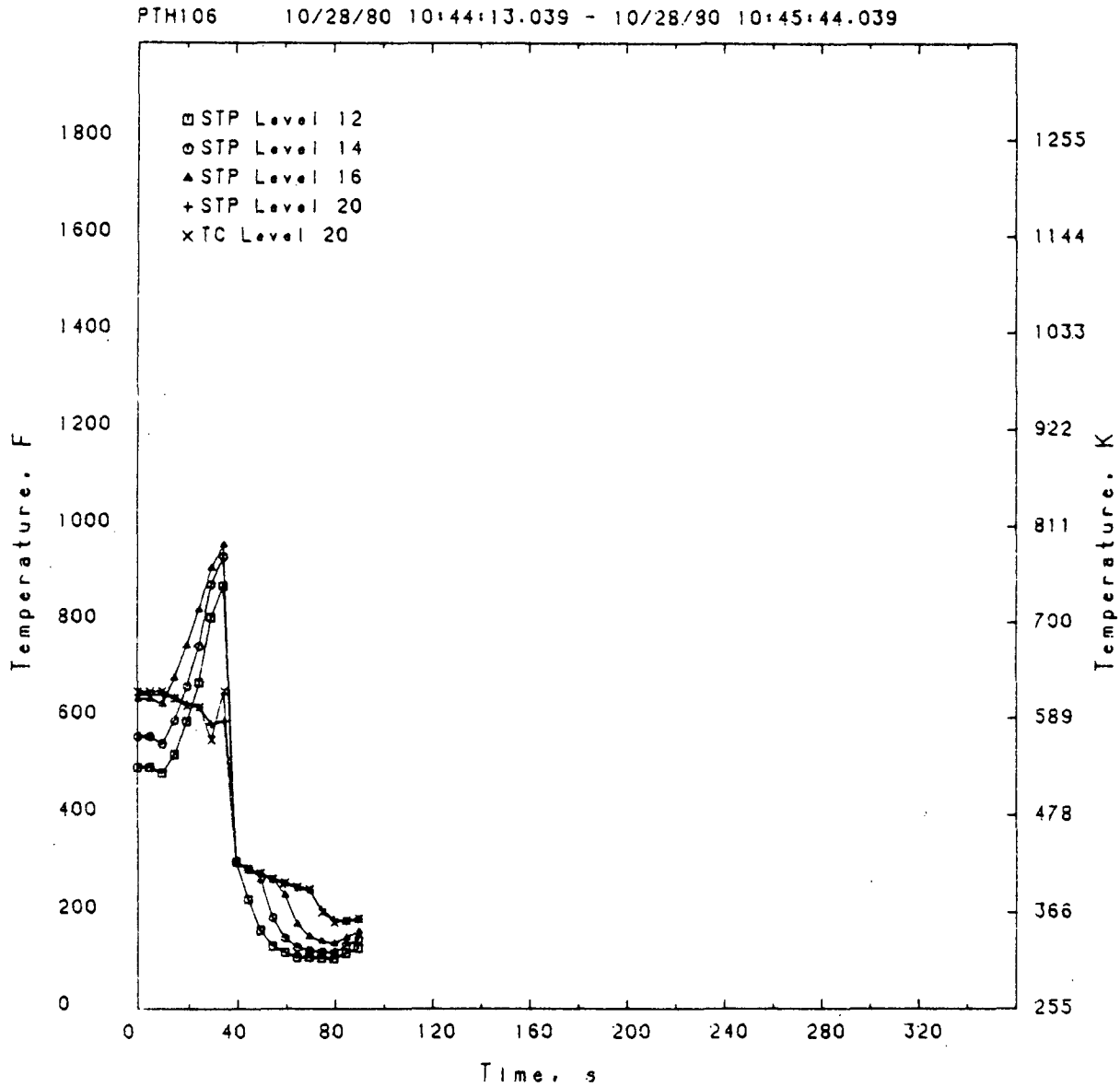

FIGURE 3.2.2.06 STEAM TEMPERATURE PROBE HISTORY DURING TRANSIENT PTH106

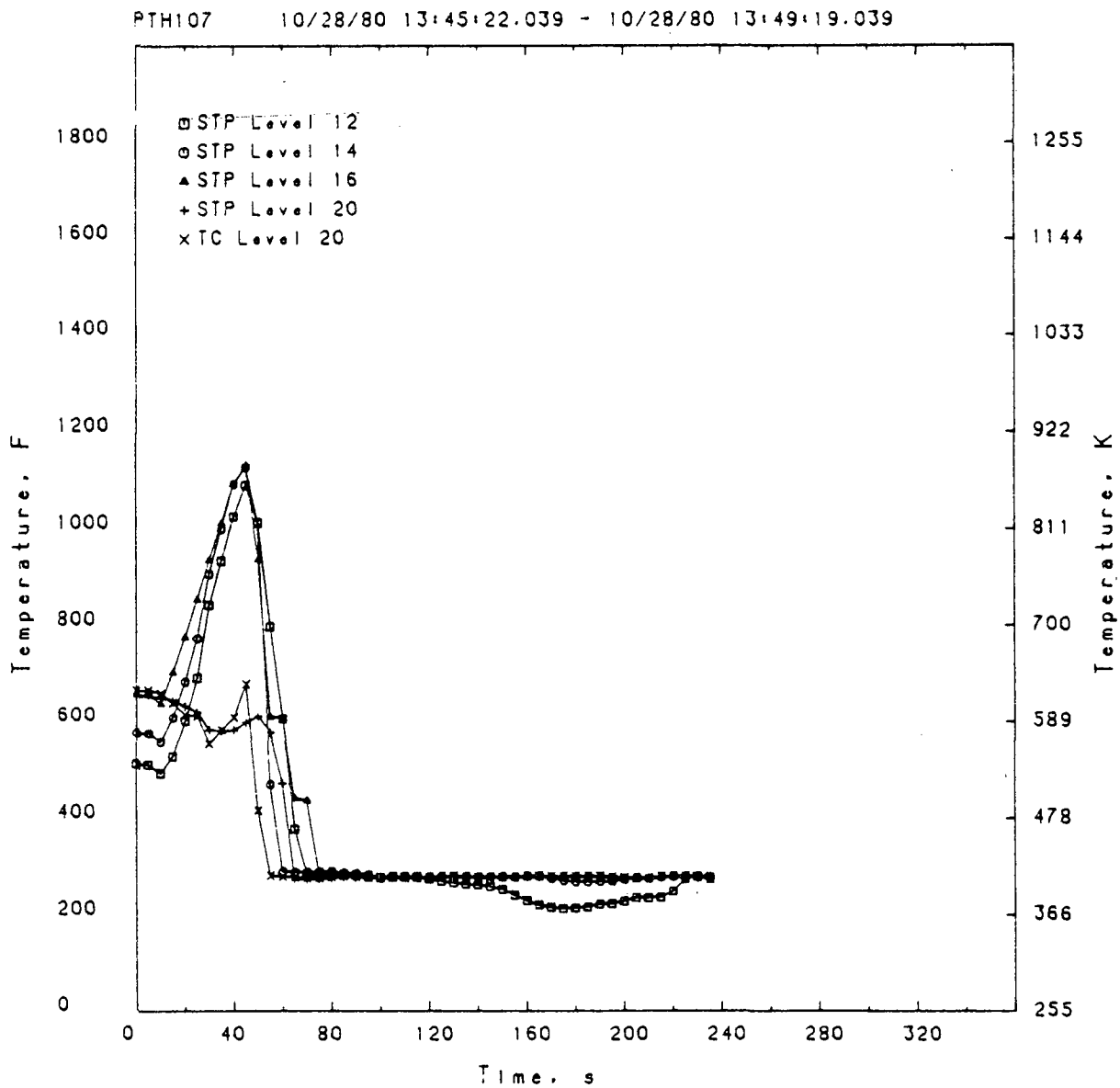

FIGURE 3.2.2.07 STEAM TEMPERATURE PROBE HISTORY DURING TRANSIENT PTH107

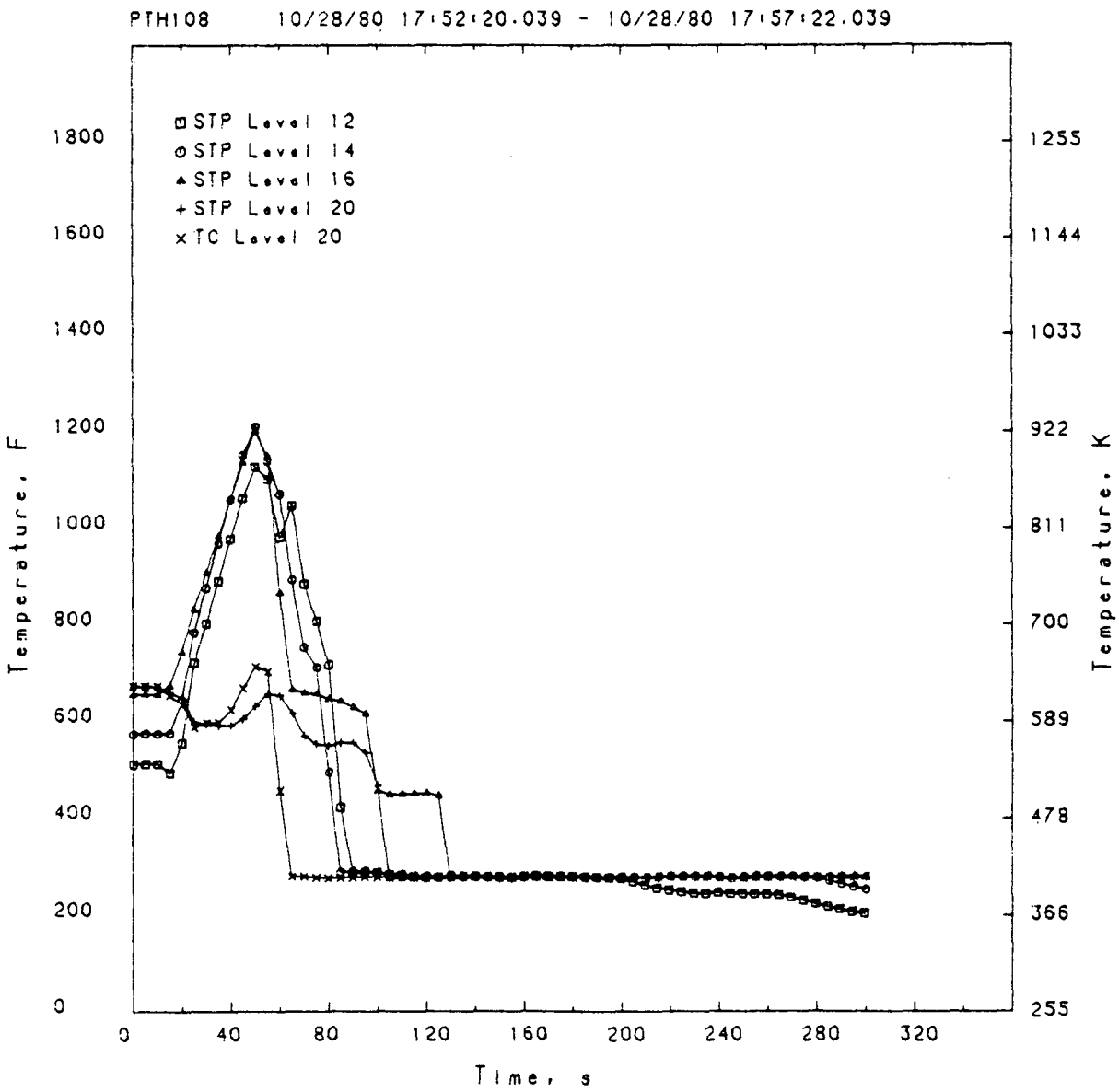

FIGURE 3.2.2.08 STEAM TEMPERATURE PROBE HISTORY DURING TRANSIENT PTH108

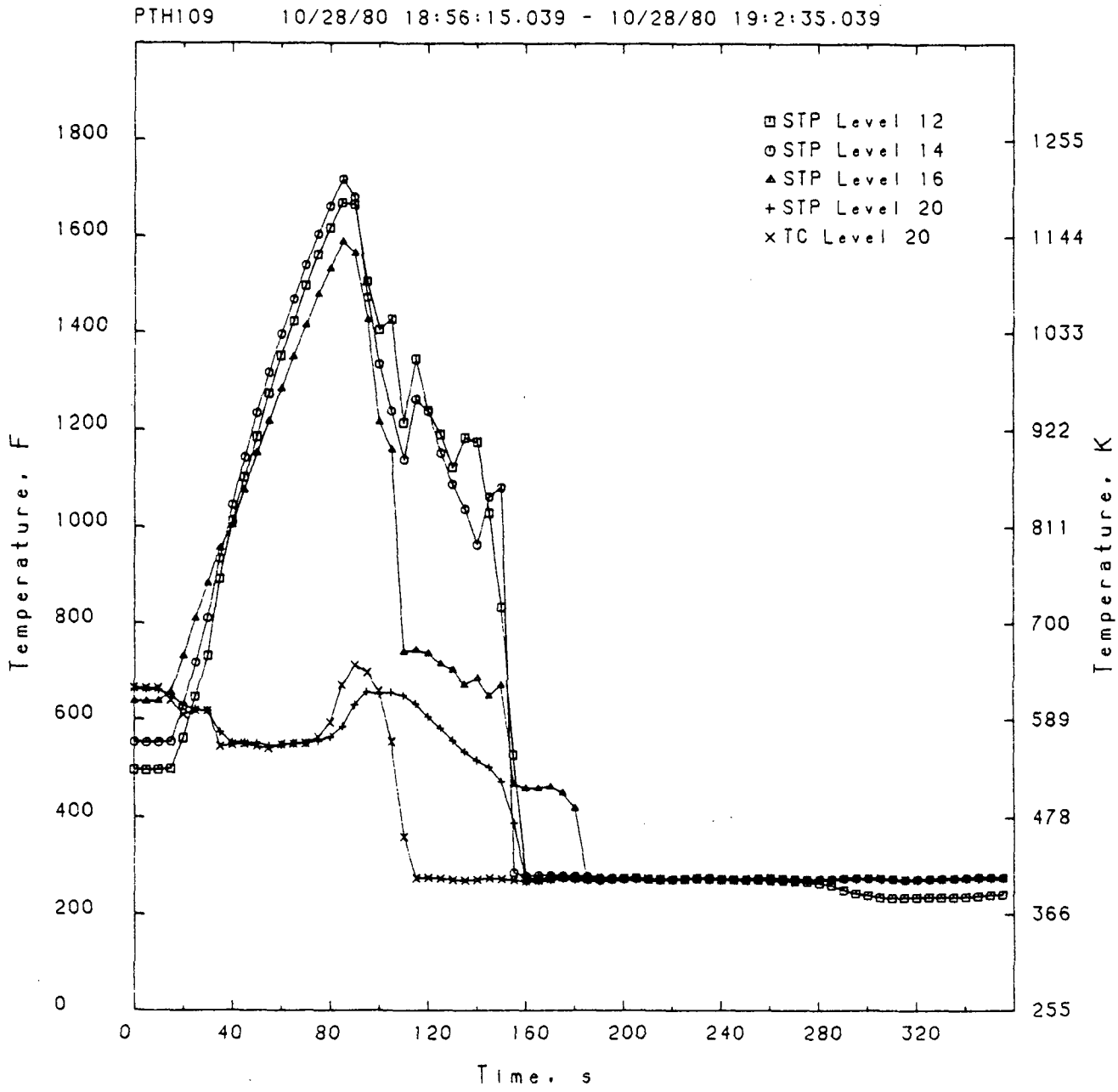

FIGURE 3.2.2.09 STEAM TEMPERATURE PROBE HISTORY FOR TRANSIENT PTH109

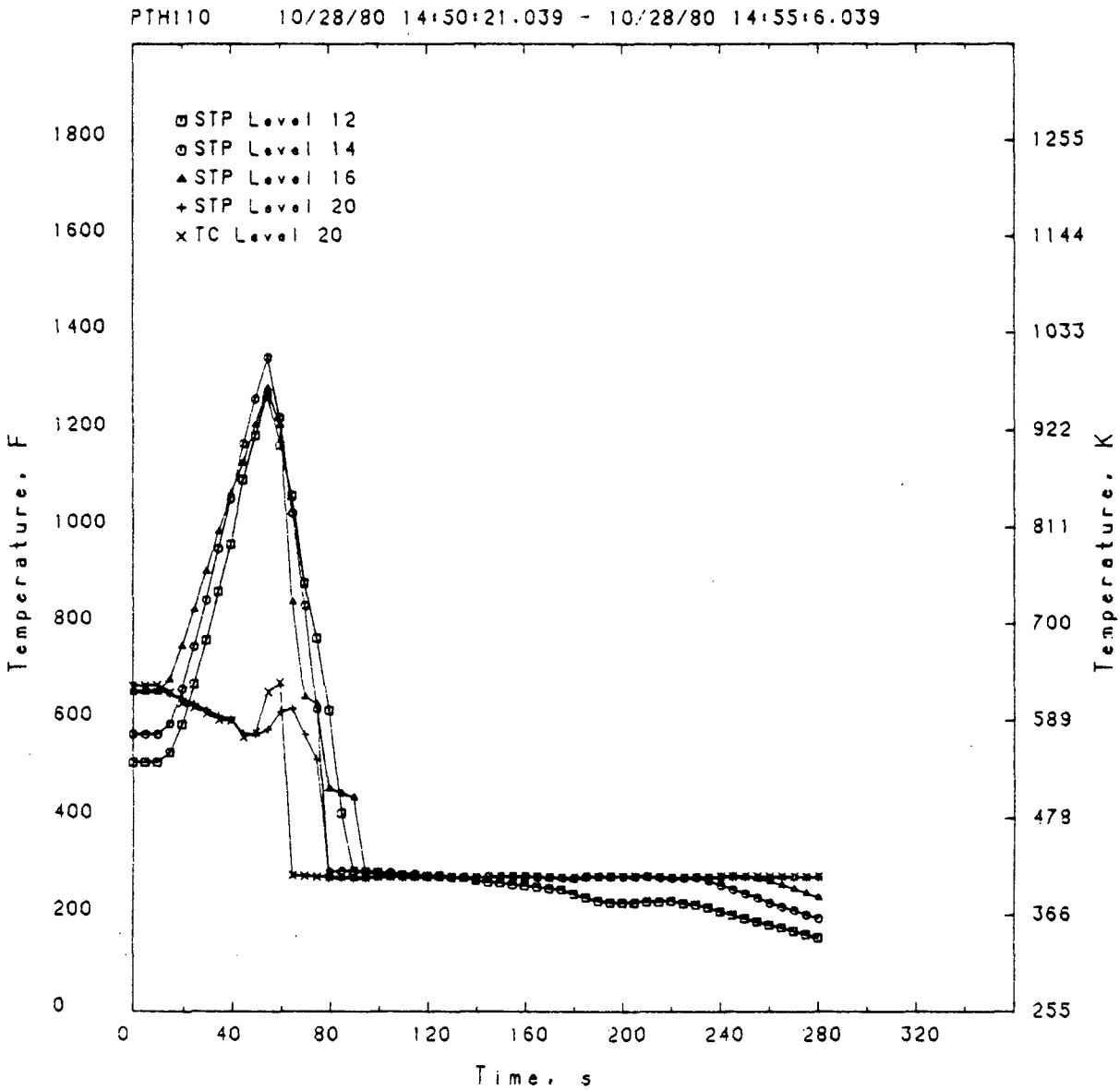

FIGURE 3.2.2.10 STEAM TEMPERATURE PROBE HISTORY DURING TRANSIENT PTH110

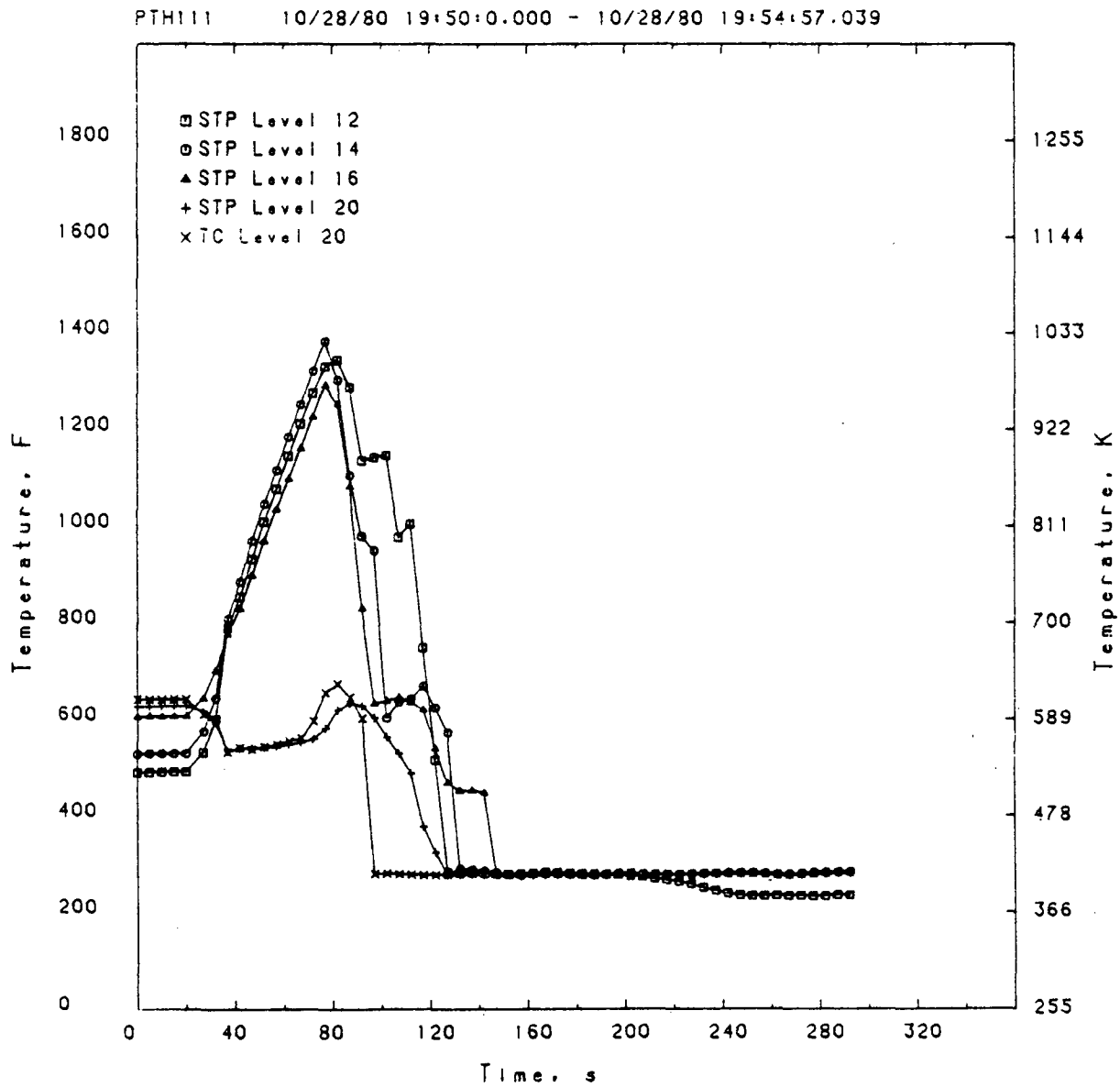

FIGURE 3.2.2.11 STEAM TEMPERATURE PROBE HISTORY DURING PTH111

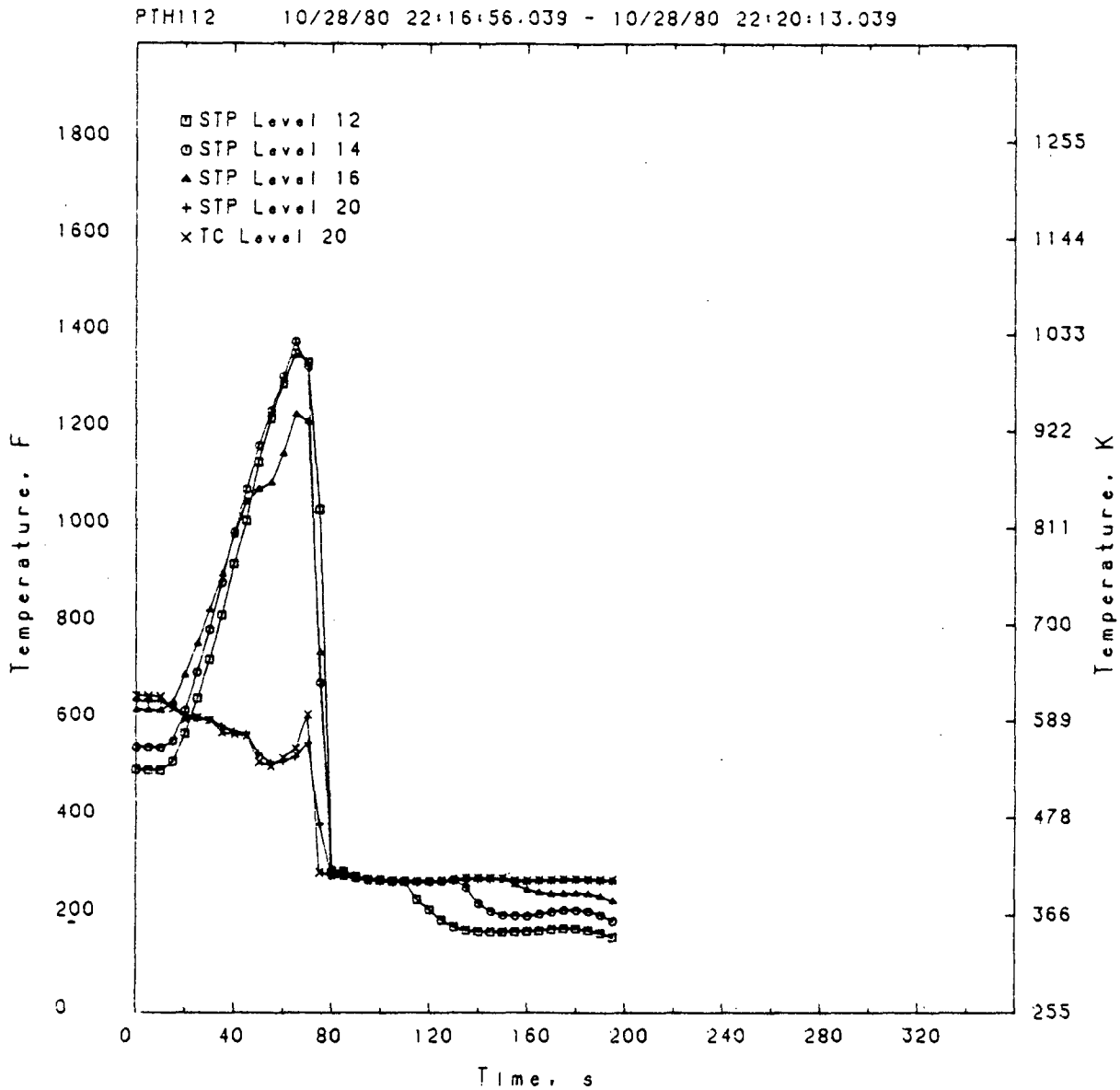

FIGURE 3.2.2.12 STEAM TEMPERATURE PROBE HISTORY DURING TRANSIENT PTH112

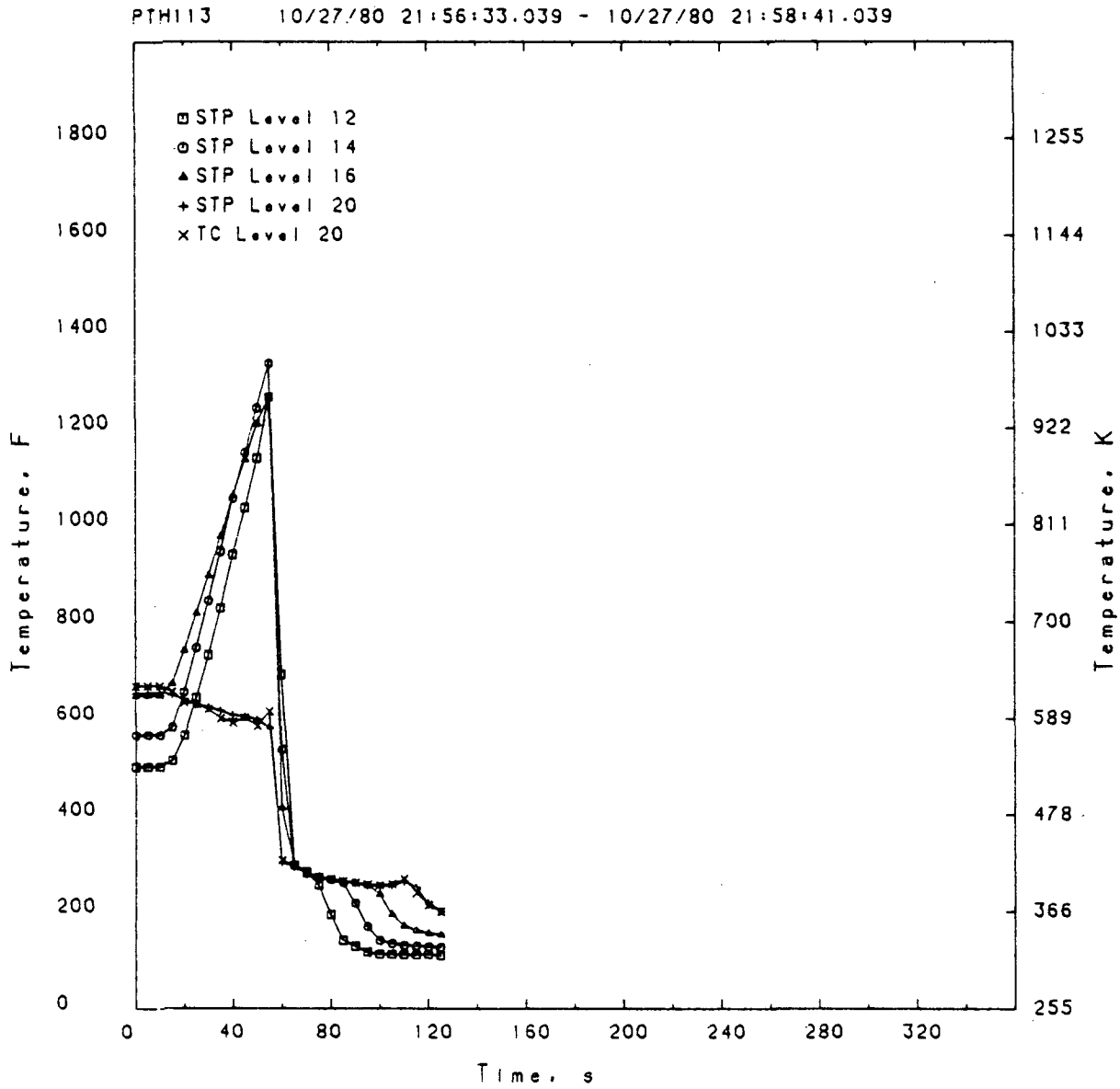

FIGURE 3.2.2.13 STEAM TEMPERATURE PROBE HISTORY DURING TRANSIENT PTH113

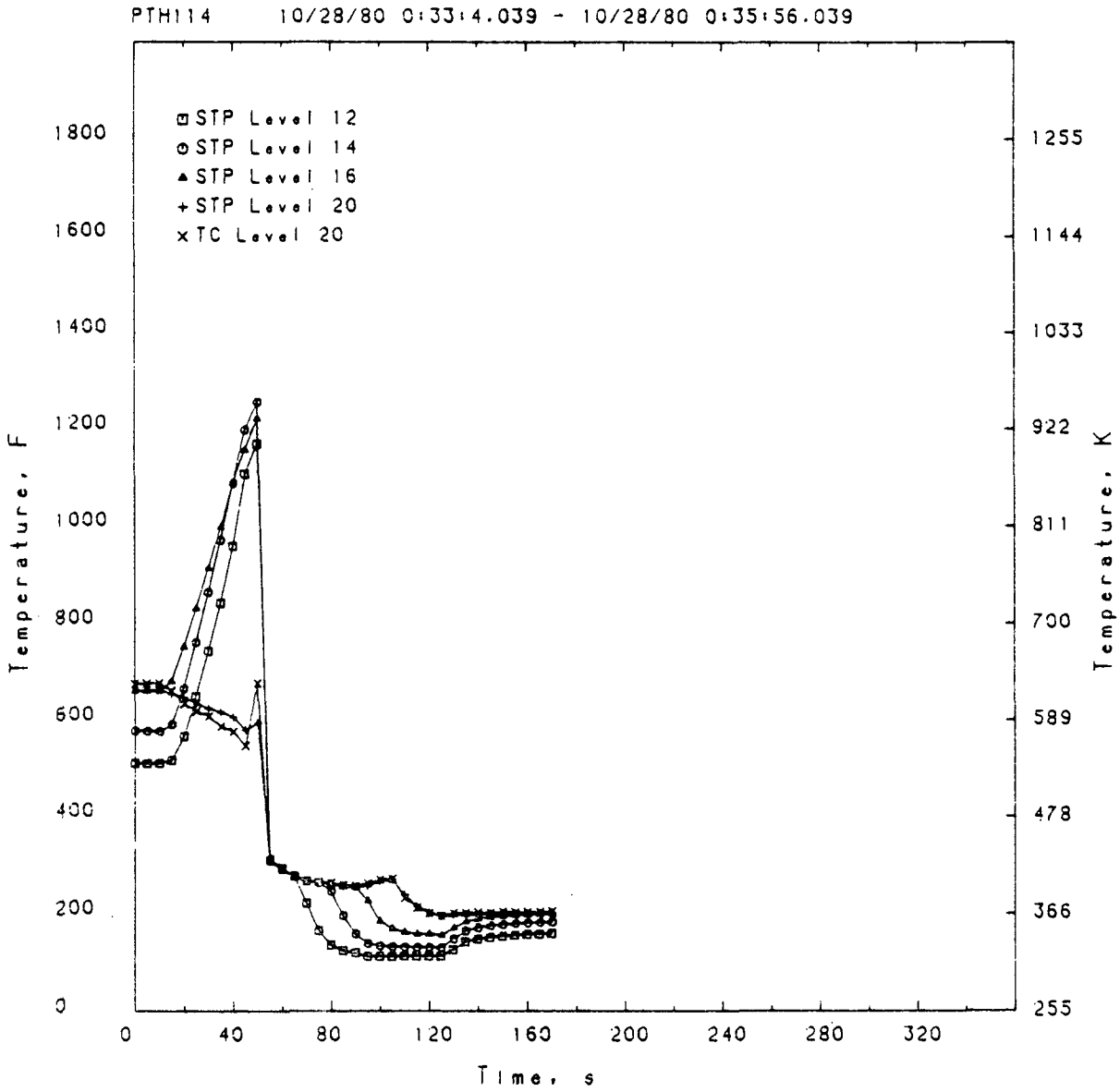

FIGURE 3.2.2.14 STEAM TEMPERATURE PROBE HISTORY DURING TRANSIENT PTH114

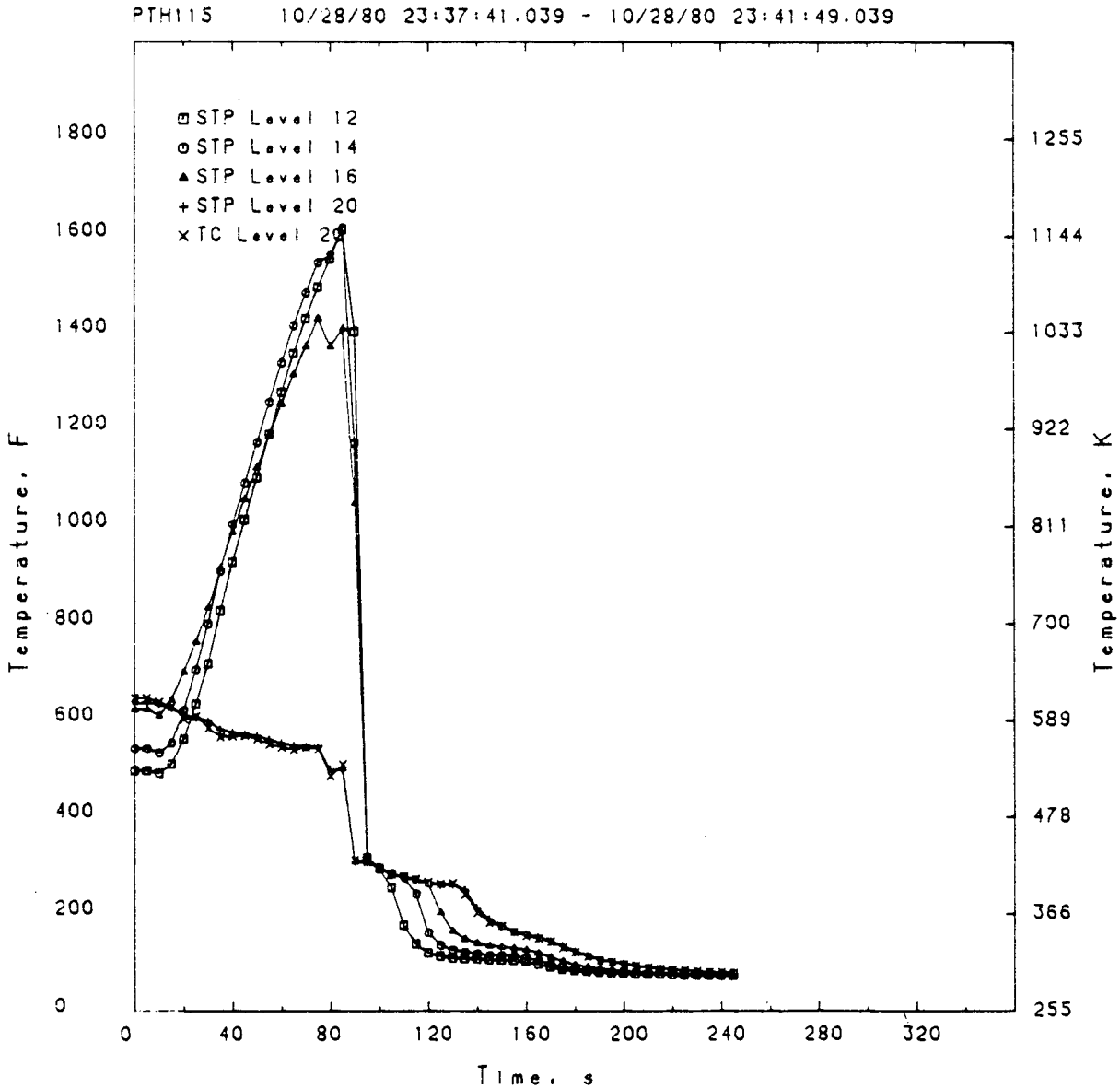

FIGURE 3.2.2.15 STEAM TEMPERATURE PROBE HISTORY DURING TRANSIENT PTH115

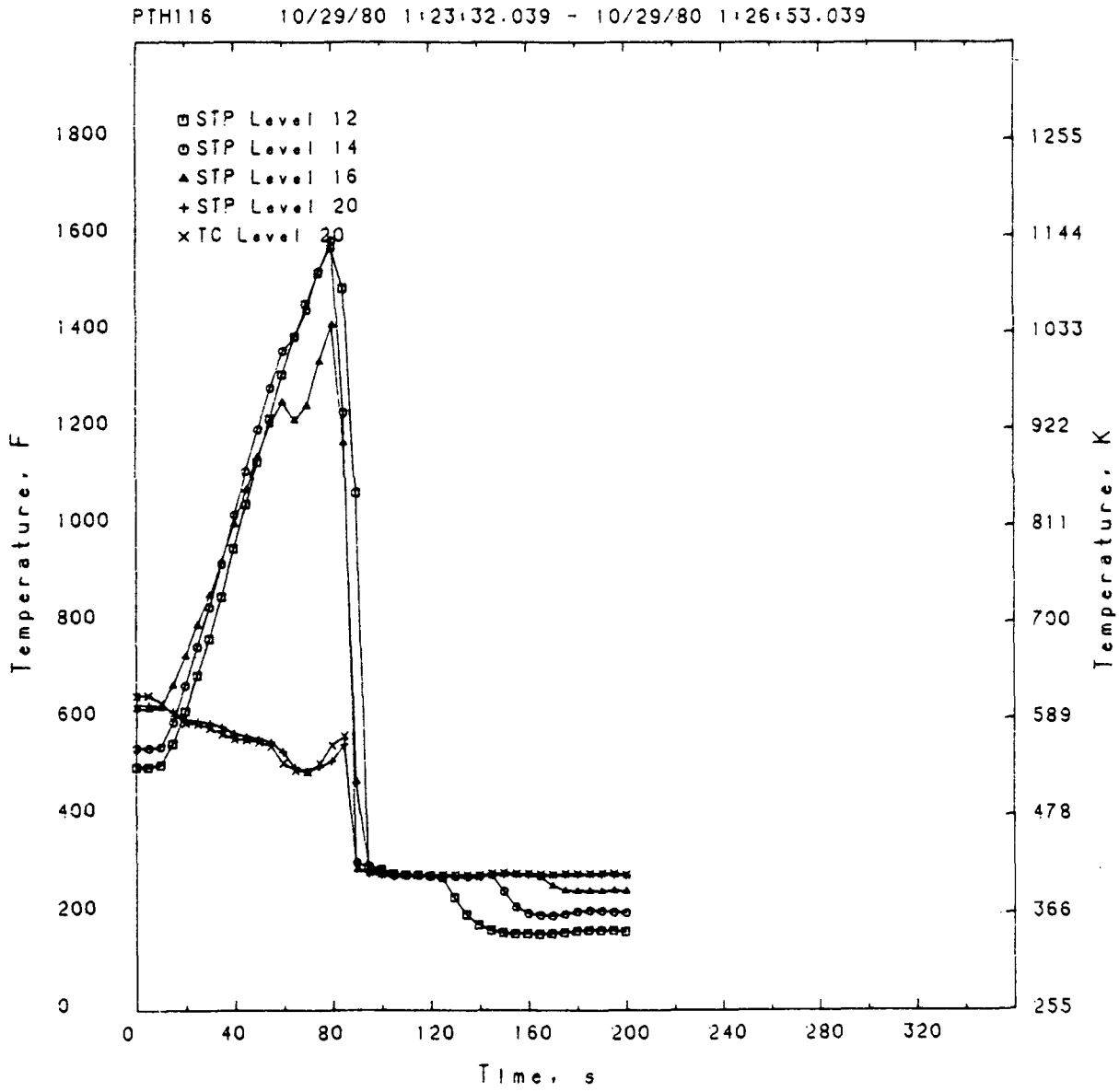

FIGURE 3.2.2.16 STEAM TEMPERATURE PROBE HISTORY DURING PTH116

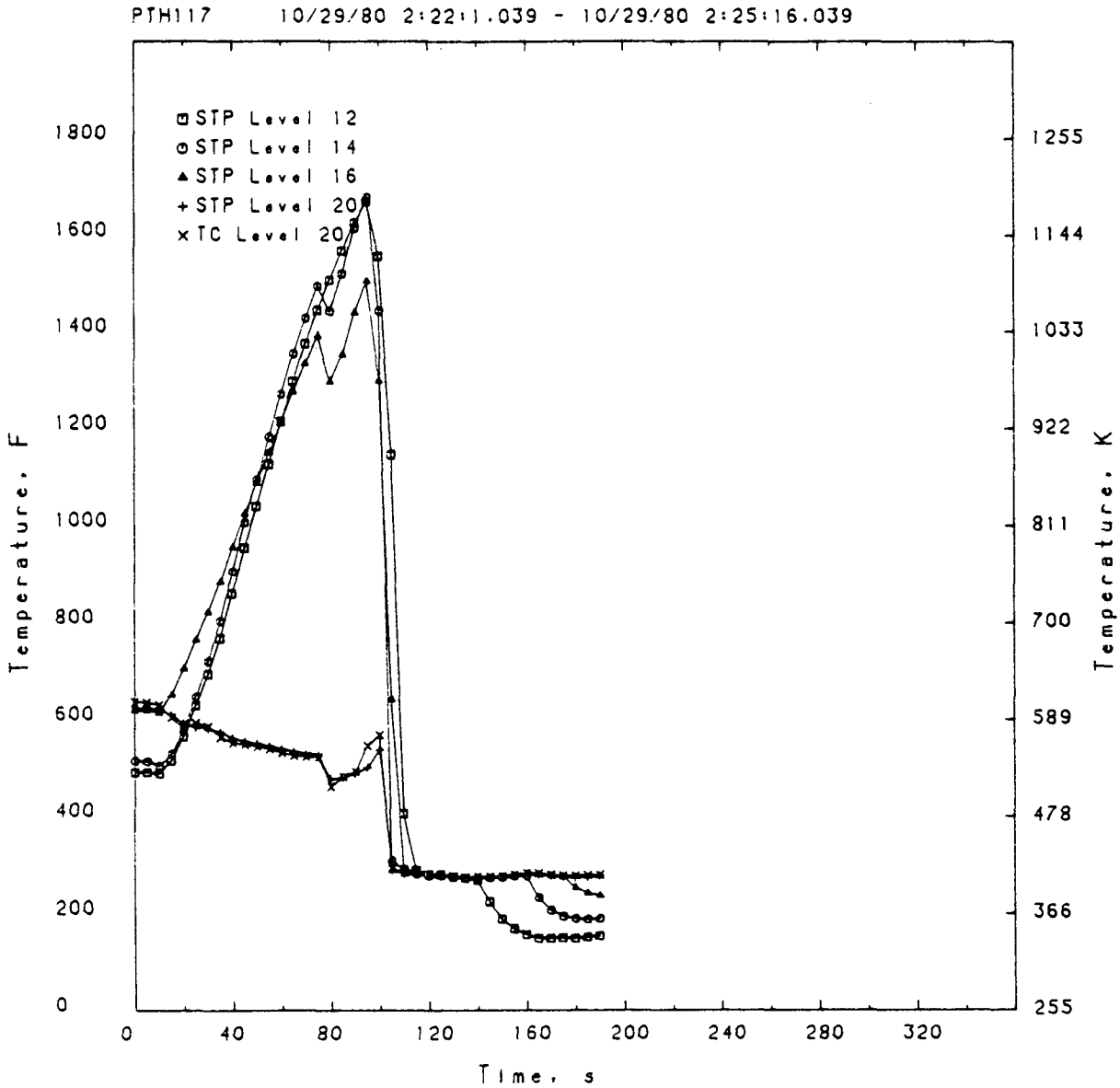

FIGURE 3.2.2.17 STEAM TEMPERATURE PROBE HISTORY DURING TRANSIENT PTH117

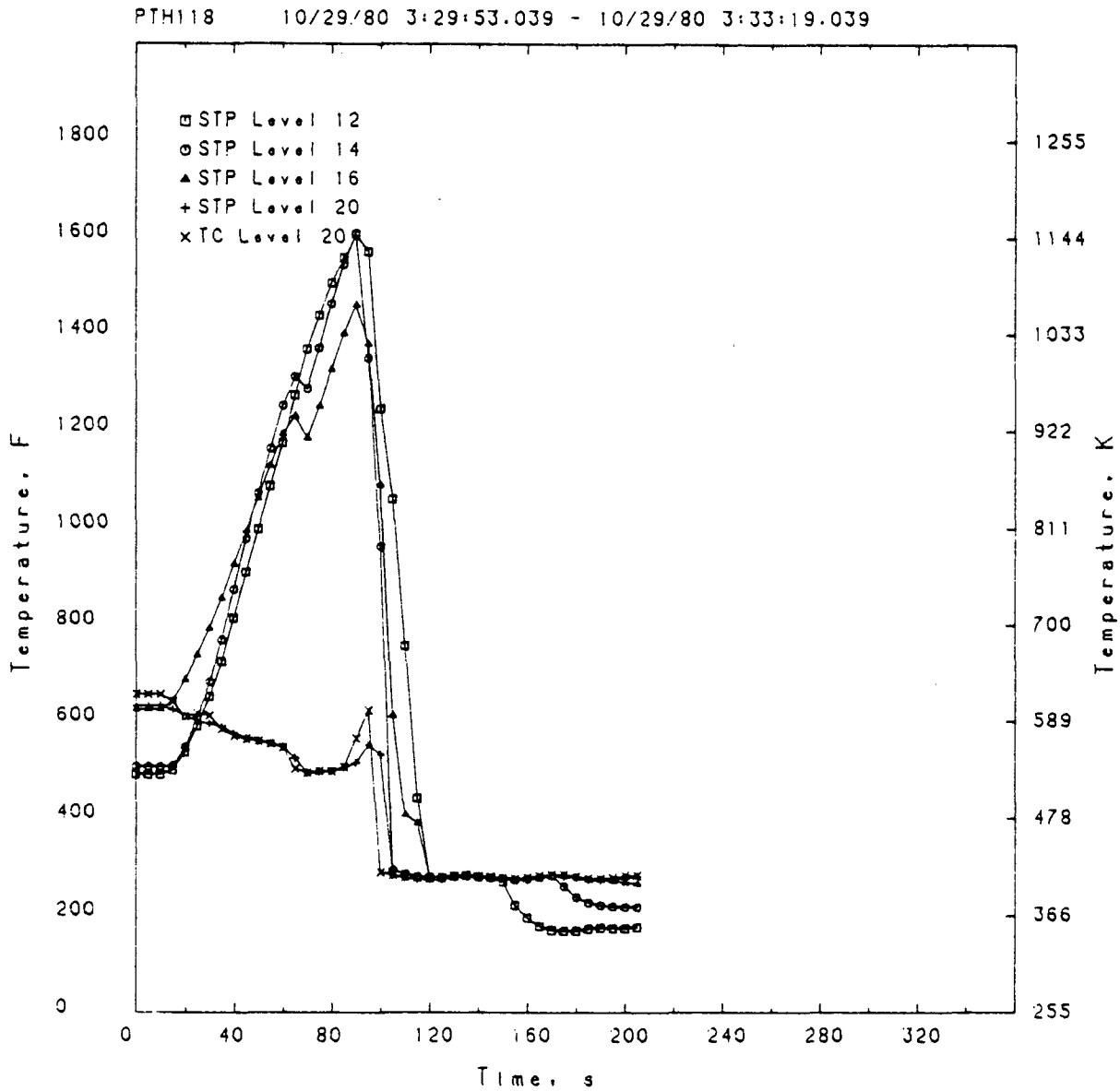

FIGURE 3.2.2.18 STEAM TEMPERATURE PROBE HISTORY DURING TRANSIENT PTH118

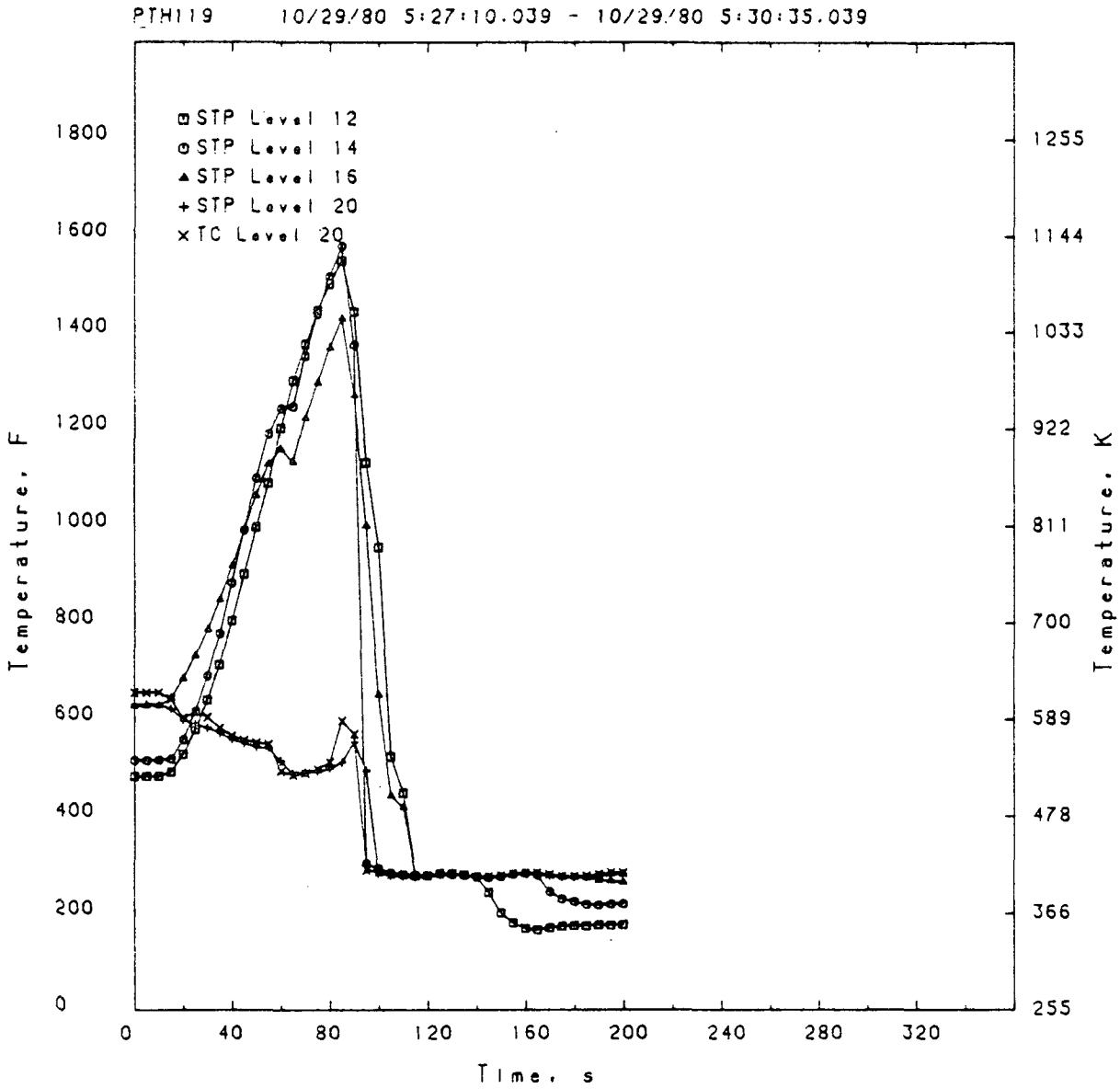

FIGURE 3.2.2.19 STEAM TEMPERATURE PROBE HISTORY DURING TRANSIENT PTH119

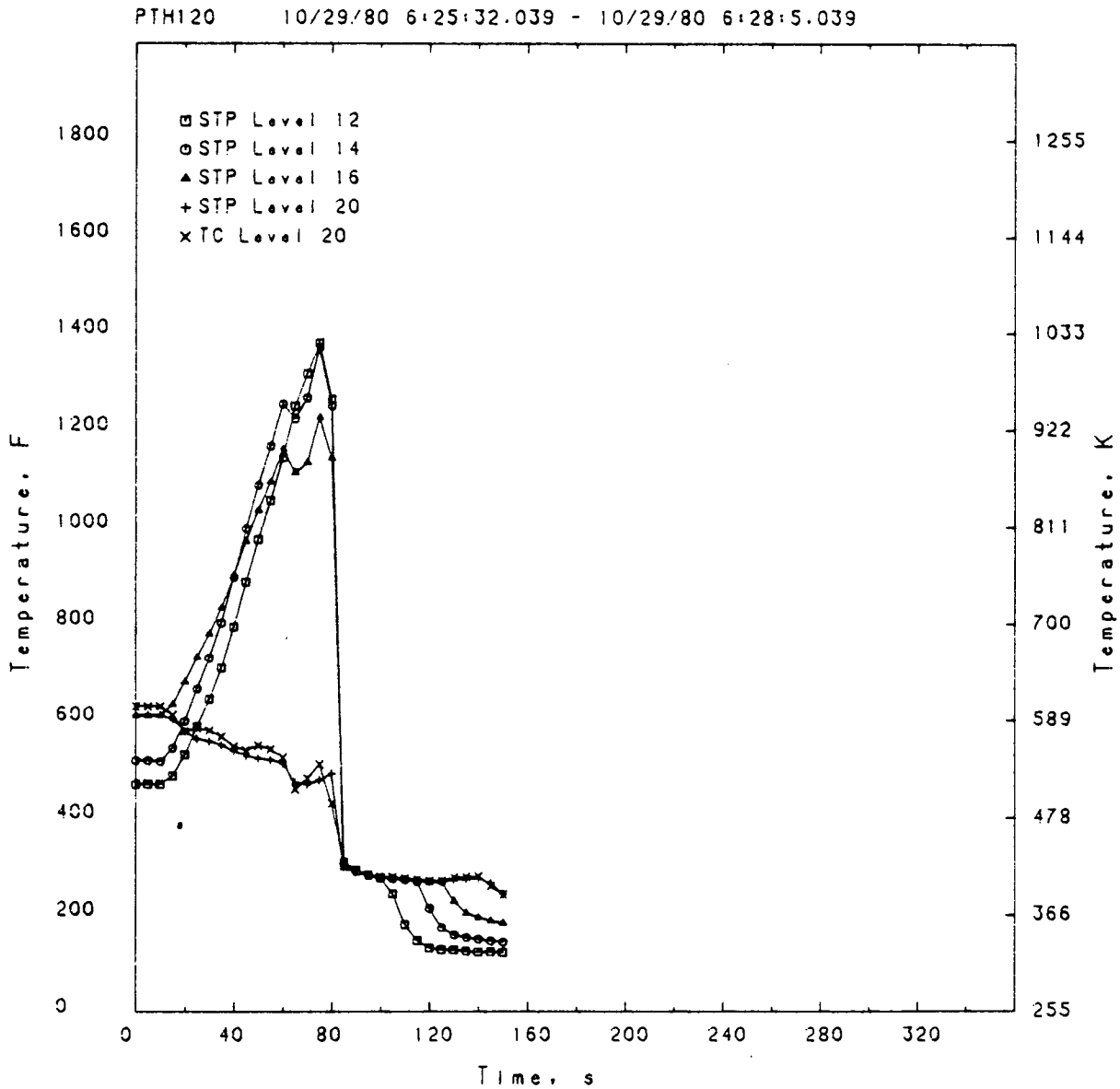

FIGURE 3.2.2.20 STEAM TEMPERATURE PROBE HISTORY DURING TRANSIENT PTH120

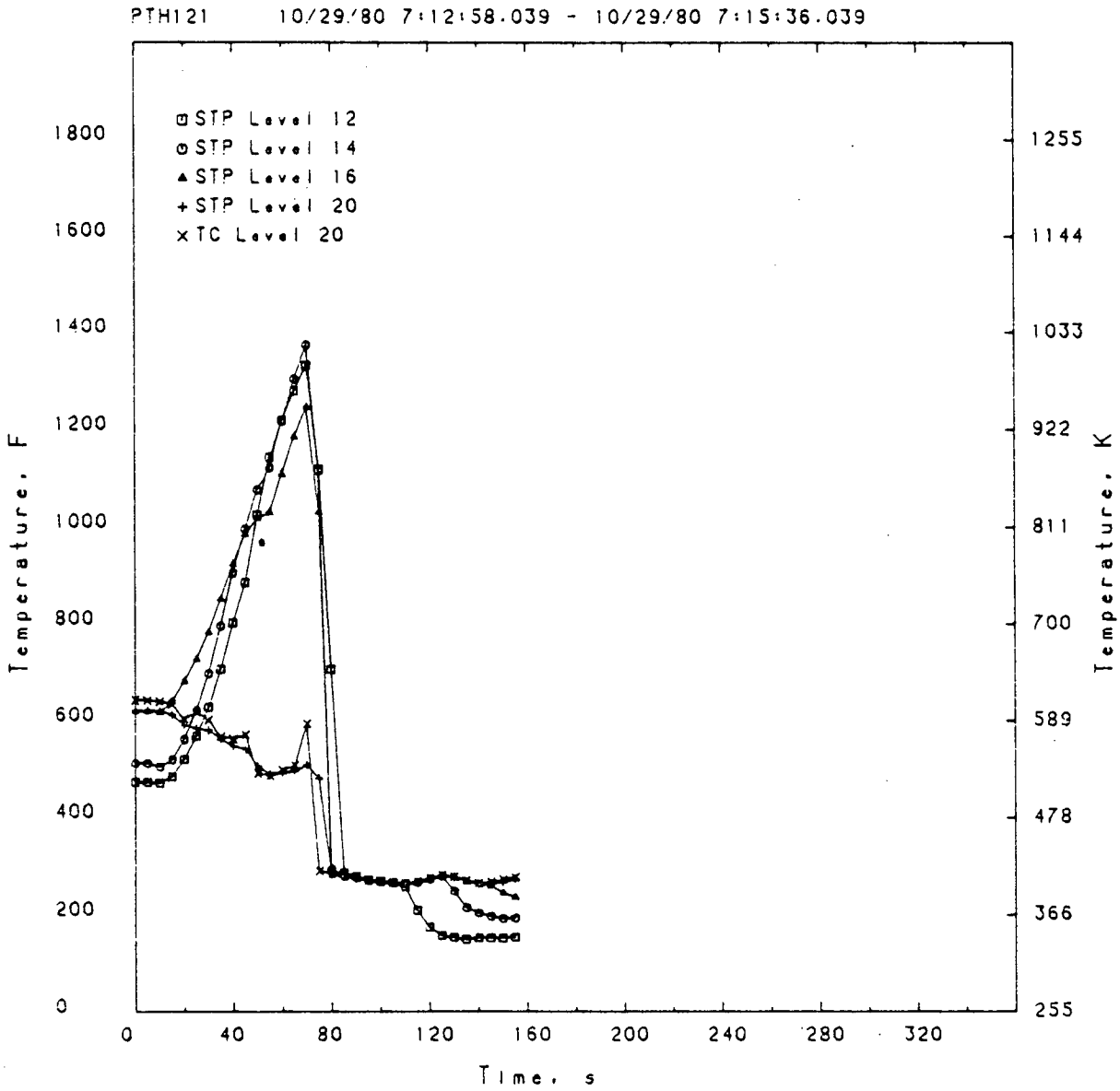

FIGURE 3.2.2.21 STEAM TEMPERATURE PROBE HISTORY DURING TRANSIENT PTH121

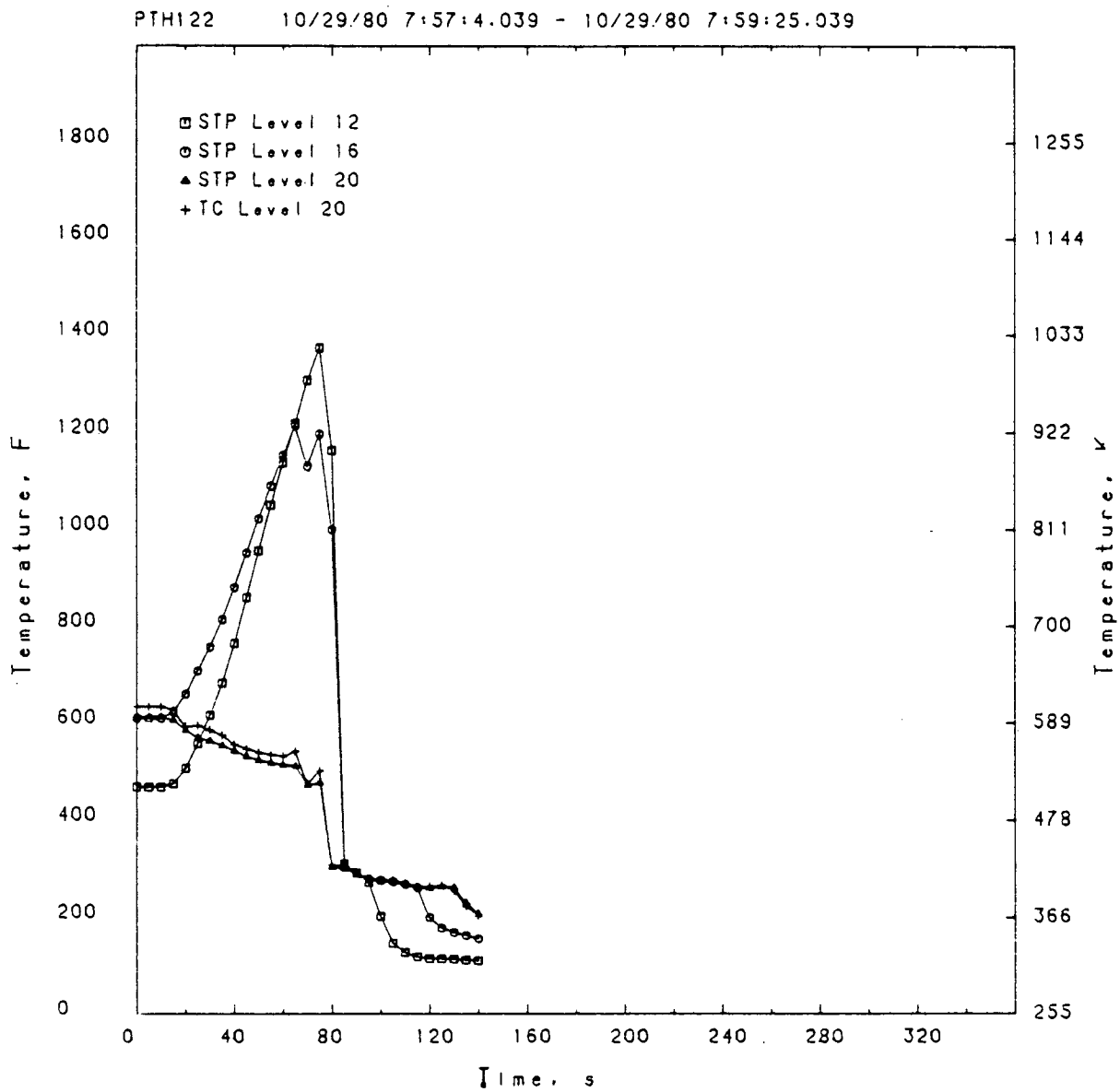

FIGURE 3.2.2.22 STEAM TEMPERATURE PROBE HISTORY DURING TRANSIENT PTH122

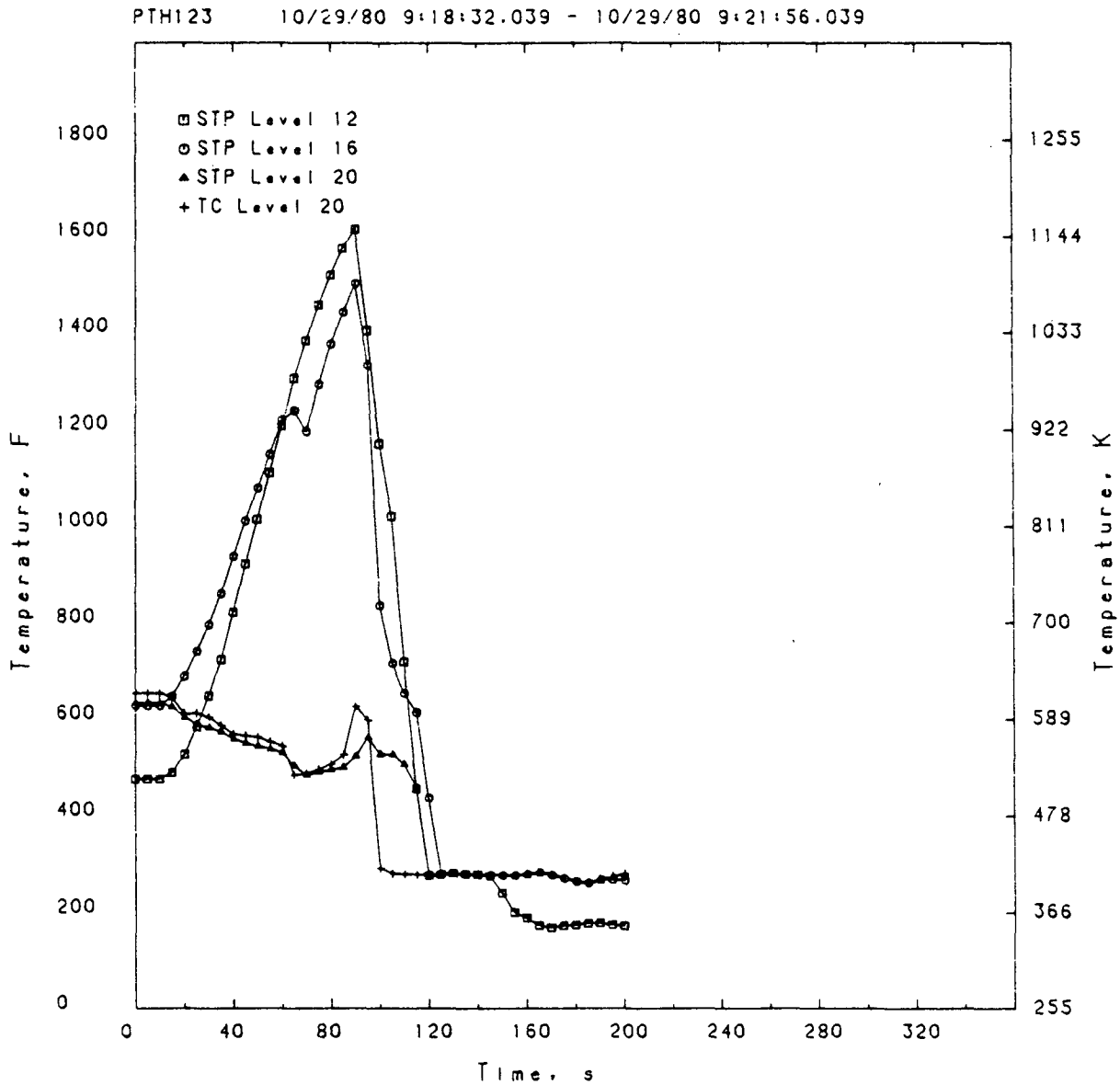

FIGURE 3.2.2.23 STEAM TEMPERATURE PROBE HISTORY DURING TRANSIENT PTH123

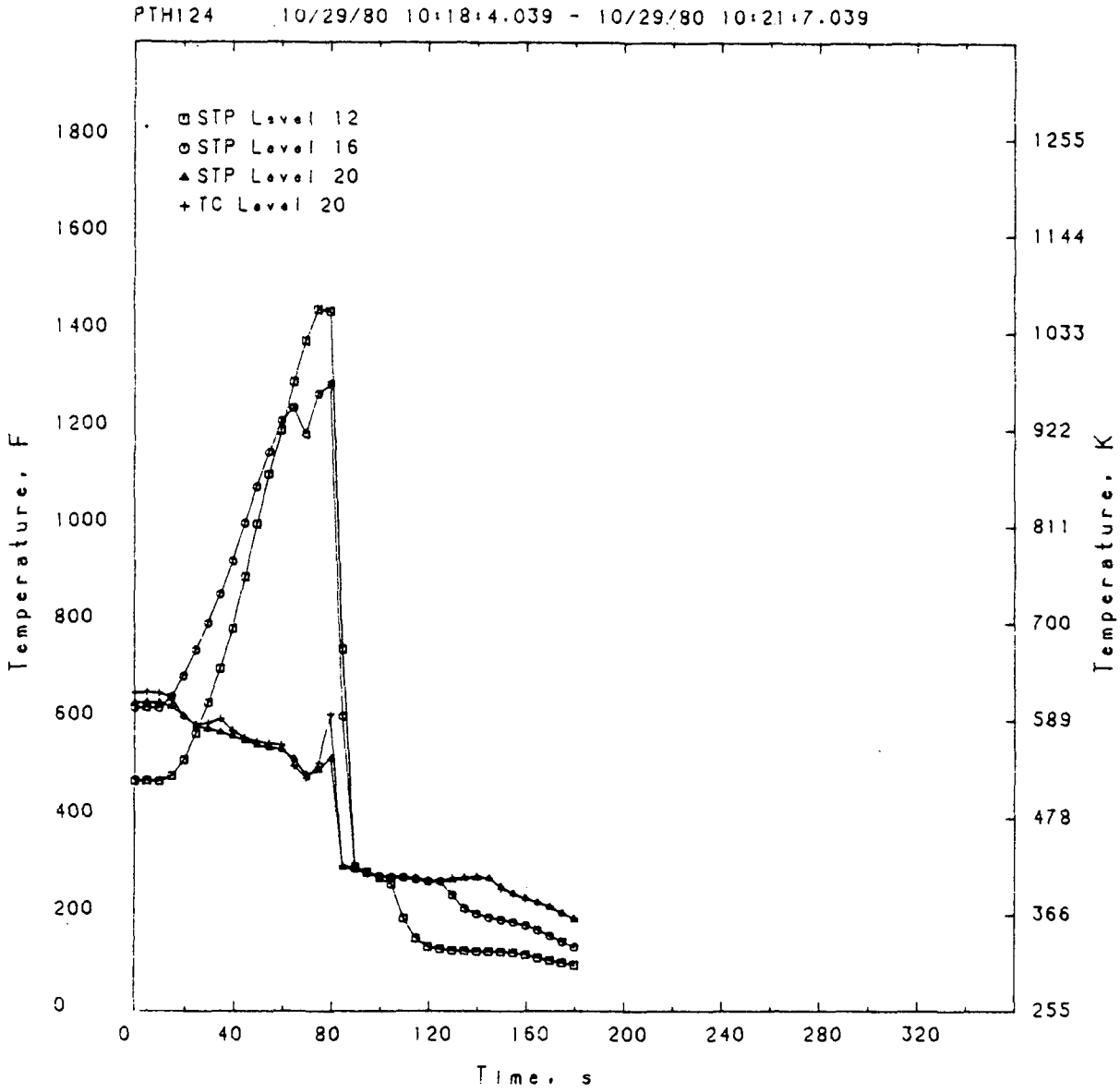

FIGURE 3.2.2.24 STEAM TEMPERATURE PROBE HISTORY DURING TRANSIENT PTH124

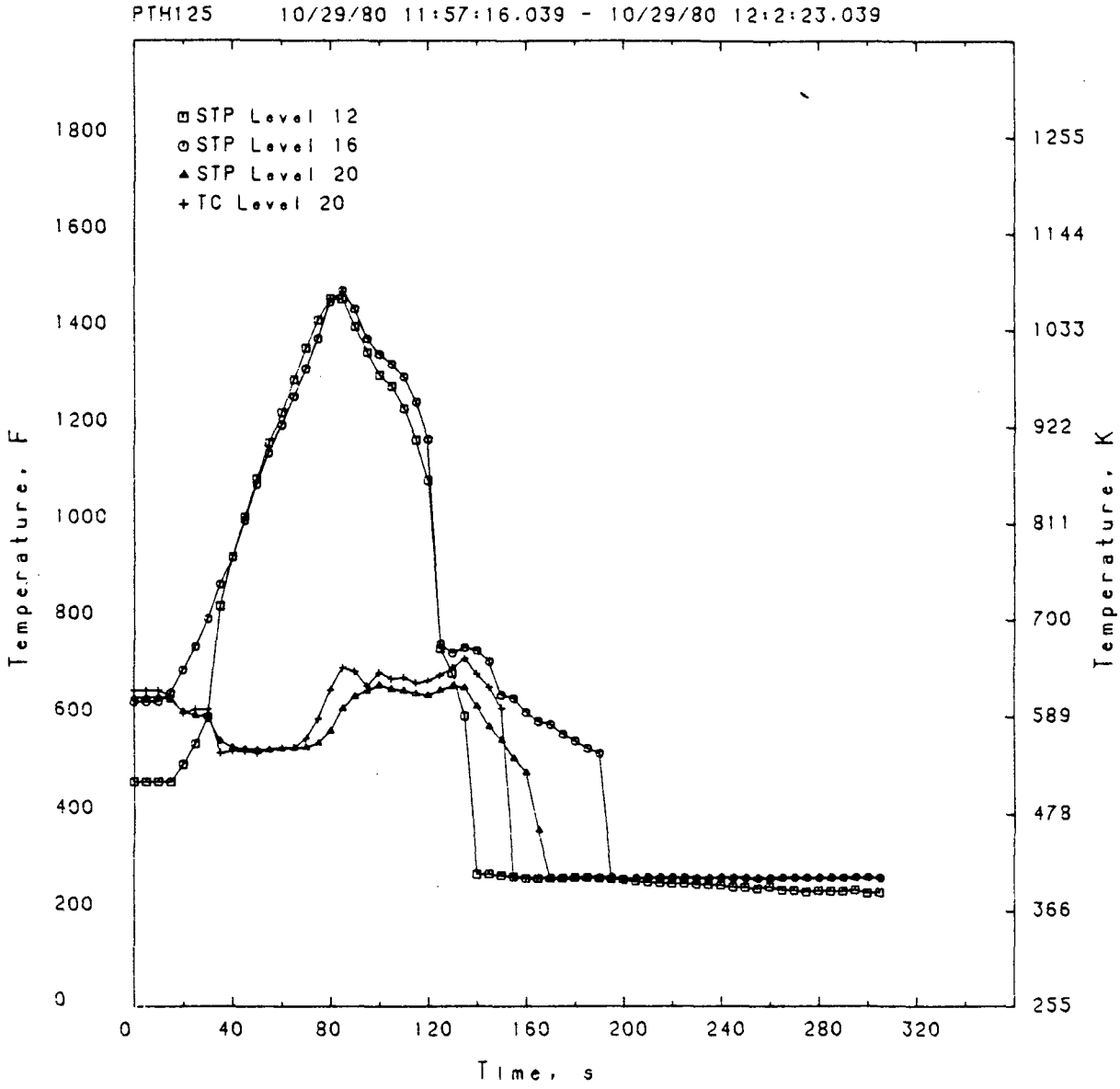

FIGURE 3.2.2.25 STEAM TEMPERATURE PROBE HISTORY DURING TRANSIENT PTH125

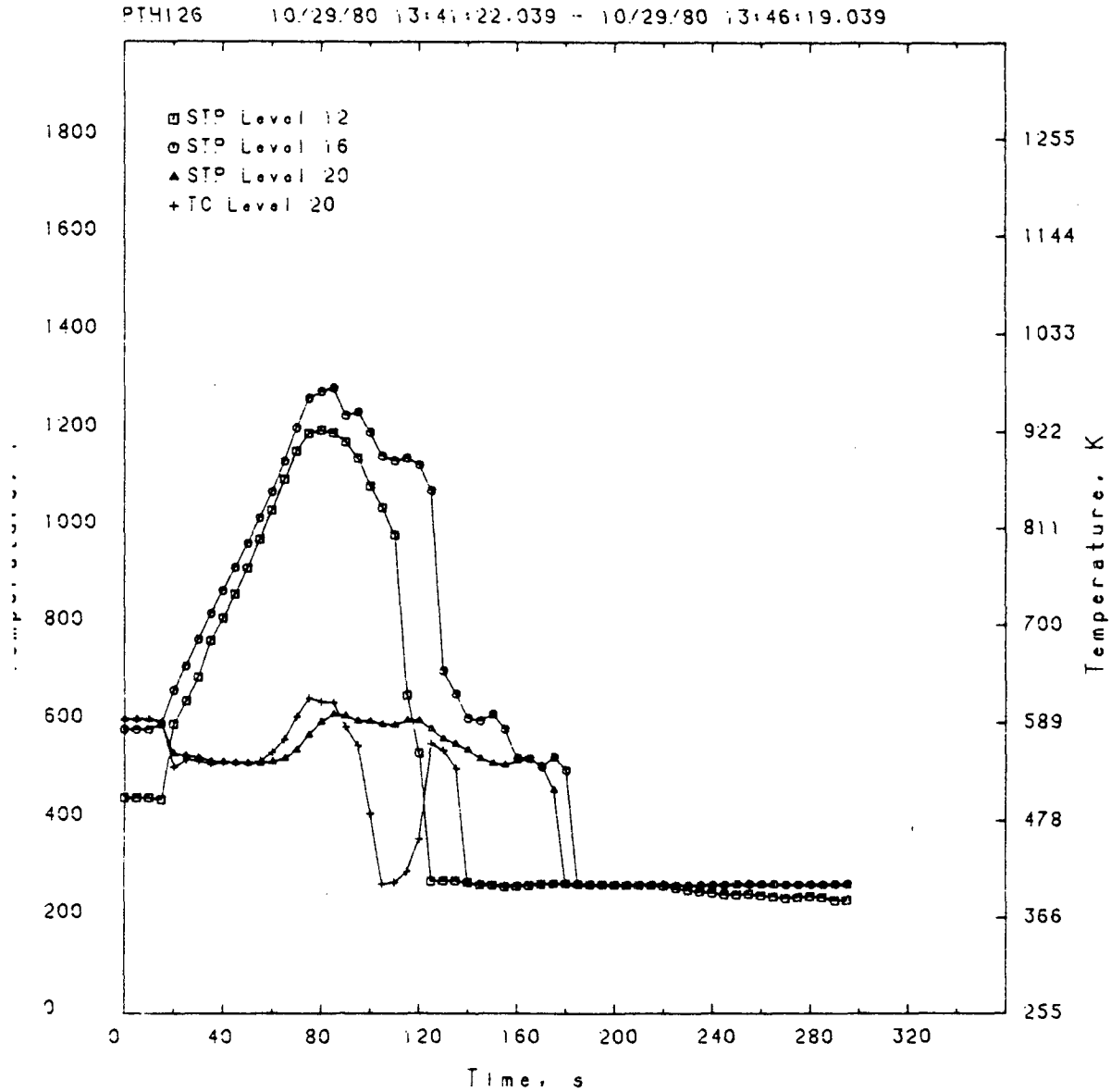

FIGURE 3.2.2.26 STEAM TEMPERATURE PROBE HISTORY DURING TRANSIENT PTH126

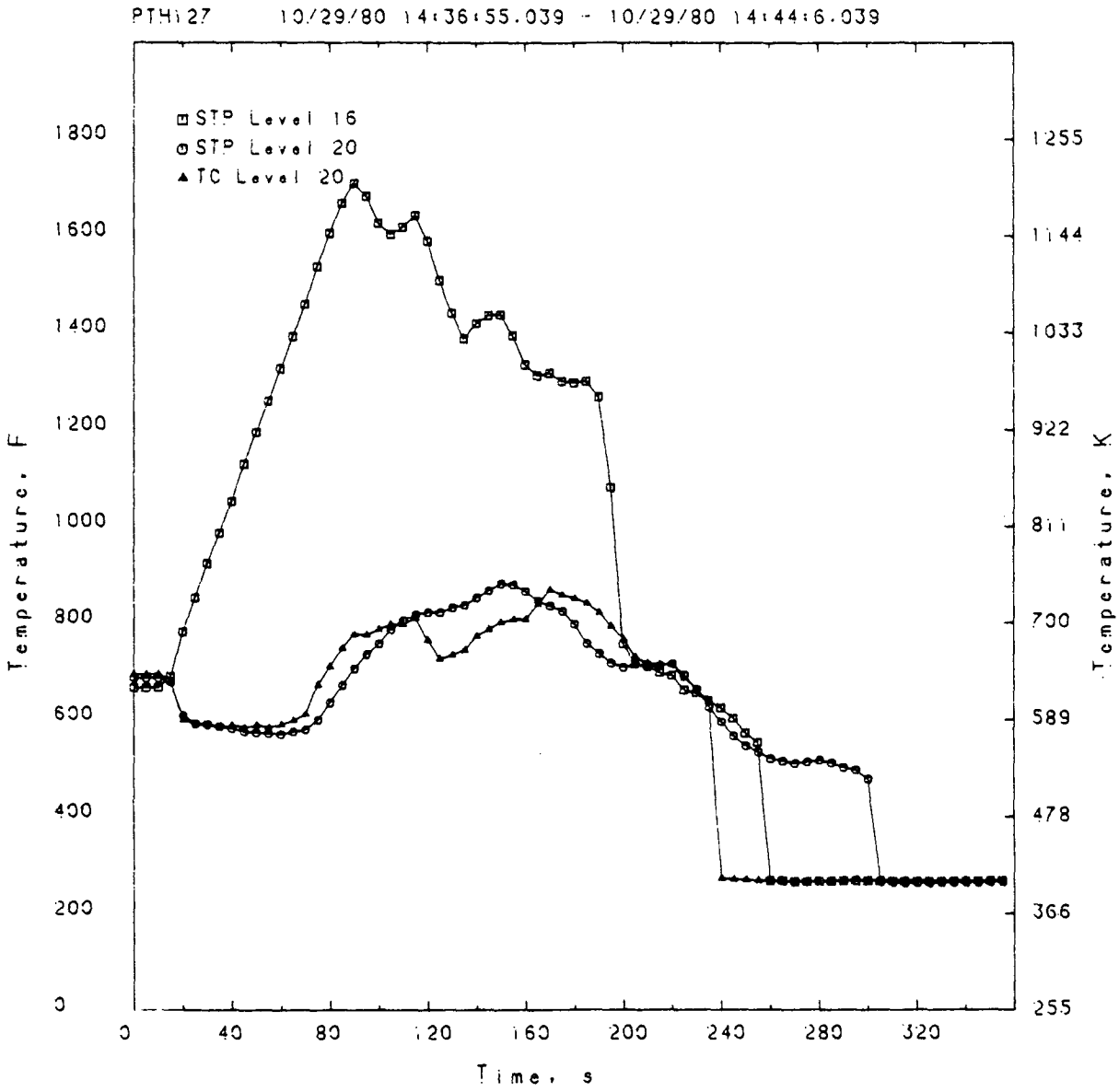

FIGURE 3.2.2.27 STEAM TEMPERATURE PROBE HISTORY DURING TRANSIENT PTH127

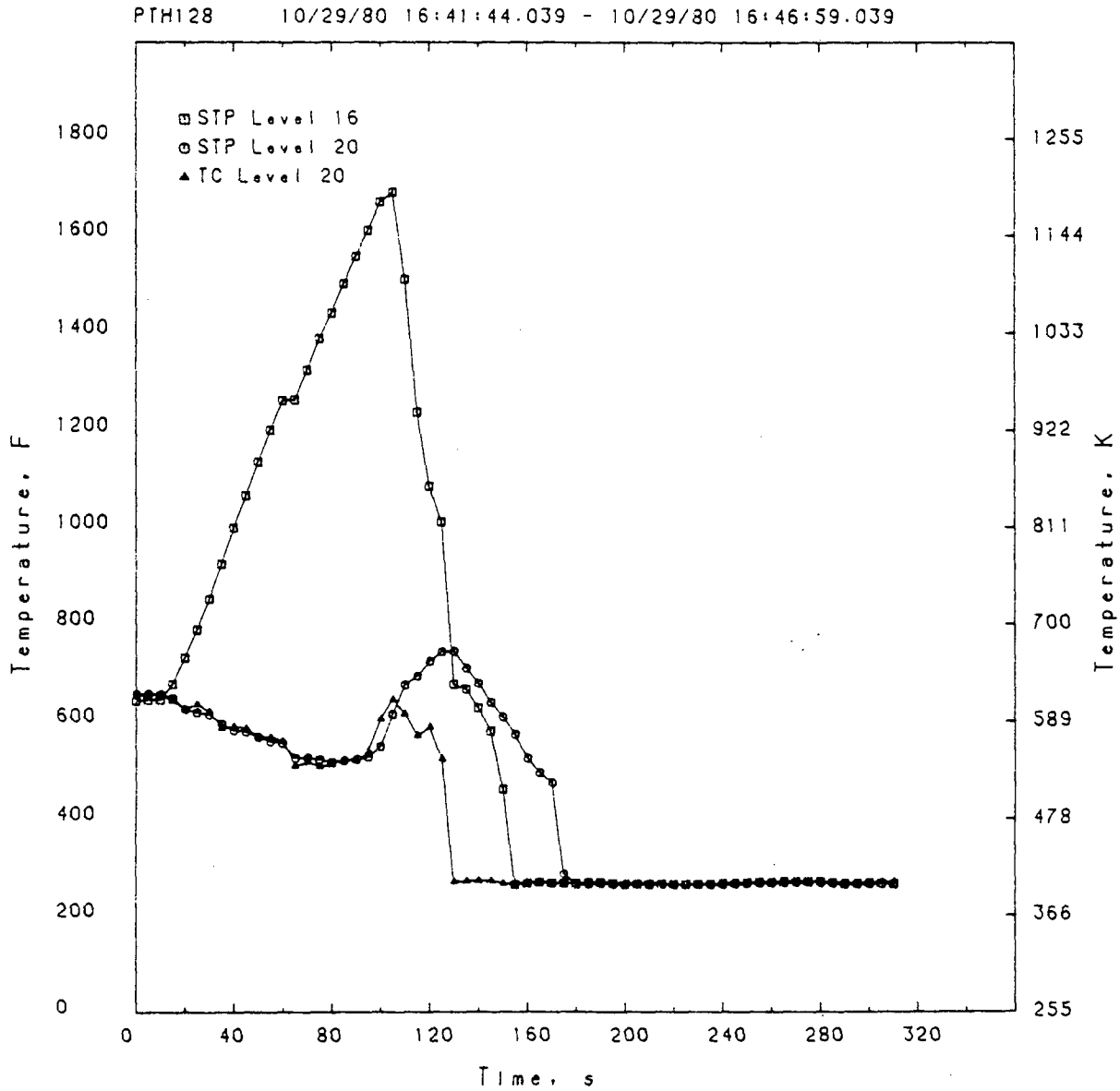

FIGURE 3.2.2.28 STEAM TEMPERATURE PROBE HISTORY DURING TRANSIENT PTH128

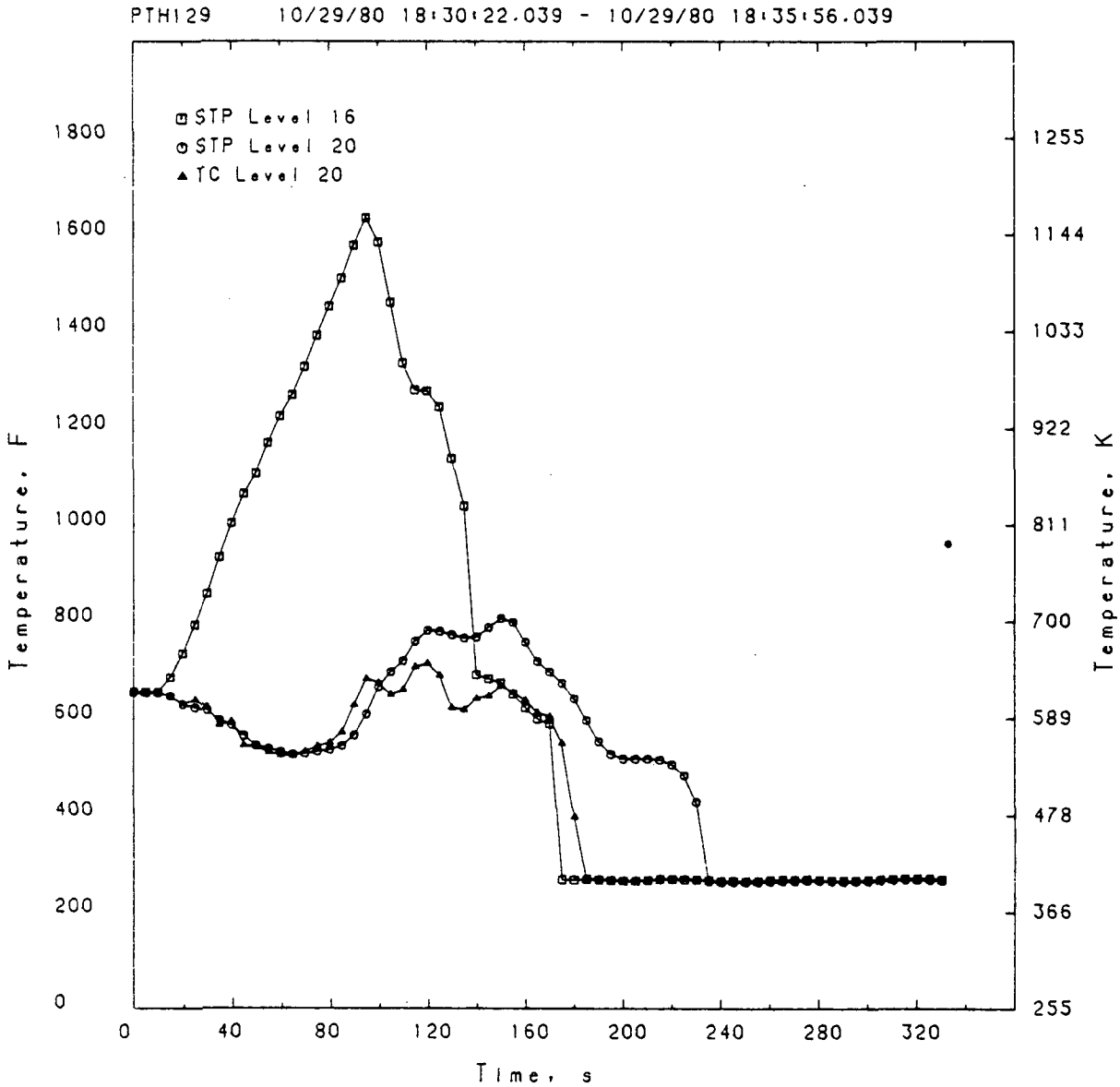

FIGURE 3.2.2.29 STEAM TEMPERATURE PROBE HISTORY DURING TRANSIENT PTH129

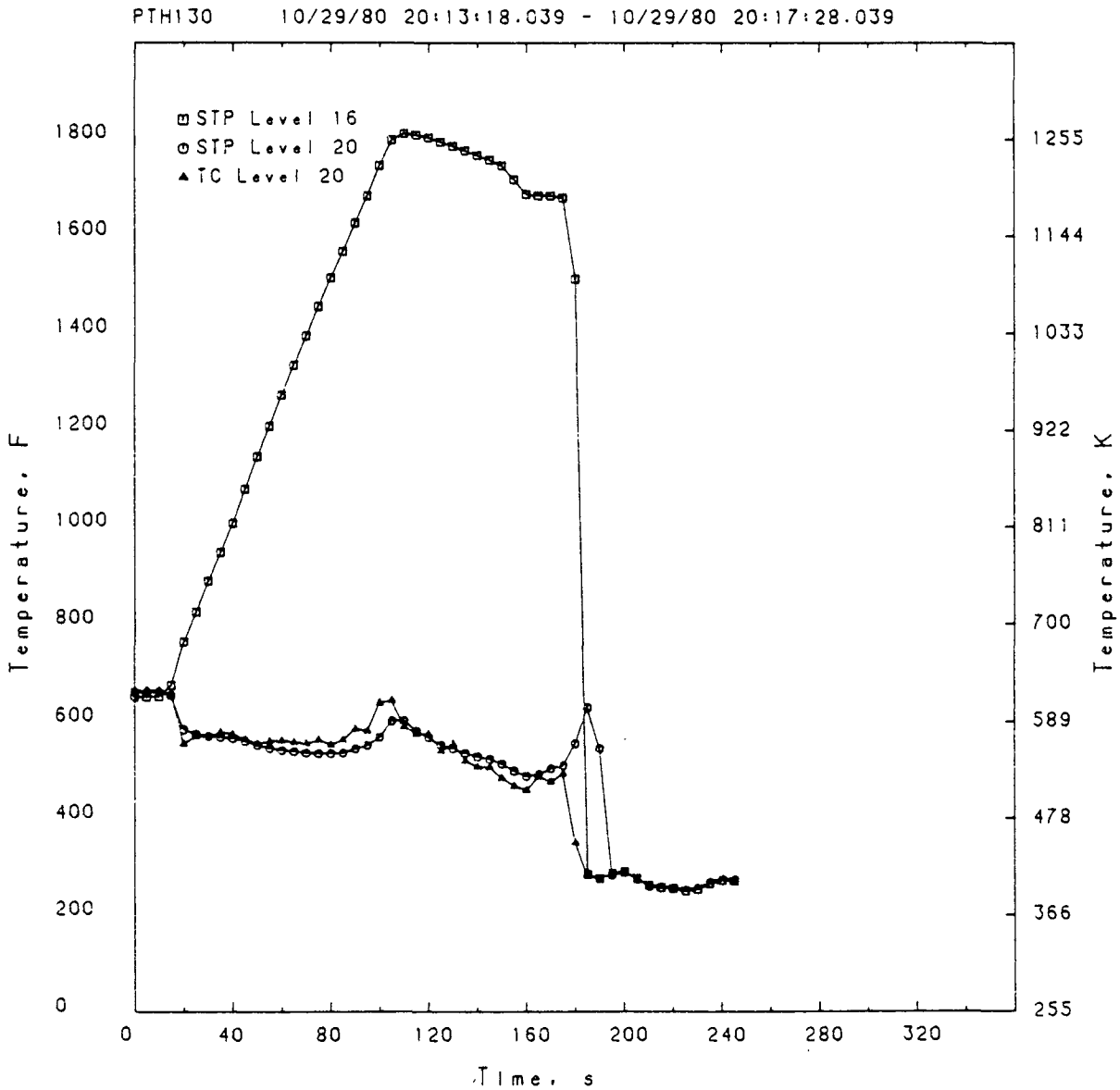

FIGURE 3.2.2.30 STEAM TEMPERATURE PROBE HISTORY DURING TRANSIENT PTH130

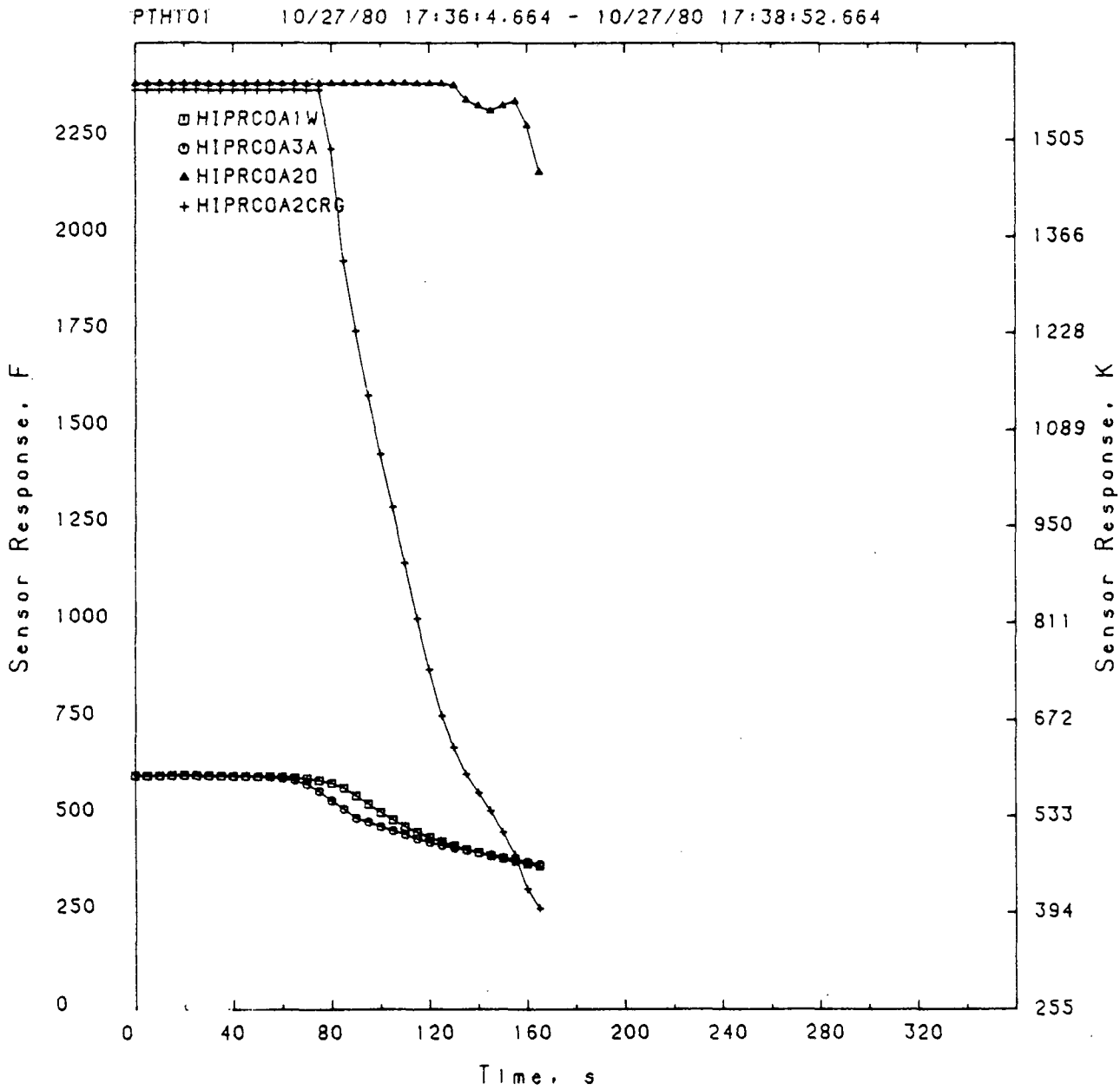

FIGURE 3.2.3.01 HIGH PRESSURE CONNECTOR TC RESPONSE HISTORY DURING TRANSIENT PTH101

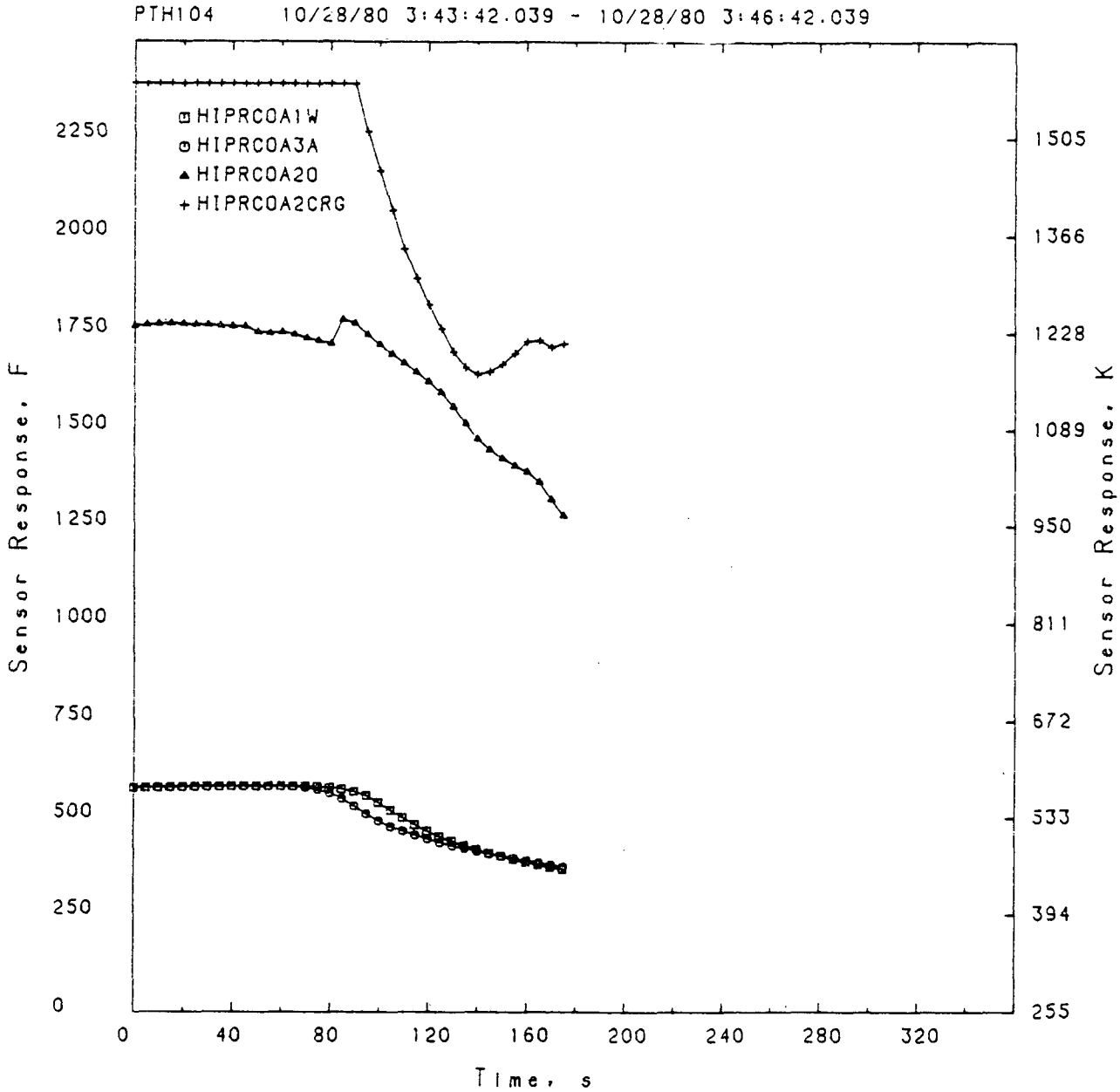

FIGURE 3.2.3.04 HIGH PRESSURE CONNECTOR TC RESPONSE HISTORY DURING TRANSIENT PTH104

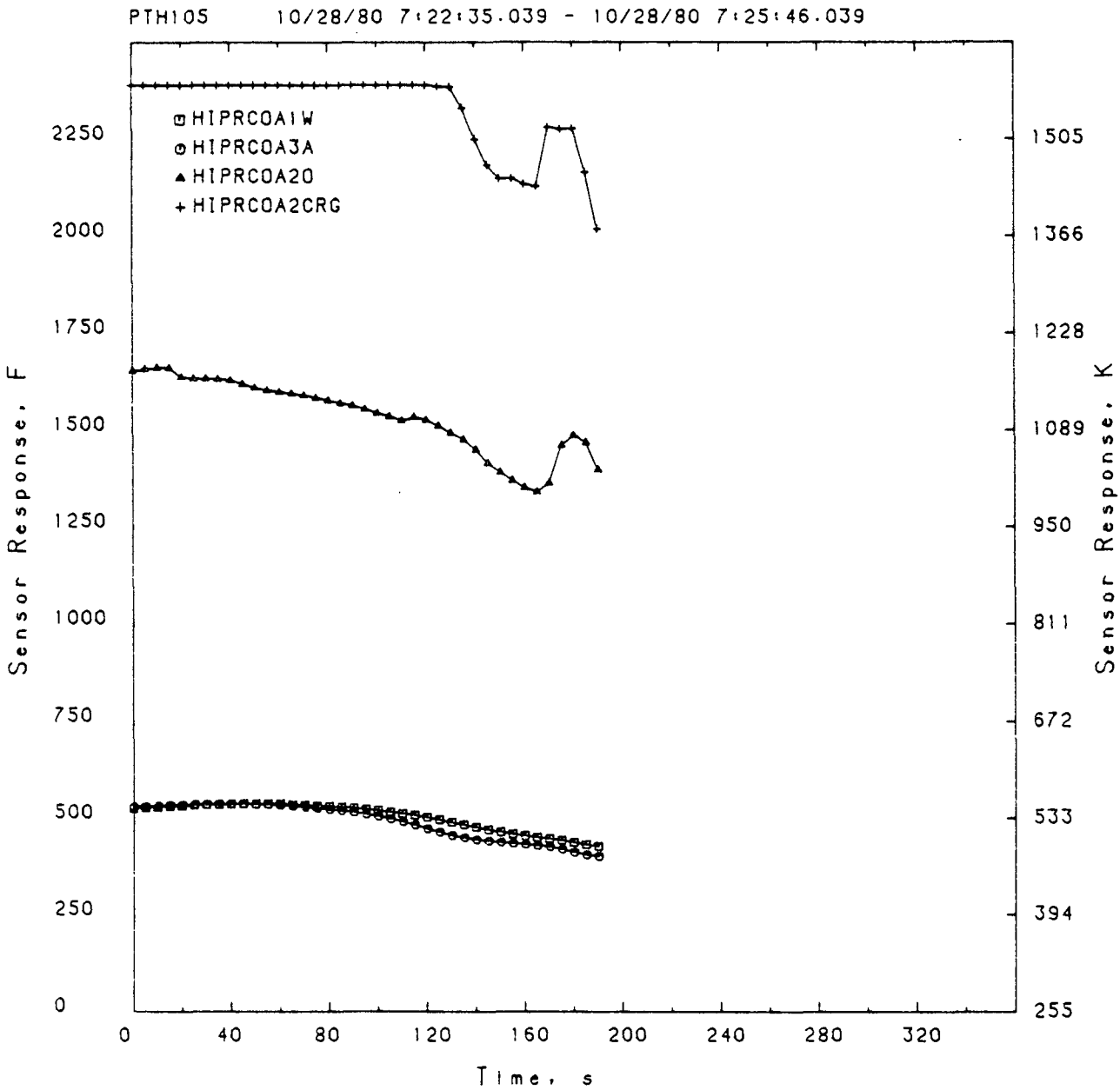

FIGURE 3.2.3.05 HIGH PRESSURE CONNECTOR TC RESPONSE HISTORY DURING TRANSIENT PTH105

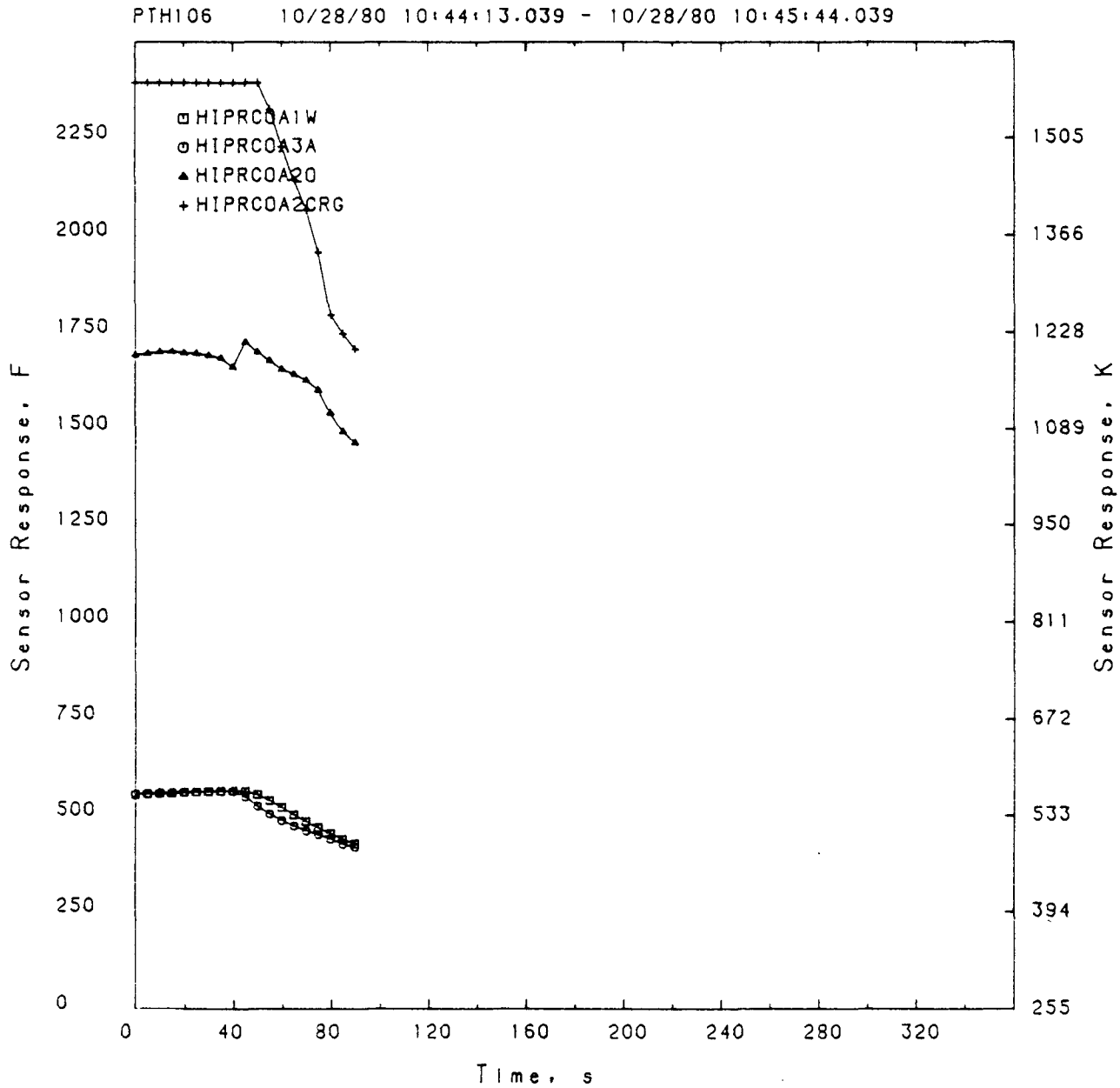

FIGURE 3.2.3.06 HIGH PRESSURE CONNECTOR TC RESPONSE HISTORY DURING TRANSIENT PTH106

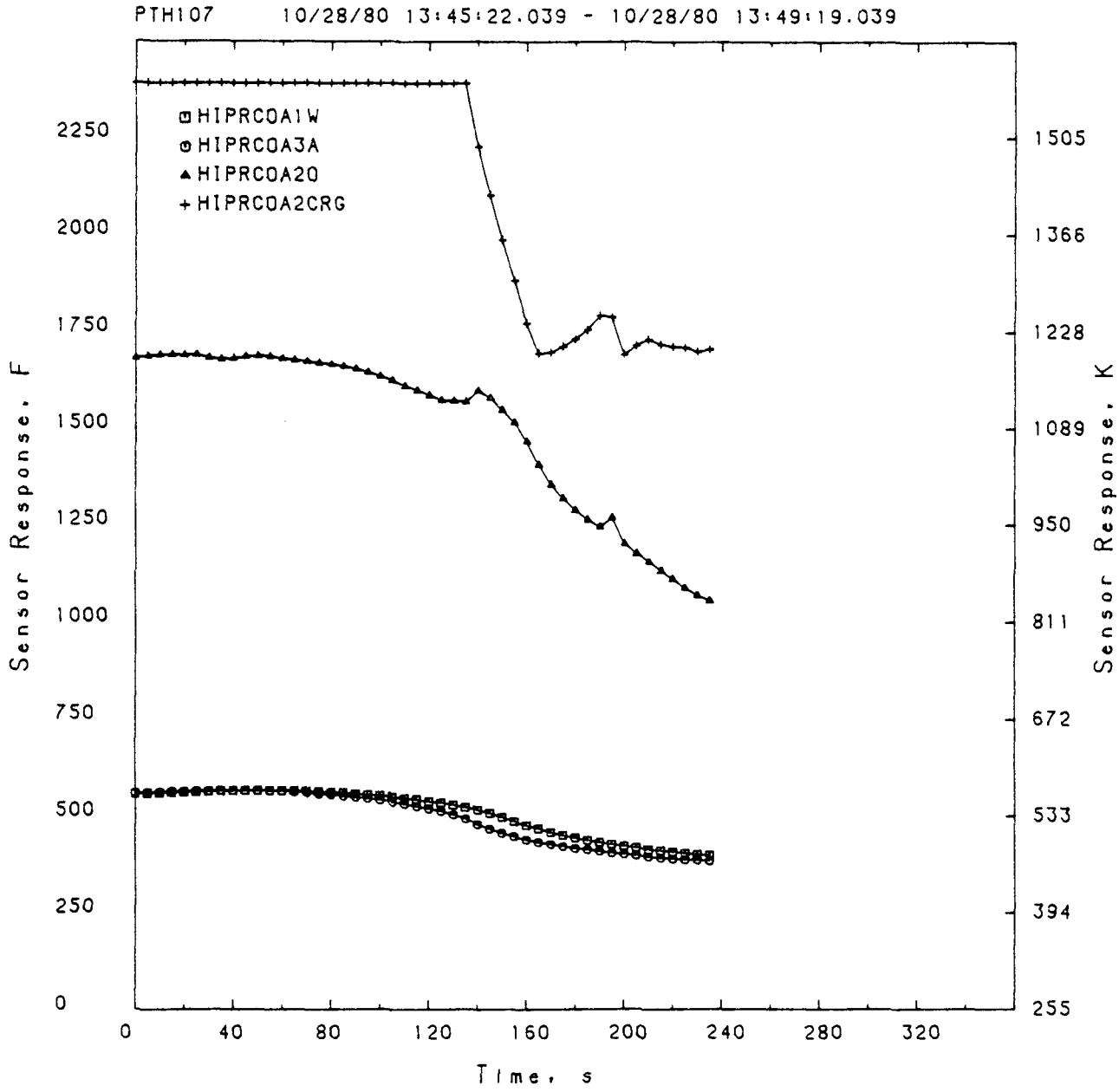

FIGURE 3.2.3.07 HIGH PRESSURE CONNECTOR TC RESPONSE HISTORY DURING TRANSIENT PTH107

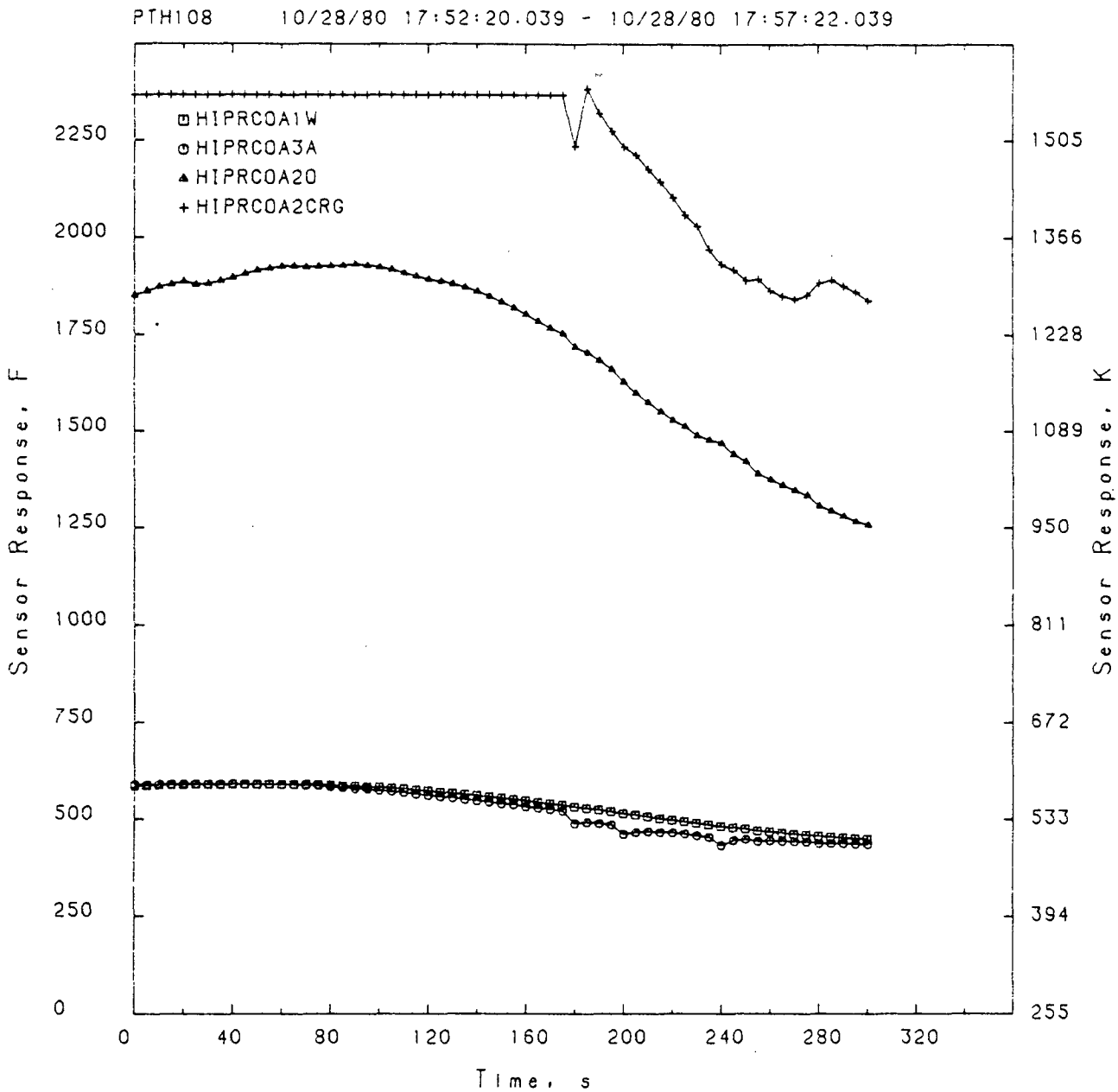

FIGURE 3.2.3.08 HIGH PRESSURE CONNECTOR TC RESPONSE HISTORY DURING TRANSIENT PTH108

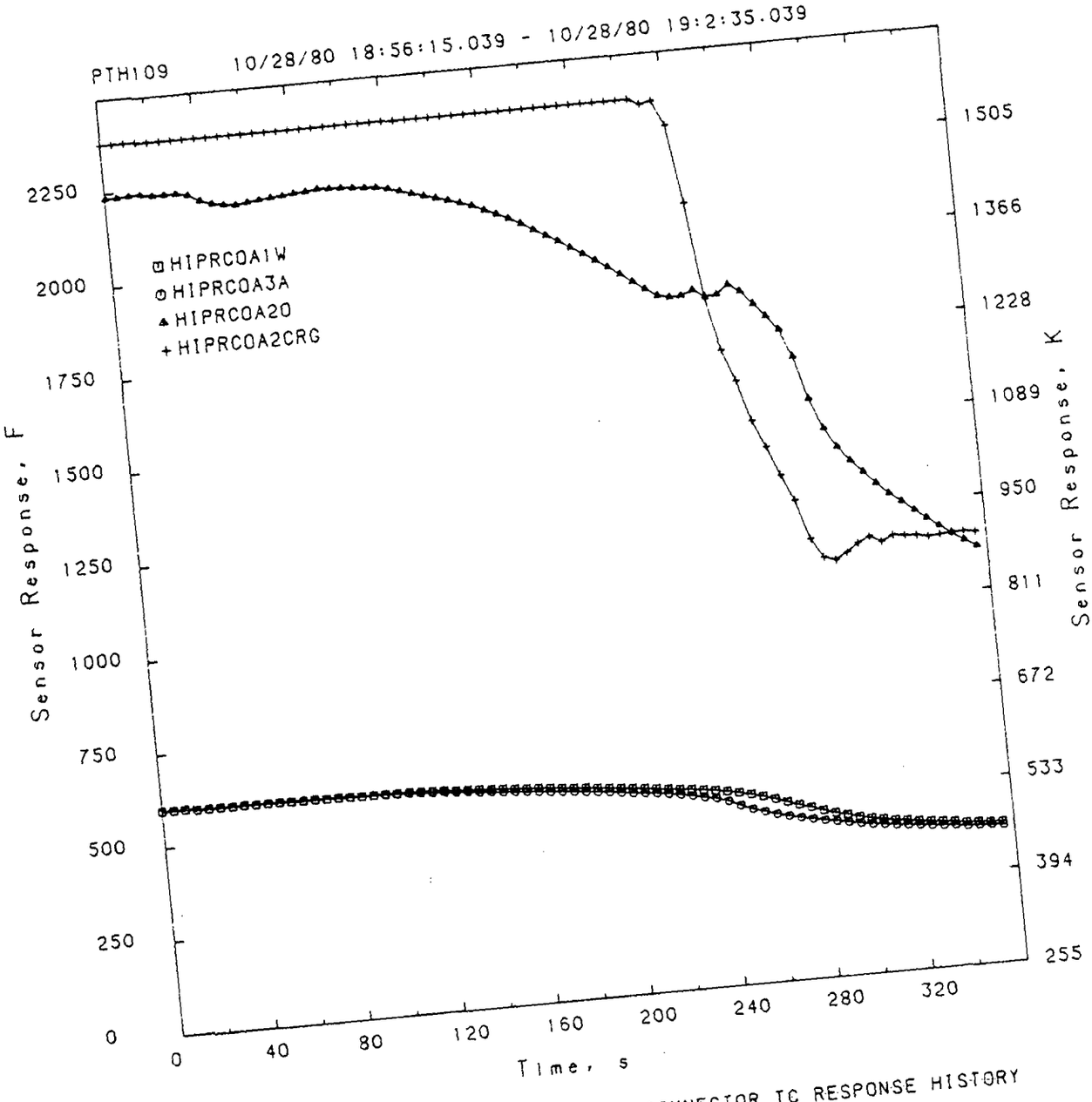

FIGURE 3.2.3.09 HIGH PRESSURE CONNECTOR TC RESPONSE HISTORY DURING TRANSIENT PTH109

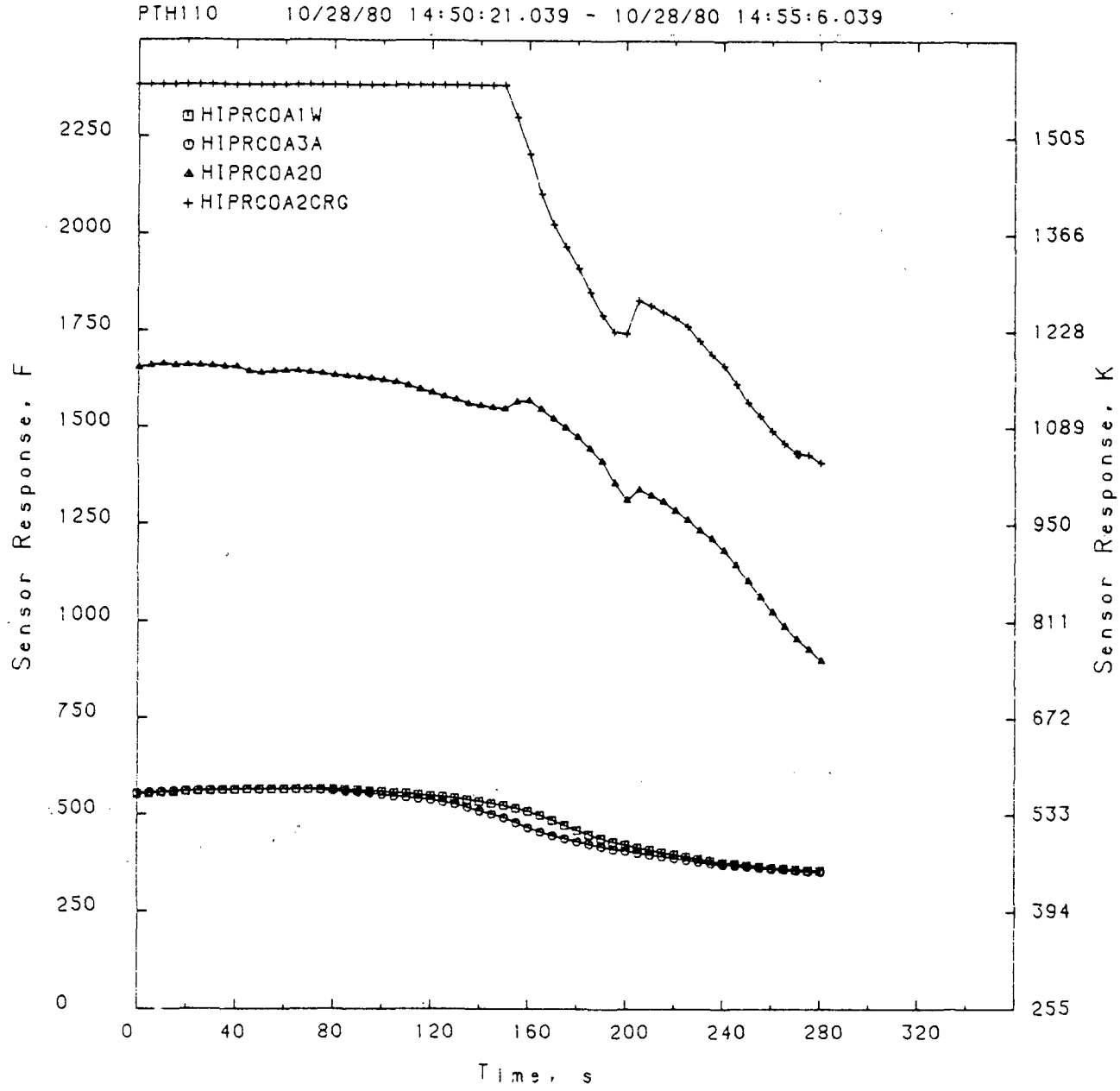

FIGURE 3.2.3.10 HIGH PRESSURE CONNECTOR TC RESPONSE HISTORY DURING TRANSIENT PTH110

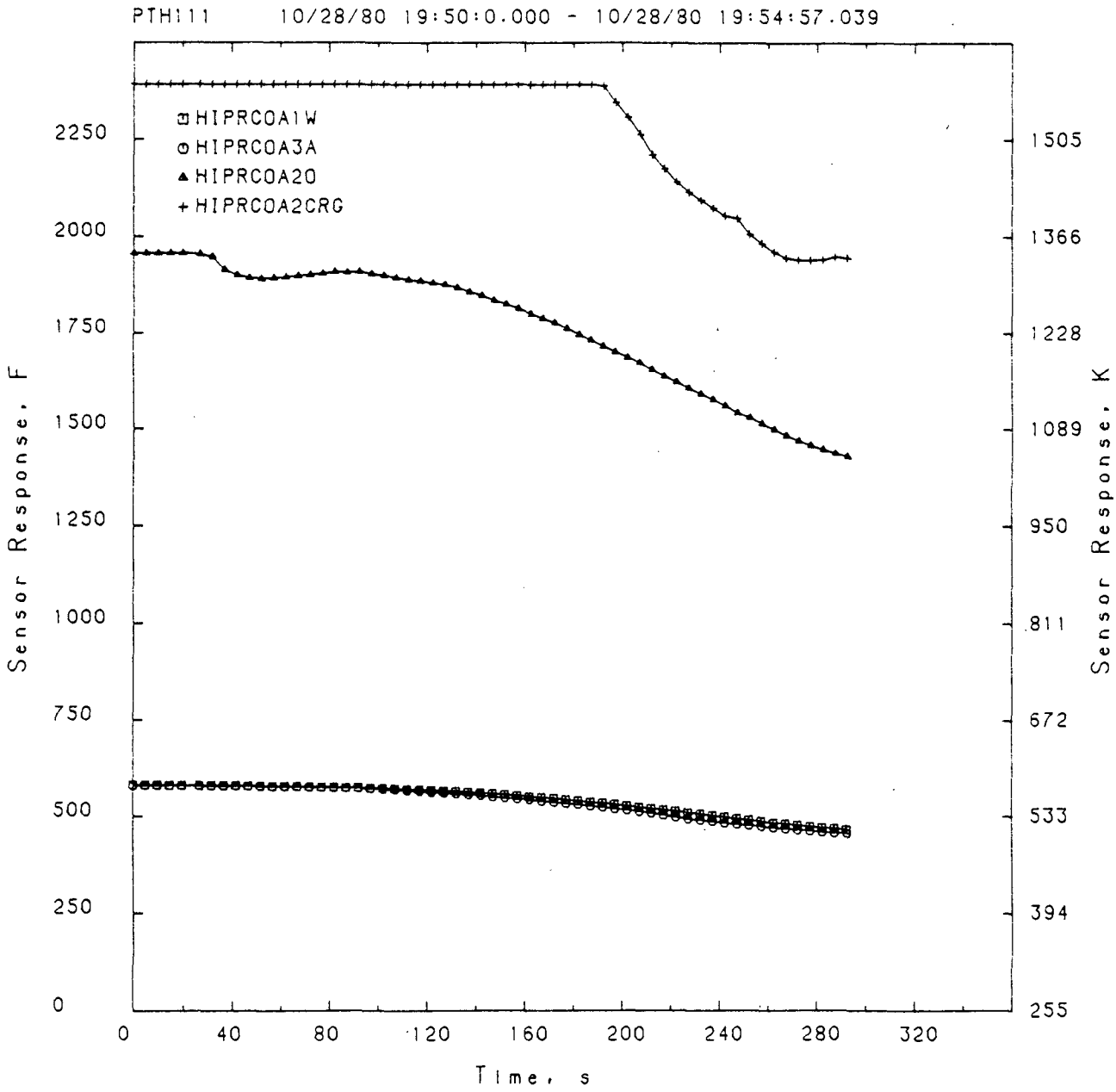

FIGURE 3.2.3.11 HIGH PRESSURE CONNECTOR TC RESPONSE HISTORY DURING TRANSIENT PTH111

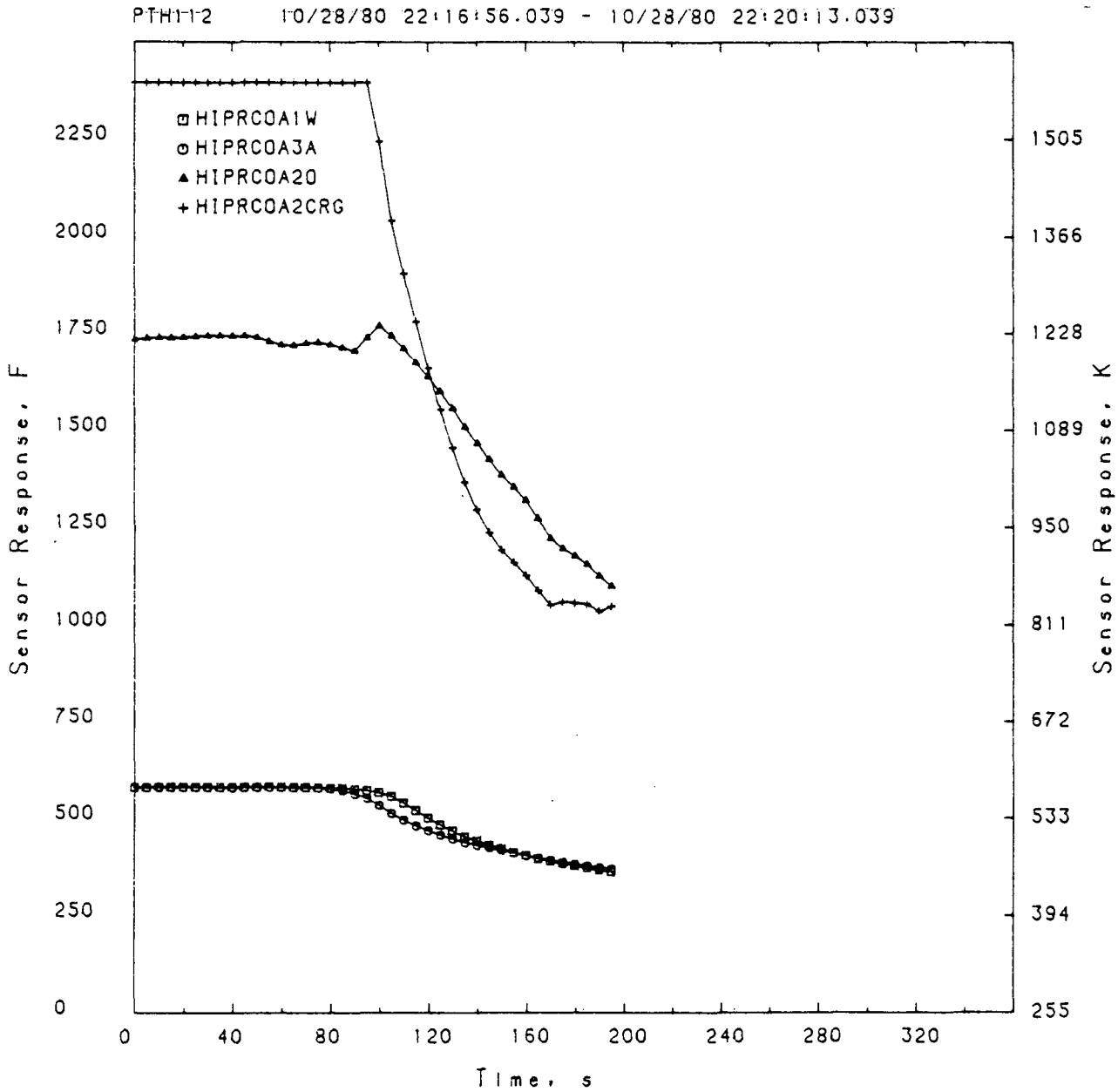

FIGURE 3.2.3.12 HIGH PRESSURE CONNECTOR TC RESPONSE HISTORY DURING TRANSIENT PTH112

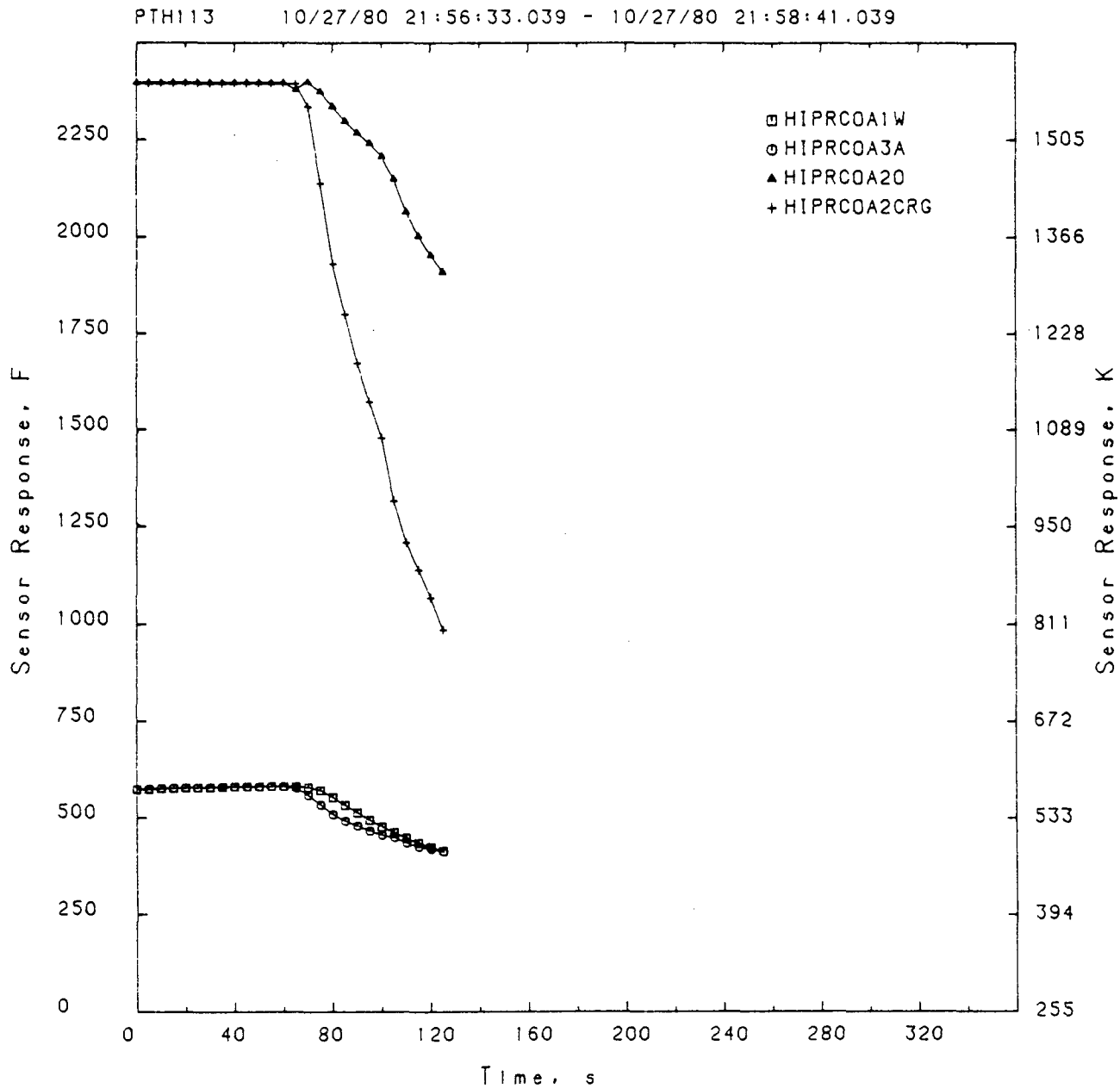

FIGURE 3.2.3.13 HIGH PRESSURE CONNECTOR TC RESPONSE HISTORY DURING TRANSIENT PTH113

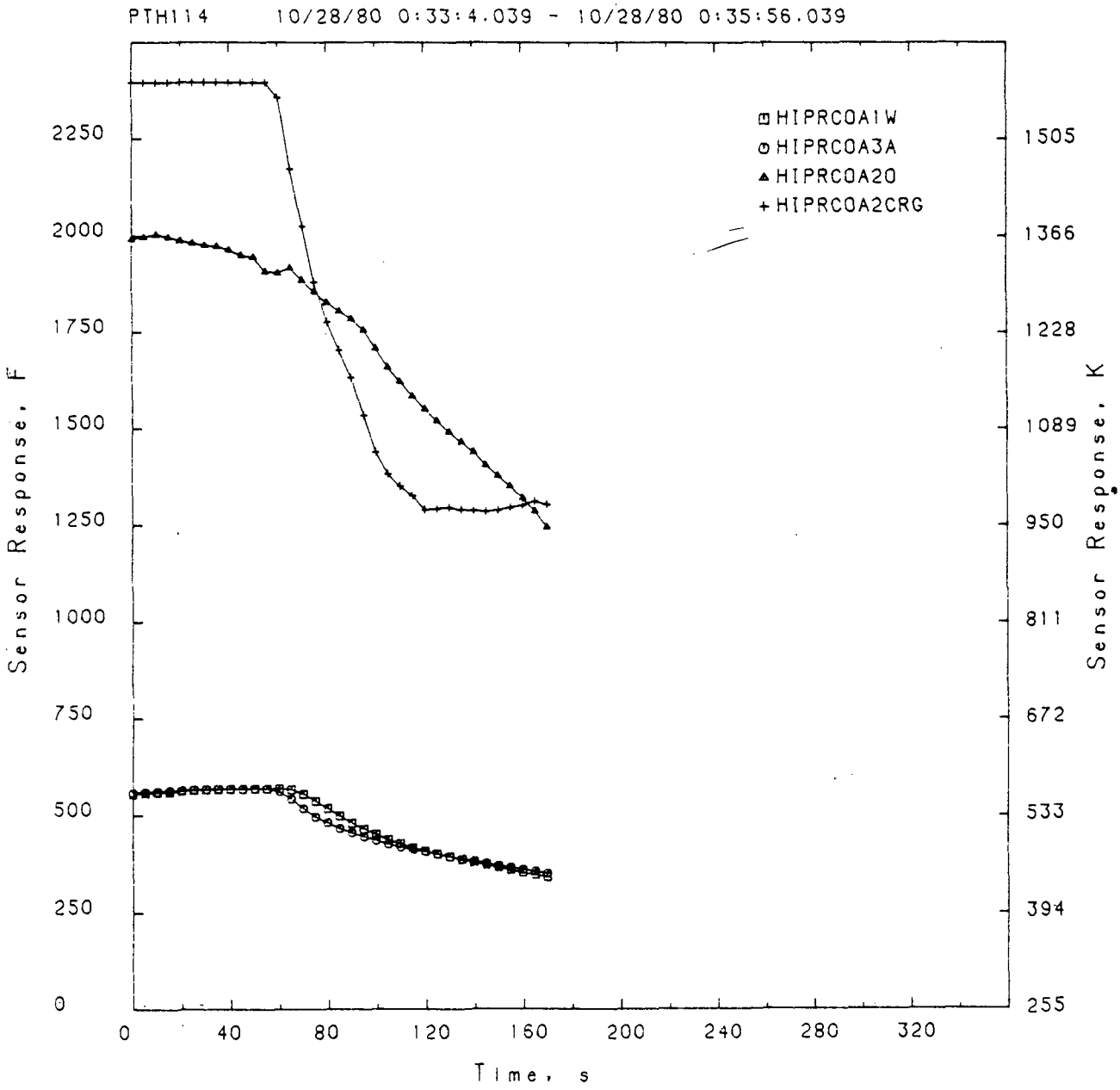

FIGURE 3.2.3.14 HIGH PRESSURE CONNECTOR TC RESPONSE HISTORY DURING TRANSIENT PTH114

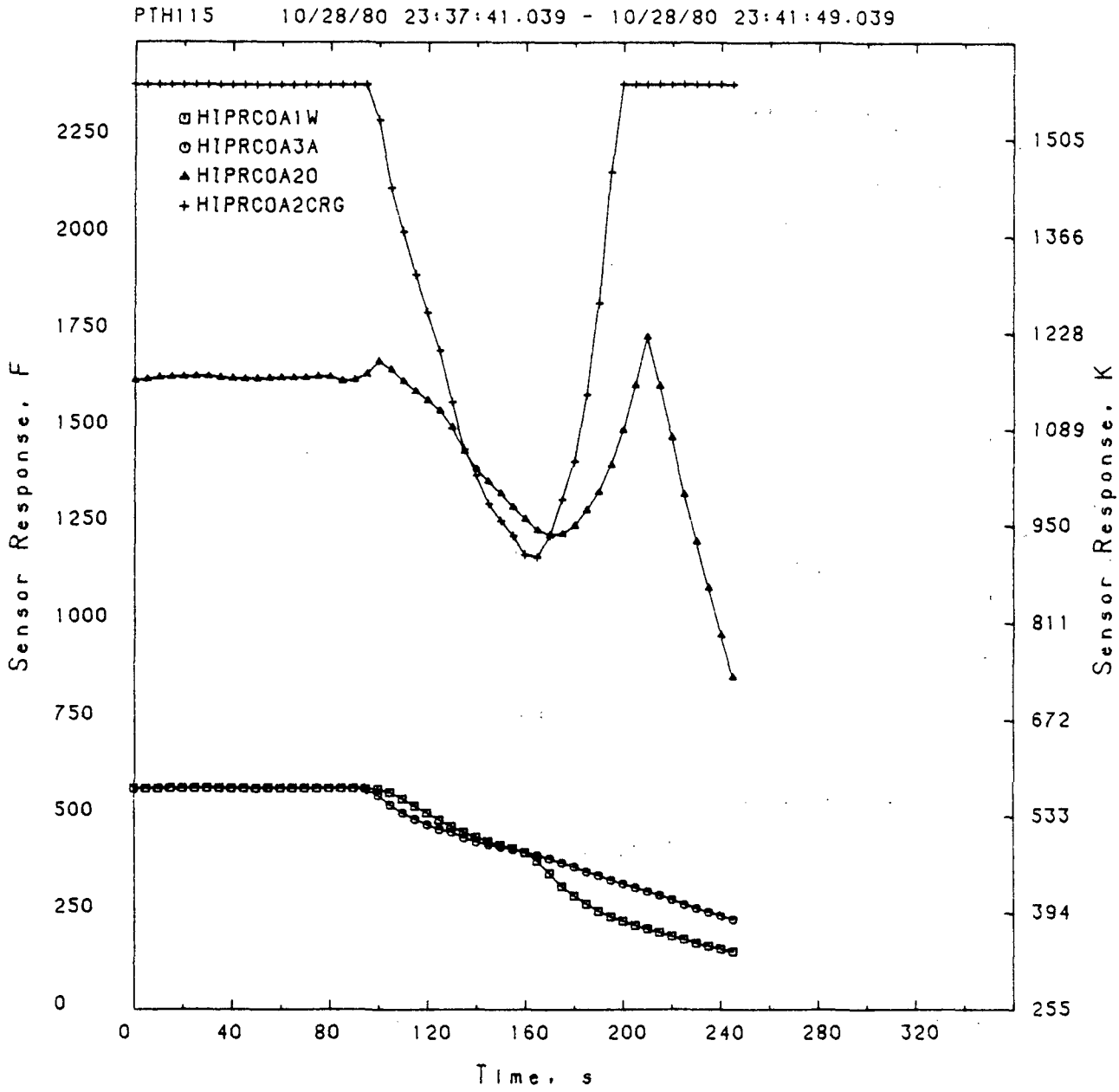

FIGURE 3.2.3.15 HIGH PRESSURE CONNECTOR TC RESPONSE HISTORY DURING TRANSIENT PTH115

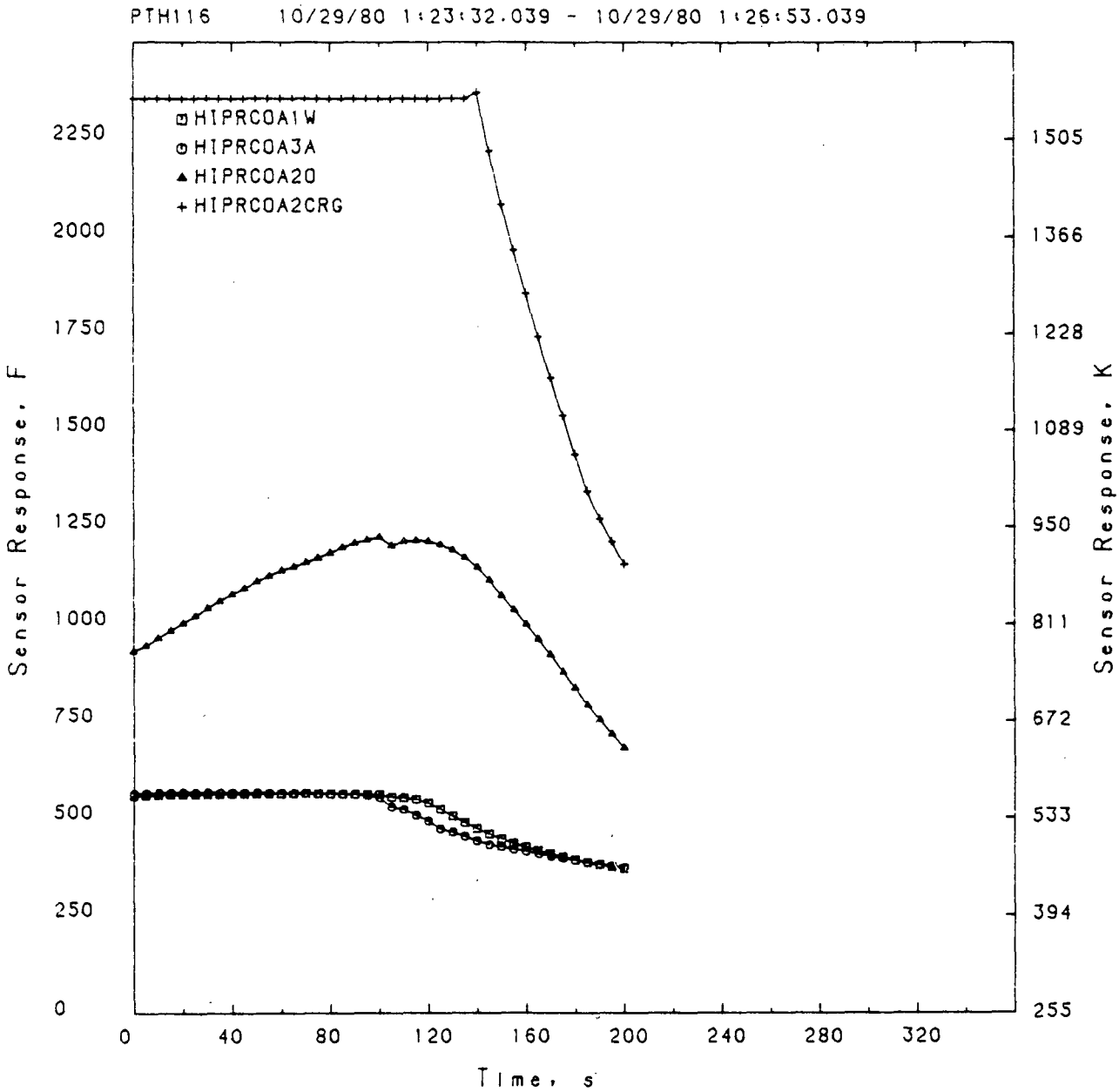

FIGURE 3.2.3.16 HIGH PRESSURE CONNECTOR TC RESPONSE HISTORY DURING TRANSIENT PTH116

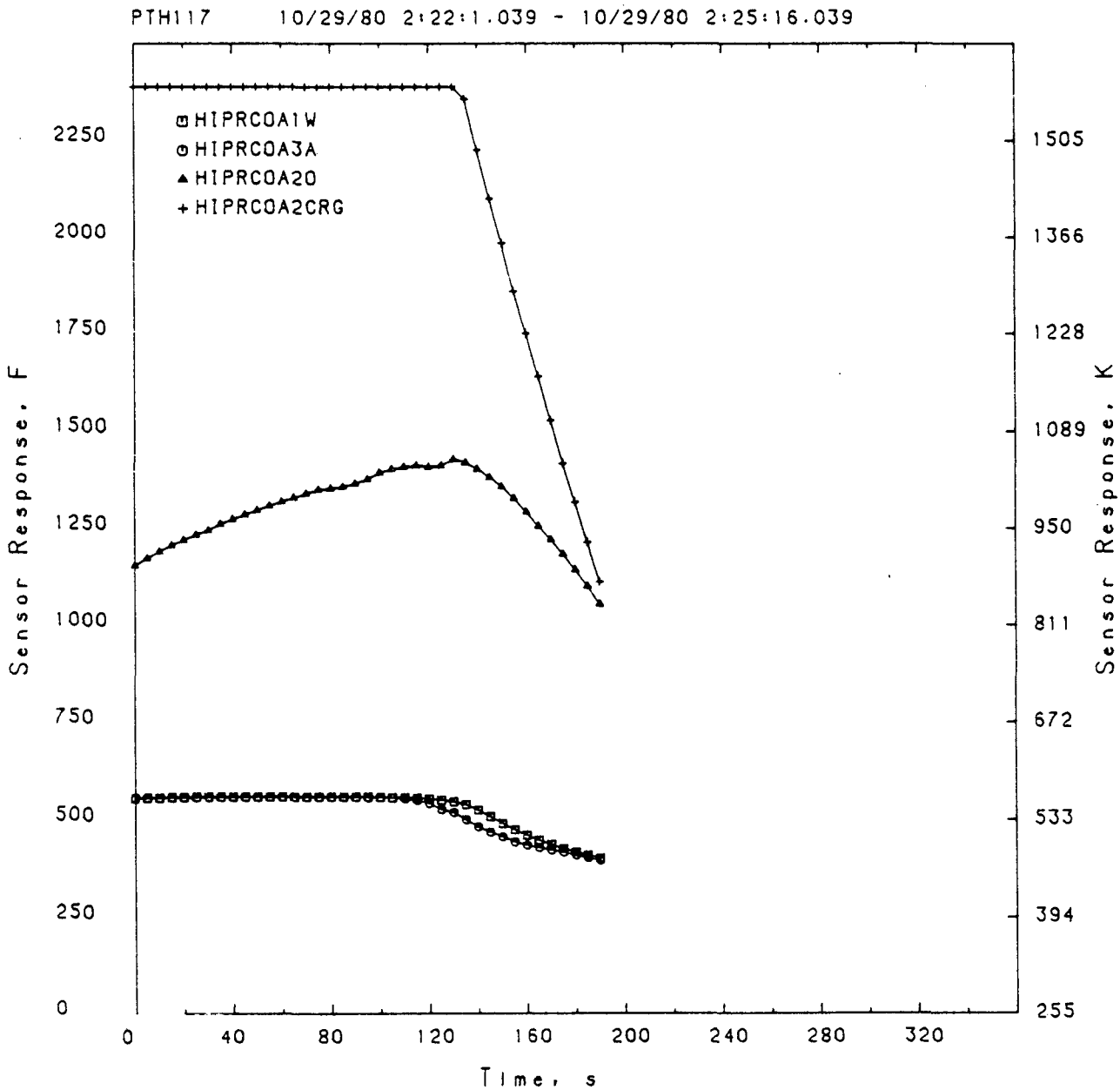

FIGURE 3.2.3.17 HIGH PRESSURE CONNECTOR TC RESPONSE HISTORY DURING TRANSIENT PTH117

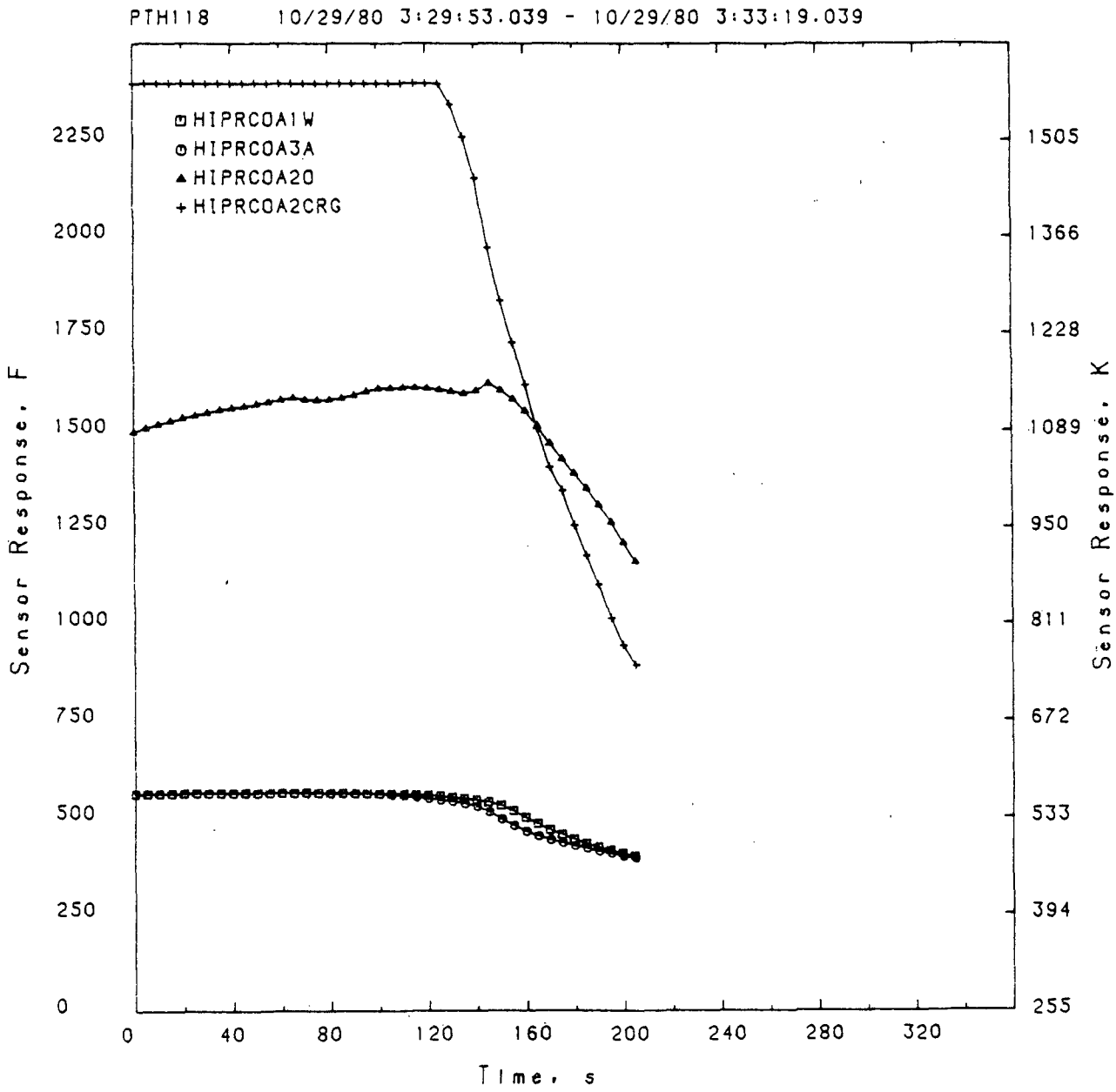

FIGURE 3.2.3.18 HIGH PRESSURE CONNECTOR TC RESPONSE HISTORY DURING TRANSIENT PTH118

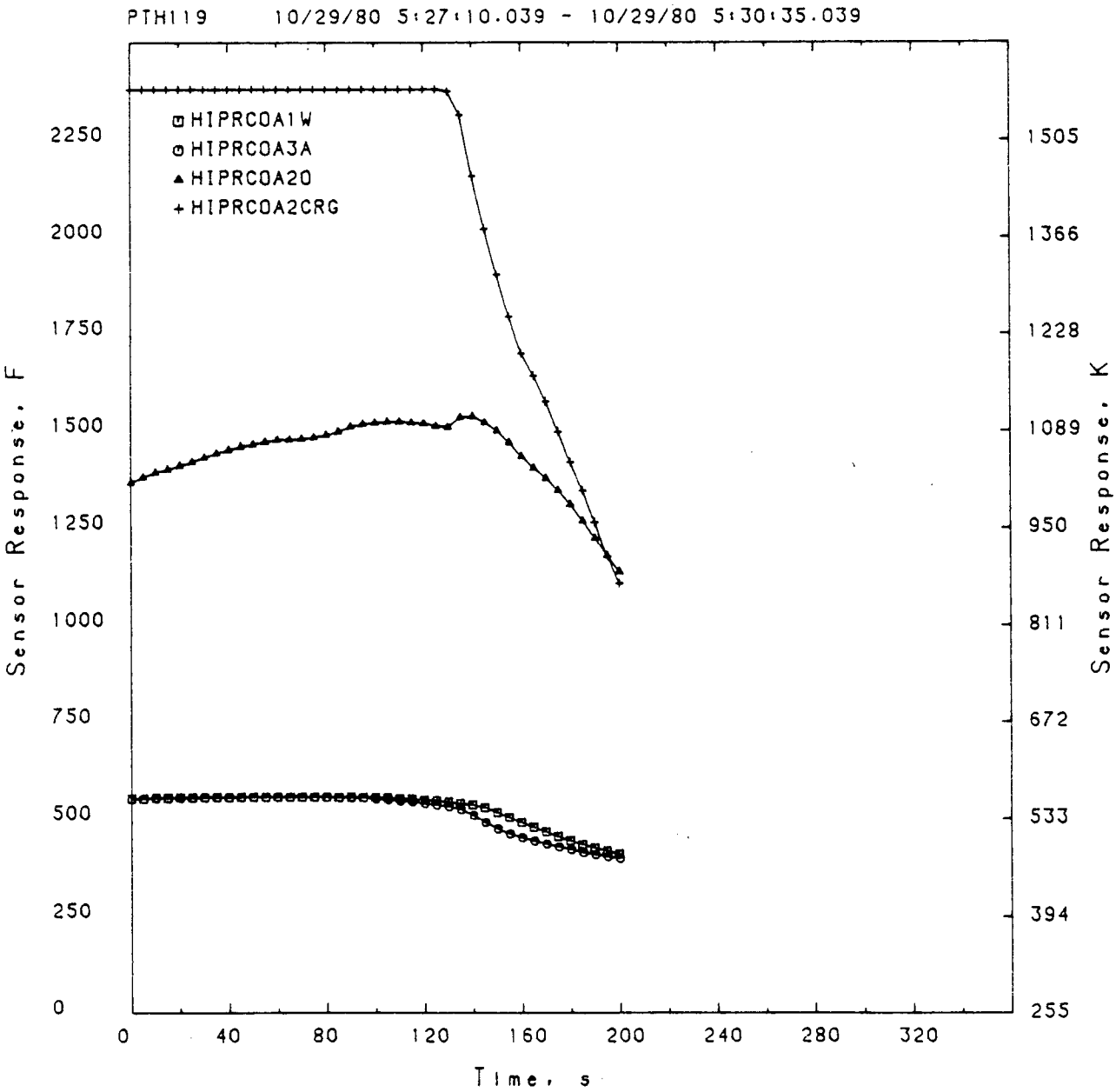

FIGURE 3.2.3.19 HIGH PRESSURE CONNECTOR TC RESPONSE HISTORY DURING TRANSIENT PTH119

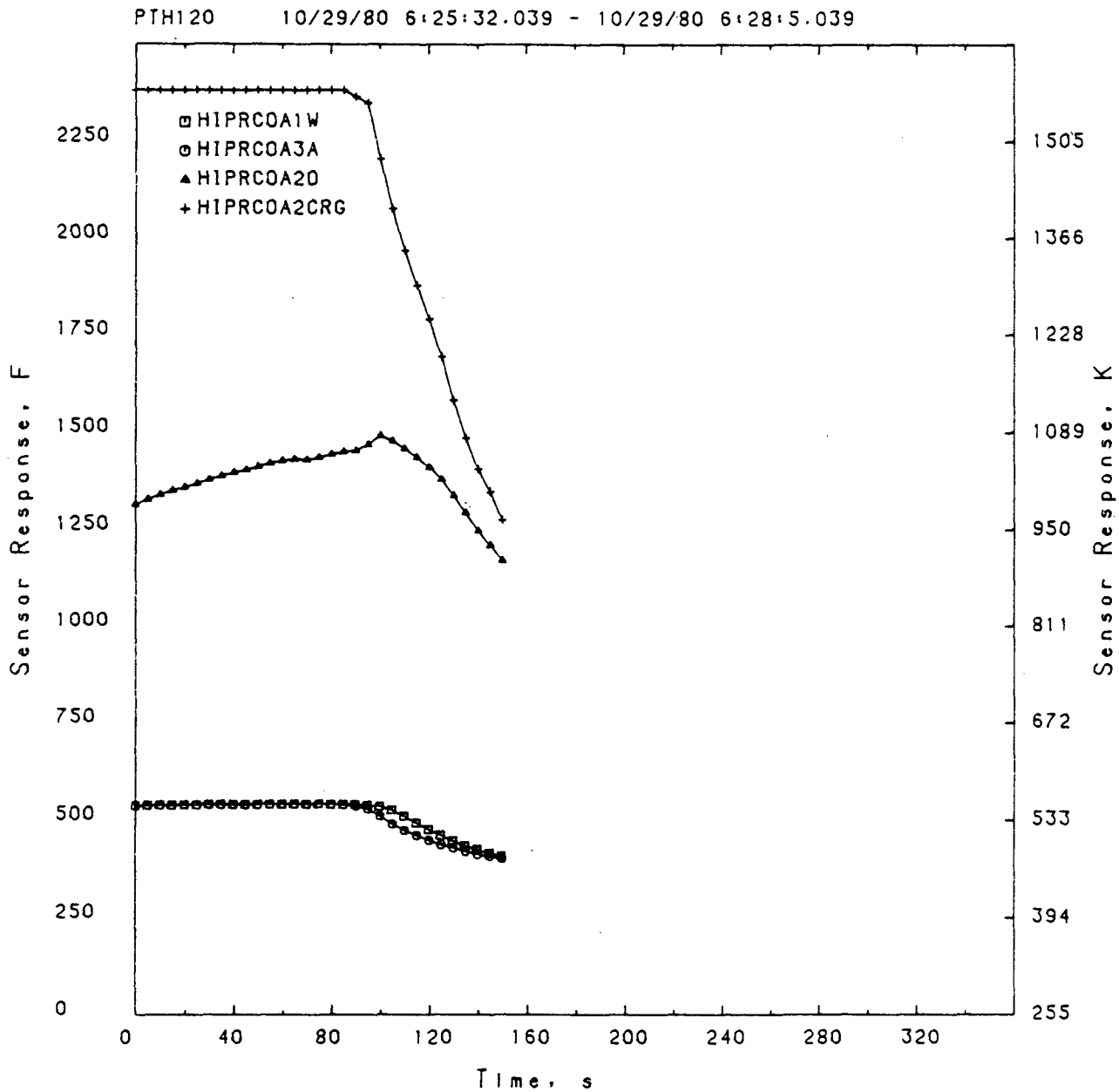

FIGURE 3.2.3.20 HIGH PRESSURE CONNECTOR TC RESPONSE HISTORY DURING TRANSIENT PTH120

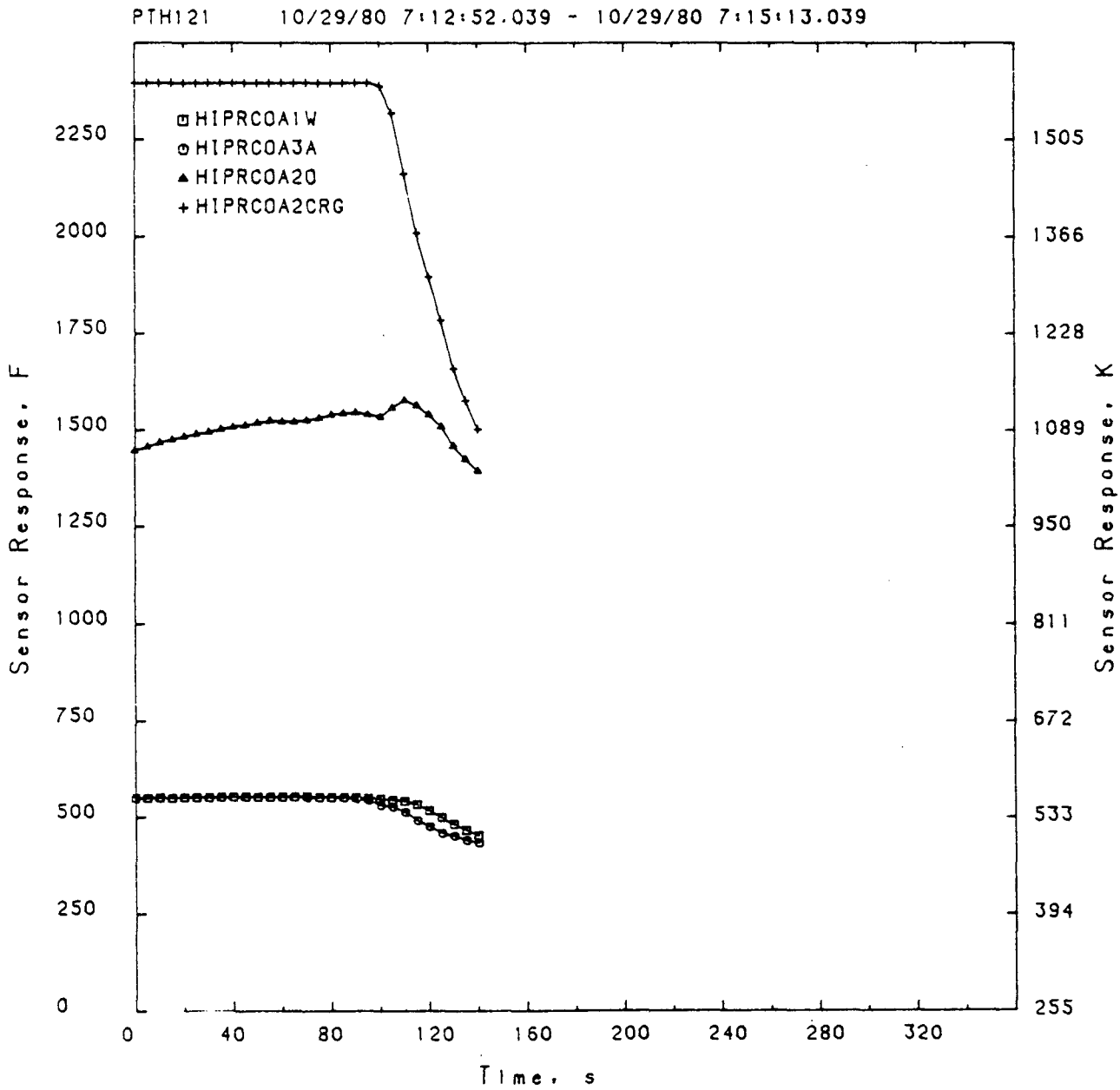

FIGURE 3.2.3.21 HIGH PRESSURE CONNECTOR TC RESPONSE HISTORY DURING TRANSIENT PTH121

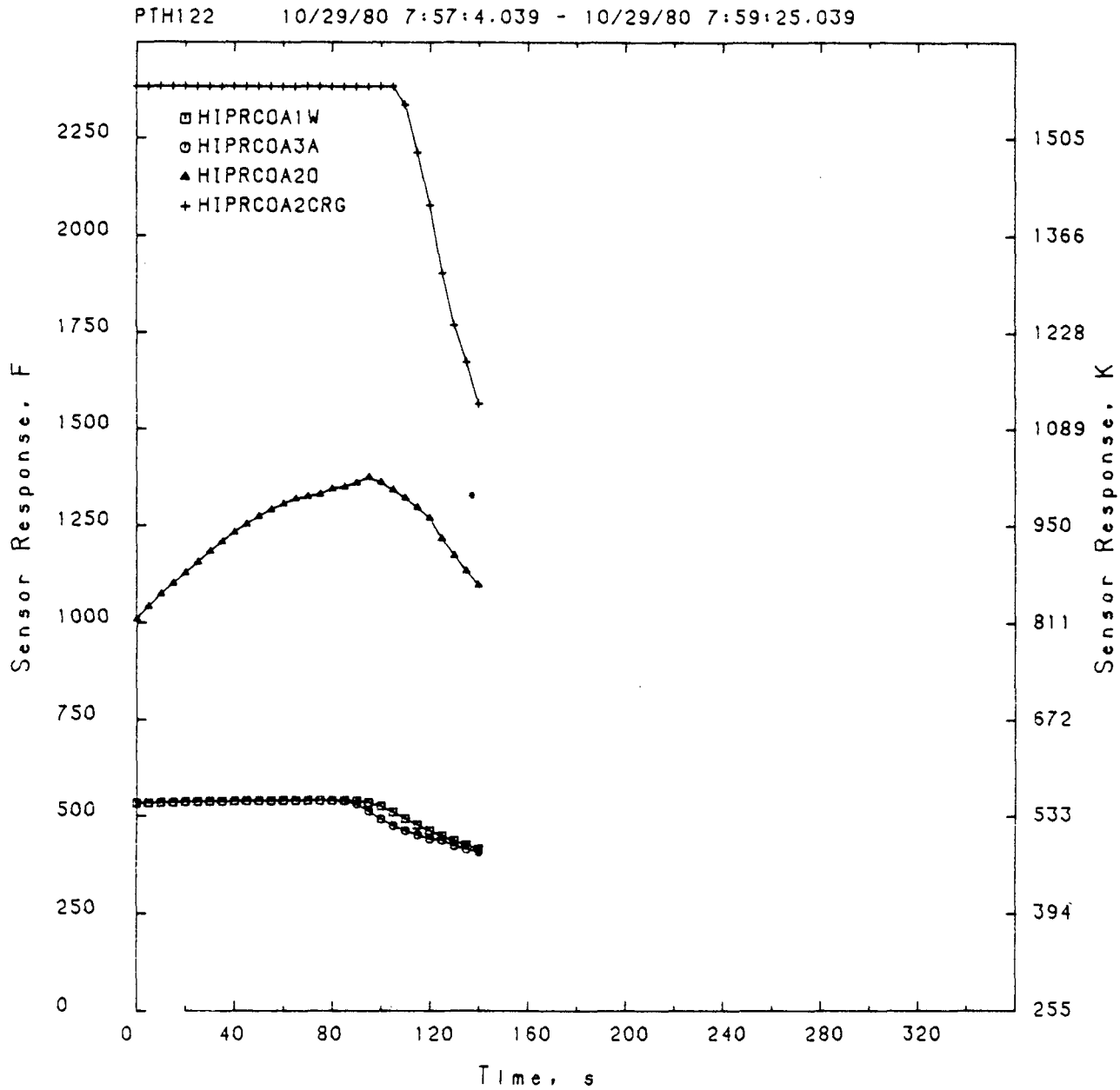

FIGURE 3.2.3.22 HIGH PRESSURE CONNECTOR TC RESPONSE HISTORY DURING TRANSIENT PTH122

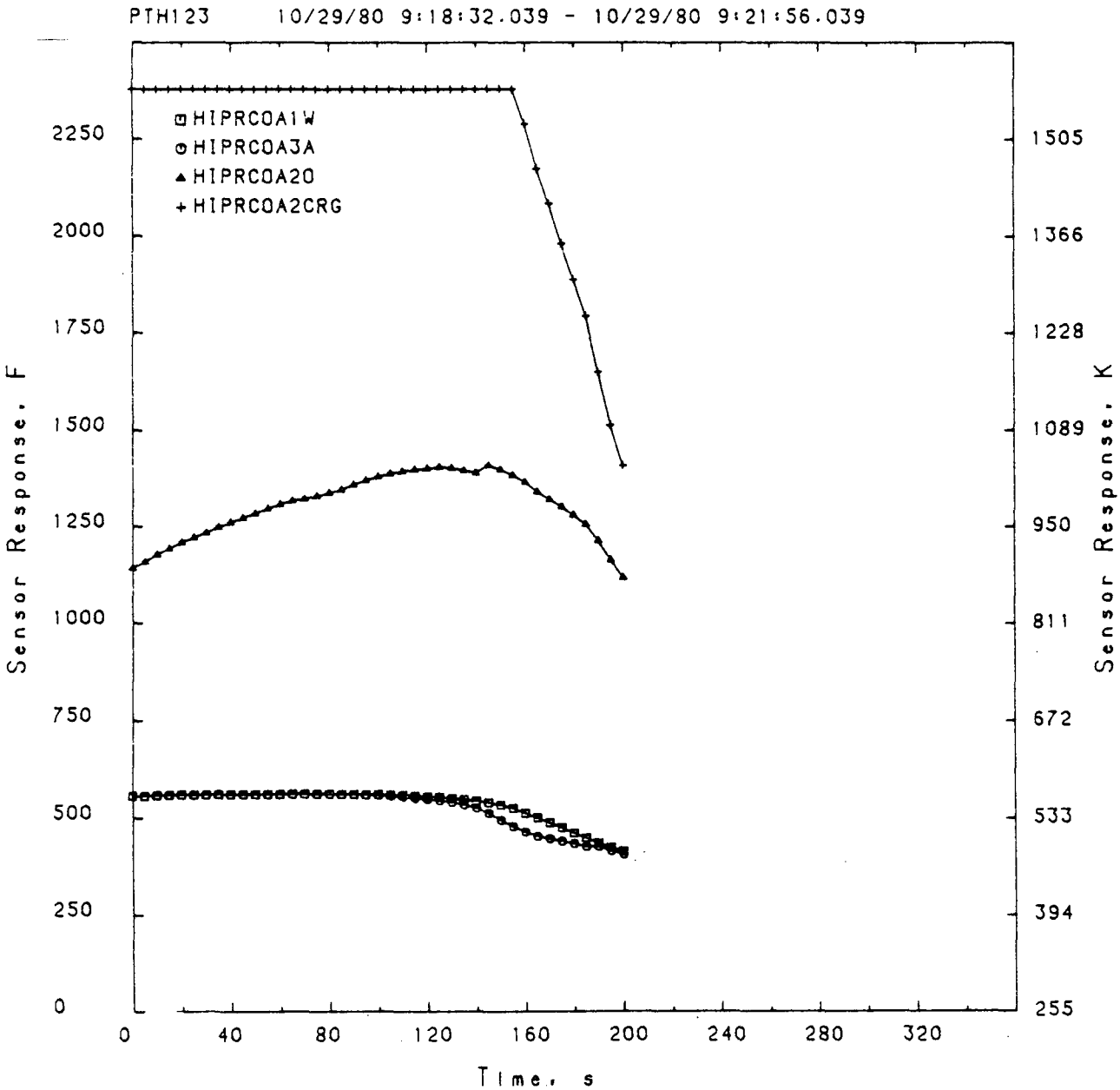

FIGURE 3.2.3.23 HIGH PRESSURE CONNECTOR TC RESPONSE HISTORY DURING TRANSIENT PTH123

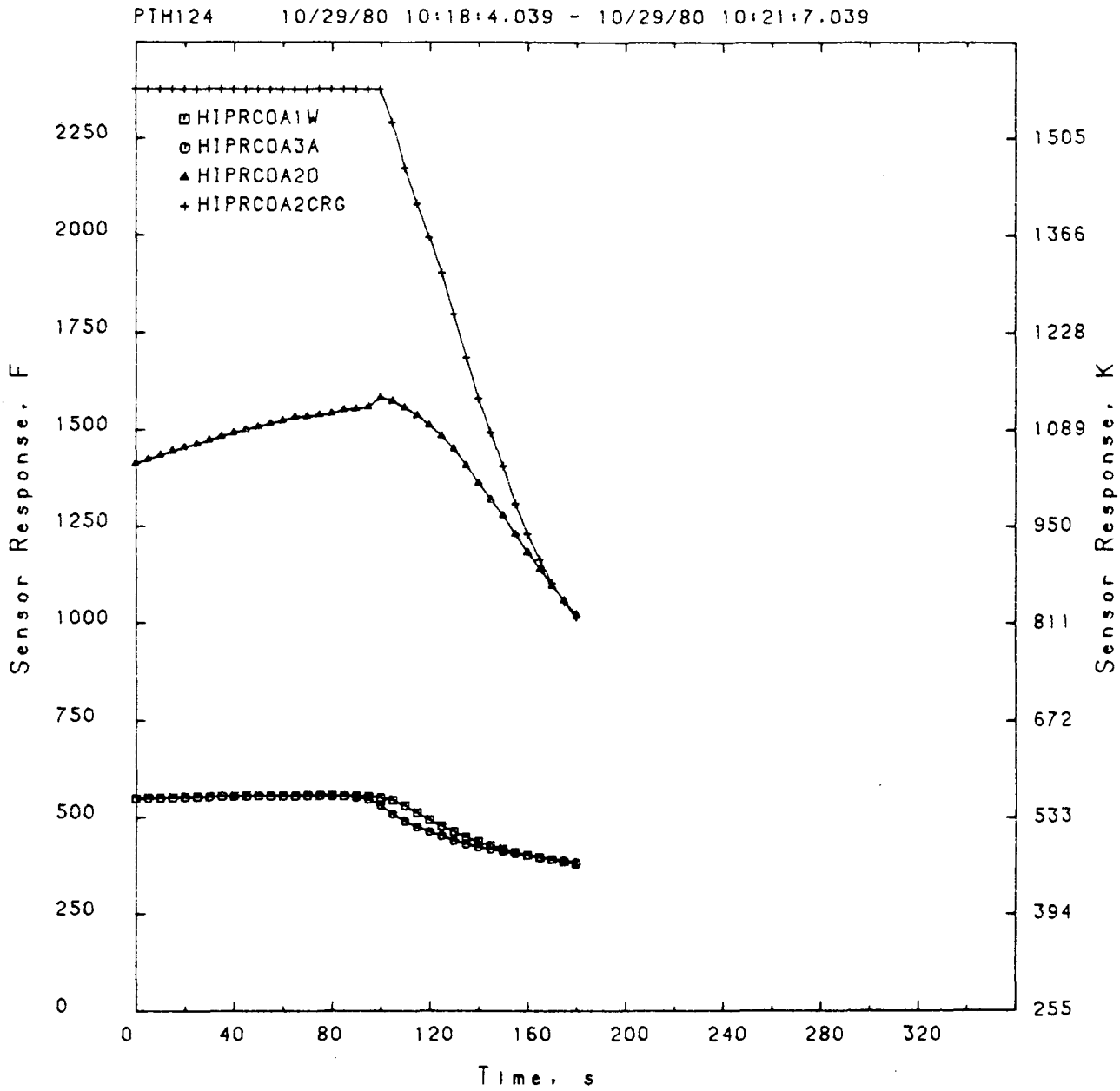

FIGURE 3.2.3.24 HIGH PRESSURE CONNECTOR TC RESPONSE HISTORY DURING TRANSIENT PTH124

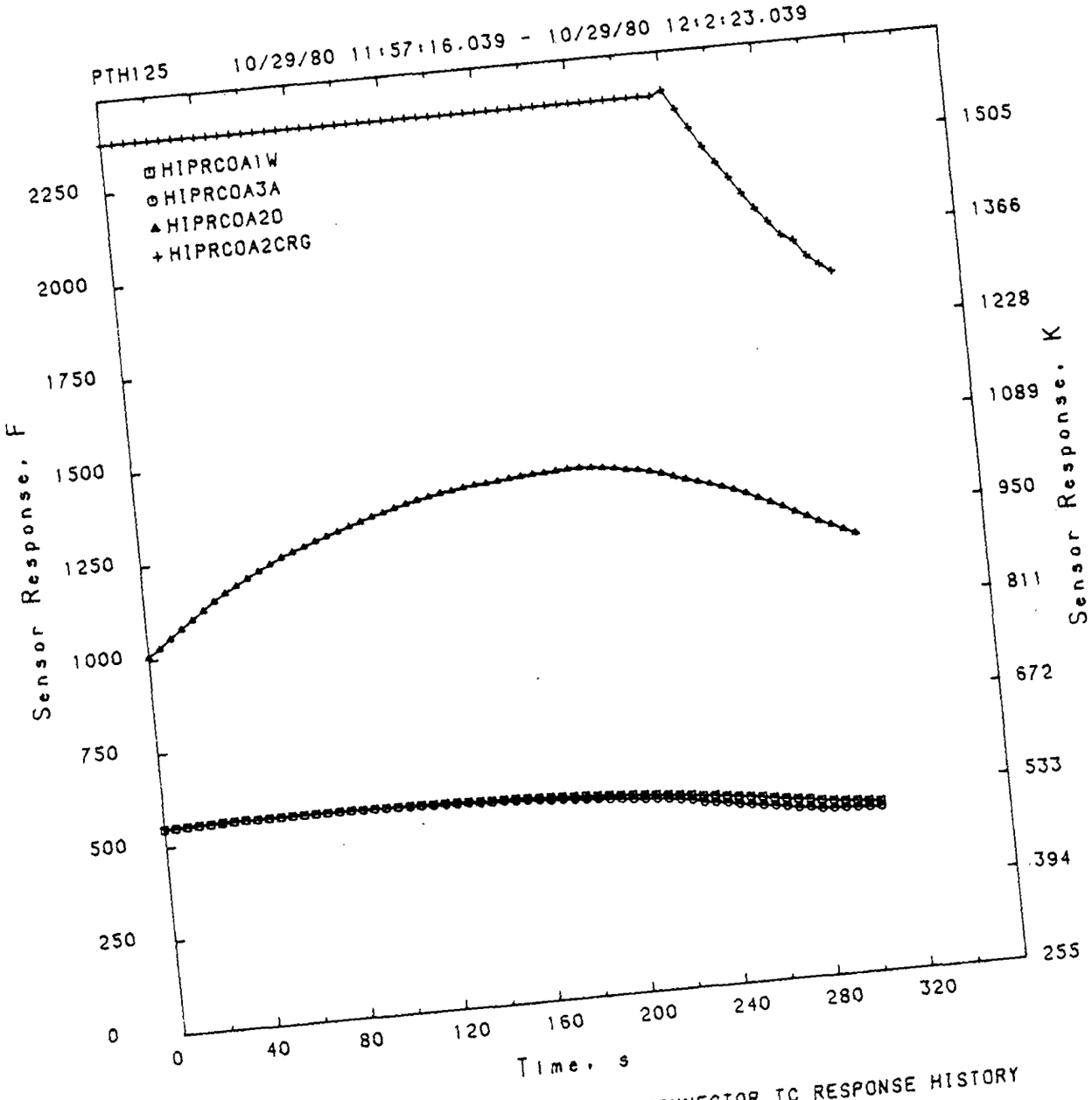

FIGURE 3.2.3.25 HIGH PRESSURE CONNECTOR TC RESPONSE HISTORY DURING TRANSIENT PTH125

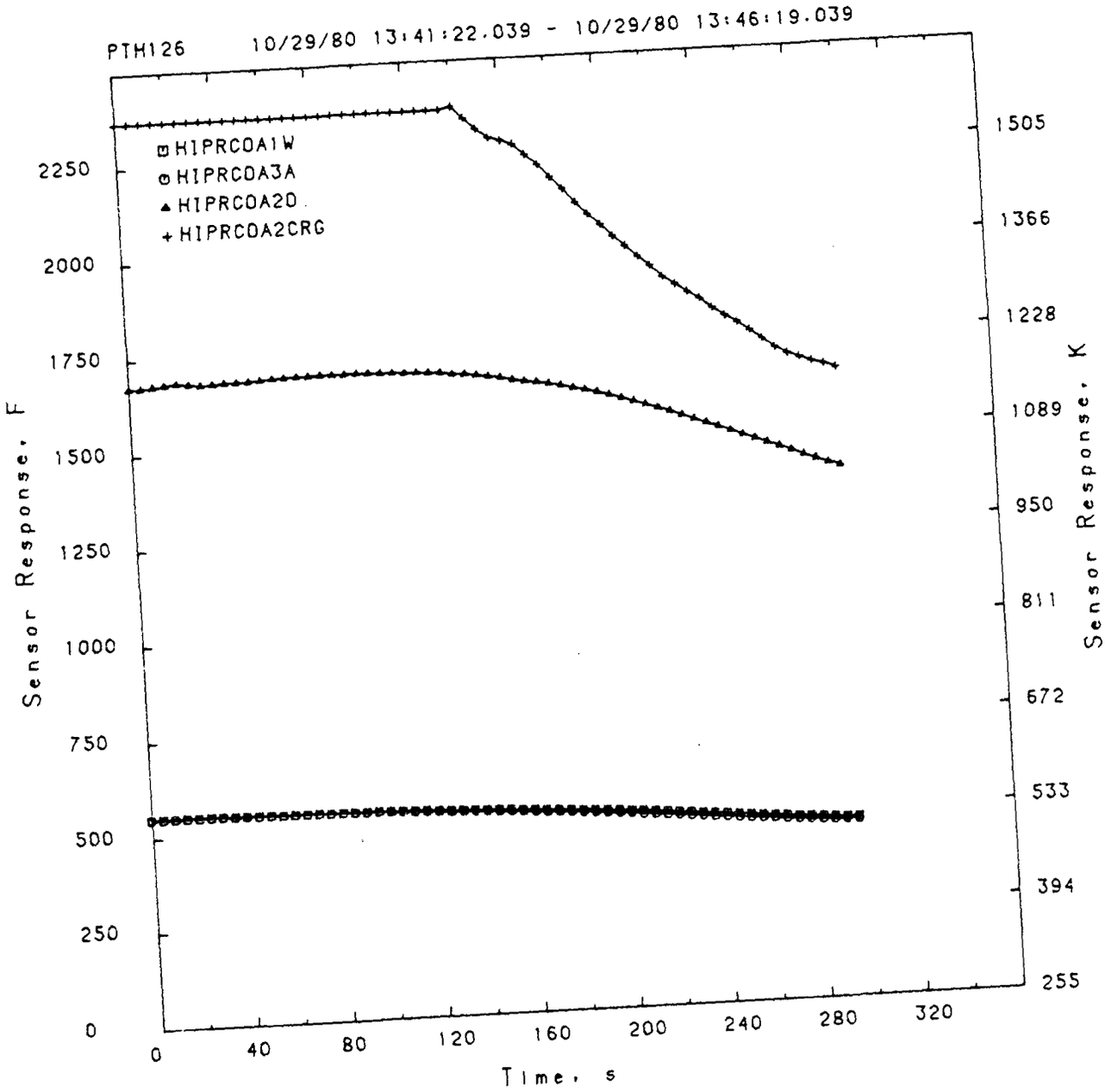

FIGURE 3.2.3.26 HIGH PRESSURE CONNECTOR TC RESPONSE HISTORY DURING TRANSIENT PTH126

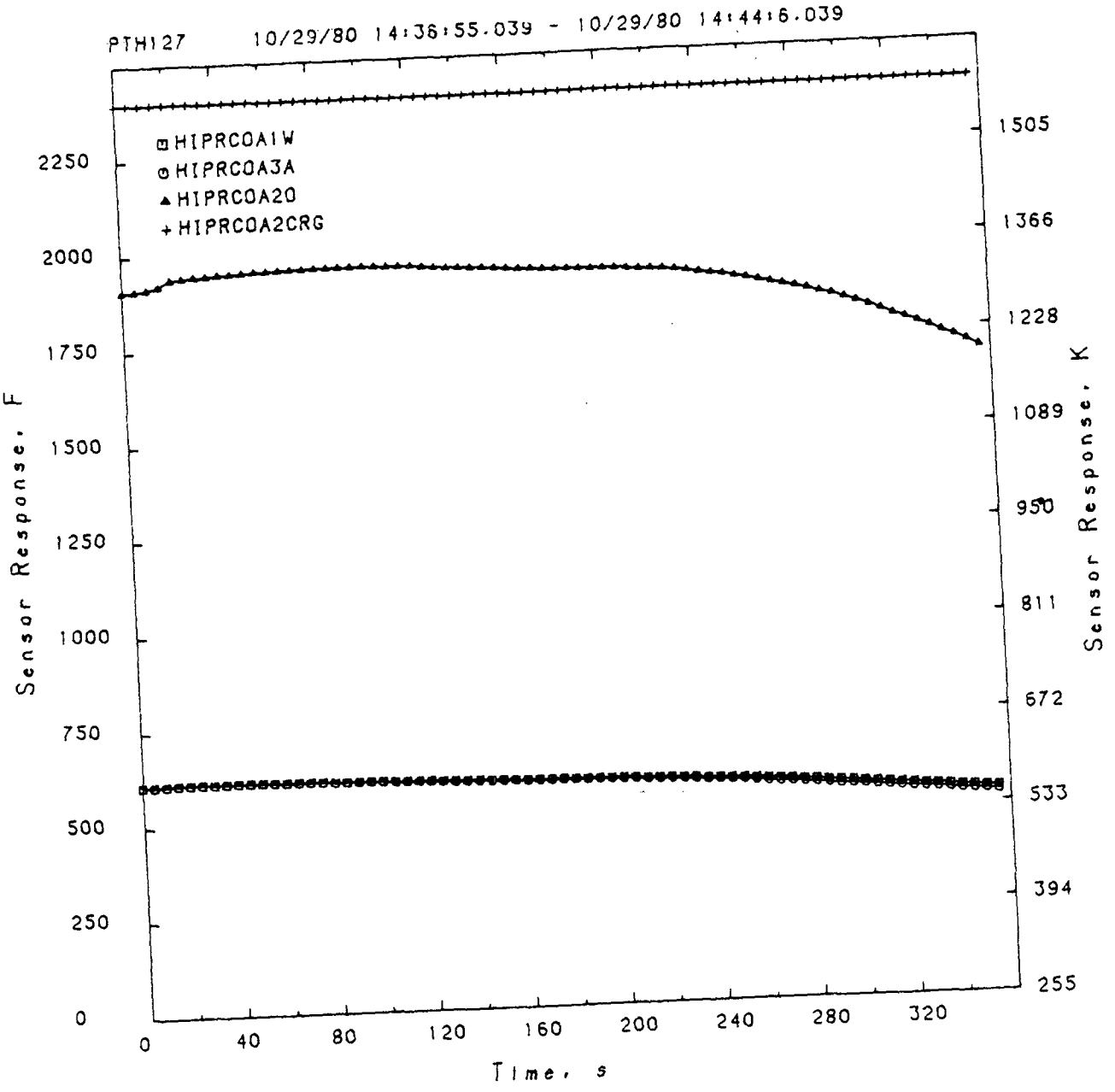

FIGURE 3.2.3.27 HIGH PRESSURE CONNECTOR TC RESPONSE HISTORY DURING TRANSIENT PTH127

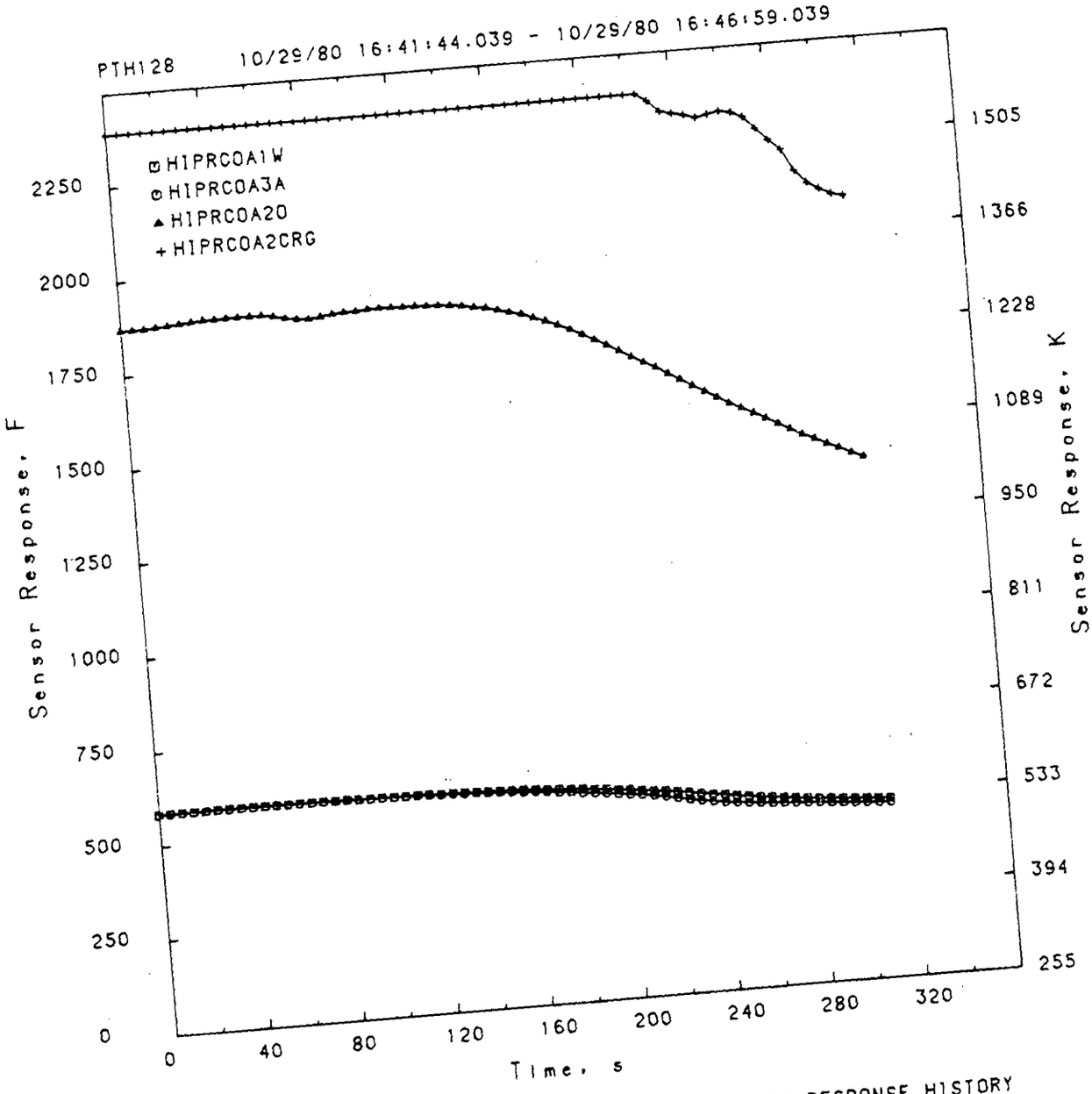

FIGURE 3.2.3.28 HIGH PRESSURE CONNECTOR TC RESPONSE HISTORY DURING TRANSIENT PTH128

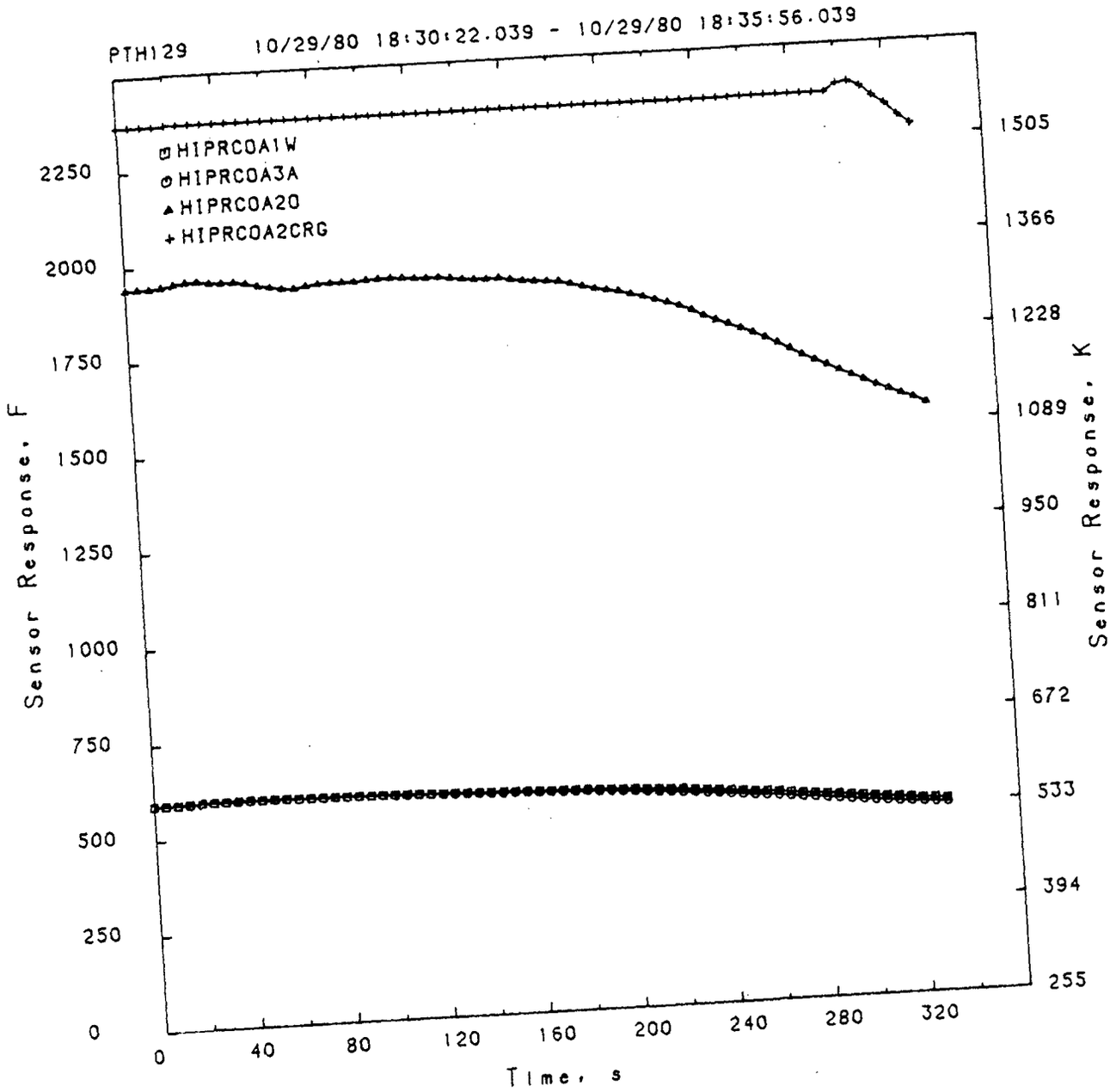

FIGURE 3.2.3.29 HIGH PRESSURE CONNECTOR TC RESPONSE HISTORY DURING TRANSIENT PTH129

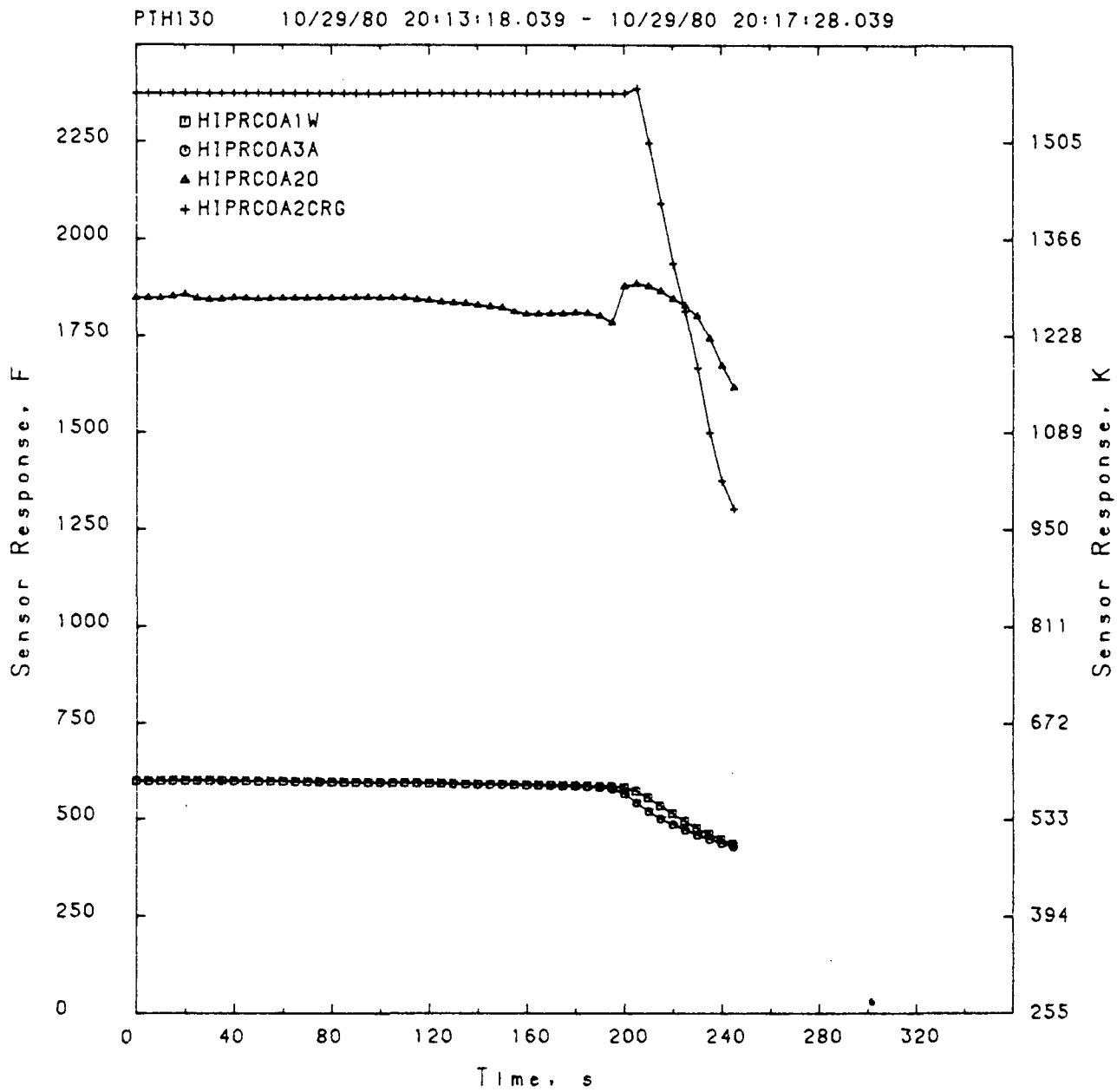

FIGURE 3.2.3.30 HIGH PRESSURE CONNECTOR TC RESPONSE HISTORY DURING TRANSIENT PTH130

PART 4

SHROUD LEAK RATE CHARACTERISTICS

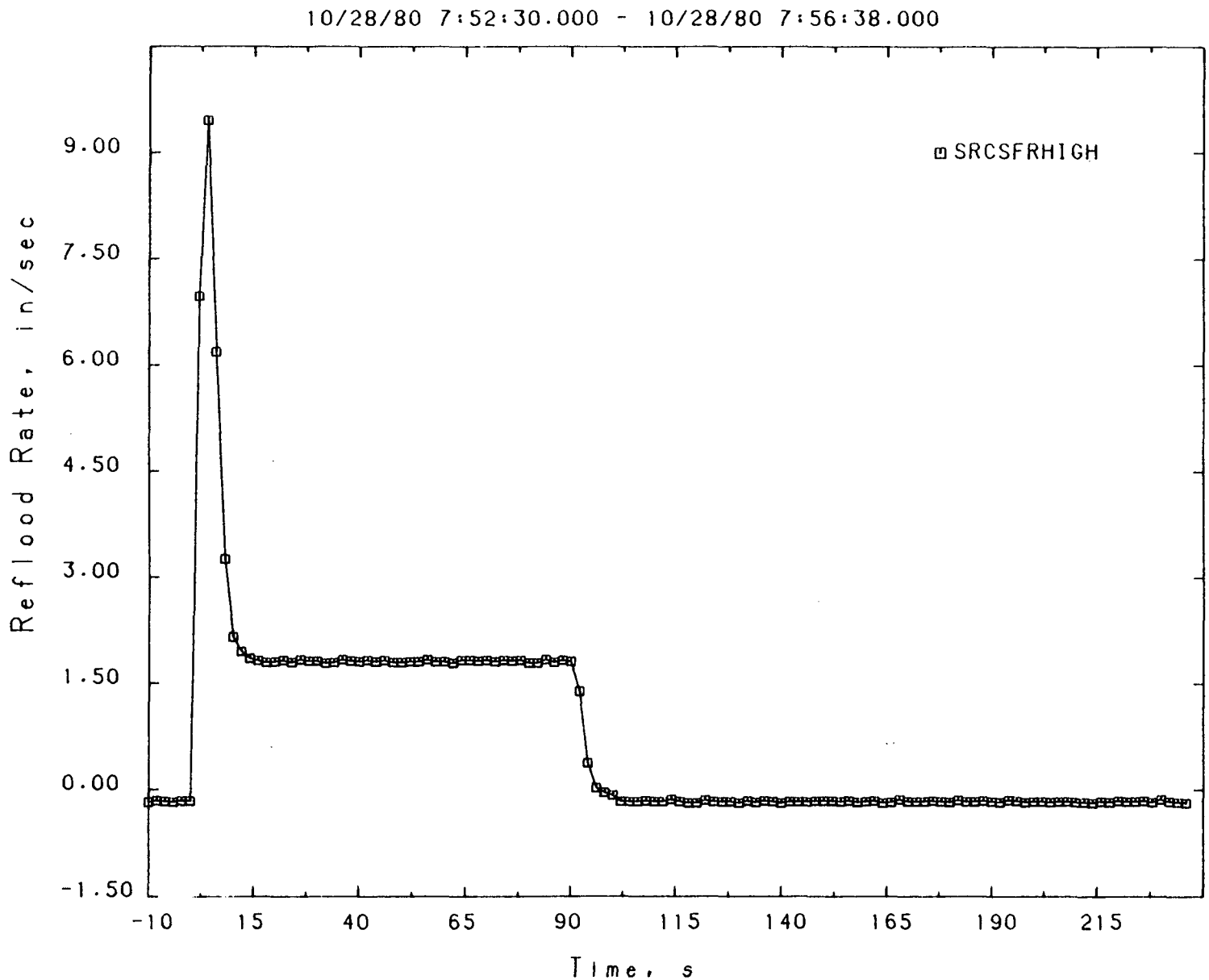

FIGURE 4.1.1 TURBINE FLOW METER - 2 IN/SEC SHROUD LEAK TEST NUMBER 1

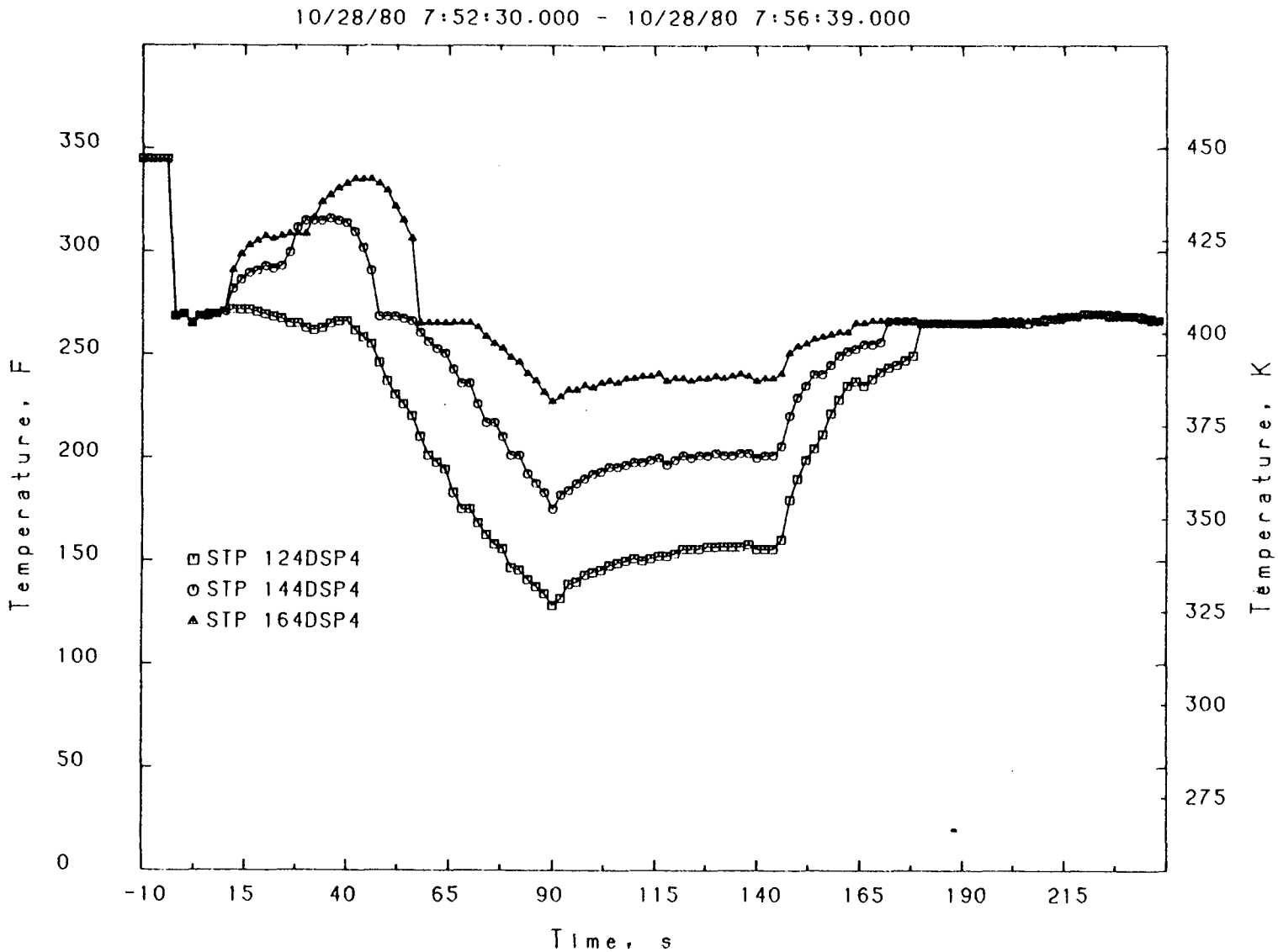

FIGURE 4.1.2 STEAM PROBE TEMPERATURES FROM THE THIMBLE TUBE
2 IN/SEC SHROUD LEAK TEST NUMBER 1

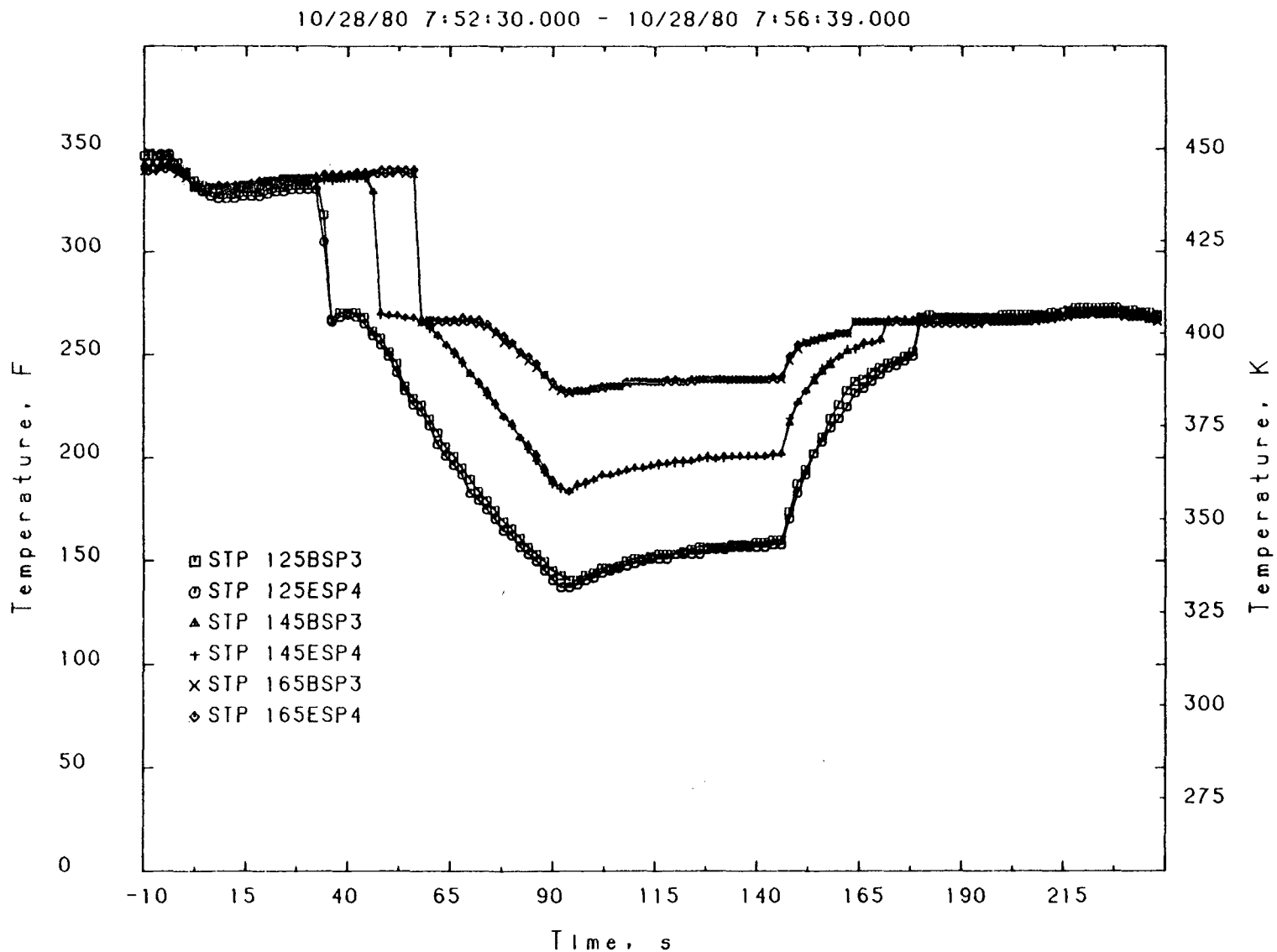

FIGURE 4.1.3 STEAM PROBE TEMPERATURES FROM THE GRID SPACERS - 2 IN/SEC SHROUD LEAK TEST NUMBER 1

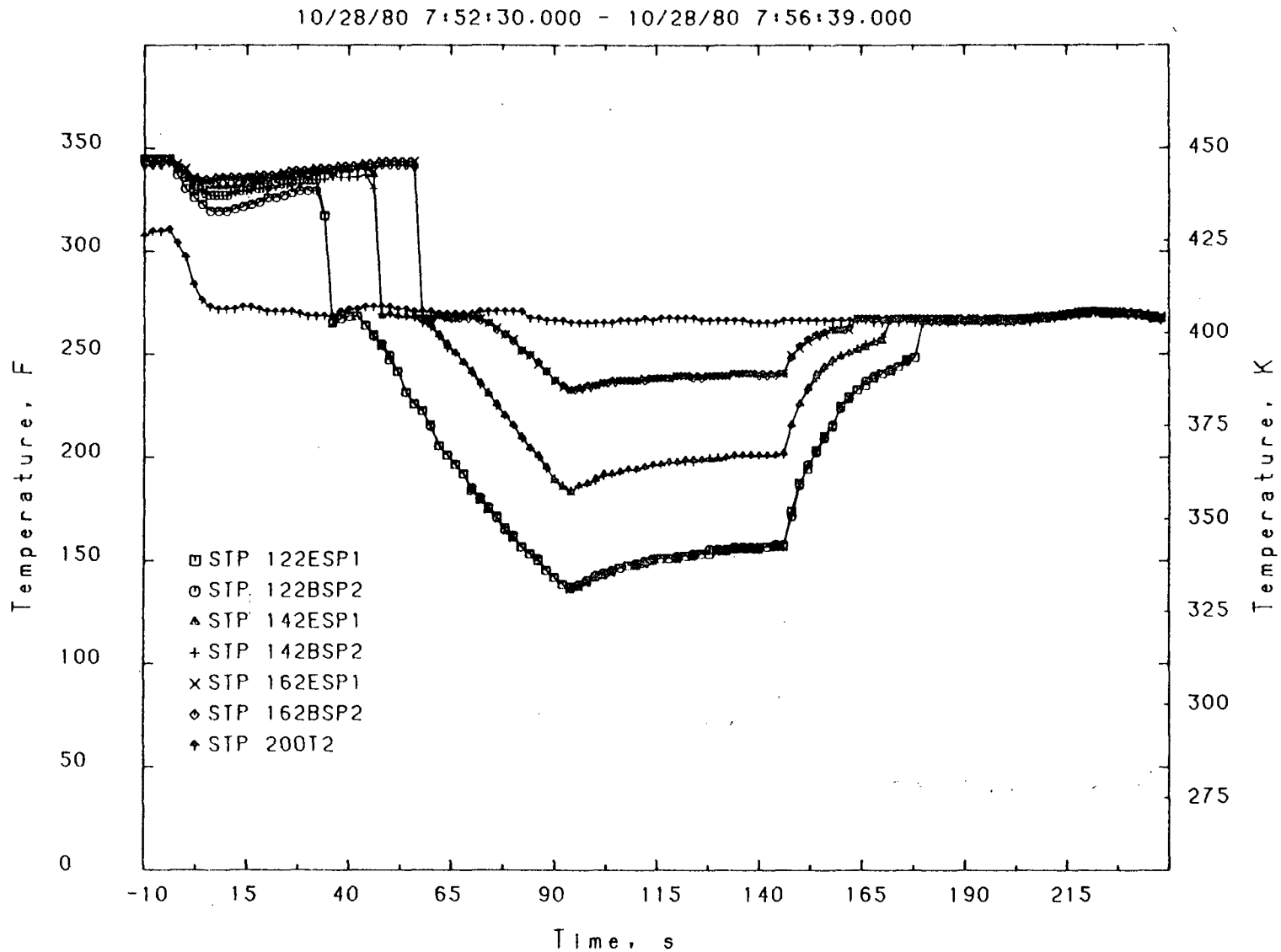

FIGURE 4.1.4 STEAM PROBE TEMPERATURES FROM THE GRID SPACERS - 2 IN/SEC SHROUD LEAK TEST NUMBER 1

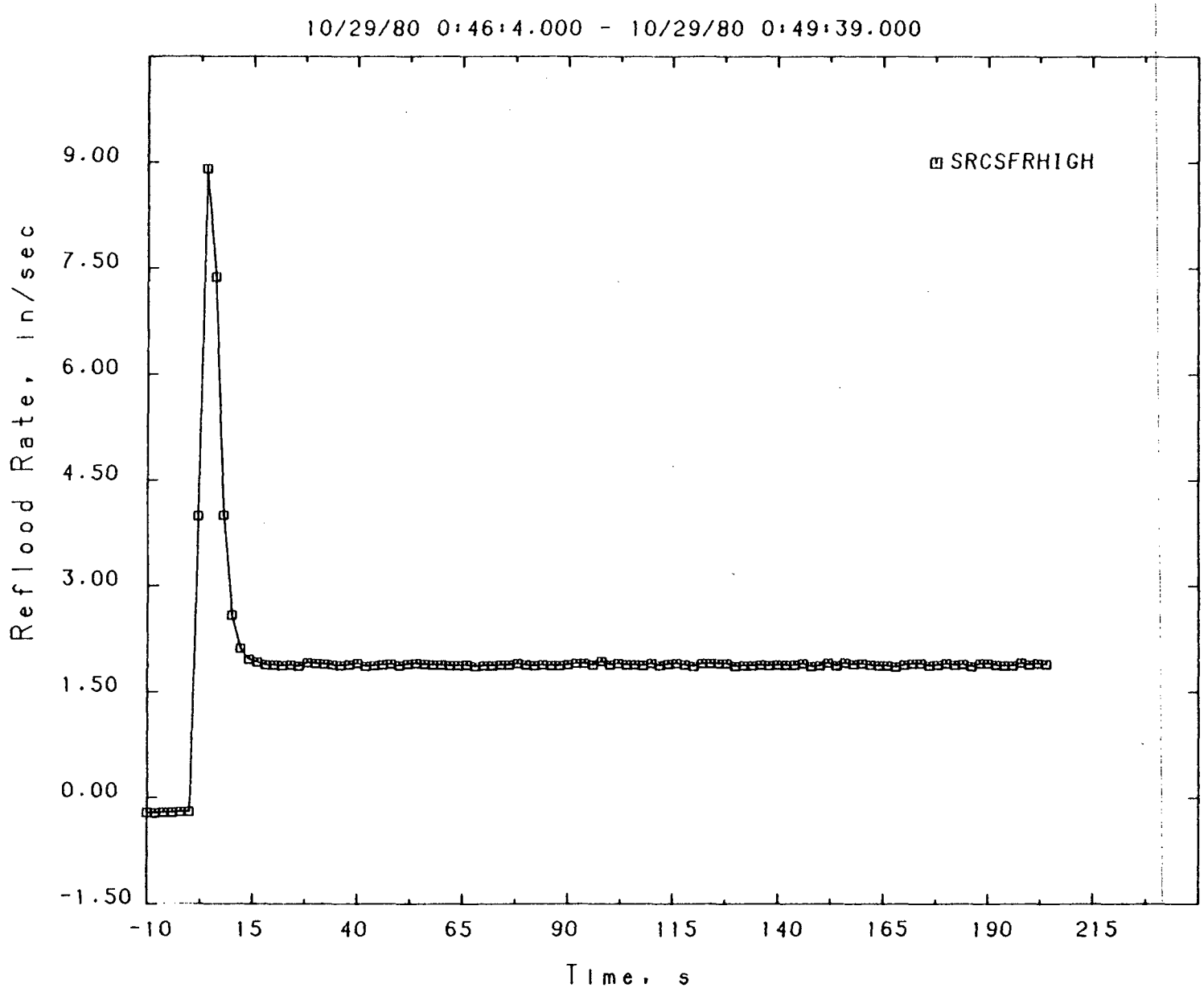

FIGURE 4.2.1 TURBINE FLOW METER - 2 IN/SEC SHROUD LEAK TEST NUMBER 2

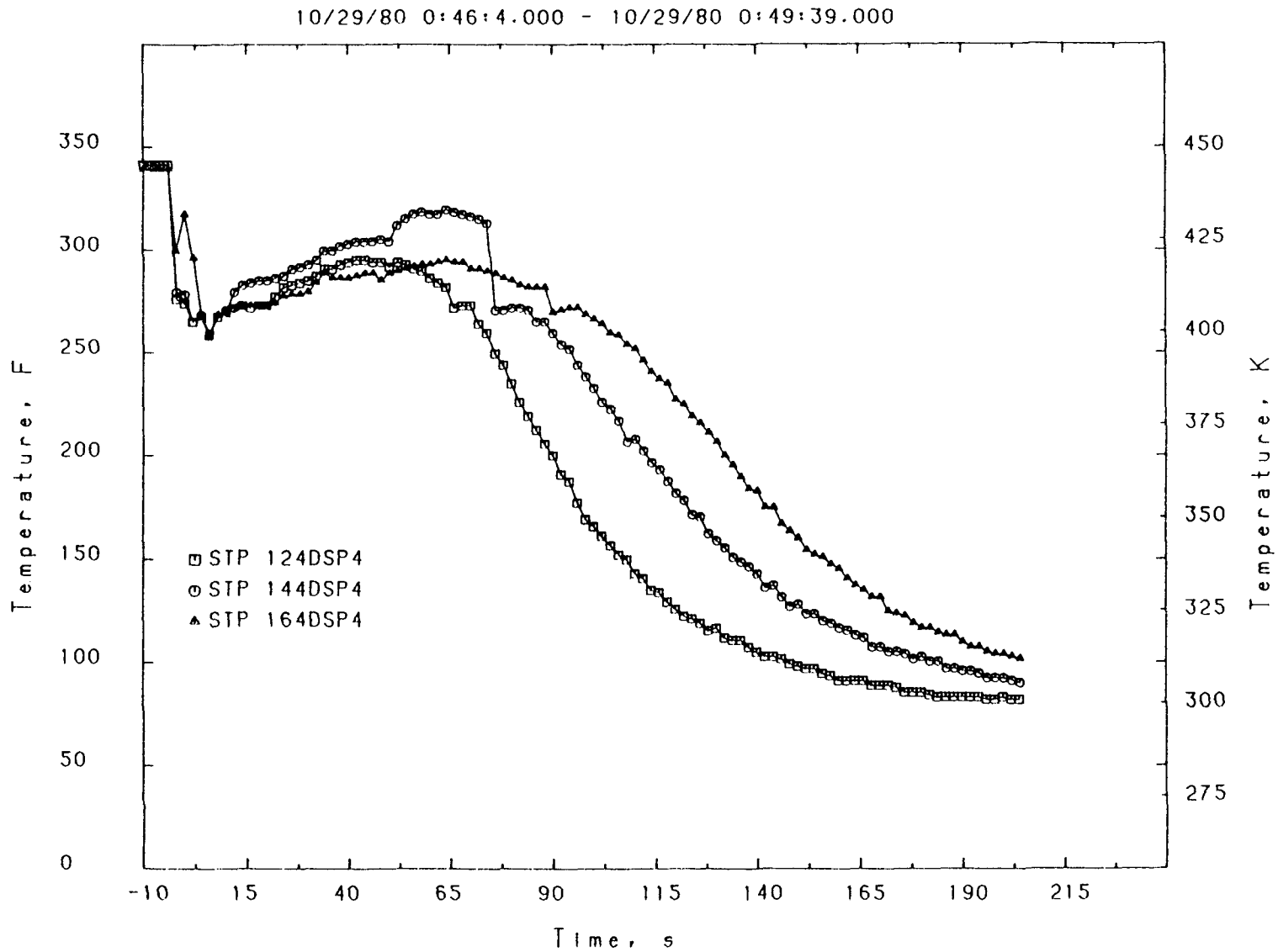

FIGURE 4.2.2 STEAM PROBE TEMPERATURES FROM THE THIMBLE TUBE - 2 IN/SEC SHROUD LEAK TEST NUMBER 2

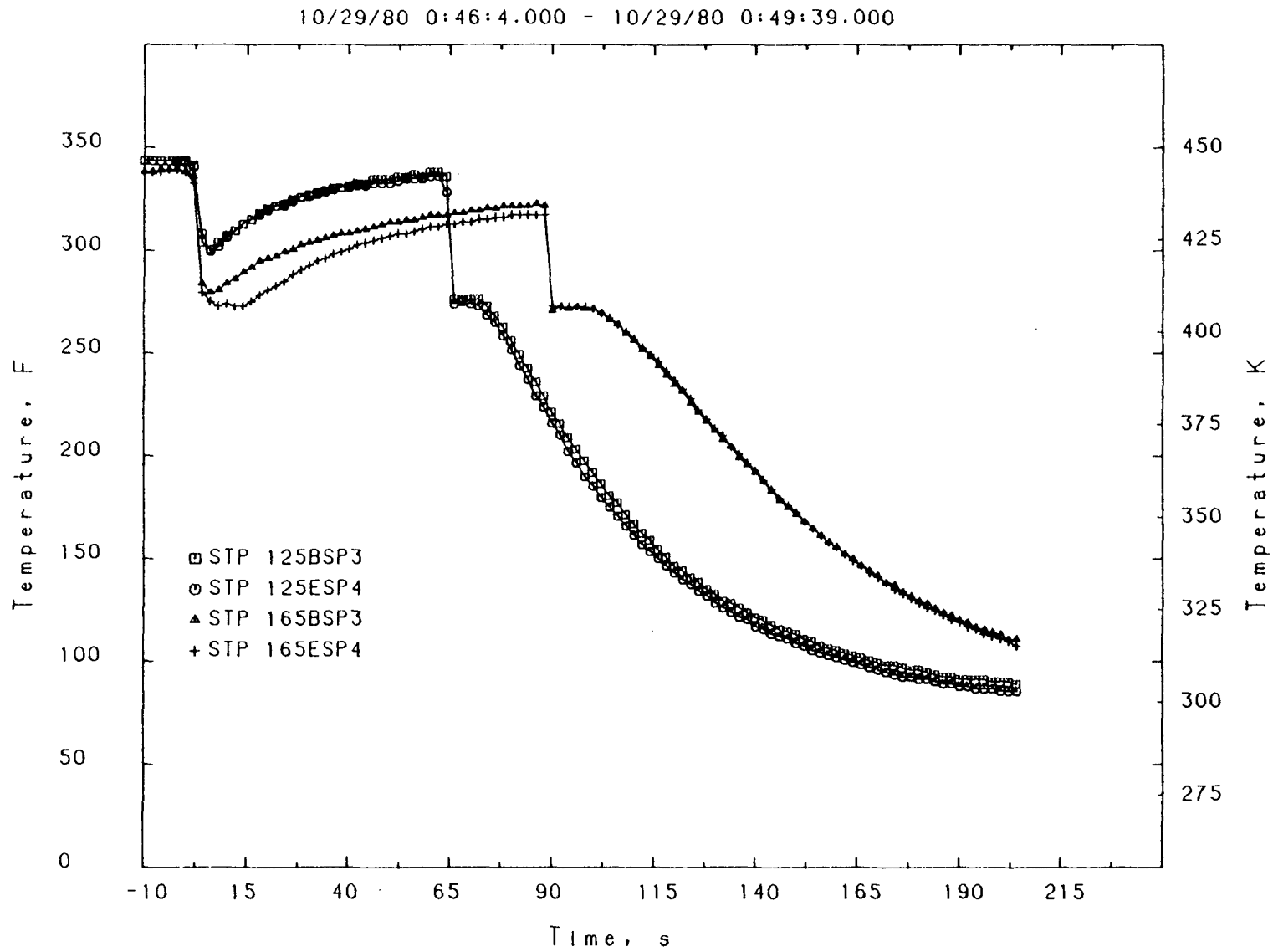

FIGURE 4.2.3 STEAM PROBE TEMPERATURES FROM THE GRID SPACERS - 2 IN/SEC SHROUD LEAK TEST NUMBER 2

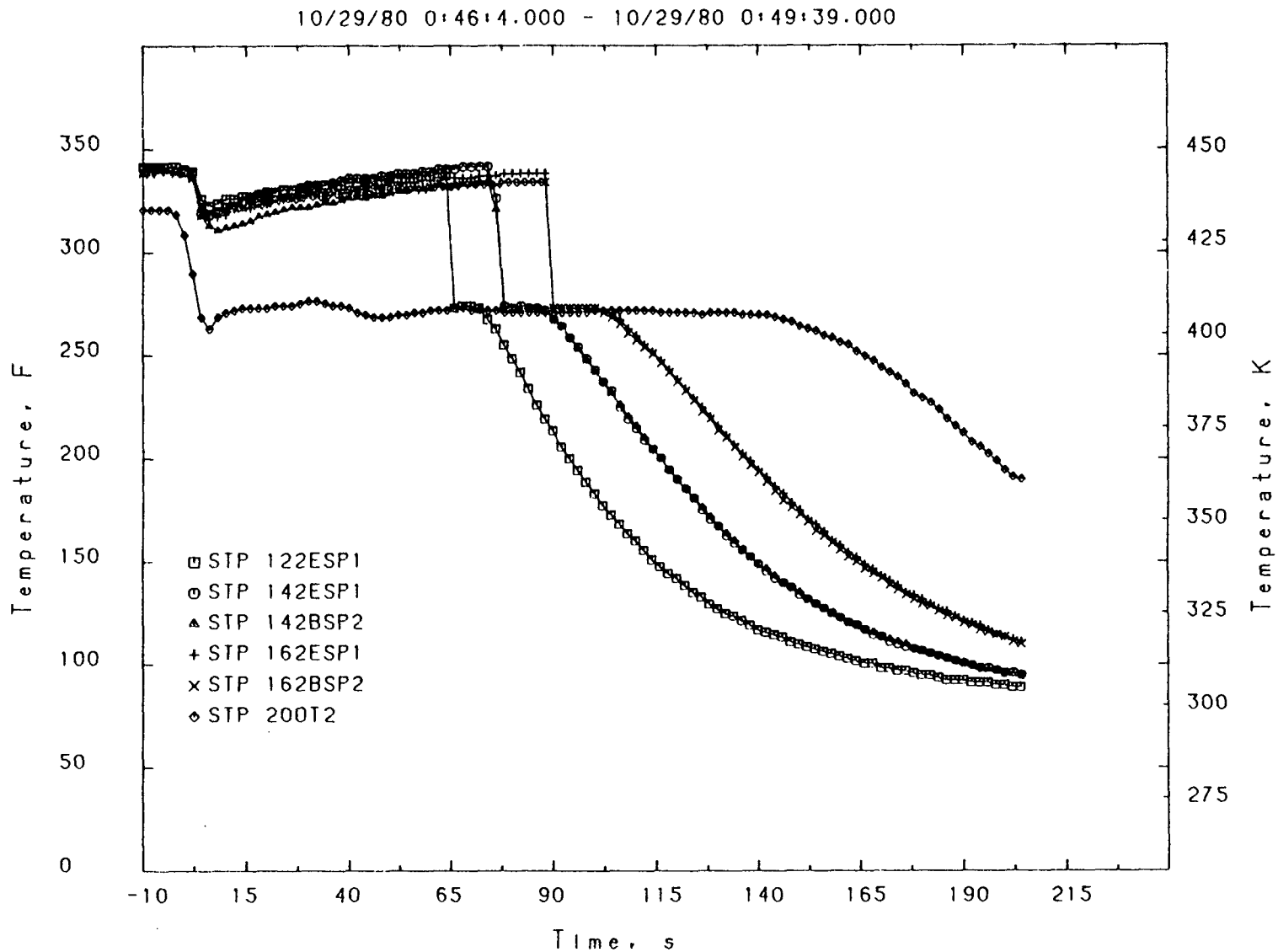

FIGURE 4.2.4 STEAM PROBE TEMPERATURES FROM THE GRID SPACERS - 2 IN/SEC SHROUD LEAK TEST NUMBER 2

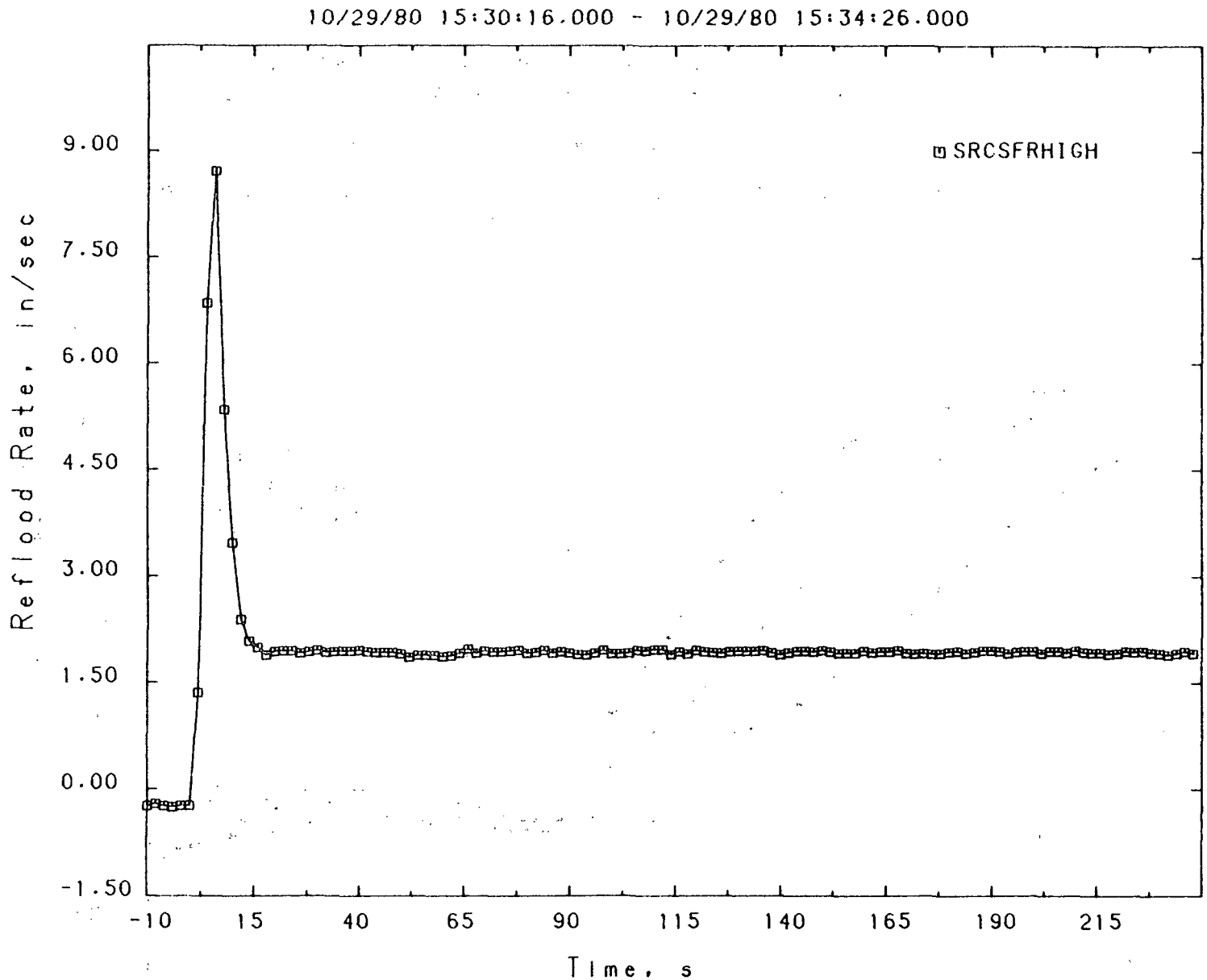

FIGURE 4.3.1 TURBINE FLOW METER - 2 IN/SEC SHROUD LEAK TEST NUMBER 3

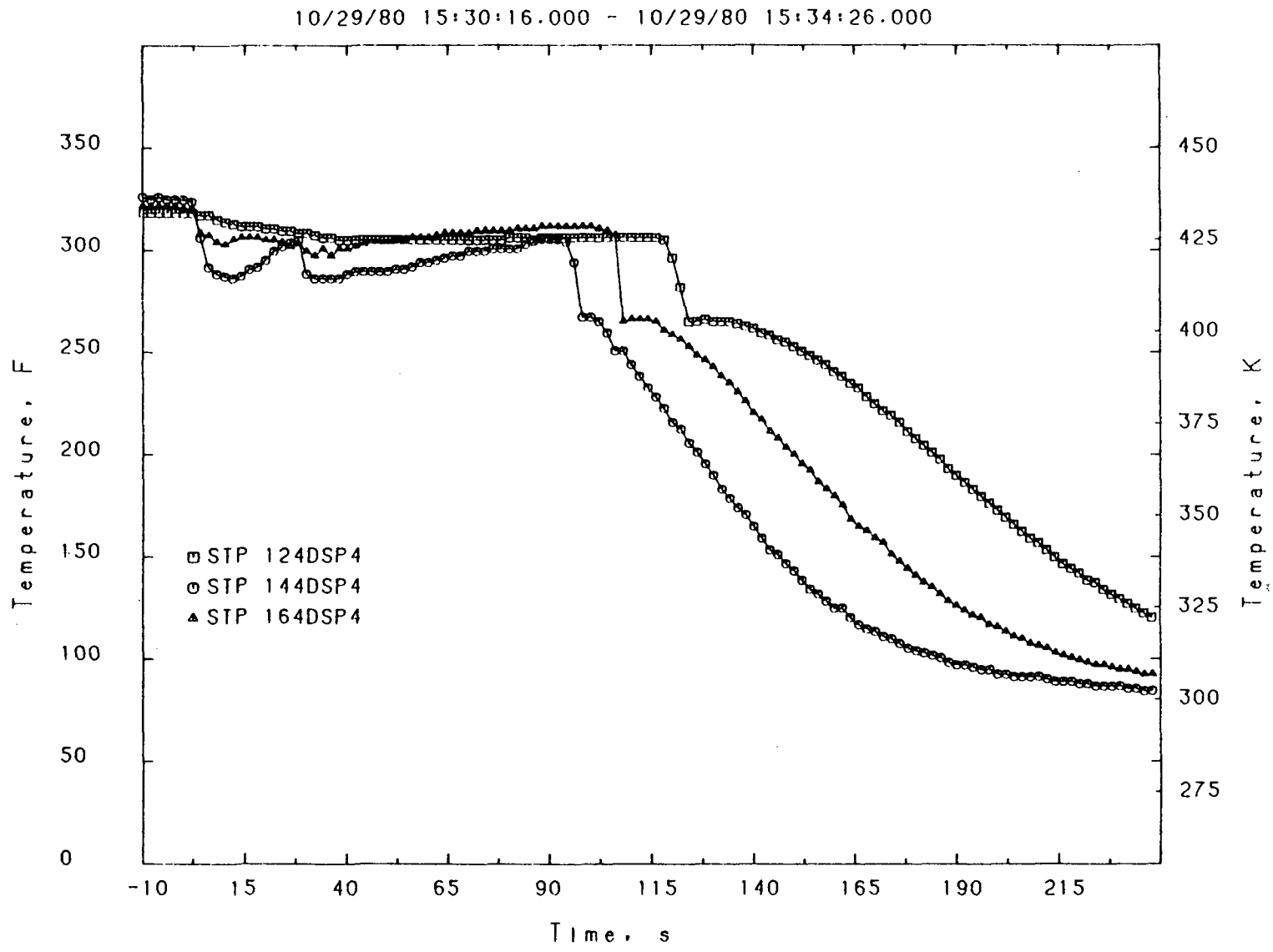

FIGURE 4.3.2 STEAM PROBE TEMPERATURES IN THE THIMBLE TUBE - 2 IN/SEC SHROUD LEAK TEST NUMBER 3

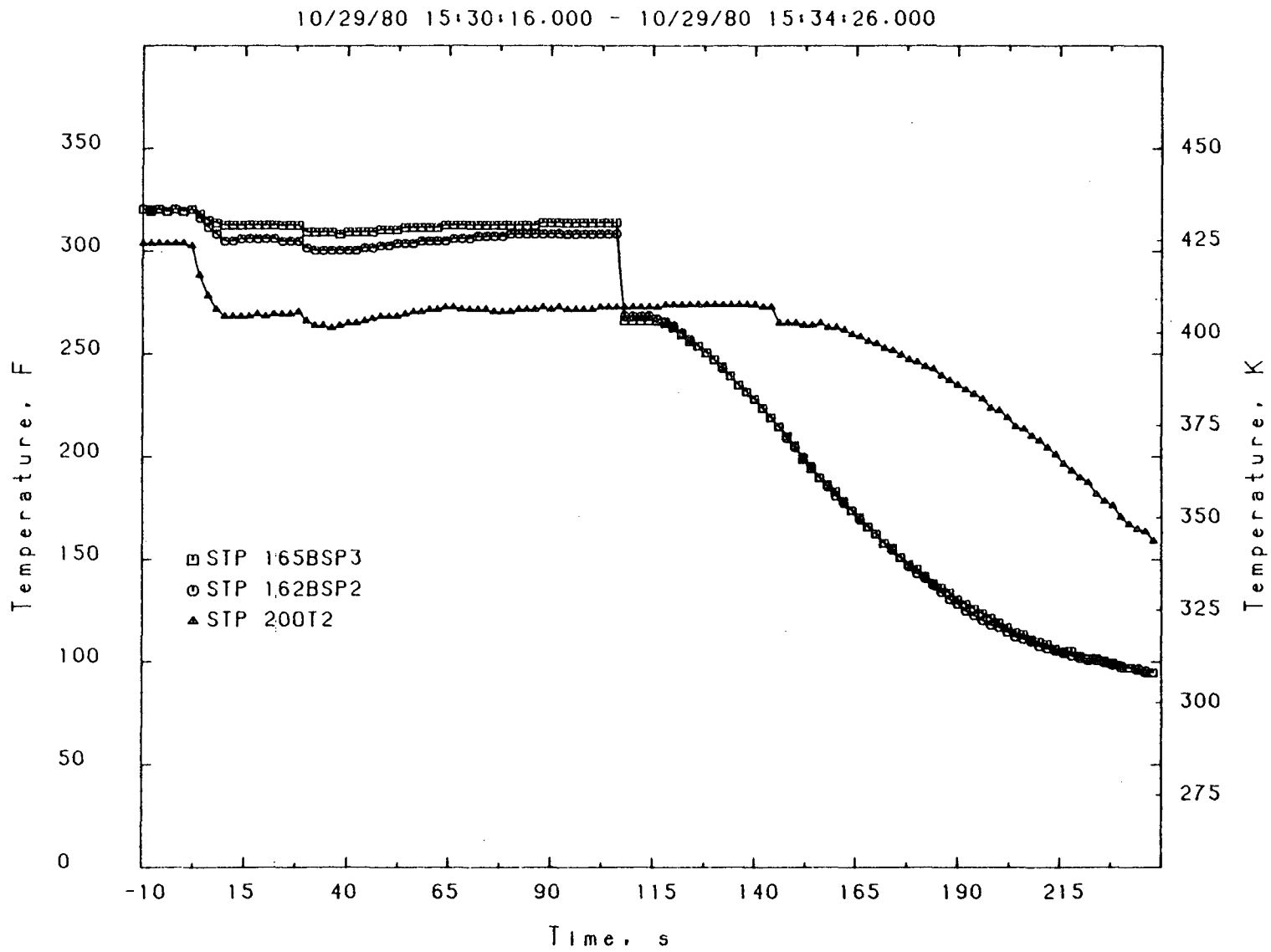

FIGURE 4.3.3 STEAM PROBE TEMPERATURES FROM THE GRID SPACERS
2 IN/SEC SHROUD LEAK TEST NUMBER 3

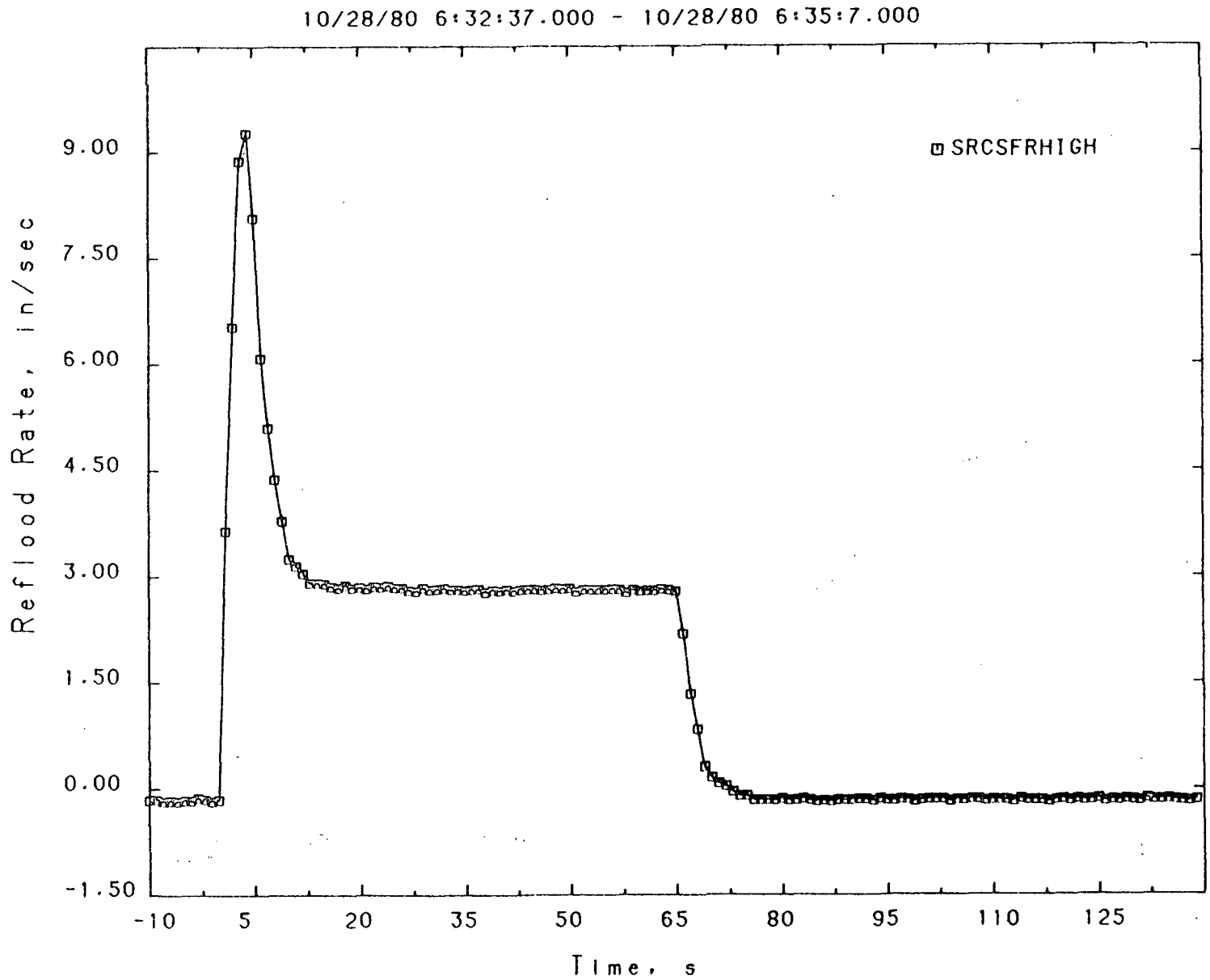

FIGURE 4.4.1 TURBINE FLOW METER - 3 IN/SEC SHROUD LEAK TEST NUMBER 1

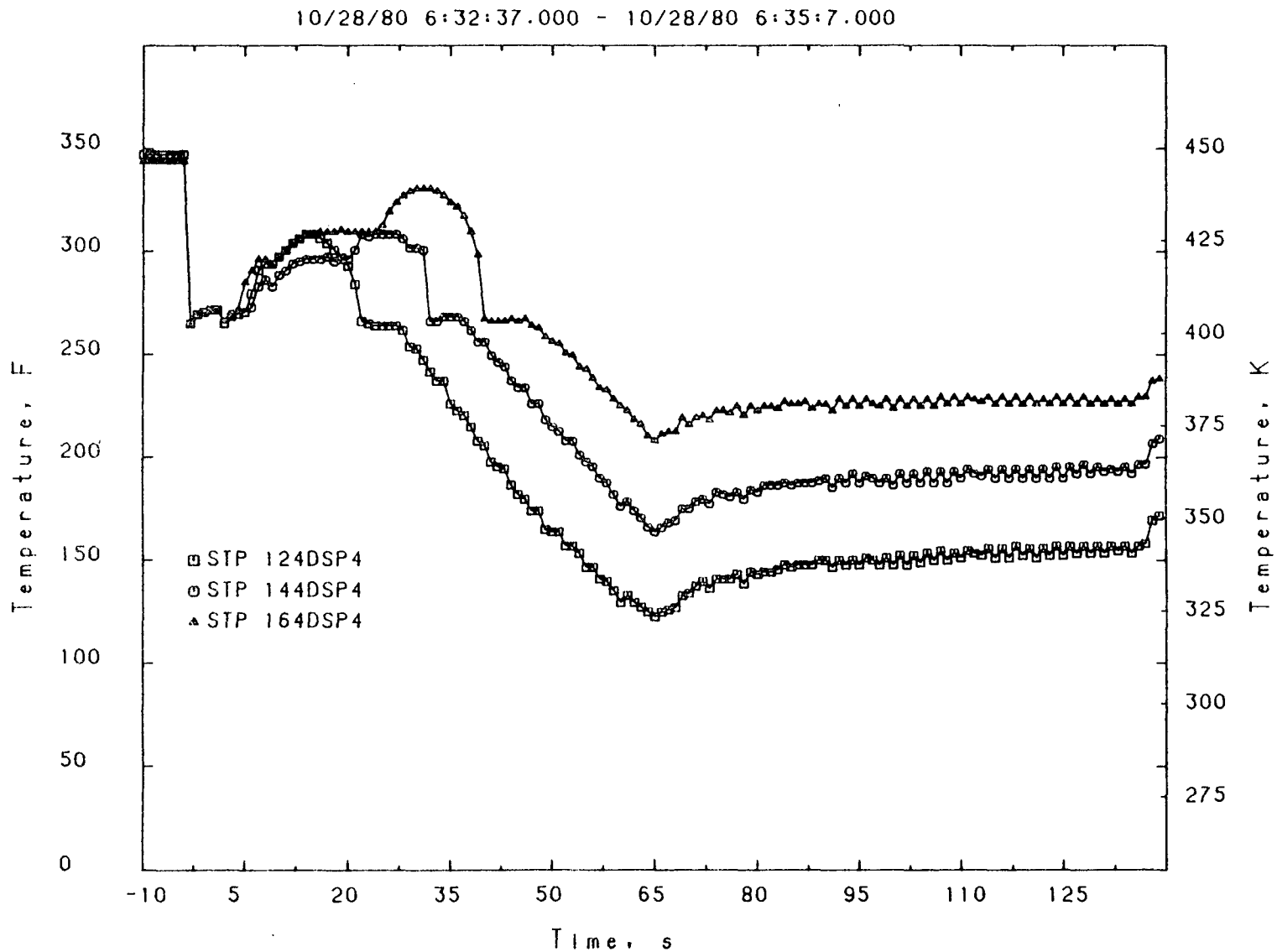

FIGURE 4.4.2 STEAM PROBE TEMPERATURES FROM THE THIMBLE TUBE - 3 IN/SEC SHROUD LEAK TEST NUMBER 1

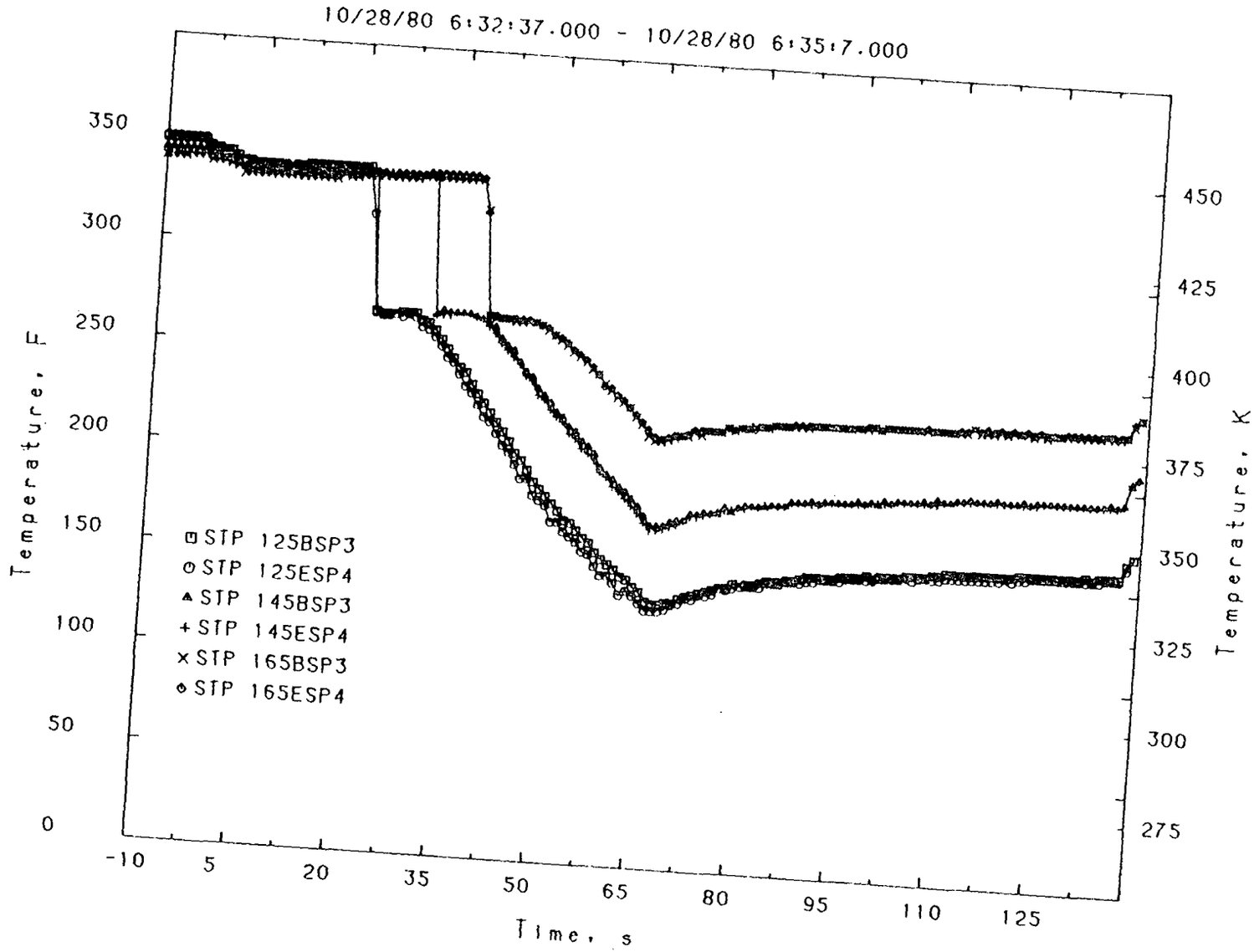

FIGURE 4.4.3 STEAM PROBE TEMPERATURES FROM THE GRID SPACERS - 3 IN/SEC SHROUD LEAK TEST NUMBER 1

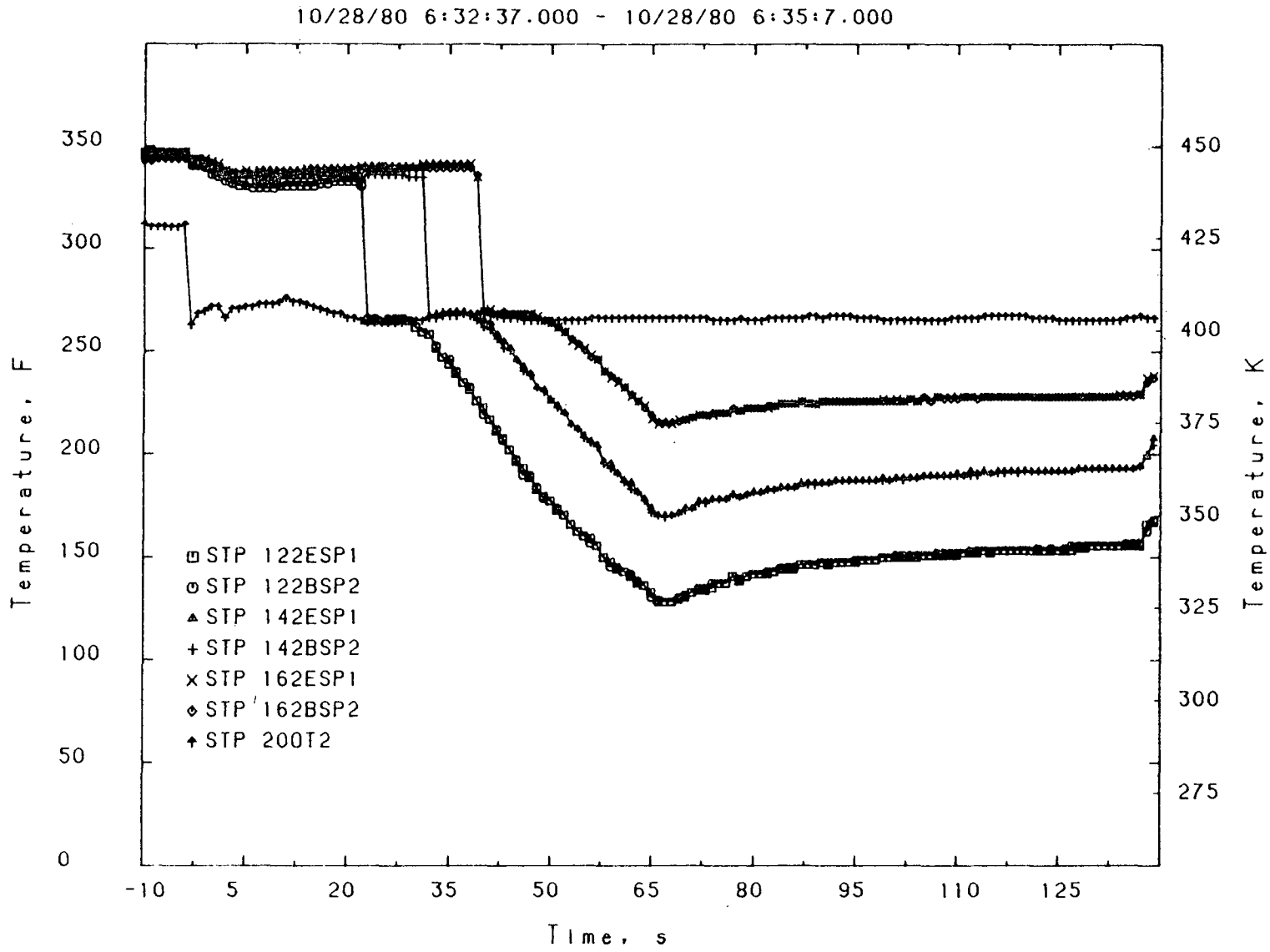

FIGURE 4.4.4 STEAM PROBE TEMPERATURES FROM THE GRID SPACERS - 3 IN/SEC SHROUD LEAK TEST NUMBER 1

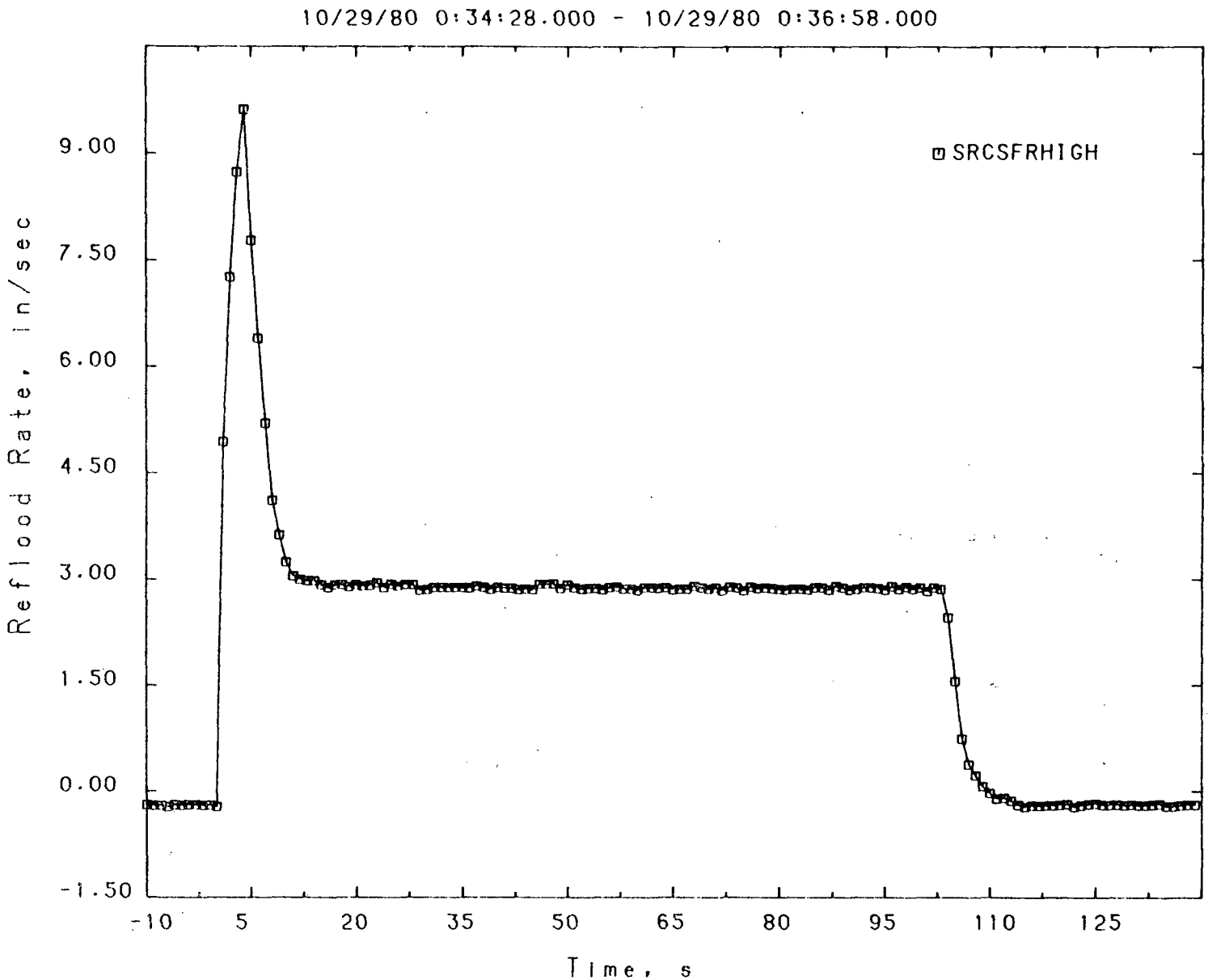

FIGURE 4.5.1 TURBINE FLOW METER - 3 IN/SEC SHROUD LEAK TEST NUMBER 2

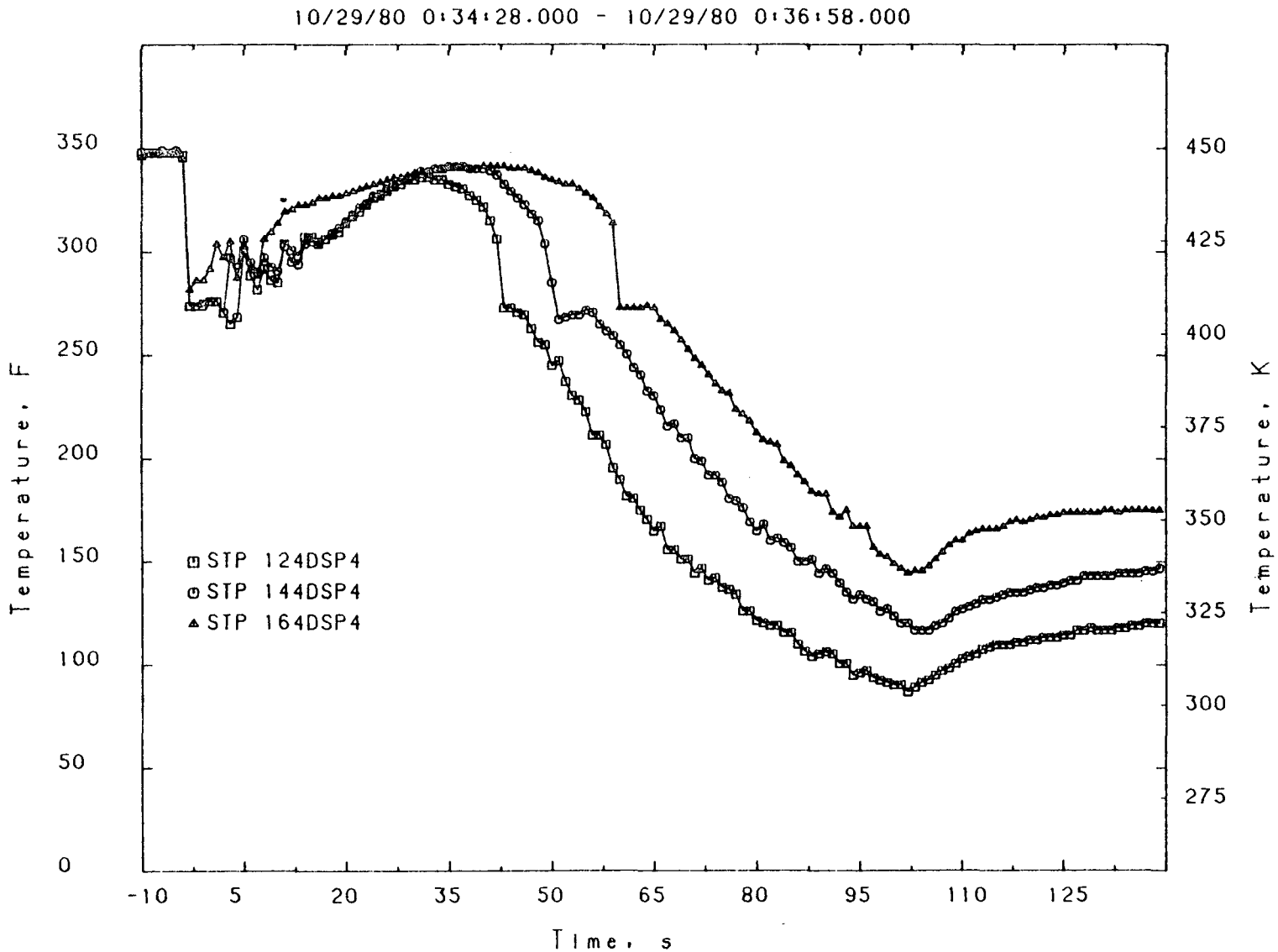

FIGURE 4.5.2 STEAM PROBE TEMPERATURES FROM THE THIMBLE TUBE - 3 IN/SEC SHROUD LEAK TEST NUMBER 2

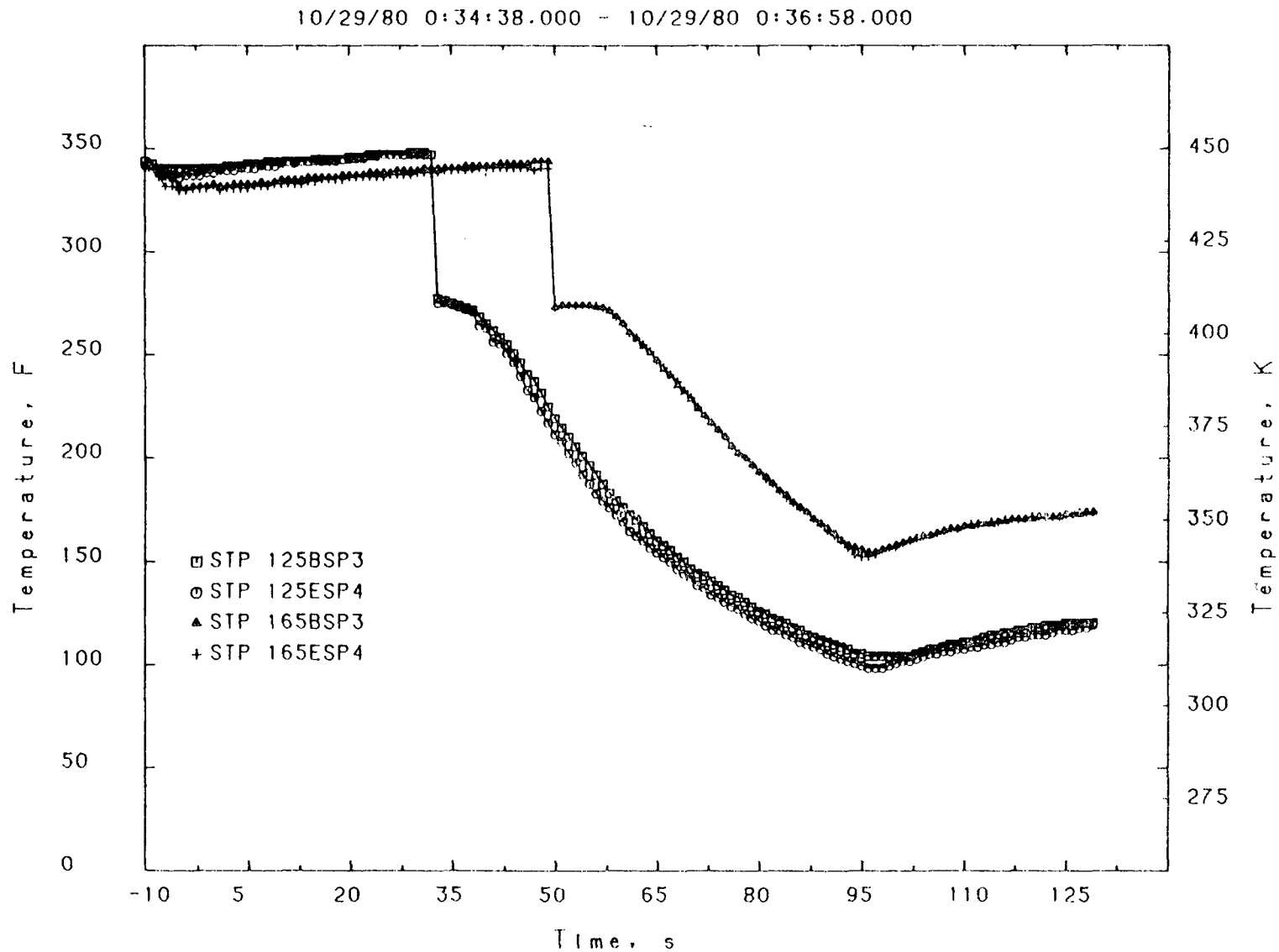

FIGURE 4.5.3 STEAM PROBE TEMPERATURES FROM THE GRID SPACERS - 3 IN/SEC SHROUD LEAK TEST NUMBER 2

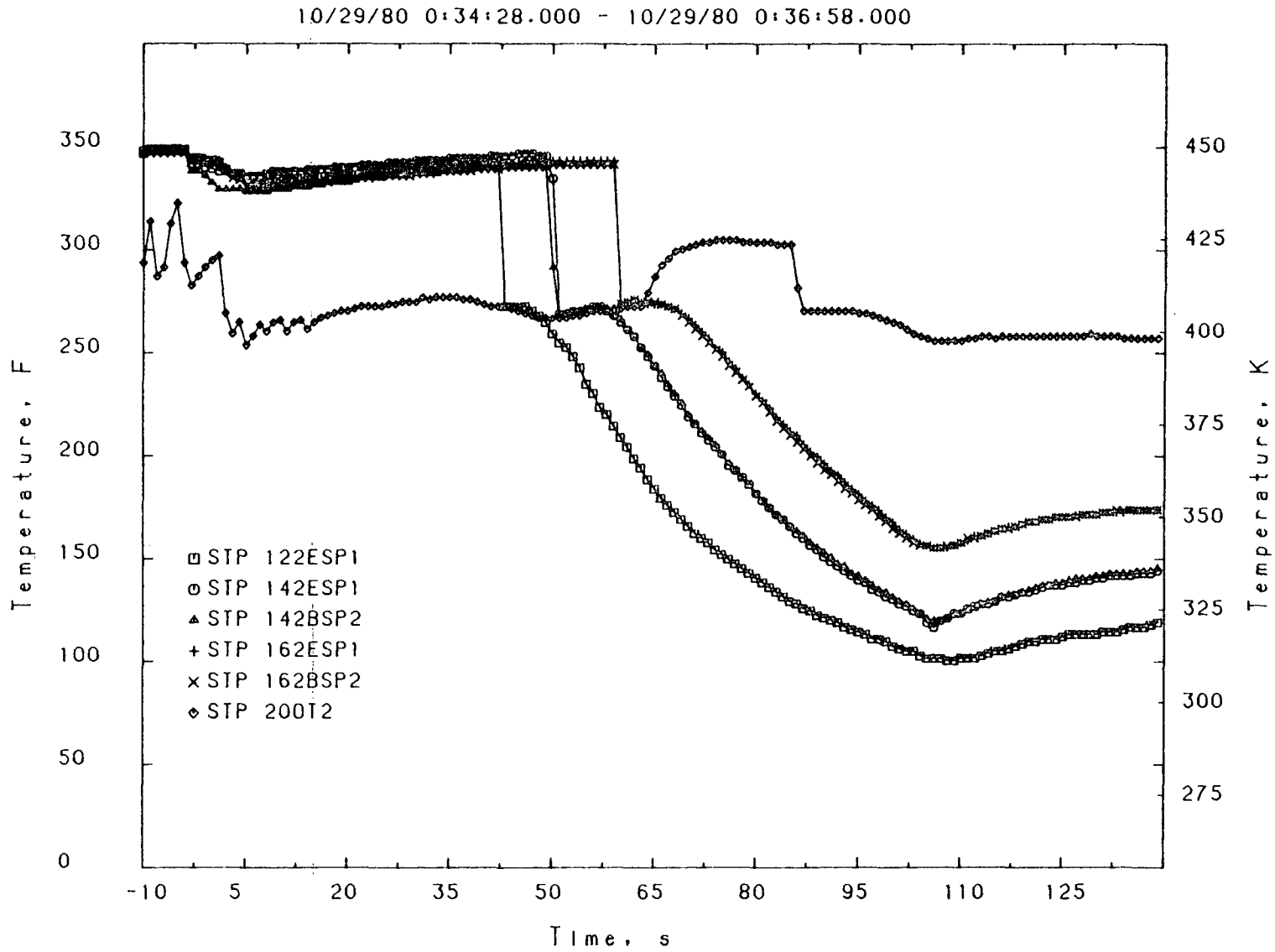

FIGURE 4.5.4 STEAM PROBE TEMPERATURES FROM THE GRID SPACERS - 3 IN/SEC LEAK RATE TEST NUMBER 2

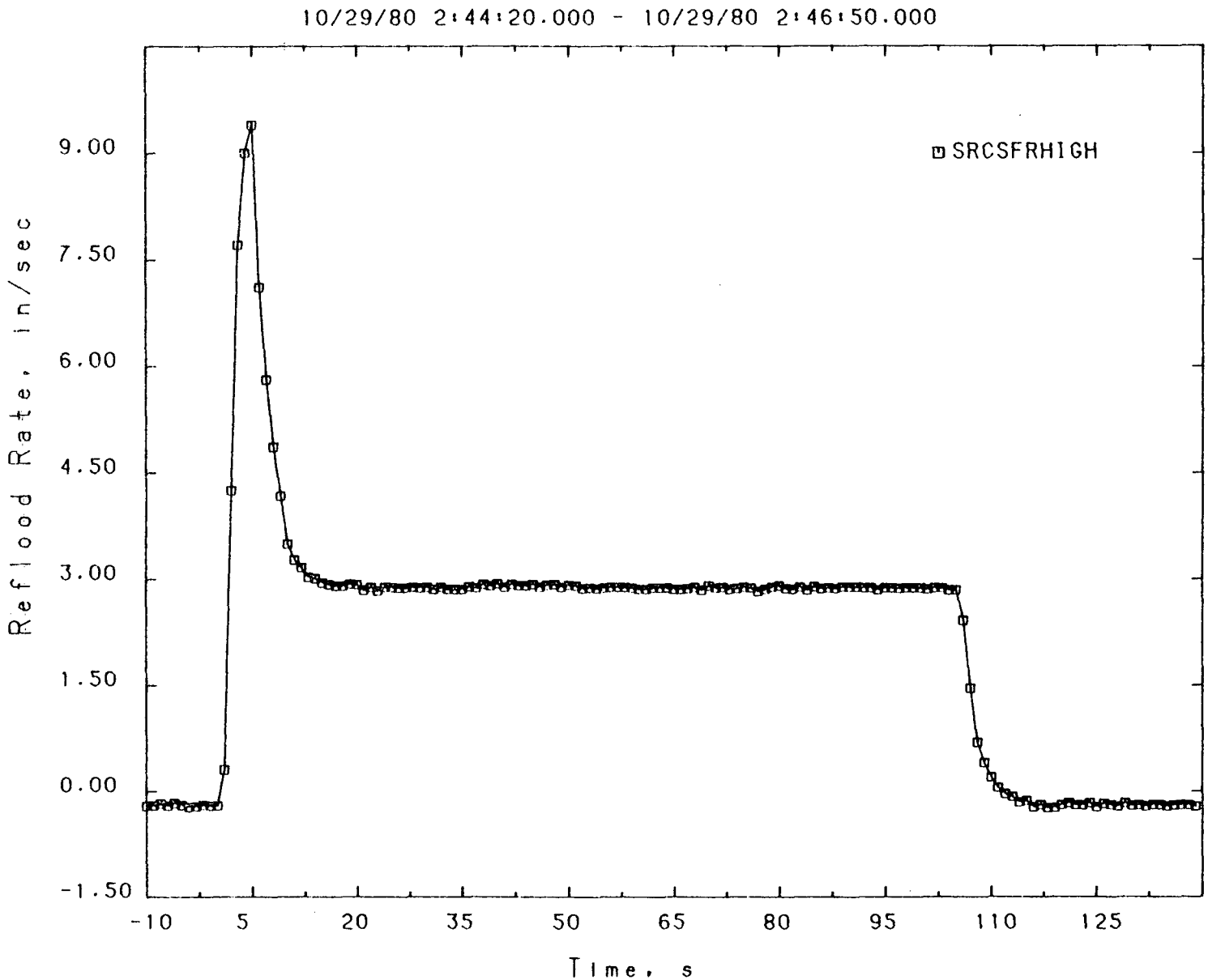

FIGURE 4.6.1 TURBINE FLOW METER - 3 IN/SEC SHROUD LEAK TEST NUMBER 3

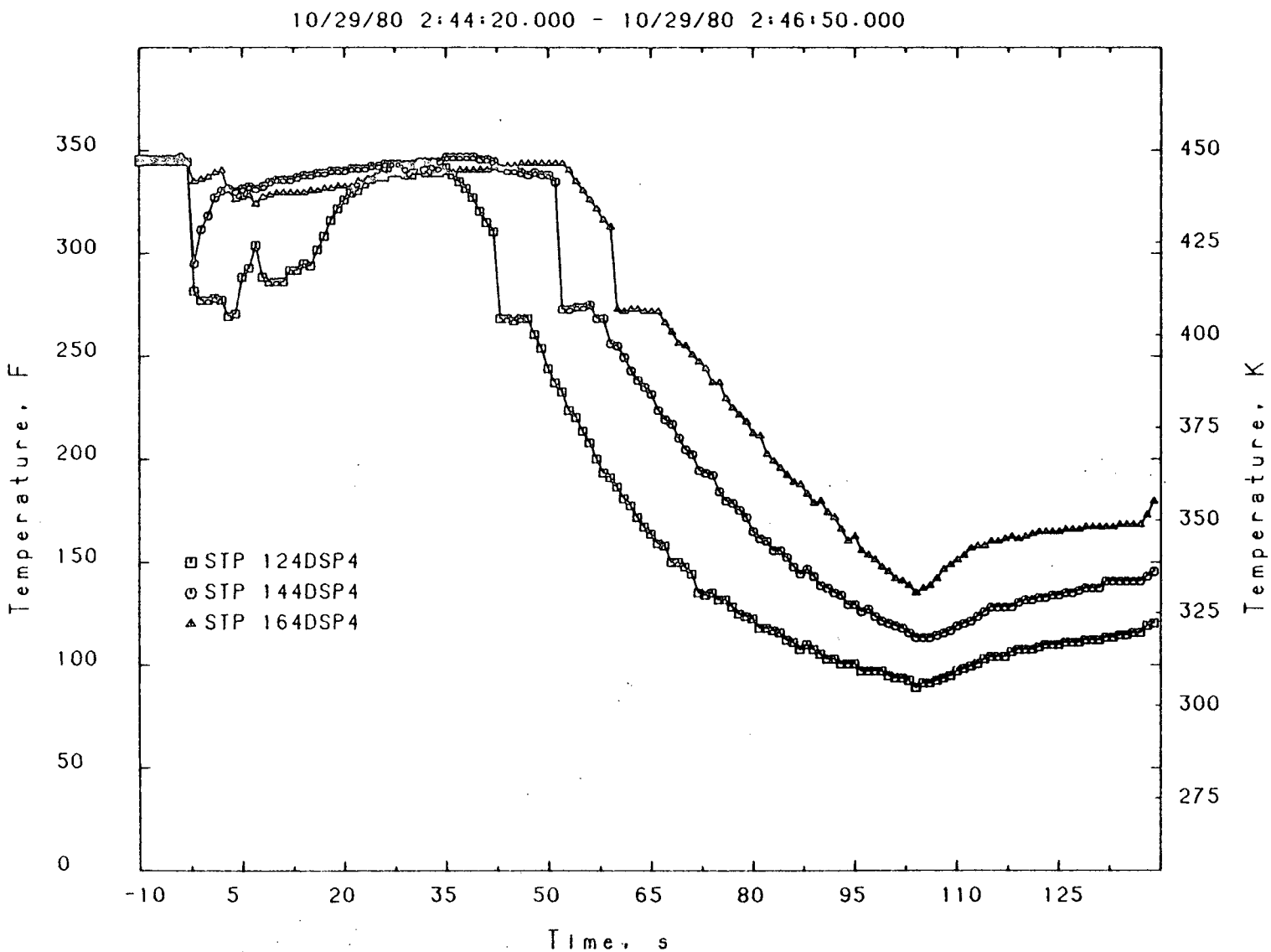

FIGURE 4.6.2 STEAM PROBE TEMPERATURES FROM THE THIMBLE TUBE - 3 IN/SEC SHROUD LEAK TEST NUMBER 3

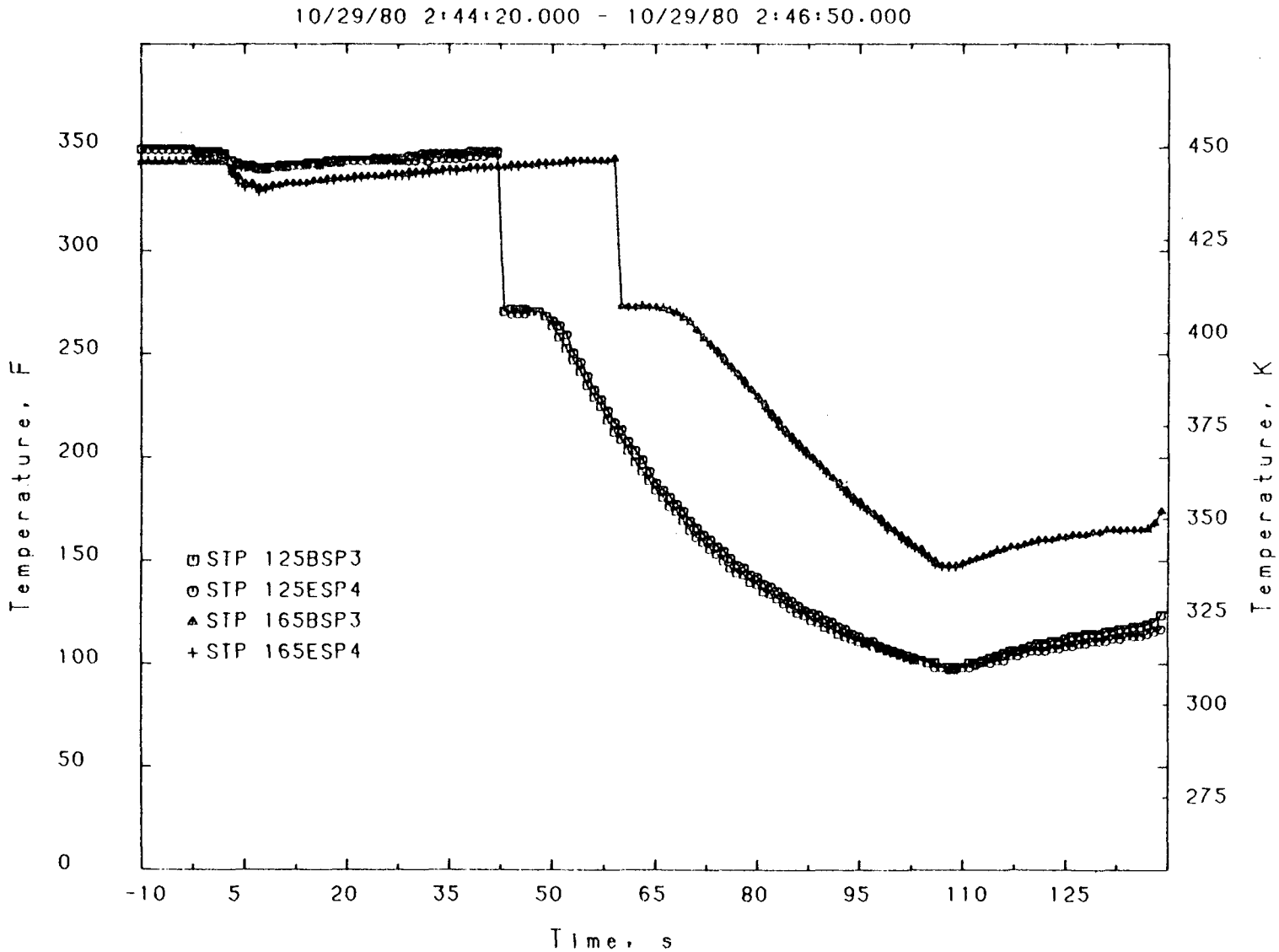

FIGURE 4.6.3 STEAM PROBE TEMPERATURES FROM THE GRID SPACERS - 3 IN/SEC SHROUD LEAK TEST NUMBER 3

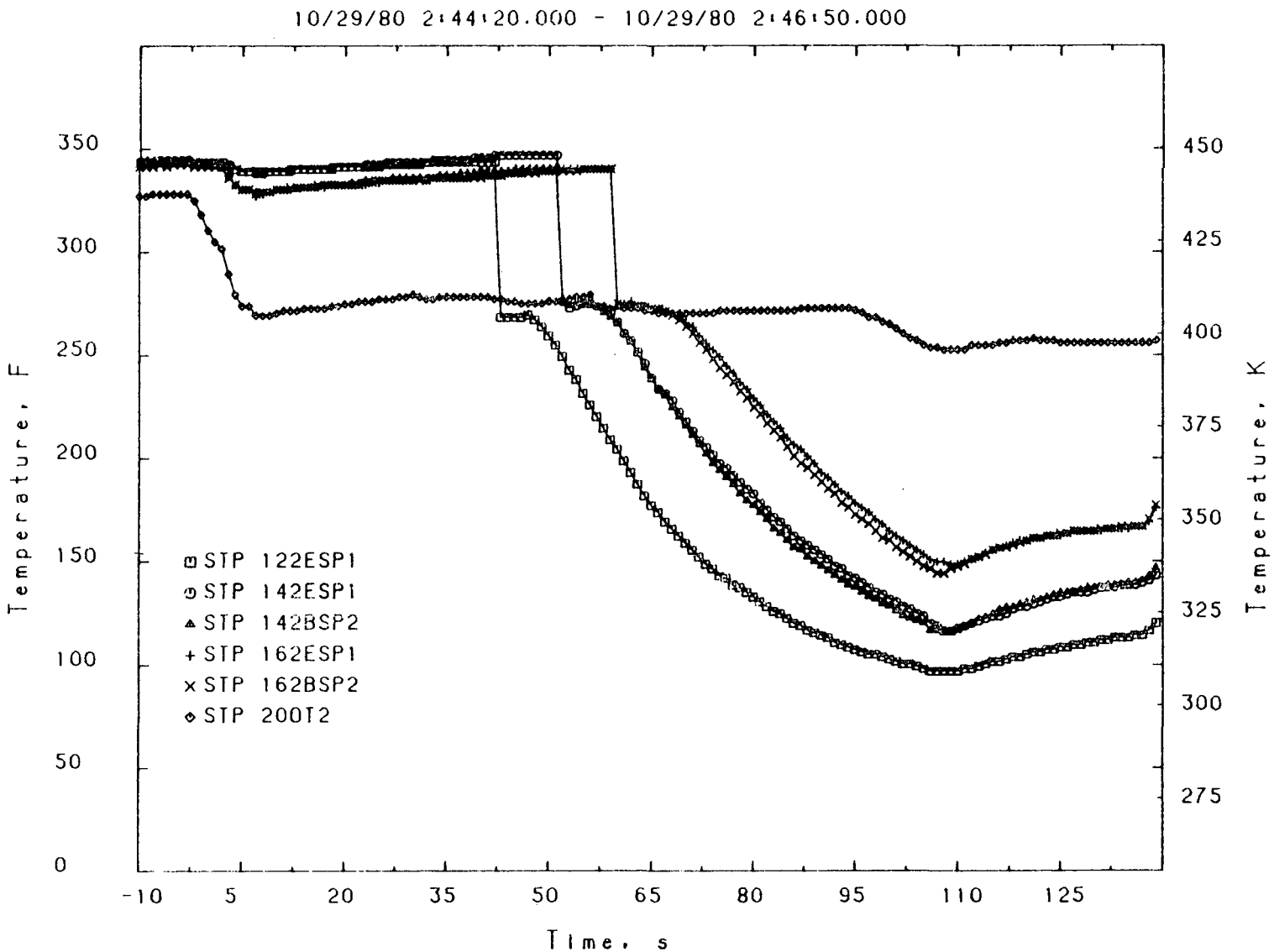

FIGURE 4.6.4 STEAM PROBE TEMPERTURES FROM THE GRID SPACERS - 3 IN/SEC SHROUD LEAK TEST NUMBER 3

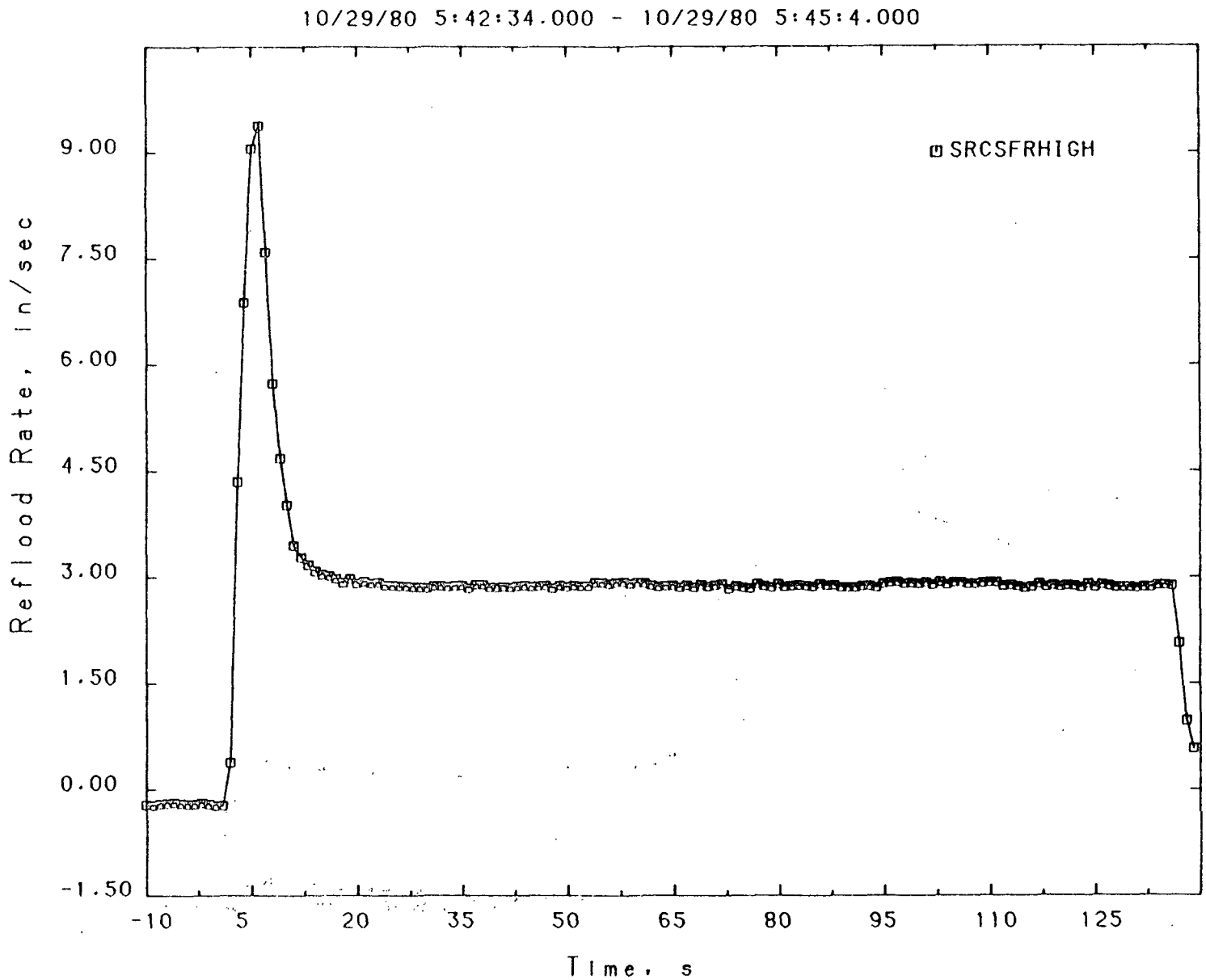

FIGURE 4.7.1 TURBINE FLOW METER - 3 IN/SEC SHROUD LEAK TEST NUMBER 4

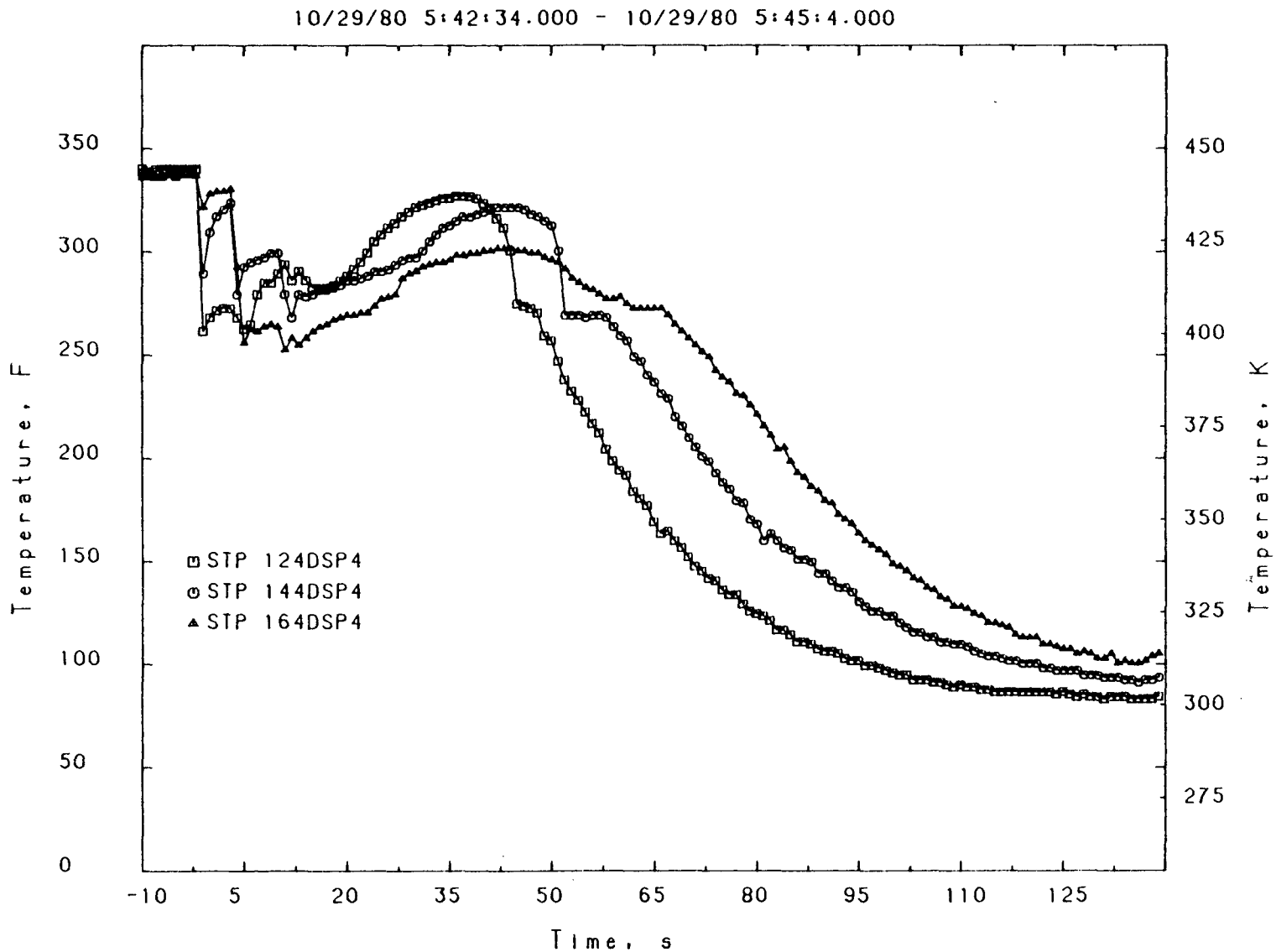

FIGURE 4.7.2 STEAM PROBE TEMPERATURES FROM THE THIMBLE TUBE - 3 IN/SEC SHROUD LEAK TEST NUMBER 4

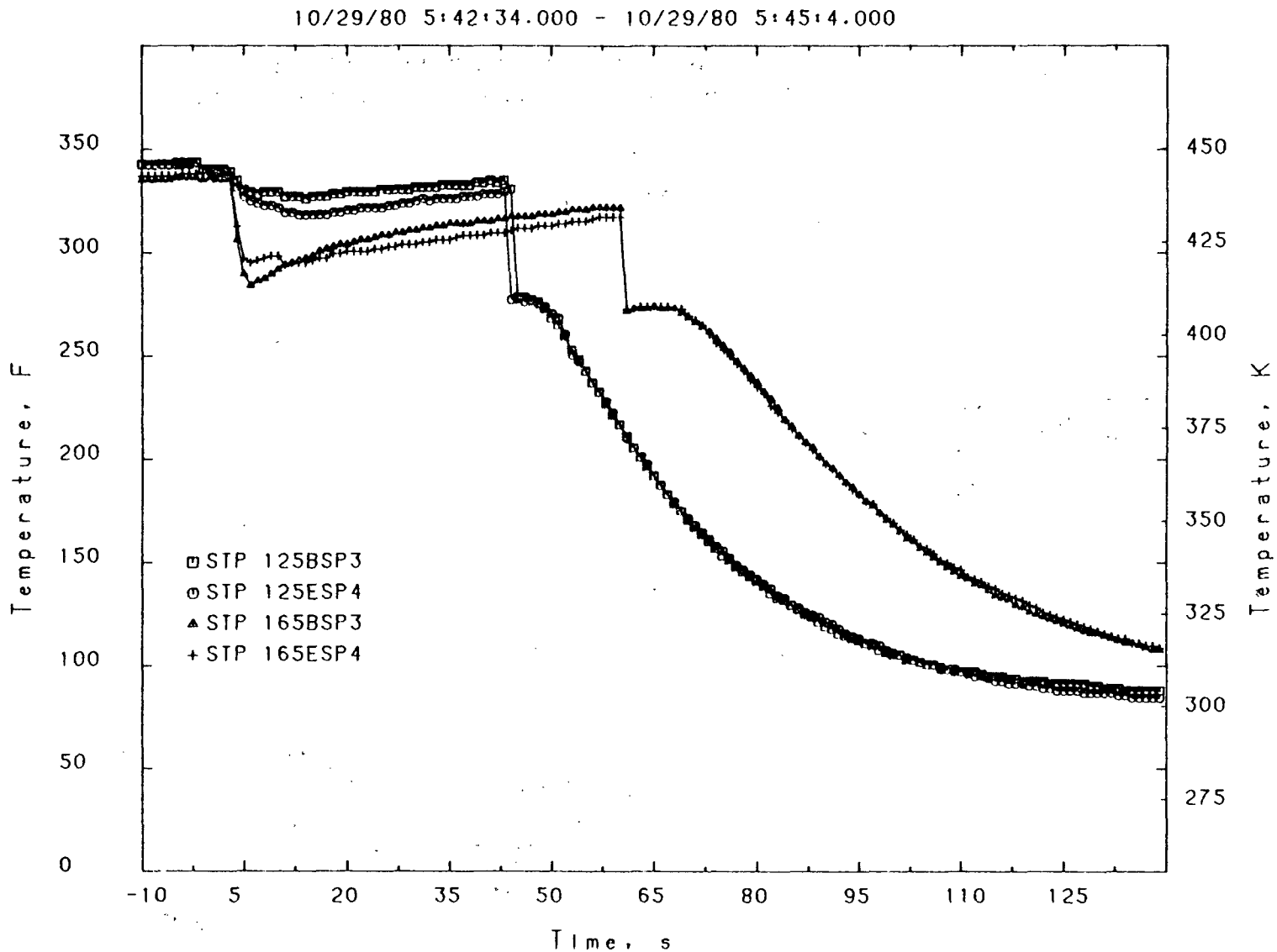

FIGURE 4.7.3 STEAM PROBE TEMPERATURES FROM THE GRID SPACERS - 3 IN/SEC SHROUD LEAK TEST NUMBER 4

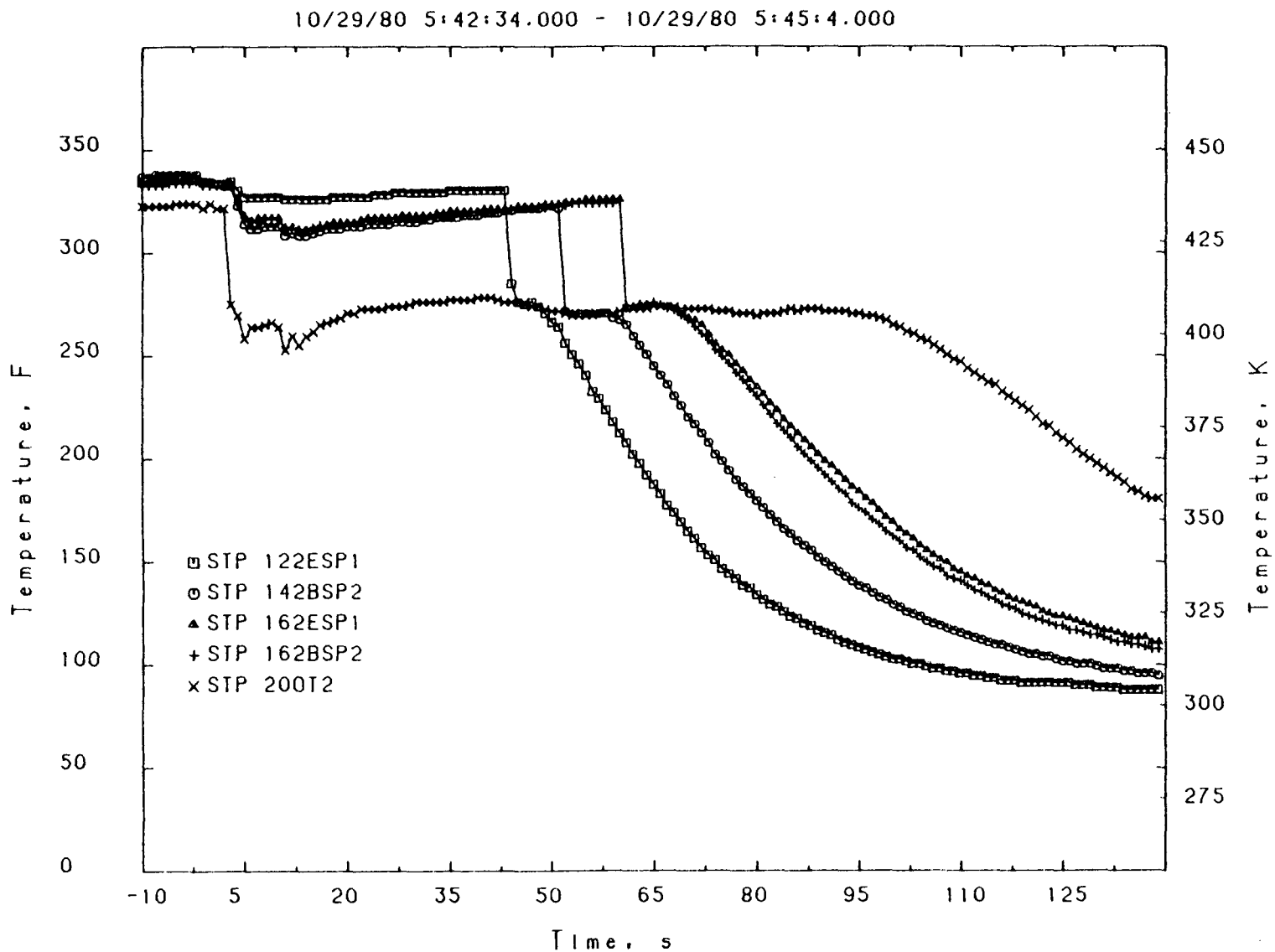

FIGURE 4.7.4 STEAM PROBE TEMPERATURES FROM THE GRID SPACERS - 3 IN/SEC SHROUD LEAK TEST NUMBER 4

PART 5

FLOWMETER RATES FOR THE FLECHT COMPARISON TEST SERIES

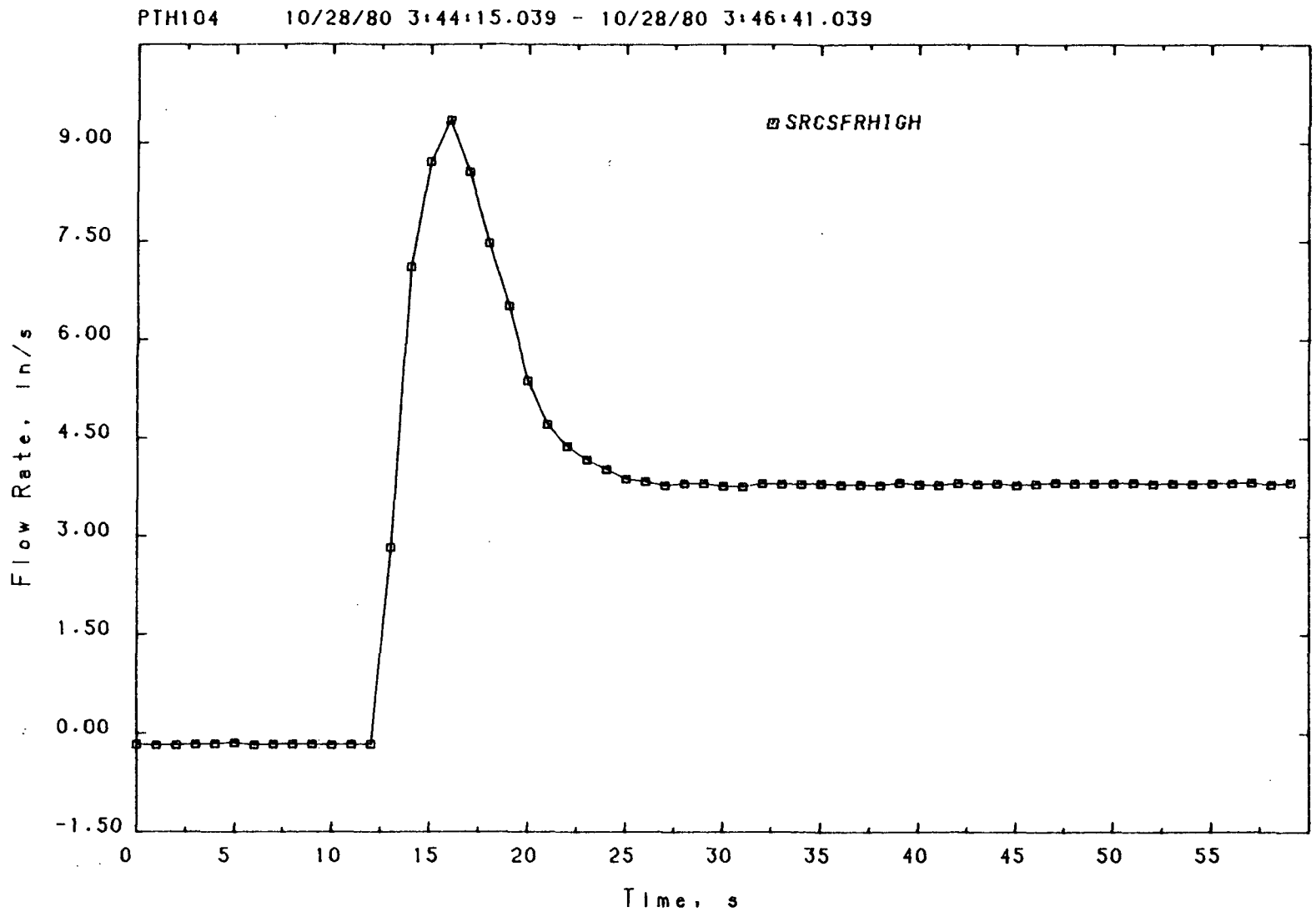

FIGURE 5.1.04 TEST ASSEMBLY REFLOODING RATE (NORMAL PREFILL)

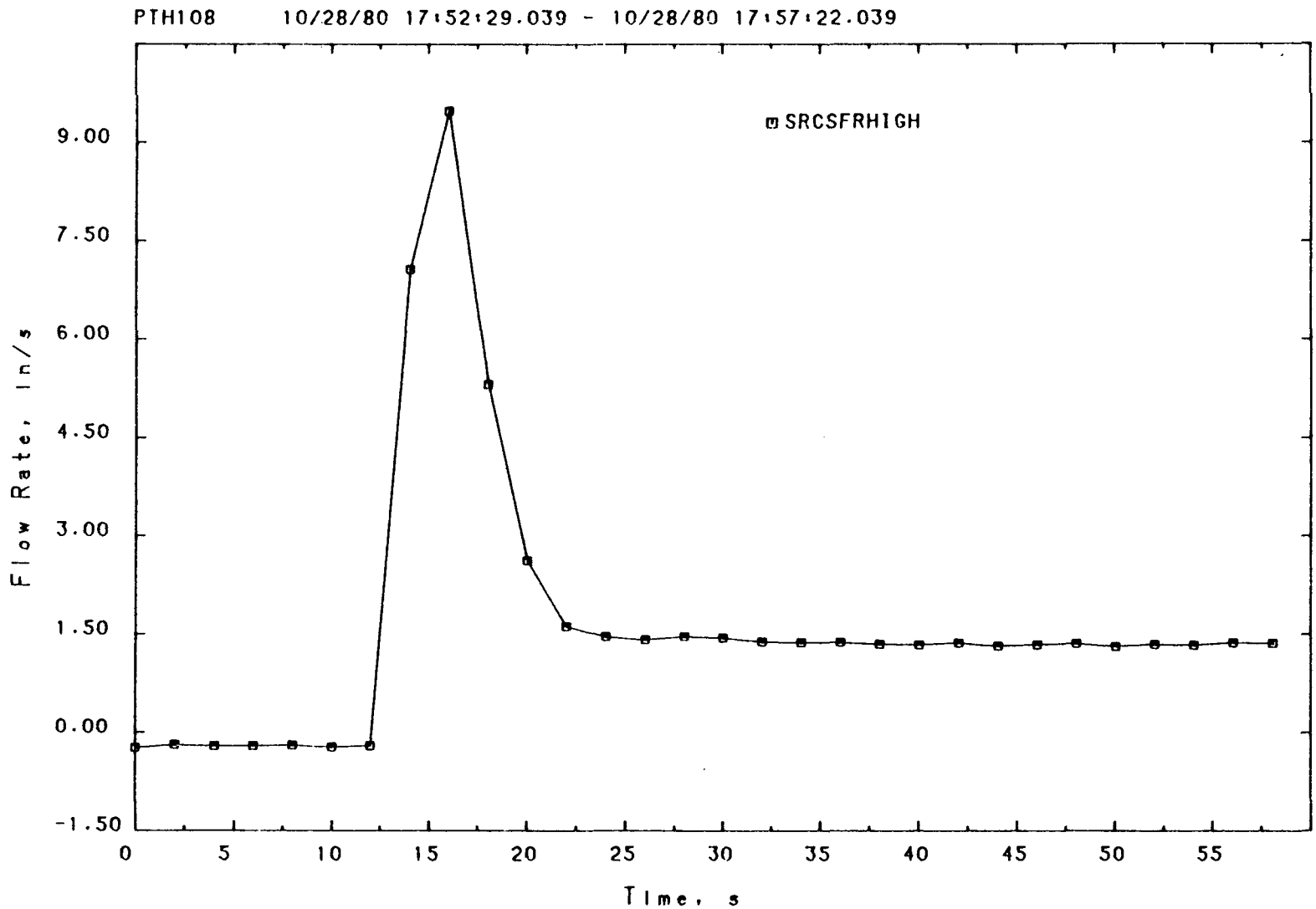

FIGURE 5.1.08 TEST ASSEMBLY REFLOODING RATE (NORMAL PREFILL)

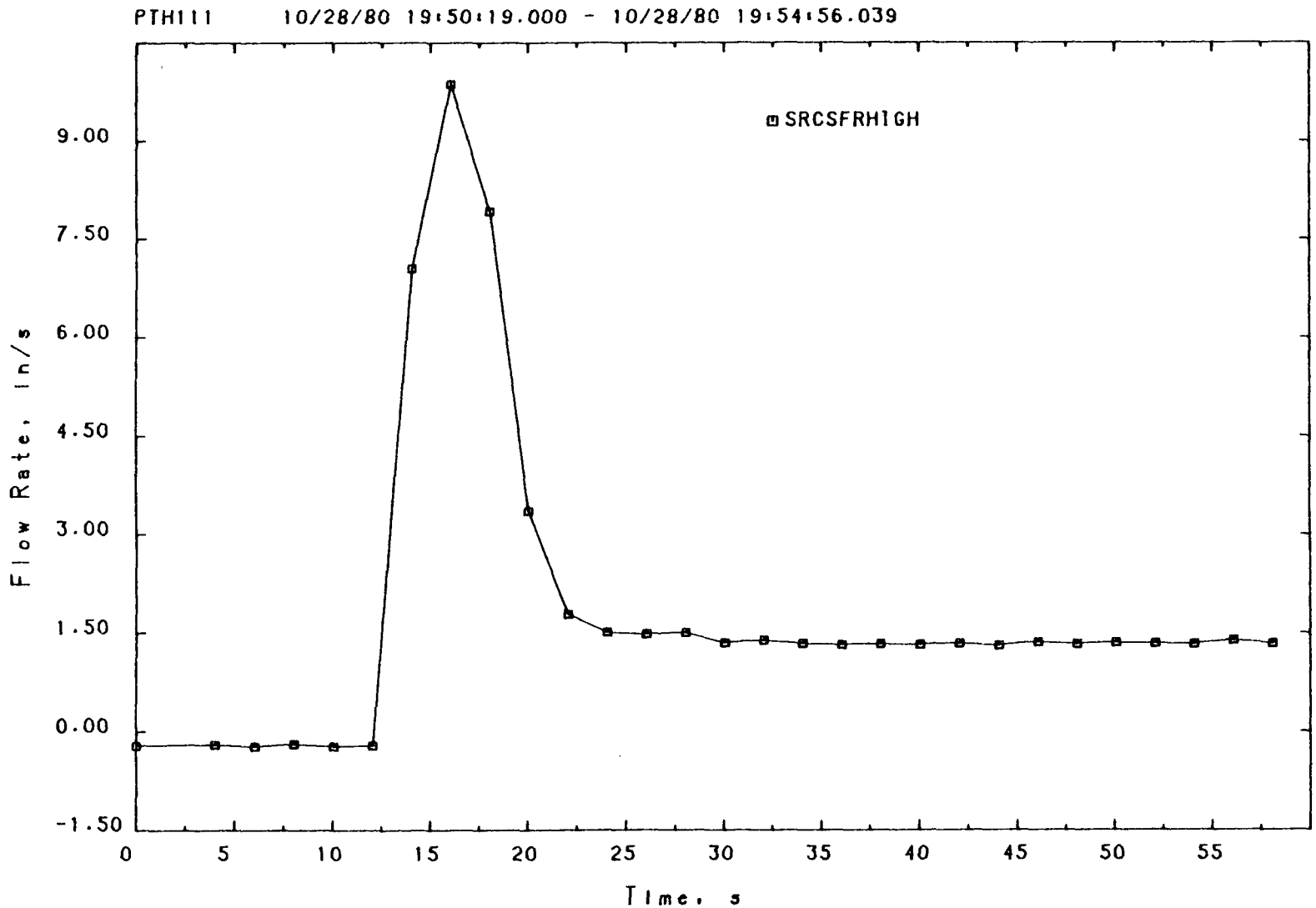

FIGURE 5.1.11 TEST ASSEMBLY REFLOODING RATE (FAST FILLED)

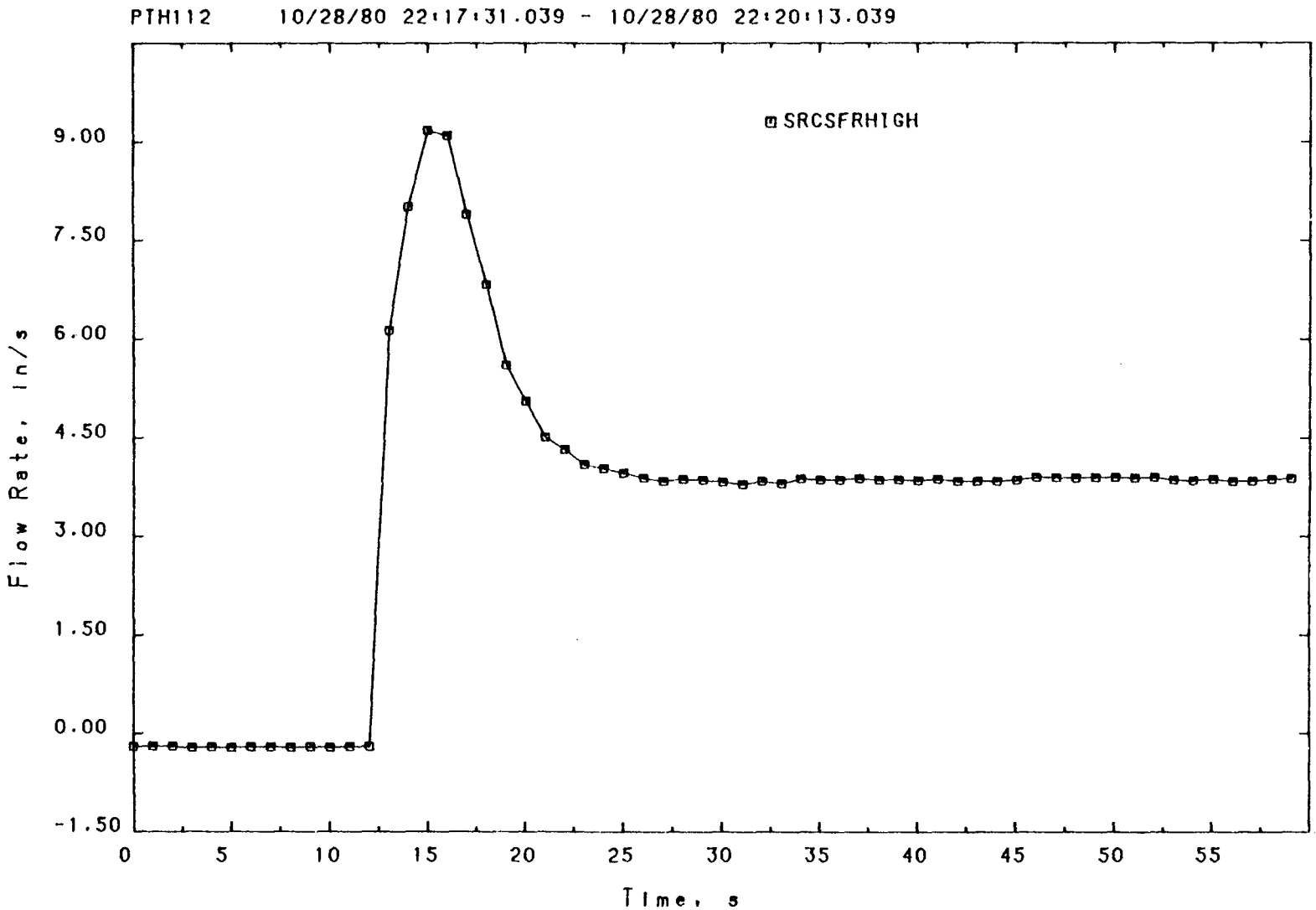

FIGURE 5.1.12 TEST ASSEMBLY REFLOODING RATE (NORMAL PREFILL)

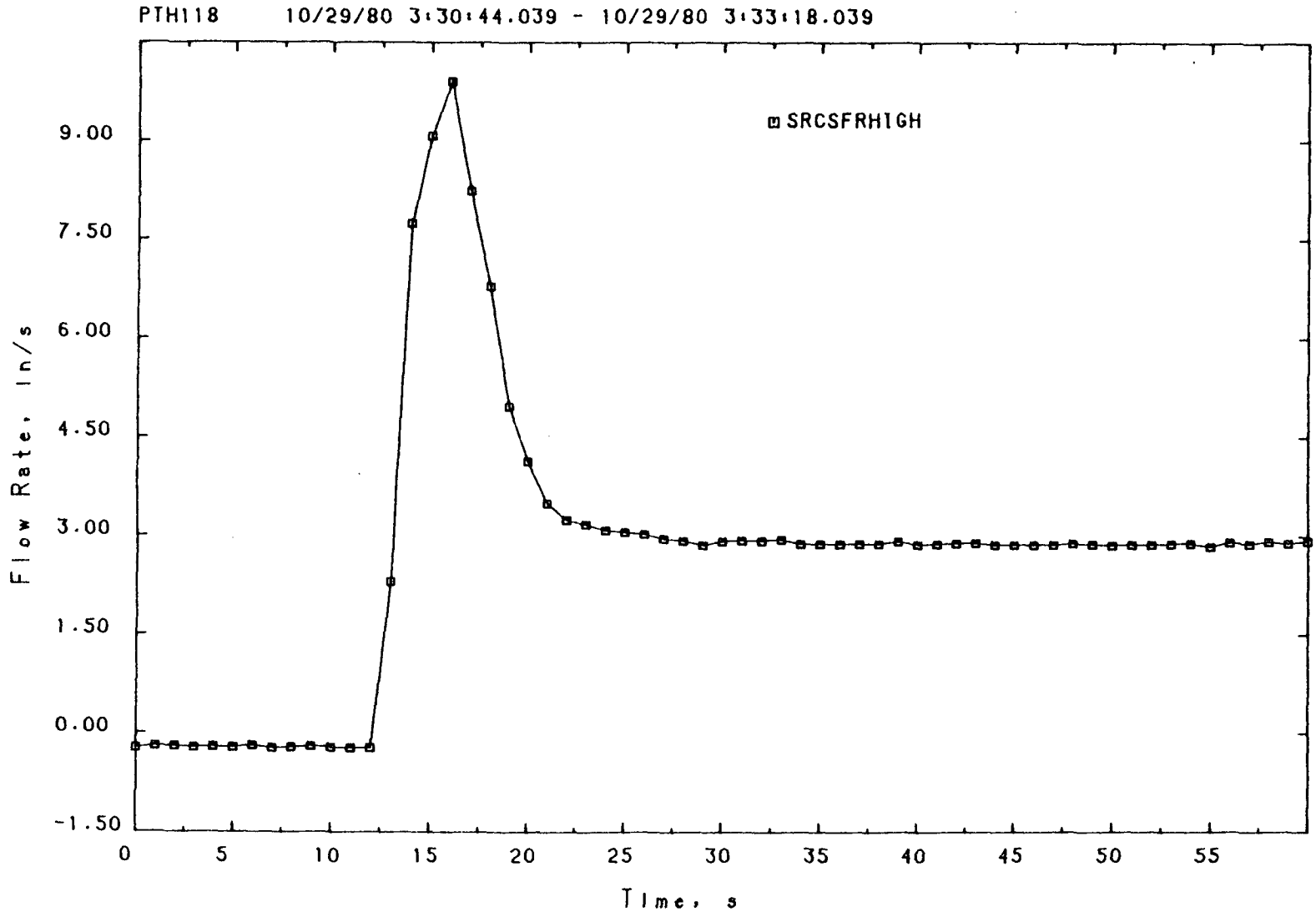

FIGURE 5.1.18 TEST ASSEMBLY REFLOODING RATE (NORMAL PREFILL)

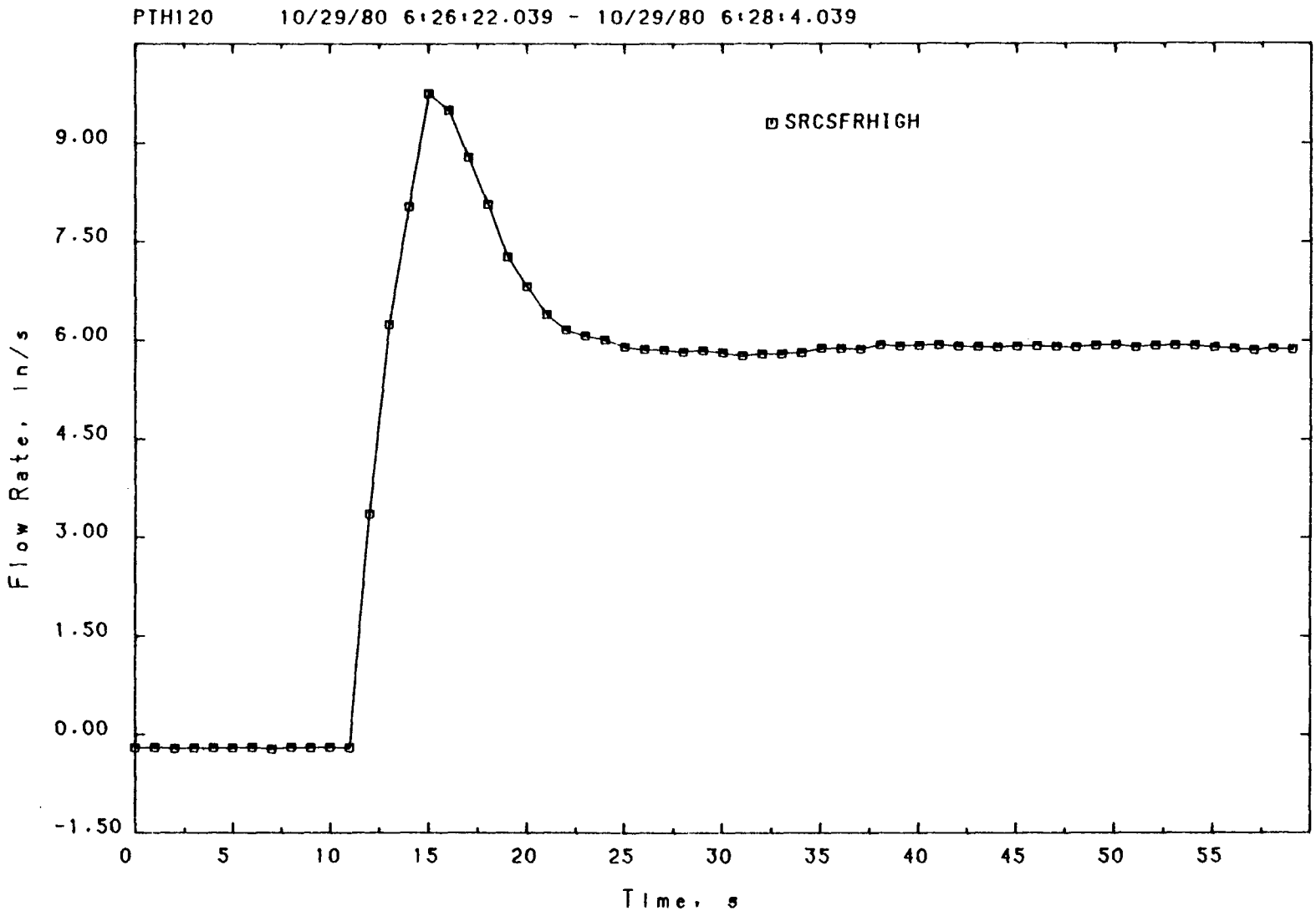

FIGURE 5.1.20 TEST ASSEMBLY REFLOODING RATE (NORMAL PREFILL)

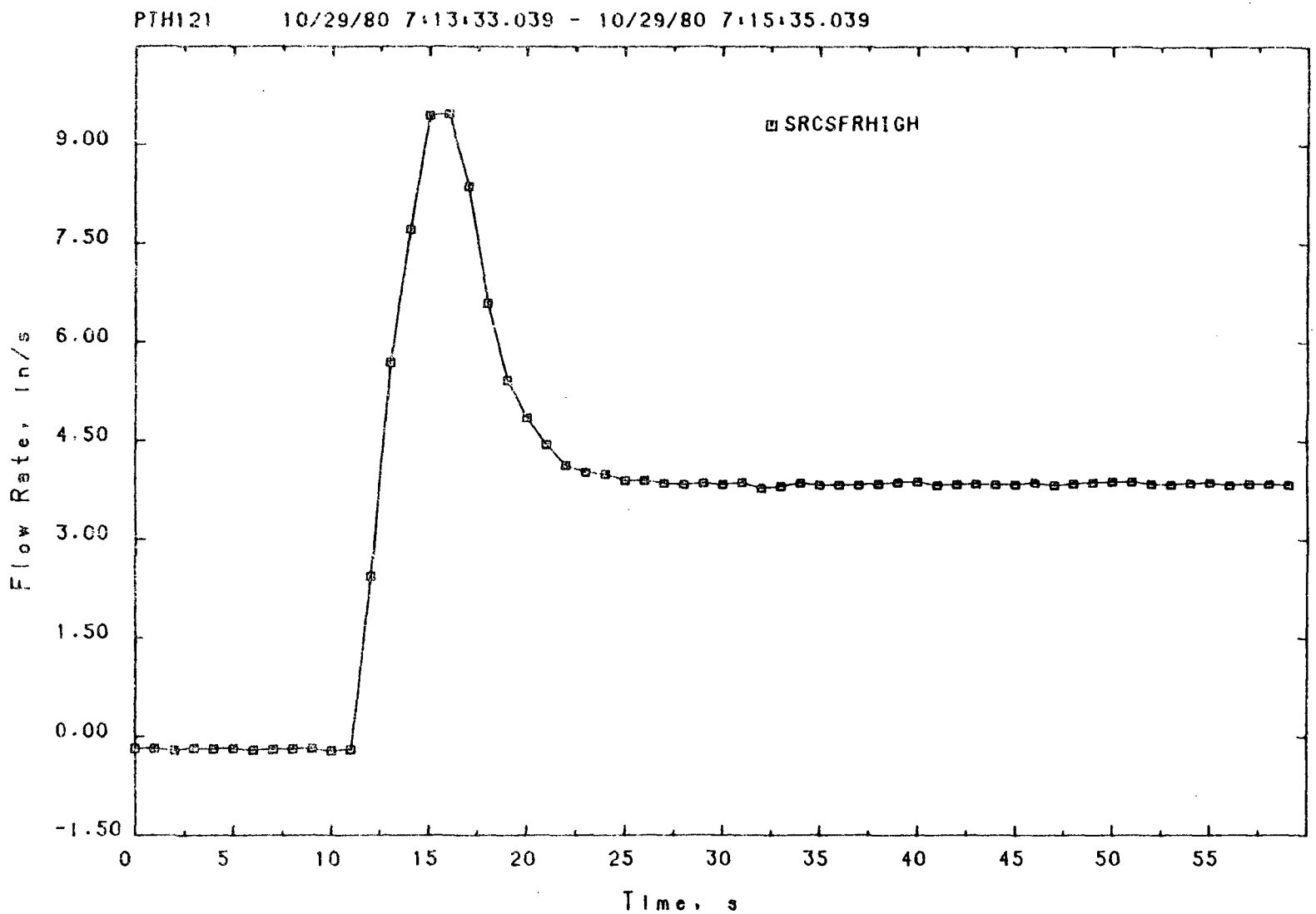

FIGURE 5.1.21 TEST ASSEMBLY REFLOODING RATE (NORMAL PREFILL)

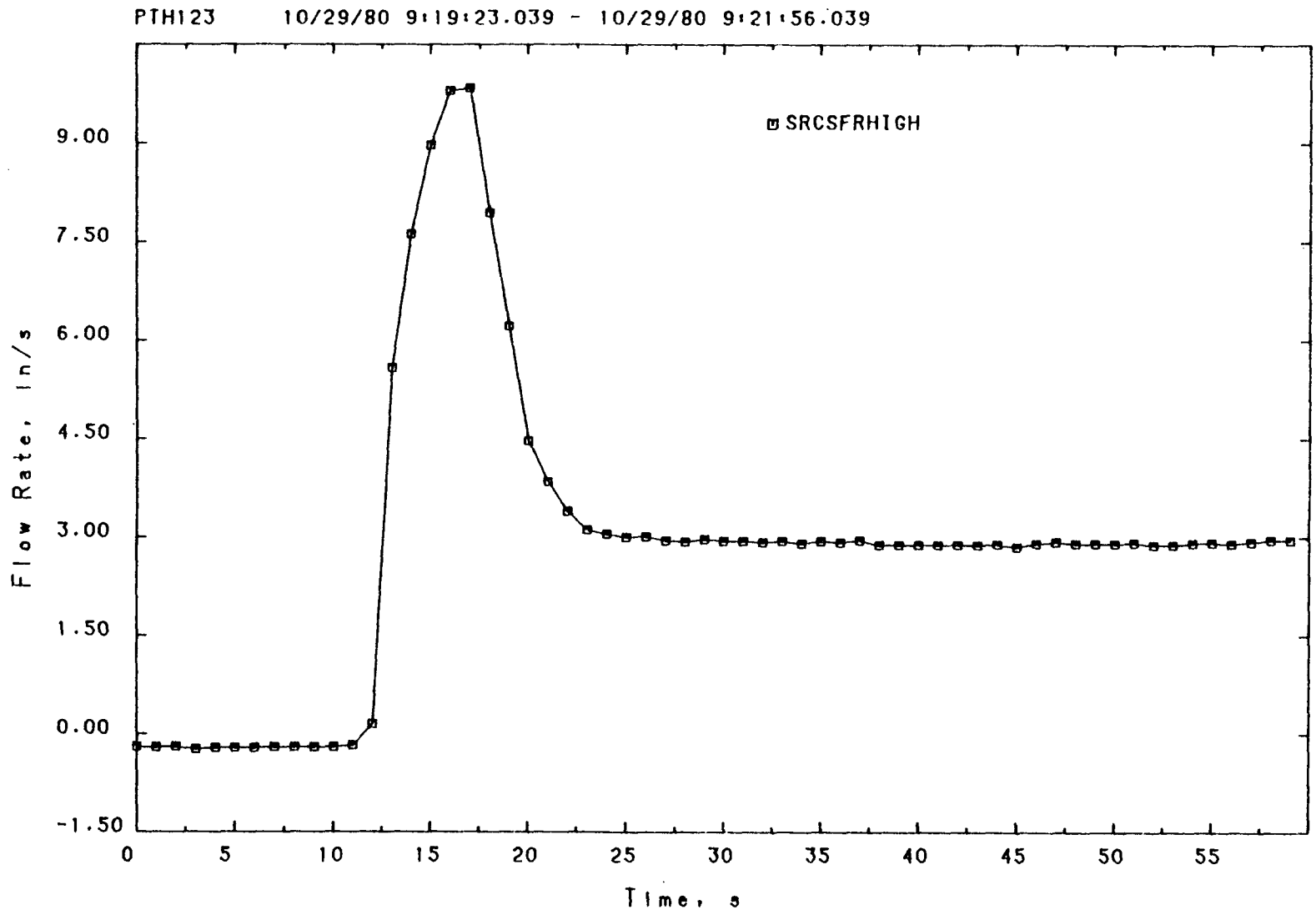

FIGURE 5.1.23 TEST ASSEMBLY REFLOODING RATE (FAST FILLED)

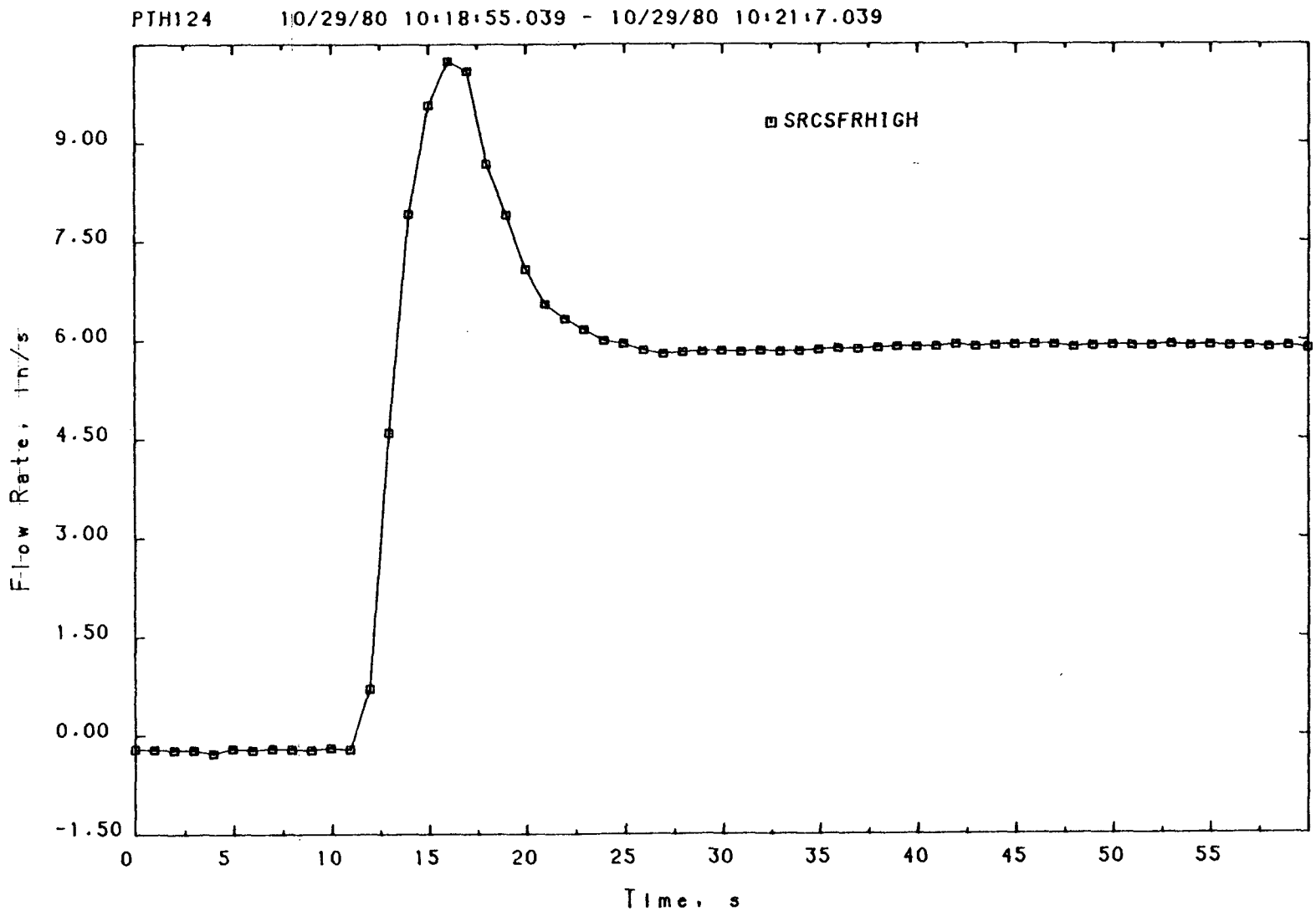

FIGURE 5.1.24 TEST ASSEMBLY REFLOODING RATE (FAST FILLED)

DISTRIBUTION

U.S. Nuclear Regulatory Commission
Washington, D.C. 20555
Mail Stop

L. Shotkin	Mail Stop - 1130-SS
N. Zuber	Mail Stop - 1130-SS
R. Meyer	Mail Stop - P-1114
R. Van Houten (3)	Mail Stop - 1130-SS
G. Marino	Mail Stop - 1130-SS
G. McPherson	Mail Stop - 1130-SS
J. Norberg	Mail Stop - NL-5650
N. Lauben	Mail Stop - P-1132
W. Hodges	Mail Stop - P-1132
L. Phillips	Mail Stop - P-1114
A. Hon	Mail Stop - 1130-SS
Y. Hsu	Mail Stop - 1130-SS
W. Johnston	Mail Stop - P-1114
D. Power	Mail Stop - P-1114
M. Picklesimer	Mail Stop - 1130-SS
L. Tong	Mail Stop - 1130-SS
T. Murley	Mail Stop - P-1102

Electric Power Research Institute (6)
3412 Hillview Avenue
Palo Alto, CA 94022

W. Sun
P. Davis (ITI)
L. Thompson
R. Oehlberg
G. Thomas
R. Duffey

Westinghouse Electric Corporation (3)
P. O. Box 355
Pittsburgh, PA 15230

L. Hochreiter
R. Rosal
D. Burman

Oak Ridge National Laboratory (3)
P. O. Box X
Oak Ridge, TN 37830

F. Mynatt
R. Chapman (2)

Combustion Engineering (2)
1000 Prospect Hill Road
P. O. Box 500
Windsor, CT 06095

R. Duncan
S. Ritterbush

Babcock and Wilcox (2)
P. O. Box 1200
Lynchburg, VA 24505

C. Morgan
B. Bingham

General Electric Company (5)
175 Curtner Avenue
San Jose, CA 95114

S. Armijo
R. Williams
L. Noble
G. Sozzi
N. Shirley

Exxon Nuclear, Inc. (4)
2101 Horn Rapids Road
Richland, WA 99352

W. Nechodom
W. Kayser
T. Doyle
J. Morgan

U.S. Nuclear Regulatory Commission
Advisory Committee on Reactor Safeguards
Washington, D.C. 20555
Mail Stop - H-1016

P. Boehnert
P. Shewmon
D. Okrent

Kernforschungzentrum Karlsruhe (4)
Weberstrasse 5
75 Karlsruhe 1
Federal Republic of Germany

H. Rininsland (2)
A. Fiege
F. Erbacher

JRC-ISPRA (4)
EURATOM
CCR ESSOR Division
21020 Cento Euratom Di Ispra (Varese)
Italy

T. Doyle
R. Klersy
J. Randles
S. Finzi

Central Electricity Generating Board
Berkeley Nuclear Laboratories
Berkeley, Gloucestershire GL13 9PB
England

T. Healey (2)

M. Ishikawa, Chief (4)
Reactivity Accident Laboratory
Japan Atomic Energy Research Institute
Tokai Research Establishment
Tokai-Mura, Naka-Gun
Ibaraki-Ken
Japan

D.M. Chapin
MPR Associates, Inc.
1140 Connecticut Avenue, NW
Washington, D.C. 20036

D. Ogden
EG&G Idaho, Inc.
P.O. Box 1625
Idaho Falls, ID 83401

J. Davis
Nuclear Engineering Department
Potomac Electric Power Company
1900 Pennsylvania Avenue, NW
Washington, D.C. 20068

C.A. Herriot/M. Notley (6)
Chalk River Nuclear Laboratories
Atomic Energy of Canada, Limited
Chalk River, Ontario, Canada KOJ 1JO

P. Griffith
Massachusetts Institute of Technology
Department of Nuclear Engineering
Cambridge, MA 02139

W. Kirchner
Los Alamos Scientific Laboratory
P.O. Box 1663
Los Alamos, NM 87544

J. Gittus
Springfields Nuclear Power Development Laboratory
United Kingdom Atomic Energy Authority
Springfields, Salwick
Preston PR 4 ORR
England

Mr. Mann
Springfields Nuclear Power Development Laboratory
United Kingdom Atomic Energy Authority
Springfields, Salwick
Preston PR 4 ORR
England

C.L. Mohr (30)
Battelle, Pacific Northwest Laboratories
P. O. Box 999
Richland, Washington 99352

NRC FORM 335 (7-77)

U.S. NUCLEAR REGULATORY COMMISSION

BIBLIOGRAPHIC DATA SHEET

1. REPORT NUMBER (Assigned by DDC)
NUREG/CR-1882
PNL-3681

4. TITLE AND SUBTITLE (Add Volume No., if appropriate)
Prototypic Thermal-Hydraulic Experiment in NRU to Simulate Loss-of-Coolant Accidents

2. (Leave blank)

3. RECIPIENT'S ACCESSION NO.

7. AUTHOR(S) C. L. Mohr, G. M. Hesson, G. E. Russcher, R. K. Marshall, L.L. King, N.J. Wildung, W.N. Rausch, W. D. Bennett

5. DATE REPORT COMPLETED
MONTH December YEAR 1980

9. PERFORMING ORGANIZATION NAME AND MAILING ADDRESS (Include Zip Code)
Pacific Northwest Laboratory
Richland, Washington 99352

DATE REPORT ISSUED
MONTH April YEAR 1981

6. (Leave blank)

8. (Leave blank)

12. SPONSORING ORGANIZATION NAME AND MAILING ADDRESS (Include Zip Code)
Division of Reactor Safety Research
Office of Nuclear Regulatory Research
U.S. Nuclear Regulatory Commission
Washington, DC 20555

10. PROJECT/TASK/WORK UNIT NO.

11. CONTRACT NO.
NRC FIN No. B2277

13. TYPE OF REPORT
Preliminary Test Report

PERIOD COVERED (Inclusive dates)
Reactor Tests of October 28-30, 1980

15. SUPPLEMENTARY NOTES

14. (Leave blank)

16. ABSTRACT (200 words or less)

A series of 28 nuclear heatup and reflood tests were performed on a 32-rod bundle of unpressurized, full-length, commercial enrichment, Zircaloy clad fuel rods. These tests were performed in the NRU reactor in October 1980. Reflood rates ranged from 1.88cm/sec (.074 in/sec) to 28 cm/sec (11 in/sec), with delay times to initiate reflood of 3 sec. to 66 sec. Measured peak clad temperatures ranged from 840K (1050°F) to 1370K (2007°G). Preliminary observations are that actual quench times are much less than predicted while peak temperatures are in general agreement with predicted values. There is no evidence of any test rod failure.

17. KEY WORDS AND DOCUMENT ANALYSIS
Peak Clad Temperature, LOCA Heatup, Clad Temperature Turnaround, Rewet, Quench, Thermal-Hydraulics, Clad Temperature Profile

17a. DESCRIPTORS
Loss of Coolant Accident (LOCA), Experimental Data, Reactor Test Data, Rewet, Quench, Cladding Temperature Profiles

17b. IDENTIFIERS/OPEN-ENDED TERMS

18. AVAILABILITY STATEMENT
Unlimited

19. SECURITY CLASS (This report)
Unclassified

20. SECURITY CLASS (This page)
Unclassified

21. NO. OF PAGES

22. PRICE
$

NRC FORM 335 (7-77)

UNITED STATES
NUCLEAR REGULATORY COMMISSION
WASHINGTON, D. C. 20555

OFFICIAL BUSINESS
PENALTY FOR PRIVATE USE, $300

POSTAGE AND FEES PAID
U.S. NUCLEAR REGULATORY
COMMISSION

U.S. MAIL